ANCHORAGE HOUSTON
ATLANTA LOS ANGELES
BETHESDA NEW YORK
CHICAGO PHOENIX
CINCINNATI PORTLAND
CRANFORD SALT LAKE CITY
DENVER SAN FRANCISCO
FAIRBANKS SANTA BARBARA
HONOLULU SEATTLE
WASHINGTON, D. C.

DAMES & MOORE

CONSULTANTS IN THE ENVIRONMENTAL AND APPLIED EARTH SCIENCES

CALGARY PERTH
GUAM SEOUL
JAKARTA SINGAPORE
JOHANNESBURG SYDNEY
LAGOS TEHRAN
LONDON TORONTO
MADRID TOKYO
VANCOUVER, B. C.

6 COMMERCE DRIVE · CRANFORD, NEW JERSEY 07016 · (201) 272-8300
CABLE: DAMEMORE TWX: 710-996-5959

December 5, 1975

Consolidated Edison Company of
New York, Inc.
4 Irving Place
New York, New York 10004

Gentlemen:

We are pleased to submit herewith copies of our report entitled, "Supplemental Geological Investigation of the Indian Point Generating Station for Consolidated Edison Company of New York, Inc.".

Should you have any questions concerning this report, please do not hesitate to contact us.

Yours very truly,

DAMES & MOORE

Joseph A. Fischer (TLS)

Joseph A. Fischer
Partner

Bernard Archer (TLS)

Bernard Archer
Associate

JAF/BA:elf

SUPPLEMENTAL GEOLOGICAL INVESTIGATION

OF THE INDIAN POINT GENERATING STATION

FOR CONSOLIDATED EDISON CO.
OF N.Y., INC.

DAMES & MOORE

NOVEMBER, 1975

484

Offices in principal cities

ANCHORAGE
ATLANTA
BILLINGS
BOCA RATON
BOSTON
CHICAGO
CINCINNATI
CRANFORD
DENVER
FAIRBANKS
HONOLULU
HOUSTON
LOS ANGELES
NEW ORLEANS
NEW YORK
PHOENIX
PORTLAND
SALT LAKE CITY
SAN FRANCISCO
SANTA BARBARA
SEATTLE
SYRACUSE
WASHINGTON D.C.
WHITE PLAINS

BEIRUT
CALGARY
JAKARTA
JOHANNESBURG
LAGOS
LONDON
MADRID
MELBOURNE
PERTH
SINGAPORE
SYDNEY
TEHRAN
TOKYO
TORONTO
VANCOUVER

DAMES & MOORE

Consultants in the Environmental and Applied Earth Sciences

SUPPLEMENTAL GEOLOGICAL INVESTIGATION OF THE INDIAN POINT GENERATING STATION

FOR CONSOLIDATED EDISON CO.
OF NEW YORK, INC.

Prepared by

DAMES & MOORE
CONSULTANTS IN THE ENVIRONMENTAL
AND APPLIED EARTH SCIENCES
CRANFORD, NEW JERSEY

Job. No. 0874-050-10

November 1975

TABLE OF CONTENTS

TABLE OF CONTENTS (Continued)

TABLE OF CONTENTS (Continued)

TABLE OF CONTENTS (Continued)

TABLE OF CONTENTS (Continued)

TABLE OF CONTENTS (Continued)

LIST OF PLATES

LIST OF PLATES (Continued)

LIST OF PLATES (Continued)

LIST OF PLATES (Continued)

LIST OF PLATES (Continued)

LIST OF PLATES (Continued)

LIST OF TABLES

1.0 INTRODUCTION

During the period of July, 1975 to October, 1975, Dames & Moore conducted a supplementary geologic investigation of the Indian Point Generating Station site and surrounding area (Plate C3-1). The investigation was authorized by Consolidated Edison Company of New York.

The intent of the investigation was to obtain additional evidence to establish, if possible, whether or not there is any evidence of recent displacement along the N-S trending fault identified onsite north of reactor unit No. 3.

The purpose of the study was to identify all significant site-associated structural features and to establish the origin and history of these features. The immediate objectives were to:

1) Determine whether or not there is any evidence of recent displacement along the N-S-trending fault identified onsite north of unit No. 3.
2) Explore the possible relationship of the fault onsite to any other significant faults in the region; and
3) Determine the date, absolutely or relatively, of the fault onsite and any others found to be associated with it or, alternatively, generate a sufficient weight of circumstantial evidence to resolve questions which may be raised by governmental agencies concerned with the safety aspects of these faults.

To achieve these objectives an integrated program of geological and geophysical investigations was conducted. This program included:

1) A review of the literature.
2) The preparation of lithological and structural plans of outcrops onsite.
3) The examination of available drill cores and foundation records onsite.
4) The generation of a geologic map of the site and surrounding area.
5) The study of fractures and faults both onsite and offsite.
6) Petrographic, mineralogic and fluid inclusion studies.
7) A regional reconnaissance of rock types, fractures and faults within a 10-mile radius from the site.
8) Radiometric dating of rock samples onsite and offsite.
9) The identification of linear features on remote sensing imagery.
10) The investigation of Pleistocene deposits and geomorphological features within a 10-mile radius of the site.
11) Seismic profiling in the Hudson River; and
12) A ground magnetic survey immediately northeast of the site.

Consultants with specialized technical skills were retained to supplement the investigations. Principal among these were: Dr. Lowell A. Douglas, consultant in pedology; Dr. Andreas Haji Vassiliou consultant in x-ray diffraction mineral identification; Krueger Enterprises, Inc., radiometric age determination; Dr. H. L. Barnes and Mr. R. K. McLimans consultant for fluid inclusion analysis and E.G.&G., contracted to perform marine seismic survey under Dames & Moore's supervision.

This report is presented in two parts. The first part, Introduction and Summary (Section 1.0 and 2.0), describes Dames & Moore's conclusions and interpretations in general terms - an overview, not an in-depth evaluation. The second part, which include all Appendices, is technical and provides the documentation necessary for a thorough evaluation.

2.0 SUMMARY

2.1 GENERAL

The Inwood Marble and Manhattan Schist Formations of the Manhattan Prong are the dominant litho-stratigraphic units cropping out at, and around the Indian Point Generating Station. These metasediments were initially deposited (during upper Precambrian and Lower Paleozoic) as flat lying undisturbed sedimentary layers on an existing metamorphosed and deformed Precambrian basement surface. Since their deposition, these rocks have been metamorphosed, folded, intruded by igneous rocks, faulted, and fractured during several orogenic and tectonic events.

During this study, the relative sequence of the development of fractures and faults that have affected these rocks since their deposition has been established. This was done to identify the nature and character of the youngest tectonic movement that has affected the area. The successively younger deformed rocks of the late Ordovician Cortlandt complex, the Devonian Peekskill Granite, and the sediments and intrusives of the Triassic Newark Basin were also studied to provide, whenever possible, a definite time correlation to a radiometrically dated geologic event.

It should be noted that the summary presented here is a synthesis of Dames & Moore's field effort integrated with the available published information on the geology of the region.

2.2 SEQUENCE OF REGIONAL DEFORMATION

Subsequent to sediment deposition and induration, the lithologic layers, which today are represented by the rocks of the Inwood and Manhattan Formations, were deformed. This initial phase of ductile deformation (F_1) developed isoclinal folds by passive flow, and a dominant axial plane foliation parallel to layering. F_1-deformation was coeval with the most intense period of metamorphism that these rocks have undergone. The minimum age for this event has been dated at 450 m.y. in the literature. A possible minimum age of 514 m.y. was obtained (by radiometric methods) during this investigation. West-striking normal faults, which produced monoclinal flexures in the overlying rocks were recognized in the Fordham Gneiss. Due to the ductile behavior of the overlying rocks, these faults are inferred to have formed during cooling following the peak of regional metamorphism and represent the initiation of brittle deformation within the Manhattan Prong.

A second period of folding (F_2) refolded the F_1-folds and is characterized by more open, concentric folds. The F_2-folds formed by flexural slip, implying a relatively brittle fold mechanism. The following fault and fracture directions were correlated with F_2-folds:

1) A conjugate pair of faults and fractures orientated about a compression direction that is normal to the layering and foliation (S_o/S_1);

2) Fractures oriented NW parallel to the extension direction; and

3) Thrust faults and extension fractures striking northeast and parallel to the strike of S_o/S_1.

The Cortlandt Complex was intruded during the period of F_2-folding. Locally, within the site area, it appears that both the fractures described above and the F_2-structural elements (axes and axial planes) have been equally rotated in the same direction by this intrusion. A radiometric age determination of 435 m.y. for the Cortlandt intrusion provides a minimum age for the genetic development of these fractures and faults onsite.

Regionally, conjugate strike-slip faults oriented WNW and NS, and orthogonal vertical extension fractures that bisect the acute and obtuse angles of the conjugate fault system may also be interpreted as being related to F_2-folding. Although the period of F_2-folding and fracturing was initiated prior to the intrusion of the Cortlandt Complex, it is possible that the stress system responsible for these faults endured long enough to have also affected the rocks of the Cortlandt Complex (Plate 1A).

Post-Cortlandt, the effects of a counterclockwise rotation of the regional compression direction resulted in the development of the following fractures and faults:

1) A conjugate pair of faults in which the dextral set strikes ENE to EW and the sinistral set

strikes WNW to EW. Regionally, these faults are also interpreted to be associated with local small-scale reverse faulting in Silurian rocks (Plate 1B).

2) A conjugate pair of faults in which the sinistral set strikes ENE to NE and the dextral set strikes NS to NNE (Plate 1C). Regional relationships also indicate that this conjugate pair is younger than the F_2-related fractures.

3) Steeply dipping to vertical extension fractures trending NW and NE (Plate 1C). Andesitic, diabasic, rhyolitic and lamprophyric dikes fill predominently steeply dipping NW-trending fractures and a few steeply dipping NE-trending fractures. A NW-trending lamprophyric dike has been dated at 398 m.y.

4) Shallow dipping NE-trending fractures which together with steeply dipping NW-trending fractures are intruded by pink granitic to pegmatitic dikes (Plate 1C). These dikes have been recognized in the area of the Cortlandt Complex. It is therefore inferred that these fractures were open prior to the intrusion of the Peekskill Granite.

Most of the faults and fractures described above may be interpreted as being geometrically related to open, concentric, steeply plunging F_3-folds. Although these folds have not yet been recognized in the study area, they have been described in other areas, one being the New York City area.

Both left-lateral and right-lateral senses of movement have been recognized along NNE and NNW-trending faults onsite and nearsite. Cross-cutting relationships onsite suggest that left-lateral NNE and right-lateral NNW may constitute a conjugate fault system with the regional compression direction oriented approximately NS (Plate 1D). The intrusion of the Peekskill Granite, which has been dated at 369 m.y., is interpreted to have occurred before the dissipation of the NS compression. Steeply dipping NNE and NNW fracture orientations have been recorded in the Peekskill Granite as joints only and no definite conjugate pair relationship can be established between these two trends. Extensional EW-striking fractures were also recognized in the Peekskill Granite.

Reactivation of the tectonic stresses occurred during the Lower Triassic and resulted in the development of the Triassic Newark-Basin. The Triassic sediments were deposited against the footwall of a normal fault, referred to in the literature as the Triassic Border Fault. This normal fault strikes northeast with the downthrown side to the southeast (Plate 2A). The Newark strata unconformably overlie pre-Triassic rocks along the northeastern and eastern margins of the basin.

The initial deformation of the Triassic rocks within the Basin was in response to a regional compression oriented approximately N25° to 30°E. A conjugate pair of faults developed, in which the sinistral set strikes NE to ENE and the dextral set strikes NNE. The regional distribution of this conjugate pair within the Triassic Basin makes it likely that rocks outside the Basin experienced the same deformation. It can also be postulated that the Triassic Border Fault experienced left-lateral, strike-slip movement at this time. Additionally, extensional fractures and normal faults striking between WNW and EW developed (Plate 2B).

Based on the structural interpretation of deformational features observed in the Manhattan Prong at and near the Indian Point Generating Station, the last tectonic event appears to have been in response to a simple shear system of sinistral polarity. The main shear of this system is oriented northeast. As a result, left-lateral reactivation of movement occurred along many northeast-trending faults (main shears) and numerous minor NNE to NNW-trending associated faults (synthetic shears). It should be mentioned, however, that during this investigation no left-lateral movement has been recognized on NNE to NNW-trending faults in the northern terminus of the Triassic Newark Basin. It is also interpreted that as deformation progressed, small increments of finite normal movement eventually occurred on NS- and NW-trending faults. Numerous NS-trending faults with steep-to-vertical slickensides have been recorded in the Hudson Highlands and lend support to this hypothesis. Some pre-existing WNW to EW-trending fractures and faults may also have inherited some of the tensional component associated with antithetic shears (Plate 2C).

To date, no unconsolidated deposits or soils older than Late Wisconsin (15,000 to 17,000 years old) have been identified in the area. These Late Wisconsin deposits consist mainly of thin glacial deposits on interstream uplands, and thicker, more extensive morainal, glacio-fluvial, glacio-lucustrine and ice contact deposits confined to the bottoms and walls of the principal valleys. Most of the faulting and folding observed in the unconsolidated sediments can be attributed to sedimentary and early diagenetic processes. The origin of a few faults and diapiric structures, described in detail in Appendix D, has not been determined conclusively.

Field and aerial photographic examination has revealed the presence of bedrock benches along the Hudson River. These benches represent remnants of an old, relatively flat valley bottom on strath which was cut by lateral planation of the Hudson River. The age of this bedrock (strath) terrace can be definitely shown to predate the Late Wisconsin ice advance, indicating a minimum age greater than 10,000 to 20,000 years. It appears that the bedrock terrace can be traced on both sides of the river from Cold Spring to Peekskill and on the east side of the river from Peekskill to Haverstraw. This terrace, which crosses several regional faults, occurs at about the same elevation ($\pm$10-20 feet) on opposite sides of the river and appears to have a constant uninterrupted slope between Cold Spring and Haverstraw.

Glacial striations on polished bedrock surfaces have been observed in the region. No vertical or horizontal displacement has affected the glacial features which extend across the faults. In one case, a half-inch vertical offset of striations on polished red sandstone does not appear to be the result of fault displacement (see Appendix D).

A soil horizon over the exposure north of reactor unit No. 3 developed as a result of the alteration of the underlying bedrock. Since the area was glaciated some 15,000 years ago and since the accumulation of clay is a time-dependent property, it is interpreted that the soil is 8,000 to 10,000 years old. The NNW-trending fault mapped in the trench at the foot of the exposure north of reactor unit No. 3 splays into two branches. The horizonation of the soil over one branch indicate that the soil has not been displaced by faulting (this determination has a precision of about ± 2 inches). Because of soil creep and differences in the rate of erosion of the underlying bedrock, no conclusion could be arrived at from soil information over the second branch.

2.3 SITE

The N-S striking fault described at the outcrop north of reactor unit No. 3 lies inbetween and terminates along two parallel NNW-trending faults. It is interpreted that the last movement on these faults occurred as a result of left-lateral reactivation along pre-existing faults in response to left-lateral displacement along northeast-trending shears.

Small euhedral crystals of undeformed calcite occur within the NS and NNW-trending faults north of reactor unit No. 3. Samples were collected from both the NNW and NS fault planes. The crystals are small (1 mm) and display well developed crystal faces. Textural relationships indicate post-tectonic formation in an open-fracture system. The results of homogenization tests, performed during fluid inclusion studies, yielded filling temperatures of 160° to 170°C. The minimum corresponding depths (pressures) to attain such boiling points is on the order of 150 feet.

The undeformed nature of the calcite crystals and the range of depths required for their formation indicates that the faults containing these crystals have not moved since they were buried at those depths. By applying a denudation rate of 2.7 inches/1000 years (Judson and Ritter, 1964) to the corresponding depth required for the formation of the fluid inclusions, the time required to unearth these crystals is 730,000 years. Meade (1969) contends that a denudation rate of 2.7 inches/1000 years is too high by a factor of two. This area was subjected to glacial scouring and the rate of erosion cannot be precisely determined. However, by using a conservative estimate of 6 inches/1,000 years, to qualitatively account for unknowns such as glacial scouring, it can be concluded that the NS to NNW-trending faults north of reactor unit No. 3 have not moved during the past 330,000 years. In addition, the suggestion of an even older age can, at the present time, be predicated on the filling temperatures of primary inclusions in unstrained crystals (160° to 170°C). These temperatures reflect a significant thermal episode probably related to igneous activity which is not known to have occurred in this area during the last 500,000 years.

FRACTURES ASSOCIATED WITH F_2

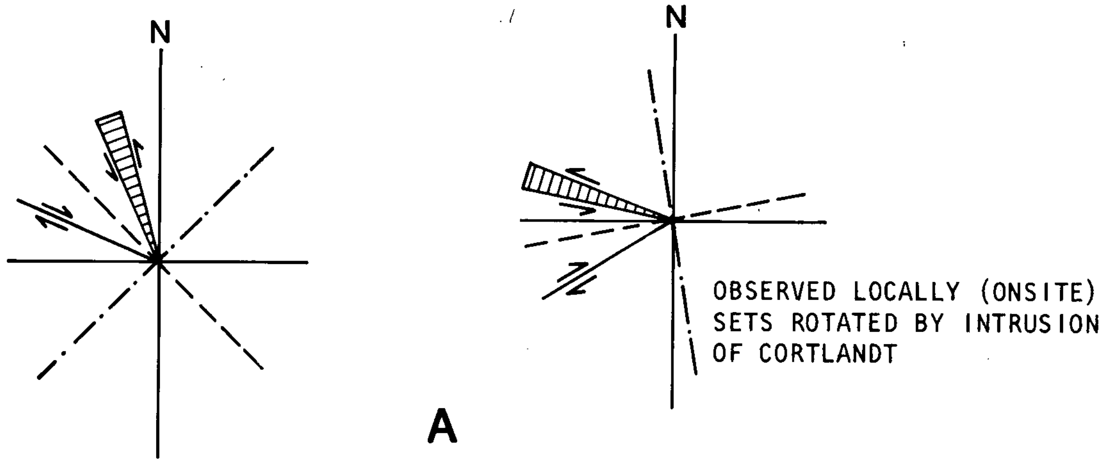

POST-CORTLANDT -- PRE-PEEKSKILL (> 369 m.y.)

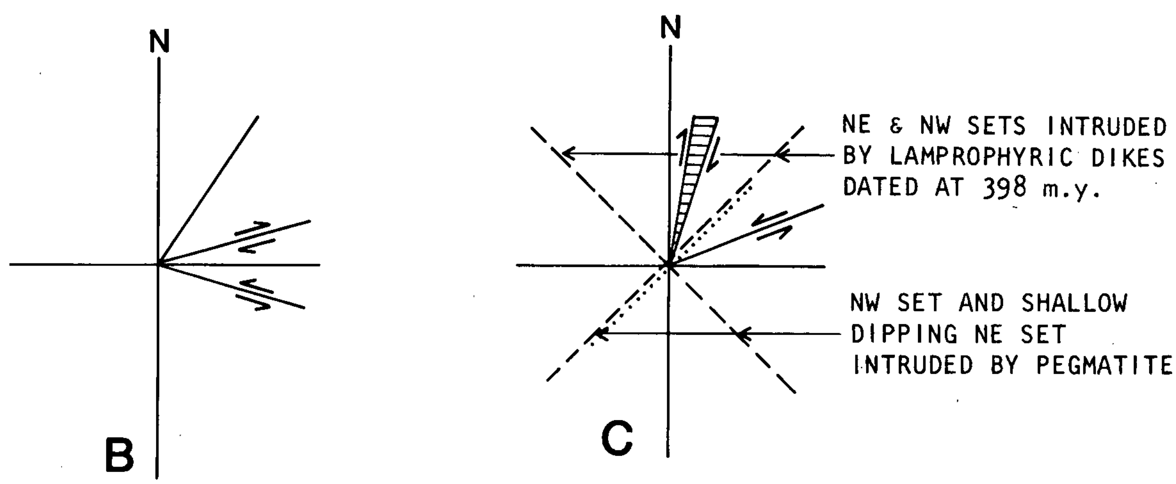

POST-PEEKSKILL (< 369 m.y.)

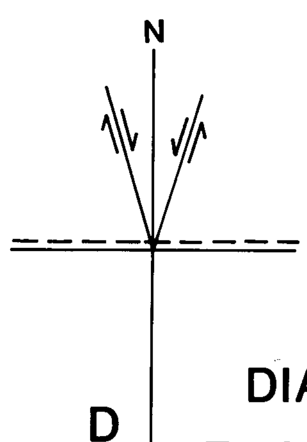

TENSION OR EXTENSION

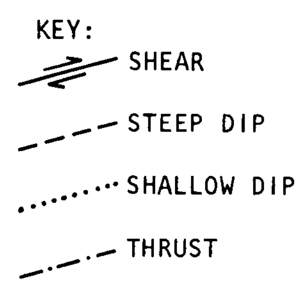

DIAGRAMMATIC SEQUENCE OF FRACTURE DEVELOPMENT WITHIN THE STUDY AREA

DAMES & MOORE

PLATE 1

DEVELOPMENT OF TRIASSIC BASIN (~200 m.y.)

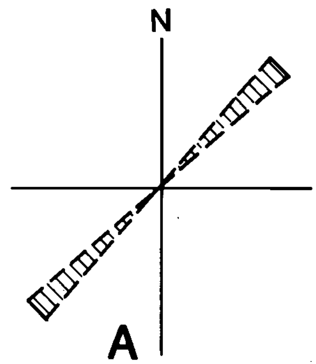

DEFORMATION OF TRIASSIC BASIN

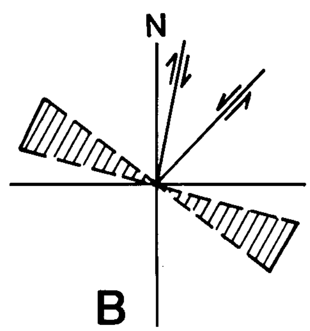

INTERPRETED LAST TECTONIC EVENT AT THE
INDIAN POINT GENERATING STATION

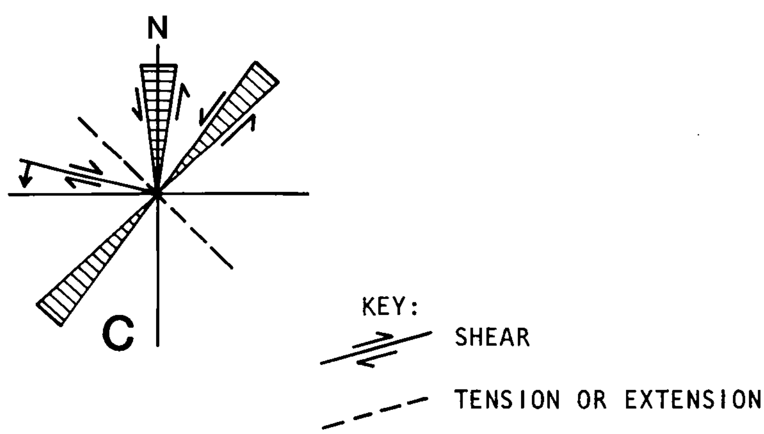

DIAGRAMMATIC SEQUENCE OF FRACTURE DEVELOPMENT WITHIN THE STUDY AREA

DAMES & MOORE

APPENDIX A

LITERATURE REVIEW

APPENDIX A1

GENERAL STATEMENT

The Indian Point Generating Station of the Consolidated Edison Company, Inc. of New York is located approximately two miles southwest of the City of Peekskill, Westchester County, New York, on the east bank of the Hudson River.

The following 7-1/2' U.S.G.S. Quadrangle maps, surrounding the site area, served as base maps for the geologic investigation:

Cornwall	West Point	Oscawana Lake
Popolopen Lake	Peekskill	Mohegan Lake
Thiells	Haverstraw	Ossining

These maps cover the area between latitude N41°07'30" and N41°30', and longitudes W73°45' and W74°07'30".

This section presents a summary of the geologic literature that discusses the rock types and stratigraphic relationships as well as the geologic structures and isotopic age determinations of the rocks that crop out at and around the Indian Point Generating Station.

APPENDIX A2

ROCK TYPES

A2.1 MANHATTAN PRONG

The Inwood Marble and Manhattan Schist Formations of the Manhattan Prong crop out onsite. Hall (1968) studied the stratigraphic relationships of the Manhattan Prong in the White Plains area. He recognized a gneiss complex, consisting predominantly of the gneisses and amphibolites of the Yonkers Gneiss and Fordham Gneiss, and a sequence of cover rocks consisting of lowerre Quartzite, Inwood Marble, and Manhattan Schist.

The Yonkers Gneiss is granitic in composition, whereas metamorphosed clastic sedimentary rocks compose most of the gneisses in the Fordham Gneiss. The gneiss complex, then, is interpreted as a predominantly clastic and volcanic eugeosynclinal sequence that has undergone high-grade metamorphism.

The Yonkers and Fordham Gneisses are truncated at the Inwood contact which is interpreted as a major angular unconformity. The scattered distribution of the Lowerre Quartzite in the Manhattan Prong is the result of deposition on an irregular topographic surface with high areas shedding clastic debris into local low areas. The Manhattan schist is in contact with different members of the Inwood Marble and locally even with the gneiss complex. This discordance between the base of the Manhattan and the older rocks, as well as the gneiss complex, is interpreted as another angular unconformity.

Since both the Inwood Marble and Manhattan Schist crop out onsite, the detailed stratigraphic classification presented by Hall (1968) for the White Plains area is included.

A2.1.1 Inwood Marble

The Inwood Marble is composed predominantly of clean dolomite marble and clean calcite marble with smaller amounts of calcite-dolomite marble, tan-to-brown weathering granular calcite marble, tan weathering calc-schists and, granular dolomitic siliceous rocks as well as some tan mica schist. The maximum apparent thickness of the Inwood Marble is 2000 feet (600 m) in the White Plains area. The Inwood Marble has been divided into five members, in the White Plains area. The following brief description of each member is in order of sequence from the base:

1) Inwood-A - White, gray, or bluegray dolomite marble composes member A of the Inwood.
2) Inwood-B - Interbedded white, gray, buff, or pinkish dolomite marble, tan and reddish-brown calcschist, purplish-brown or tan siliceous calc-schist, and gray calcite-dolomite marble are common. Bedding is one-half inch (1 cm) to 3 feet (1 m) thick. The upper and lower contacts of Inwood-B are gradational.
3) Inwood-C - White or blue-gray clean dolomite marble in beds 6 inches (15 cm) to 8 feet (2.4 m) thick are characteristics; in some places, member C is massively bedded and it is locally fetid. Irregular pods and lenses of quartz may be present.

4) Inwood-D - This consists of thin-bedded, tan dolomite marble, gray calcite marble, and tan calcschist.

5) Inwood-E - Gray or white calcite marble that commonly weathers tan is characteristic of member E.

Units B and C are the most commonly exposed members of the Inwood. There are some places where, apparently as a result of sedimentary facies changes, one or more of the Inwood members were not deposited. Such lensing in and out is apparently common for Inwood members D and E.

A2.1.2 <u>Manhattan Schist</u>

This is an assemblage of schists, schistose gneisses, and amphibolites. Three members of the Manhattan have been recognized and mapped in the White Plains area. These three members are here briefly described, beginning with the oldest.

1) Manhattan-A - Manhattan A is a predominantly gray or dark-gray fissile sillimanite-garnet-muscovite-biotite schist with interbedded white calcite marble at the base. It should be noted that these marble beds have heretofore been considered part of the Inwood Manhattan Schist. The schist is locally rusty or brown on the weathered surface. The entire unit has an apparent maximum thickness of 900 feet (300 m).

2) Manhattan-B - Dark greenish-gray or black amphibolite makes up member B. This unit is discontinuous, being absent or only a few feet (meters) thick in many places, but as much as 100 feet (30 m) thick elsewhere.

3) Manhattan-C - Brown weathered garnet-muscovite-biotite schist or schistose gneiss characterizes Manhattan C. These rocks are typically feldspar rich and commonly contain sillimanite nodules. Bedding is distinguished with difficulty in most exposures, but siliceous beds are prominent in some places.

Prucha (1956) studied the stratigraphic relationships of the metamorphic rocks in southeastern New York, south of the Hudson Highlands. He considers the Fordham, Inwood, and Manhattan conformable. These Formations can be traced almost continuously from New York City to Danbury, Connecticut. Some workers have suggested that this conformity is structural; but Prucha believed it unreasonable to expect that this conformity would be so complete and persistent over 60 miles, if due solely to deformation. Furthermore, he argued that the stratigraphic position should not be so consistent if conformity were due only to tectonism. He considers the local presence of Inwood and Manhattan type rocks in the Fordham to be due to tight infolding. He also prefers not to consider the Lowerre Quartzite as a Formation but as the upper quartzitic facies of the Fordham. The Fordham, Inwood, and Manhattan are considered to be part of the New York City Group.

Ratcliffe and Knowles (1969) studied the stratigraphic relationships in the Manhattan Prong, along the western edge of the Cortlandt intrusives. They described the following rock types:

1) Fordham Gneiss (Basement Rocks)

"Pinkish gray, poorly foliated, K-feldspar-quartz-biotite gneiss, granitic gneiss or granulite layered, biotite-plagioclase-quartz gneiss; massive, hornblende-biotite-plagioclase gneiss and related layered hornblende gneisses and amphibolites.

2) Lowerre Quartzite

White quartzite - weathers tan to pinkish-tan. Possible basal conglomerate present closest to the contact with the underlying Fordham Gneiss. No actual contact with Fordham seen.

3) Inwood Formation

Due to varying degrees of metamorphism, the Inwood differs from place-to-place in color and crystallinity.

Unit A "White to gray crystalline dolostone or dolomitic marble, without sandy or argillaceous impurities."

Unit B - "Gray to dark-gray, layered dolostone with thin, orange, weathering quartzite in one-inch beds, and numerous phyllitic partings... Minor three-to-five-foot thick quartzites along with biotitic, mottled calc-dolstone."

Unit C - "White crystalline dolomitic marble, locally sandy at base..." "...tremolite-diopside rich bed near the top at Crugers."

4) Manhattan Formation

A dark to light-bluish gray crystalline limestone or marble occurs at the base of the Formation. This basal carbonate thins or is absent where the Manhattan and Fordham are in close proximity. The Manhattan can be subdivided into two units:

The Lower Manhattan (Unit A) is principally a dark colored "graphitic" biotite-rich phyllite or schist containing interbedded black, calcite quartzites, calcareous phyllite, and phyllitic marbles. Rustyweathered sooty-black schists and calcareous graywackes occur near the base. Based on fossil content and lithologic characteristics, this unit is considered correlative with Annsville Phyllite of the Peekskill Valley.

Upper Manhattan (Unit B) is lighter colored than the Lower Manhattan. The Unit is characterized by abundant garnets and larger mica crystals. Biotite-muscovite-quartz-plagioclase granulites are common and account for a considerable thickness of this unit.

Lithostratigraphic mapping along the western border of the Cortlandt Complex (Ratcliffe and Knowles, 1969) supports the correlation of metasediments at Crugers, south of Cortlandt, with the rocks exposed at Verplanck Point, Tomkins Cove, and Stony Point. The following mineralogical assemblages were recognized within the Manhattan:

1) In the Tomkins Cove - Stony Point area: quartz-muscovitechlorite-opaque (Annsville, equivalent to Lower Manhattan); quartz-muscovite-biotite-plagioclase-opaque (Lower Manhattan); quartz-muscovite-biotite-plagioclase-garnet (Upper Manhattan).

2) At Verplanck Point: quartz-biotite-muscovite-plagioclasegarnet-opaque and quartz-biotite-muscovite-garnet-staurolite-calcite (Lower Manhattan); quartz-biotite-muscovite-plagioclase-garnet-staurolite (Upper Manhattan).

3) At Crugers: Quartz-biotite-muscovite-plagioclase-garnet-staurolite, quartz-biotite-muscovite-plagioclase-K-feldspar-calcite-

epidote, and quartz-biotite-muscovite-plagioclase-calcite-actinolite (Lower Manhattan); quartz-biotite-muscovite-plagioclase-staurolite-garnet-kyanite (Upper Manhattan).

These mineralogical changes appear to indicate normally progressive regional metamorphism to the east-southeast. Further southeast sillimanite was reported. The contact metamorphic effect induced by the Cortlandt Complex is local.

A2.2 HUDSON HIGHLANDS

The Precambrian rocks of the Reading Prong extend 140 miles from Reading, Pennsylvania, north to Connecticut. The metamorphic complex of the Hudson Highlands extends northeastward from Peapack, New Jersey, across the Hudson River, to Connecticut (Ratcliffe, 1970). Whereas Dallmeyer (1968) considered the Hudson Highlands to be part of the Reading Prong, Harwood and Zietz (1974) suggest that the weakly magnetic rocks of the Hudson Highlands appear to extend westward and overlie the more magnetic rocks of the main mass of the Reading Prong.

The mineral assemblages of the Highlands rocks are typical of the upper amphibolite-lower granulite facies of regional metamorphism. The metamorphic rocks in the Bear Mountain area are inhomogeneous and can be classified as:

1) biotite-quartz-feldspar gneiss;
2) hypersthene-quartz-oligoclase gneiss; and
3) hornblende-quartz-feldspar gneiss.

The predominant rock type is a rusty-weathering, well-foliated, biotite-quartz-feldspar-gneiss. Lenses of marble and local gradation into lenses or layers rich in sillimanite, garnet and/or graphite have been recognized. The hypersthene-quartz-oligoclase-gneiss has a faint foliation, is gray green on fresh surfaces and light gray on weathered surfaces. Free K-feldspar is rare. The hornblende-quartz-feldspar-gneiss is greenish, well-foliated, and shows a strong compositional layering.

Dallmeyer (1968) considered the biotite-quartz-feldspar gneiss a metasediment and the hypersthene-quartz-oligoclase-gneiss a meta-igneous rock. The hornblende-quartz-feldspar-gneiss is of unknown origin. Both the paragneiss and hornblende-quartz-feldspar gneiss were metamorphosed to the sillimanite-almandine subfacies of the almandine-amphibolite facies. The orthogneiss was metamorphosed to the granulite facies. Although the effects of retrogressive metamorphism have been recognized in the orthogneiss, these effects are localized and only one period of regional metamorphism is implied.

A2.3 MAJOR IGNEOUS INSTRUSIONS

The Storm King Granite is a hornblende granite that intrudes the Canada Hill Gneiss of the Hudson Highlands. Perthite, quartz, plagioclase and hornblende are the major constituents, and clinopyroxene, apatite, zircon, biotite, sphene, and opaques are accessories. A weak foliation, defined by hornblende, biotite, and flaty quartz crystals, is most conspicuous near the contacts. This foliation is conformable to that in the surrounding gneisses (Dallmeyer, 1968).

The Canopus Pluton, a highly differentiated dioritic to quartz monzonitic pluton, approximately 3.5 km long and 0.5 km wide, was emplaced as an elongated sill within an already well-developed fracture zone in Canofus Hollow. Ratcliffe and others (1972) considered this fracture zone part of the Ramapo fracture system. Northwest-southwest trending shears that cross the igneous rocks are filled with undeformed, late-stage pegmatitic differentiates, ranging in composition from hornblende diorite pegmatite to granite pegmatite.

The diverse igneous rocky types, ranging from diorite to peridotite, that make up the Cortlandt complex near Peekskill, New York, are intrusive into a series of metasedimentary rock of lower Paleozoic or late Precambrian age (Ratcliffe, 1968). Based on his mapping, Balk (1927) considered the complex to represent the upper part of a funnel-shaped magma chamber. Biotite diorite, remarkably uniform in both texture and composition, constitutes the earliest part of the pluton. This rock as well as the metasediments are intruded by layered cortlandite, pyroxenite, hornblende, pyroxenite, and hornblendite. Lamprophyre and diorite dikes and sills occupy definite joint sets in the biotite diorite and follow axial plane cleavage or compositional layering in the metasediments. Aplite dikes, several inches thick, cross the dikes in both the biotite diorite and the phyllite. Late-stage serpentinization of the Cortlandite is restricted to local areas and is of minor signifance (Ratcliffe, 1968).

The Rosetown is a composite pluton which has an older funnel-shaped mass of hornblendite and hornblende diorite. This older pluton and the surrounding Precambrian gneisses have been fractured along a shear zone that trends N40°E, coplanar with the nearby Ramapo Fault at Tomkins Cove (Ratcliffe, 1971). Blocks of Precambrian geniss, rocks of the older pluton, Waffinger limestone, and Annsville phyllite are found as xenoliths in the younger diorite that forms the major part of the Rosetown pluton. North and south of the pluton, unsheared lamprophyric dikes (largely spessartites) and small pods of diorite intrude the shear zone. These dikes intrude gneissic rocks in the vicinity of the Ramapo Fault near Tomkins Cove. Although foliated near the fault, these dikes and small diorite pods have not been as intensely mylonitized as the country rocks.

The Peekskill Pluton has an irregular, elongated shape aligned approximately east-west. Except for contacts with the Inwood Marble, there are no physiographic expressions of contacts between the Peekskill Pluton and adjacent rocks. Granodiorite occupies the center and western portions of the pluton. Eastward, it grades into a granite. Because of poor exposures, contacts are not accurately located. Inclusions from the Cortlandt Complex are rare and no xenoliths of Inwood have been found.

The granodiorite is a light-colored, fine-to-medium grained rock, generally massive, though locally a slight-to-moderate foliation can be recognized. The rock is more noticeably foliated and richer in biotite near the contact. The granite phase is a massive, high, fine-to-medium grained rock which is homogeneous in most places but locally shows a slight foliation due to the orientation of mica flakes.

A series of isomineralogical contour maps, showing the distribution of quartz and feldspar, suggest that the pluton is a skewed body. Espejo (1969) concluded that no evidence of faulting exists at the borders of the pluton, and interpreted the truncation of the isomineralogical contours to tilting of the pluton towards the northeast.

APPENDIX A3

STRATIGRAPHIC RELATIONSHIPS

Many geologists have proposed that the cover rocks of the Manhattan Prong correlate with the Cambrian and Ordovician clastic and carbonate sequence north of the Hudson Highlands. The Lowerre Quartzite correlates with the Poughquag Quartzite as well as the fossiliferous Dalton and Cheshire further north. Therefore, the Yonkers-Fordham gneiss complex is, therefore, Precambrian, but not necessarily coeval with the gneisses of the Hudson Highlands.

Prucha (1956) doubted that any definite stratigraphic correlation of the New York City Group can be made directly across the Hudson Highlands. However, he thought that, ultimately, some units may be proved to be correlative with the Cambro-Ordovician rock north of the Highlands. Paige (1956) mapped the rocks along a northeast-trending strip extending from Tomkins Cove, west of the Hudson River to near Annsville, east of the River. He accepted unequivocally as Cambro-Ordovician the Poughquag Quartzite (200± feet), Wappinger Limestone (200± feet), and the Hudson River Phyllite (Annsville, thickness unknown).

The sequence and thickness of many units are strikingly similar among rocks of the Stony Point-Tomkins Cove area, Verplanck Point, and Crugers. All workers agree that marbles and schists exposed south of the Cortlandt Complex (at Crugers) belong to the Inwood Marble-Manhattan Schist sequence that was developed in the type sections in Manhattan. The carbonate rocks and schists at Verplanck Point are generally thought to belong to the Manhattan Schist and Inwood Marble sequence. The discovery of Pelmatozoan columnals in the lower part of the Manhattan Schist (Ratcliffe and Knowles, 1969) strengthens the conclusion that the lower part of the Manhattan is Middle Ordovician at Verplanck Point. However, bedrock continuity of this fossiliferous unit to Crugers and to Tomkins Cove is everywhere broken by the Hudson River. At Tomkins Cove, the fossiliferous Trenton limestone indicates that the base of the Annsville Phyllite is also of Middle Ordovician age and may be correlative with the Manhattan Schist.

The Cambrian and Lower Ordovician deposits, represented by the Inwood Marble, comprise a sequence of clean dolomite and calcite limestone with some argillaceous and arenaceous beds. The thickness of the carbonate section beneath the Manhattan is highly variable, ranging from at least 400 feet at Crugers to total absence at Maiden Lane. At Maiden Lane the basal Manhattan is in contact with Unit A of the Inwood. Furthermore, at Maiden Lane the combined Inwood and Lowerre are only 45 feet thick, and are situated between the basal Manhattan and the Fordham. An unconformity beneath the basal Manhattan is, therefore, consistent with the regionally unconformable relations known in the Middle Ordovician of adjacent areas of New York State and New England (Ratcliffe and Knowles, 1969).

APPENDIX A4

ISOTOPIC AGE DETERMINATIONS

Isotopic mineral ages in the Manhattan Prong indicate that the rocks underwent a final thermal event involving pegmatite formation at about 360 m.y. ago. Ages obtained from various pegmatites and the Peekskill Granite support the conclusion that they were not emplaced later than 360 m.y. (Long and Kulps, 1962). They use the K-ar ages of 480± 15 m.y., 455 m.y., and 445 m.y. for the Fordham Gneiss near Crotonville and at Terrytown, and the 43.5 m.y. age of the Cortlandt Complex to suggest that the 360 m.y. event was superimposed on an existing metamorphic terrane. The minimum age of this terrane must have been 460 to 480 m.y. Pb-Pb and U-Pb ages of detrital zircons (well-rounded) from the Fordham Gneiss indicate a time of formation at about 1,150 m.y. It should be noted that this isotopic information does not establish a Precambrian age of either the original sedimentation or the metamorphism(s) of the Manhattan Prong.

Pb-Sr whole rock analyses of Pound Ridge Granite Gneiss, within the Fordham Gneiss, indicate that the granite gneiss formed 596±19 m.y. ago. This age is very similar to the Rb-Sr whole-rock isochron age of 575± 30 m.y., obtained from the Yonkers Granite Gneiss by Long (1969). The Yonkers and Pound Ridge Granite Gneisses, therefore, constitute an accumulation of Avalonian migmatitic fluids that permeated the pre-Avalonian Fordham Gneiss (Mose and Hayes, 1975). They also indicate that, on the basis of $^{40}Ar/^{39}/Ar$ incremental heating studies, the 360 m.y. regional metamorphism reported by Long and Kulp (1962) took place about 450 m.y. ago. The 360 m.y. age represents the time at which the micas were uplifted and cooled enough to retain radiogenic argon.

In the New Jersey-New York Highlands west of the Hudson River, concordant U-Pb ages from zircon suggest that the Highlands were metamorphosed at about 1,150 m.y. ago. A later metamorphism or reheating is suggested by K-Ar and Rb-Sr mica ages which agree at roughly 835 ± 35 m.y. The Storm King Granite north of Bear Mountain, which intrudes the 1150 m.y. old "Canada Hill Gneiss", yields discordant zircon ages. The Pb^{207}/Pb^{206} age of 1060 m.y. was considered a minimum for the Storm King by Long and Kulp (1962).

Dallmeyer (1972) noted that retrograde alteration is locally developed in the Highlands, west of the Hudson River (particularly in paragneisses), and is more widespread to the east. Total gas $^{40}Ar/^{39}Ar$ biotite ages from western paragneisses are 799 ± 10 m.y.; 805 ± 10 m.y.; and 810 ± 15 m.y. Hornblende ages range from 915 to 950 m.y. (Sutter and Dallmeyer, 1972). Pb^{207}/Pb^{206} Zircon ages are 1150 m.y. $^{40}Ar/^{39}Ar$ incremental gas release patterns show negligible variation in the $^{40}Ar/^{39}Ar$ ratio, and the total gas and incremental ages are similar. This correlation is not consistent with episodic gas loss (i.e. a distinct 800 m.y. retrograde event) but suggests the discordancy between Zircon and biotite ages resulted from continuous gas-diffusion during slow uplift. Biotite $^{40}Ar/^{39}Ar$ total gas ages also decrease in age from west to east, whereas coexisting hornblendes generally record slightly older ages. In the easternmost areas, both biotite and hornblende show plateau incremental release patterns. In the western areas, incremental release patterns (345-380 m.y.) with hornblendes give older total gas ages (545-580 m.y.). The release patterns and age distribution suggest only one Paleozoic thermal event increasing in intensity from west to east. The range of ages in easternmost areas suggests that this occurred prior to Late Ordovician (Dallmeyer and others, 1974 and 1975).

A whole-rock isochron, based on samples ranging from pyroxene diorite to quartz morzonite, yields an age of 1032± 45 m.y. for the Canopus Pluton. Biotite separated from the Canopus diorite yielded a K-Ar minimum age of 700±28 m.y. (Ratcliffe 1971, 1972). Therefore, this pluton postdates the 1150 m.y. dynamo-thermal event that affected the Precambrian gneisses. A phlogopite K-Ar age of 893±10 m.y. from the fault zone at the west side of Canopus Hollow is probably a minimum age for Precambrian fault activity on the Canopus Fault (Ratcliffe and others, 1972).

Biotite from biotite norite of the Cortlandt Complex near Montrose Station, on the east side of the Hudson River, yielded an age of 435 m.y. Long and Kulp (1962) concluded that this date represents the minimum age of intrusion of the Cortlandt Complex. K-Ar ages of 810± m.y. on hornblende from the older part of the Rosetown Pluton and 580± 20 m.y. from the diorite were interpreted as excessively old ages because xenoliths of Annsville phyllite and Wappinger limestone occur in the diorite (Ratcliffe, 1971). Therefore, the Cortlandt and the Rosetown may be, at least in part, correlatives.

The youngest granitic type rock recognized in this area is the Peekskill Granite. Concordant K-Ar and Rb-Sr muscovite ages of 355 ± 15 m.y. were obtained from this Granite (Ratcliffe, 1971). Mose and others (1974) also reported that a five-point isochron from the Peekskill Granite yielded an age of 369 ± 27 m.y. with an initial Sr_{87}/Sr_{86} ratio of 0.7076 ± 0.0005.

APPENDIX A5

STRUCTURE

A5.1 PRECAMBRIAN

Dallmeyer (1972) recognized that the first event in the tectonic history of the Bear Mountain area, in the Hudson Highlands metamorphic complex, was the formation of east-northeast plunging isoclinal folds (B_1) that eradicated most of the primary structures and produced a well-developed axial plane foliation. The foliation is mostly, but not always, parallel to compositional layering that reflect either original sedimentary layering or metamorphic differentiation (Dallmeyer, 1968). The axial planes of B_1 strike northwest and dips 30° to 50° northeast. Various lineations (bondinage, sillimanite and hornblende C-axes, and rodding of quartz and feldspar) are associated with B_1-folding. Sillimanite lineations display a maximum of S80E-25°, whereas bondinage lineations trend nearly N75E-35°. The others are randomly oriented.

A subsequent increase in rock competence led to the superposition of a set of more open folds (B_2) which distorted the earlier fold set. The northeast trend of these structures (N35° to 45°E, plunging 30° to 45°) is the dominant structural orientation in the Highlands. Most lineations are related to B_2-folds. These lineations are: preferred orientation of sillimanite and hornblende C-axes, and crests and troughs of mesoscopic B_2-folds. These lineations define a single N36E-35° maximum. Megascopic folds show that $\beta + B_2$ and that B_2-fold axes and B_2-lineations are nearly identical in orientation implying that B_2 was cylindrical.

The tightness of the B_1-folds, plus their strong axial plane foliation, suggest that the first movements in the Bear Mountain area consisted of slip (shear) folding during which S_o-surfaces were passively folded. Rodding parallel to B_1 indicates some translation of material along B_1-axes, most likely due to dehydration that left the rocks mobile and incapable of supporting laminar-glide movements. Consequently, the early shear folding gave way to a transitional stage where movements were accomplished by a combination of shear and flexural-slip folding. This increase in competence, during the transitional period, was accomplished by a reorientation of the regional stress field which is recorded in the spread of quartz and biotite girdles in the petrofabric projections and in the elongated maxima of B_1-projections. The transitional period was followed by development of B_w-folds. B_1-axial plane foliation is rotated about the B_2-folds. All B_1-lineations and fold axes were rotated along a small circle during B_2, indicating flexural-slip folding (Dallmeyer 1968).

The B_1 and B_2-folds recognized in the Bear Mountain area of the Central Highlands (Dallmeyer 1969, 1972) are correlative with the F_2 and F_3 features described by him in the Sloatsburg-Ramsey area (Dallmeyer, 1972). Mesoscopic F_1-folds related to the earliest deformation throughout the Highlands were identifield in the Bear Mountain area by Helenek (1971), and in the Sloatsburg-Ramsey area by Dallmeyer (1972). These folds are typically appressed, nearly recumbent, often rootless isoclinal folds whose axial planes parallel or subparallel the southeast dipping foliation (Dallmeyer, 1972).

The folding events occurred during a single episode of regional metamorphism at upper amphibolite to lower granulite facies intensity (Dallmeyer, 1972). The Canopus Pluton cross-cuts F_1-folds in the Precambrian gneisses and crystallized during a phase of right-lateral, strike-slip faulting which accompanied F_2-folding along a N40°E trend. At Bear Mountain the Storm King Granite forms a phacolith that is believed to have intruded the keel of a N40°E plunging synform (Lowe, 1950). Similarly, a large "phacohithic" hornblende granite body occupies the core of the High Torne (F_3) synform. Th granite was either synchronous with F_3-folding or at least mobile at that time (Dallmeyer, 1972). Consequently, the F_1 and F_2-folds in the Precambrian rocks did not form during a Phanerozoic orogenic event (Ratcliffe and others, 1972). Detailed structrual studies at the northern end of the Highlands may reveal Paleozoic refolding of Precambrian structures.

A5.2 <u>PALEOZOIC</u>

In the Tomkins Cove dolomite quarry, west of the Hudson River, the rocks are isoclinally folded. The axial planes of major and minor folds are overturned to the northwest. Beds strike N35° to 40°E, and dip approximately 70°SE. Dips on the eastern limb of folds are gentler than those on the western limb. Phyllites and mica schists appear in the northeast part of the quarry and dip steeply southeast. The dolomites and phyllites are interpreted to be on the western flank of a major tight, overturned fold. In a quarry north of Verplanck, on the east side of the Hudson River, closely folded dolomites strike N35° to 45°E, and dip approximately 70°SE. The dolomite is interpreted to occupy the eastern limb of an overturned fold. Mica schists overlie the dolomites and also dip 70°SE. The dolomites on both sides of the Hudson River differ only in the degree of recrystallization, with the dolomite on the east side being more recrystallized than that on the west side. This difference is interpreted to have resulted from the contact metamorphic effect imposed by the intrusion of the Cortlandt Complex (Paige, 1956). Paige was convinced that the dolomites and phyllites (schists) on both sides of the Hudson River are correlative and that the Cambro-Ordovician sequence is identical to the InwoodManhattan sequence of the Peekskill area. He also thought that some evidence existed for a second period of folding.

Mapping by Ratcliffe (1968) supports Paige's contention that Stony Point represents the upright limb of a major northeasterly trending anticline that runs through the Tomkins Cove quarry. A calcite marble, interbedded at the base of the dark phyllite, which, in turn, rests on dolostones just west of Stony Point, forms a unique three-part stratigraphic sequence that is repeated on the west limb of the proposed structure at the Tomkins Cove quarry. This correlation is further supported by right-side-up, southeast facing crossbeds in the dolostone on the southeast limb of the anticline west of Stony Point. The anticline is interpreted as an F_1-structure with an axial trace that extends from Verplanck through Tomkins

Cove to Crugers (Ratcliffe, 1968).

The orientation of the axial planes of F_1-folds is not consistent, owing to a later phase of folding that warped the earlier axial planes. F_2-folds vary in intensity and orientation from one locality to the next. These late structures seem to be genetically related to the intrusion of the Cortlandt Plutons. Indeed, F_2-structures may have resulted from interference between small "mushrooming" plutons (Ratcliffe, 1968).

The effects of three phases of folding with associated fabric changes have been recognized in the Manhattan Formation of Manhattan Island and in the Schists of the Bronx, in New York City (Bowes and Langer, 1969; and Langer and bowes, 1969). The first recognized phase of deformation was characterized by isoclinal folds (F_1) with a strong axial planar foliation, associated with regional metamorphism. The most prominent and commonly developed folds, which deform both the lithological layering and the dominant foliation, were formed during a second phase (f_2). The fold axes of these second-phase folds consistently plunge at a moderately shallow angle, and their trend generally correspond with that of the Appalachian Mountain belt. Deformation took place by both flexural-flow and flexural-slip mechanisms; there was some new mineral growth and the development of pegmatitic material. In a third phase of deformation (f_3), open, steeply plunging, symmetrical folds were formed. The major structures in the New York City area, shown to be the result of deformation during F_2 (Langer and Bowes, 1969), can be traced northwards through the White Plains district to the Peekskill district (Bowes and Langer, 1969).

A5.3 FAULTS

The term "border fault system" is used by Ratcliffe (1971) to describe collectively the various faults that trend N30° to N50°E, and either mark the northwest border of the Triassic sediments or lie close to the depositional edge of the Newark Basin. He considers that the Ramapo Fault proper, a part of this sytem, extends for 50 miles from Stony Point, New York to Peapack, New Jersey.

At Stony Point the Ramapo Fault downdrops both Triassic and Paleozoic rocks against the Precambrian on the west. This portion of the fault extends across the Hudson River to the Peekskill Hollow area. From Annsville, New York, a complex fracture zone along Canopus Creek extends northeastward across the entire width of the Hudson Highlands. The Ramapo Fault proper and the northeastern extensions are referred to collectively as the "Ramapo fault system" (Ratcliffe, 1971).

Estimates of maximum dip-slip displacement on the border fault in post-Brunswick time range from 30,000 to 200 feet. In support of a maximum 200 to 500-foot vertical net slip, Ratcliffe (1971) observed that the Triassic fanglomerate is only in fault contact for a distance of 700 feet. Paleozoic rocks form the hanging wall along most of the fault. Moreover, the strike of the Triassic rocks parallels its contact with the Paleozoic rocks, thus suggesting it is an erosional-depositional contact rather than a faulted contact. This interpretation is consistent with the observation that the Triassic fanglomerate within 50 feet of the fault are noncataclastic and are undeformed except for small west-dipping antithetic faults.

Pre-Triassic fault movements along the north end of the Ramapo Fault are inferred predominantly from the relationship of igneous intrusives to regional faults. The eastern and western contacts of the Canopus Pluton with the bordering Precambrian gneisses are extensively mylonitized along N30° to 40°E right-lateral transcurrent faults. Biotite separated from the Canopus diorite yielded a K-Ar minimum age of 700±28 m.y. The filling of subsidiary right-lateral shears by late differentiates suggest that faulting was active at the time of intrusion, in late Precambrian (Ratcliffe, 1971).

The Rosetown is a composite pluton which has an older funnel-shaped mass of hornblendite and hornblende diorite in the southeast. This older pluton and the surrounding Precambrian gneisses have been fractured along a shear zone that trends N40°E, coplanar with the nearby Ramapo Fault at Tomkins Cove. To the southeast of this zone, Precambrian hornblende-biotite-granite gneiss trend N40°E, whereas to the northwest these gneisses trend N45°W. Rb/Sr whole-rock studies indicate that this older part is coeval with the Reading Prong-Grenville rocks: paragneiss = 1,141±60 m.y. old; metavolcanics = 1,141±111 m.y. old; and hornblende granite = 1,061±12 m.y. old (Mose and others, 1975). Blocks of Precambrian gneiss, rocks of the older pluton, Waffinger limestone, and Annsville Phyllite are found as zenoliths in the younger diorite that form the major part of the Rosetown pluton. Therefore, the age of the diorite is post-Middle Ordovician. Rb/Sr whole-rock studies also show that the younger part of the Rosetown Complex was emplaced in the Ramapo Fault zone 444±15 m.y. ago, indicating that this part of the fault zone ceased movement by ordovician time (Mose and others, 1975). North and south of the pluton, unsheared lamprophyric dikes (largely spessartites) and small pods of diorite intrude the shear zone. These dikes intrude gneissic rocks in the vicinity of the Ramapo Fault near Tomkins Cove. Although foliated near the fault, these dikes and small diorite peds have not been as intensely mylonitized as the country rocks. Ratcliffe (1971) thinks that the 810±8 m.y. K-Ar ages on hornblende from the older part of the pluton and the 580± m.y. age from the diorite may be excessively old (because xenoliths of Annsville phyllite and Wappinger limestone occur in the diorite). Therefore, Ratcliffe believes that the Cortlandt and the Rosetown may be, at least in part, correlatives.

The change in the basal limestone facies in a northwest direction as the Ramapo Fault is approached (at the latitude of Tomkins Cove) suggests that an uplift area existed in that direction during Middle Ordovician time. This evidence and the observable unconformity at Annsville (reported by Bucher, 1957) suggest that block faulting may have been active on the Ramapo system in pre-Middle Ordovician time.

The following tectonic history along the Ramapo fracture sytem has been suggested by Ratcliffe (1970):

1) Fault activity along the Ramapo trend began as late as Precambrian time, when right-lateral, strike-slip faulting was important;

2) Middle Ordovician normal fault activity produced uplift along the Ramapo fracture system at Annsville, N.Y., and the unconformable relationship cited by Bucher;

3) Post-Annsville (Middle Ordovician) right-lateral, strike-slip faulting resumed in Late Ordovician but pre-Devonian time, producing cataclasis of rocks ranging in age from Precambrian to Middle Ordovician; and

4) Triassic faulting followed the older, well-established trends and downdropped the Newark Basin along a system of hinged normal faults.

On the basis of bedrock mapping in the area, Ratcliff (1975) classified the faults he recognized into three relative age groups, described below.

A5.3.1 <u>Precambrian to Ordovician Faults</u>

These faults are largely confined to Precambrian rocks. They trend N40°E and are curvilinear in map trace. Cataclasis is pronounced in the faults, and dioritic, andesitic and locally diabasic dikes intrude the shear zones in the Dunderberg area. They are commonly healed and show positive topographic expression. Locally, zones of tightly appressed folds parallel the faults with axial planes dipping in the same direction as the faults. The Canopus faults, the Lake

Peekskill fault, and the Gallows Hill fault belong to this group.

A5.3.2 Devonian Fault

The Peekskill fault, which trends N60°E from Peekskill and extends southwestward across the Hudson River, is regarded as Devonian in age. The displacement on the fault is unknown, but the slickensides and geology would be consistent with a normal fault with a large component of left-lateral, strike-slip movement. This is supported by the apparent left-lateral offset of older faults west of the Hudson River.

A5.3.3 Young High-Angle Faults

These faults offset older faults and commonly are topographically expressed by narrow zones of deep weathering. A large component of dip-slip movement is indicated for most of these faults, although, locally, strike-slip movement predominates. The "Triassic border fault" at Tomkins Cove has downdropped the Annsville Phyllite against Precambrian gneiss. This fault forms the northern extension of the Ramapo Fault as classically interpreted and may extend northward as the Dickiebusch Lake Fault. North of Tomkins Cove numerous N10° to 30°W trending cross-faults extend up Dunderberg Mountain. Slickensides indicate dip-slip and right-lateral movement. A north-south, steeply west-dipping normal fault crosses Jones Point, and may extend southward across the river and continue through Verplanck to Greens Cove. The fault cutting the norite of the Cortlandt Complex and a group of four north-south high-angle faults extend from Buckberg Mountain northward to the Doodletown

Bight. These faults have left-lateral and west-side-down displacement senses, contrary to the sense of movement on the "Triassic border fault."

A small north-south trending fault, dipping to the southeast with approximately two feet of offset measured in the direction of the northeast plunging slickensides, is exposed in the rockcut between Units No. 2 and No. 3.

The preliminary data indicate that the Triassic border faults and related fractures, when traced northeastward, pass into a north-south series of faults that may extend north-northeastward along the Hudson River, rather than extending N45°E as previously assumed (Ratcliffe, 1975).

APPENDIX A6

TRIASSIC

A6.1 INTRODUCTION

The question of whether the Triassic rocks of the New Jersey Basin and the Connecticut Valley were deposited in two separate basins or in a larger connected basin has been reviewed by deVries Klein (1969). He concludes that a "half-graben" distribution of sedimentary facies can occur in a simple graben where structural and physiographic boundaries do not coincide. He favors the deposition of Triassic sedimentary rocks in separate basins, and adds that care should be exercised when reconstructing the location and size of fossil faults in the Triassic basins of Eastern North America.

What is known (or hypothesized) about the structure of the Triassic rocks in Rockland County is directly related to the origin and history of the Palisades intrustion. Dalton (1890) and Kümmel (1900) noted that there are relatively sharp changes in elevation of the intrusion across present topographic breaks in the ridge. They attributed this to a change in the mode of intrusion. As one proceeds northward from New Jersey, the sill either changes to a dike or to a step-like configuration of dike-sill-dike which migrates upsection to the north and west. Lowe (1959) believes that north of Nyack the intrusion is a wing dike which dips to the southwest. Thompson (1959) believes the intrusion remains a sill and is faulted.

All seem to agree that there is a fault at Short Clove. Kümmel interpreted an oblique slip fault at Sparkill

Gap and discussed the possibility of a fault at Trough Hollow. Lowe described minor north-south faults at West Nyack. He conceded the possibility of faulting at Long Clove and Trough Hollow, but feels there are insufficient data to substantiate faulting at these localities. Thompson interprets all topographic gaps and the topographic expression of Little Mountain and the end of the ridge at Mt. Ivy, New York as related to block faulting. He also postulates a northwest-trending set parallel to South Mountain.

Thompson (1959) and Lowe (1959) noted glacial striations in valleys which were eroded in fault zones prior to glaciation.

A6.2 EVIDENCE OF FAULTING

Thompson (1959) presents four lines of evidence of faulting in the Triassic basins of Eastern North America.

1) Joint Spacing, Patterns and Attitudes

   In undisturbed portions of the Palisades, columnal jointing is classic: columns are generally 1 to 3 feet in diameter, normal to the upper and lower sill contacts, and are broken by cross-joints parallel to the sill contacts at several feet. In faulted areas, columnal jointing is obscured by closely spaced secondary (i.e. tectonic) fractures. The most common secondary fractures are:

"(1) a steeply dipping set of platy joints that may be regarded as subsidiary faults parallel to a high-angle normal fault; (2) flat-lying, sheet-like fractures that are typical tension (feather) joints of high angle reverse; and (3) diagonal shear fractures that may accompany either normal or reverse faults...."

2) <u>Size, Shape and Abundance of Talus Fragments</u>
Unfaulted areas have large columnal blocks. In faulted areas talus is much more abundant, consisting of smaller, often wedge-shaped blocks.

3) <u>Fault Plane Phenomena</u>
Slickensides, breccia, gouge and mineralized joints occur in the faulted areas.

4) <u>Topography</u>
Faulted zones, being broken, are more easily eroded. Thus, the gaps in the ridge indicate where the faults are. If the changes in diabase elevation are due to stratigraphic migration of the intrusion (dike), the rock would not be broken. Also, the surrounding sediments would be strengthened by contact metamorphism.

Lowe (1959) points out that all the topographic gaps have roughly the same elevation at the ridge crest, and believes they are related to a higher (Pleistocene) base level of erosion.

Lowe states categorically that he saw no feather joints. He believes that Thompson's diagonal shear fractures are widely spaced, primary fractures which may have taken minor movements during later tectonic events (i.e. slicks do not always prove major faulting). Breccia, gouge and "platy joints" are observed within only a few feet of faults of minor displacement, i.e. if they are found in the talus near a gap, they do not signify a major fault in the gap.

APPENDIX A7

PLEISTOCENE

Flint (1963) attempted to correlate midwestern glacial stratigraphy with features in Eastern New York and New England. He pointed out that the general knowledge of glacial stratigraphy in the northeast is poor because of a lack of end moraines and stratigraphic sections that include deposits from more than one drift sheet. The lack of moraines results from great relief, steep slopes, resistant bedrock, and thin glacial drift which are unfavorable conditions for unhindered ice flow, and the creation and preservation of thick stratigraphic sections.

Two main Wisconsin advances were followed by a readvance in the New York-Long Island area. A retreat in the Connecticut River Valley and a readvance to Middletown followed; these were characterized by till and ice-contact drift overlying disturbed varved sediments in a 16-mile wide belt grading northward to kame terrace deposits and a pitted outwash valley train (terrace remnants). Another retreat followed and extensive lacustrine varved clay and silt were laid down in Northern Connecticut, Massachusetts, Vermont, and New Hampshire. Similar histories are indicated in Massachusetts and Eastern New York, but direct correlation has not been accomplished. The readvance to Middletown, in Connecticut (Cary substage) is thought by Flint (1963) to have been synchronies with an advance into the Hudson Gorge between Newburgh and Peekskill. No deposits remain above river level to prove this correlation. Flint does not recognize a Lake Hudson, only a Lake Hackensack extending from New York City to Haverstraw, and a later Lake Albany extending from Newburgh to Glens Falls. He tentatively correlates Lake Albany with the large Connecticut Valley Lake.

In a study of the pleistocene geology at Croton Point, New York, Markl (1971) describes deposits of deltaic sediments and till. The materials consist of till, deposited as a terminal or lateral moraine, overlain by glacial lake clays and deltaic sand. Other till deposits were found overlying a sand terrace on the south bank of the Croton River. Clays, 3 to 10 feet thick, were observed at Croton Point. However, Markl thinks that much greater thicknesses probably existed at one time. Similar clays, up to 200 feet thick near Haverstraw, are referenced and lesser thicknesses near Ossining and Peekskill are also mentioned. Stratified sands overlie the clays and occur as terraces with surfaces up to 100 feet in elevation from Croton-on-Hudson to Harmon Park, Harmon, and Crotonville. Contorted beds were found to be common and were explained in terms of cohesion and high-flow velocity. Microfaults (less than five inches of displacement) of both normal and reverse senses of movement were observed in a sand pit. Markl (1971) speculates that the Croton Point deposits represent delta deposits in glacial Lake Hudson at the mouth of the Croton River. Some of the materials further north, near Croton-on-Hudson and Harmon, may represent sediments deposited by a stream emerging from a small valley followed by Highway 129, through Croton-on-Hudson. The deposits of Lake Hudson, cropping out "near Haverstraw" or "near Peekskill," are described as stratified sand and gravel (2 to 25 feet thick) resting on varved clay delta deposits. At Croton Point, Harmon, and Peekskill, the deposits rise to elevations of a little over 100 feet, which make up the approximate shoreline of Lake Hudson (Reads, 1972).

A summary of Lake Wisconsin glacial history was presented by Weiss (1974):

1) 20,000 B.P. - Late Wisconsin glacial maximum in New England and Long Island.

2) 17,000 B.P. - Beginning of ice retreat from the Harbor Hill moraine on Long Island.

3) 15,000 B.P. - Wallkill moraine formed, the Lower Hudson Valley is ice-free south of New York Highlands, glacial Lake Hudson formed.

On the basis of pollen and forams studies in cores, taken between Peekskill and the Narrows of New York Bay (Weiss 1974), the following additional events were recognized:

1) Well before 12,000 B.P. - Dissipation of glacial Lake Hudson and establishment of tidal conditions in the estuary.

2) 11,500 B.P. - Increased salinity, high enough to support foraminifers.

3) 10,000 B.P. - Slightly decreased salinity, followed by an increase to previous level by 9,000 B.P.

4) 6,500 B.P. - Maximum transgression of brackish water into the estuary.

5) 3,000 to 1,500 B.P. - Decrease in salinity due to a faster sedimentation rate, and a slower rise in sea level or crustal subsidence.

In a study of the Hudson River gorge in the Highlands, Thompson (1936) recognized the following apparent erosion levels:

1) 400 to 480 ft. - Presumably correlative with the Harrisburg Peneplain.

2) 220 ft. - A bench and terrace bordering the river in the Highlands.

3) 160 to 199 ft. - Includes a narrow bench and stratified Pleistocene deposits along the Hudson River around Newburgh and Cornwall.

4) 140 ft. or less - Terrace deposits around Peekskill and at Verplanck.

Thompson (1936) also noted that no upland (Schooley) peneplain is evident in the area, and points out that summit elevations are discordant and lithologically controlled. He concludes that the present course of the Hudson River follows joints, faults, foliation, and basic dikes.

APPENDIX B

SITE GEOLOGIC INVESTIGATIONS

APPENDIX B1

INTRODUCTION

This report documents the results of a comprehensive geologic field investigation, laboratory research program, and presents new information pertinent to the Indian Point Generating Station site geology.

The principal objectives of the study were to:

1) Determine if there exists any evidence of recent displacement along the recently identified N-S trending fault north of Unit No. 3;
2) Explore the possible relationship of the fault onsite to any other significant faults in the region; and
3) Determine, absolutely or relatively, the age of last movement of this fault and any other faults found to be associated with it; or alternatively, generate a sufficient weight of circumstantial evidence to resolve questions which may be raised by governmental agencies concerning the safety of these faults.

Comprehensive geologic field investigation and laboratory programs were implemented to address the above stated objectives. The program consisted of the following tasks:

1) Review of available published and unpublished geologic literature, geophysical and geological maps, photographic records of containments,

excavations, and logs of existing borings;

2) Detailed geologic mapping at a scale of 1:30 and 1:60 of all rock exposures present within the site proper;

3) Surficial geologic mapping at a scale of 1:2,400 and 1:6,000 of the area situated east of the Hudson River and west of the New York-Albany Post Road;

4) Mapping at a scale 1:24,000 and examination of the Pleistocene sediments and geomorphic features within a 4-mile radius of the site;

5) Study of folds development in the rocks of the Cambro-Ordovician Inwood and Manhattan Formations.

6) Study of joints, fractures, and faults.

7) Laboratory analyses of representative samples of whole rock and mineralization along joints, fractures and faults. X-ray diffraction, microscopic petrography, geothermometry and geobarometry, and isotopic age determination were used for these analyses;

8) Hand-held magnetometer survey to establish the accurate position of geologic contact between the Cortlandt Complex and Manhattan Schist; and

9) Data reduction, analysis, and interpretation.

APPENDIX B2

STRATIGRAPHY, PETROGRAPHY, AND MINERALOGY OF THE ROCK UNITS AND THE FRACTURE-FAULT FILLING MINERRALS

B2.1 GENERAL

The site is located upon the Cambro-Ordovician schists and dolostones of the Manhattan Prong. The older unit, the Inwood Formation, consists of dolostones and marbles that are exposed onsite and along the Hudson River to the southwest. The dark schists of the Manhattan Formation lie unconformably, and are probably in fault contact, above and to the east of the Inwood Formation. Both of these formations were regionally metamorphosed to medium grade prior to the intrusion of the Cortlandt Complex, now exposed to the north, east, and south of the metasediments. The emplacement of this complex has resulted in the overprinting of a contact aureole of variable width and intensity upon the regional metamorphism.

Several periods of hydrothermal activity, either related to these metamorphic episodes or to later intrusive events, have caused the deposition of minerals along fractures and faults onsite. Detailed field observations and results of laboratory analyses related to metamorphism and hydrothermal activity are reported in Attachment B5.4. Plate B5-1 is a diagramatic stratigraphic column which shows the general relationship between the rock units in and around the Indian Point Generating Station. Plate B3-1 and B3-2 show the areal data gathered during the mapping program, and Plates B3-3 and B3-4 suggest, as of to date, the most probable interpretation.

B2.2 STRATIGRAPHIC AND PETROGRAPHIC DESCRIPTIONS OF THE ROCK UNITS

B2.2.1 The Inwood Formation

The oldest of the three major rock types in the site area, the Inwood Formation, consists of dolostones which were probably deposited in a shelf environment during Cambrian through Early Ordovician time (Hall, 1967). This unit is observed to overlie unconformably the Fordham Gneiss in other parts of the Manhattan Prong. Onsite, the Inwood consists of buff to blue-gray dolostones, dolomitic limestone, and white marble, with small layers of chert and siliceous phyllite. The dolostones are commonly siliceous and/or feldspathic in some beds. The common minerals are dolomite, calcite, muscovite, quartz, pyrite, and microcline. Lithologic layers range in thickness from 0.5 to 15 feet.

Hall (1967) has divided the Inwood into five members in the White Plains area and suggests that it reaches a maximum thickness of 2000 feet. The exposures in the site area were not divided and classified but a correlation between the rock types here and at White Plains can be made. Hall's two most common units were the B and C members. Calc-schist, typical of the B-member, does not occur onsite but does crop out to the southwest (down section). Therefore, the rocks onsite probably are correlative to the C member of Hall's classification.

Texturally, the Inwood is a medium-grained, recrystallized, micaceous dolostone that contains no observed index minerals. It is, therefore, difficult to define the grade of metamorphism that it reached. At localities where the dolostones are adjacent to an intrusive contact, they are metamorphosed to a diopside or tremolite zone of contact metamorphism.

B2.2.2 <u>The Manhattan Formation</u>

The metamorhpic rocks of the Manhattan Formation reflect an original sequence of trough-type shales, feldspathic sands, and volcanics. These rocks are shown to lie unconformably on the Fordham Gneiss, the Lowerre Quartzite, and the Inwood Formation. Therefore, they have been interpreted to be younger than the Middle Ordovician regional unconformity. A recent interpretation by Hall (1967) suggests that the Lower Member of the Manhattan is indeed of Middle Ordovician age, but that the Middle and Upper Members are possibly the trough equivalents of the Inwood Formation and have later been thrust into their present position. A younger limit for the age of the Manhattan is obtained from the age of regional metamorphism (450 m.y.) as interpreted from $^{40}Ar/^{39}Ar$ incremented heating studies (Mose and Hayes, 1975).

From the geologic mapping performed during this study, three members of the Manhattan Formation have resulted, any one of which may not always be present.

The Lower Member of the Manhattan consists of thin interbeds of white marble, gray quartzite, and fine-grained metapelite. This distinctive unit is commonly up to 30 feet thick and is fairly continuous north of the site, but does not occur at the Verplanck Quarry. Instead, at this locality, a blue dolostone with Pelmatozoan columnals, as reported by Ratcliffe (1968), crops out at the contact and is less than five feet thick. It is probable that the Middle Member of the Manhattan (with calc-schist lenses) is in thrust contact with the Inwood Formation, and the distinctive unit of the Lower Member is faulted away in the Verplanck area.

The Middle Member commonly overlies the Lower Member, but the nature of the contact is not known. Its observed maximum outcrop thickness is 200 feet, consisting of a commonly rusty-weathering, fine-grained, biotite-quartz schist and a two-mica schist. The rocks are occassionally quite dense, sulfidic and magnetic, and relict euhedral garnets reflect a medium grade of regional metamorhpism. These denser, more magnetic horizons are non-continuous and probably consist of metavolcanics.

The Upper Member overlies both other members, but it has been observed to be in conformable contact with the Middle Member. The Upper Member consists of a gray, two-mica, garnet schist with feldspathic-quartzite laminae. Wherever observed, this member was affected by the contact metamorphism of the Cortlandt intrusions. The rocks closest to the intrustion have been partially melted, and a fairly broad band of sillimanite grade metamorphism occurs around the central body of the Complex. Two cases of relict grains of minerals, reflecting an earlier medium grade regional metamorphism, were observed in these rocks. One case was a relict staurolite grain that is now surrounded by fresh recrystallized sheets of muscovite and biotite. The other example was the ghost outline of a euthedral garnet with only a core of the relict garnet left surrounded by quartz and feldspar.

Hall (1967), mapping in the White Plains area, has defined very similar rock types within the Manhattan. The subdivision suggested for that area differs slightly from the ones presented in this report in that the Middle Member, B, in the White Plains area is reserved for just the metavolcanics. This unit is discontinuous however, and is not useful as a persistent stratigraphic marker. Hall's Lower Member, A, has two distinctively different rock types included within it. These two units which are much more persistent and, therefore, more useful as stratigraphic markers, should be divided in the site area. In this study the upper part (rusty schist) of Hall's A member and the B member (dense rusty schist - metavolcanics), both of which are similar in appearance in the field, are grouped into the Middle Member of the Manhattan Formation. The Lower Member in this report consists only of the basal unit of Hall's, which is a very distinctive lithology.

B2.2.3 The Cortlandt Complex

The Cortlandt Complex consists of mafic and ultramafic igneous rocks that were emplaced in multiple injections. Balk's (1928) classical study of the igneous foliation defined two main funnel-shaped intrusions and a large basinal pluton. Shand (1942) mapped the rock types according to the occurrences of critical mineral phases such as hornblende (poikilitic or prismortic), olivine, hypersthene, and augite. He found that the magmatic rock types that were defined reflected the borders of the different intrusions defined earlier by Balk.

The rock types encountered within the Cortlandt during these investigations were a medium to very coarse-grained, biotite, hornblende gabbro, and a two-pyroxene norite which commonly had large poikilitic hornblendes. Most samples of the Cortlandt are fresh and have not experienced a later metamorphic event. Where faults cut the complex, severe alteration has occurred.

A biotite from the biotite norite in Montrose has been dated at 435 m.y. by the K/Ar method (Long and Kulp, 1962). They suggest that this is probably a minimum age for the intrusion. Biotite from the contact aureole was dated by the K/Ar method and yielded an age of 405 m.y. A maximum estimate for the age of the Cortlandt comes from the 450 m.y. interpreted age of the regional metamorphism that occurred prior to the intrusion and metamorphic overprinting by the Cortlandt (Mose and Hayes, 1975).

Along with causing a narrow-to-broad contact aureole, the main bodies of the Cortlandt partially melted the metasedimentary country rocks. Hybrid rocks along the margins reflect assimilation of the restites, yielding anomalous mineralogy.

Late granitic dikes have intruded along fractures within the Cortlandt. These dikes are composed of the typical granitic phases: quartz, two feldspars, and muscovite.

B2.3 STRATIGRAPHIC CORRELATION OF THE INWOOD AND MANHATTAN FORMATIONS

The lithologic descriptions and divisions of the rock units, mapped onsite and in the surrounding area match quite well the classification of Hall (1967) from the White Plains area. These also appear to be very similar to the descriptions of rocks at Tomkins Cove, Stony Point, Crugers, and Annsville, mapped by Paige (1956) and Ratcliffe (1968). A limestone unit has been mapped at the base of the "Manhattan - Annsville" unit, near Annsville (Bucher, 1951), at Verplanck Quarry (Ratcliffe, 1968), and at Tomkins Cove (Ratcliffe, 1968). At all three places, a regional unconformity has been interpreted to underlie this basal limestone. Middle Ordovician fossils in the latter two localities were identified in the limestone (Bucher, 1957 and Ratcliffe and Knowles, 1969).

It is apparent that the correlation from the site area to White Plains, Tomkins Cove, and to Annsville is quite sound, and that the Inwood and Manhattan Formations are correlative to the Wappinger and Annsville Formations.

The main argument against correlation from Verplanck Point to Tomkins Cove has been the grade of metamorphism exhibited by the rocks. It has been argued that the gradient across the 1-1/2 miles of the Hudson River is too steep to account for by regional metamorphism (Berkey and Rice, 1919). Ratcliffe explained that the higher crystallinity of the rocks at Verplanck is due to the contact effect of the Cortlandt.

Even though the contact aureole is large, the rocks were at medium grade of regional metamorphism prior to the intrusion. In fact, the phyllites at Tomkins Cove and the fine-grained schists at Verplanck Quarry are not drastically different in regional metamorphic grade. It is also possible that a post-regional-metamorphism structural event, such as F_2-folding or subsequent faulting, could have shortened the distance.

B2.4 MINERALOGY OF THE FAULT-FRACTURE FILLING MATERIAL

Veins and coarsely recrystallized concentrations of minerals occur along many of the faults and fractures onsite. The fracture planes that appear to be mineralized are commonly parallel or subparallel to the bedding. The minerals that are abundant in such associations are calcite, muscovite, phlogopite, quartz, sulfides, feldspars, amphiboles, and zeolites.

The uni- or polymodal mineral concentrations, commonly found along fractures in the Inwood Marble onsite, occur most frequently along NNW to NE fractures and faults. In several cases the polymodal concentrates are the result of metamorphism of a quartz-feldspar-muscovite-rich horizon within the dolostone. More commonly, material has been transported by hydrothermal activity. This transport could be very local in extent, being related to either regional or contact metamorphism, since all the mineral phases are common constituents in the local dolostone wall rock. During such a thermal event, the partial pressures of several different fluid phases increase, and material is "sweated out" of the rock and deposited along open surfaces, where the pressure is lower.

Several periods of hydrothermal acitvity have been differentiated on the basis of the overgrowth of different mineral phases. These events are probably related to the igneous activity during Silurian, Devonian, and Triassic times.

Muscovite and phlogopite commonly occur as medium-to-coarse disseminated grains, coating a fracture surface. They also occur intergrown with either quartz or calcite in more massive deposits. Both sheet silicates have generally been deformed in the fault zones that were examined. Sulfides occur as coatings on fracture surfaces or as pyrite crystals intergrown with other mineral phases. Amphiboles are rare and commonly weathered, but appear to belong to the tremolite-actinolite family. Feldspars occur as large crystalline growths and as medium-grained intergrowths with quartz, calcite, and muscovite. The least deformed occurrences have growth twins which fade away, suggesting slight deformation.

Both deformed and undeformed quartz crystals occur onsite. The undeformed crystals are not associated with faults. At least three periods of calcite growth can be defined onsite and in the surrounding area. The first, and commonly the most massive, is a generation of pink calcite. Onsite it is deformed, and has been overgrown by a second generation of deformed white calcite and a later third generation of undeformed calcite. But in the Verplanck Quarry, a large breccia zone, at the intersection of E-W and N30E faults, is healed with massive pink calcite that is zoned and commonly contains vugs with very coarse, undeformed crystals.

Undisturbed zeolite crystals have grown along fractures onsite and in the Cortlandt Complex.

In conclusion, most of the mineralization is deformed onsite except for the last generation of calcite and the zeolites.

APPENDIX B3

STRUCTURAL SETTING OF THE INDIAN POINT GENERATING STATION

B3.1 GENERAL

The rocks of the Manhattan Prong outcropping at and near the Indian Point Generating Station have a long and complex history of multiple deformation. The rocks comprising the Inwood and Manhattan Formations were originally deposited as sediments in Late Cambrian to Middle Ordovician time with intermittent periods of uplift and erosion. These rocks were subsequently metamorphosed, folded, intruded by igneous rocks, faulted, and intensely fractured during several episodes of regional crustal compression. This polyphase deformation has resulted in a very complex tectonic picture composed of many structural elements of different age, orientation, and character. The following discussion consists of a general description of these different structural features as well as the geologic history of their development.

B3.2 THE STRUCTURAL ELEMENTS

B3.2.1 General

The tectonic emplacement of the Cortlandt pluton caused a local rotation of structural elements formed during the initial phases of deformation. Thus, the structural elements recognized in the area may be conveniently subdivided into two groups:

1) structural elements which have been rotated by the effects of the Cortlandt intrusion; and

2) structural elements which have not been rotated and are younger than the Cortlandt Complex.

B3.2.2 The Pre-Cortlandt Structural Elements

B3.2.2.1 F_1-Folds

Field work in the rocks of the Manhattan Prong within two miles of the site has revealed a number of mesoscopic folds which have been termed F_1-folds, i.e. first-phase folds (see Attachment B5.2). The folds of this early phase are commonly asymmetric, tight-to-closed, isoclinal folds, and locally they are symmetric folds whose axes correspond to the true dip of bedding. These folds formed as a result of passive flow folding in the Inwood Formation and passive slip folding in the Manhattan Formation. Continuous slip along the dominant axial plane foliation to F_1-folds, S_1, has resulted in the unfolding of the tight isoclinal folds (Bowes and Langer, 1969). The strikes of the axial planes to F_1-folds vary as a result of subsequent folding, but they generally trend NNW to NE. Additionally, F_1-fold axes, where they are relatively undeformed, plunge 30° to 50° ENE to SSW. There are no fractures genetically associated with the F_1-folds because of the ductile nature of their formation.

B3.2.2.2 F_2-Folds

The second-phase folds, F_2, are typically small, asymmetric concentric folds which have locally folded the older F_1 structures and regional foliation, S_1. These folds occur in several orders, of which the lower order folds have axial planes that fan around the higher order F_2-folds (Plate B5.2-3). In the Indian Point area, F_2-fold-axes have variable trends and plunge from 10° to 30° north or south.

This phase of folding was semi-ductile in nature, resulting in an incipient axial plane foliation and (on the lower order folds) an axial plane fracture cleavage which strikes N20 to 60E and dips 30° to 60° NW or SE, thus forming a cleavage fan around a NE-striking, upright axial plane to F_2-folds. In addition to these axial fractures, there is a set of conjugate shears, faults, and fractures about a compression direction which is consistently normal to S_0/S_1. These shear planes have a 20 to 30-degree dihedral angle and are oriented generally from ENE to NW. They are characterized by strike-slip movement and healed breccias where exposed in the Inwood Formation, with some calcite and minor mineralization in the fault zones. Examples illustrating this relationship are discussed in greater detail in Attachment B5.3.

B3.2.3 Rotation by the Cortlandt Intrusion

The structural featues described above have been locally rotated by the intrusion of the Cortlandt pluton. The geologic maps (ref. Plates B3-1 through B3-4) of the Indian Point area show the rotational effect of the Cortlandt Complex on the rocks of the Manhattan Prong. This rotation is partially responsible for the variable orientation of fractures parallel to the axial plane of the f_2-folds and the conjugate shears normal to S_0/S_1.

B3.2.4 Post-Cortlandt Structural Elements

B3.2.4.1 General

There are three major groups of faults with associated fractures that postdate the intrusion of the Cortlandt Complex. These structures have the common characteristic of a consistent orientation in the Indian Point area, i.e. they have not been rotated by the Cortlandt intrusion.

The three major fault groups are oriented ENE-WNW, NE, and NNE-NNW. All of the post-Cortlandt faults found in the area can be classified into one of these three major groups. Subdivision into these groups has been made on the basis of a fracture study made in successively younger rocks of Cambro-Ordovician to Triassic age (see Attachment B5.3). The general characteristics of the faults and fractures comprising each group, as well as the major faults of each group found at or near the site are discussed below in their interpreted sequence of development.

B3.2.4.2 ENE-WNW Faults

The rocks of the Indian Point-Verplanck area are deformed by numerous faults which have an average E-W strike. This major group consists of a system of conjugate faults where the sinistral set strikes E-W to N70W dipping southward, and the dextral set strikes E-W to N75E dipping southward. With very few exceptions, faults of both sets are offset or truncated by younger faults. The E-W striking faults in the Inwood Formation are typically characterized by breccias which have been healed by a re-crystallized calcite cement.

There are four major zones of E-W faults near the Indian Point site that have been mapped (ref. Plates B3-1 through B3-4). The northernmost zone of E-W faults is exposed in a series of railroad cuts in the Cortlandt Complex at Travis Point and at the Peekskill Railroad Station. Several faults, 1 to 3 feet thick, were observed at this locality. Breccias were preserved in some of these faults, but not in others. Fault strikes in this locality averaged N80E. Two N75W faults with preserved breccias were found. One fault with a preserved breccia was observed to be crosscut by a granitic dike 1-foot thick.

Another fault was found to offset a granitic dike, but there was no preserved breccia present. The E-W fault structures cannot be traced across a N30E trending fault exposed along the railroad tracks. They are traceable and exposed to the west of this northeast-trending fault.

A second major fault zone is exposed at Lent's Cove, and also at the roadcut beside the exit ramp off the New York-Albany Post Road at Welcher Avenue in Buchanan. This fault zone does not contain a preserved breccia, but consists of closely-spaced fractures with interstitial crushed rock. The fault at Welcher Avenue strikes E-W to N80W, and at Lent's Cove it strikes N80E to N70E. The geometry of fractures and the shallow plunge of slickensides suggest a dextral strike-slip movement.

The third major fault zone is exposed at the corner of Bleakley and Broadway Avenues in Buchanan. Remanants of this fault zone are exposed again 400 feet eastward near the pond.

This fault consists of a zone of closely-spaced fractures striking E-W to N80E, with interstitial crushed rock and subhorizontal slickensides. This fault zone cannot be traced westward; however, there appears to be a dextral offset of the Cortlandt-Manhattan contact on the south side of Bleakley Avenue.

The fourth major E-W fault zone occurs in the Verplanck Quarry and possibly again to the west on the west edge of Lake Meahagh. The fault strikes N80E and dips southward. It is exposed on both the east and west faces of the quarry, and contains a sheared, healed breccia. On the shear planes of the fault, pink and white crystalline calcite has been sheared with subhorizontal slickensides visible on the shear surface as well as minute grains of pyrite. Crystals of free-growing, zoned, dogtooth calcite crystals (up to 1.5 inches long) are present as overgrowths on older pink and white calcite. This major fault zone appears to be offset dextrally across the quarry. The movement sense of this fault appears to be sinistral, based on offset of the Inwood-Manhattan contact at the quarry and the Manhattan-Cortlandt contact near Lake Meahagh, where small felsic veins of the contacts are sinistrally offset along a small N80 to 90E trending fault. At the quarry, the strike of bedding rotates near the fault zone in such a manner as to suggest dragging due to dextral movement along the fault. This may indicate that the latest movement on this fault has the opposite sense of the genetic movement.

The four fault zones described above are genetically the oldest post-Cortlandt structural features in the vicinity of the Indian Point site. Regardless of their age of development, their existance is important because they may have been reactivated during later fault movements.

B3.2.4.3 <u>Northeast Faults</u>

The next successively younger faults are part of a conjugate system with a N50 to 60E sinistral set and a N20 to 30E dextral set. Faults of this conjugate system consistently offset the ENE-WNW faults. The sinistral set is characterized by healed breccias and white calcite mineralization, slickensides, and gray-green gouge. The dextral set is characterized by healed breccias and soft, loose, crushed breccia and gouge. The faults themselves exhibit both dextral and sinistral strike-slip movement senses with numerous subhorizontal slickensides. Numerous faults of each set are present as can be seen on the geologic plans of the rock exposures onsite (see Attachment B5.1). An analysis of fractures in the Inwood, Manhattan, and Cortlandt rocks has shown that there is a set of N40 to 60W east-dipping fractures which are approximately orthogonal to the compression direction which formed the NE conjugate faults. The orientation of these fractures is similar to that of the axial plane of F_3-folds recognized in New York City (Bowes and Langer, 1969). There are a few NW-striking fractures which exhibit gently plunging slickensides indicating some strike-slip shear fracturing.

Numerous granitic veins and dikes were measured in the outer zone of the Cortlandt Complex. One set strikes NE and dips gently NW, and the other strikes NW and dips steeply NE. Two interpretations of these veins are possible. They may have formed along axial plane fractures and low-angle release fractures during F_3-folding. On the other hand, they may have formed during emplacement of the Peekskill Granite in Devonian time. The proximity of the Peekskill Granite suggests this body as the source of granitic fluids which filled these fractures.

B3.2.4.4 NNE-NNW Faults

All of the structural features described above, both pre- and post-Cortlandt in age, are offset by younger faults whose strikes range from N40E to N15W. Fracture studies have shown that this major group consists of three sets of faults: N15W to N-S, N5E to N15E, and N20E to N40E (Attachment B5.3). Faults of all three sets have been mapped in detail in the rock exposures at the Indian Point Generating Station, as well as in the rocks of the Inwood, Manhattan, and Cortlandt Formations which crop out near the site (ref. Plates B3-1 through B3-4). Fault relationships onsite and in the region have shown both dextral and sinistral movement senses on faults of this group. Faults of each set also offset or are offset by other faults of this group. These faults are rarely healed; breccias are commonly soft, and one or more sets of slickensides are common. Both pink and white calcite, and, less commonly, mica, pyrite, feldspar, and quartz occur in some faults.

Field mapping at and near the site has identified several major faults of each set in this group which may be throughgoing structures:

1) <u>N10W to N-S Set</u>. Excavations between Nuclear Reactors No. 1 and No. 3 in the Inwood Formation have revealed a zone of faulting bounded by two N10W striking faults. Both of these faults contain healed breccias which have been sheared; gray-green and orange gypsiferous, clayey gouge, and pyrite, mica, feldspar mineralization. The movement sense along these faults is both dextral and sinistral. Structurally associated with these faults is a N-S fault which was first described by Ratcliffe (1975). This N-S sinistral fault terminates within the zone bounded by the NNW faults. The NNW fault zone is traceable southward to the edge of Nuclear Reactor No. 3, and northward apparently to the gas turbine building of Nuclear Reactor No. 1.

2) <u>N5E to N15E Set</u>. A N5 to 10E striking fault in the rock exposure beside Nuclear Reactor No. 3 is traceable up to 6 feet from the containment structure (see Attachment B5.1). This fault clearly truncates a N50 to 60E sinistral fault zone, and a number of NNW striking shear planes, one of which demonstrates 5 to 6 inches of dex-

tral displacement. The movement sense of this fault is uncertain, although a sinistral sense may be interpreted. This fault may be exposed further north in the rock cut beside the gas turbine of Reactor No. 1 (Fault 17, Attachment B5.1). This fault contains pyrite and mica, and sinistrally offsets a dextral N-S fault.

Another prominent N5 to 10E dextral fault is exposed in the southernmost outcrop onsite (see Attachment B5.1). This fault contains breccia, mica, and feldspar. The continuity of this fault is not known.

3) N20E to N40E Set. Four major N20 to 40E *en echelon* faults, two of them bordering the site and the other two transecting the site, have been recognized in the Inwood, Manhattan, and Cortlandt rocks (ref. Plates B3-1 through B3-4).

The westernmost fault is exposed on the eastern bank of the Hudson River in the Inwood Formation approximately 1500 feet south of the site. The fault zone is about 10 feet thick, intensely brecciated with numerous subhorizontal slickensides, and contains soft clay matrix in the breccia. The geometric arrangement of shear fractures along the fault zone suggests sinistral movement. The southwest projection of this fault coincides with a strong topographic depression between the northwest side of the Verplanck Quarry and the river.

The easternmost fault (NE striking) is exposed in a railroad cut in Cortlandt rocks across Travis Point up to the Peekskill Railroad Station. The same fault was mapped as a sinistral oblique-slip fault by Ratcliffe (1975). The southwest projection of this fault passes through a linear belt of glaciofluvial sediments which may have filled a topographic depression (see Attachment B5). Further south, a strong photolinear at Verplanck lies along the projection of this main N20 to 30E fault.

Two faults which appear to pass through the site area are exposed in the north wall of the Verplanck Quarry. The largest fault is exposed in the northeast corner of the quarry as a 50-foot thick limestone breccia in the Inwood Formation with several smaller parallel faults. The movement sense is apparently dextral based on the apparent offset of a large N80E fault zone which transects the quarry. Parallel to this fault along the east wall, a discontinuous breccia occurs just below the Inwood-Manhattan contact, and the contact itself is a highly weathered zone. A quartz-muscovite vein crosses this zone and suggests mineralization there. This contact zone is traceable southward halfway to the south wall where the zone intersects a N80E fault which has offset the contact. This zone is not exposed to the north except at the site where the Inwood-Manhattan contact has been located by drilling near Unit 2 (see Plate B3-2). The other N30E fault is exposed approximately in the center of the north wall of the Verplanck Quarry. This fault is exposed further north also in the Inwood Formation, just outside the north end of the Georgia Pacific property. This fault is 4 to 5 feet thick with a sheared, healed breccia at the edges, and a central crushed breccia in a soft clay matrix. Gash veins indicate an old dextral movement sense, but the geometric arrangement of frictional shears indicates a later sinistral movement sense. This fault may coincide with the N30E fault found on site in the trench which was mapped in detail (see Attachment B5.1). The fault in the trench also exhibits an old dextral and a later sinistral movement sense, based on the geometry and cross-cutting relationship of associated frictional shear fractures. The true size of the fault in this trench is not known, but the continuity and the physical and geometrical properties of the fault are very similar to the other two exposures of this zone further south. A N40E striking fault is exposed in the rock cut beside Nuclear Reactor No. 3.

B3.3 FRAMEWORK OF FAULTING IN THE VERPLANCK PENINSULA

A series of *en echelon* faults striking between N20 to 40E have been mapped in the Verplanck Peninsula. These faults have a predominant strike-slip component of movement and dip 60° to 90° east. A sinistral sense of movement, indicated by the offset of stratigraphic rock units, is interpreted as the latest sense. Some of the faults also show evidence of older dextral movement. Generally, the N20 to 40E faults offset numerous ENE-WNW striking faults (ref. Plate B3-2). Also, a number of N-S striking faults are interpreted as being terminated at each end by a N30E fault (ref. Plate B3-4).

Irrespective of exactly when they developed, the N-S and WNW faults are favorably oriented for reactivation by sinistral simple shearing of the N30E main shears. The pervasive nature of the main shears partly explains the abundance of these associated faults.

The site is bordered by two main N30E shears and is transected by at least two others (ref. Plates B3-1 through B3-4). The westernmost N30E fault is located on the east edge of the Hudson River, and is exposed in the Inwood Formation just south of the site area. It projects southward to a zone of faults in the Inwood Marble, exposed near the river just west of the Verplanck Quarry.

Several hundred feet east of this fault is a smaller but pervasive N20E sinistral fault, which is exposed near the center of the north wall of the Verplanck Quarry; it is also exposed in outcrops bordering the north side of the Geogria Pacific Company, and again at the site in a trench mapped immediately west of the rock cut beside Reactor Unit No. 3. Field observations at two exposures show that younger sinistral movements along this fault have been overprinted on older dextral movements.

There are several major faults exposed in the rock cut immediately north of Reactor Unit No. 3, but one N40E fault appears to be through-going. The northern extension of this N40E fault coincides with a possible dextral displacement of the Manhattan-Cortlandt contact (see Attachment B5.4 and B3-4). This fault probably passes through Reactor Unit No. 3, but has not been found again further south, possibly because it merges with the N30E-trending fault located further west.

The second main N30E shear occurs parallel to and, in places, coincident with the Inwood-Manhattan contact which borders the eastern edge of the site. The only exposures of this fault occur at the Verplanck Quarry, but it trends northward toward a possible sinistral offset of the Manhattan-Cortlandt contact north of the site (see Attachment F). Where this fault coincides with the Inwood-Manhattan contact, the basal member of the Manhattan Schist appears to be either absent or anomalously thin.

The most pervasive N30E fault in the en echelon system occurs between Travis Point and Verplanck Point. This fault appears to be a major sinistral shear which truncates or offsets numerous ENE to WNW fault zones (ref. Plates B3-1 through B3-4). The sinistral fault at Travis Point is exposed in the Cortlandt Complex. A projection of this fault coincides with a possible sinistral offset of the Manhattan-Cortlandt contact near the Bleakley-Broadway intersection (see Attachment F and Plate B3-4). Further south, the fault is aligned with a linear belt of glaciofluvial sediments which appear to have filled an old topographic depression (see Appendix D and Plate B3-4). Still further south, between the quarry and Verplanck Point, the fault is aligned with a pronounced photolinear which coincides with a major offset of folded Inwood and Manhattan rocks (ref. Plates B3-1 and B3-4). All of these features are along a N30E trend and have been interpreted as resulting from a major N30E shear in this en echelon system.

It should be noted that this system of en echelon shears transects two prominent E-W fault zones. One E-W fault zone occurs at the corner of Broadway and Bleakley Avenues, but cannot be found west of the Travis Point-Verplanck Point fault. This fault was mapped as dextral based on the possible displacement of the Manhattan-Cortlandt contact (see Attachment F). The intensity of shearing along this fault suggests that it may have been reactivated during sinistral movement on the main shears. Another continuous E-W fault extends from Lake Meahagh to the Verplanck Quarry. This fault is sinistral, but is offset by at least two of the *en echelon* main shears (ref. Plate B3-2).

In summary, the overall structural framework indicates a 1000 to 2000-foot zone of subparallel, *en echelon* N30E shears, with smaller associated faults trending N-S and WNW-ENE. Although they are genetically old, they are pervasive and may have been used for the youngest tectonic movements in response to regional sinistral simple shearing.

APPENDIX B4

THE YOUNGEST TECTONIC MOVEMENTS

APPENDIX B4

THE YOUNGEST TECTONIC MOVEMENTS

B4.1 IDENTIFICATION OF THE YOUNGEST TECTONIC MOVEMENTS

The structural significance of the N-S-trending fault, identified north of Reactor No. 3 (Ratcliffe, 1975), can be better understood if it is related to the detailed field observations made during this investigation.

As has been described in the preceding sections major, through-going NNE-NE faults have been mapped in the vicinity of the Indian Point Generating Station. These faults have experienced, predominantly strike-slip movements and show evidence of both dextral and sinistral senses of movement. They were developed in response to a roughly NE-directed principal horizontal compression, resulting in the development of NNE-NE dextral and NE sinistral conjugate shears and a system of orthogonal extensional fractures trending NE and NW. These extensional fractures are common in the Appalachians. Lamprophyre dikes are commonly emplaced along these trends. A potassium-argon age determination on kaersutite, from a lamprophyre dike in Orange County, New York (Monroe Quadrangle), yields an age of 398±17 m.y.; this represents the minimum age of emplacement of the dike. Thus, it is reasonable to conclude that the tectonic system, which includes the dextral NNE-NE trending faults, was developed during a Lower Paleozoic tectonic event, prior to 400 m.y. ago.

These faults, however, have experienced sinistral, strike-slip movements subsequent to their formation. It has been explained that these movements could correspond to the youngest tectonic event recognized in the area, based on the cross-cutting relationships between different faults recorded and mapped at and near the Indian Point Generating Station. This youngest tectonic event could be correlated with the tectonic event postulated by de Boer, based on a paleomagnetic study of Mesozoic dikes (de Boer, 1967). A simple shear system of sinistral polarity was interpreted by de Boer, for the northern Appalachians on the basis of the fan-shaped distribution of Mesozoic mafic dikes. This approximately NE-oriented stress system would have been operative in the northeastern Appalachians during Jurassic and possibly Early Cretaceous times. This shear system could have been responsible for the emplacement of the mafic dikes and caused the sinistral reactivation of pre-existing NNE-to-NE trending faults. Such strike-slip movements could also induce synthetic shearing and dip-slip movements along faults and fractures oriented NNW-NNE.

B4.2 INTERPRETATION OF THE MINIMUM AGE OF THE YOUNGEST TECTONIC MOVEMENT

It is reasonable to propose that the stress system which would facilitate the sinistral strike-slip faulting along faults trending NNW-NE has dissipated in Early Cretaceous time, when dike development ceased (approximately 100 m.y. ago). This conjecture suggests an old age for the youngest tectonic movements recognized in the vicinity of the Indian Point Generating Station, including the NS trending faults.

As mentioned in Appendix B2 and described in Attachment B5.4, a principal characteristic of the NNW-NE trending zones is the presence of hydrothermal mineralization. Detailed descriptions of this mineralization are given in Attachment B5.4. Briefly, this mineralization consists of randomly oriented medium to coarse-grained muscovite and phlogopite, crystalline growths of feldspar (adularia), and intergrowths of feldspar with quartz, calcite, pyrite and muscovite. Although, in all fault zones that were examined, this mineralization has been deformed by subsequent faulting, its presence indicates that the NNW-NE trending faults formed in the distant geologic past, possibly in Lower Paleozoic. Commonly, however, free-growing, dogtooth calcite crystals were observed along several onsite faults trending NNE-NE and E-W. These crystals are undeformed. Because many of them occur as delicate forms in vugs, on open faces and in unconsolidated fault gouge, and since they are highly prone to disturbance by the most minor movement, their lack of deformation indicates that no movement has occurred along the faults since their deposition. Therefore, the age of this calcite-mineralization provides a minimum age of last movement.

Fluid inclusions in these calcite crystals indicate that their growth was initiated under conditions of elevated temperature and pressure. Avereage filling temperatures of primary inclusions from unstrained crystals, collected from several onsite faults, ranged approximately between 160°C and 170°C (see Attachment B5.4). These temperatures reflect a significant thermal episode not known to have occurred in the region since Late Mesozoic (over 70 m.y. ago). According to Hadley (1964), the frequency distribution of a comprehensive collection of radiometric dates of the entire Appalachian region shows that the last recognizable thermal episode peaked in the mid-Mesozoic. This is further substantiated by the absence of any sign of post-Mesozoic igneous activity throughout the northeastern United States (Brown, 1968). Broughton and others (1966) verify the absence of such activity in New York. Current regional thermal conditions appear completely normal. Analysis of limited heat flow data from deep regional wells (Urban, 1972) indicates no abnormality. Furthermore, the only thermal spring in the state occurs at Lebanon, New York, east of Albany (Peterson, 1970). Even there, the constant 75° Fahrenheit temperature is probably due to ground-water plumbing, unrelated to a geothermal abnormality. A minimum age of crystallization on the order of 330,000 years has been estimated for these undeformed calcite crystals (see Attachment B5.4).

Soil and weathering profiles developed over some NS-trending faults, situated northwest of Reactor No. 3, do not appear to have been disturbed by faulting. It is interpreted that this soil is 8,000 to 10,000 years old (see Appendix E).

ATTACHMENTS
TO
APPENDIX B

(ATTACHMENTS B5.1 TO B5.4)

ATTACHMENT B5.1

DETAILED GEOLOGIC MAPPING AT THE

INDIAN POINT GENERATING STATION

B5.1.1 INTRODUCTION

This attachment describes all pertinent geologic information obtained during the detailed geologic mapping of five bedrock exposures at the Indian Point Generating Station. Lithologic, stratigraphic, and structural data gathered during this mapping combined with previous investigations were utilized to produce the interpreted geologic map, shown on Plate B5.1-1. Outcrop locations, shown on this geologic map are referred to as: Outcrop North of Nuclear Reactor No. 2; Outcrop in the Trench Northwest of Nuclear Reactor No. 3; Outcrop Adjacent to Turbogenerator Building No. 1; Outcrop North of Nuclear Reactor No. 3; and Outcrop South of Nuclear Reactor No. 3.

Detailed geologic plans were prepared for each of these outcrops, at scales of 1:30 or 1:60. These plans are presented on Plates B5.1-3 through B5.1-7 (at a reduce scale). Base lines, generally outlining these exposures, were measured by steel tapes and oriented by compass to facilitate mapping. Brunton compasses were used for structural measurements. At the western portions of the outcrop north of Nuclear Reactor No. 3, in the trench located northwest of Reactor No. 3 and at the outcrop adjacent to Turbogenerator Building No. 1, abnormal magnetic fields, produced by electric currents, dictated the use of an alternative method of mapping. At locations, where abnormal magnetic fields were produced by electric currents, a steel tape and a protractor were used to measure the acute angle, in a horizontal plane, between the projection of structural features and the base line. As a result of this technique, the accuracy of these measurements can only be considered to be within $\pm 10°$.

All other pertinent structural data, recorded at each outcrop, have been plotted on lower hemisphere, equal area projections, illustrated on Plates B5.1-8 through B5.1-12. This data consist of poles or planes representing foliation and/or bedding, the axial planes and plunges of folds, lineations and slickensides, slickensided surfaces, fracture planes, fault planes, and an interpretation of fault and fracture geometry based on information contained in Attachment B5.3.

The locations of samples taken for laboratory examination and analysis are shown on the geologic plans. Information regarding the results of this laboratory investigation is presented in Attachment B5.4.

B5.1.2 <u>LITHOLOGY AND STRATIGRAPHY</u>

The Indian Point Generating Station is underlain by two Cambro-Ordivician rock formations, the Inwood Marble and the Manhattan Schist. The Inwood Marble is exposed at all outcrops examined onsite, while the Manhattan Schist outcrops only north of Nuclear Reactor No. 2.

At the site, the Inwood Marble is composed of three interbedded lithologies, a blue grey-to-light grey (often buff-colored) dolostone; a limestone similar in appearance to the dolostone; and several thick beds of white marble. These rocks exhibit a weak mineral foliation defined by light-colored micas. Within these lithologies are minor layers of chert and phyllite, which are usually folded and boudined.

Within approximately 20 feet of its contact with the Inwood Marble, the Manhattan Schist includes thinly bedded carbonates and biotite quartzite, with minor phyllite layers. Further upsection, the Manhattan Schist is a coarse grained two-mica schist with minor quartzite layering. The presence of garnet and staurolite in this schist indicates a medium grade of regional metamorphic recrystallization.

Hydrothermal activity in this area has deposited a variety of minerals along fault and fracture surfaces (see Attachment B5.4). Pyrite, both pink and white varieties of calcite, as well as brown, white, and green micas are associated with these hydrothermal deposits. Zeolites were observed as fracture-filling material in the Manhattan Schist.

A variety of fault-filling material occur onsite, consisting of healed and unhealed breccias, gouges, and hydrothermal mineralization. Several faults in the outcrop north of Nuclear Reactor No. 3 are coated by a black greasy substance, which was determined by laboratory analysis to be rock flour (Attachment B5.4). All materials sampled along fault planes show some degree of deformation, except for a few occurrences of calcite.

B5.1.3 STRUCTURAL FABRIC

B5.1.3.1 General

Faults are described specifically and in detail for each outcrop. They are referred to by numbers shown on the geologic plan of each individual outcrop (see Plates B5.1-3 through B5.1-7). All other structural elements, such as bedding, foliation, folds, and fracture and fault geometry are described in general terms.

B5.1.3.2 Folds

The structural elements related to folding at individual outcrops are presented on lower hemisphere, equal area projections, illustrated by Plates B5.1-8 through B5.1-12, and are represented diagrammatically on the geologic plans of each outcrop, illustrated by Plates B5.1-3 through B5.1-7. A more detailed study of folding observed at and around the Indian Point Generating Station is contained in Attachment B5.2.

The orientation of the axial plane cleavage (S1) in the rocks at the site is generally subparallel to the orientation of large-scale compositional layering original bedding (SO). In the eastern portion of the site, SO/S1 generally trends NE to NNE, while in the western areas SO/S1 is oriented NNW to NW. These surfaces dip moderately to steeply eastward in both cases.

The orientation of SO/S1 in some areas changes rapidly, within a few feet. At the outcrop north of Nuclear Reactor No. 2, the orientation of SO/S1 changes from about N10W to N40 to 50W, across the contact of the Inwood Marble and the Manhattan Schist. This change in strike over a short distance may be due to faulting.

Detailed geologic mapping at the site has revealed two generations of folding. The character of the older generation (F_1) is generally tight-to-closed isoclinal folds. Locally, these folds are symmetric with axes roughly corresponding to the true dip of bedding. A weak mineral alignment (S1), parallel to the large-scale compositional layering (SO), represents the axial plane foliation of the F_1-folds. Continuous slip along this dominant axial plane foliation has resulted in unfolding some F_1 isoclinal folds. The orientation of the axial planes of the F_1-folds varies as a function of subsequent folding and faulting, but generally trend NNE to NE.

The second generation of the F_2-folds, best exposed north of Reactor No. 2, are commonly concentric folds which locally fold the F_1 structures and SO/S1. At this exposure the axes of the F_2-folds generally trend N40 to 50W, and plunge 10° to 30° to the southeast. Their axial planes strike NW and dip gently to the north or south.

An analysis of folding at the outcrop north of Nuclear Reactor No. 2 is presented on Plates B5.1-8A and B5.1-8B. It should be noted that a total of 72 fractures were observed either parallel to the axial planes or perpendicular to the axes of F_2-folds. These fractures probably represent tensional and extensional fracturing, genetically related to F_2-folding. Spatial geometric relationships also reveal that when the axial planes and axes of the F_2-folds change orientation, there is a directly related change in the orientations of these fractures.

B5.1.3.3 Faults

B5.1.3.3.1 Outcrop North of Nuclear Reactor No. 2

The geologic plan of this outcrop is illustrated on Plate B5.1-3. All structural elements from this outcrop are represented on lower hemisphere, equal area projections, illustrated on Plates B5.1-8A and B5.1-8B.

Six faults were observed in the Inwood Marble at this outcrop, and two were recorded in the Manhattan Schist.

The orientation of the F_1-fault varies from N85E to N85W, dipping 80° to 85° southward. This fault is characterized by occasional breccias, between one and three inches thick. Deformed and undeformed calcite crystals were observed along this fault; the latter were sampled for laboratory examination (Samples D-1 and D-6). The sinistral movement sense along this fault is established by stratigraphic offset and fracture geometry. A calcite vein, parallel to bedding, is displaced about seven inches along F_1. A second-order fault, truncated by F_1, is oriented N70E - 85°N and displaces two one-inch calcitic beds in a sinistral sense. Another fault, oriented N15W - 70°N, also truncated by the main shear, is interpreted as exhibiting a dextral movement sense on the basis of the relationship between this fault and the fractures (oriented NS to N20E) it truncates.

The F_2-fault consists of several parallel and subparallel planes oriented about N30E 80°S. Numerous patches of deformed and undeformed calcite were observed along this trend. The undeformed material was sampled for laboratory examination (Sample D-2). Two instances of stratigraphic offset define the sinistral nature of the movement along this fault. A one-inch thick siliceous limestone bed and the F_1-fault were both observed to be displaced by the F_2-fault.

Fault F_3 trends about N73E and dips 65° to 85° to the south, and is characterized by discontinuous healed breccias and lenses of deformed and undeformed calcite. The undeformed calcite was sampled (Sample D-3) for laboratory examination. A 2-1/2-inch wide, white limestone bed, offset about four inches, defines the dextral movement sense of this fault. The cross-cutting relationship between this fault and F_2 is unknown. However, fault F_3 bears an apparent conjugate relationship to fault F_1.

The F_4-fault zone trends generally E-W and dips 80° to 85° southward. It is characterized by patches of calcite that appear to be deformed. Stratigraphic offset, as well as associated fracture geometry, define a sinistral sense of movement along this fault. A folded dolostone bed, about one-inch thick, is displaced approximately one-half inch, and N50E-trending fractures are truncated by this zone.

Fault F_5 is a 2 to 3-foot wide zone of closely spaced, parallel-to-subparallel fractures oriented about N75 to 80E, dipping 80° to 85° to the south. Some of these fractures are filled with deformed calcite. Movement sense along this zone was interpreted as dextral, based on the similar observed displacement along the nearby subparallel fault. This smaller fault truncates a N65W - 65°N-trending fault, demonstrating a sinistral stratigraphic offset.

The F_6-fault is a well-defined plane oriented N85E - 78°S, characterized by occasional healed breccias up to 1-1/2 inches thick. Calcite along this plane appeared deformed and was sampled for laboratory examination (Sample D-5). Ten to 12 inches of stratigraphic offset of a one to two-foot wide marble bed establishes the sinistral movement sense of this fault.

Fault F_7 is composed of two faults which merge at the base of the outcrop. One is oriented N50E - 80°N and the other N30E - 86°S. Shearing of of the healed breccia suggests a reactivation of movement. Oblique-slip displacement is inferred by slickensides plunging 55°, as well as by the associated fracture geometry, while strike-slip motion could be interpreted from slickensides which plunge 15° to 20°. No definite sense of movement could be established.

The F_8-fault is characterized by a one to six-inch-thick healed breccia, oriented N70W - 82°S. Its movement sense cannot be defined.

B5.1.3.3.2 <u>Outcrop in Trench Northwest of Nuclear Reactor No. 3</u>

The geologic plan of this outcrop is illustrated on Plate B5.1-4. All structural elements from this outcrop are represented on Lower Hemisphere, Equal Area Projections, illustrated on Plate B5.1-9.

Throughout this exposure a total of four shear zones were mapped. Stratigraphic displacement was observed in only one case, the F_3-fault. The other zones are considered faults because of the combined development of breccias, slickensides, and fracture geometries along them, suggestive of movement, such as frictional shears and feather joints. In the majority of cases, the character and sense of movement were interpreted on the basis of slickensides and associated fracture geometry.

The F_1-shear zone strikes N40E and dips 65° to 75° to the southeast. The breccia developed along this zone is healed, and consists of angular to subangular limestone fragments. A shear plane with slickensides developed on it, pitching 8° to 16°, and 25° to 40° toward the northeast, cuts across the breccia. The more steeply pitching slickensides appear to be younger. The fracture geometry associated with this shear zone suggests, but does not prove that two senses of strike-slip movement occurred along this zone. The cross-cutting relationships between these fractures indicate an older dextral movement, perhaps related to the formation of the breccia and a younger sinistral movement.

The F_2-shear zone is about eight inches thick, composed of three planes trending N82E, N87E, and N72W. Each of these planes contains completely healed breccia, similar to that along the F_1-fault. The N72W fracture is bounded by the ENE-trending planes. This geometry suggests a dextral sense of strike-slip movement, with the N72W fracture being the frictional shear, and the ENE fractures, the main shear.

The F_3-fault zone consists of three sharp, well-defined planes trending about N30E, N33E, and N09E, dipping 60° to 67° southward. The N30E-trending plane truncates the other two. This geometric relationship suggests that the N30E oriented plane is the main shear which truncates the other two frictional shears, and a sinistral sense of strike-slip motion. A two-foot stratigraphic offset of a one to three-inch bed of yellow sandy limestone supports this interpretation. The sinistral shear plane cuts across the healed breccia along the main shear. Slickensides on this plane pitch 16° to 18°, and 35° to 40° to the northeast.

The F_4-shear zone is characterized by a yellowish red breccia about ten to twelve inches wide, oriented about N30 to 35W, dipping to 76° to 78° northward, subparallel to the original bedding. This ironoxide-stained, unhealed breccia consists of angular to subangular weathered limestone fragments and cobble-sized fragments of an older healed breccia. Slickensides are abundant on many planes, in the vicinity of this zone, with pitches that vary from 40° to 60° to the northwest, indicating an oblique-slip movement sense. Fracture geometry suggests that the northern side is down-dropped, and the strike-slip component of movement is sinistral.

B5.1.3.3.3 Outcrop Adjacent to Turbogenerator Building No. 1

The geologic plan of this outcrop is illustrated on Plates B5.1-5A and B5.1-5B. All structural elements from this outcrop are represented on lower hemisphere, equal area projections, illustrated on Plate B5.1-10.

Fault F_1 is oriented subparallel to bedding at about N50E - 68°SE, and marks the eastern boundary of a similarly trending healed breccia. A finer distinctive breccia is developed adjacent to the F_1-plane. Patches of deformed calcite on this surface exhibit slickensides which plunge 22° northeast. However, no movement sense could be established for this fault.

The F_2-fault is oriented subparallel to bedding at about N50E - 60°S, and is characterized by a three to four-inch thick healed breccia. Patches of calcite along the F_2-plane exhibit slickensides plunging 17° northeast. Several en-echelon calcite-filled fractures are oriented N-S - 82°E. If these represent filled tension gashes, it is possible to interpret a sinistral sense of movement along this fault.

Fault F_3 is oriented N03E - 53°S, and is characterized by a healed breccia of variable thickness. Several en-echelon calcite veins are oriented N08E to N16E and are bounded by healed breccias. These apparent tensional fractures, coupled with the orientation of smaller breccias, probably representing secondary shears to F_3, suggest a dextral sense of movement along this fault.

Fault F_4 is parallel to bedding, oriented N4E - 53°S. This surface displays slickensides on calcite which plunge 35° northeast.

The F_5-fault is characterized by a six-inch wide healed breccia, oriented N54E - 66°S. Several en-echelon calcite veins, oriented N-S - 80°E, appear to be offset about three to six inches in a sinistral sense. This displacement, as well as the geometry of the veins themselves, indicates sinistral movement along this fault. An older healed breccia, generally trending E-W, is truncated by this fault.

The F_6-fault trends generally ENE, dipping 75° to 85° to the south, and is characterized by a two to three-inch thick healed breccia. The fracture geometry associated with this fault is suggestive of a sinistral sense of movement.

Fault F_7 is a zone of closely spaced fractures oriented about N-S - 75°E. Calcite along some of these fractures exhibits horizontal slickensiding. About a six-inch displacement of the F_6 breccia defines the dextral movement along this fault.

Fault F8 is a one to two-foot wide zone oriented about N30E - 60°S. This zone is characterized by fractured siliceous, micaceous filling material, and soft fault gouge along its margins. It is possible that a number of minerals in this zone are of hydrothermal origin. Samples (CA-1, CA-2, CA-3, CA-4, and CA-7) were taken from this filling material for laboratory examination. The movement sense along this fault was not determinable, though it does truncate fault F_7.

The F_9-fault is oriented about N04E - 68°S, and characterized by occasional healed breccias developed along this trend. Calcite lenses, on the order of one inch displaced by small shears associated with this fault, indicate a sinsitral sense of movement. A sample (CA-5) was taken from this fault for laboratory examination.

Faults F_{10} and F_{11} are oriented N11W - 69°E and N49E - 54°N, respectively. Both faults are characterized by loosely cemented breccias. These faults apparently merge, although their exact relationship is unclear.

Fault F_{12} is a nearly vertical healed breccia oriented about N11W, which is sheared and offset by a number of faults, designated as F_{13}. These are a series of small discontinuous faults oriented about N05W - 64°N, which show a consistent, down to the east "normal" sense of movement.

The F_{14}-fault consists of a loosely cemented breccia parallel to bedding, oriented N07E - 63°S, which contains undeformed calcite crystals. Secondary faults trending N34E - 83°N, also characterized by loosely cemented breccia, contain vugs or undeformed calcite. This fault geometry is suggestive of a dextral sense of movement along fault F_{14}.

Fault F_{15} trends generally WNW and dips about 60° southward, characterized by a four-foot thick healed breccia. This breccia is truncated by fault F_{18} and displaced in a dextral sense by fault F_{16}.

The F_{16}-fault plane is oriented N04E - 65°S and N06W - 67°S, and is characterized by a healed breccia about six inches thick, exhibiting nearly horizontal slickensides. The stratigraphic offset by this fault of the F_{15} breccia, and a marble bed by about 4 inches establishes the dextral movement sense along this fault.

Fault F_{17} is oriented N06E - 64°E and is characterized by a two to four-inch zone of microbreccia, and an open breccia with pyrite aggregates along the fault zone. A sinistral movement sense along this fault is defined by its displacement of the F_{16}-fault, as well as by its associated fracture geometry.

The F_{18}-fault is oriented parallel to bedding at about N17E-61°S, with possibly some hydrothermal mineralization along its trend. This fault truncates fault F_{15}. Drag attributed to strike-slip movement along F_{18} suggests a sinistral sense of movement.

Fault F_{19} is oriented N14E-63°S, or parallel to bedding. This fault is characterized by healed breccia, and at the base of the outcrop, by sand and silt-filling material. A sinistral sense of movement along this fault is suggested by its associated fracture geometry.

Fault F_{20} is a healed breccia oriented about N02E-52°N, and truncated by faults F_{18} and F_{19}. The geometric relationship of these three faults implies that fault F_{20} is the frictional shear, with sinistral movement sense, developed by sinistral movement along the main shears F_{18} and F_{19}.

The F_{21}-fault is a healed breccia oriented N32E-82°S. This fault is truncated by Fault F_{20} and displaced in a dextral sense by several small faults trending about N26W.

B5.1.3.3.4 <u>Outcrop North of Nuclear Reactor No. 3</u>

The geologic plan of this outcrop is illustrated on Plates B5.1-6A and B5.1-6B. All structural elements from this outcrop are represented on lower hemisphere, equal area projections, illustrated on Plate B5.1-11.

Fault F_1 is a two-foot wide zone of intensely weathered breccia, oriented about N35E-65S. Weathering of this breccia has produced grey, green, and orange silts and clays. This fault constitutes the southeast border of a larger, generally northeast-trending breccia zone. The obvious difference in the character of the F_1 zone leads one to interpret it as a reactivation along the margin of the larger, completely healed zone. The sinistral movement sense of F_1 is indicated by about 15 feet of offset of a two-foot wide, dark grey marble bed.

The F_2-fault is poorly defined, nearly vertical plane, trending about N20W. Near its intersection with F_1, its surface is coated with a dark green mineral. The relationship of F_2 to F_1 is uncertain. However, it appears that F_1 is not offset by F_2. The dextral movement sense of F_2 is defined by about 6 inches of apparent offset of F_3.

Fault F_3 is oriented N45E-75°S. This fault is characterized by a healed breccia about six inches wide, defining the northwest border of the large, generally NE-trending breccia zone.

The offset of a marble layer with several siliceous interbeds, by about two feet, defines the dextral movement sense along this fault. Fault F_3 is truncated by fault F_6, and is offset in a dextral sense by both F_2 and F_5.

Fault F_4 is a nearly vertical zone of closely spaced fractures, oriented N65E, that cuts through the central portion of the larger breccia zone. This zone is truncated by both $F_2$and F_3-faults, although its relationship to the surrounding faults is unclear. The two-foot wide dark grey marble bed appears to be offset about three feet along this zone, in a sinistral sense.

Fault F5 is small, consisting of a single plane oriented N20W-62°N, displaying subhorizontal slickensides plunging to the north. This fault is truncated by F_6 and offsets F_3 a few inches in a dextral sense.

Fault F_6 is a well-defined plane oriented N10E, 55° to 60°E, exhibiting subhorizontal slickensides. On the east side of this fault are several pods of breccia, up to six inches thick, whose counterparts cannot be located on the west side. The offset counterpart of the F_3-fault also could not be located.

Faults F_7, F_{11}, F_{12} and F_{13} compose a zone of generally NNW faulting, which closely parallels bedding, oriented N05 to 10W, dipping 60° to 70° eastward. Faults F_9 and F_{10} appear to be related to shearing along two of the NNW-trending planes.

Faults F_7 and F_{11} are oriented about N10W-65°N. Fault F_{11} is characterized by black, sheared material along its trend, which has weathered to silts and clays in places. The movement sense along these faults is interpreted as dextral on the basis of their relationship with faults F_9 and F_{10}.

Fault F_8 consists of a sinle plane, oriented N05E to N35E, dipping 65°E and 85°E, respectively. The upper surface exhibits subhorizontal slickensiding. This fault is truncated by a bedding surface, located between faults F_7 and F_{11}. Its cross-cutting relationship to F_7 is unclear. However, neither fault appears to offset the other.

Faults F_9 and F_{10} are oriented N26E and N17W respectively, dipping 60° to 70° southward. Both faults exhibit minor stratigraphic offsets, indicating dextral movement senses. Fault F_9 is truncated by both F_7 and F_{11}. It appears that F_9 is a frictional shear resulting from dextral shearing along F_7 and F_{11}.

Fault F_{12} is oriented about N10W-66°N. This fault is characterized by a continuous nine-inch wide bed of dark grey cemented breccia. A finer and more distinctive three-inch wide breccia is developed along its western edge, while its eastern border is defined in places by black sheared material. Locally this "breccia bed" has weathered to grey, green, orange, and black silts and clays.

Fault F_{13} is oriented N10W-72°N, closely paralleling bedding. Healed and highly weathered breccias were both observed between F_{12} and F_{13} at their northern mapped extents. A dextral movement sense is interpreted for this fault on the basis of the position of the weathered breccia in this area.

Fault F_{14} is a zone of closely spaced fractures oriented about N30E-75°S. Movement sense along this trend is established as dextral by approximately two feet of displacement of a mineral pod. This fault is truncated by F_{12} and offset in a sinistral sense by F_{15}.

Fault F_{15} consists of a well-defined plane oriented generally N-S-65E, exhibiting subhorizontal slickensides. The movement sense along this fault is defined as sinistral by three separate stratigraphic offsets on the order of two to three feet. Faults F_{14} and F_{17} are both offset in this manner, as well as a two to three-inch wide mineralized bed of white marble. Undeformed crystals of calcite were observed over-growing deformed calcite between two slickensided surfaces defining the F_{15}-fault. Samples (S-1, S-2, S-15 and B-31) of the mineralization along this fault were taken for laboratory examination.

Fault F_{16} is oriented N53E-63°S, and exhibits subhorizontal slickensiding. A small breccia zone is developed along this trend near the base of the outcrop. Sinistral movement along this fault is established by a one-foot offset of the previously mentioned mineralized bed of white marble.

Fault F_{17} is a generally E-W oriented, nearly vertical healed breccia, approximately two feet wide. It is characterized further by the mineralization that crosses its northern margin and meanders through its central portion. This mineralization resembles that along faults F_{24} and F_{22}, as well as the irregularly shaped masses of minerals trending in a generally northwest direction from F_{24}. This mineralization consists of disoriented micas, pyrite, quartz and feldspar (possibly the adularia variety). Sample S-14 was taken from fault F_{17} for laboratory examination. Near its junction with F_{22}, a wedge of unbrecciated rock may indicate that two trends of brecciation merged to form F_{17}. This trend is offset in a number of places, possibly in a dextral sense by F_{13}, definitely in a sinistral sense by F_{15}, and possibly in a dextral or a sinistral sense by F_{22}.

Faults F_{18} and F_{19} are two very small faults consisting of single planes oriented N40 to 45E, and dipping approximately 70° to the south. Dextral movement along these trends is defined by three to four-inch offsets of dark grey marble beds.

Fault F_{20} consists of two planes oriented N25W-62°N and N40W-80°N. Both planes exhibit slickensides which plunge at steep and shallow angles. It is possible that both strike-slip and dip-slip movements have occurred along these surfaces. The N25W plane truncates bedding in a manner that suggests normal movement. However, faults F_{11}, F_{12} and F_{13} do not appear to be affected by any displacement along the N40W surface.

Faults F_{21}, F_{22}, and F_{23} are probably related faults composing a NNW-trending fault zone. These faults are generally characterized by healed breccia developed between them, nearly horizontal slickensides and a black greasy material. Fault F_{22} contains hydrothermal mineralization along its trend. This mineralization and the black material was sampled for laboratory examination. Movement sense along these faults (F_{22} and F_{23}) is probably dextral and sinistral. Fracture geometry and the established displacement of F_{15}, which is probably a splay of F_{21}, indicate a sinistral movement sense. The displacement across F_{22} and F_{23} of F_{17} can be interpreted as both sinistral and dextral senses of movement.

Fault F_{24} is oriented N80E-82°S. This fault is characterized by a six-inch wide, well-defined healed breccia, marking the southern border of a large, poorly defined area of brecciation. There is some hydrothermal mineralization along the northern margin of this breccia. Stratigraphic displacement across this fault is difficult to define, but is interpreted to be of sinistral sense. It is possible that this fault is a counterpart of F_{17}, offset along F_{22} and F_{23} in a dextral sense.

Fault F_{25} is characterized by a well-defined healed breccia, about one-foot thick, oriented N85W-75°N. Stratigraphic offset across this fault appears to be about one foot in a sinistral sense. It is possible that this fault is a counterpart of F_{17} offset along F_{22} in a sinistral sense.

Fault F_{26} and subparallel small faults (F_{27}, and F_{28}) are a series of en-echelon faults oriented N-S to N05E-70° to 80° E. A breccia is developed between F_{27} and F_{28}. All of these faults demonstrate a minor offset of a NW-trending mineralized surface in a dextral sense.

Fault F_{29} trends N05E-71° E, and consists of a single plane exhibiting subhorizontal slickensides. This fault shows a definite sinistral movement sense indicated by about a six-inch displacement of a black marble bed, as well as a large N35W-trending zone of hydrothermal mineralization.

Fault F_{30} is a single plane, oriented N15E-75° E, characterized by subhorizontal slickensides. This fault displays a small stratigraphic offset, with a sinistral movement sense.

Fault F_{31} comprises two subparallel planes oriented about N35 to 40W, dipping 65 to 70° N. Steeply plunging slickensides indicate oblique-slip movement along these surfaces.

B5.1.3.3.5 <u>Outcrops South of Nuclear Reactor No. 3</u>

The geologic plan of this outcrop is illustrated on Plate B5.1-7. All structural elements from this outcrop are represented on lower hemisphere, equal area projections, illustrated on Plate B5.1-12.

Fault F_1 is a healed breccia, oriented about N65E-75° N. Slickensides on this surface plunge 15° to the northeast. A dolostone bed, which is displaced about three inches, defines the dextral movement sense of this fault.

The F_2-fault is a well-defined plane, trending about N65 to 70E, dipping 60° northward. Dextral movement along this fault is defined by about six inches of stratigraphic displacement.

The F_3-fault consists of two healed breccias oriented N80E-70°N and N85W-82°S. There is some calcite mineralization along these faults. However, no sense of movement could be established for these breccias.

Fault F_4 is oriented about N10E-65°S, and is characterized by a thick healed breccia with some mineralization along the fault surface. This mineralization was sampled (SA2-4 and SA 2-5) for laboratory examination. This mineralization consists of medium-size grains of mica, probably phlogopite and muscovite, quartz, and possibly weathered amphybolites of the actinolite-tremolite family. Dextral movement sense along this fault was interpreted from its associated fracture geometry, and from the observed displacement along the nearby smaller fault F_{4A}. Fault F_{4A} displaces fault F_5 about 1-1/2 inches in a dextral sense.

Fault F_5 is a single vertical plane oriented N80E, exhibiting slickensides pitching 65° to the northeast. The geometry of fractures associated with this fault suggests a dextral sense of movement.

The F_6-fault is oriented N20E - 55S and is filled with a soft gouge material. The dextral movement sense interpreted for this fault is based on its associated fracture geometry.

Fault F_7 is also oriented parallel to bedding, about N15E - 60°S. The soft gouge material filling this fault was sampled (SA2-6) for laboratory examination. No satisfactory determination of sense of movement along this fault could be made.

B5.1.3.4 Fractures

An interpretation of the fracture and fault data taken at each outcrop is presented on lower hemisphere, equal area projections, illustrated on Plates B5.1-8 through B5.1-12. The information and interpretations from this site do not differ significantly from those which are described in greater detail in Attachment B5.3. Their sequence of development can be summarized as follows: a conjugate set, bearing a consistent, near perpendicular geometric relationship to SO/S1; a conjugate oriented ENE and WNW; a conjugate oriented NE and NNE, frequently bearing a near perpendicular relationship to a prominent NW group of fractures; and a conjugate oriented NNE and NNW.

In addition to these groups, one other significant fracture trend is observed at the outcrop adjacent to Turbogenerator Building No. 1 and the outcrops south of Nuclear Reactor No. 3. This fracture group is oriented generally N10 to 15E, dipping 10° to 30° northward and is similar to a group of fractures observed in the Cortlandt Complex, filled with granitic intrusives, possibly Devonian in age. In the eastern portion of the outcrop, south of Nuclear Reactor No. 3, these fractures cross cut the generally E-W trending fractures. However, they do not cross cut fault F_4 and F_7 (Plate B5.1-7), and cannot be observed west of them. At the present time, it is not known what these fractures represent.

ATTACHMENT B5.2

FOLD DEVELOPMENT IN THE SITE AREA

B5.2.1 GENERAL

Folds were studied at four outcrops in the rocks of the Manhattan Prong located within 2 miles of the site. Locations of these stations are shown on Plate B5.2-1 (Stations 1D, 2D, 3D, and 4D). The objectives of this study were to determine the fold geometry and to provide a basis for evaluating the relationship between folding, fracturing and faulting.

All folds encountered in this study are mesoscopic although within this category folding on different scales was observed. Two basic types of folds were recognized; they are shown diagrammatically on Plates B5.2-2 and B5.2-3. The first and more common type consists of tight, nearly isoclinal folds. The second is characterized by more open, concentric folds. Relationships between the two types, although not commonly seen, were recongized at Stations 1D and 2D. It is evident that the isoclinal folds have been refolded by the more open structures. Therefore, the tight folds are classified as F_1-folds and the concentric folds are termed F_2.

B5.2.2 DISCUSSION OF THE RESULTS

B5.2.2.1 F_1-Folds

F_1-folds are either symmetrical or asymmetrical. The axes of the symmetrical folds correspond very closely to the true dip direction of the associated larger scale bedding, whereas the axial trends and plunges of the asymmetric folds approximate more closely the apparent dips. In both cases, however, the larger scale bedding or foliation is axial planar to F_1; hence, the trends of the fold axes are essentially parallel to the strikes of the bedding or foliation. All F_1-fold data are plotted on Lower Hemisphere, Equal Area Projections (see Plate B5.2-4). Both symmetrical and asymmetrical F_1-folds were seen at Station 1D. Symmetrical folds occur with the north-striking bedding, and asymmetrical folds are associated with northwest-oriented bedding. The significance of this relationship, if any, is unknown.

B5.2.2.2 <u>F_2-Folds</u>

The F_2-folds recongized in this study are inclined mesoscopic structures in which the axial plane is approximately normal to layering. In this area, the F_2-fold axes plunge generally toward the southeast at 10° to 30°. Data on F_2-folds are plotted on lower hemisphere, equal area projections, Plate B5.2-4.

Several orders of F_2-folds were observed at Station 1D, with the orientations of the smaller folds controlled by the larger scale structures. The axial traces of the smaller folds are essentially normal to the layering, defining the larger scale fold regardless of the attitude of the layering. This geometry implies that, although F_2-folds at all scales formed in response to the same protracted stress system, the smaller structures developed earlier and were later rotated by the larger folds. It is thus inferred that the mesoscopic F_2-folds are inclined due to rotation about megascopic folds, the axial planes of which are probably upright.

B5.2.2.3 Age of Folding

The F_2-fold trend in the area of study is approximately normal to the regional grain, implying that subsequent deformation produced a local rotation of the mesoscopic folds. Minimal evidence exists in the restricted study area for postulating the age of folding. However, a small F_2-fold occurs in the Inwood Marble at the contact with the Cortlandt Complex. This contact which trends 35° to 60° is straight and appears to have been unaffected by this folding. It is, therefore, suggested that, at least, small-scale F_2-folding predated emplacement of the Cortlandt Complex.

ATTACHMENT B5.3

JOINTS, FRACTURES, AND FAULTS STUDY

B5.3.1 INTRODUCTION

This attachment documents the results of the joints, fractures, and faults study undertaken in the vicinity of the Indian Point Generating Station.

The purpose of this study was to determine the sequence of development of fractures and faults, in and around the Indian Point Generating Station, in order to define, if possible, the orientation, character, and extent of the youngest deformation in the area. These objectives were implemented by studying the senses of movement, the character of filling material, and the cross-cutting relationships of fractures and faults. It should be noted that in some cases there exist overlap between this Attachment and Appendix C.

This study involved collecting fracture data from 17 stations situated within the region adjacent to the Indian Point Generating Station. These data were collected from successively younger deformed rocks: the Cambro-Ordovician Inwood Marble and Manhattan Schist, the late-Ordovician intrusive Cortlandt Complex, the Devonian Peekskill Granite and the sediments and intrusives of the Triassic Newark Basin.

Station locations are illustrated on Plate B5.3-1. Stations are designated by a letter indicating lithology and a number indicating the sample of that rock type. For example, Station I-1 indicates the first sample of the Inwood Marble. Fracture strike frequency diagrams, generated from data at these stations, are also represented on Plate B5.3-1.

B5.3.2 METHODOLOGY

B5.3.2.1 General

Four major operations were performed during this study:

1) Data collection - field measurement of fractures and other accessory structural elements;

2) Data compilation - presentation of data on lower hemisphere, equal-area projections.

3) Data analysis - determining the orientation of data concentrations and correlating fractures and faults of similar orientations and characters.

4) Data interpretation - determining the relationship between fractures, faults and folds and interpreting the relationship on the basis of known experimental and tectonic models.

B5.3.2.2 Data Collection

The length of exposures selected as station-locations was on the order of 100 to 200 feet. When the character of the outcrop permitted, sampling was conducted along three relatively orthogonal orientations. The average number of fracture readings recorded at an outcrop was 200, varying from 134 at Station M-1 to 400 at Station I-2.

Fracture orientations were recorded in terms of strike and dip, using a Brunton compass. An arbitrary character notation of "major", "signigicant", or "minor" was also assigned. If observed, more specific characterization was recorded; for example, any indication of the shear or extensional nature of the fracture, plunges of slickensides, or mineralization, i.e. quartz, calcite, mica, or clay was noted. Two other accessory structural elements consistently measured were foliation and/or bedding and faults. The axes of F_1 and F_2-folds in this area have been shown to lie in the plane of the "large scale layering" (S_0/S_1) (see Attachment B5.2). These planes were also recorded in terms of strike and dip. Lineations on these surfaces were recorded in terms of trend and plunge.

Where demonstrable displacement was indicated, faults were defined as dextral or sinistral, normal or reverse. In cases where stratigraphic displacement across the fault could not be established with confidence, no movement sense was assigned. In addition, mineralization and/or breccia character, as well as any observed cross-cutting relationship, were also recorded.

B5.3.2.3 Data Compilation

All station-data are plotted on lower hemisphere, equal area projections (see Plates B5.3-12 through B5.3-19). In general, the following plots were generated: a plot of poles to all fracture planes, a contoured plot of poles to all fracture planes, a plot of poles to foliation (S_0/S_1) planes, a plot of poles to slickensided planes, a plot of poles to mineralized fracture planes, and a plot of poles to fault planes. In some cases where foliation varied across an outcrop, separate plots were prepared to define the relationship between fractures and foliation.

Plots for each location are designated by a plate number prefixed by B5.3, indicating this attachment. Plots of fault data collected from the Triassic rocks and the rocks exposed at the Indian Point Generating Station are presented on Plates B5.3-2 and B5.3-3.

B5.3.2.4 Data Analysis

Data analysis initially consists of plotting on separate diagrams the planes that correspond to the centers of maxima defined by the contoured plots of poles to fractures. The accessory structural information is then used to determine the relationships of dominant fracture concentrations to other collected structural elements such as foliation, observed faults, slickensided planes, and mineralized fractures. In many cases, it becomes possible to establish the shearing or extensional character of a significant fracture trend.

B5.3.2.5 Data Interpretation

The final interpretation of the characterized data was based on observed or deduced field relationships between fractures, faults, folds and igneous intrusive bodies and on the principles of rock mechanics. Summary plots of interpreted fracture and fault orientations and interpreted senses of movement are presented for each station on Plates B5.3-2 to B5.3-9 and Plates B5.3-11 to B5.3-19.

B.5.3.2.6 Method Limitations

In applying the principles of rock mechanics to interpret field data, it should be realized that we are dealing with a natural system rather than with samples deformed under controlled laboratory conditions.

The character of the large-scale deformation was arrived at by the examination of mesoscopic structural features. In some cases, it may happen that the fracture pattern at a specific outcrop is controlled by a dominant local structure. This can either mask or confuse the regional pattern. Therefore, caution must be exercised in interpolating between mesoscopic and macroscopic scales (see Section B5.3.4.2).

A biased sample can be produced by the preferred orientation of an outcrop, and sampling in three orthogonal dimensions is not always possible. This should not be considered a serious problem since data from more than one outcrop were collected for each rock type sampled.

Despite the limitations mentioned above, the interpretations and conclusions should be reliable.

B5.3.3 DESCRIPTIONS OF DATA

This section describes the relationships between faults, prominent fracture trends, and the accessory structural information.

B5.3.3.1 Fault Data

This discussion summarizes the relationships between all fault-orientations observed during the course of this study. As illustrated by Plates B5.3-2 and B5.3-3, the range of fault orientations encompasses nearly the entire perimeter of a stereonet. This fan of poles to faults was divided for analysis on the combined basis of orientation, sense of movement, mineralization and breccia character, offsetting relationships, and persistent angular relations to other observed structural elements.

Division of this fan yields four major groups of predominantly strike-slip faults: a NNW to NW group; an ENE to WNW group; a NE group; and a NNE to NNW group. Each group is discussed separately and subdivided further, as warranted.

The NNW to NW group ranges in strike from about N20W to N60W, primarily dipping to the north. This group was initially separated on the basis of an observed field relationship at Station I-3 (Plates B5.3-1, B5.3-7 and Section C2.5.1). These faults occur as a conjugate pair at high angle to the foliation. This group can be subdivided on the basis of predominant sense of movement. The two resulting faults are a sinistral set trending N20W to N35W and a second dextral set trending N40W to N60W. Both sets of faults are characterized by healed breccias, some calcite mineralization, and one occurrence of pyrite mineralization along a dextral fault.

The ENE-WNW group trends from N70E to N70W with predominantly southward dips. This group is identified by the outstanding similarities in their character. In a majority of cases, these faults are characterized by healed breccias. Where cross-cutting relationships were observed, only one member of this group was not offset by a younger fault. Continued subdivision of this group yields, on the basis of predominant sense of movement along a given orientation, two sets of faults with opposite senses of movement can be recognized. The sinistral faults of this conjugate pair are oriented between N80E and N70W, while the dextral set of faults trends from N85E to N70E (see also Section C2.6).

The NE group of faults is oriented between N40E and N60E, and dips consistently to the east. The majority of faults in this group display sinistral movement senses, and are characterized by both healed breccias and calcite mineralization. Left-lateral faults of this group were observed to consistently offset other faults, whereas right-lateral members were, in some cases, offset by other faults. This group has not been subdivided any further because no significant differences in character appear to warrant this.

The NNE to NNW group of faults fans from N30E to N15W, and dips primarily to the east. These faults are characterized by one or more of the following: healed and unhealed breccias, gouge, and hydrothermal mineralization. Various members of this group were observed to either offset or be offset by other faults. Based on fault-plane characteristics and on cross-cutting relationships, three sets of faults can be separated within this group: a N20E to N30E set, a N05E to N15E set, and a N-S to N15W set. All three orientations contain member faults showing right-lateral and/or left-lateral senses of displacement (Plate B5.3-3).

Faulting in the Triassic basin is described separately because it may reflect the most recent tectonic event.

On the basis of orientation and movement sense and on information provided by the New York State Geologic Map (1970), Triassic faults can be subdivided into four groups: a N-S group; a NNE group; a NE group; and a WNW to NW group.

The N-S group trends between N5W and N15E. The faults that were observed have a dextral sense of movement and are vertical or steeply dipping eastward (Plate B5.3-2).

The second group, oriented about N30E, was derived entirely from the New York State Geologic Map where neither sense of movement nor amount of dip were indicated.

The NE group trends from N50E to N70E, and all faults have subvertical dips. Faults of this orientation displayed sinistral senses of movement (Plate B5.3-2).

The WNW to NW group trends from N45W to N70W. These faults have a predominant normal sense of movement and dip consistently to the southwest (Plate B5.3-2).

B5.3.3.2 <u>Fracture Data</u>

B5.3.3.2.1 <u>The Inwood Marble and Manhattan Schist</u>

The major fracture trends of the Inwood Marble and Manhattan Schist are combined in this description. Information from five stations located on both the east and west sides of the Hudson River (Plate B5.3-1) provide the data base for this discussion. Combined data from all five outcrops (Plates B5.3-4 to B5.3-9) indicate five major groups of fractures: a group that has variable trends and fractures oriented ENE to

WNW; NE; NW; and NNE to NNW.

Over the areal extent of this study, foliation varied in trend from about N20W to N50E. At station I-3 (Plate B5.3-7) these planes were nearly vertical, but everywhere else they dipped moderately to the east (50° to 70°). At most locations, S_0/S_1 displayed subhorizontal slickensides. Where the foliation was trending NNE to NE, some indication of faulting was observed along these surfaces. At station I-2 (Plate B5.3-5) a number of foliation planes were coated with a soft, gray-green gouge.

The first group of fractures has variable trends. The members of this group were identified on the basis of their consistent, near perpendicular relationship to S_0/S_1. The fractures in this group can be subdivided into two sets that constitute a conjugate pair. The basis for this division is the conjugate pair of faults observed at Station I-3 that bear a similar relationship to S_0/S_1 (Plate B5.3-7). Fractures of these sets at several locations exhibit subhorizontal slickensides. At locations I-1, I-2, and I-3, this group represents a prominently filled fracture direction (Plates B5.3-4, B5.3-5, and B5.3-7).

The ENE to WNW group of fractures varies in orientation from about N75E to N75W, with predominantly southward dips. At Station I-2 there are a number of faults which parallel this trend (Plate B5.3-5). There are several occurrences of subhorizontal slickensides on fractures within this group. This group can probably be subdivided into two trends, oriented ENE and WNW, reflecting the generally East-West trending conjugate pair of faults.

The NE group of fractures range in orientation from about N40E to N60E, generally dipping to the east. This trend is characterized by subhorizontal slickensides, and is subparallel to the previously mentioned fault trend of primarily sinistral displacement. This group also represents a preferred trend of calcite mineralization. At Station M-2 several mafic dikes with sheared contacts follow this trend (Plate B5.3-9). Fractures of this group at Station I-2 contain gray-green gouge material (Plate B5.3-5).

The NW group of fractures, ranging from N40W to N60W and dipping both north and south, is probably associated with the NE group because of its orthogonal relationship to it. At Station I-1 this NW group represents a prominent pink and white calcite mineralization trend (Plate B5.3-4).

The NNE to NNW fracture group trends from about N30E to N15W, with generally eastward dips. This entire trend is characterized by subhorizontal slickensides, gouge, and some calcite mineralization. Faults paralleling this group display both dextral and sinistral senses of movement. On the basis of fracture character alone, it is impossible to subdivide this large group. However, it seems proper to divide it on the basis of fault group orientation as discussed in Section B5.3.3.1. This subdivision provides three narrower trends of fractures, oriented N20E to N30E; N5E to N15E; and N-S to N15W, which parallel the fault trends.

B5.3.3.3.2 The Cortlandt Complex

Four stations were located in the Cortlandt Complex (Plate B5.3-1). At Stations C-1 and C-2 on the east side of the Hudson River, the rock is generally described as a Cortlandite of noritic composition. At Stations C-3 and C-4 on the west side of the Hudson River, the rock is a diorite intruded by various "lamprophyric" dikes.

Two general trends of faulting were observed in the Complex: a generally East-West trend of which one was defined as sinistral (Plate B5.3-11), and a N50 to 60E trend also sinistral in character (Plates B5.3-13 and B5.3-14).

Four major groups of fractures are reflected in the stereonets of the Cortlandt samples: an ENE to WNW group; a NE group; a NW group; and a NNE to NNW group. While the general trend does not vary across the river, the dips on the west side are generally lower.

The ENE to WNW fracture group varies in strike from N70E to N70W, with generally subvertical dips. A number of lamprophyric dikes, faults, and subhorizontally slickensided planes parallel this trend. This group could be subdivided into two fracture sets, reflecting the previously discussed conjugate pair. These sets would trend ENE and WNW, or about N80E and N80W.

The NE group of fractures is also a prominent trend in the Cortlandt Complex. This group trends about N40E to N60E, and dips generally eastward. These are several sinistral faults, as well as surfaces with low-to-moderately plunging slickensides parallel to this direction. The majority of lamprophyric dikes are oriented parallel to this trend (Plates B5.3-13 and B5.3-14).

A NW fracture group trending about N45W and dipping both north and south is characterized by planes exhibiting moderate to steeply plunging slickensides (Plates B5.3-11 and B5.3-13). This group is probably genetically associated with the NE group, based on their nearly orthogonal relationship.

The NNW to NNE group of fractures in the Cortlandt Complex trends from abut N15W to N30E, with predominantly eastward dips. This group is characterized by sinistral faulting, a number of planes with low-to-moderately plunging slickensides, and a few lamprophyric dikes. Any subdivision of this group would be similar to that previously proposed for the NNE to NNW faults.

A group of less significant NE trending fractures, trending from about N30E to N60E and dipping shallowly to the north, was observed only at Station C-1. This group constitutes an orientation of granitic vein intrusions in the Cortlandt Complex (Plate B5.3-11).

B5.3.3.3.3 <u>The Peekskill Granite</u>

Three stations were located in the intrusive Peekskill Granite (Plate B5.3-1). Only one small fault was found during the sampling of this granitic body. It is oriented N8E and its sinistral movement was interpreted by offset fractures. No other accessory information was observed.

There are two major fracture trends apparent in the plot of the Peekskill Granite data: an ENE group, and a NNE to NNW group (Plates B5.3-15 and B5.3-16).

The ENE group trends from about east-west of N60E, dipping north and south. There is one occurrence of a south dipping N60W-trending fracture at Station P-2. Little more can be said of these fractures, considering the lack of accessory information.

The NNE to NNW group varies from about N30E to N15W in trend, and dips mainly to the east. Based on previous information, it is probably correct to assume that this is the consistently occurring NNE to NNW group of fractures and faults, and to subdivide it similarly.

B5.3.3.3.4 The Triassic Basin

Three stations were located in the Triassic rocks (Plate B5.3-1). Sedimentary rocks were sampled at all three stations, with diabase being sampled at TR-3 as well. Stereoplots from Triassic stations illustrate a fanning of fracture poles (Plates B5.3-17 to B5.3-19). Although no distinct clusters are apparent in this fan, subgrouping is performed on the basis of previously described Triassic fault information (Section B5.3.3). These groups generally trend NNW to NNE, NNE, NE, and WNW to NW.

The NNW to NNE group ranges in orientation from N10W to N15E, and is subparallel to the direction of dextral faulting. This group is further characterized by calcite filled fractures (Plate 5.3-17), some of which were slickensided at low-to-moderate angles of plunge.

The NNE group trends about N30 to 35E and is parallel to a fault group of unknown dip and movement plan. This group is characterized by calcite mineralized fractures which display low-to-moderately plunging slickensides.

The NE fracture group is subparallel to the NE trend of sinistral faulting, and is characterized by calcite minearlization and subhorizontal slickensides.

The ENE to WNW group of fractures is somewhat similarly oriented to the WNW to NW group of dip-slip faults, and has little other characteristics associated with it.

Two unique sets of fractures are apparent from plots of the diabase sampled at Station TR-3 (Plate B5.3-19). The average planes to these sets are oriented N85E to 50S and N10W to 65N; both are characterized by quartz-filling material.

B5.3.4 INTERPRETATION OF DATA

B5.3.4.1 General

The plots on Plates B5.3-2 and B5.3-3 represent the interpreted sets of fracture- and fault-planes, showing the sense of movement for each orientation. This interpretation was made on the combined basis of the analyzed fault and fracture data presented above.

The sequence of development of faults and their associated fracture sets are presented from oldest to youngest.

B5.3.4.2 Rotated Faults and Fractures

The oldest group of fractures found in the Cambro-Ordovician rocks have a variable trend. These faults and their associated fractures bear a consistent sub-perpendicular relationship to the S_0/S_1 surface and/or the overall gentle plunge of the F_2-folds to the south. This group of conjugate faults is interpreted as genetically associated with F_2-folding. The local change in the orientation of these fractures at and near the site was probably induced by the intrusion of the Cortlandt Complex. Therefore, these fractures and faults can be dated as Pre-Cortlandt.

The best example of these rotated faults was observed at Station I-3, where S_0/S_1 trends N50 to 55E. At this location, a definite set of conjugate faults is oriented about N20W and N50W. Indication of dextral movement was observed on the N50W faults, and sinistral movement on those oriented N20W.

At location M-2, there are two basic trends of S_0/S_1, planes oriented N40E and N20W, both dipping eastward. Although, in this case, data collection was not designed to separate these rotated fractures. By separate fracture collection in areas of observably different S_0/S_1 trends, two sets of fractures can be associated with each major S_0/S_1 orientation. By sub-perpendicular relationship, a N30W and a N60W set is apparently associated with the N40E trending S_0/S_1. Sets oriented N65E and N85E are likewise probably related to the N20W trending S_0/S_1.

Data collection at Station I-2 was designed to detect this rotation by collecting data separately in areas of different S_0/S_1 orientation (Plates B5.3-5 and B5.3-6). It is apparent at this station that, as S_0/S_1 changes from N10E to N30E, these fractures maintain their near perpendicular relationship to foliation (see also Plates B5.1-8A and B).

B5.3.4.3 ENE to WNW Faults and Fractures

The next oldest group of faults and fractures recognized in the area are consistent in orientation, ranging from about N70E to N70W, and generally dipping to the south. This group is dated as Post-Cortlandt because of its occurrence in the Cortlandt Complex, and as Pre-Devonian because of its weaker expression (as joints) in the Peekskill Granite.

The conjugate relationship of these fractures is established by fault data. Plate B5.3-3 illustrates the sinistral nature of the WNW set and the dextral character of the ENE set. These faults are categorized as the oldest group of constant orientation for two reasons. First, wherever cross-cutting relations could be observed, these faults were offset by younger faults. Secondly, their predominant character, containing healed breccias, indicates that they are primarily old faults.

At Station C-1 there are four faults of this orientation, one of which has been established to have a sinistral movement sense. None of them project across the railroad cut immediately to the west. It is indicated by intense slickensiding and by this anomalous situation that a younger NNE fault, probably beneath the roadbed, has offset or truncated the E-W trending faults.

A number of strike-slip ENE-WNW trending faults were observed at location I-2. Movement senses could not be determined. These faults consist primarily of healed breccias. Observation at this station also revealed the presence of a number of normal faults along this same trend, with a consistent down to the south movement plan.

B5.3.4.4 NE Faults and Fractures

The next successively younger fault and fracture group is oriented generally NE. This probable pair of conjugate faults is oriented N20 to 30E, and N40 to 60E. It is probable that the development of this group was initiated in Pre-Devonian time because of its lack of consistent expression in the Peekskill Granite. The conjugate relationship of these two sets was established by interpretation of the fault data.

The N40 to 60E trend is characterized primarily by sinistral movements, healed breccia and/or calcite mineralization. Where cross-cutting relationships were observed, faults of this trend were either offset or did offset other faults. This fracture trend is well reflected in plots from stations I-1, M-2, C-2, and C-4, commonly exhibiting subhorizontal slickensides.

The N20 to 30E trend is characterized by healed and unhealed breccias, and displays both dextral and sinistral movement senses. This trend of faulting is predominantly offsetting in nature. The associated fracture group is well reflected at stations I-1 and C-1. At both locations, these fractures are characterized by subhorizontal slickensides.

Another fracture trend oriented N40 to 60W is interpreted as genetically related to the NE conjugate faults, because of its orthogonal relationship to the acute bisectrix of the conjugate pair. This trend is interpreted as the direction of extensional fracture. At C-1 and C-3, NW fractures display steeply plunging slickensides. At stations I-1 and I-2, this NW trend represents the predominant direction of calcite filling.

B5.3.4.5 <u>NNE to NNW Faults and Fractures</u>

The next youngest group of faults and fractures is oriented NNE and NNW. Because of its consistent occurrence in all rocks studied, little can be said about its age and origin, except that it is most likely Devonian or younger.

This conjugate pair is oriented N-S to N15W, and N20 to 30E. Each set of the conjugate pair demonstrates both dextral and sinistral movements. Offsetting and offset relationships are also common to both NNE and NNW-trending faults.

NNE and NNW trends of fracturing are well developed throughout the study area, and comprise the major fracture orientations in the Peekskill Granite and Triassic rocks. At station I-3, both sinistral and dextral faulting were observed along the NNW trend. At station M-2, this trend is associated with a number of subhorizontally slickensided planes, one of which was recognized as a dextral fault. The NNE trend of fractures at Stations I-1 and I-2 display some subhorizontal slickensiding. At the same location, numerous faults, parallel to this trend, were observed, one of which was sinsitral in character.

At station C-1, slickensides plunging at low angles were observed on NNE-trending fractures, and at station C-4 a sinistral fault trends NNE.

B5.3.4.6 Identification of the Youngest Deformation

B5.3.4.6.1 General

One of the principal objectives of this study was to determine the orientation, character, and extent of the youngest deformation in the area. It was not within the scope of this study to define movement along fault and fracture systems beyond their genesis. Utilizing the methods of this study, it is impossible to determine the exact sequence of multiple movement along pre-existing fracture planes. In addition, it was not within the scope of this study to perform the large-scale mapping required to define a regional fault system and determine its cross-cutting relationships. Thus, the information in this study can only lend itself to an interpretation of what the youngest deformation may have been. The youngest rocks involved in this study are of Triassic age. Because their deformation may reflect the last tectonic event in this area, they are discussed separately.

B5.3.4.6.2 Interpretation of the Triassic Deformation

The fault data presented in Section B5.3.3.2 suggest that the Triassic basin has been deformed by a compression oriented NNE to NE. This compression produced a conjugate fault system composed of dextral faults oriented NS to NNE and sinistral faults oriented NE. There are a number of dip-slip faults oriented approximately orthogonal to this conjugate pair, or about WNW to NW. Furthermore, there are several faults of unknown movement sense and character paralleling this compressional direction.

Although there are fractures in Triassic rocks which parallel these N-S, NNE, NE, and generally E-W fault trends, there is no well-defined clustering of these orientations. The trends of subhorizontally slickensided, generally calcite-filled fractures vary from NNW to ENE. In addition, the poles to the fractures are distributed along the trace of the bedding plane which probably indicates that the fractures developed prior to the general tilting of the basin.

B5.3.4.6.3 <u>Interpretation of the Youngest Deformation</u>

Deformation of the Triassic rocks by NNE to NE oriented compression does not explain several observations that are listed below:

1) Plots of fracture poles in Triassic rock show a fanning of orientation. In a conjugate shear system, concentrated groups of fracture poles would be expected;
2) The presence of subhorizontally slickensided, calcite-filled fractures, as well as several faults oriented parallel to what is an expected extension direction of the conjugate system;
3) The existence of NNE to NNW sinistral faults that are not observed to be offset both onsite and in the vicinity of the site.

Therefore, it is hypothesized that another tectonic event followed the development of this NE-oriented conjugate fault system that affected the Triassic rocks. Two possible hypotheses are presented here, the second of which is more plausible, since it explains more of the anomalies previously stated.

The first hypothesis is that frictional shearing accompanying the conjugate system produced the fanning of orientation noted above. The second, and preferred, hypothesis is comparable to that proposed by Jelle de Boer (1967). According to de Boer, a simple shear system of sinistral polarity was dominant in the Northeastern Appalachians during the late Paleozoic and Mesozoic. The main shear direction was oriented about NE. The existence of that system can satisfactorily account for most of the observations made onsite and in the Triassic Basin.

Assuming this hypothesis is correct, this simple shear system resulted in the emplacement of Late Triassic to Early Cretaceous mafic dikes. It then might be possible to extrapolate further and propose that this shear system dissipated in the Lower Cretaceous, when dike emplacement ceased. This conjecture indicates that this proposed tectonic event occurred between Late Triassic to Early Cretaceous.

Irrespective of these hypotheses, it is probably accurate to state that the youngest tectonic fractures are oriented between the NNW to NE.

B5.3.5 CONCLUSIONS

The conclusions stated herein are summarized from the previously stated interpretations supported by direct field observations.

At least four genetically unique fault systems are reflected in the fracturing of the Inwood Marble in and around the Indian Point Generating Station. These fault systems are listed below in their proposed sequence of development:

A rotated pair of conjugate faults, of variable orientation, related to F_2-folding. These faults are dated as Pre-Cortlandt, because their rotation was probably induced by the intrusion of the Cortlandt Complex. This rotation could have also been induced by subsequent deformations.

A non-rotated conjugate pair of faults, oriented ENE to WNW, is dated as being Post-Cortlandt and Pre-Devonian in age.

A conjugate pair of faults, oriented generally NE, is also probably of Pre-Devonian age, but younger than the ENE to WNW system, as demonstrated by observed cross-cutting relationships.

A conjugate pair of faults, oriented about NNE and NNW, can only be dated as Post-Devonian.

The last two fault systems, proposed to be Post-Triassic, are: (1) A conjugate pair of faults that developed in response to a principal horizontal compression oriented NNE; and (2) A fault system that developed in response to simple shear of sinistral polarity. This stress system, in which the main shear was oriented NE, reactivated many pre-existing fractures and faults.

Conflicting senses of movement along NNE (N20E to N30E) trending faults can be interpreted as follows: Genetically, these faults were developed as the dextral component of a generally NE-oriented conjugate fault system, with the sinistral component oriented N40E to N60E. Following this, the N20E to N30E fault trend was reactivated as the sinistral component of a NNW to NNE-oriented conjugate fault system, with the dextral component oriented NNW. The proposed Triassic deformation contributes further to this reactivation scheme by initiating dextral faulting along a generally N-S trend related to the NE conjugate fault system. Sinistral simple shear along a N30E trend with possibly syntectonic, sinistral synthetic faulting along NNE- to NNW-trends reverses once more the sense of movement.

ATTACHMENT B5.4

MINERALIZATION OF FAULTS AND METAMORPHISM

B5.4.1 INTRODUCTION

The objectives of this phase of the investigation were:

1) Evaluate methods of dating the different periods of tectonic activity; and
2) Determining if possible, existence of anomalous patterns in the apparent geometry of regional metamorphic isograds, and if these anomalies could be interpreted to have resulted from faulting.

To accomplish objective 1), all exposed faults at the Indian Point Generating Station were examined for the presence of fault-filling material. The mineralogy, textures, and parageneses of the mineral assemblages along the faults were studied. Key samples were collected, thin-sectioned, and analyzed by use of a petrographic microscope. Dr. A. Haji-Vassiliou, of Rutgers University, performed X-ray diffraction studies on select mineral and fine-grained aggregates. Dr. H.L. Barnes and R. McLimans, of Pennsylvania State University, performed fluid inclusion studies on calcite crystals.

Location of samples is shown on the Geological Plans (see Attachment B5.1 and Plate B5.4-1). Samples were collected from Verplanck, Tomkins Cove, and Annsville Creek to determine metamorphic grade and identify anomalous geometric conditions of the regional metamorphic isograds. Due to the interference caused by thermal overprinting of the Cortlandt Complex, in the Verplanck Area, a total of twenty-five samples were needed from that area. These samples represent several grades of contact metamorphism. They were examined under the petrographic microscope to ascertain if the grade of regional metamorphism that existed prior to intrusion could be determined from relict minerals.

B5.4.2 COMPARATIVE STUDY OF THE REGIONAL METAMORPHIC GRADES ACROSS THE HUDSON RIVER

B5.4.2.1 General

Cambro-Ordovician rocks on both sides of the Hudson River appear to be stratigraphically correlative, but show different degrees of metamorphic recrystallization. The difference in metamorphic grade appears to change quickly over an anomolously short distance (1.5 miles). Therefore, this study was performed to determine if the apparent rapid change in metamorphic grade could be attributed to:

1) Contact metamorphism caused by the emplacement of the Cortlandt Complex;
2) Structural shortening of regional isograds, or
3) Both 1) and 2) above.

The units of importance are: (1) the Inwood and the Manhattan Formations, and (2) their postulated equivalents, the Wappinger and Annsville Formations. Preliminary analysis of the Inwood and Wappinger Formations showed that these dolostones lacked index minerals. Therefore, their usefulness to this phase of the study was restricted. The metapelites of the Annsville and Manhattan Formations were used in this comparative study. Table B5.4-1 lists the mineral assemblages studied.

B5.4.2.2 Metamorphism at Verplanck

Samples of various metamorphic grades, as defined in the field, were collected at Verplanck for thin-sectioning (see Plate B5.4-1). These samples were studied microscopically in an attempt to differentiate the effects of contact metamorphism from that of regional metamorphism.

The following metamorphic zones were identified to be the product of contact metamorphism associated with the intrusion of the Cortlandt Complex:

1) Inner Zone - variable in width consisting of partially melted granofelsic rocks;
2) Broad sillimanite schist zone;
3) Two-mica garnet schist $\pm$ staurolite zone; and
4) Outer Zone - not characterized by a persistent new mineral phase, but the breakdown of the regional metamorphic minerals is observed.

The Inner Zone is composed mainly of granofelsic and very coarse grained, schistose rocks with high concentrations of garnet, locally developed. Anatectic melting has resulted in mobilization of felsic components and concentration of the mafic mineral residuum.

In the sillimanite zone, sillimanite is of fibrolitic habit, commonly associated with biotite, but also occurs as "mats" and scattered needles. Coarse muscovite is ubiquitous and tends to be discordant to the biotite foliation. Muscovite is commonly porphyroblastic or poikiloblastic. Petrographic evidence indicates that the muscovite formed during either late-stage regional metamorphism or contact metamorphism associated with the intrusion of the Cortlandt. The latter alternative is the preferred interpretation.

The two-mica garnet schist zone is characterized by finer texture and less mobilized micaceous schist with disseminated garnets.

The Outer Zone rocks commonly are two-mica schists with garnet and staurolite occurring locally.

Relics of the regional metamorphic assemblages persist within the higher grade Cortlandt aureole. Under the near thermal conditions, staurolite became unstable and, in one observed case, remnants of staurolite are surrounded by recrystallized mica.

The garnets associated with the two-mica garnet zone and the sillimanite and muscovite zone are fresh; while in the outer portions of the Cortlandt aureole, at Verplanck Quarry, garnets show definite signs of instability. Frequently, the outlines of original euhedral garnets are preserved. Residual garnet grains are surrounded by feldspar, quartz, and opague impurities.

Deformed grains of biotite and muscovite that have not recrystallized occur just north of the site in staurolite schist. This texture suggests post-crystallization movement.

The information presented above suggests that this area had experienced a regional metamorphic grade that crystallized garnet and staurolite prior to the emplacement of the Cortlandt Complex.

B5.4.2.3 Metamorphism at Tomkins Cove

The contact aureole of the smaller intrusions at Tomkins Cove has similar mineral assemblages to the one at Verplanck; however, the gradient is much steeper. The phyllites of the Annsville Formation, away from the intrusions, reflect the true grade of the regional metamorphism in the area. These rocks are very fine grained phyllites that contain only low-grade mineral assemblages such as sericite and chlorite and quartz. The metamorphic foliation is defined by the sheet silicates.

The rocks of the Annsville Creek area are similar in texture and mineralogy to the rocks at Tomkins Cove. These occurrences of phyllites are on strike with one another and probably belong to some low-grade regional metamorphic isograd.

B5.4.2.4 Conclusion

Even though the Cortlandt Complex has increased the metamorphic grade of many of the rocks at Verplanck, it appears that the regional metamorphic grade of these rocks, determined from the relict mineral assemblages prior to the Cortlandt Complex, was medium grade.

The difference in metamorphic grade between the medium grade rocks at Verplanck and the low-grade equivalents at Tomkin's Cove would indicate a temperature difference in excess of 100°C. Considering the distance between these locations, it would appear that the metamorphic gradient is too steep to be representative of normal regional metamorphism.

Therefore it is proposed that structural shortening, post-dating regional metamorphism, could have produced what now appears to be an anomalously steep regional metamorphic gradient.

B5.4.3 MINERALIZATION ALONG FAULT ZONES

B5.4.3.1 General

Many of the NS to NE faults onsite contain crystals and mineral aggregates. Some of these mineral occurrences lie along bedding planes and could be interpreted to be the result of metamorphism of a more pelitic or feldspathic layer within the dolostone. It appears, however, that most of the examples studied were deposited along open faults and fractures by hydrothermal fluids. Many of the mineral phases have been deformed, but there are generations that have formed after the last movement along the surface of interest. Samples of vein materials were collected from the site and their locations are marked on the geologic plans (see Attachment B5.1).

The structural setting and location for each sample is described in Table B5.4-2. Thin sections were prepared from key samples, and were examined microscopically to identify the generations of crystal growth and to determine whether the crystals were deformed. X-ray diffraction analysis of certain mineral phases was performed to aid in their identification.

Subsequent subsections of this attachment are divided into three parts. The first subsection describes the various generations of mineral deposition. The second subsection describes the results of X-ray studies, and the third describes the fluid inclusion studies on the undeformed calcite crystals.

B5.4.3.2 Mineral Assemblages Along Faults

The observed mineral assemblages are as follows:

- Calcite + muscovite + pyrite;
- Quartz + phlogopite + muscovite + calcite + pyrite + amphibole;
- Adularia (?) + calcite + muscovite + pyrite + quartz;
- Calcite + gypsum + illite + paragonite + pyrite;
- Stilbite + heulandite (aeolites); and
- Calcite.

In the NS fault zone recognized in the rock cut north of the Nuclear Reactor No. 3, hydrothermal activity altered the host rock and formed a coarse crystalline incrustation of potassium feldspar (adularia variety), calcite, quartz, muscovite and pyrite (Sample SB-3). Large anhedral to euhedral crystals of potassium feldspar (1 to 2 cm) are penetrated and overgrown by pink calcite. Calcite, in turn, is overgrown by a large muscovite (up to 1 cm) intermixed with recrystallized irregular, randomly oriented mass of muscovite and microcline plus massive pyrite.

Under the microscope, large crystals of adularia show patchy extinction and faint "microcline" like or diffused polysynthetic twinning, which appears to be identical with combined albite and pericline twinning of microcline.

In the NNW fault plane at the same exposure, Sample B-20 contains less ordered white micas (than those found in the wall rocks) associated with calcite and minor brown micas.

Table B5.4-2 presents the results of the mineralogical identification of fault-filling material samples gathered during the course of these investigations.

B5.4.3.3 Summary of X-ray Studies

X-ray diffraction studies were conducted to aid the field study and microscope identification of certain minerals. These studies were performed by Dr. A. Haji-Vassiliou of Rutgers University. Several mineral phases were X-rayed to check their composition.

Green, elongated prisms of "actinolite" from a NE fault in the outcrop adjacent to Turbogenerator Building No. 1, and from a NS fault in the outcrop south of Reactor No. 3, were found to be an altered hydrous Mg-Al silicate (samples SCA-10 and S-2). These samples were of limited use in the study of paragenesis. Pink calcite from NS faults at both exposures was checked for the presence of isomorphous $MnCO_3$ which is useful in determining the depth of formation. None was found in this sample.

White and brown mica samples (SCA-2 and SB-3) from the outcrops, adjacent to the Turbogenerator building and north of Nuclear Reactor No. 3, were checked for composition and the degree of crystallinity. X-ray analysis identified two phases of muscovite, metamorphic and hydrothermal, and confirmed the presence of only one pleochroic phlogopite. Two dark, very thin, fine-grained gouges along the NS faults north of Reactor No. 3, were analyzed.

The basic mineralogy of this cohesive material is:

- Quartz + microcline + dolomite + paragonite/ phengite;
- Quartz + microcline + dolomite + pyrite; and
- Quartz + dolomite + gypsum + kaolin.

The use of these assemblages to aid in our interpretation appears to be restricted at this point.

Feldspar from a NS zone in this exposure was X-rayed to determine the state of ordering and, therefore, the temperature of crystallization. A diffractogram pattern for the X-rayed portion of this sample infers a triclinic lattice. This suggests a primary origin for the triclinic adularia, which crystalized at temperatures far below the order-disorder transformations temperature.

A sample from a NNW striking fault plane north of the Reactor No. 3 shows that the fault plane is coated by two generations of white muscovite plus pyrite and calcite.

In the NNE striking fractured zone in the exposure adjacent to the Turbogenerator Building, the observed mineral assemblage consists of: phlogopite + muscovite + quartz + pyrite + calcite and amphibole (samples SCA-2, SCA-10). Phlogopite occurs here in large deformed aggregates (up to 2 cm) with characteristic curved cleavage traces. Highly strained, pseudo-mosaic textures of quartz, deformed pyrite and calcite, and fine muscovite are the common constituents.

North of Reactor No. 2 in the Manhattan Schist, several fracture planes of different orientations are coated with zeolite mineralization. Stilbite crystals occur in the form of fibrous and radially arranged crystals up to 1-cm long. Heulandite occurs in small clear prisms. Stilbite and heulandite belong to the group of platy zeolites which exhibit a strong property for base exchange, permitting the replacement of the cations by others (potassium among others).

B5.4.3.4 Fluid Inclusion - Geothermometry and Geobarometry

B5.4.3.4.1 General

Fluid inclusion studies (Appendix H.2) were performed to obtain an estimate of the minimum age of last movement on specific faults. The faults studied contained undeformed calcite crystals which are interpreted to have been deposited on the fault surfaces after last movement. Analysis of the fluid inclusions within the calcite crystals provide temperature-pressure relations which can be converted to depth of burial. A summary of the fluid inclusion studies is given in Table B5.4-3 with sample locations.

B5.4.3.4.2 Theory and Method

The presence of fluid inclusions in crystals infers that the depositing brine was at its boiling point when the crystals grew. To determine what these temperatures were, samples were placed in a microscope heating stage, and the temperature was increased until homogenization of fluid and gas was obtained within the inclusions. This work was done by Dr. H.L. Barnes and R. McLimans of Pennsylvania State University, discussed in greater detail in Appendix H.2.

Once the homogenization temperatures are obtained, pressure conditions for formation can be interpreted from knowledge of the salinities and by use of a genetic model. None of the fluids present in inclusions in the calcite contained daughter minerals. This indicates that the salinity of the fluids is between 0 and 26 weight percent equivalents. Values of 2 wt. percent and 25 wt. percent NaCl were used in estimating depth of burial.

A hydrostatic model is the most applicable to the data, due to the open nature of the fault zones and the continuous deposition of the mineralization by hydrothermal fluids. Since hydrostatic conditions are assumed, Haas' curves (1971) can be used to obtain depths of burial from our data (Plate B5.4-2). The most conservative values are used in all computations, and values for both end members of salinity content are presented below.

B5.4.3.4.3 Results

Calcite is the only mineral which is both suitable as a host for fluid inclusions and present in the undeformed state along faults at the Indian Point site. Generally, it occurs as small euhedral crystals within the fractured zones. In the rock cut adjacent to Reactor No. 3 samples were collected from both the NNW and NS fault planes (Samples B-35 and B-31, Plate B5.1-6A). The latest mineral phase at these locations are small crystals of calcite (1 mm), displaying well-developed crystal faces. Textural relationships indicate post-tectonic formation in an open fracture system. The results of homogenization tests yielded filling temperatures of 160° to 170°C.

The corresponding depths of pressure required to attain such boiling points are 50 to 60 meters. This is a conservative estimate since the average temperature (not the highest temperature) was used to determine depth.

Other samples, collected from NS trending faults and representing the post-tectonic undisturbed phase of calcite crystallization, indicate similar ranges of filling temperatures.

From the rock cut north of Reactor No. 2, Sample ND-2, (D-2, Plate B5.1-3) was obtained from NNE striking fault plane that offset an EW-trending fault plane. Fluid inclusion studies of these large, euhedral, and unstrained calcite crystals indicate an average filling temperature of 194°C. This temperature would correspond to a minimum depth of burial of 200 meters.

From the same outcrop north of Reactor No. 2, Sample ND-6 (D-6, Plate B5.1-3) from the above mentioned EW-trending fault was obtained. This sample contained small euhedral crystals overgrown by pyrite which, in turn, is overgrown by lower temperature calcite. Fluid inclusion studies of these crystals indicate an average filling temperature of 317°C.

B5.4.3.4.4 <u>Conclusion</u>

The field and microscopic studies indicate that the last mineral phase to form along the NNW, NS, NNE and EW onsite faults was calcite. The calcite is undeformed and it is interpreted that the fault planes from which the samples were taken have experienced no movement since the formation of the calcite.

The fluid inclusion studies indicate average filling temperatures of 101°C to 317°C for primary inclusion in the above mentioned samples. Due to the nature of fluid inclusion studies, it is generally assumed that the highest temperature derived from a primary inclusion within a single crystal is most representative of the true temperature of formation. The logic for this assumption is similar to that for K/A dating where Ar loss results in a minimum age. Similarly loss of gas from within a fluid inclusion gives an apparent lower filling temperature. Therefore, it could easily be argued that depths of burial in excess of 100 meters were required for the calcite crystals studied. In order to be conservative, a lower filling temperature of about 171°C corresponding to a depth of burial of 50 meters will be used to derive an estimate of the minimum age of formation of the calcite crystals. Assuming 50 meters for depth of burial and applying a denudation rate of 2.7 inches/1000 years (Judson and Ritter, 1964), the time required to unearth the samples studied would be 730,000 years. Meade (1969) contends that a denudation rate of 2.7 inches/1000 years is too high by a factor of two. Thus, a minimum age of the crystals studied would be 1,460,000 years. Since the study area has been glaciated, the true rate of denudation cannot be precisely determined. To qualitatively account for unknowns, such as glaciation, we have assumed a conservative rate of denudation of 6 inches/1000 years. This rate would allow about 75 feet of material to be removed by forces other than those used to determine the rate of 2.7 inches/1000 years (Judson and Ritter 1964). It is therefore concluded, based on the above assumptions, that the minimum age of formation for the calcite crystals, and therefore the age of last movement along the onsite faults mentioned above, is about 330,000 years.

In addition, the suggestion of an even older age can be predicted on the filling temperatures of primary inclusions in undeformed calcite crystals. The temperatures (in excess of of 160°C) reflect a significant thermal espisode probably related to igneous activity which is not known to have occurred during the last 500,000 years.

TABLE B5.4-1

MINERAL ASSEMBLAGES OF METAMORPHIC AND IGNEOUS ROCKS

Sample	Location	Typical Mineral Assemblages
		Manhattan Schist Samples
N-8	Verplanck	Plagioclase + Biotite + Garnet + Sphene + Hercynite
N-44A	Verplanck	Plagioclase + Orthoclase + Biotite + Garnet + Quartz + Sphene + Opaque
N-44B	Verplanck	Plagioclase + Orthoclase + Biotite + Quartz + Sillimanite + Pyroxene + Hornblende
N-44D	Verplanck	Plagioclase + Biotite + Epidote + Hornblende + Sphene
N-45A	Verplanck	Plagioclase + Biotite + Muscovite + Garnet + Sillimanite + Opaque
N-45B	Verplanck	Plagioclase + Biotite + Quartz + Garnet + Sillimanite + Opaque
N-46	Verplanck	Plagioclase + Microcline + Quartz + Biotite + Muscovite + Sillimanite + Tourmaline + Quartz
N-47	Verplanck	Plagioclase + Quartz + Biotite + Muscovite + Garnet + Sillimanite + Staurolite + Tourmaline + Ilmenite
N-48	Verplanck	Plagioclase + Microcline + Quartz + Biotite + Opaque
N-49	Verplanck	Plagioclase + Microcline + Muscovite + Sphene + Apatite + Opaque
N-1	Verplanck	Plagioclase + Quartz + Garnet + Biotite + Muscovite + Sillimanite + Opaque
N-2	Verplanck	Plagioclase + Quartz + Biotite + Muscovite + Sphene + Tourmaline + Apatite + Opaque
Z-5	Verplanck	Plagioclase + Microcline + Quartz + Biotite + Muscovite + Apatite + Zircon + Opaque
N-9	Verplanck	Plagioclase + Quartz + Garnet + Biotite + Muscovite + Opaque
N-10	Verplanck	Quartz + Microcline + Epidote + Sphene + Opaque
N-32A	Verplanck	Microcline + Amphibole + Quartz + Biotite + Epidote + Opaque
N-32B	Verplanck	Microcline + Biotite + Hornblende + Sphene + Epidote + Opaque
N-40	Verplanck	Feldspar + Quartz + Biotite + Garnet + Amphibole + Pyroxene + Epidote + Sphene + Opaque
ND-8	Verplanck	Feldspars + Quartz + Biotite + Muscovite (sericite)
ND-9	Verplanck	Plagioclase + Quartz + Biotite + Tourmaline
ND-7A	Verplanck	Plagioclase + Quartz + Biotite + Muscovite + Garnet + Staurolite
ND-10	Verplanck	Plagioclase + Quartz + Biotite + Muscovite + Tourmaline + Garnet + Staurolite
N-16	Verplanck	Feldspar + Biotite + Quartz + Sphene + Opaque
VQ-1	Verplanck	Plagioclase + Biotite + Muscovite + Quartz + Garnet + Opaque
VQ-2	Verplanck	Feldspar + Carbonate + Biotite + Muscovite + Quartz
		Inwood Marble Samples
N-32C	Verplanck	Calcite + Tremolite + Diopsiole + Microcline + Biotite + Sphene
N-37	Verplanck	Carbonate + Muscovite (Talk?) + Tremolite + Diopsiole + Quartz
SA1-2	Verplanck	Carbonate + Quartz + Feldspar (Microcline) + Muscovite + Opaque

TABLE B5.4-1 (Continued)

Sample	Location	Typical Mineral Assemblages
SA1-4	Verplanck	Carbonate + Quartz + Feldspar + Muscovite
SA1-5	Verplanck	Carbonate + Quartz + Feldspar + Muscovite + Opaque
S-2	Verplanck	Dolomite + Quartz
SA2-3	Verplanck	Carbonate (Dolomite) + Quartz + Feldspar + Muscovite + Opaque
SA2-5	Verplanck	Carbonate + Quartz + Feldspar + Muscovite + Opaque
S-4	Verplanck	Carbonate (Calcite) + Quartz + Muscovite + Phlogopite
S-5	Verplanck	Carbonate (Calcite) + Dolomite) + Quartz + Muscovite + Opaque
S-7	Verplanck	Carbonate + Microcline + Muscovite + Phlogopite + Opaque
S-8	Verplanck	Carbonate + Feldspar + Muscovite + Opaque
S-10	Verplanck	Carbonate + Mircocline + Quartz + Muscovite + Opaque
S-11	Verplanck	Carbonate + Microcline + Quartz + Muscovite + Opaque
S-15	Verplanck	Carbonate + Feldspar + Quartz
S-21	Verplanck	Carbonate + Feldspar + Quartz + Muscovite + Phlogopite + Opaque
CA-2	Verplanck	Carbonate + Quartz + Muscovite + Opaque
CA-3	Verplanck	Carbonate + Quartz + Micas (Phlogopite + Muscovite) + Opaque
CA-5	Verplanck	Carbonate + Quartz + Muscovite + Opaque
CA-6	Verplanck	Carbonate + Quartz + Microcline + Opaque
CA-8	Verplanck	Carbonate (Dolomite) + Quartz + Microline + Muscovite + Opaque
ND-3	Verplanck	Carbonate (Calcite) + Quartz + Feldspar + Muscovite + Opaque
ND-4	Verplanck	Carbonate (Calcite) + Feldspar + Muscovite + Opaque
ND-5	Verplanck	Carbonate + Feldspar + Quartz + Micas
		Annsville Phyllite Samples
AP-1	Annsville Creek	Quartz + Feldspar (Albite) + Sericite + Calcite + Chlorite + Tourmaline + Opaque
AP-2	Annsville Creek	Quartz + Feldspar (Albite) + Calcite + Sericite + (Chlorite + Biotite + Epidote) + Opaque
AP-3	Annsville Creek	Quartz + Carbonates + Sericite + Chlorite + Tourmaline
TC-6	Tomkins Cove	Quartz + Carbonates (Calcite + Ankerite [?]) + Sericite + Chlorite + Tourmaline + Routite (?) + Graphite (?)
TC-8	Tomkins Cove	Quartz + Calcite + Feldspar (Albite [?]) + Mica (Sericite [?]) + Opaque
		Wappinger Limestone Samples
TC-2B	Tomkins Cove	Calcite + Quartz + Sericite + Graphite (?)
WL-1	Annsville Creek	Carbonate (Calcite + Dolomite) + Quartz + Muscovite + Opaque
WL-2	Annsivlle Creek	Carbonate + Quartz + Muscovite + Opaque

TABLE B5.4-1 (Continued)

Sample	Location	Typical Mineral Assemblages
WL-3	Annsville Creek	Carbonate + Tremolite + Diopside + Brown Mica + Epidote
WL-4	Annsville Creek	Carbonate + Quartz + Muscovite + Opaque
WL-5	Annsville Creek	Carbonate + Microcline + Tremolite + Diopsiole + Ziosite
SPL-1	Stony Point	Carbonate (Calcite) + Mg Chlorite + Muscovite + Opaque
SPL-2	Stony Point	Carbonate + Muscovite + Quartz + Opaque
SPL-3	Stony Point	Carbonate + Tremolite + Quartz
		Stony Point Metamorphic Rocks
SP-5	Stony Point	Microcline + Plagioclase + Biotite + Muscovite + Opaque
SP-10	Stony Point	Microcline + Plagioclase + Biotite + Muscovite + Quartz + Garnet
SP-11	Stony Point	Microcline + Plagioclase + Biotite + Quartz + Garnet + Sillimanite
SP-12	Stony Point	Microcline + Plagioclase + Quartz + Biotite + Tourmaline
SP-13	Stony Point	Microcline + Plagioclase (Sauss. Epidote + Actinolite?) + Quartz + Biotite + Muscovite + Opaque
		Cortlandt Intrusive Rocks
N-39	Verplanck	Pyroxene (Opx + Cpx) + Biotite + Plagioclase + Opaque
N-41	Verplanck	Amphibole (Hornblende) + Pyroxene (Cpx) + Plagioclase + Opaque
N-42A	Verplanck	Amphibole (Hornblende) + Pyroxene (Cpx) + Plagioclase + Opaque
N-42B	Verplanck	Amphibole (Hornblende) + Pyroxene (Cpx) + Plagioclase + Opaque

TABLE B5.4-2

FAULT FILLING MINERAL ASSEMBLAGES

Sample	Structural Setting	Mineral Assemblage - Deformed	Mineral Assemblage - Undeformed
S-2	NS Fault	Quartz + Calcite + Muscovite + Phylogopite + Amphibolite + Pyrite	-
SA2-1	FW Fault	Calcite	Calcite
SA2-2	EW Fault	Calcite	Calcite (?)
SA2-3	EW Fault	Quartz + Muscovite + Pyrite	
SA2-6	NE Fault	Calcite + Muscovite + Phlogopite	
SA2-4	EW Fault	Calcite + Quartz + Muscovite	
SB-3	NS Fault	Aduloria + Calcite + Muscovite + Pyrite + Quartz + Phlogopite	
SB-4B	NS Fault	Muscovite + Pyrite + Calcite	Calcite
B-6	NS Fault	Calcite	Calcite
B-7	NE Fault	Calcite + Pyrite	
B-9	NE Fault	Calcite	
B-10B	NE Fault	Calcite	
B-14	EW Fault	Calcite	
B-15B	NE Fault	Calcite	
B-20	NNW Fault	Muscovite + Phlogopite + Calcite + Pyrite	
B-21	NNW Fault	Muscovite + Calcite + Pyrite	
B-30	NS Fault	Pyrite + Limonite	
B-31	NS Fault	Calcite	Calcite
B-35	NNW Fault	Calcite	Calcite
B-36	NNE Fault	Calcite	Calcite
SCA-2	NE Fault	Calcite + Quartz + Muscovite + Phlogopite + Pyrite	
SCA-10	NS Fault	Calcite + Quartz + Phlogopite + Muscovite + Pyrite + Amphibole	Calcite
S-13B	NS Fault	Calcite + Muscovite	
S-D1	NS Fault	Calcite + Muscovite	Calcite
CA-4	NE Fault	Calcite + Pyrite	Calcite (?)
CA5(30+03)	NS Fault	Calcite	Calcite
ND-2	NS Fault	Calcite	Calcite
ND-2	EW Fault	Calcite	Calcite
DN-6	EW Fault	Calcite	Calcite
ND-7A			Stilbite + Heulandite

TABLE B5.4-3

INCLUSION FILLING TEMPERATURES AND DEPTHS OF FORMATION

Sample	Structural Setting	Size of Calcite Crystals Analyzed (mm)	Type of Inclusion	Number of Inclusions	Filling Temperature (°C)	Average Filling Temp. (°C)	Corresponding Pressure Bars	Depth of Formation 2Wt%NaCl (Meters)	Depth of Formation 25Wt%NaCl (Meters)
4B	NS Fault	5 to 10	Primary	7	171 to 186	117	1.3	85	60
B-6	NS Fault	0.5 to 1.5	Secondary (?)	1	118	118	.9	9	5
B-31	NS Fault	1 to 2	Primary	7	151 to 169	161	1.2	60	35
B-35	NNW Fault	1 to 2	Primary	3	141 to 195	171	1.3	74	49
30-03	NS Fault	0.1 to 1.5	Primary	5	159-201	174	1.3	79	55
D-1	NS Fault	0.2 to 1	Primary (?)	2	94.95	94.5	.7	0	0
ND-2 (D-2)	NNE Fault	2 to 20	Primary	12	171-226	194	1.5	160	107
ND-1 (D-1)	EW Fault	0.2 to 1	Primary	5	225-250	232	2	320	205
ND-6	EW Fault	0.5 to 1	Primary	3	274-352	317	3.5	1350	840
SA2-1	EW Fault	0.4 to 1.2	Primary	8	131-188	168	1.3	67	40
SA2-2	EW Fault	10 to 15	Primary (?)	5	92-167	139	1.0	35	16

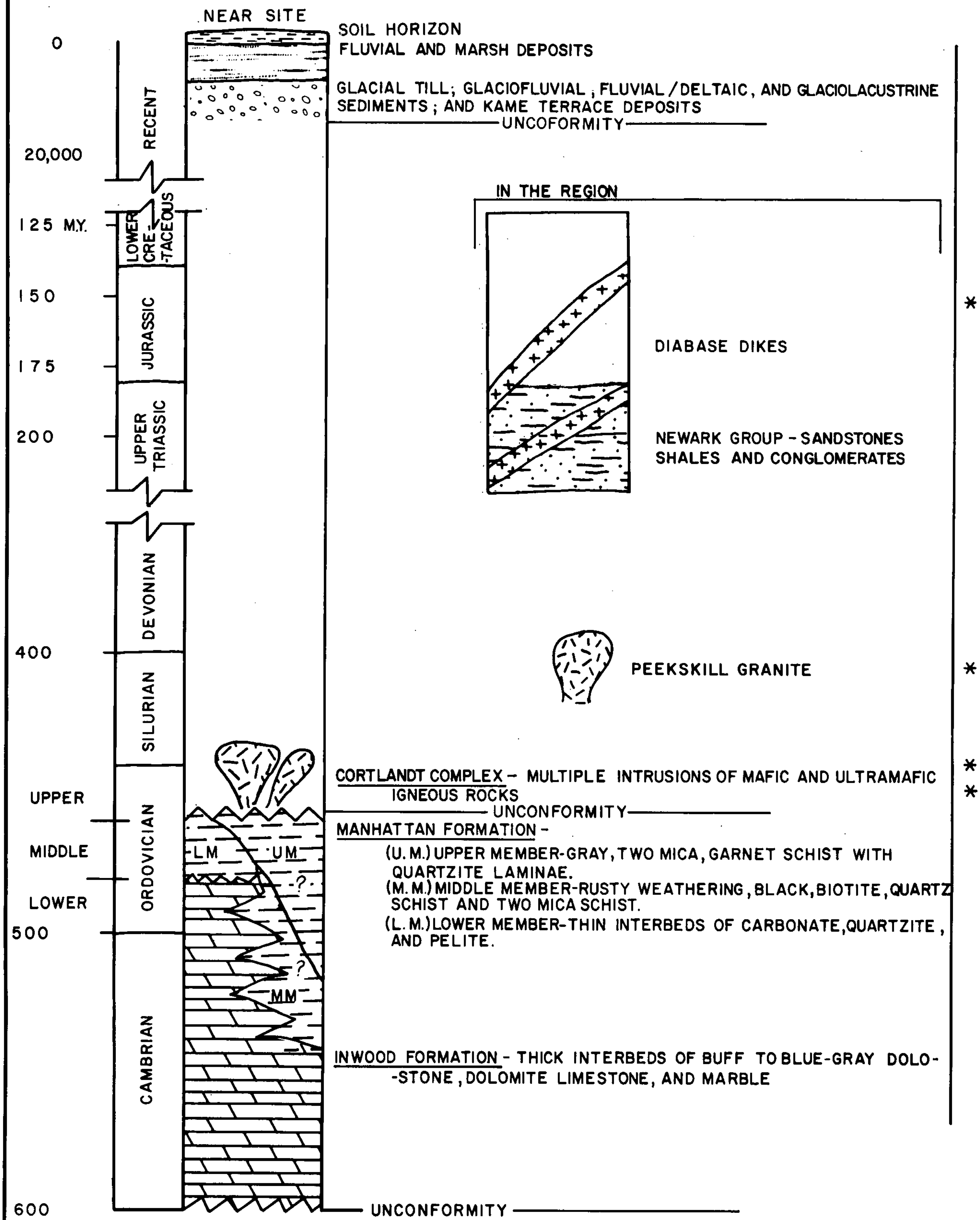

STRATIGRAPHIC COLUMN OF THE ROCKS AND SURFICIAL MATERIALS NEAR INDIAN POINT, NEW YORK

NOTE:
* POSSIBLE HYDROTHERMAL ACTIVITY

DAMES & MOORE

PLATE B2-1

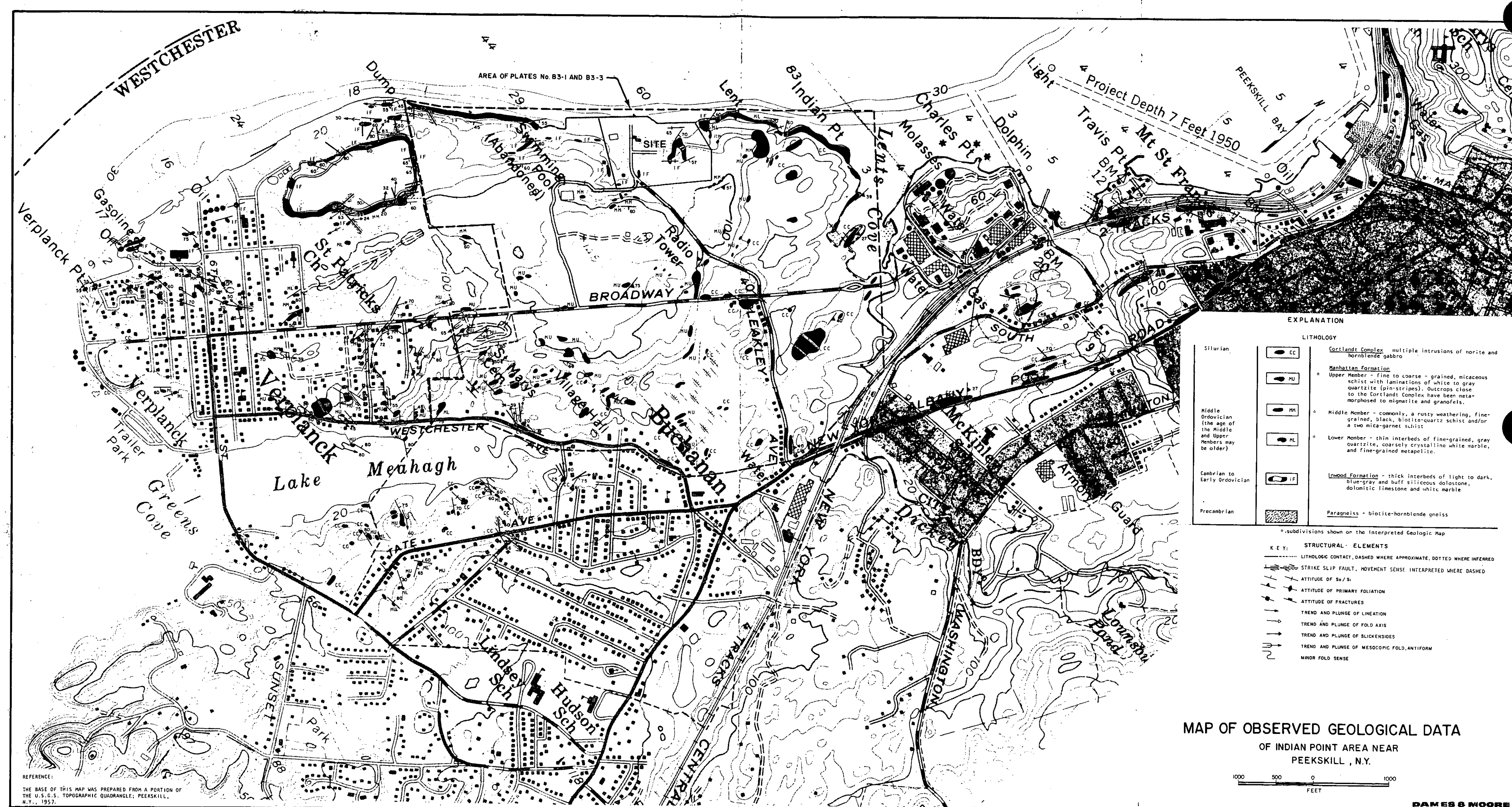
WESTCHESTER
AREA OF PLATES No. B3-1 AND B3-3
Project Depth 7 Feet 1950
PEEKSKILL BAY
Indian Pt
Charles Pt
Lents Cove
Verplanck Pt
Verplanck
Buchanan
Lake Meahagh
Greens Cove
BROADWAY
WESTCHESTER AVE
EXPLANATION
LITHOLOGY
Silurian
CC
Cortlandt Complex multiple intrusions of norite and hornblende gabbro
Manhattan Formation
MU
* Upper Member - fine to coarse - grained, micaceous schist with laminations of white to gray quartzite (pin-stripes). Outcrops close to the Cortlandt Complex have been metamorphosed to migmatite and granofels.
Middle Ordovician (the age of the Middle and Upper Members may be older)
MM
* Middle Member - commonly, a rusty weathering, fine-grained, black, biotite-quartz schist and/or a two mica-garnet schist
ML
* Lower Member - thin interbeds of fine-grained, gray quartzite, coarsely crystalline white marble, and fine-grained metapelite.
Cambrian to Early Ordovician
IF
Inwood Formation - thick interbeds of light to dark, blue-gray and buff siliceous dolostone, dolomitic limestone and white marble
Precambrian
Paragneiss - biotite-hornblende gneiss
* subdivisions shown on the Interpreted Geologic Map
KEY: STRUCTURAL ELEMENTS
LITHOLOGIC CONTACT, DASHED WHERE APPROXIMATE, DOTTED WHERE INFERRED
STRIKE SLIP FAULT, MOVEMENT SENSE INTERPRETED WHERE DASHED
ATTITUDE OF So / S1
ATTITUDE OF PRIMARY FOLIATION
ATTITUDE OF FRACTURES
TREND AND PLUNGE OF LINEATION
TREND AND PLUNGE OF FOLD AXIS
TREND AND PLUNGE OF SLICKENSIDES
TREND AND PLUNGE OF MESOCOPIC FOLD, ANTIFORM
MINOR FOLD SENSE
MAP OF OBSERVED GEOLOGICAL DATA
OF INDIAN POINT AREA NEAR
PEEKSKILL, N.Y.
1000 500 0 1000
FEET
REFERENCE:
THE BASE OF THIS MAP WAS PREPARED FROM A PORTION OF THE U.S.G.S. TOPOGRAPHIC QUADRANGLE; PEEKSKILL, N.Y., 1957.
DAMES & MOORE

PLATE B3-2

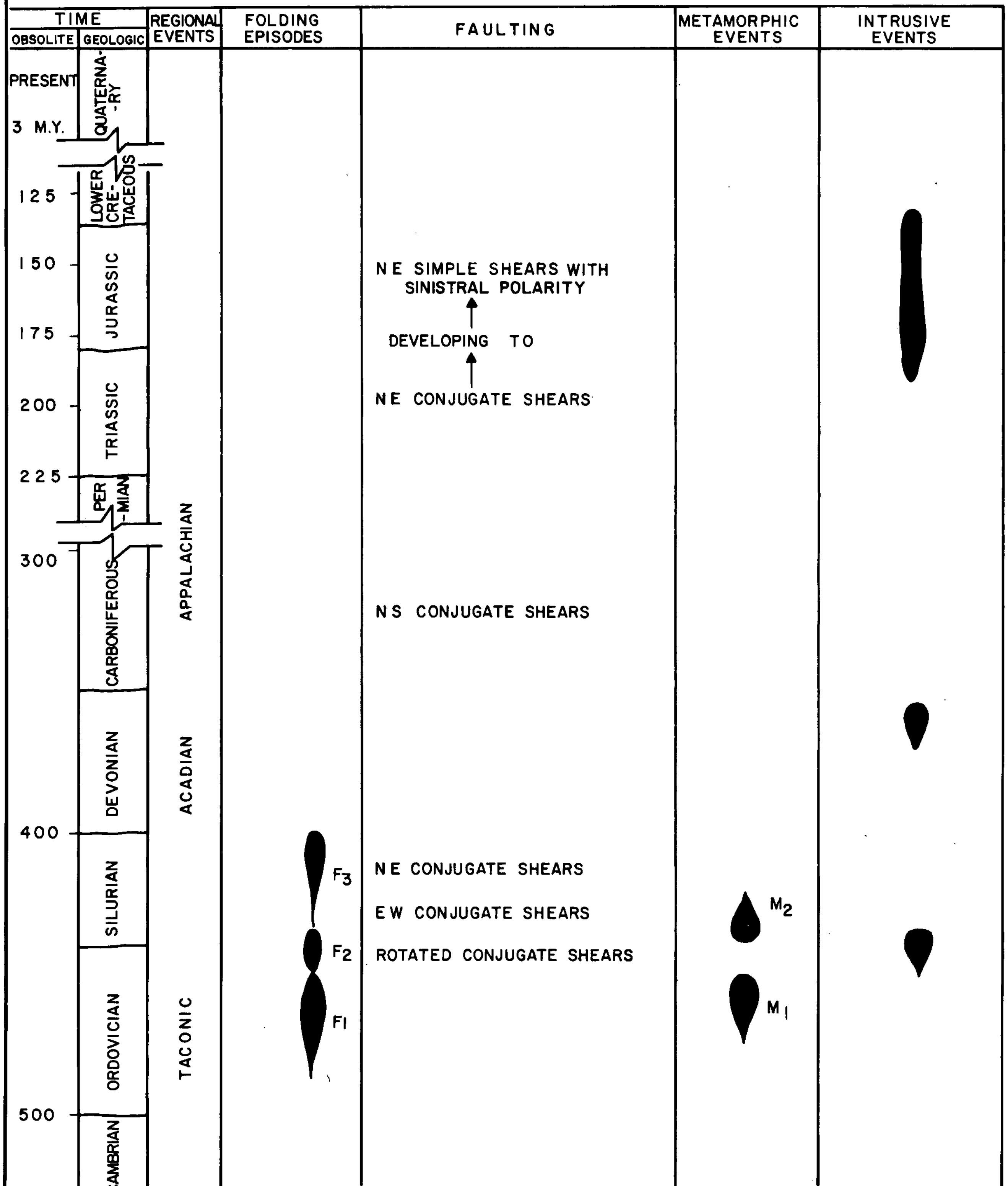

DIAGRAMMATIC REPRESENTATION OF THE DEFORMATIONAL HISTORY OF THE SITE AREA

DAMES & MOORE

PLATE B4-1

or B - WELL DEFINED HEALED BRECCIA

or PB- POORLY DEFINED HEALED BRECCIA

or Ub- UNHEALED BRECCIA

or M - MINERALIZATION: PYRITE, MICA, K-FELDSPAR, PINK CALCITE

- STRATIGRAPHIC MARKER

- LOCATION OF SAMPLE TAKEN FOR PETROGRAPHIC STUDY (SAMPLE NUMBER SHOWN ON OUTCROP PLANS)

70° 70° - STRIKE AND DIP OF PREDOMINANTLY STRIKE SLIP FAULT; DASHED WHERE INFERRED.

70° 70° - STRIKE AND DIP OF PREDOMINANTLY STRIKE SLIP FAULT; ARROWS INDICATE OBSERVED SENSE OF MOVEMENT; DASHED WHERE INTERPRETED.

60° 60° - STRIKE AND DIP OF PREDOMINANTLY DIP SLIP FAULT; DASHED WHERE INFERRED. HATCHURES INDICATE DOWNTHROWN SIDE.

65° - STRIKE AND DIP OF JOINT OR FRACTURE

65° - STRIKE AND DIP OF JOINT OR FRACTURE; ARROW INDICATES RAKE OR PLUNGE OF SLICKENSIDES

- STRIKE OF VERTICAL JOINT OR FRACTURE

60° - STRIKE AND DIP OF ORIGINAL BEDDING (S_o)

60° - STRIKE AND DIP OF FOLIATION (S_1)

60° - STRIKE AND DIP OF FOLIATION (S_2)

20 - DIRECTION AND AMOUNT OF PLUNGE OF AXIS OF F_1 FOLDING; OR LINEATION ASSOCIATED WITH F_1 FOLDING

30 - DIRECTION AND AMOUNT OF PLUNGE OR AXIS OF F_2 FOLDING; OR LINEATION ASSOCIATED WITH F_2 FOLDING

20 40 - STRIKE AND DIP OF AXIAL PLANE OF MINOR FOLD; ARROW INDICATES DIRECTION AND AMOUNT OF PLUNGE

- MATCH LINE

EXPLANATION OF SYMBOLS UTILIZED ON GEOLOGIC PLANS OF SITE OUTCROPS

DAMES & MOORE

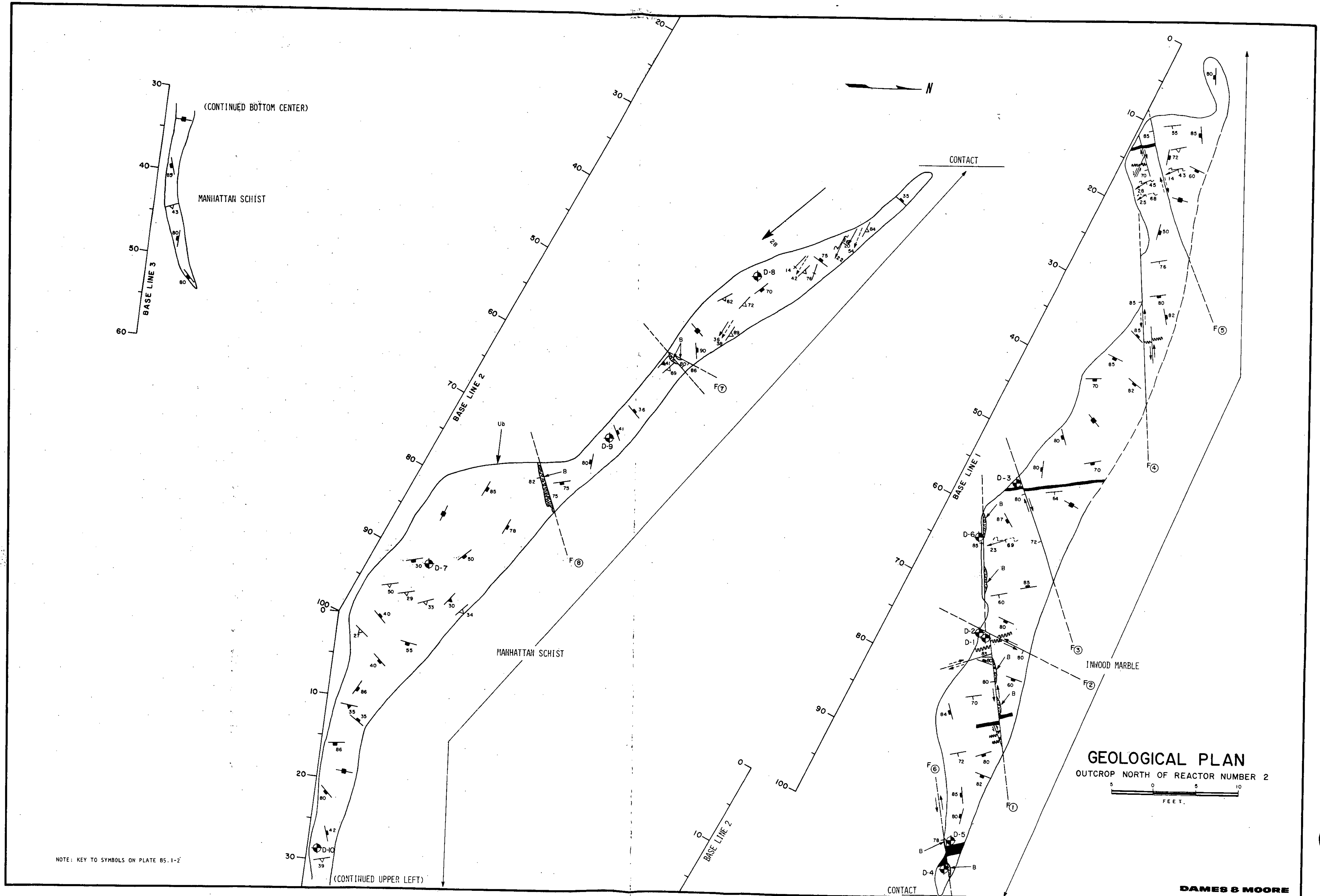

GEOLOGICAL PLAN

OUTCROP NORTH OF REACTOR NUMBER 2

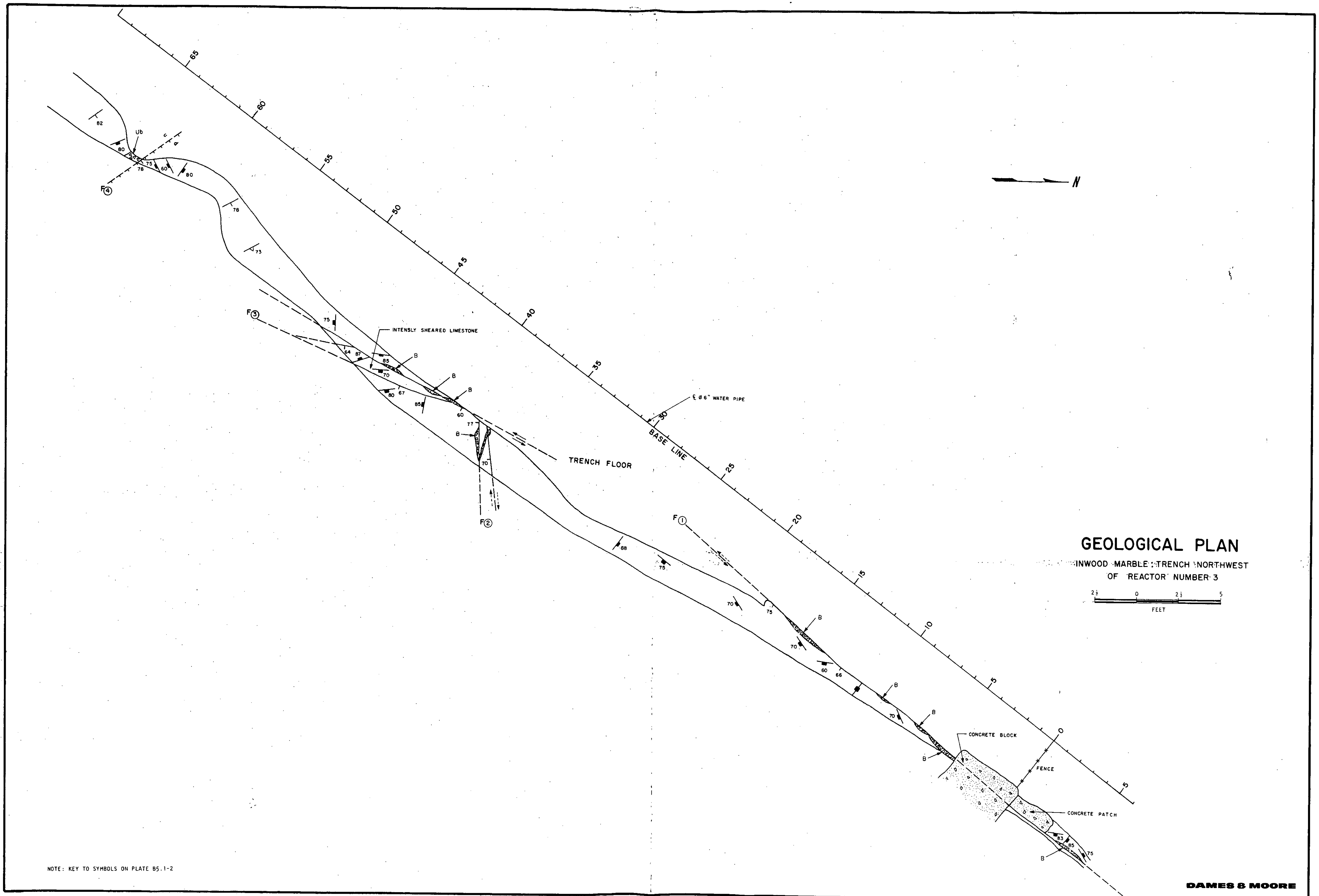

GEOLOGICAL PLAN

INWOOD MARBLE : TRENCH NORTHWEST
OF REACTOR NUMBER 3

NOTE: KEY TO SYMBOLS ON PLATE B5.1-2

DAMES & MOORE

PLATE B5.1-4

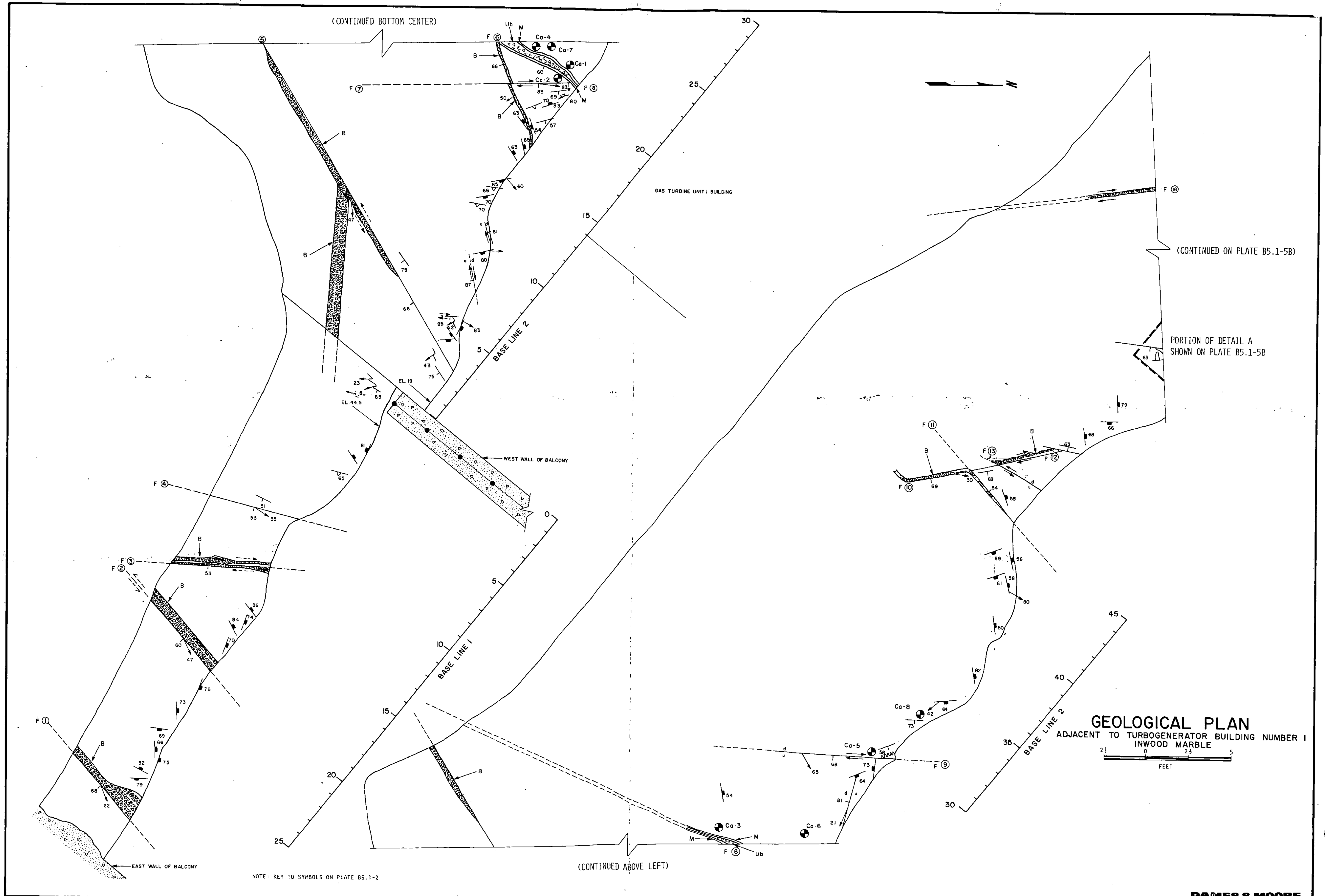

GEOLOGICAL PLAN

ADJACENT TO TURBOGENERATOR BUILDING NUMBER I
INWOOD MARBLE

DAMES & MOORE

PLATE B5.1-5A

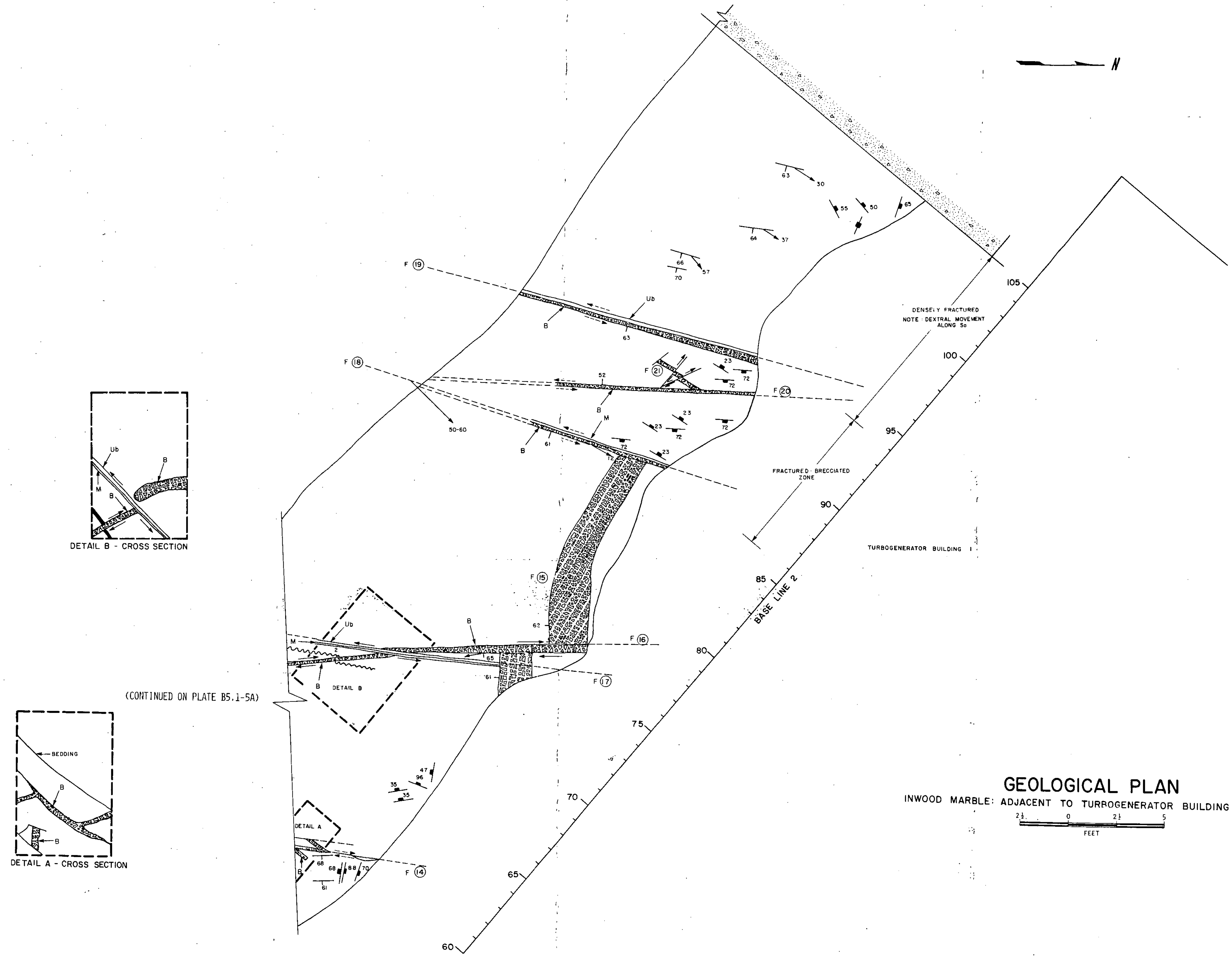

(CONTINUED ON PLATE B5.1-5A)

GEOLOGICAL PLAN

INWOOD MARBLE: ADJACENT TO TURROGENERATOR BUILDING NUMBER I

NOTE: KEY TO SYMBOLS ON PLATE B5.1-2

DAMES & MOORE

PLATE B5.1-5B

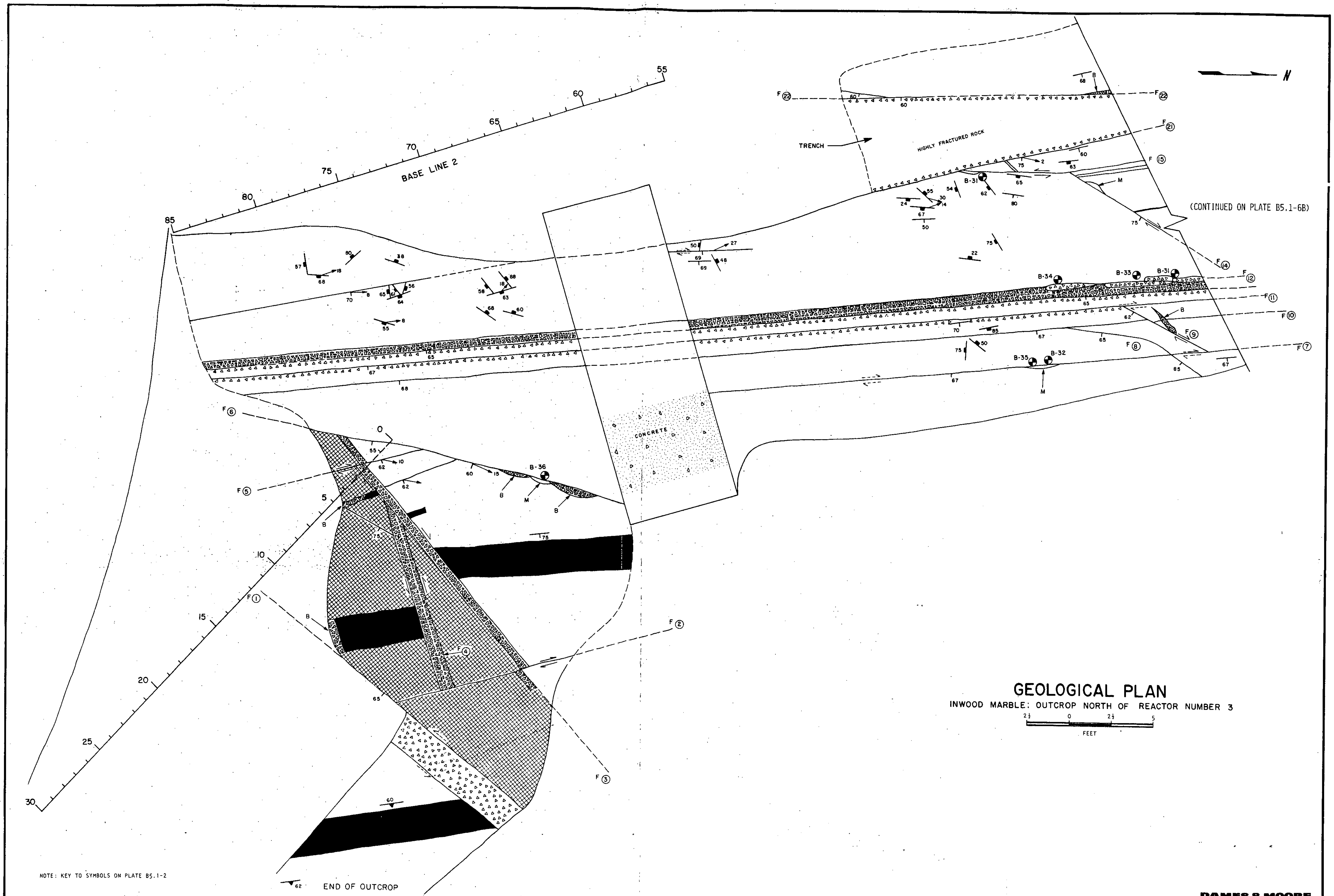

GEOLOGICAL PLAN

INWOOD MARBLE: OUTCROP NORTH OF REACTOR NUMBER 3

2½ 0 2½ 5 FEET

DAMES & MOORE

PLATE B5.1-6A

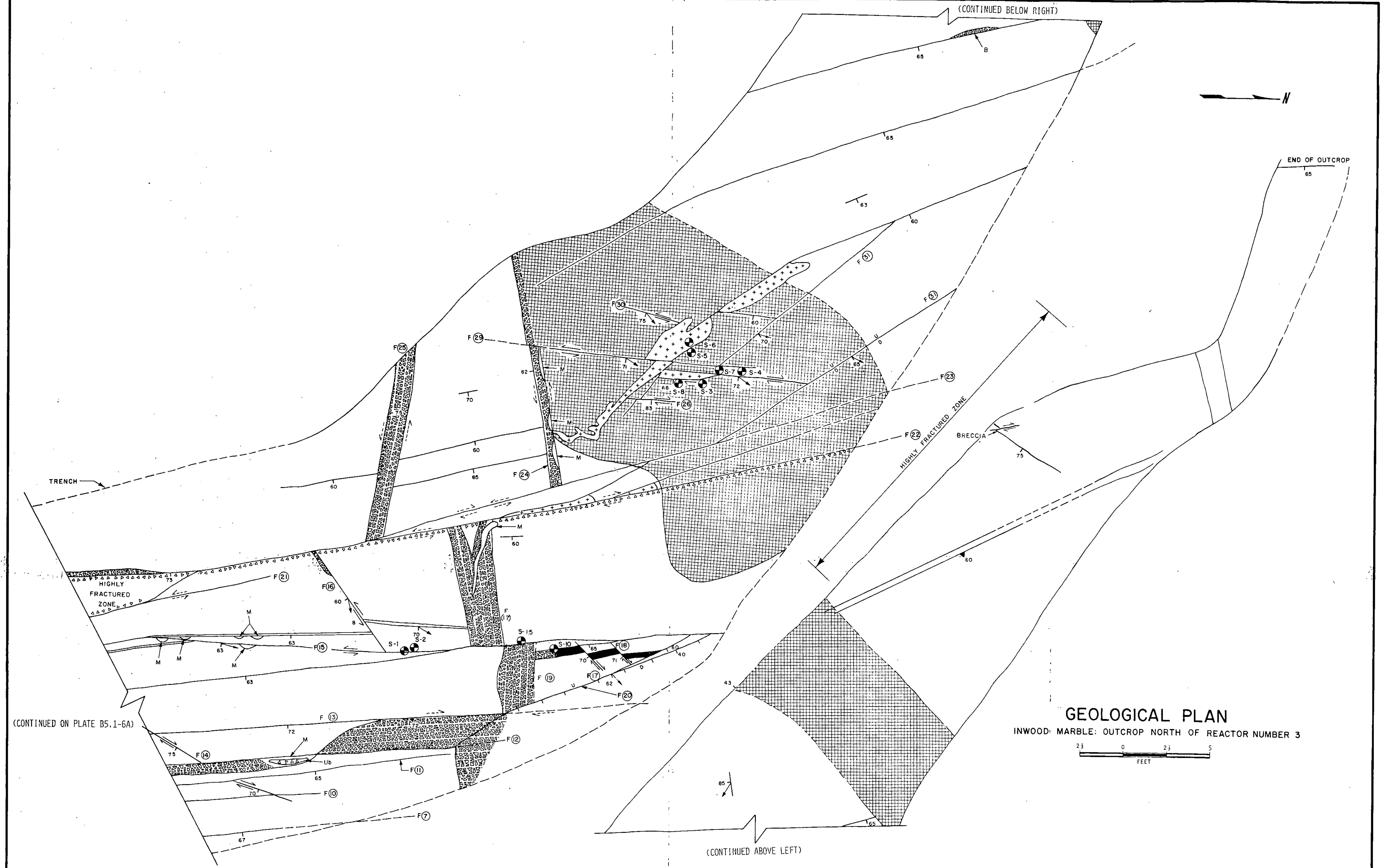

GEOLOGICAL PLAN

INWOOD MARBLE: OUTCROP NORTH OF REACTOR NUMBER 3

FEET

NOTE: KEY TO SYMBOLS ON PLATE B5.1-2

DAMES & MOORE

PLATE B5.1-6B

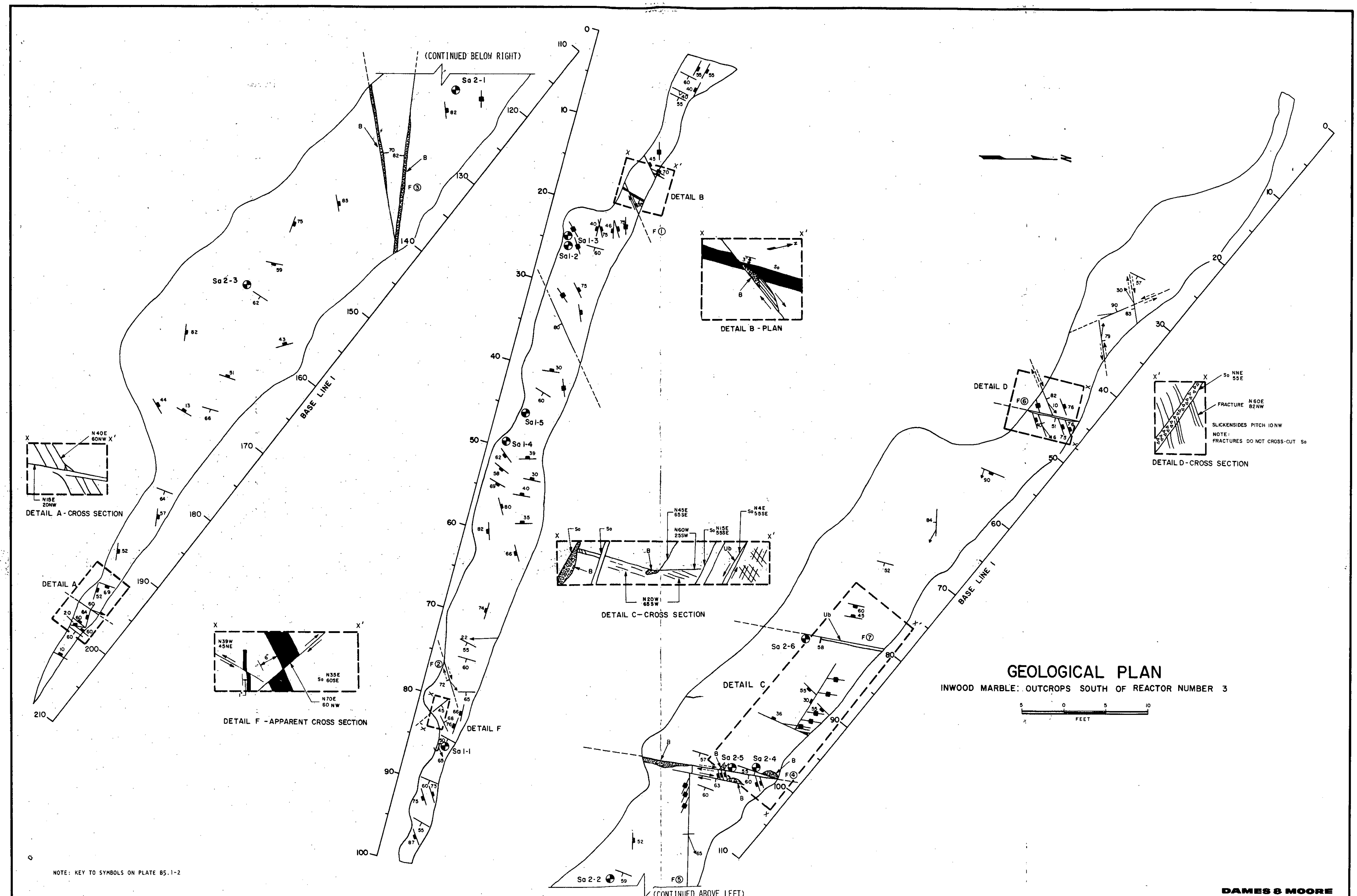

(CONTINUED BELOW RIGHT)
DETAIL A - CROSS SECTION
DETAIL B
DETAIL B - PLAN
DETAIL C
DETAIL C - CROSS SECTION
DETAIL D
DETAIL D - CROSS SECTION
DETAIL F
DETAIL F - APPARENT CROSS SECTION
BASE LINE I
FRACTURE N60E 82NW
SLICKENSIDES PITCH 10NW
NOTE: FRACTURES DO NOT CROSS-CUT So
(CONTINUED ABOVE LEFT)
NOTE: KEY TO SYMBOLS ON PLATE B5.1-2
GEOLOGICAL PLAN
INWOOD MARBLE: OUTCROPS SOUTH OF REACTOR NUMBER 3
FEET
DAMES & MOORE

PLATE B5.1-7

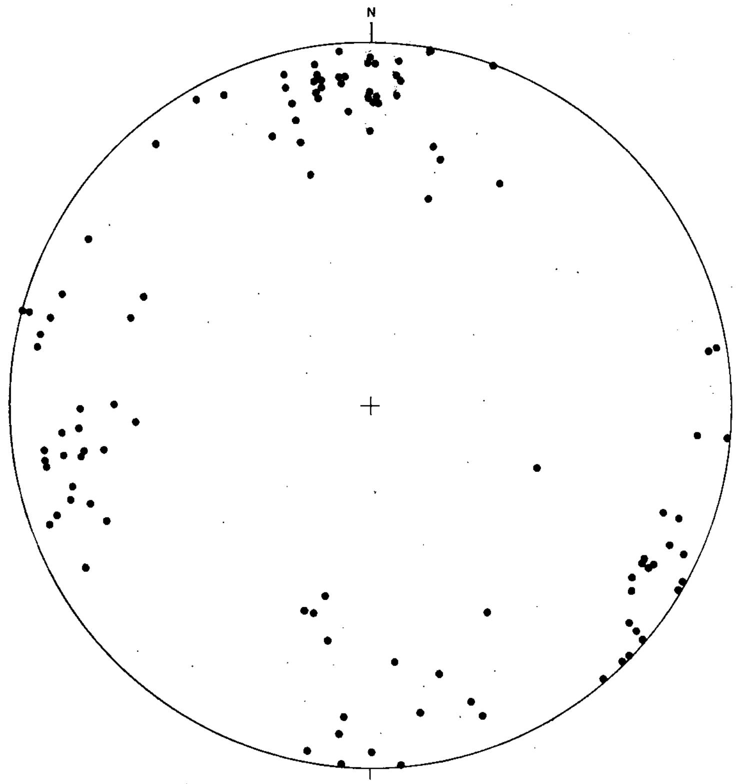

108 POLES TO FRACTURE PLANES

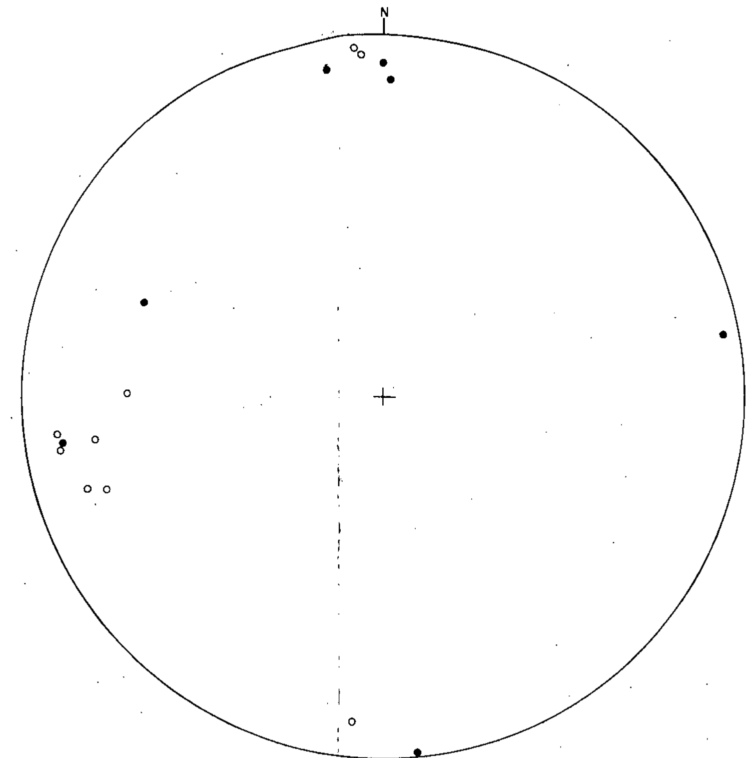

16 POLES TO SLICKENSIDED SURFACES

○ PITCH 0°-45°
● PITCH 45°-90°

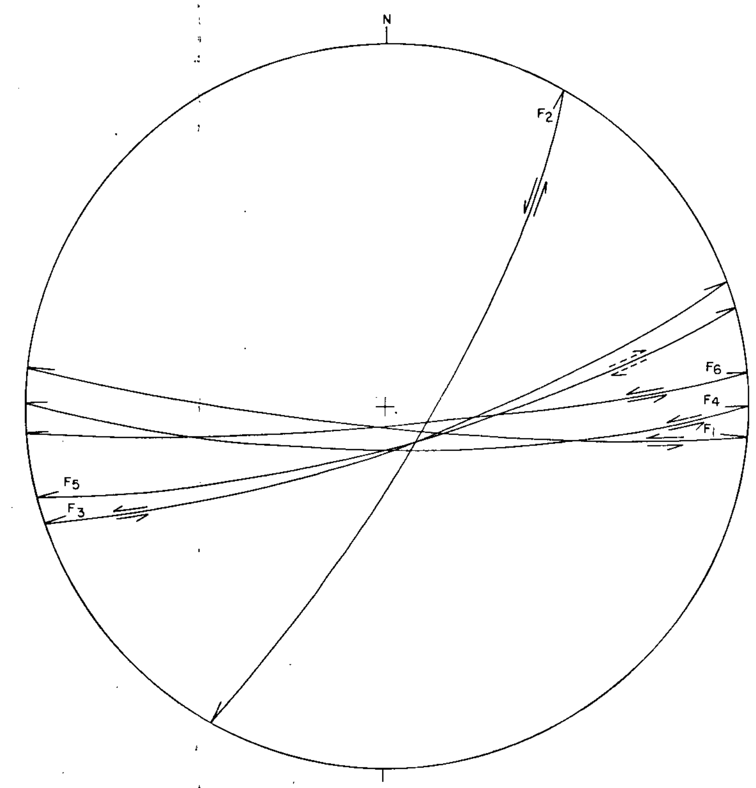

PLANES REPRESENTING OBSERVED FAULTS

⇄ SENSE OF MOVEMENT, DASHED WHERE INTERPRETED
F_4 INDICATES NUMBER OF FAULT REFERRED TO IN TEXT

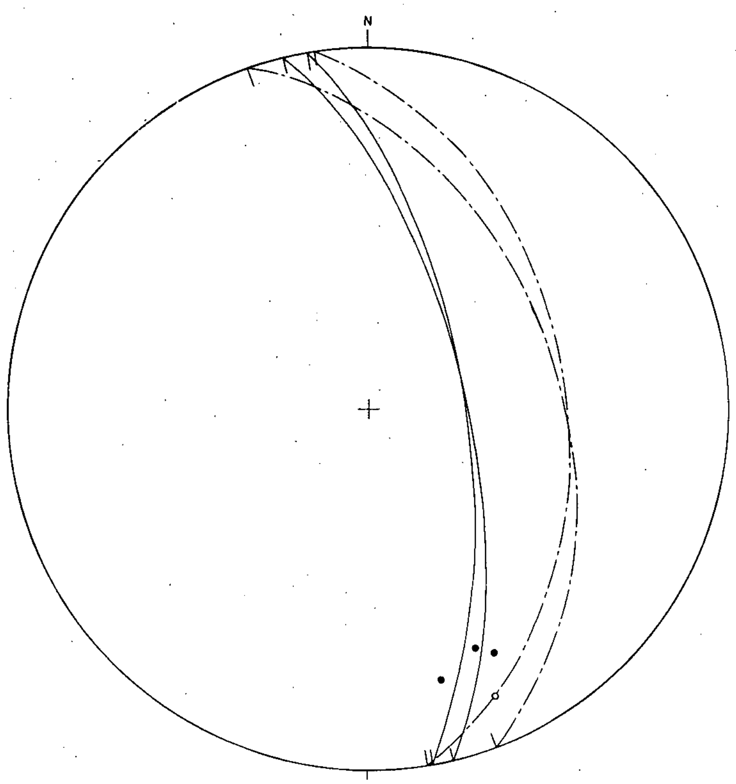

PLANES REPRESENTING AXIAL PLANES OF F_1 AND F_2 FOLDS

——— AXIAL PLANE OF F1 FOLDS
– – – AXIAL PLANE OF F2 FOLDS
● PLUNGE OF F1 FOLDS
○ PLUNGE OF F2 FOLDS

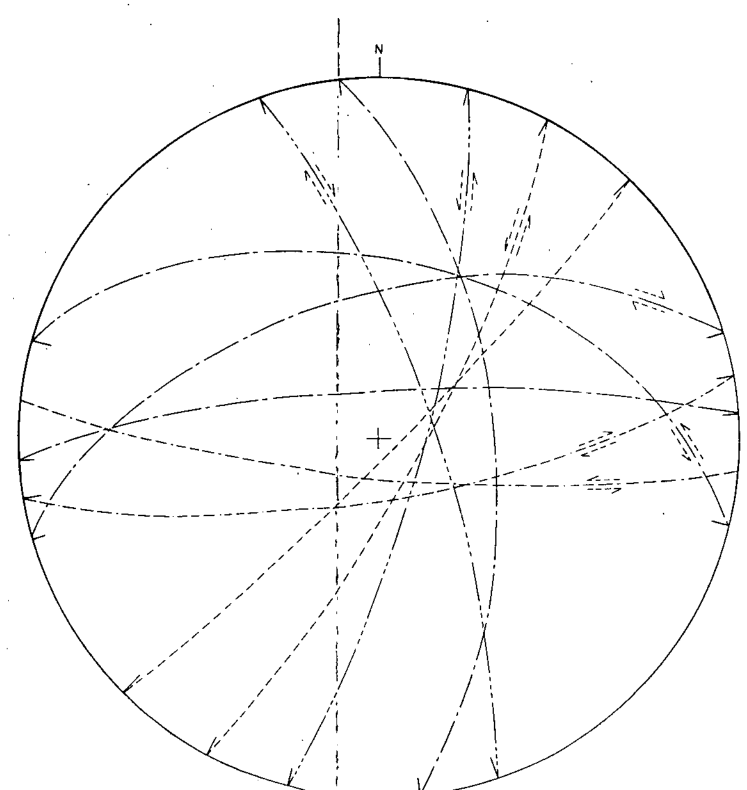

INTERPRETED FRACTURE AND FAULT GEOMETRY
INTERPRETED SENSES OF MOVEMENT SHOWN, RELATED PLANES DENOTED BY SAME SYMBOL

STRUCTURAL ELEMENTS

REPRESENTED ON LOWER HEMISPHERE EQUAL AREA PROJECTIONS
INWOOD MARBLE: OUTCROP NORTH OF REACTOR NUMBER 2

DAMES & MOORE

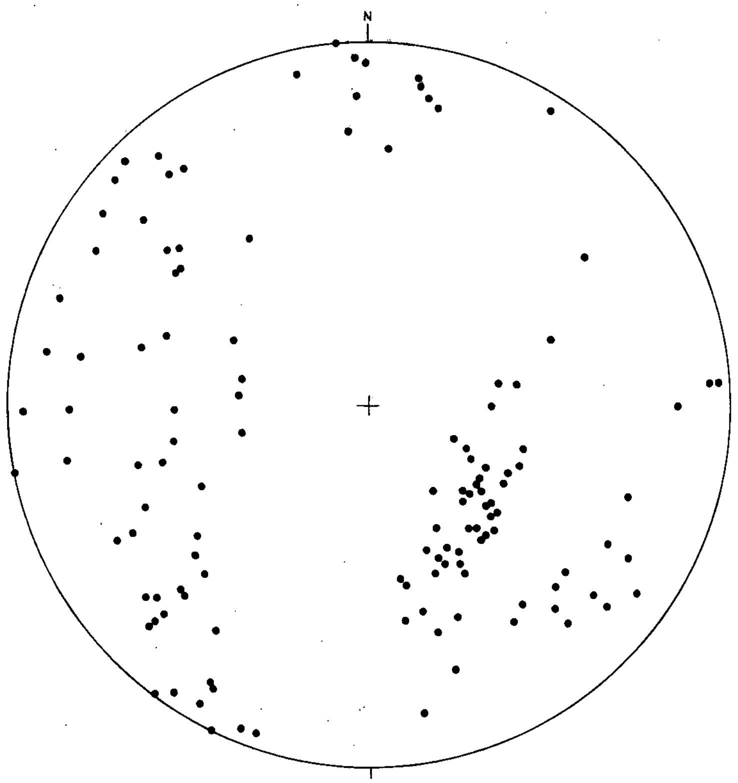

126 POLES TO FRACTURE PLANES

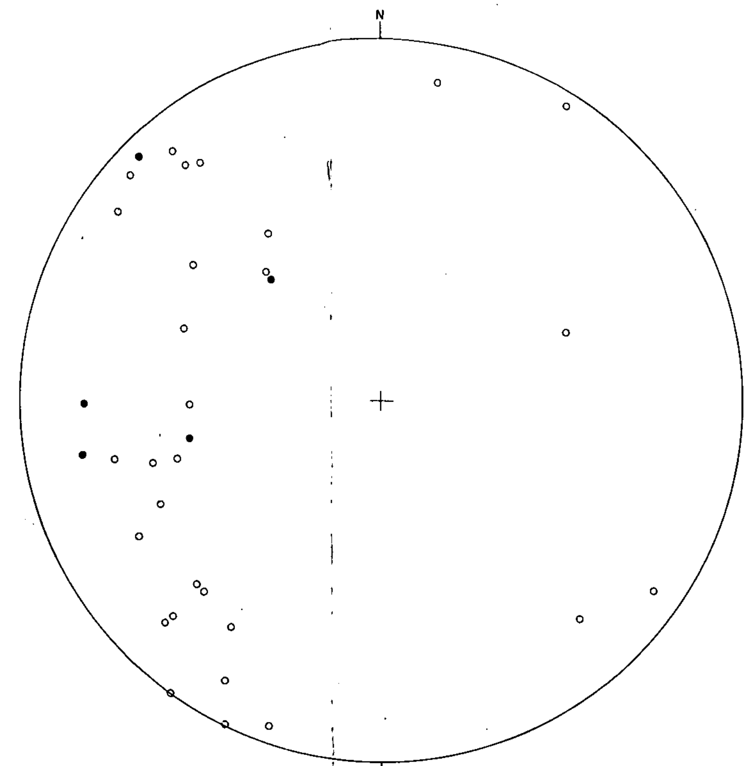

34 POLES TO SLICKENSIDED SURFACES

○ RAKE 0° - 45°
● RAKE 45° - 90°

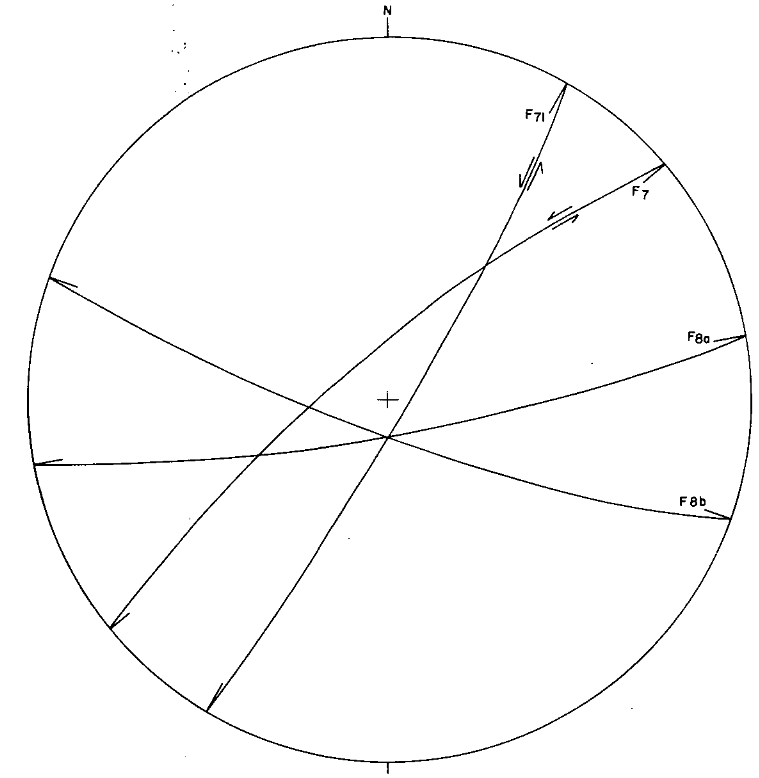

PLANES REPRESENTING OBSERVED FAULTS

⇌ SENSE OF MOVEMENT
F8a INDICATES NUMBER OF FAULT REFERRED TO IN THE TEXT

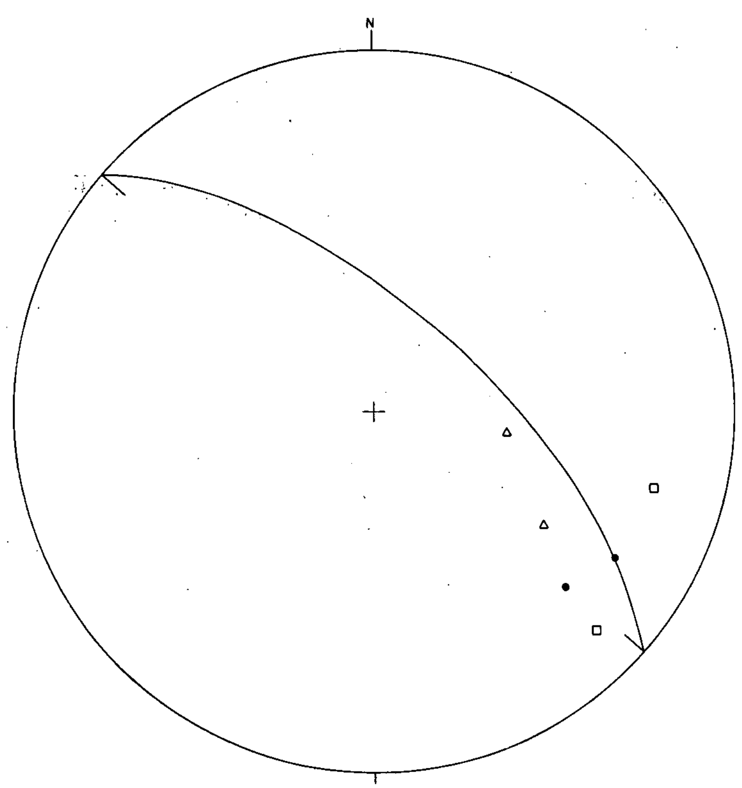

PLANE REPRESENTING S_0/S_1 SURFACES

● PLUNGE OF F2 FOLD AXES
△ L1-LINEATION ASSOCIATED WITH F1 FOLDING
□ L2-LINEATION ASSOCIATED WITH F2 FOLDING

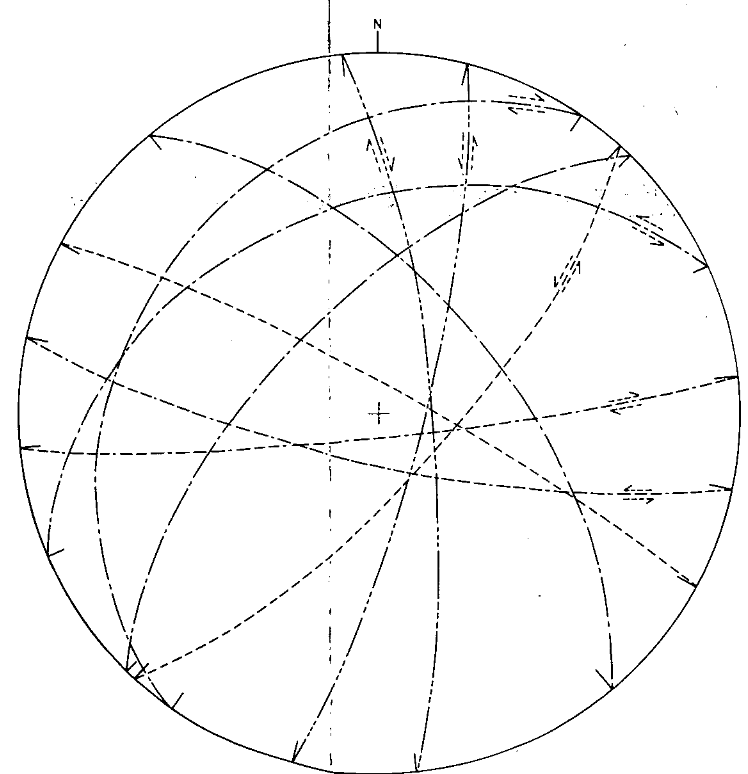

INTERPRETED FRACTURE AND FAULT GEOMETRY
INTERPRETED SENSES OF MOVEMENT SHOWN. RELATED PLANES DENOTED BY SAME SYMBOL

STRUCTURAL ELEMENTS
REPRESENTED ON LOWER HEMISPHERE EQUAL AREA PROJECTIONS
MANHATTAN SCHIST: OUTCROP NORTH OF REACTOR NUMBER 2

DAMES & MOORE

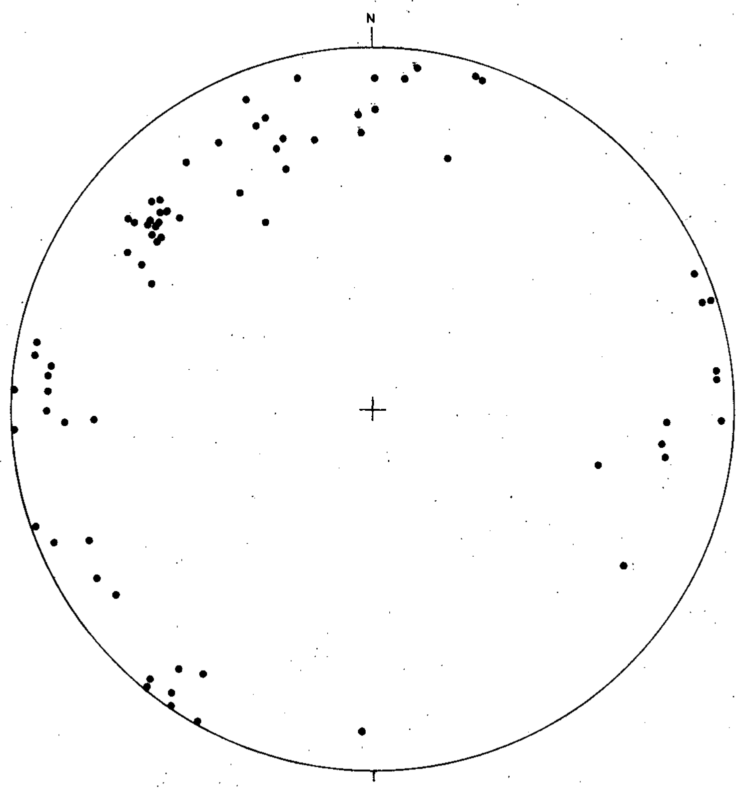

72 POLES TO FRACTURE PLANES

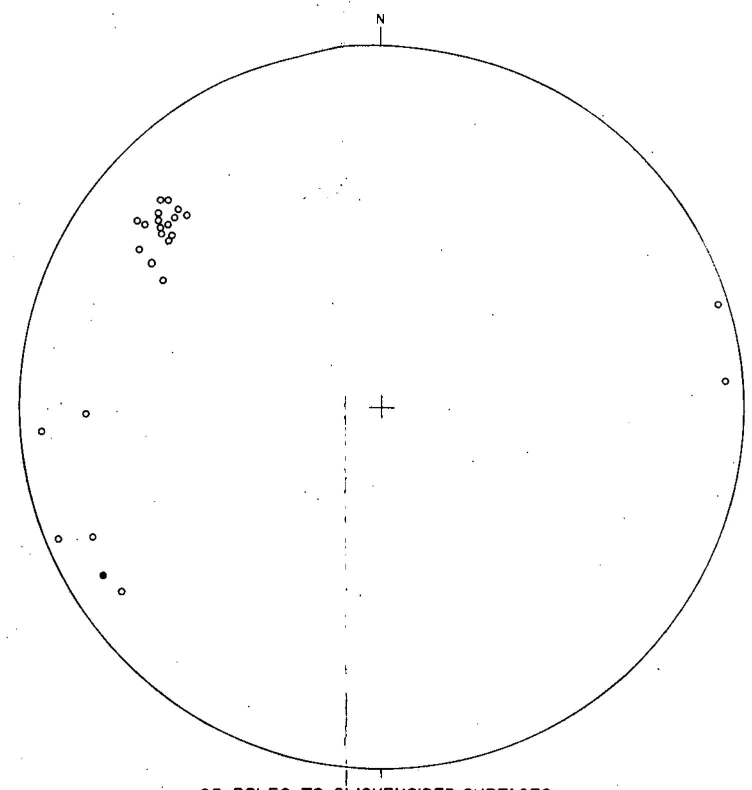

25 POLES TO SLICKENSIDED SURFACES

○ RAKE 0°-45°
● RAKE 45°-90°

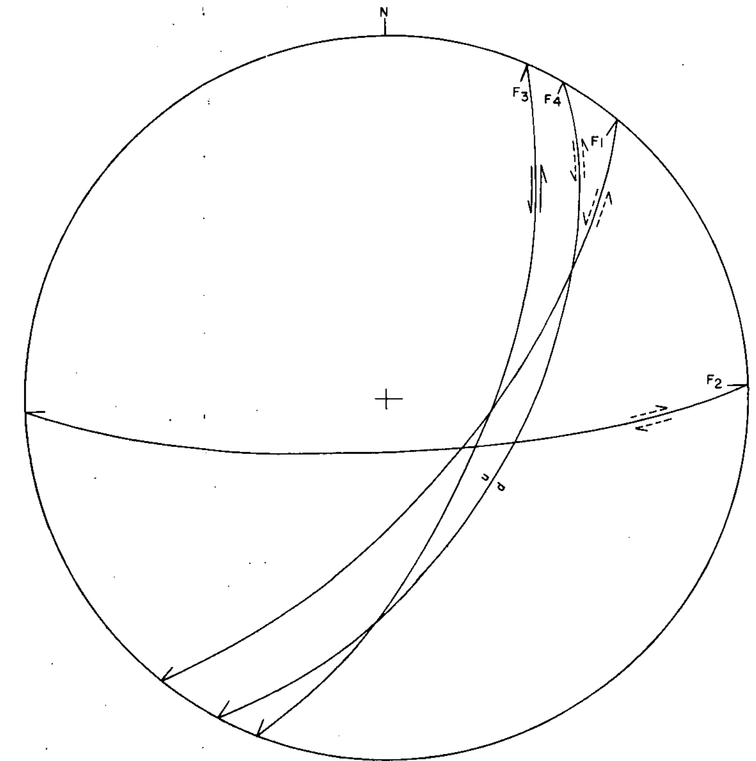

PLANES REPRESENTING OBSERVED FAULTS

SENSE OF MOVEMENT: DASHED WHERE INTERPRETED
TWO SENSES OF MOVEMENT SHOWN WHERE OBSERVED OR INTERPRETED
F_2 INDICATES NUMBER OF FAULT REFERRED TO IN THE TEXT

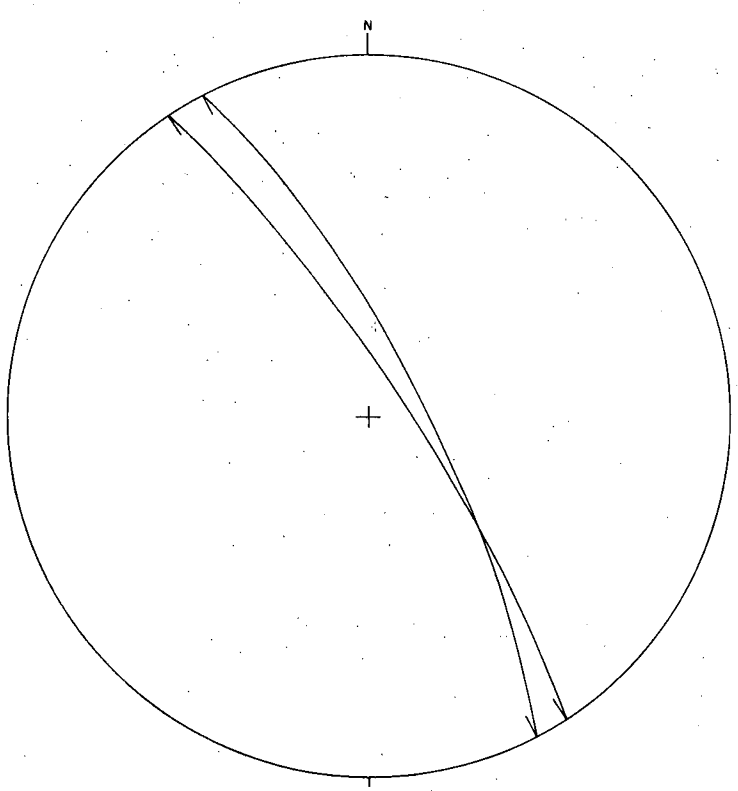

PLANES REPRESENTING So/S1 SURFACES

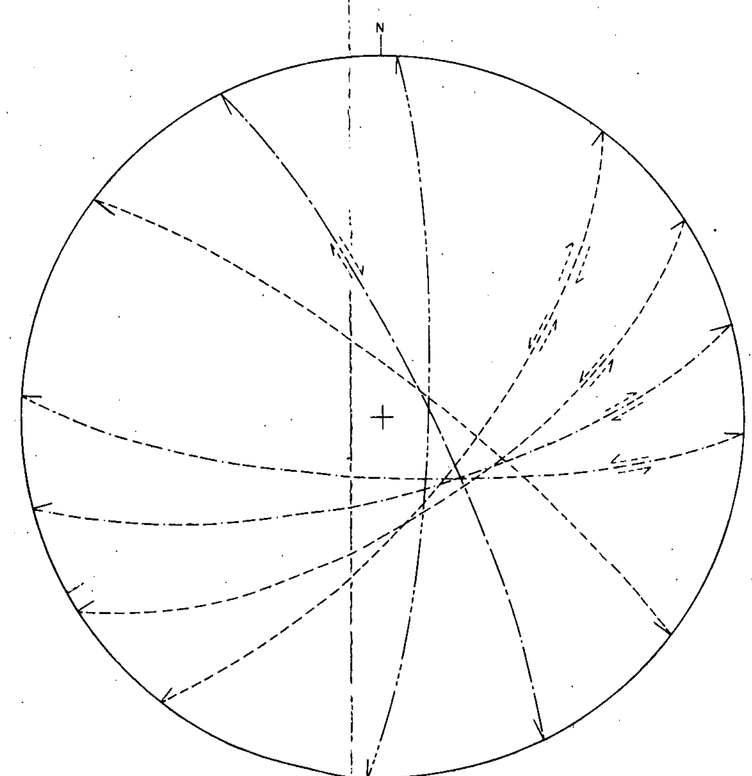

INTERPRETED FRACTURE AND FAULT GEOMETRY
INTERPRETED SENSES OF MOVEMENT SHOWN, RELATED PLANES DENOTED BY SAME SYMBOL

STRUCTURAL ELEMENTS

REPRESENTED ON LOWER HEMISPHERE EQUAL AREA PROJECTIONS
INWOOD MARBLE: TRENCH NORTHWEST OF REACTOR NUMBER 3

DAMES & MOORE

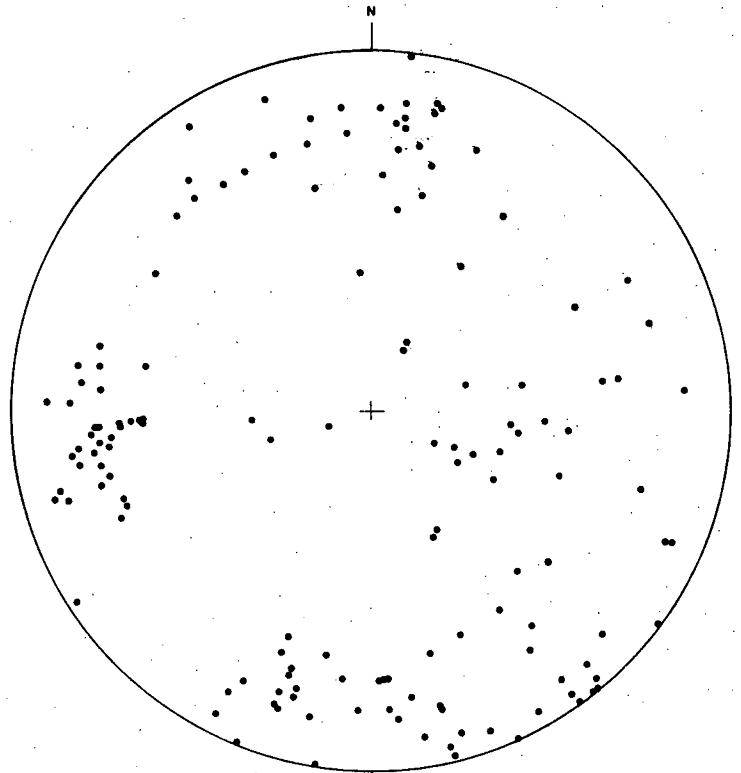

145 POLES TO FRACTURE PLANES

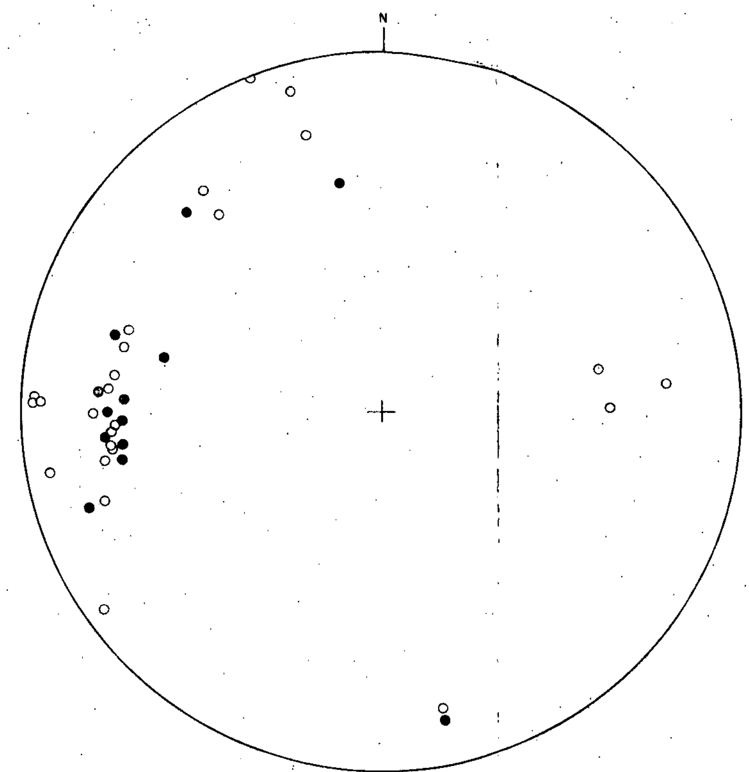

38 POLES TO SLICKENSIDED SURFACES

KEY:
○ RAKE 0-45°
● RAKE 45°-90°

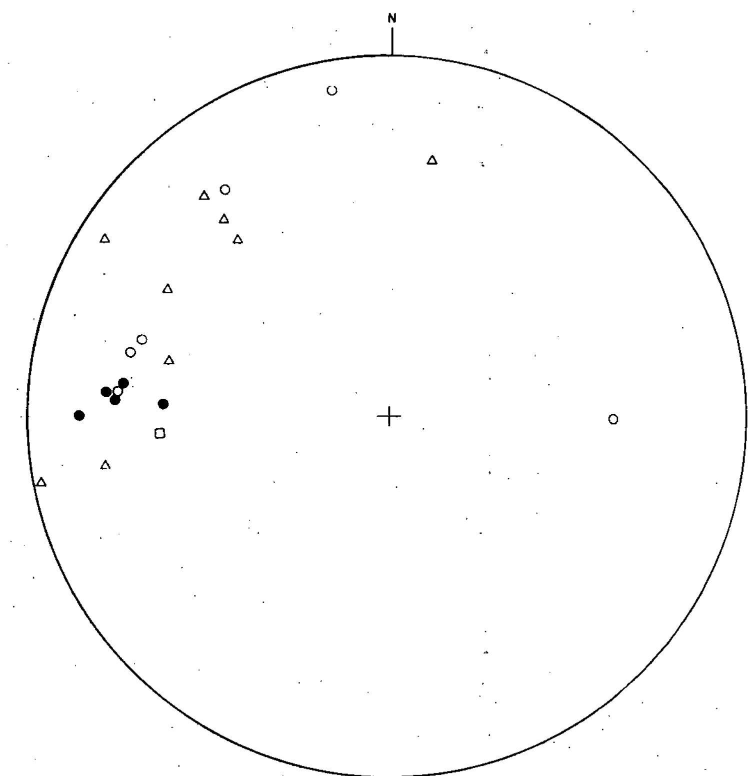

21 POLES TO OBSERVED FAULT PLANES

KEY:
● DEXTRAL
○ SINISTRAL
□ NORMAL
△ UNDEFINED

STRUCTURAL ELEMENTS

REPRESENTED ON LOWER HEMISPHERE EQUAL AREA PROJECTIONS

INWOOD MARBLE: OUTCROP ADJACENT TO TURBOGENERATOR BUILDING NUMBER 1

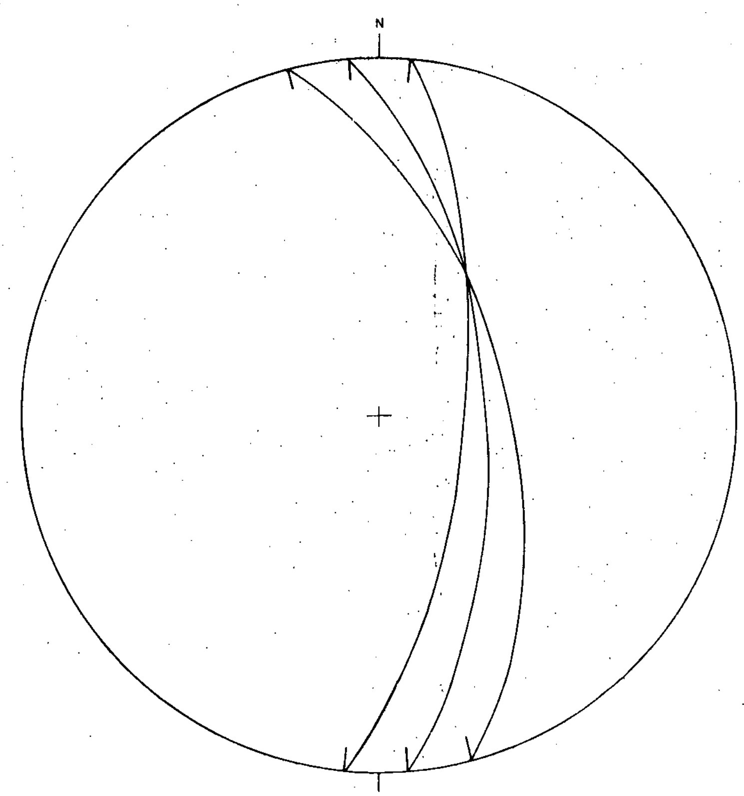

PLANES REPRESENTING S_0/S_1 SURFACE

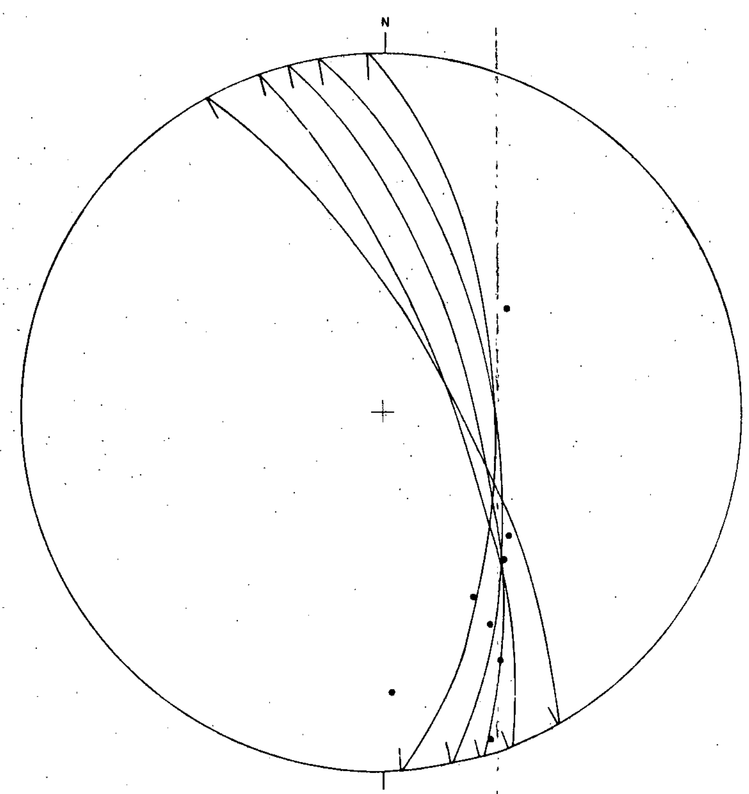

F2 FOLDS

KEY:
/ AXIAL PLANE OF F2 FOLD
• PLUNGE OF AXIS OF F2 FOLD

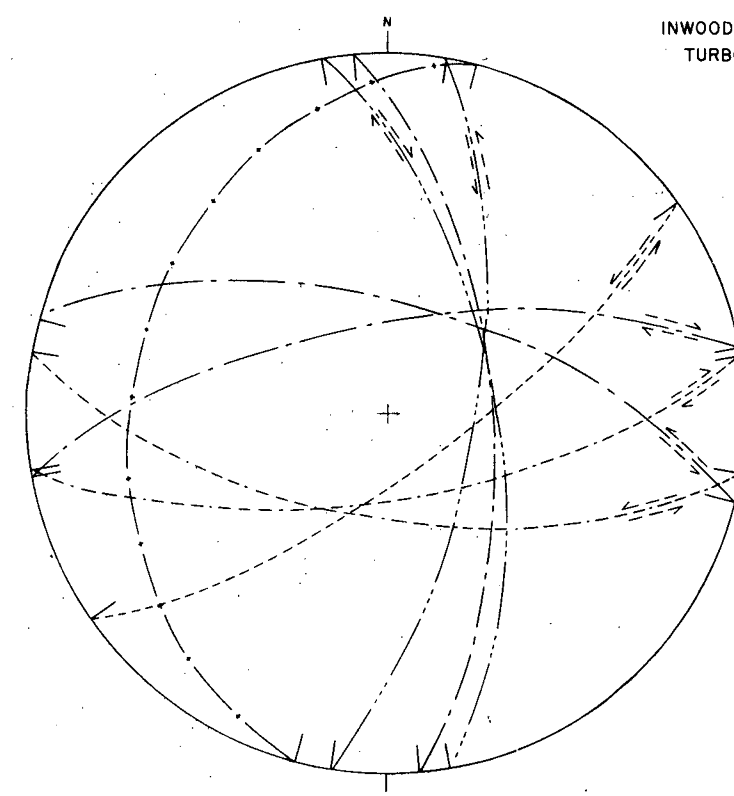

INTERPRETED FAULT AND FRACTURE GEOMETRY

INTERPRETED SENSES OF MOVEMENT SHOWN
RELATED PLANES DENOTED BY SAME SYMBOL

DAMES & MOORE

PLATE B5.1-10

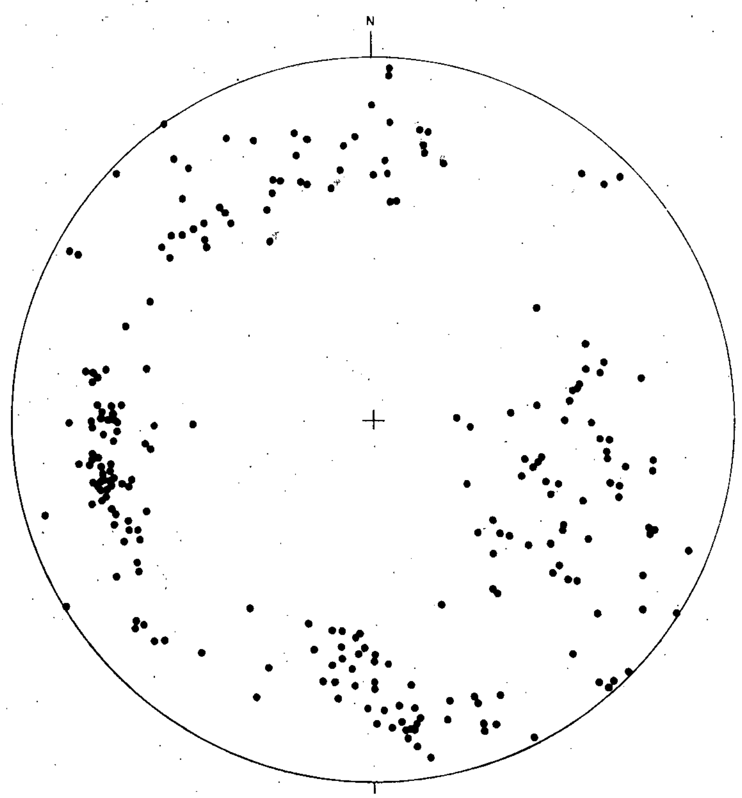

235 POLES TO FRACTURE PLANES

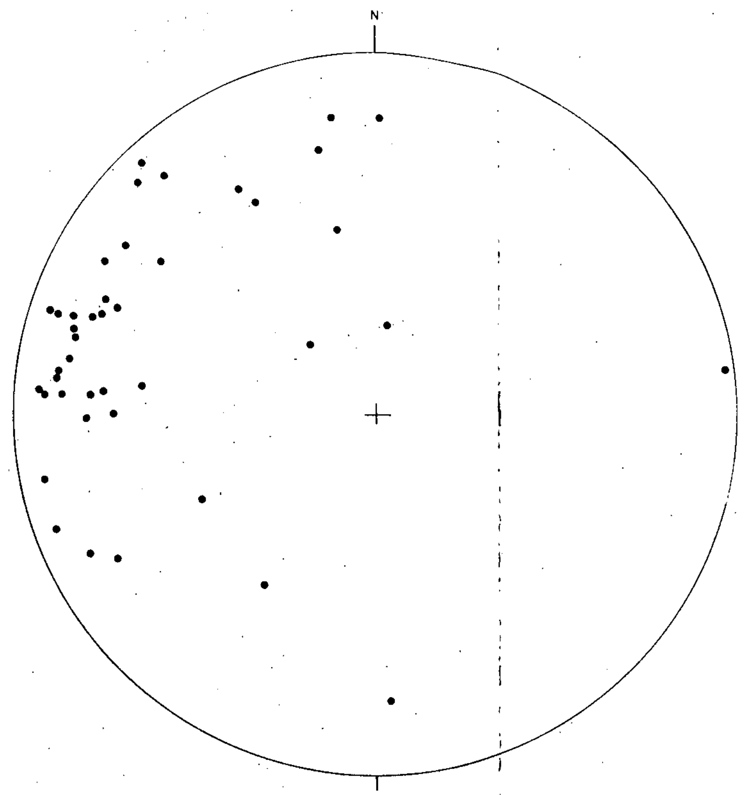

40 POLES TO SLICKENSIDED SURFACES

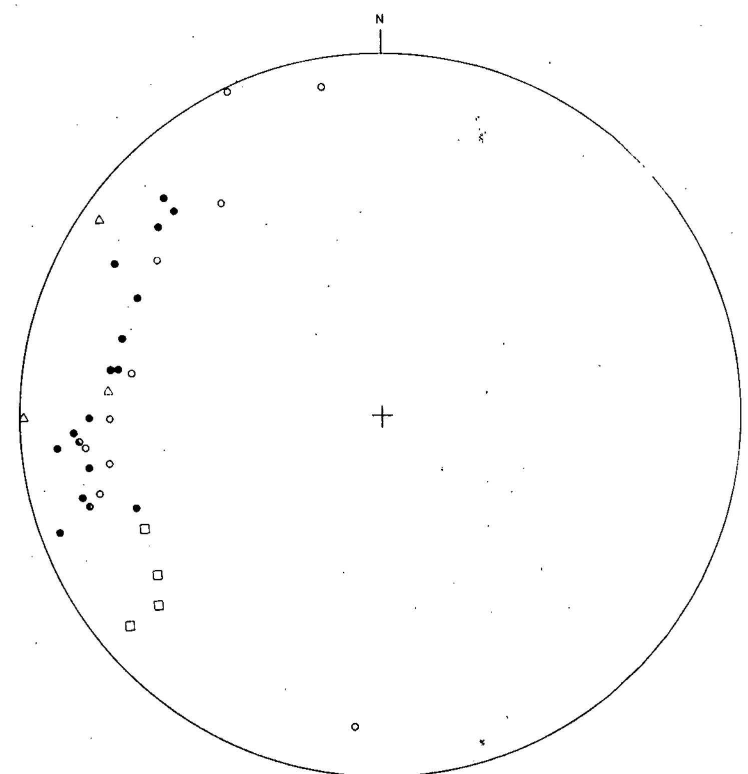

34 POLES TO OBSERVED FAULT PLANES

- ● DEXTRAL
- ○ SINISTRAL
- □ NORMAL
- △ UNDEFINED

STRUCTURAL ELEMENTS

REPRESENTED ON LOWER HEMISPHERE EQUAL AREA PROJECTIONS
INWOOD MARBLE : OUTCROP NORTH OF
REACTOR NUMBER 3

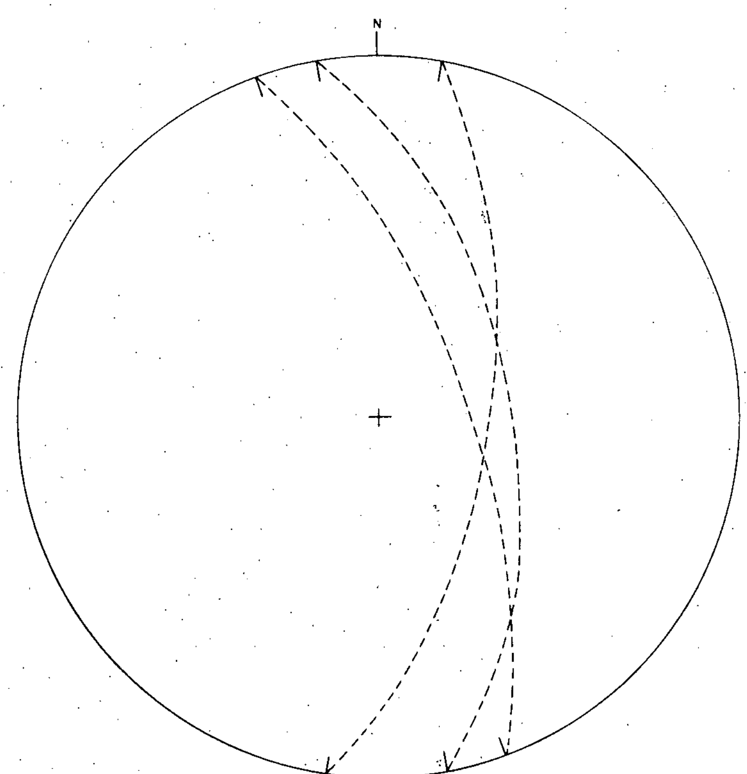

PLANES REPRESENTING S_0/S_1 SURFACES

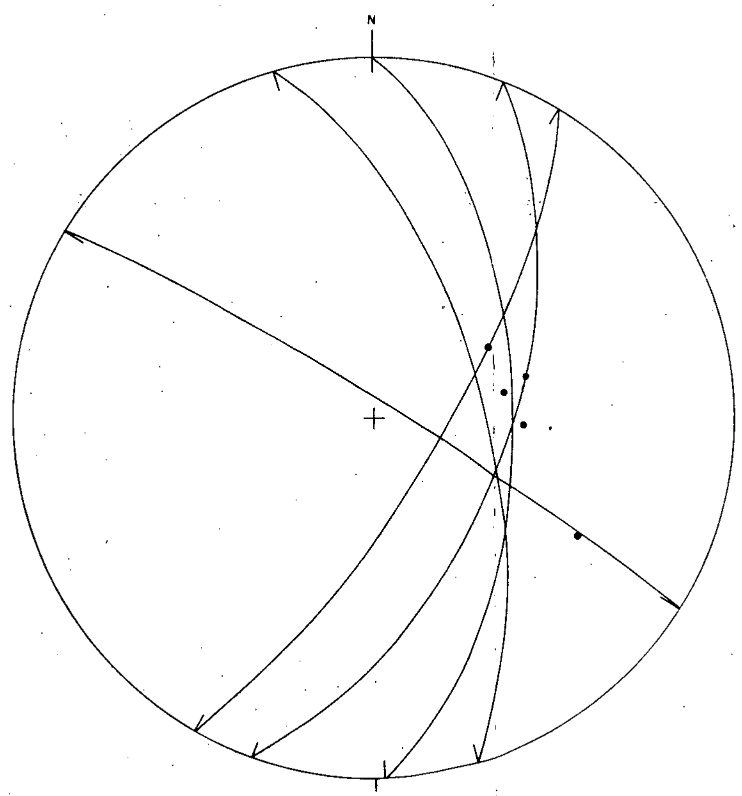

F_2 FOLDS

— AXIAL PLANE OF F2 FOLD
● PLUNGE OF AXIS OF F2 FOLD

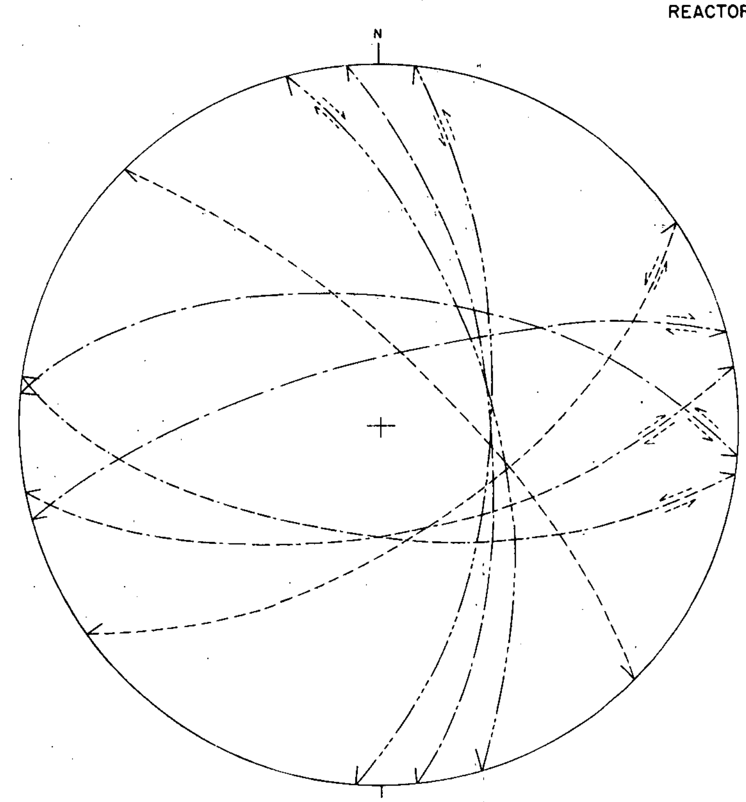

INTERPRETED FRACTURE AND FAULT GEOMETRY
INTERPRETED SENSES OF MOVEMENT SHOWN. RELATED PLANES DENOTED BY SAME SYMBOL

DAMES & MOORE

PLATE B5.1-11

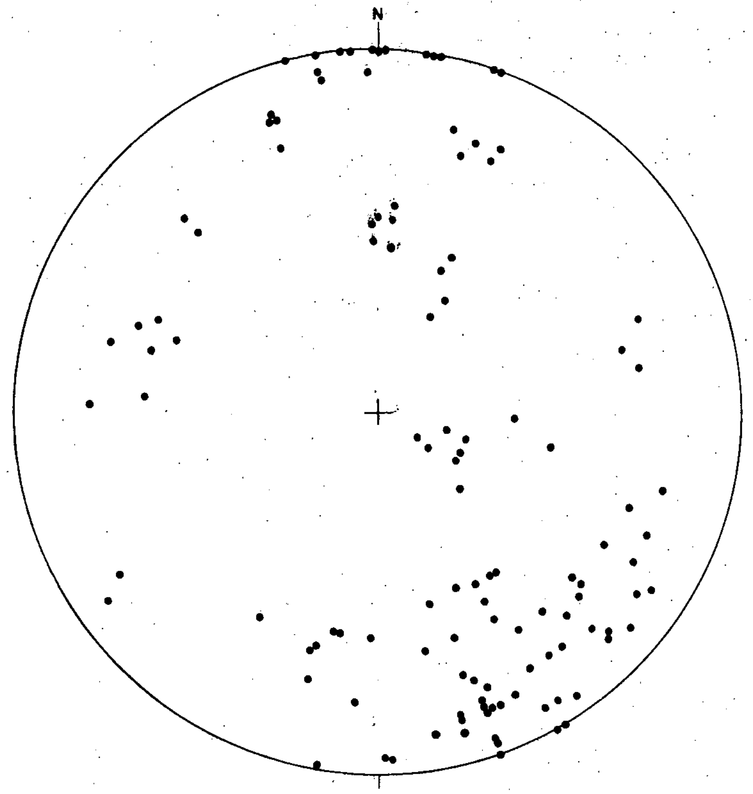

120 POLES TO FRACTURE PLANES

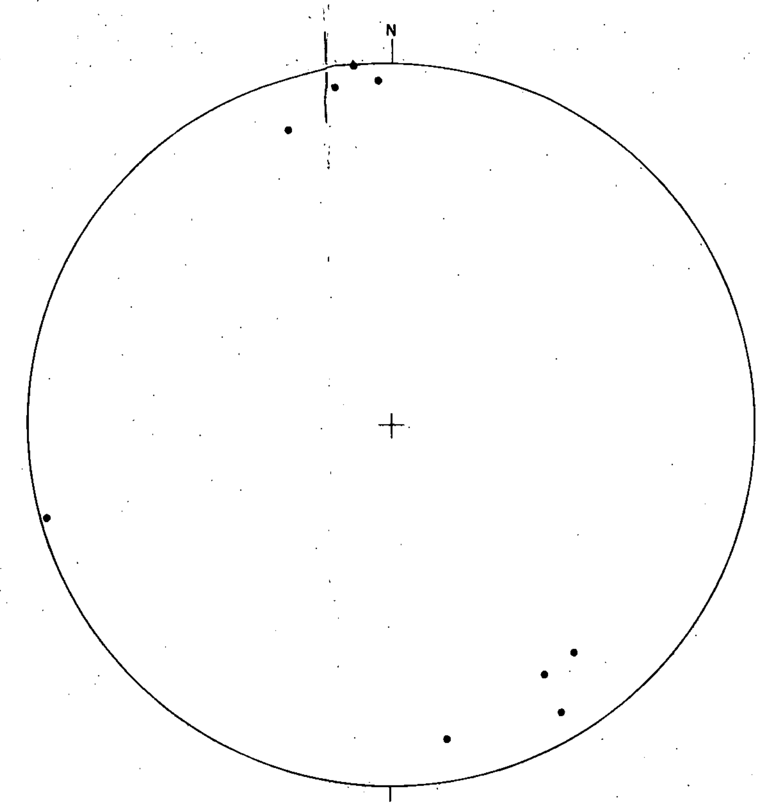

9 POLES TO SLICKENSIDED SURFACES

● RAKE 45°-90°

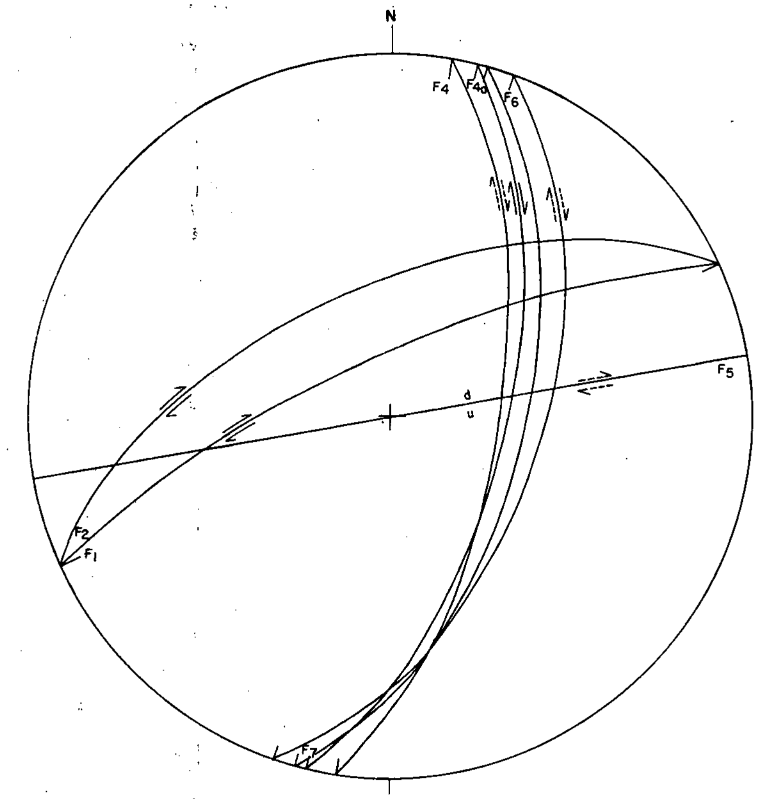

PLANES REPRESENTING OBSERVED FAULTS

SENSE OF MOVEMENT. DASHED WHERE INTERPRETED

d / u — TWO SENSES OF MOVEMENT SHOWN WHERE OBSERVED OR INTERPRETED

F_2 INDICATES NUMBER OF FAULT REFERRED TO IN THE TEXT

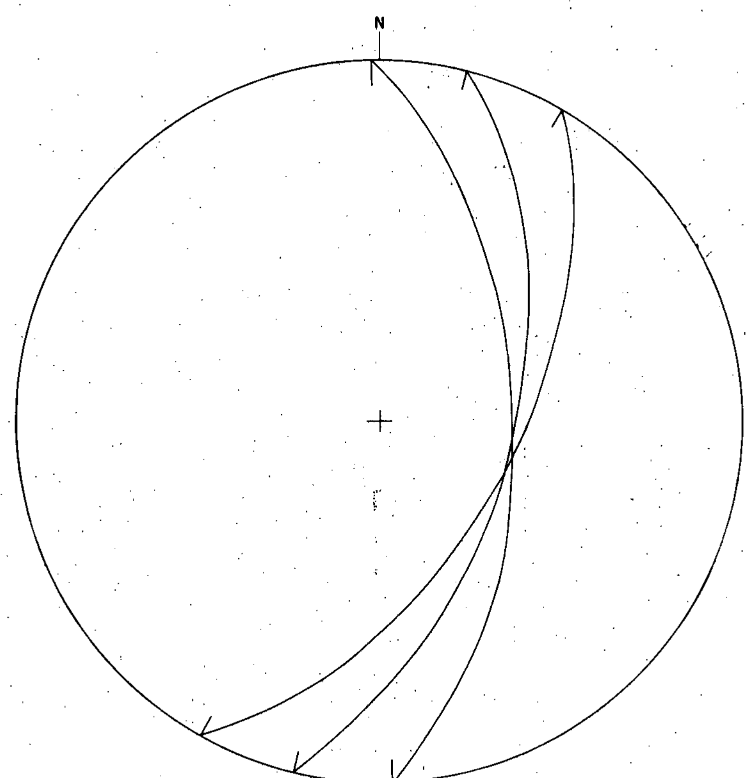

PLANES REPRESENTING So/Si SURFACES

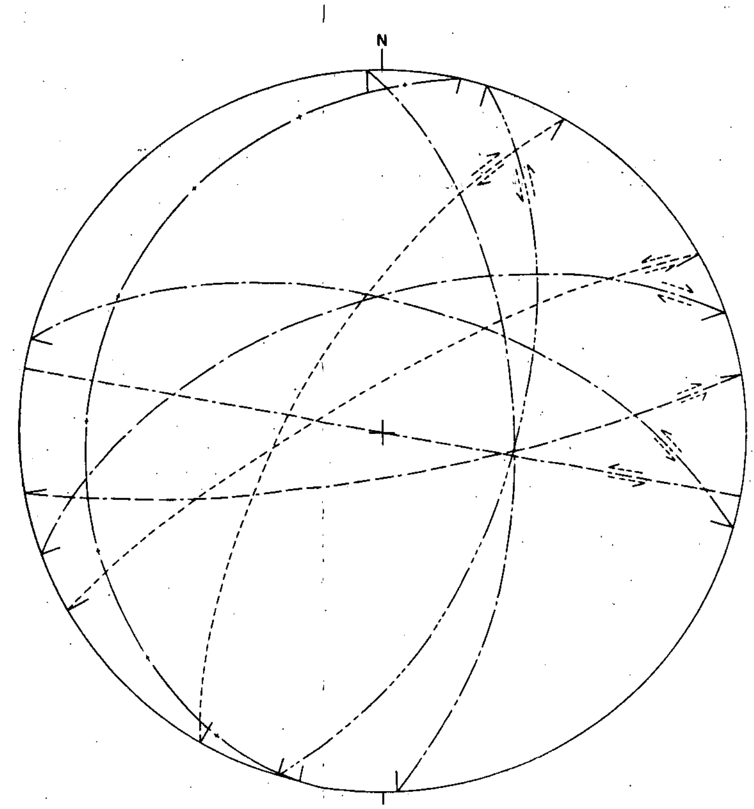

INTERPRETED FRACTURE AND FAULT GEOMETRY

INTERPRETED SENSES OF MOVEMENT SHOWN, RELATED PLANES DENOTED BY SAME SYMBOL

STRUCTURAL ELEMENTS

REPRESENTED ON LOWER HEMISPHERE EQUAL AREA PROJECTIONS
INWOOD MARBLE: OUTCROPS SOUTH OF REACTOR NUMBER 3

DAMES & MOORE

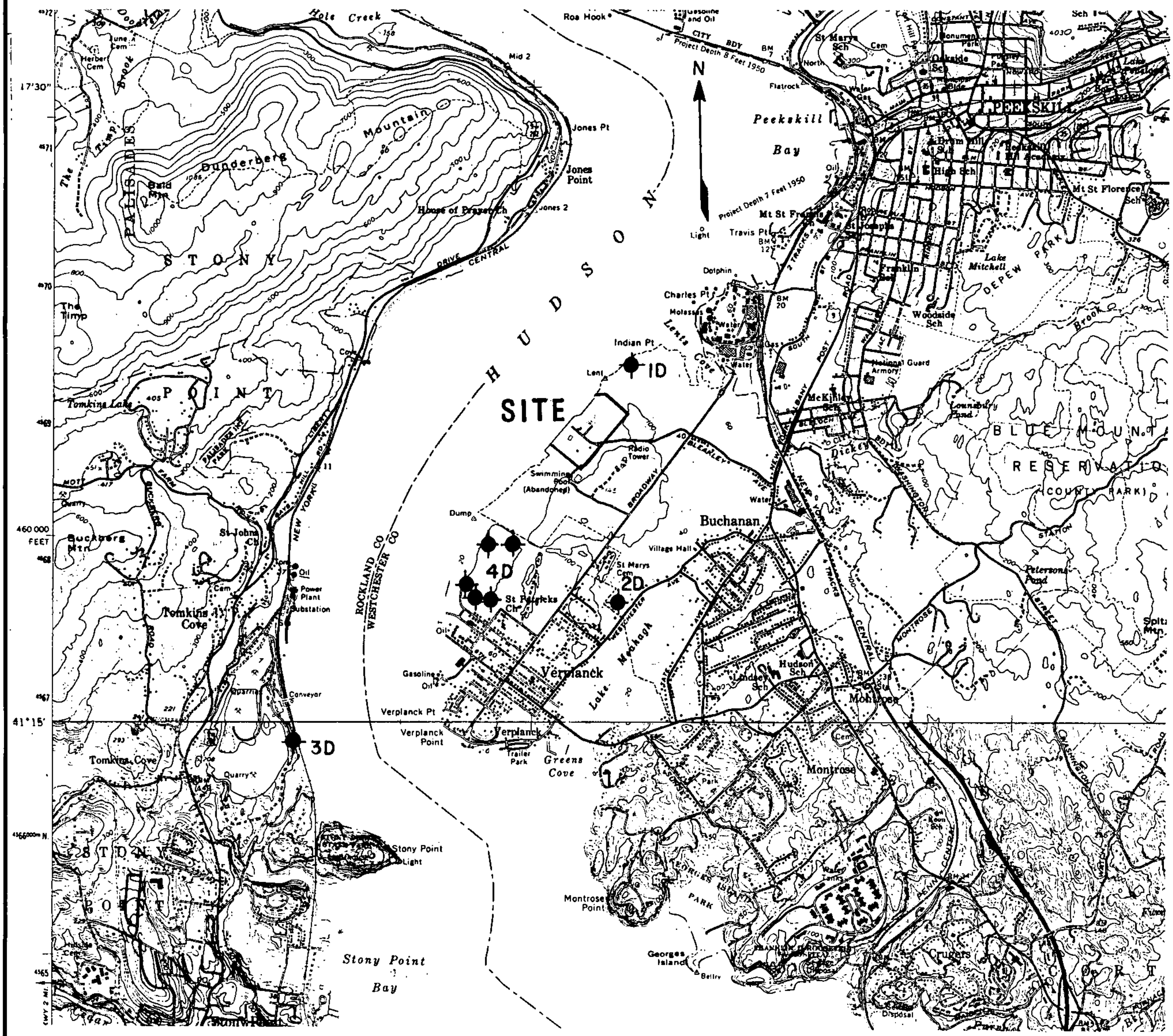

LOCATION MAP FOR FOLD STUDY

KEY:

◆ LOCATION OF STATION WHERE FOLDS WERE STUDIED

Reference: The base for this map was produced from the following U.S.G.S. Topographic Maps Peekskill, N.Y., 1957; Haverstraw, N.Y., 1967.

DAMES & MOORE

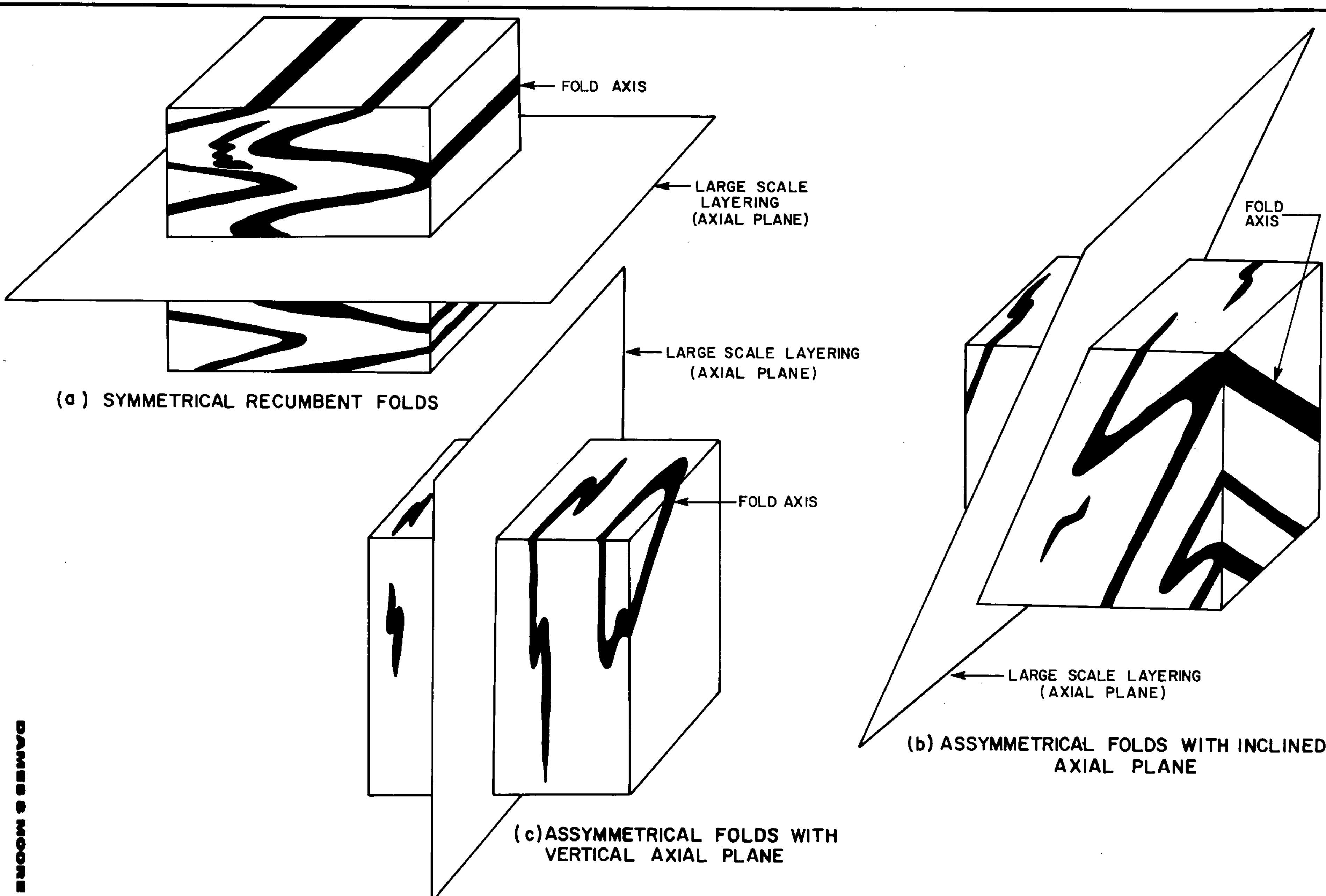

SCHEMATIC BLOCK DIAGRAMS OF F1-FOLDING

DAMES & MOORE

PLATE B5.2-2

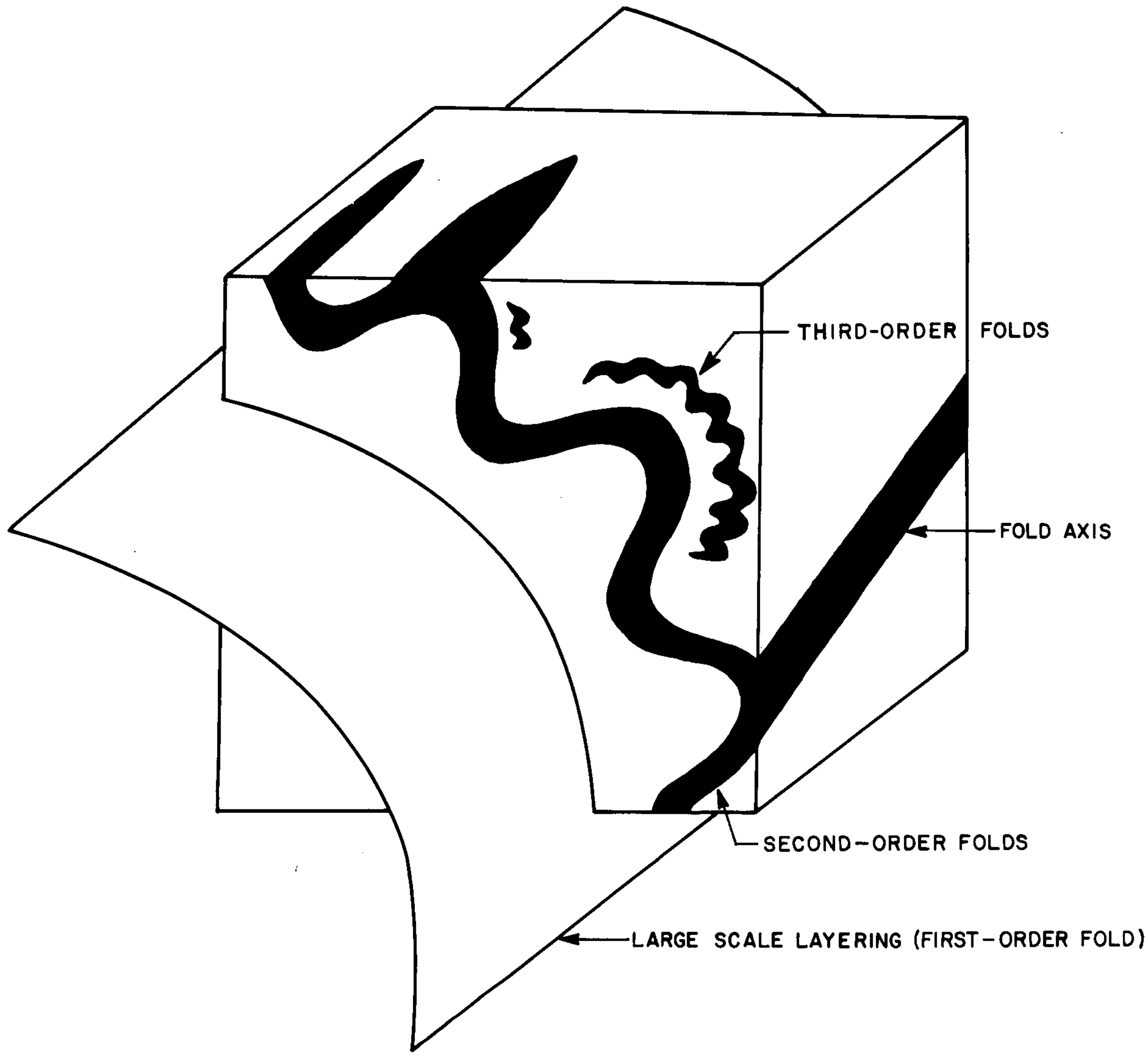

SCHEMATIC BLOCK DIAGRAM SHOWING THREE ORDERS OF F_2-FOLDS

DAMES & MOORE

PLATE B5.2-3

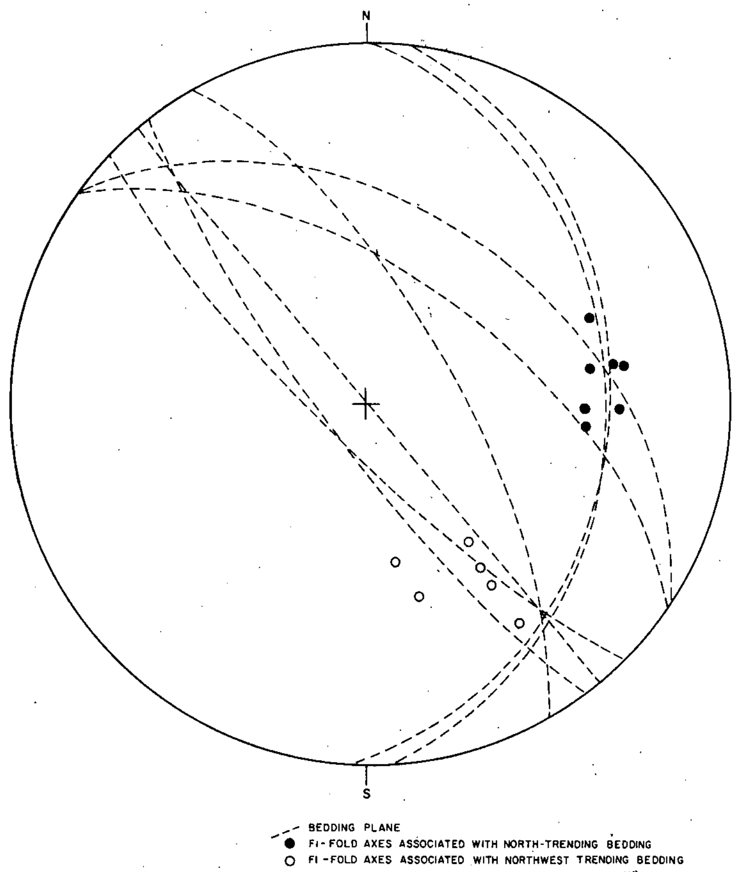

STATION 1D
F1-FOLD AXES

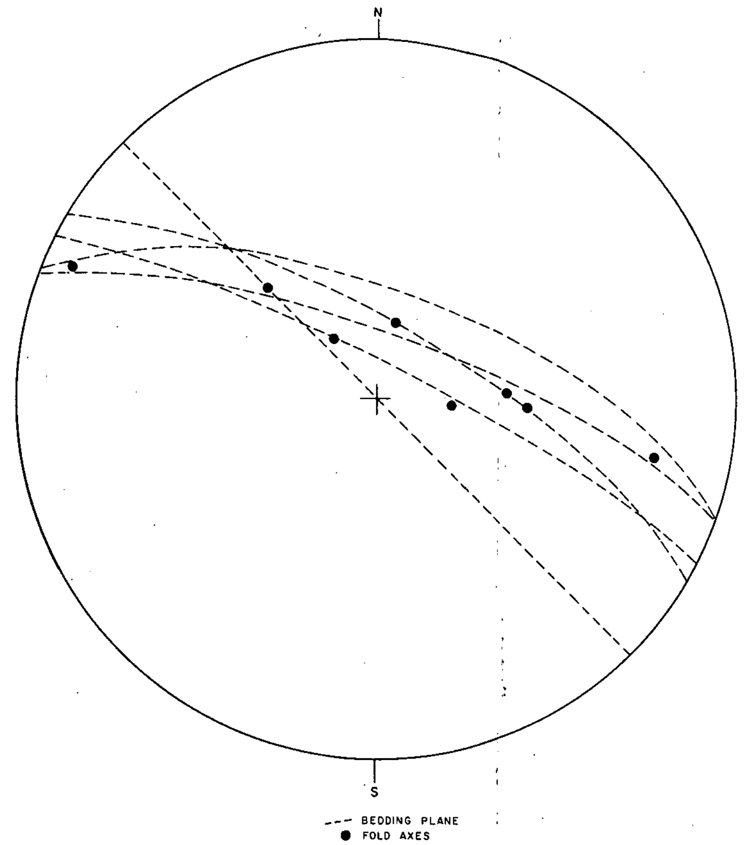

STATION 2D
F1-FOLD AXES

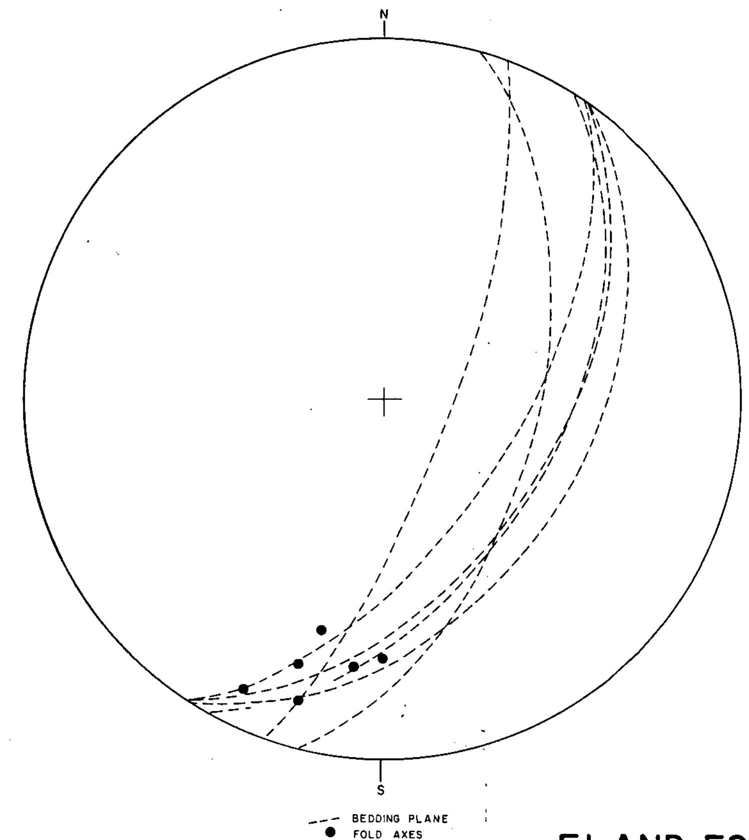

STATION 3D
F1-FOLD AXES

F1 AND F2 FOLD AXES AND BEDDING PLANES REPRESENTED ON LOWER HEMISPHERE EQUAL AREA PROJECTIONS

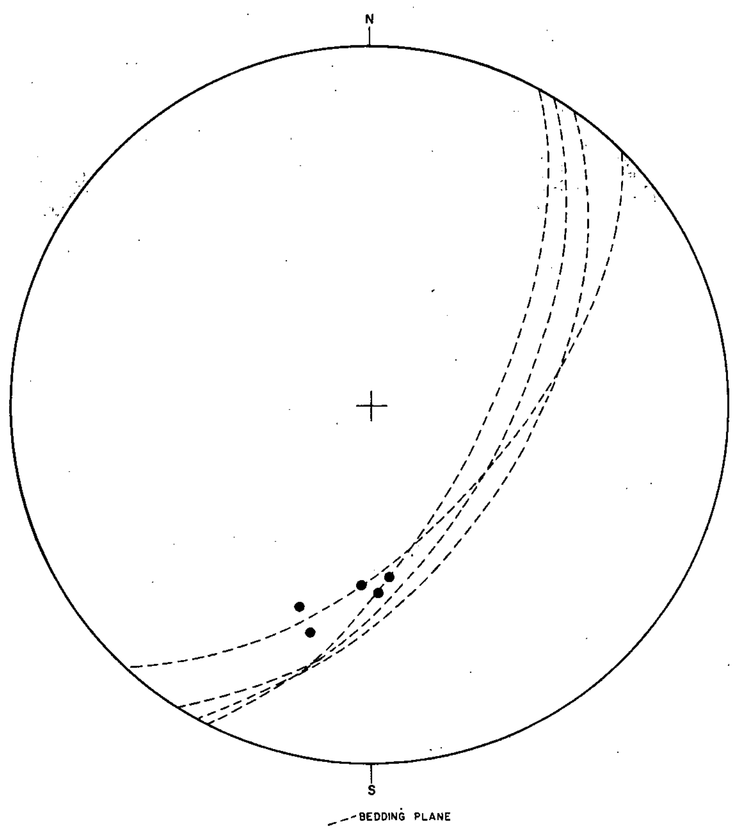

STATION 4D
F1-FOLD AXES

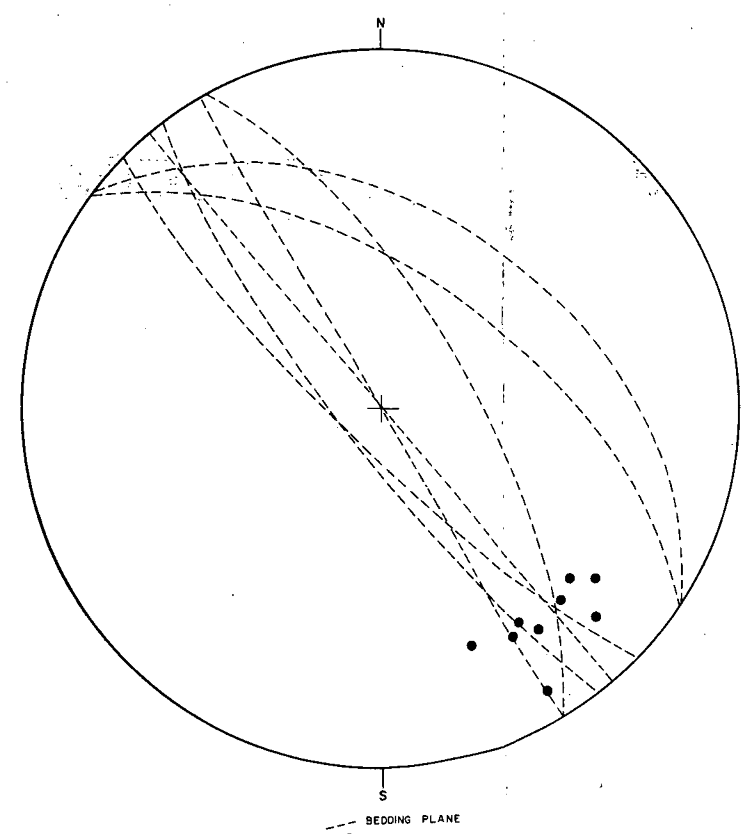

STATION 1D
F-2 FOLD AXES

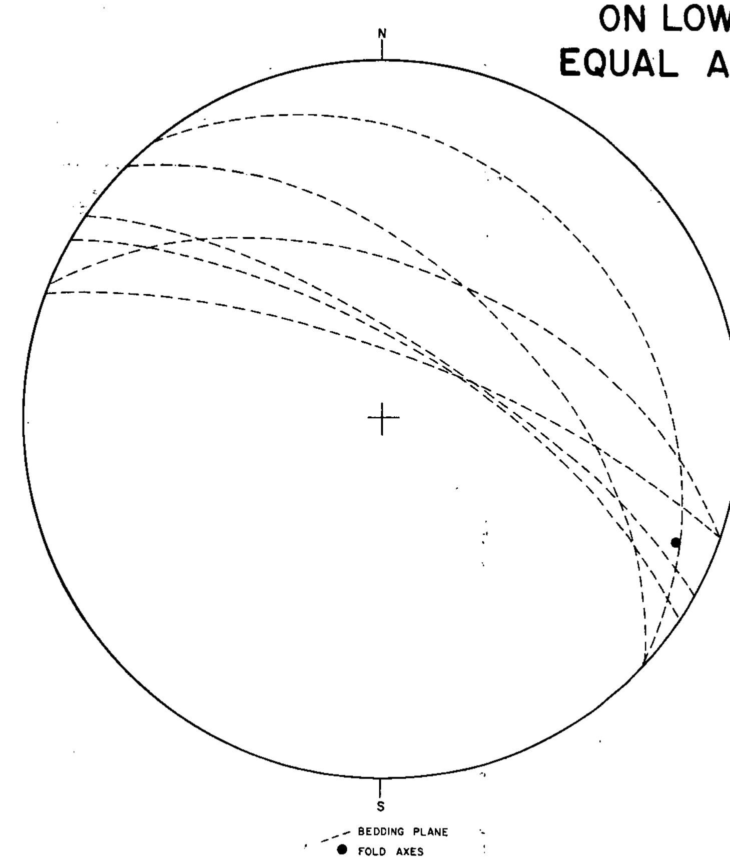

STATION 2D
F2-FOLD AXES

DAMES & MOORE

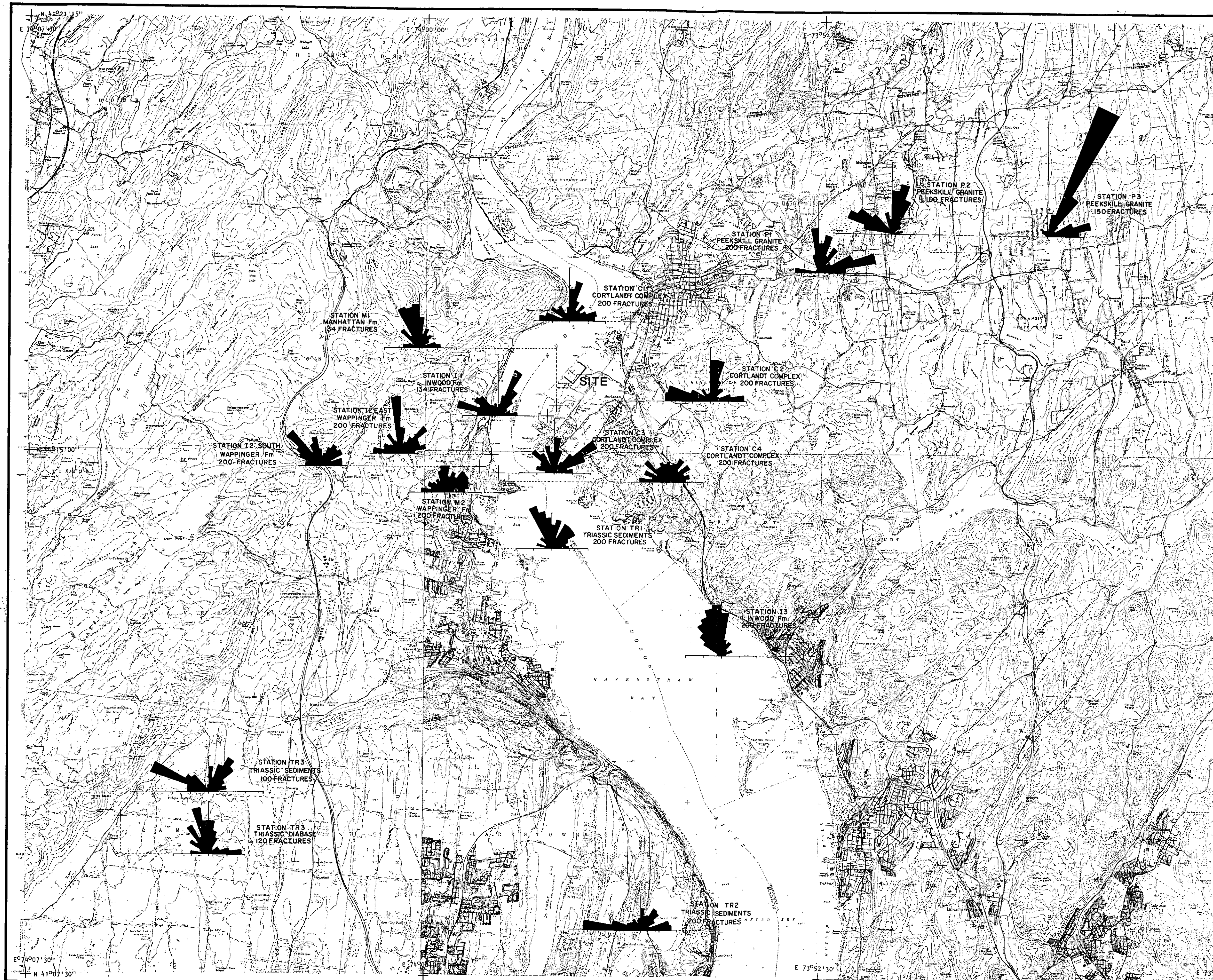

N

FRACTURE STUDY LOCATION MAP SHOWING AREAL DISTRIBUTION OF FRACTURE FREQUENCY DIAGRAMS

KEY:

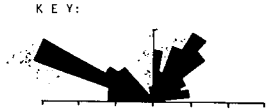

FRACTURE FREQUENCY ROSETTE SHOWING INTERVALS OF 5%.

1 0 1

MILES

REFERENCE:

THE BASE FOR THIS MAP WAS PREPARED FROM THE FOLLOWING U.S.G.S. TOPOGRAPHIC QUADRANGLES: THIELLS, N.Y., 1955; POPOLOPEN LAKE, N.Y., 1957; HAVERSTRAW, N.Y., 1967; PEEKSKILL, N.Y., 1957; OSSINING, N.Y., 1967; MOHEGAN LAKE, N.Y., 1956.

DAMES & MOORE

PLATE B5.3-1

(LOWER HEMISPHERE EQUAL AREA PROJECTIONS)

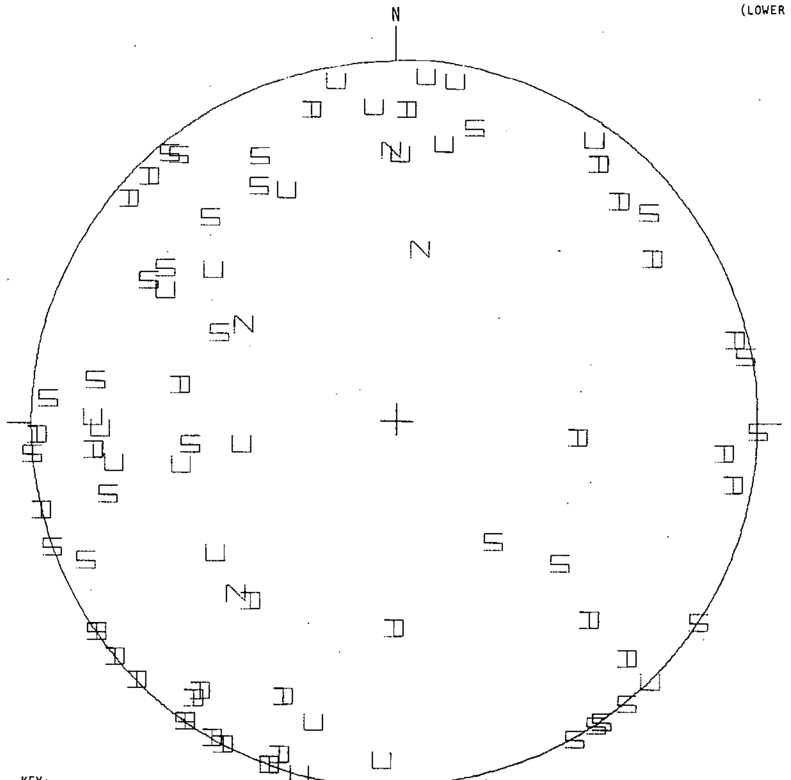

KEY:
D POLE TO FAULT OF DEXTRAL MOVEMENT SENSE
S POLE TO FAULT OF SINISTRAL MOVEMENT SENSE
U POLE TO FAULT OF UNDEFINED MOVEMENT SENSE
N POLE TO FAULT OF NORMAL MOVEMENT SENSE

NUMBER OF POLES = 87

POLES TO FAULTS

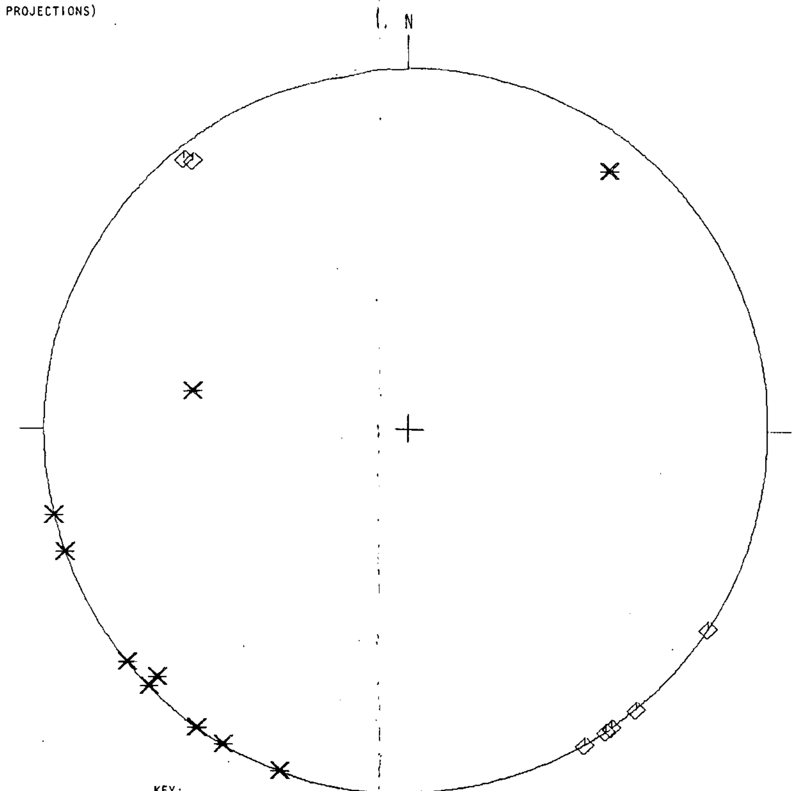

KEY:
OFFSET FAULT
OFFSETTING FAULT

NUMBER OF POLES = 22

POLES TO FAULTS (CROSS-CUTTING RELATIONS)

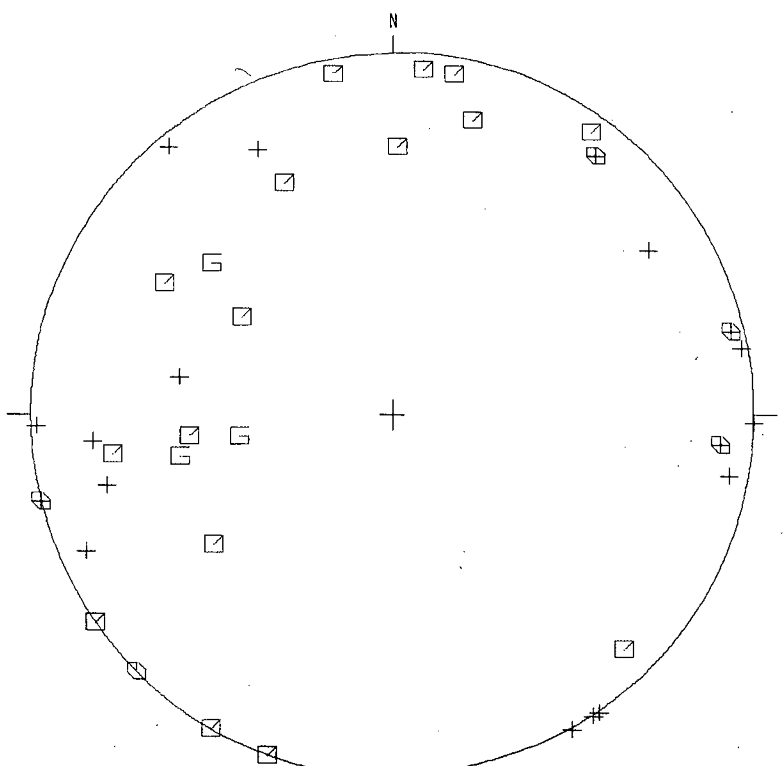

KEY:
G GOUGE FILLING MATERIAL
HEALED BRECCIA
CALCITE MINERALIZATION
PYRITE MINERALIZATION

NUMBER OF POLES = 45

POLES TO MINERALIZED FAULTS

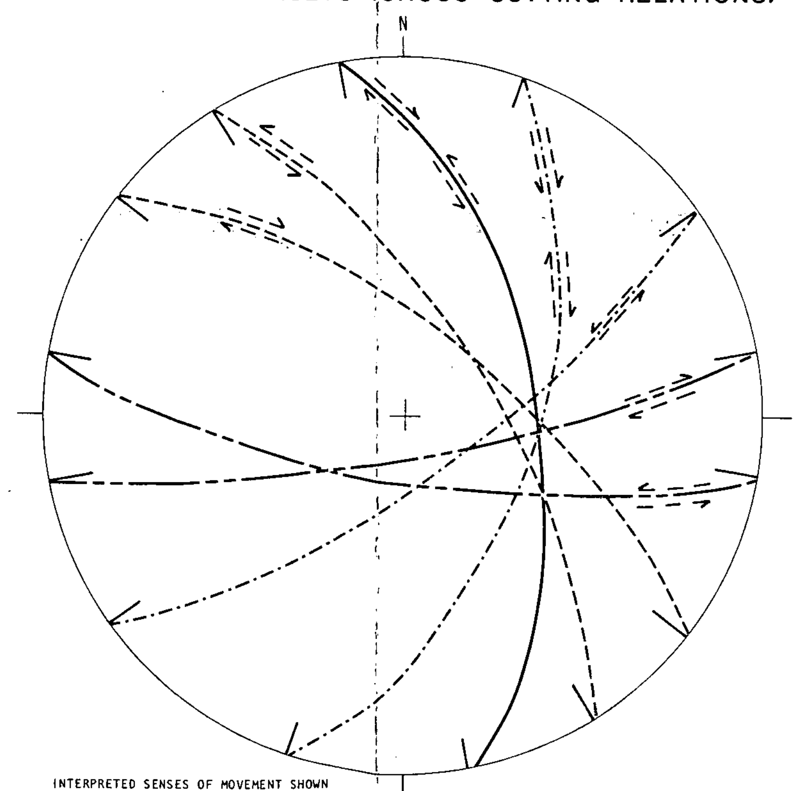

INTERPRETED SENSES OF MOVEMENT SHOWN
RELATED PLANES REPRESENTED BY SAME SYMBOL.

INTERPRETED FAULT GEOMETRY

SUMMARY OF FAULT DATA FROM PALEOZOIC ROCKS IN THE STUDY AREA (SITE EXCLUDED)

(LOWER HEMISPHERE EQUAL AREA PROJECTIONS)

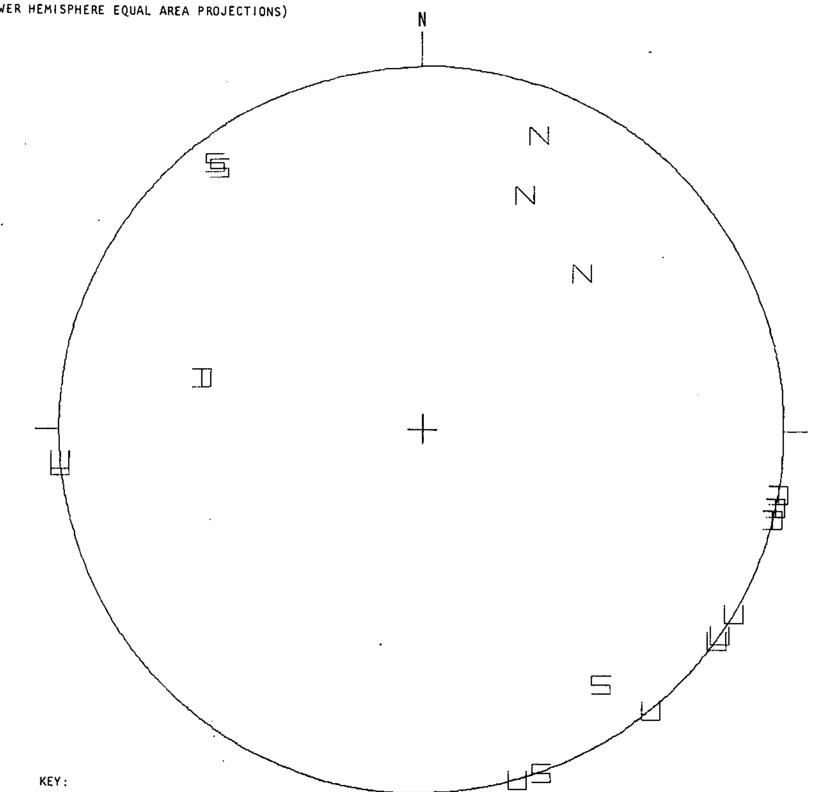

KEY:
D POLE TO FAULT OF DEXTRAL MOVEMENT SENSE
S POLE TO FAULT OF SINISTRAL MOVEMENT SENSE
U POLE TO FAULT OF UNDEFINED MOVEMENT SENSE
N POLE TO FAULT OF NORMAL MOVEMENT SENSE

REFERENCE: NEW YORK STATE GEOLOGIC MAP.

NUMBER OF POLES = 18

(STATION TR-1 AND TABLE C6-1)

POLES TO FAULTS (TRIASSIC)

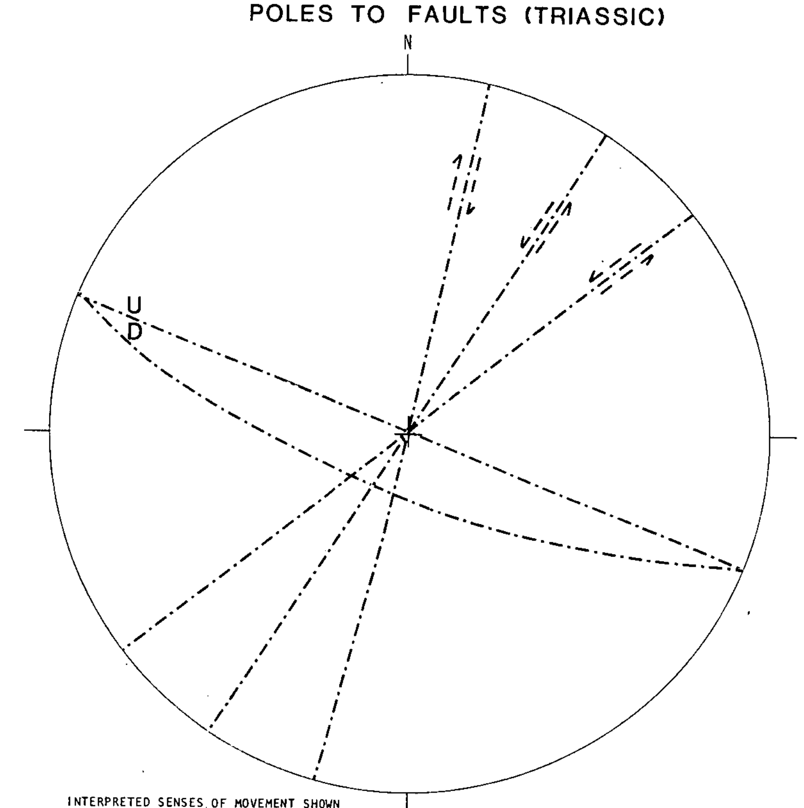

INTERPRETED SENSES OF MOVEMENT SHOWN
RELATED PLANES REPRESENTED BY SAME SYMBOL.

INTERPRETED FAULT GEOMETRY (TRIASSIC)

SUMMARY OF FAULT DATA FROM TRIASSIC ROCKS IN THE STUDY AREA

DAMES & MOORE

SUMMARY OF FAULT DATA FROM OUTCROP STUDIES AT THE INDIAN POINT SITE

(LOWER HEMISPHERE EQUAL AREA PROJECTIONS)

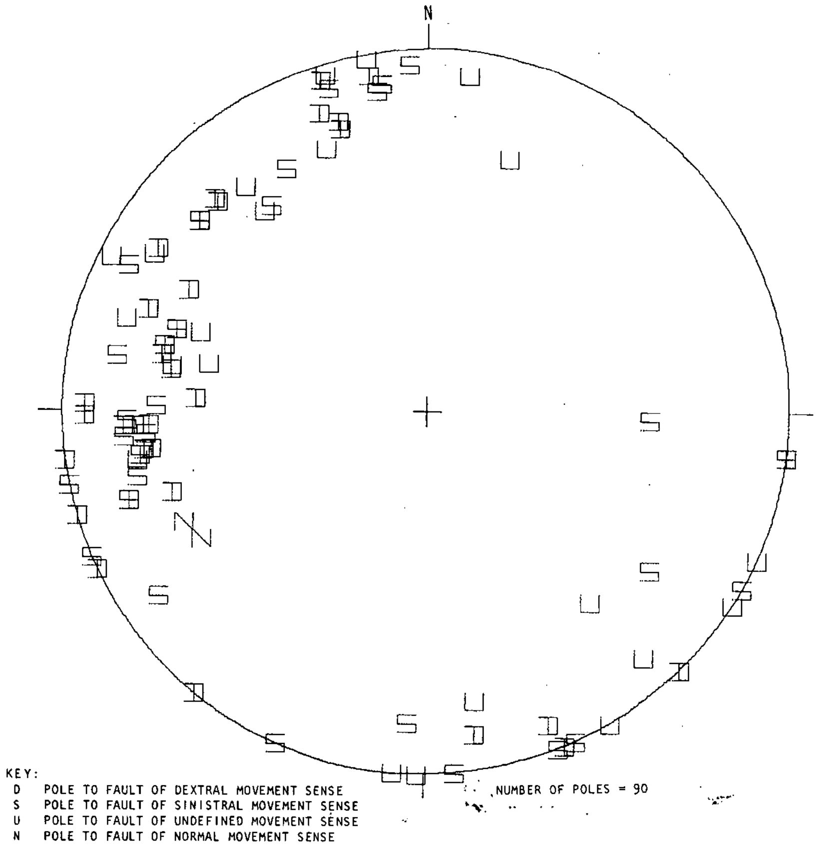

POLES TO FAULTS (SITE)

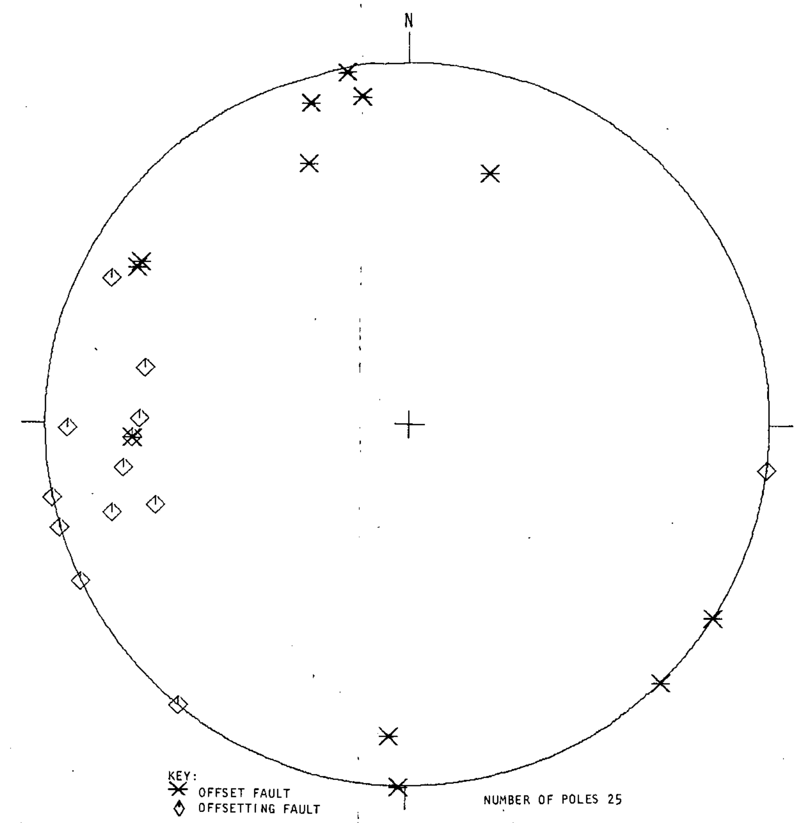

POLES TO FAULTS ONSITE (CROSS-CUTTING RELATIONS)

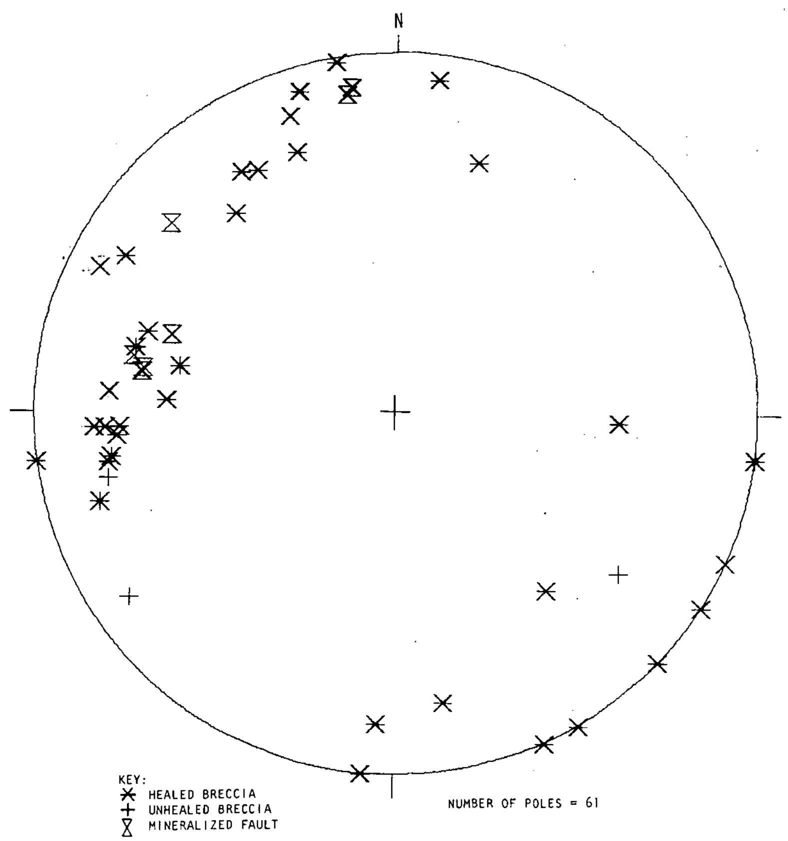

POLES TO MINERALIZED FAULTS (SITE)

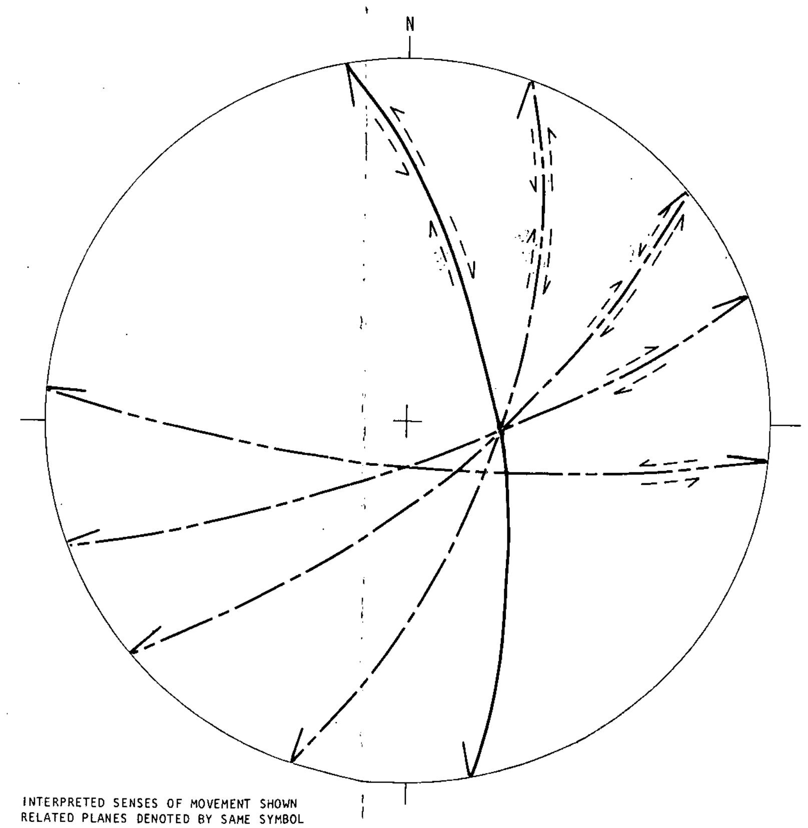

INTERPRETED FAULT GEOMETRY (SITE STUDIES)

DAMES & MOORE

PLATE B5.3-3

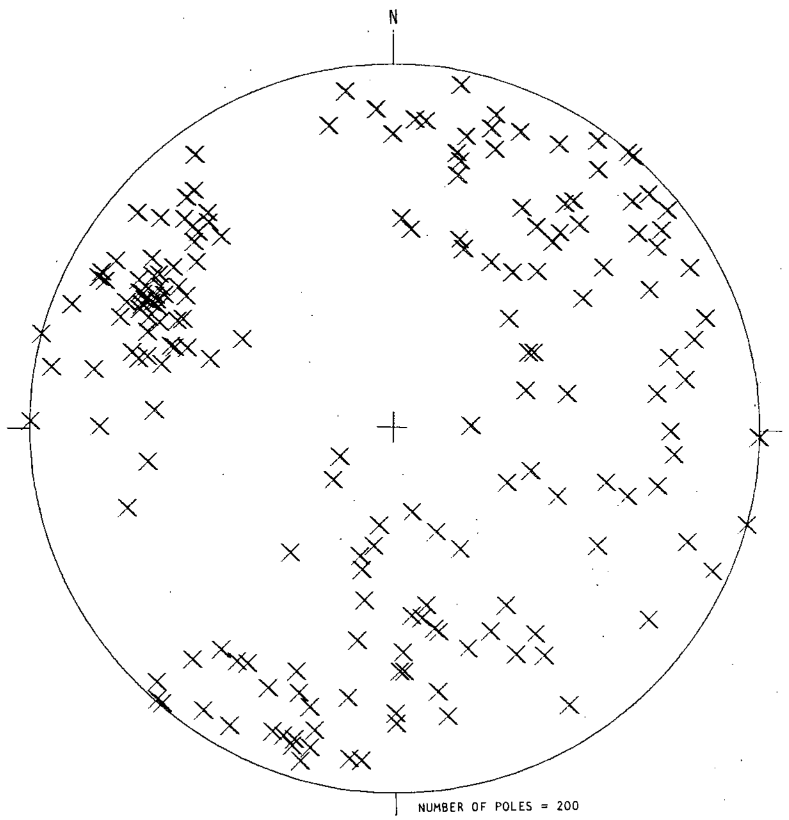

I.1.1 PLOT OF POLES TO ALL FRACTURE PLANES

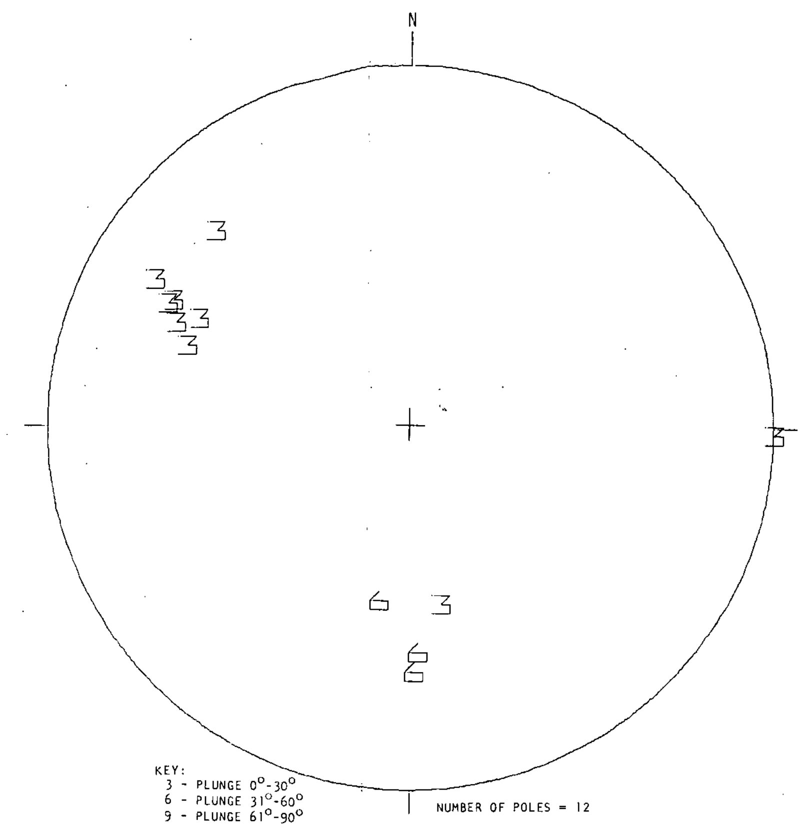

I.1.3 PLOT OF POLES TO SLICKENSIDED PLANES

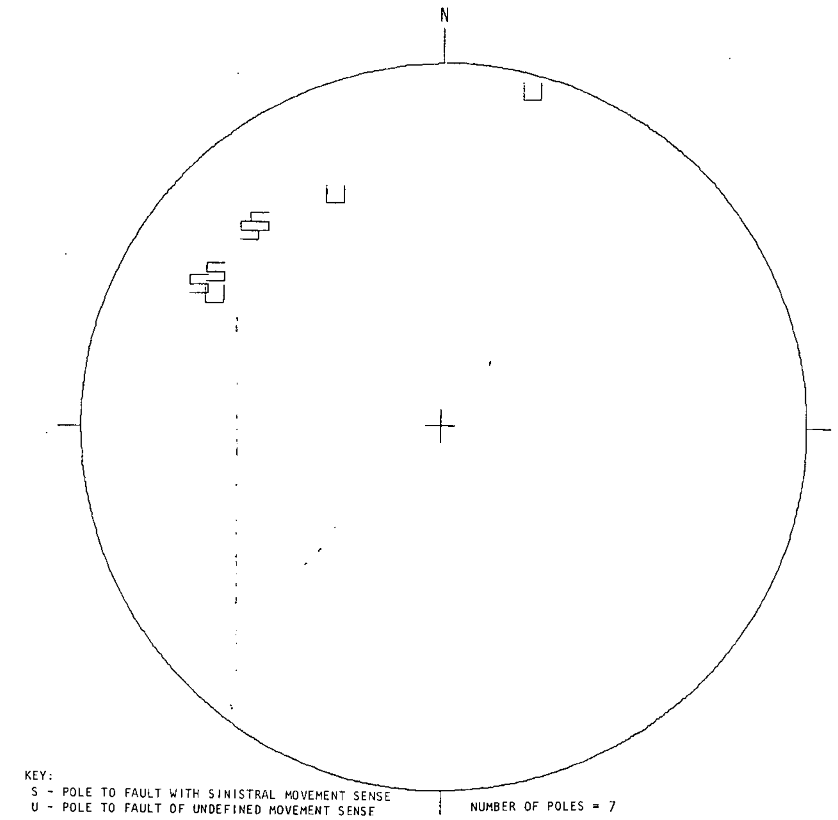

I.1.5 PLOT OF POLES TO FAULT PLANES

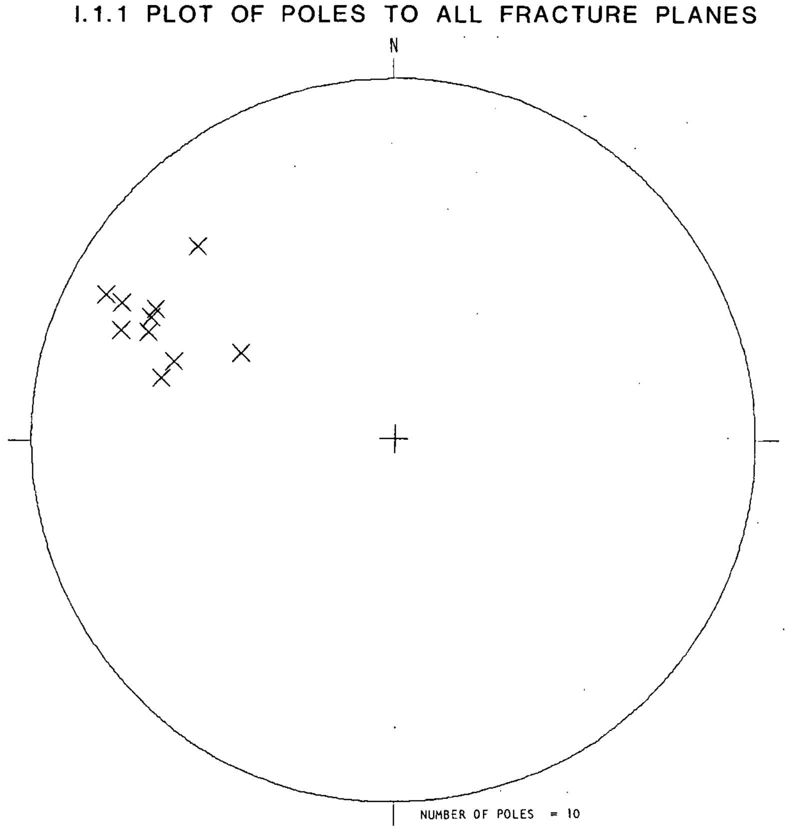

I.1.2 PLOT OF POLES TO FOLIATION (S0/S1) PLANES

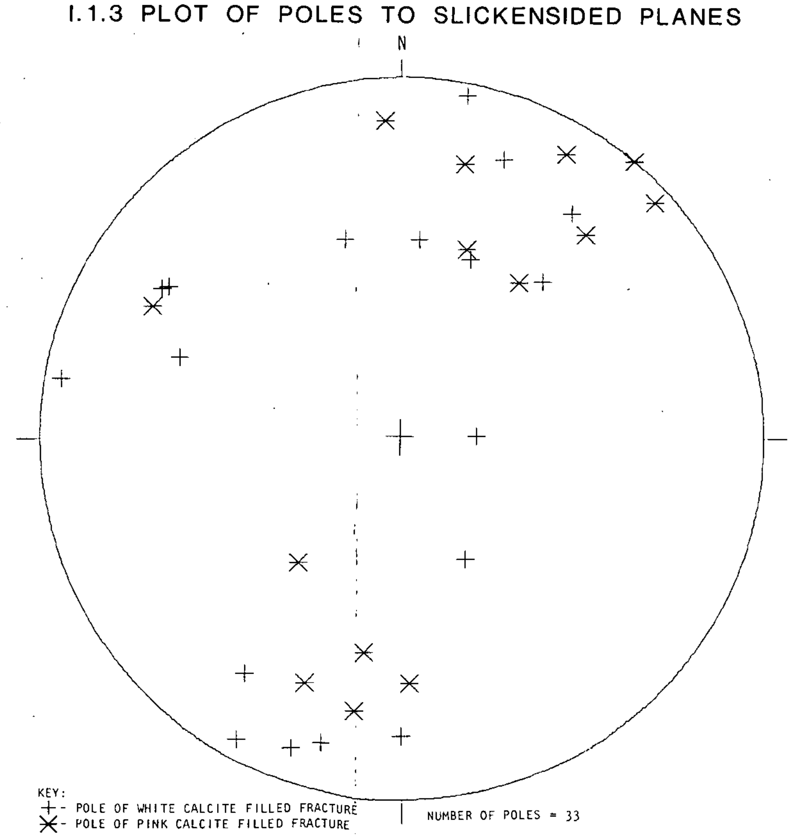

I.1.4 PLOT OF POLES OF MINERALIZED FRACTURES

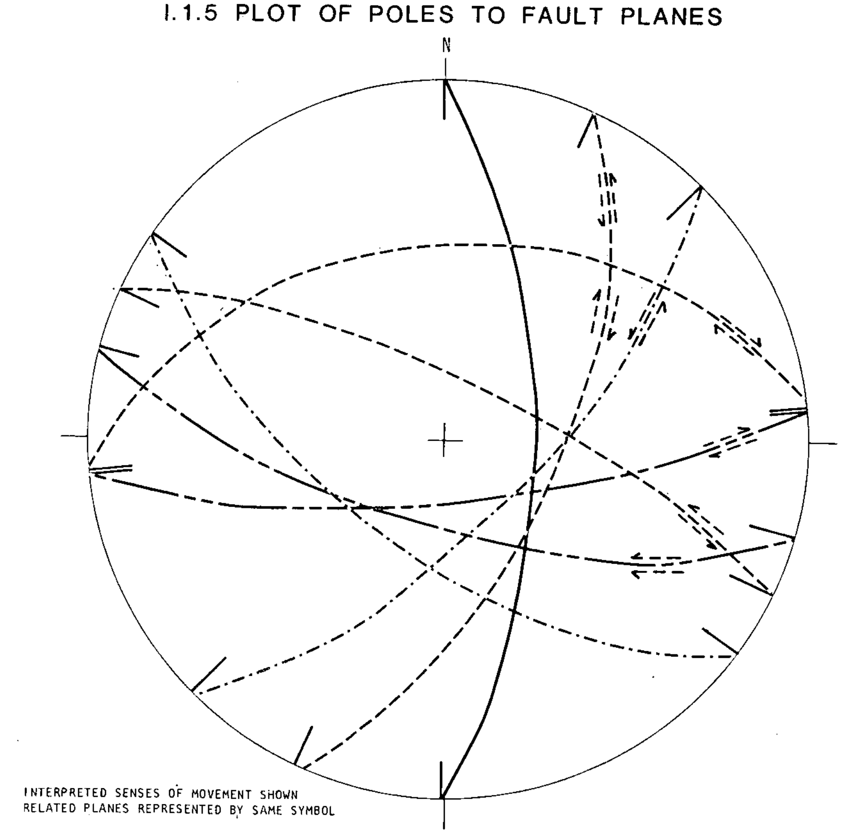

I.1.6 INTERPRETED FRACTURE AND FAULT GEOMETRY

NOTE: STATION LOCATION SHOWN ON PLATE B5.3-1

STRUCTURAL ELEMENTS
STATION I-1 INWOOD MARBLE

(LOWER HEMISPHERE EQUAL AREA PROJECTIONS)

DAMES & MOORE

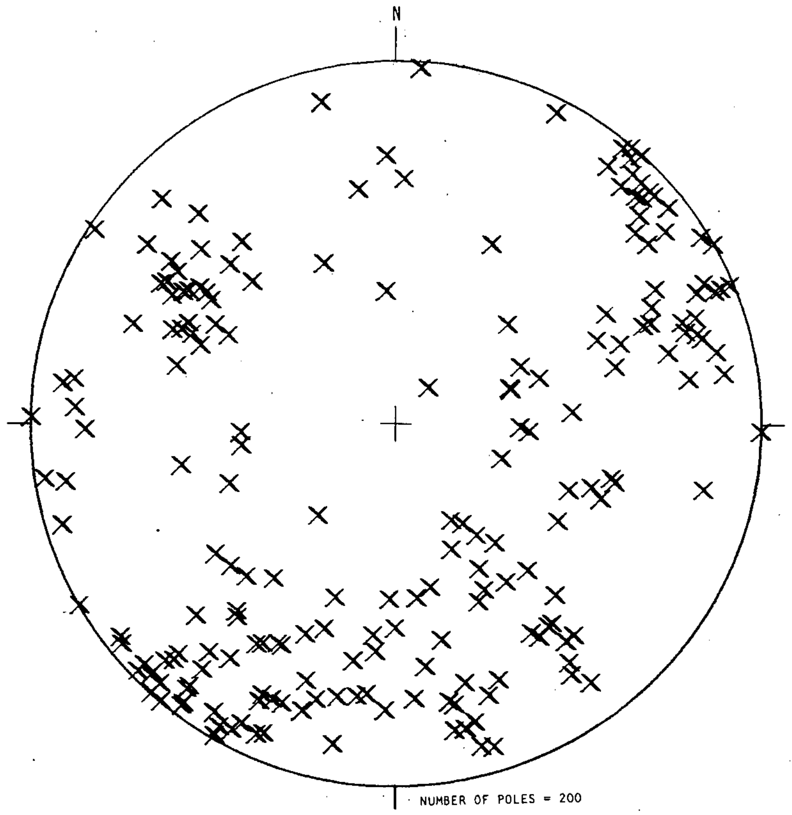

I.2.1.1 PLOT OF POLES TO ALL FRACTURE PLANES

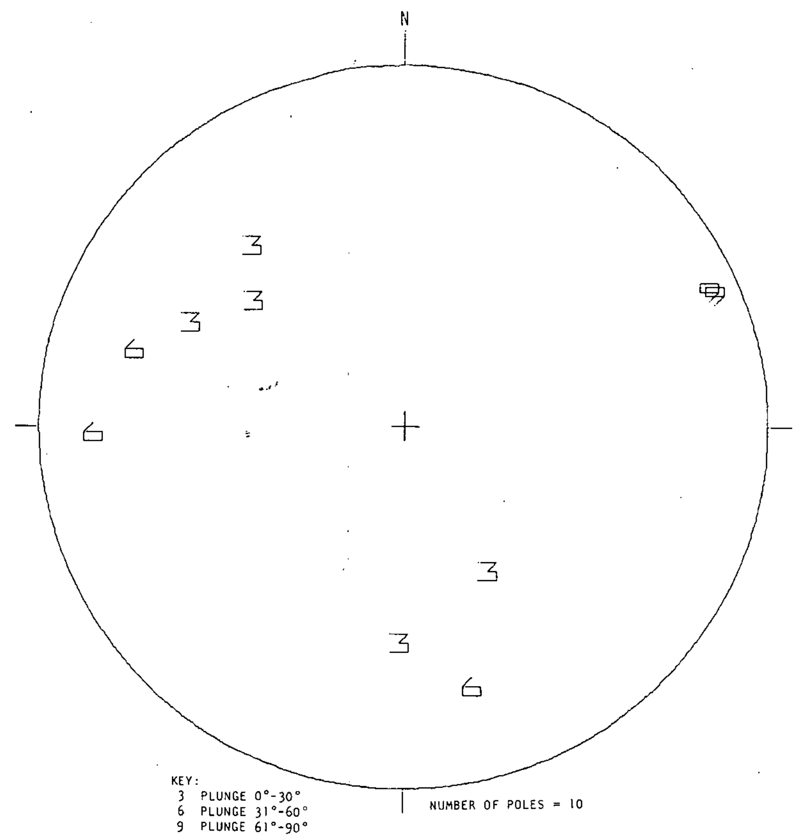

I.2.3 PLOT OF POLES TO SLICKENSIDED PLANES

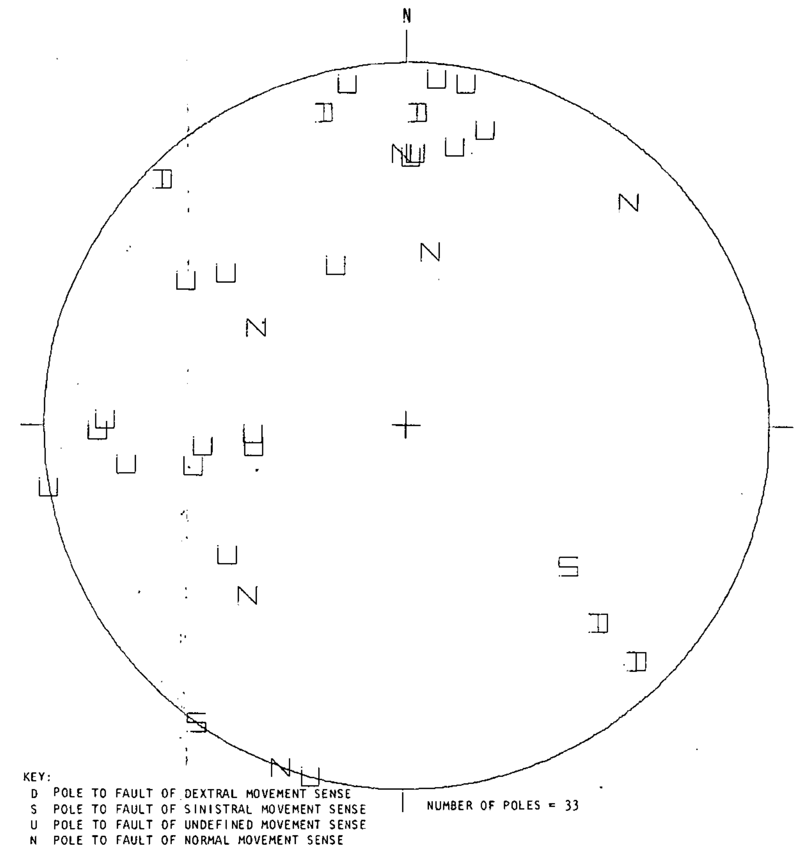

I.2.5 PLOT OF POLES TO FAULTS

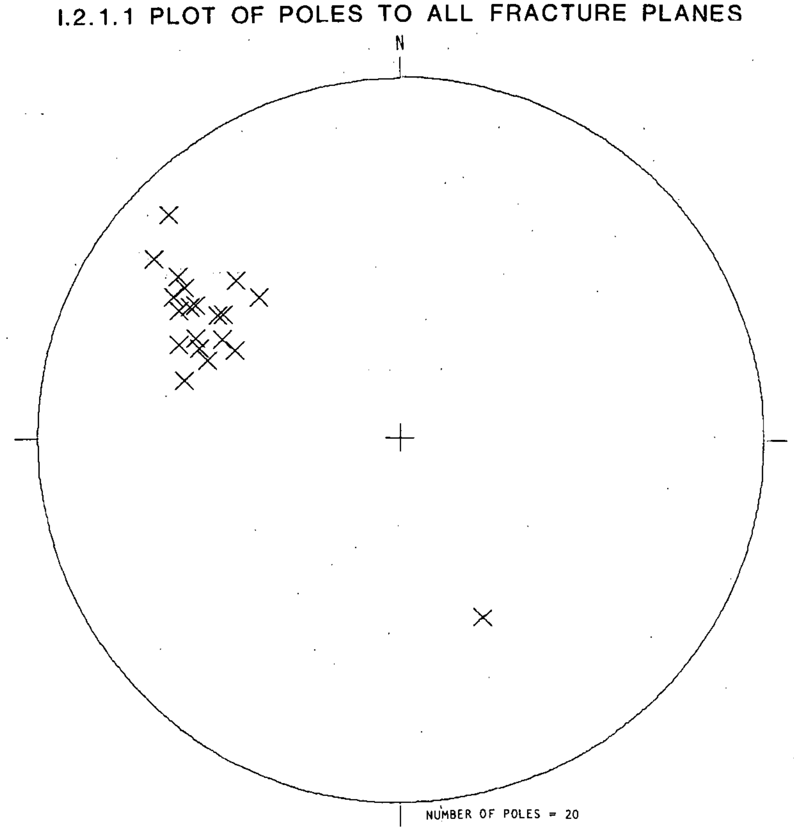

I.2.2.1 PLOT OF POLES TO FOLIATION (S0/S1) PLANES

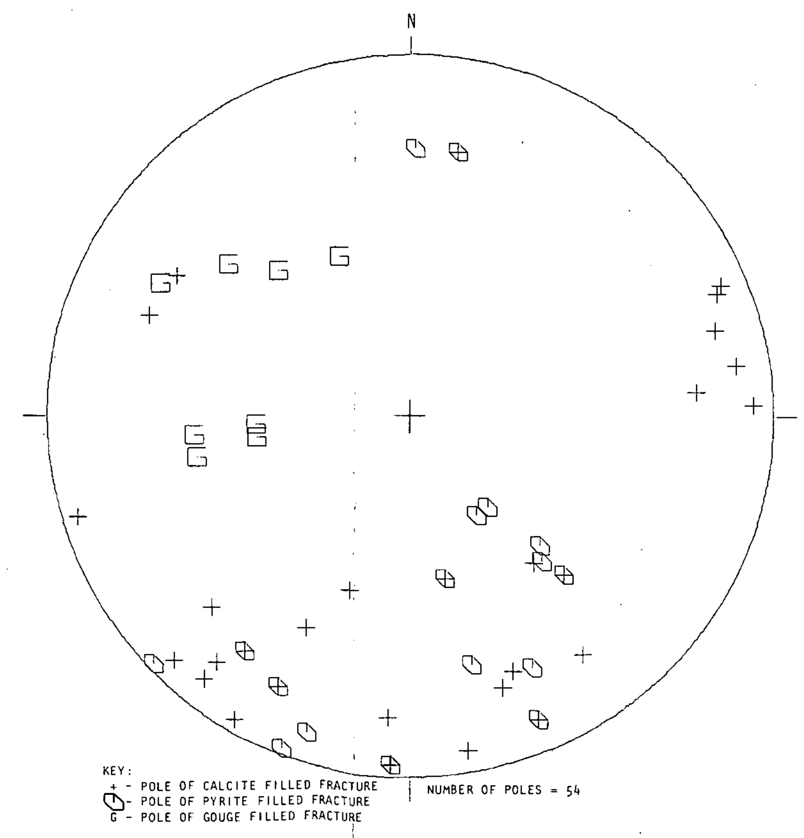

I.2.4 PLOT OF POLES TO MINERALIZED FRACTURE PLANES

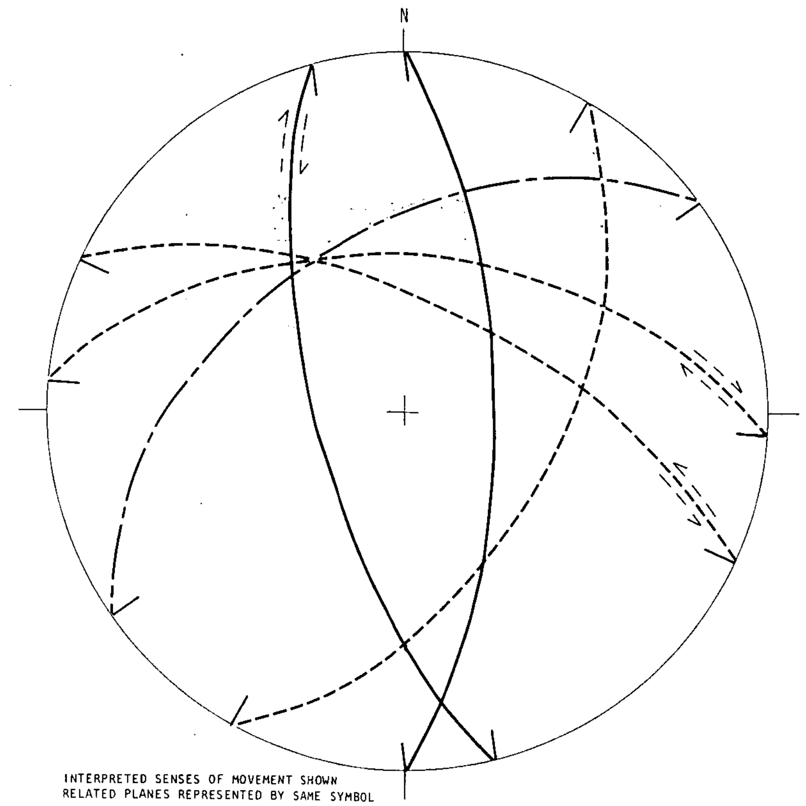

I.2.1.6 INTERPRETED FRACTURE AND FAULT GEOMETRY

NOTE: STATION LOCATION SHOWN ON PLATE B5.3-1

STRUCTURAL ELEMENTS
STATION I-2 (SOUTH WALL) WAPPINGER LIMESTONE

(LOWER HEMISPHERE EQUAL AREA PROJECTIONS)

DAMES & MOORE

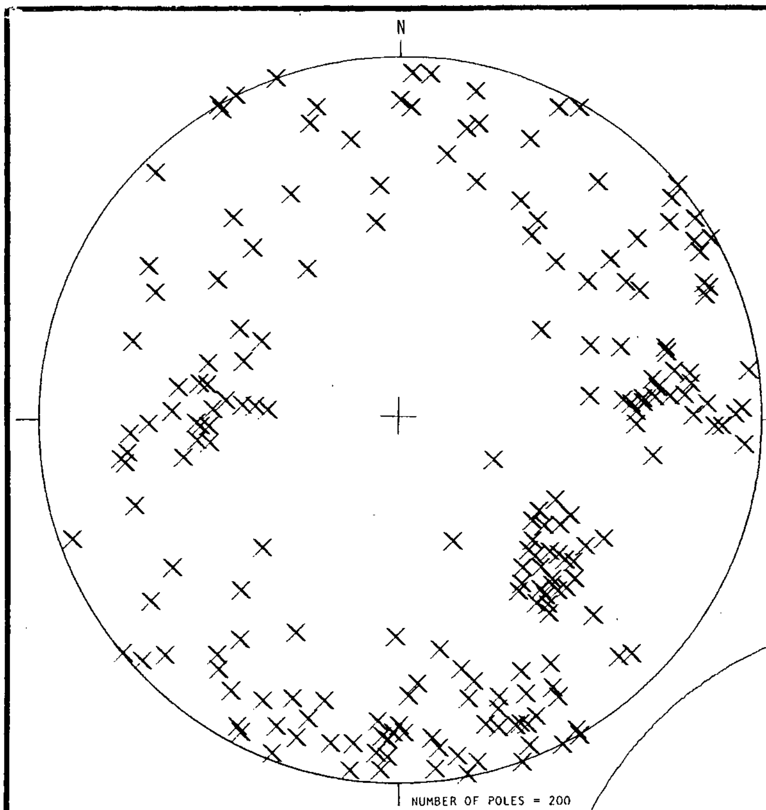

I.2.1.2 PLOT OF POLES TO ALL FRACTURE PLANES

NOTE: STATION LOCATION SHOWN ON PLATE B5.3-1

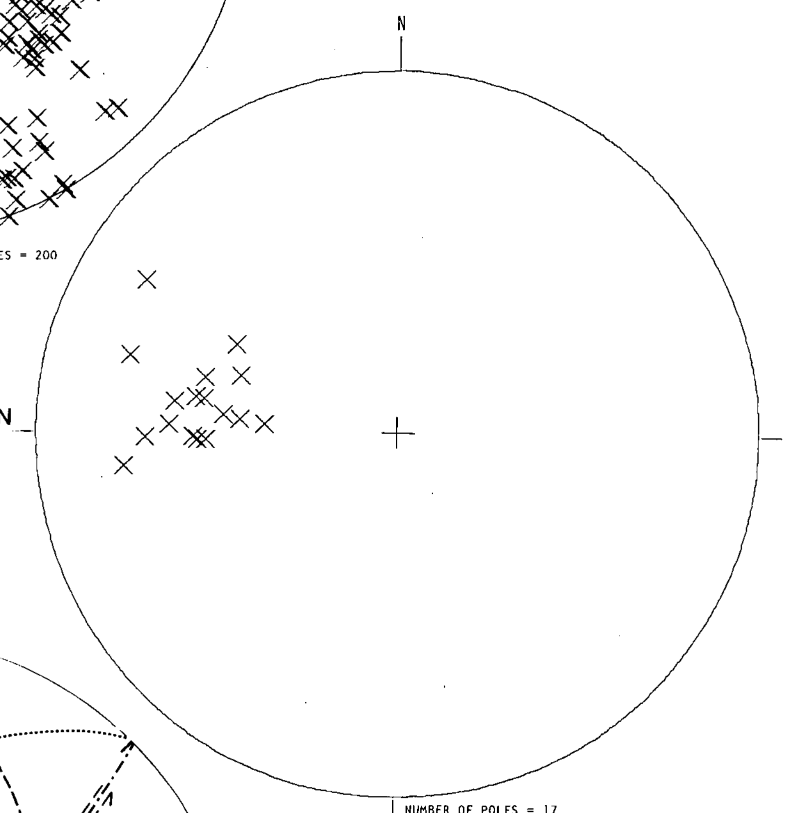

I.2.2.2 PLOT OF POLES TO FOLIATION (S0/S1) PLANES

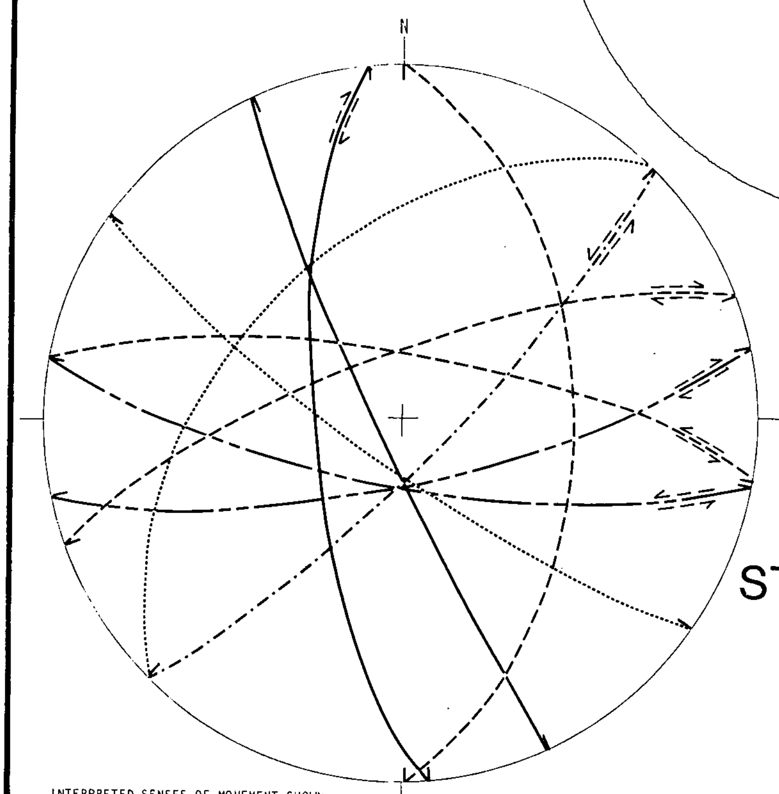

I.2.2.6 INTERPRETED FRACTURE AND FAULT GEOMETRY

INTERPRETED SENSES OF MOVEMENT SHOWN
RELATED PLANES REPRESENTED BY SAME SYMBOL.

STRUCTURAL ELEMENTS
STATION I-2 (EAST WALL)
WAPPINGER LIMESTONE

(LOWER HEMISPHERE EQUAL AREA PROJECTIONS)

DAMES & MOORE

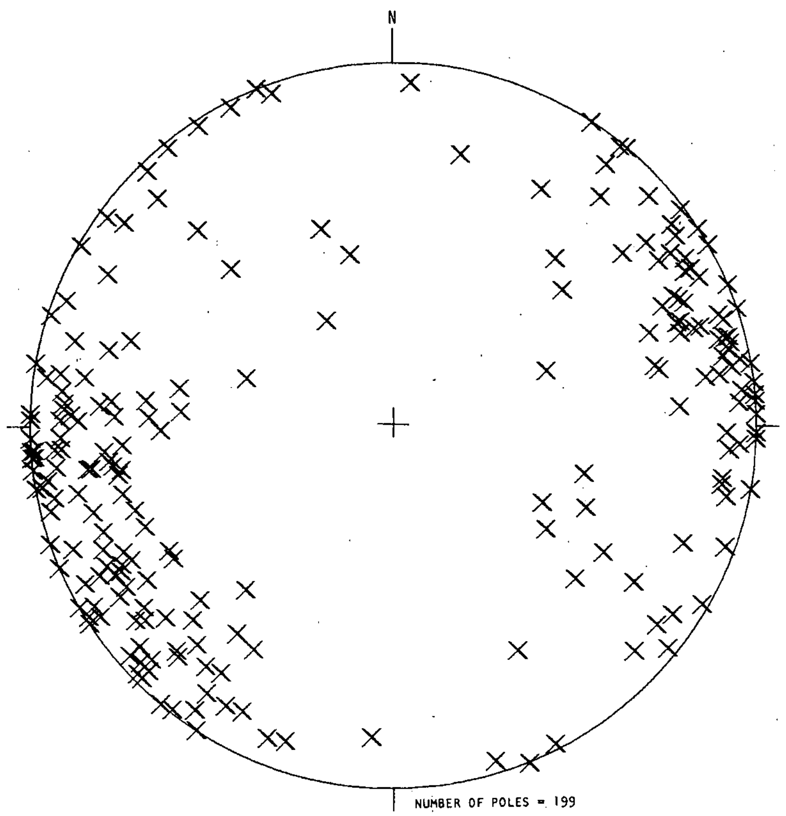

I.3.1 PLOT OF POLES TO ALL FRACTURE PLANES

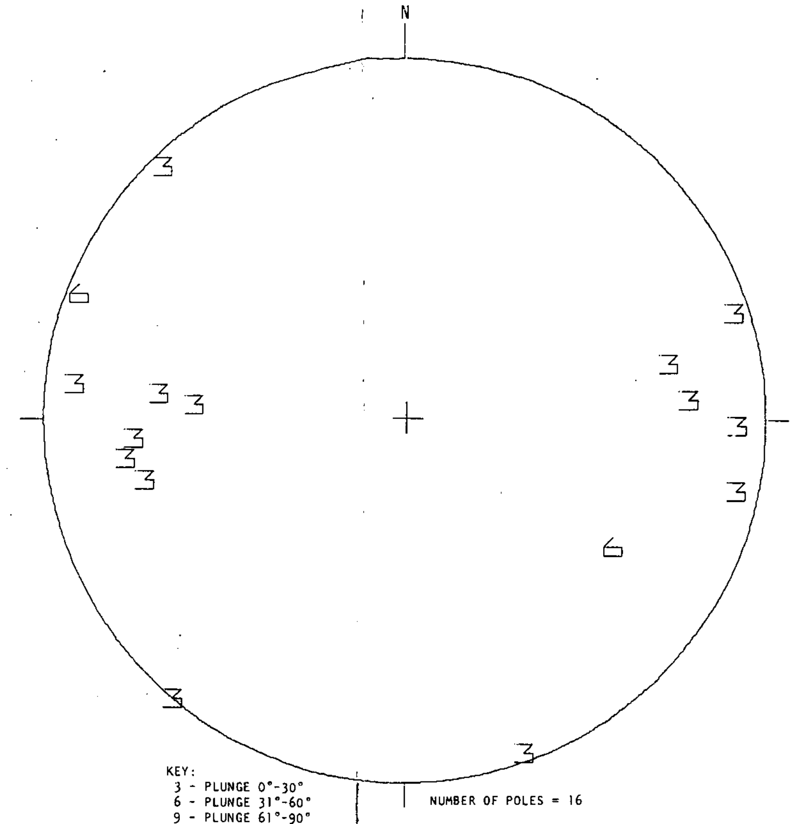

I.3.3 PLOT OF POLES TO SLICKENSIDED PLANES

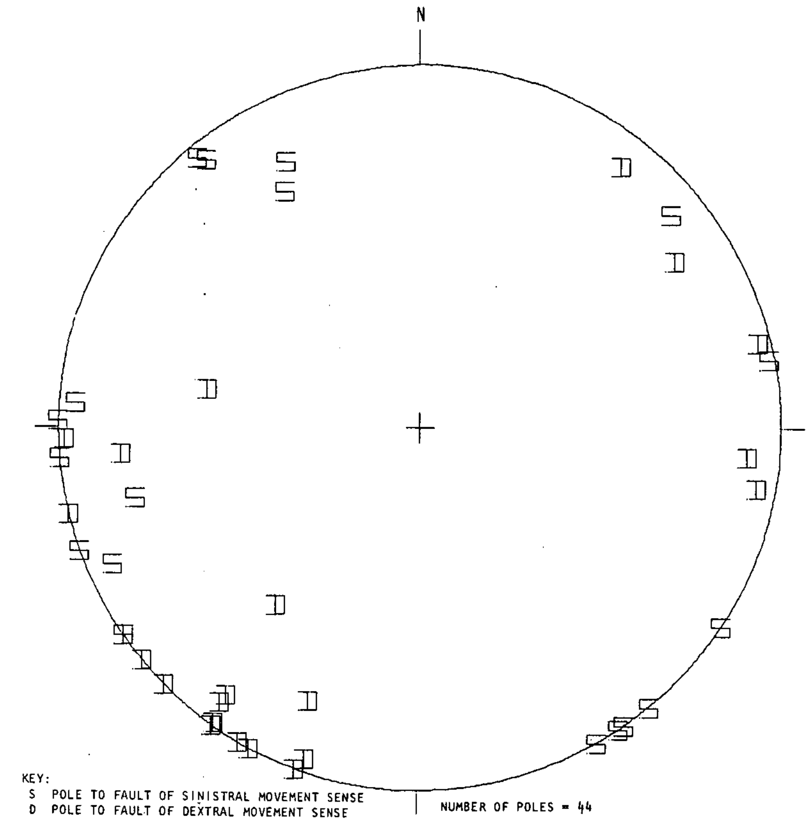

I.3.5 PLOT OF POLES TO FAULT PLANES

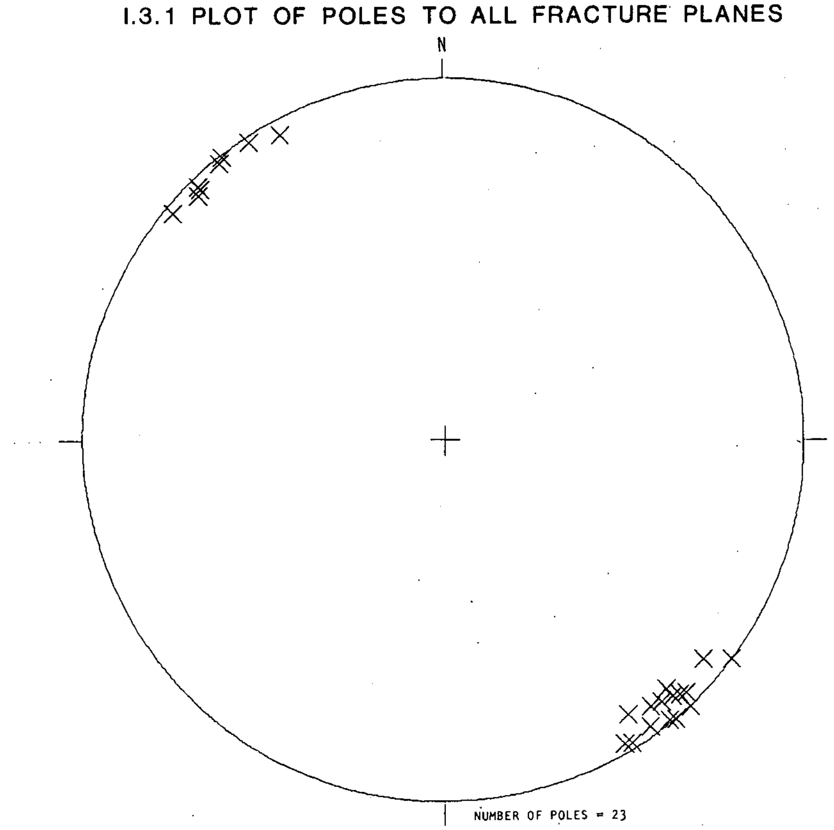

I.3.2 PLOT OF POLES TO FOLIATION (S0/S1) PLANES

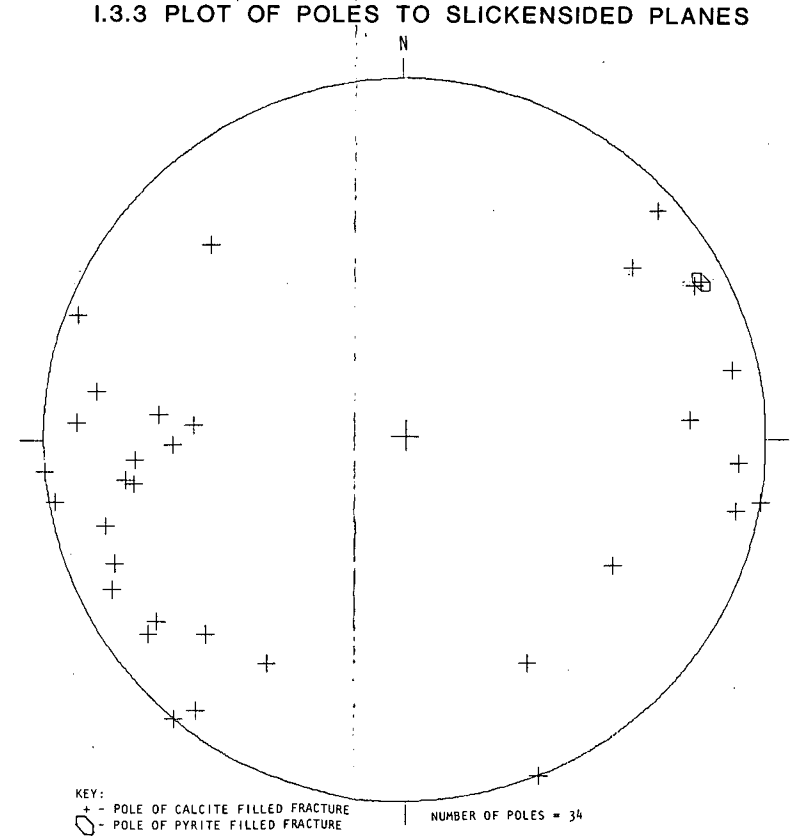

I.3.4 PLOT OF POLES TO MINERALIZED FRACTURE PLANES

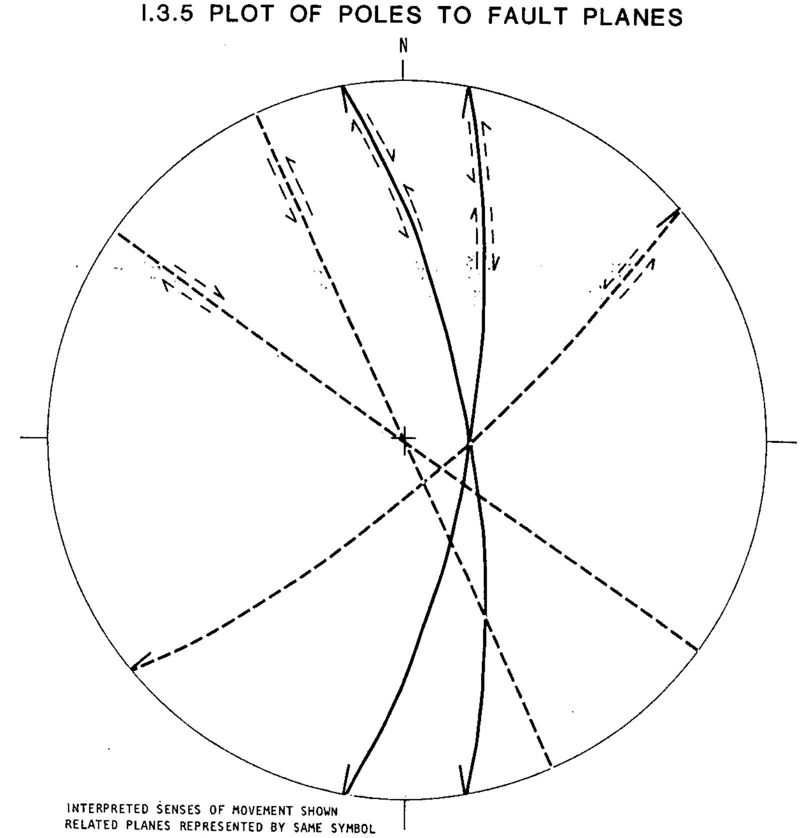

I.3.6 INTERPRETED FRACTURE AND FAULT GEOMETRY

NOTE: STATION LOCATION SHOWN ON PLATE B5.3-1

STRUCTURAL ELEMENTS
STATION I-3 INWOOD MARBLE

(LOWER HEMISPHERE EQUAL AREA PROJECTIONS)

DAMES & MOORE

PLATE B5.3-7

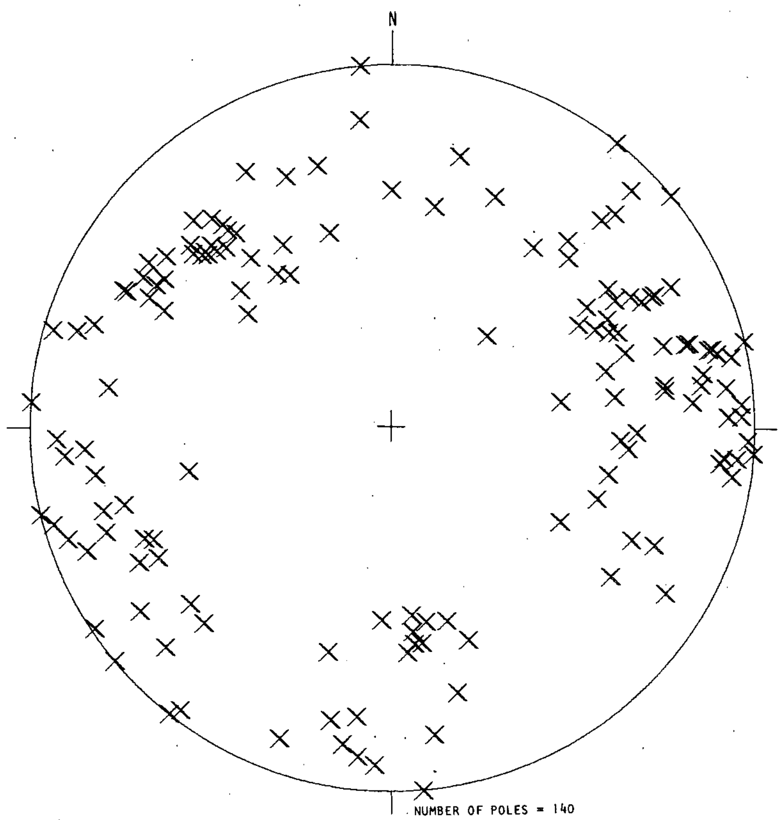

M.1.1 PLOT OF POLES TO ALL FRACTURE PLANES

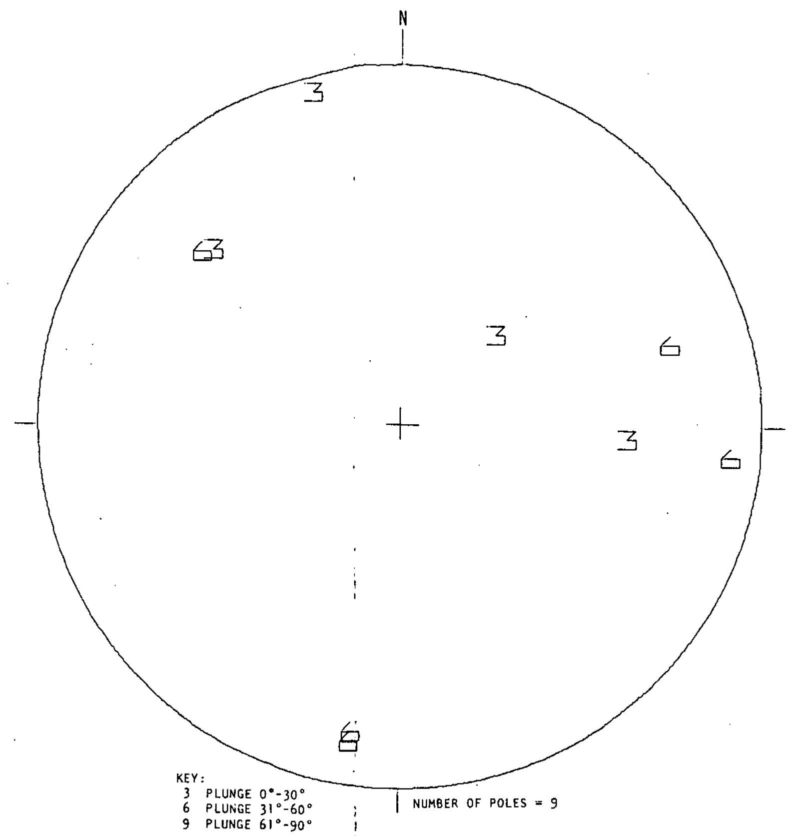

M.1.3 PLOT OF POLES TO SLICKENSIDED PLANES

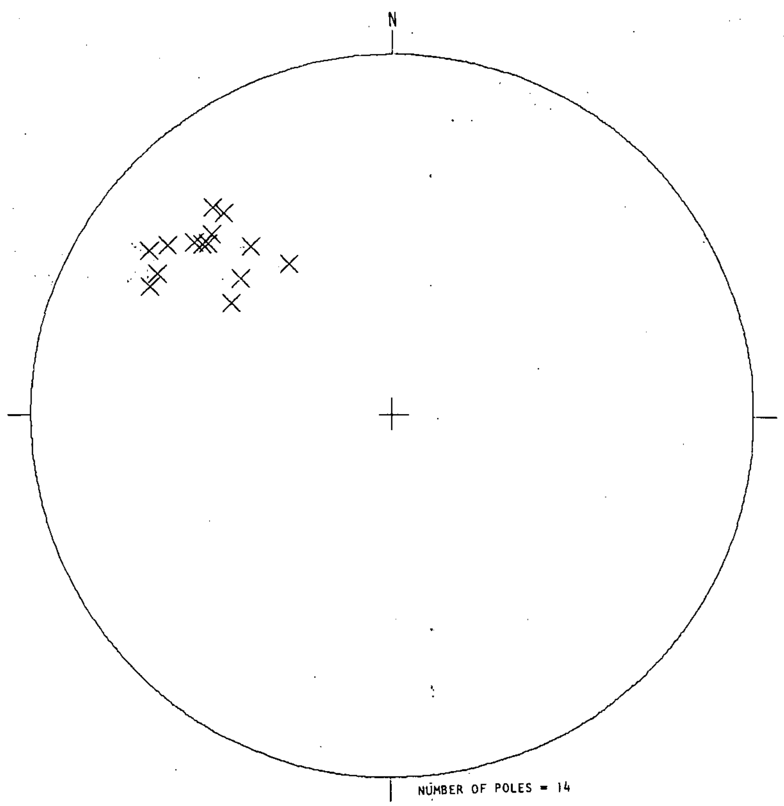

M.1.2 PLOT OF POLES TO FOLIATION (S0/S1) PLANES

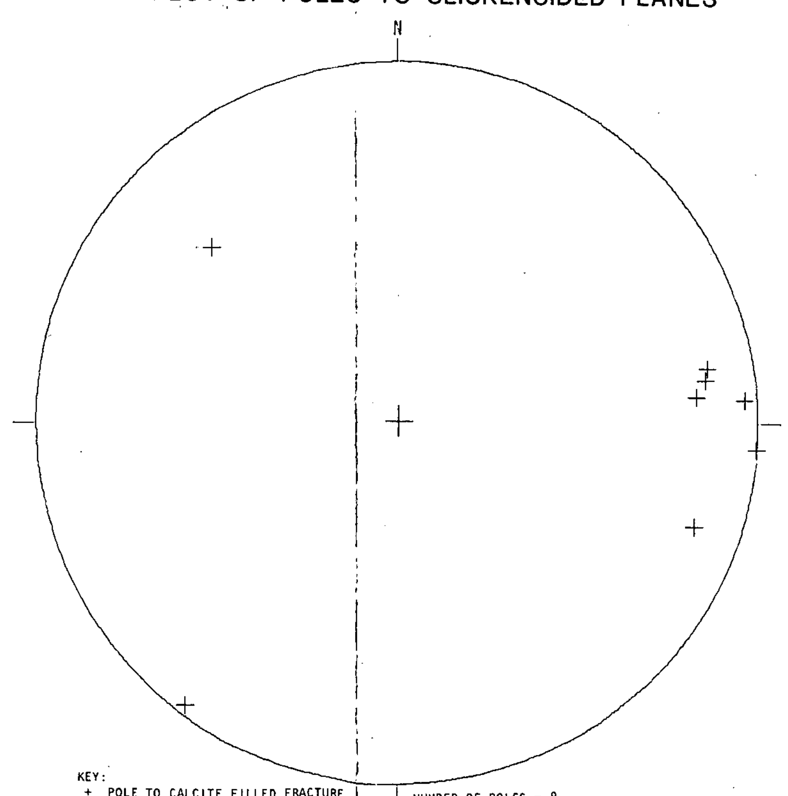

M.1.4 PLOT OF POLES TO MINERALIZED FRACTURE PLANES

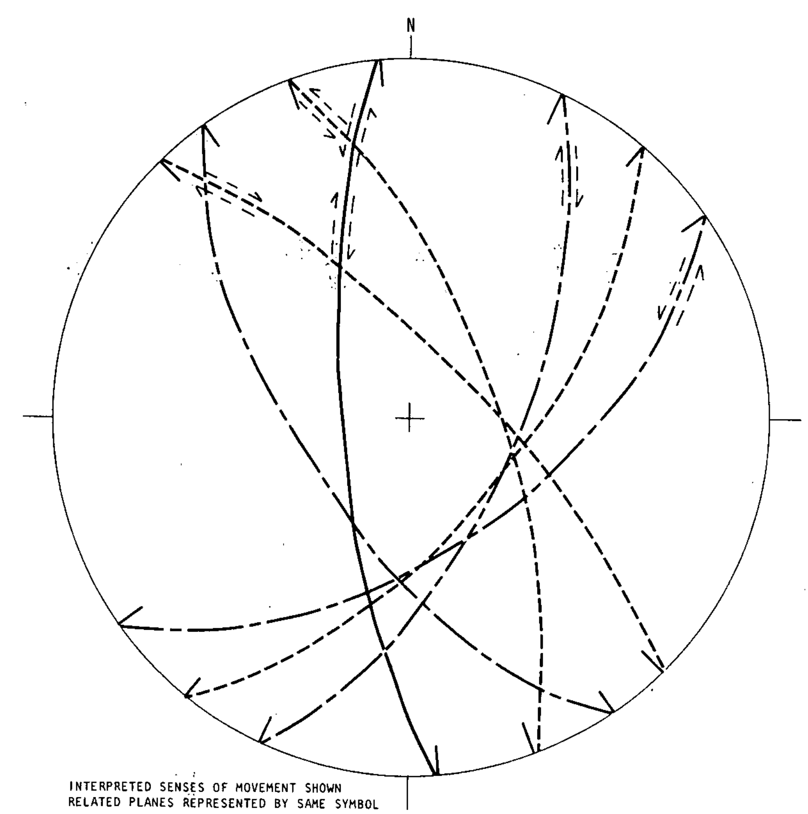

M.1.6 INTERPRETED FRACTURE AND FAULT GEOMETRY

NOTE: STATION LOCATION SHOWN ON PLATE B5.3-1

STRUCTURAL ELEMENTS
STATION M-1 MANHATTAN SCHIST

(LOWER HEMISPHERE EQUAL AREA PROJECTIONS)

DAMES & MOORE

PLATE B5.3-8

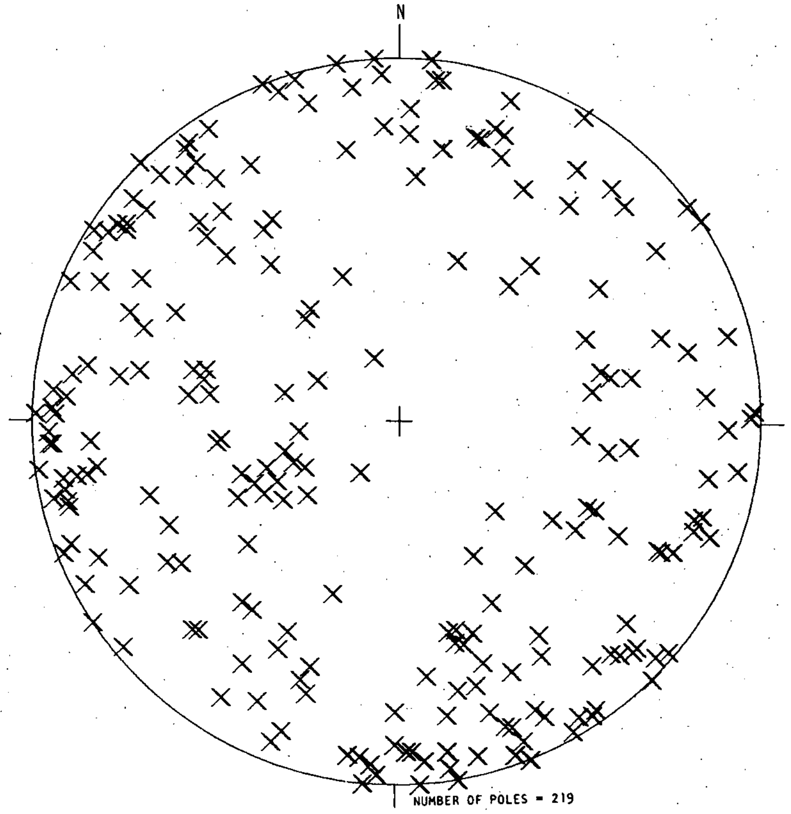

M.2.1 PLOT OF POLES TO ALL FRACTURE PLANES

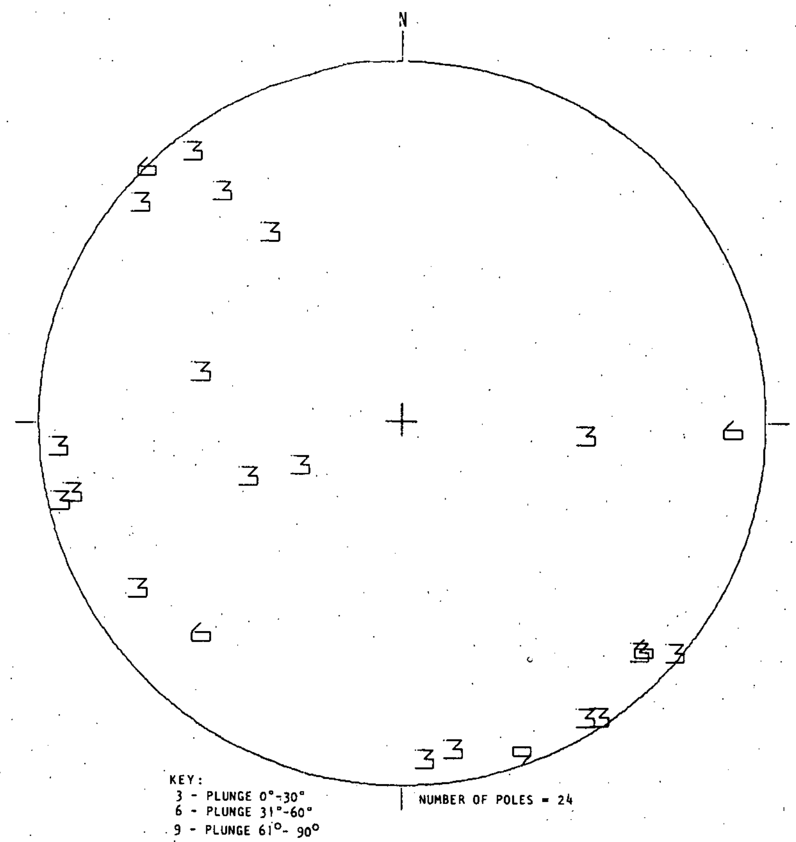

M.2.3 PLOT OF POLES TO SLICKENSIDED PLANES

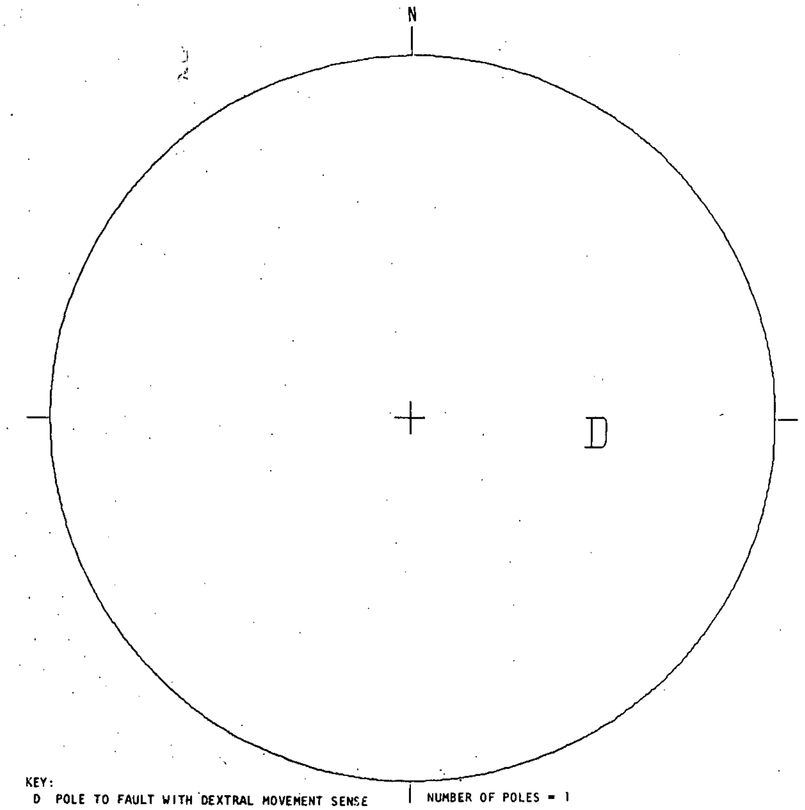

M.2.5 PLOT OF POLE TO FAULT PLANE

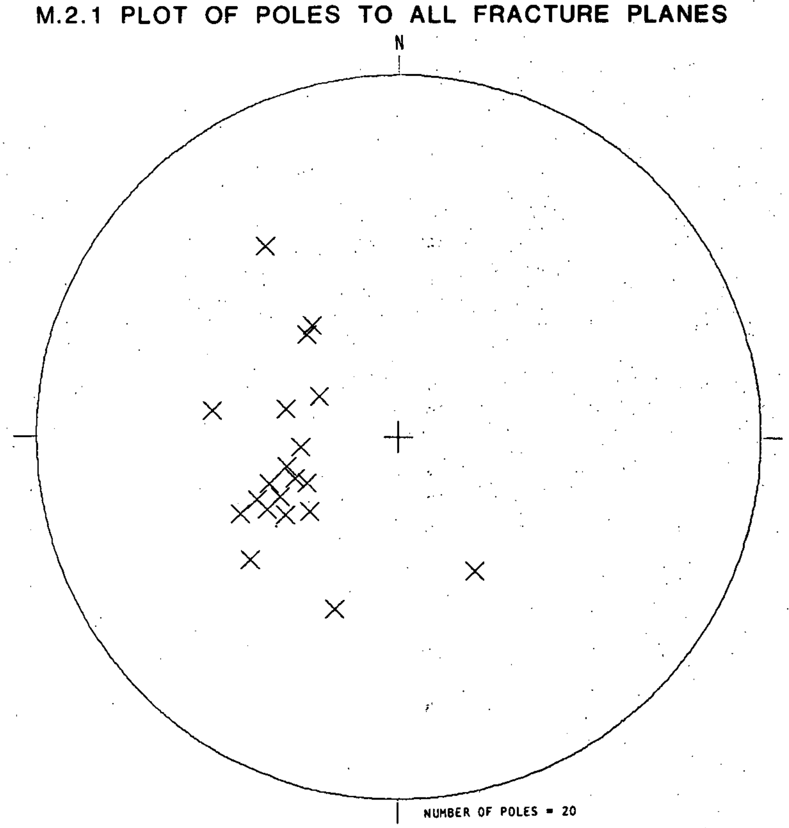

M.2.2 PLOT OF POLES TO FOLIATION (S0/S1) PLANES

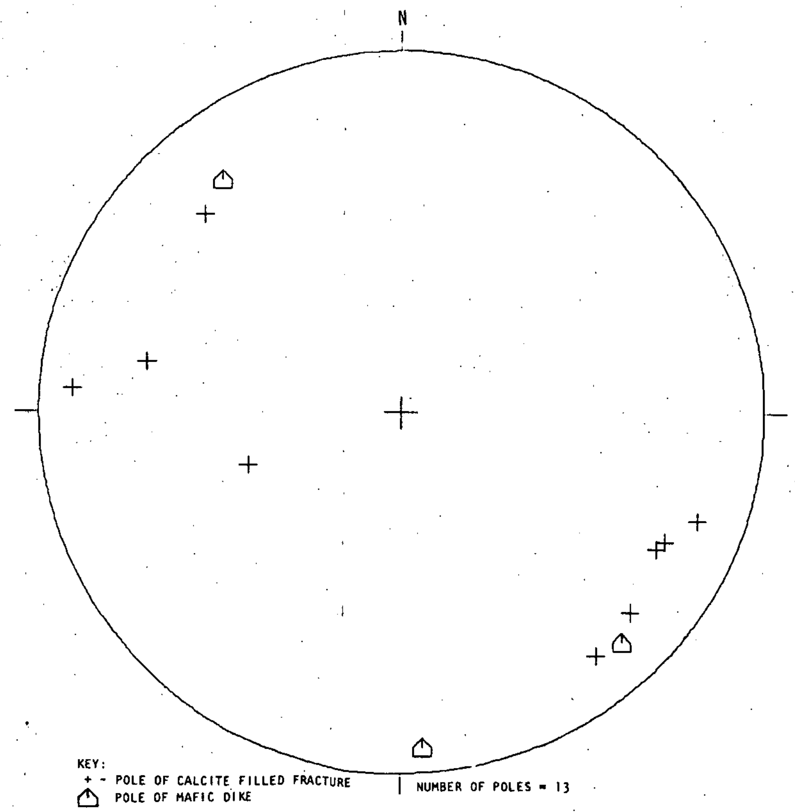

M.2.4 PLOT OF POLES TO MINERALIZED FRACTURE PLANES

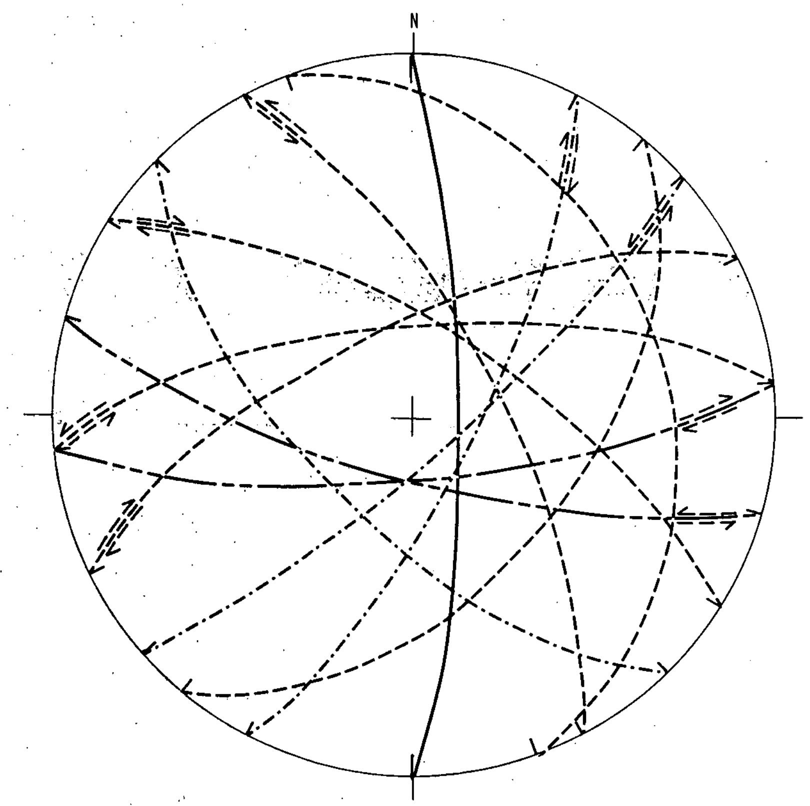

INTERPRETED FRACTURE AND FAULT GEOMETRY

NOTE: STATION LOCATION SHOWN ON PLATE B5.3-1

STRUCTURAL ELEMENTS
STATION M-2 ANNSVILLE PHYLLITE

(LOWER HEMISPHERE EQUAL AREA PROJECTIONS)

DAMES & MOORE

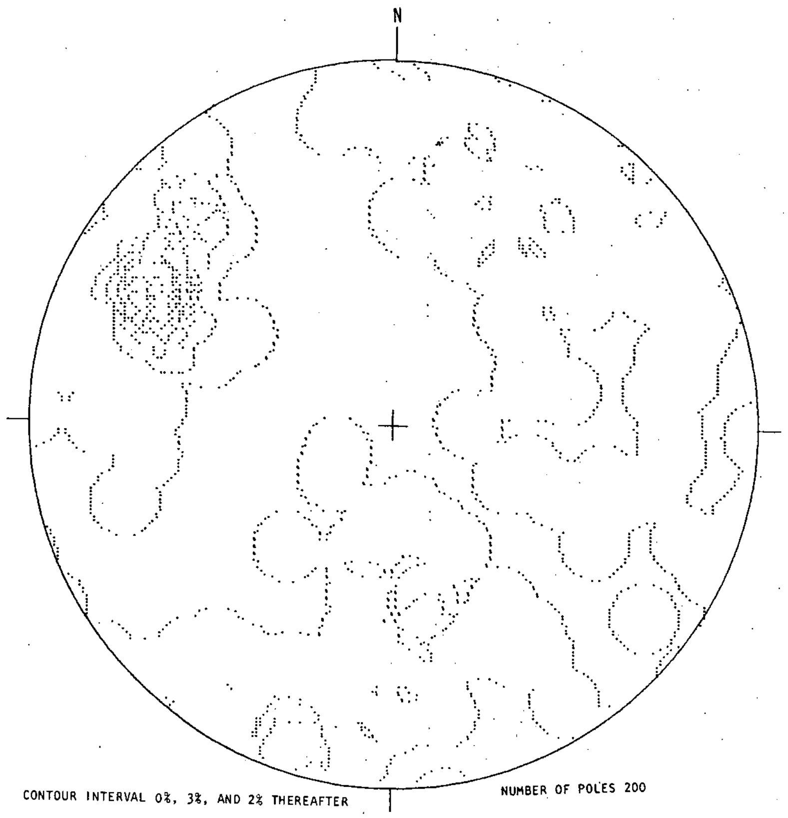

I.1.1 CONTOURED PLOT OF POLES TO FRACTURE PLANES

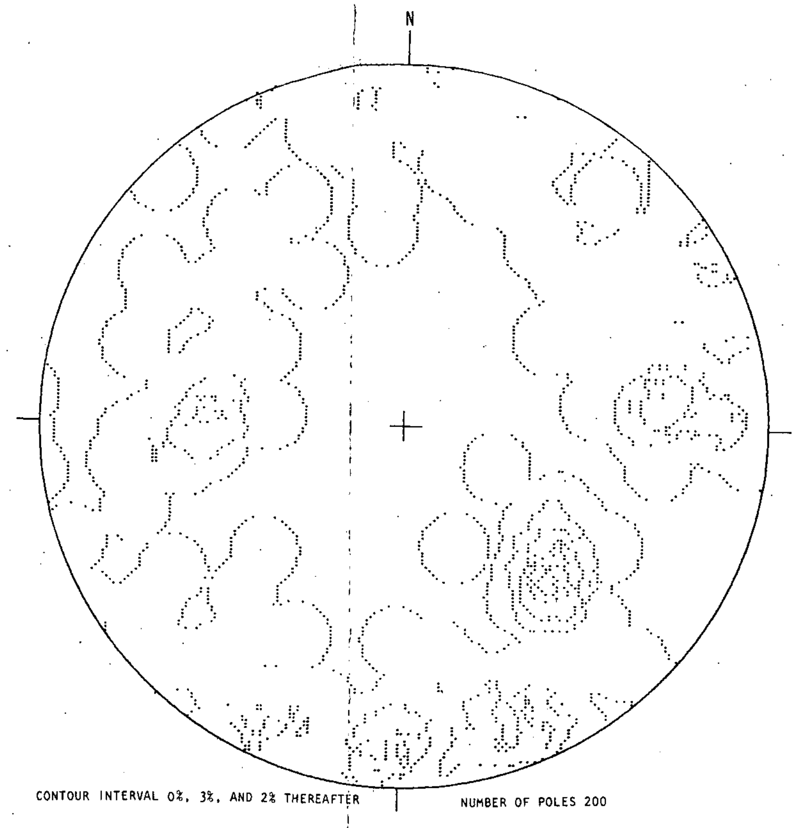

I.2.1.2 CONTOURED PLOT OF POLES TO FRACTURE PLANES (EAST WALL)

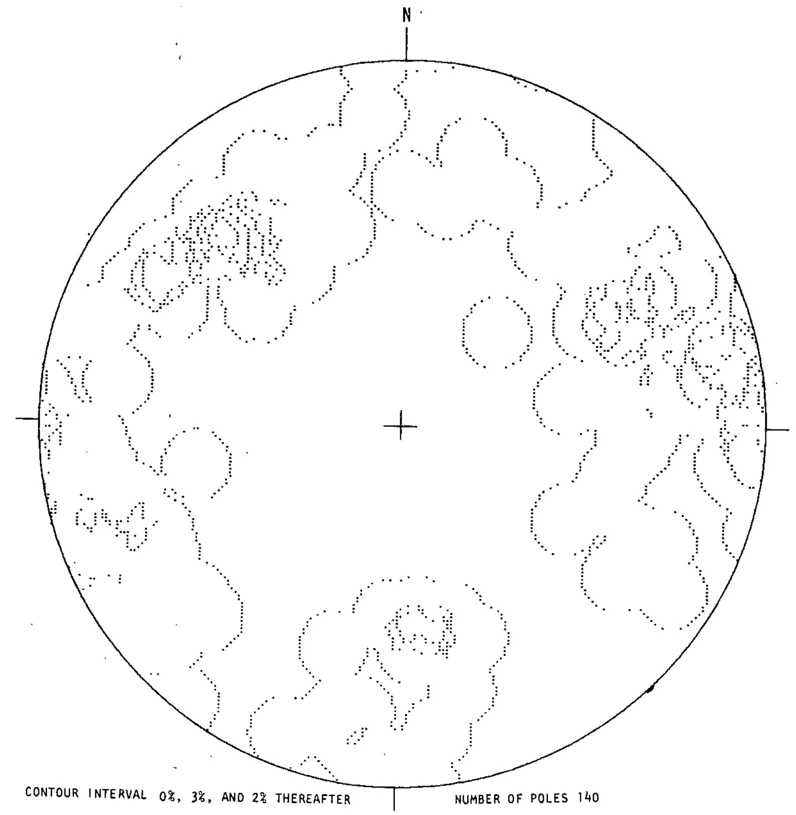

M.1.1 CONTOURED PLOT OF POLES TO FRACTURE PLANES

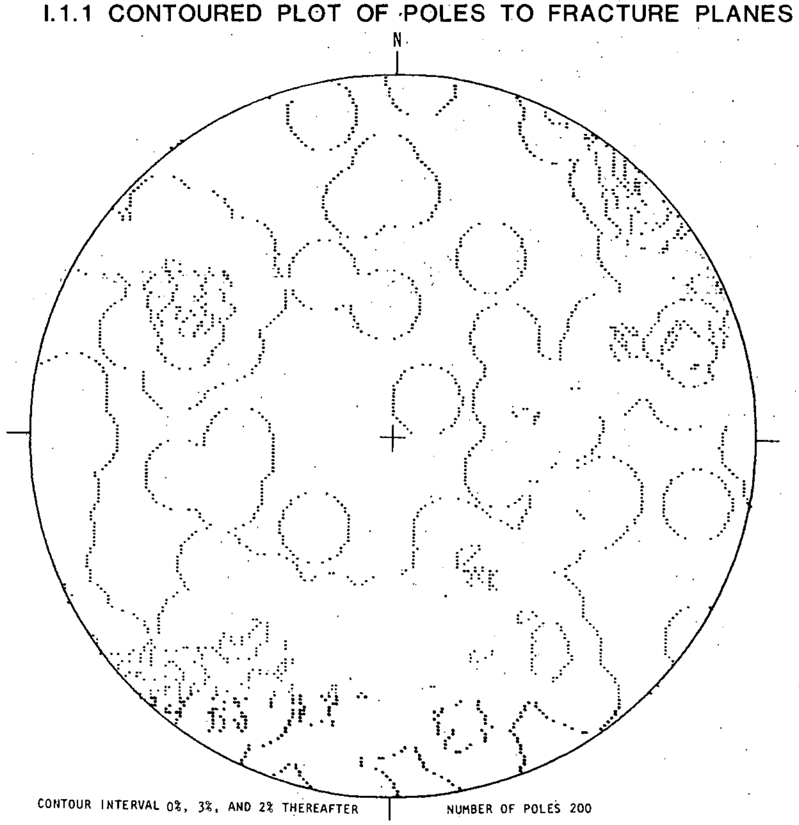

I.2.1.1 CONTOURED PLOT OF POLES TO FRACTURE PLANES

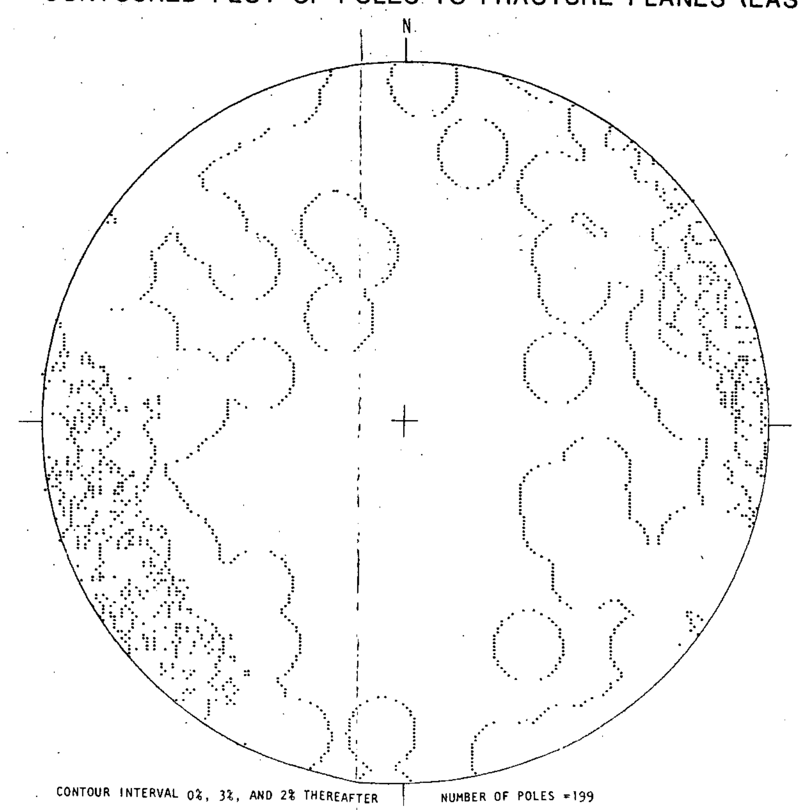

I.3.1 CONTOURED PLOT OF POLES TO FRACTURE PLANES

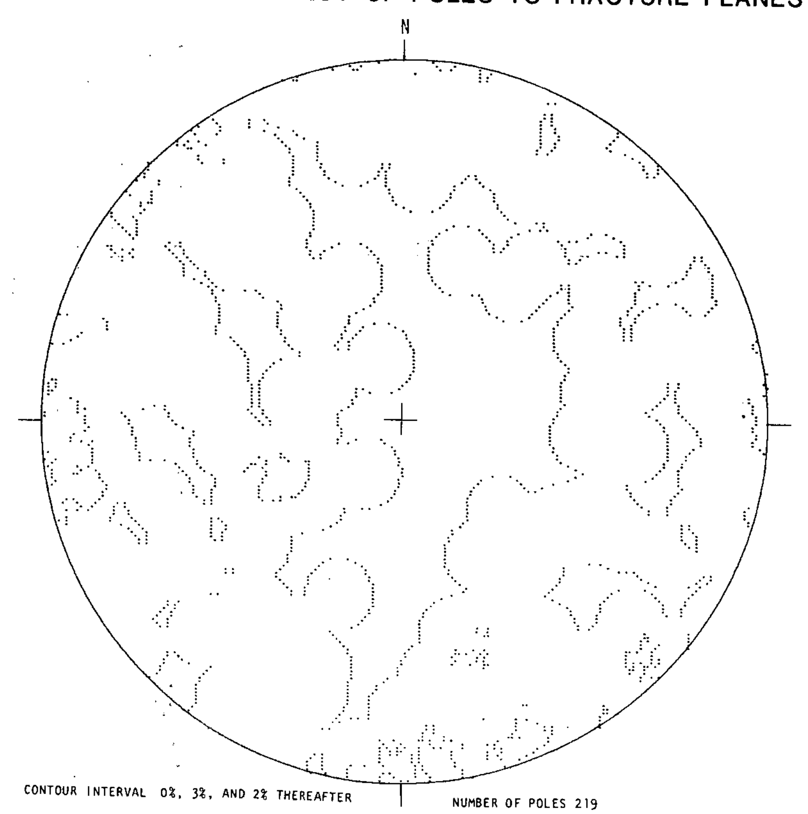

M.2.1 CONTOURED PLOT OF POLES TO FRACTURE PLANES

(LOWER HEMISPHERE EQUAL AREA PROJECTIONS)

CONTOURED PLOTS OF POLES TO FRACTURE PLANES FOR INWOOD - WAPPINGER AND MANHATTAN - ANNSVILLE OUTCROPS

NOTE: STATION LOCATION SHOWN ON PLATE B5.3-1

DAMES & MOORE

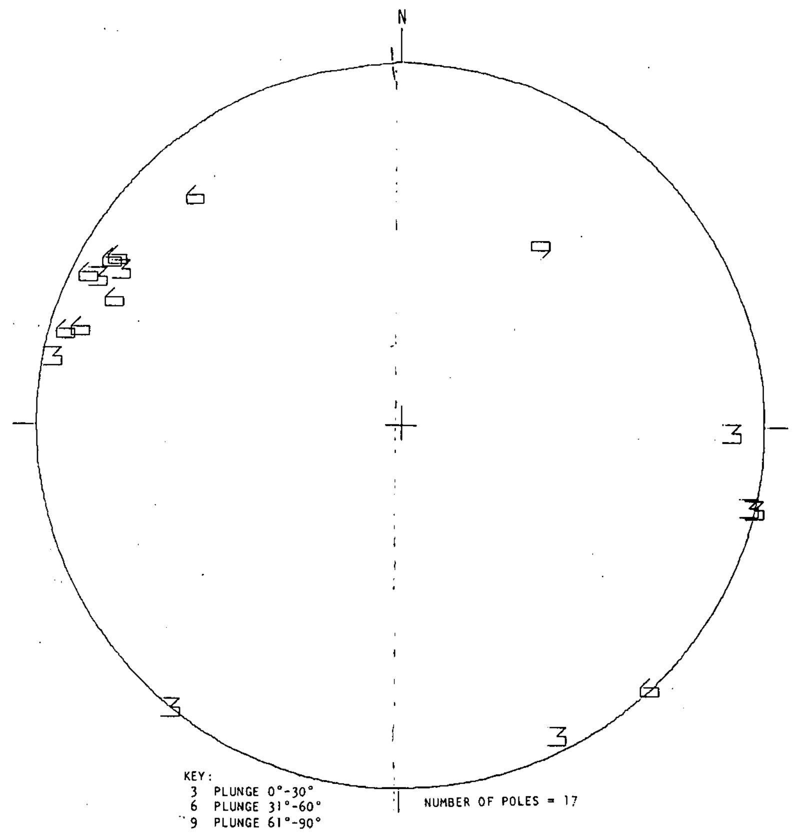

C.1.3 PLOT OF POLES TO SLICKENSIDED PLANES

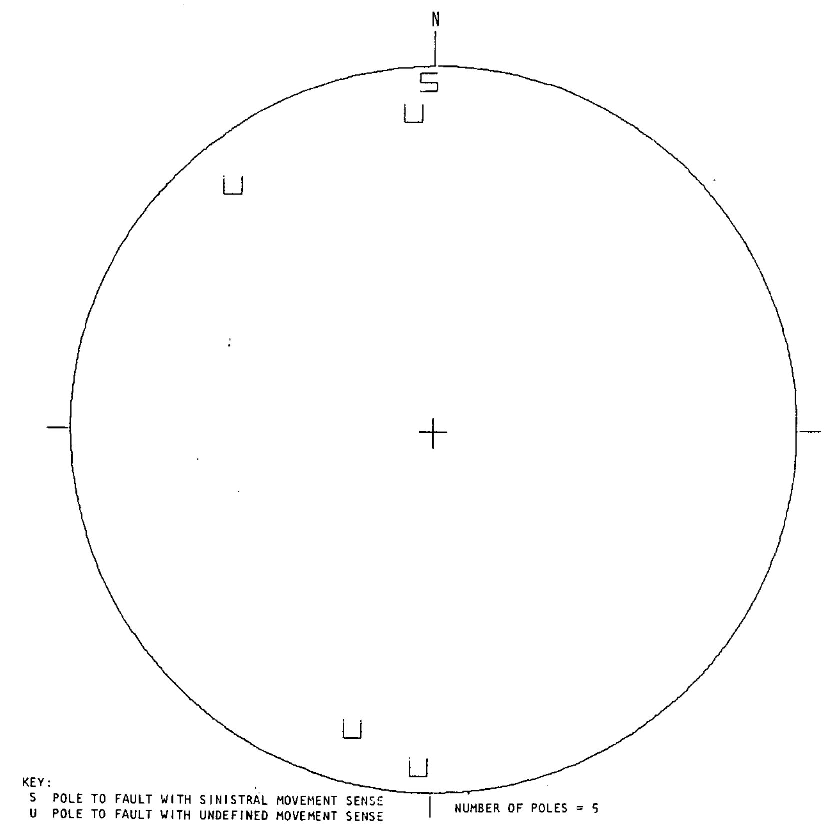

C.1.5 PLOT OF POLES TO FAULT PLANES

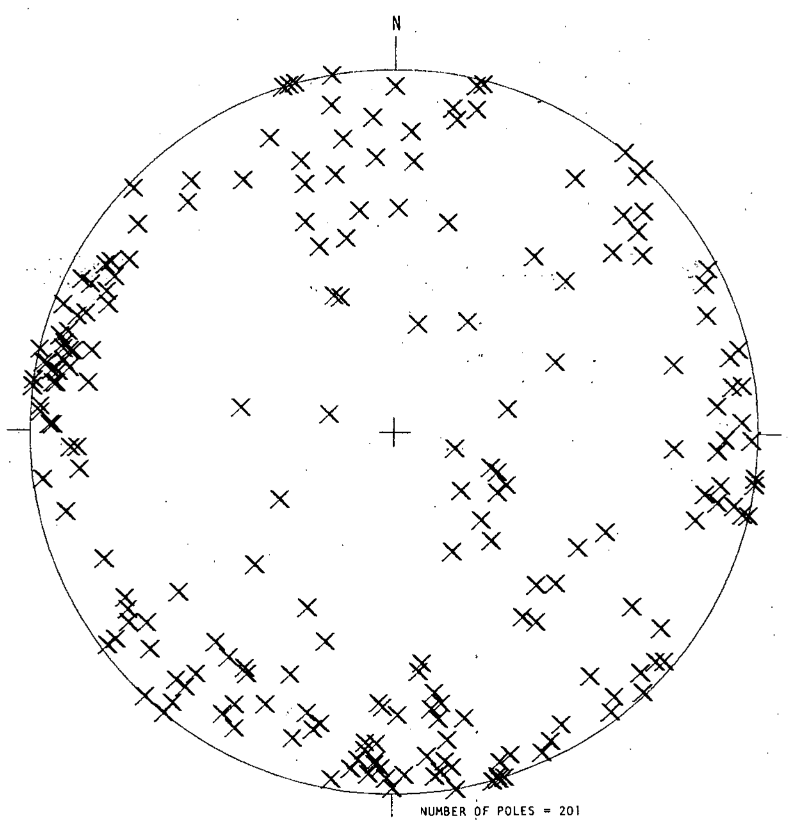

C.1.1 PLOT OF POLES TO ALL FRACTURE PLANES

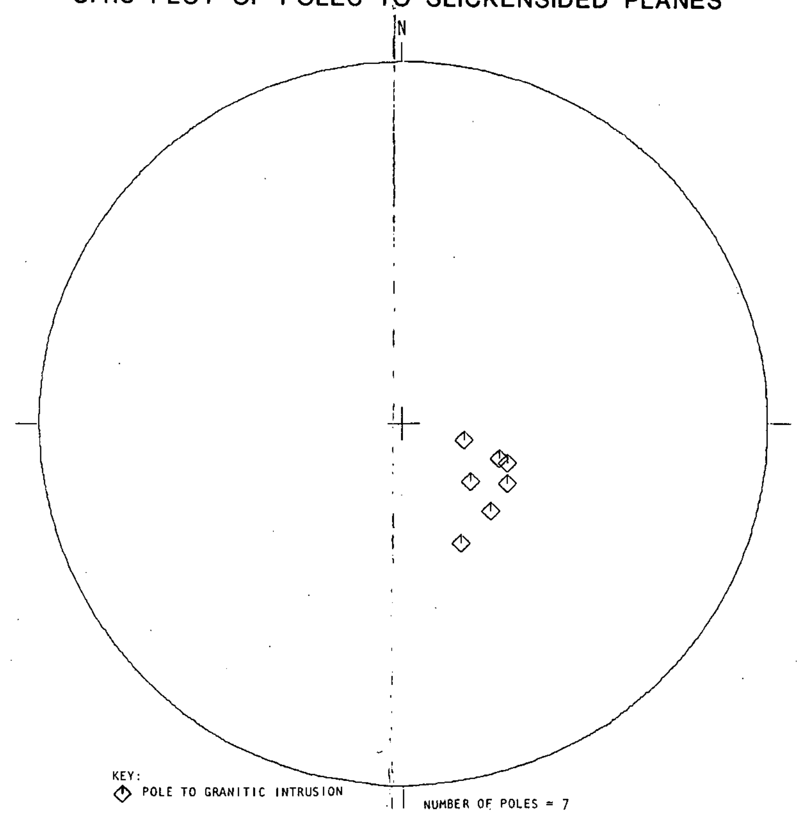

C.1.4 PLOT OF POLES TO MINERALIZED FRACTURE PLANES

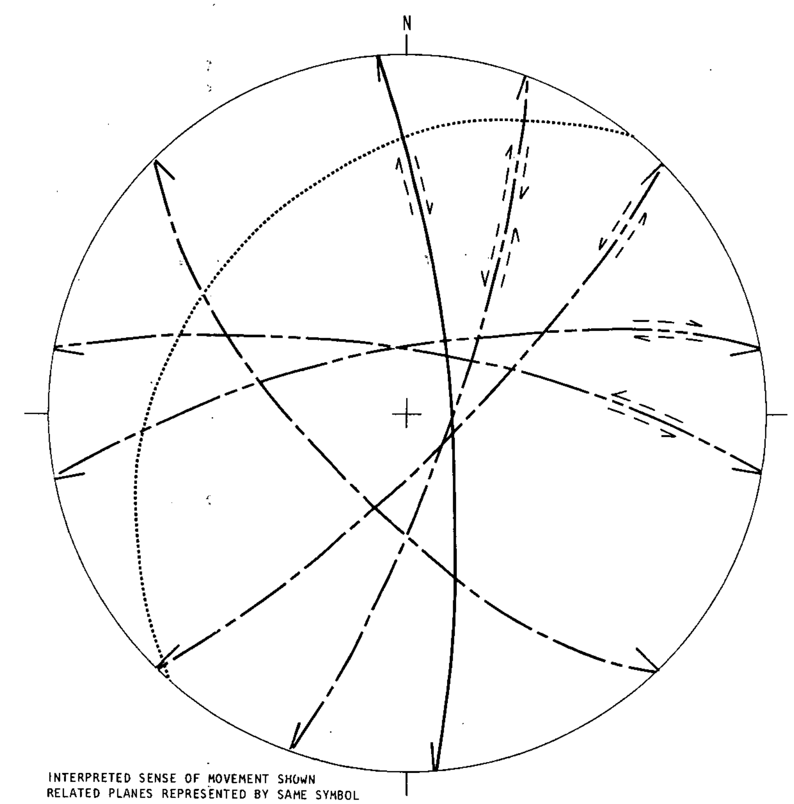

C.1.6 INTERPRETED FAULT AND FRACTURE GEOMETRY

NOTE: STATION LOCATION SHOWN ON PLATE B5.3-1

STRUCTURAL ELEMENTS
STATION C-1 CORTLANDT COMPLEX

(LOWER HEMISPHERE EQUAL AREA PROJECTIONS)

DAMES & MOORE

PLATE B5.3-11

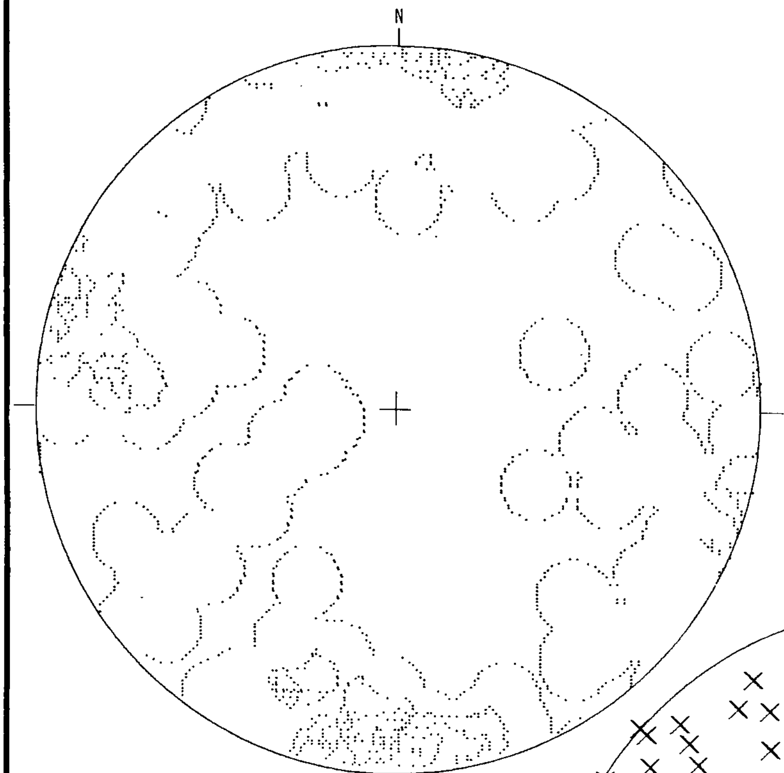

C.2.1 CONTOURED PLOT OF POLES TO FRACTURE PLANES

NOTE: STATION LOCATION SHOWN ON PLATE B5.3-1

CONTOUR INTERVAL 0%, 3%, AND 2% THEREAFTER ; NUMBER OF POLES = 202

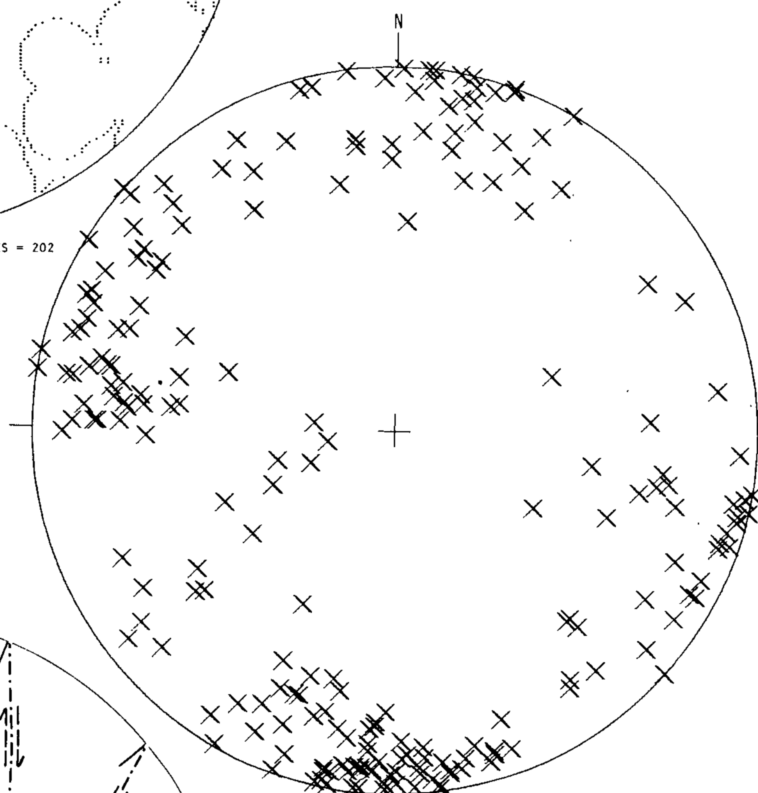

C.2.1 PLOT OF POLES TO ALL FRACTURE PLANES

NUMBER OF POLES = 202

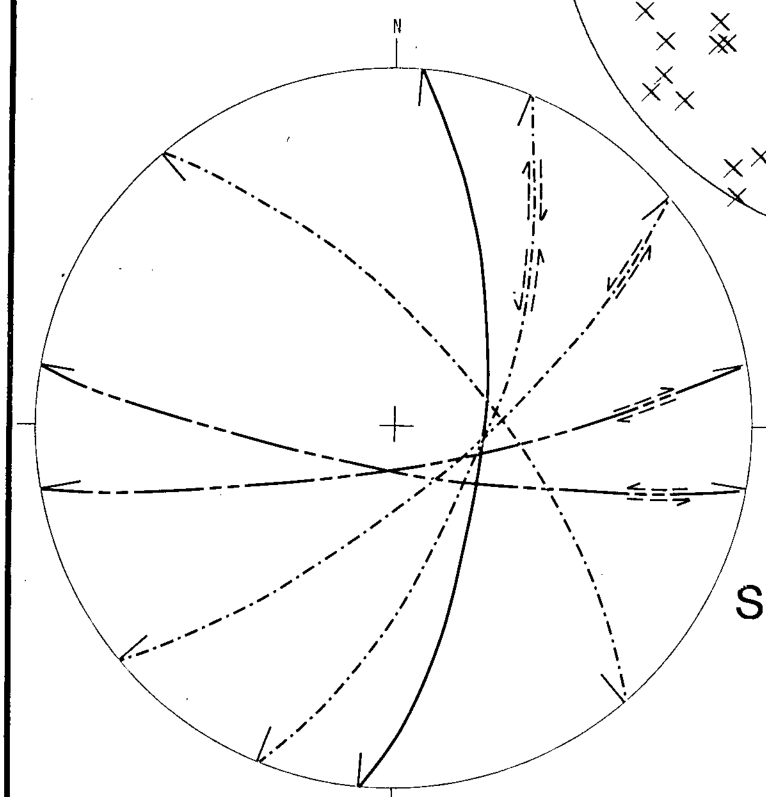

C.2.6 INTERPRETED FRACTURE AND FAULT GEOMETRY

INTERPRETED SENSES OF MOVEMENT SHOWN
RELATED PLANES REPRESENTED BY SAME SYMBOL

STRUCTURAL ELEMENTS
STATION C-2
CORTLANDT COMPLEX

(LOWER HEMISPHERE EQUAL AREA PROJECTIONS)

DAMES & MOORE

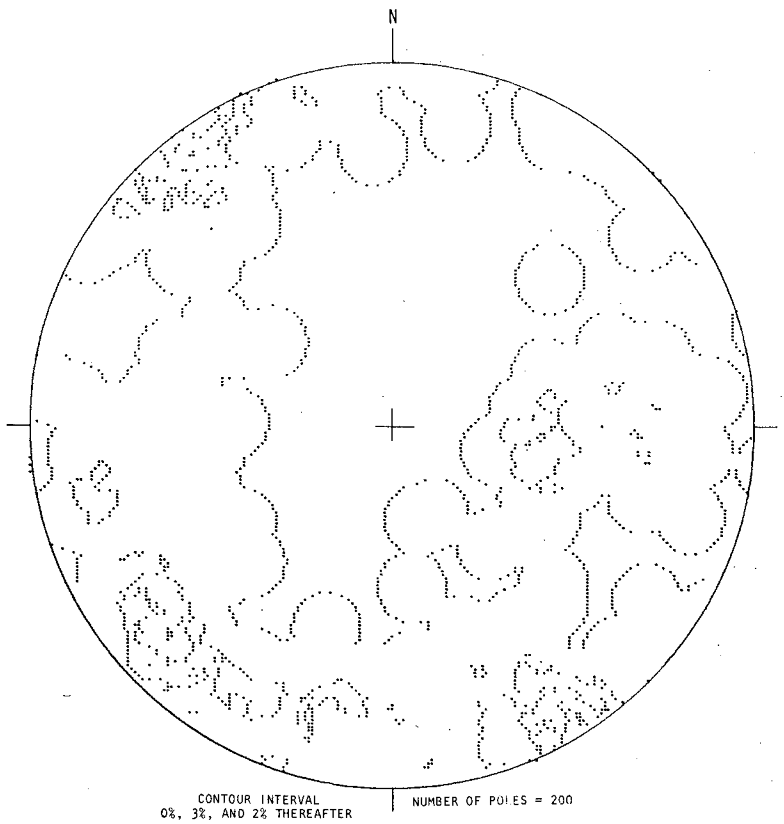

C.3.1 CONTOURED PLOT OF POLES TO FRACTURE PLANES

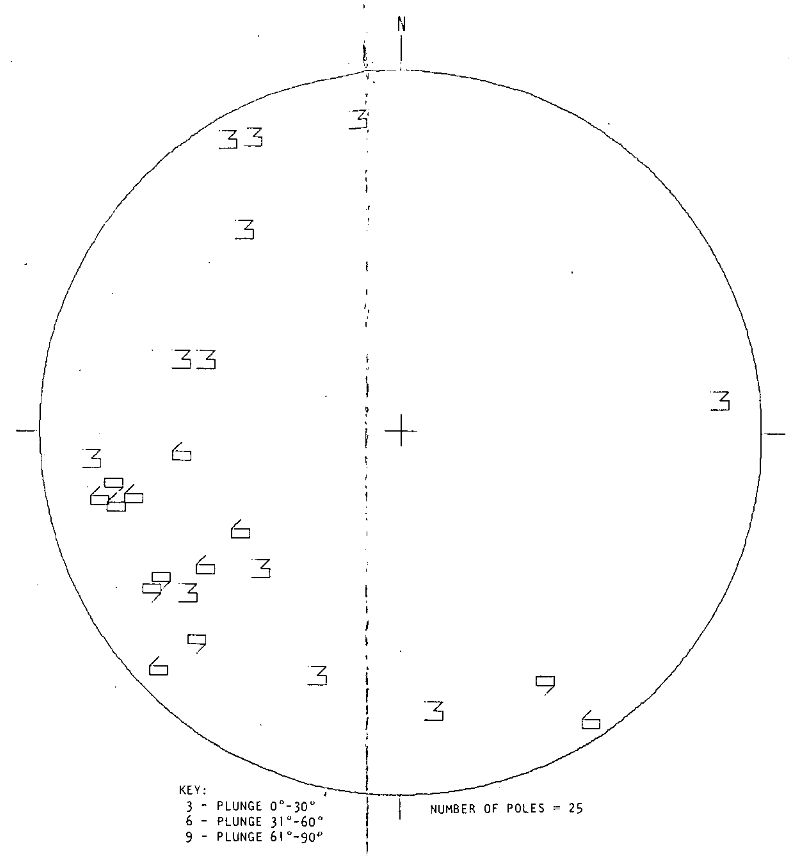

C.3.3 PLOT OF POLES TO SLICKENSIDED PLANES

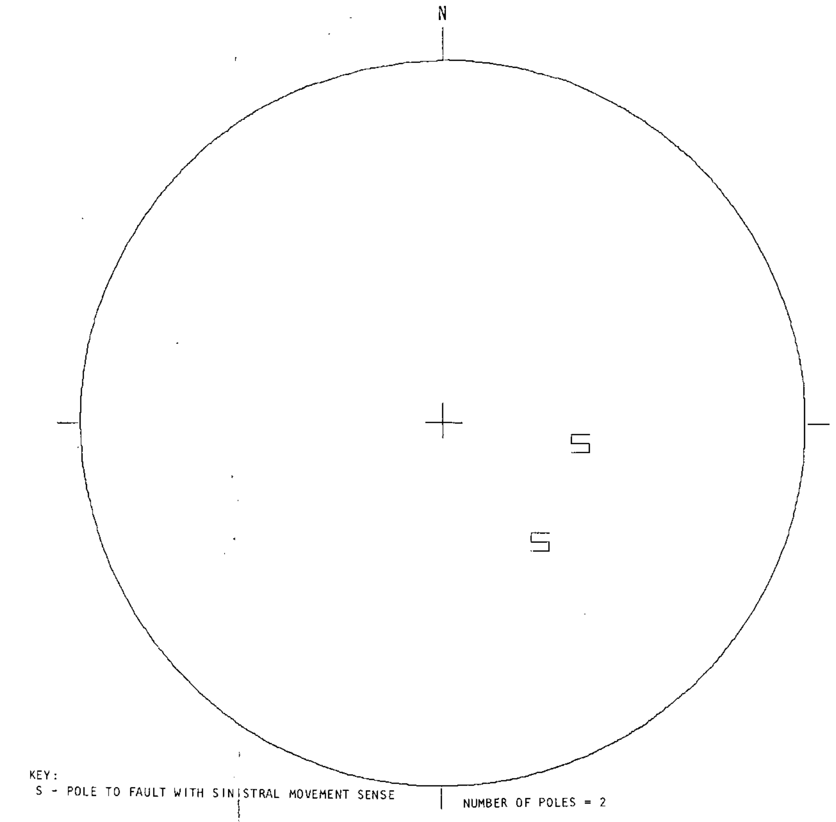

C.3.5 PLOT OF POLES TO FAULT PLANES

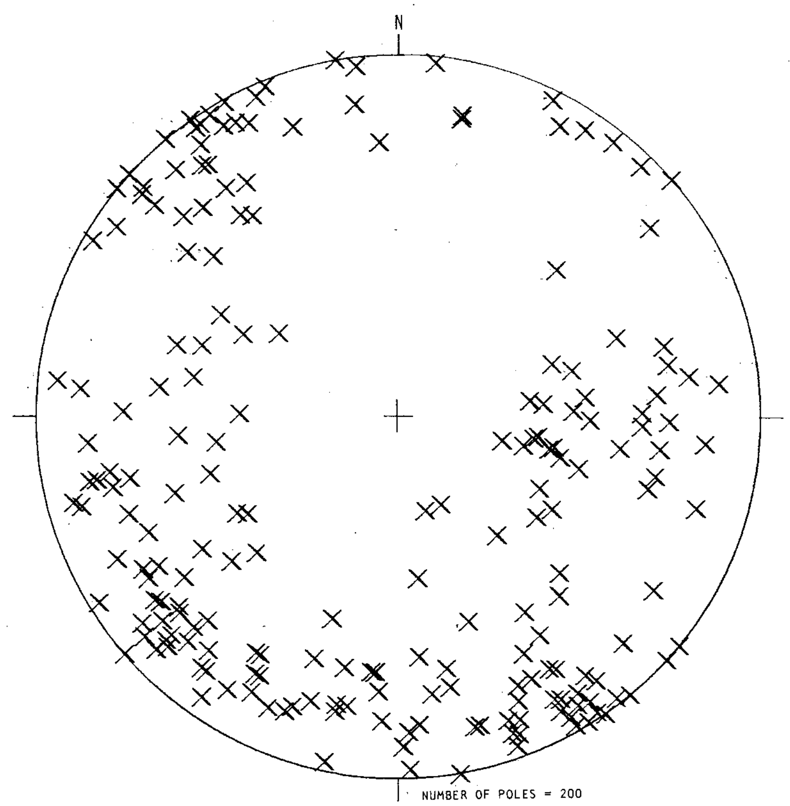

C.3.1 PLOT OF POLES TO ALL FRACTURE PLANES

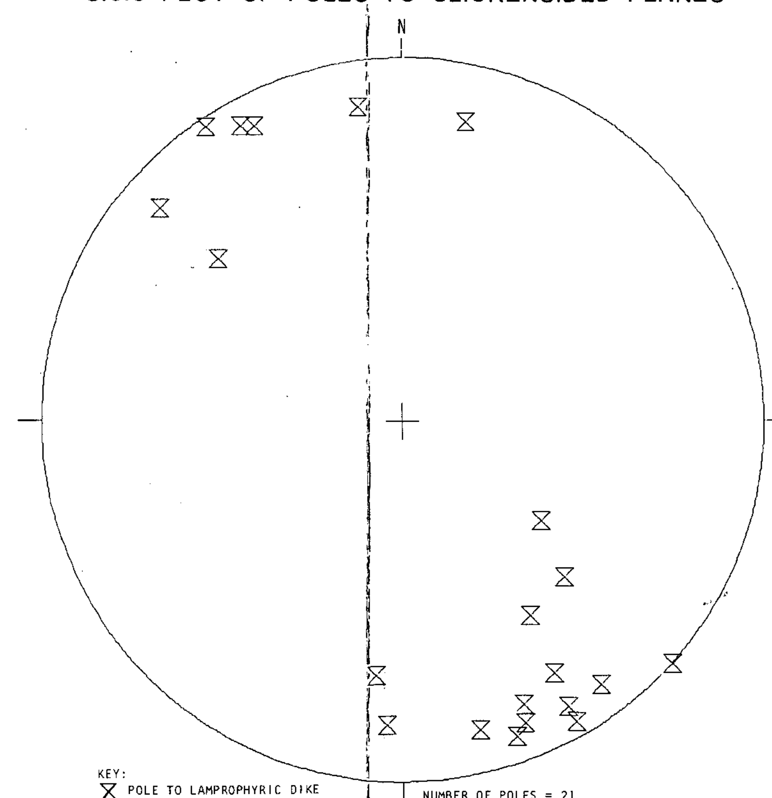

C.3.4 PLOT OF POLES TO MINERALIZED FRACTURE PLANES

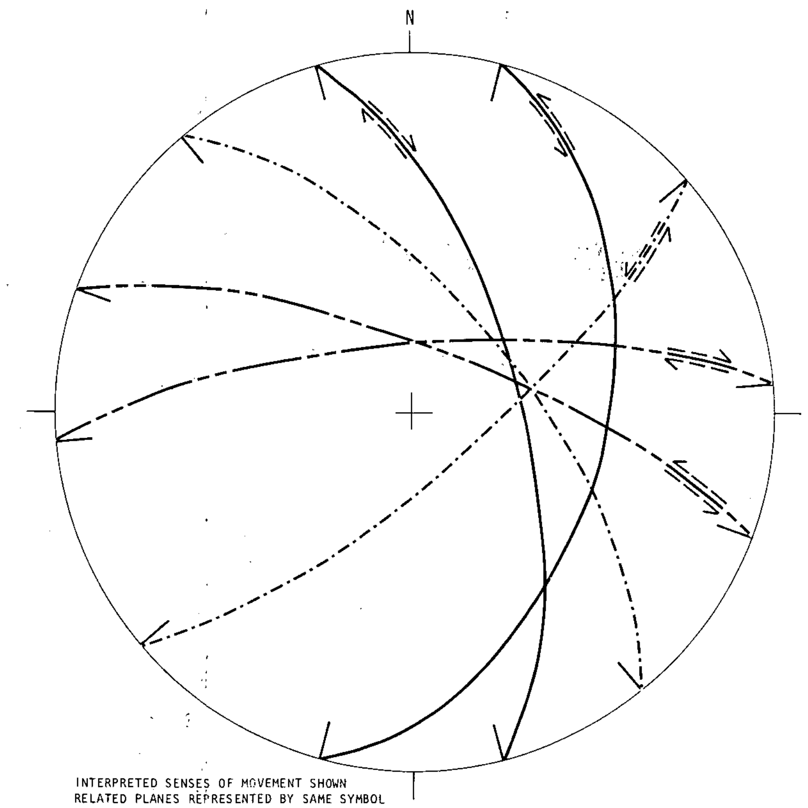

C.3.6 INTERPRETED FAULT AND FRACTURE GEOMETRY

NOTE: STATION LOCATION SHOWN ON PLATE B5.3-1

STRUCTURAL ELEMENTS
STATION C-3 CORTLANDT COMPLEX

(LOWER HEMISPHERE EQUAL AREA PROJECTIONS)

DAMES & MOORE

PLATE B5.3-13

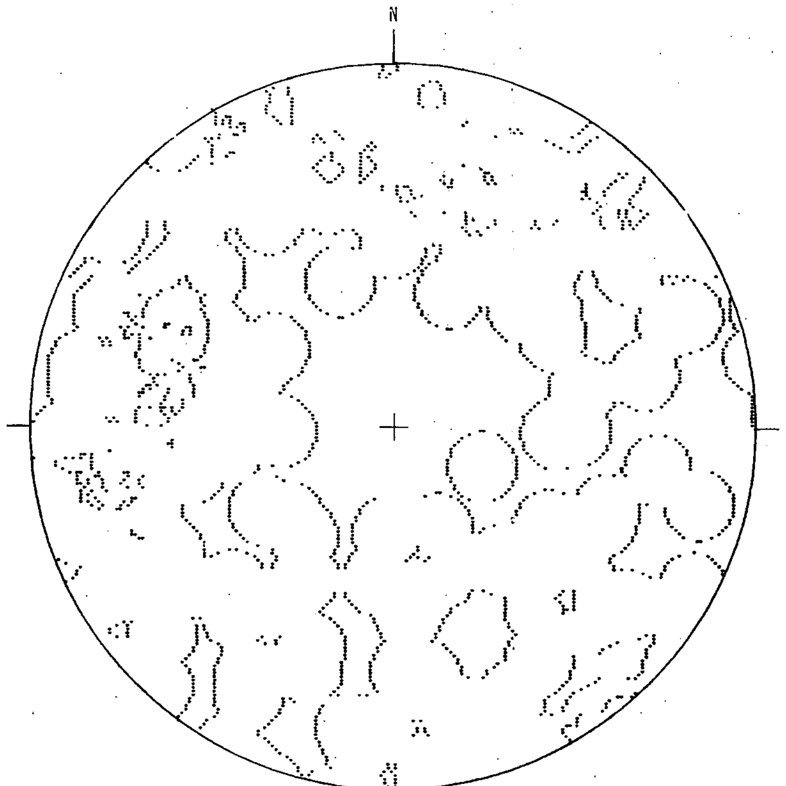

C.4.1 CONTOURED PLOT OF POLES TO FRACTURE PLANES

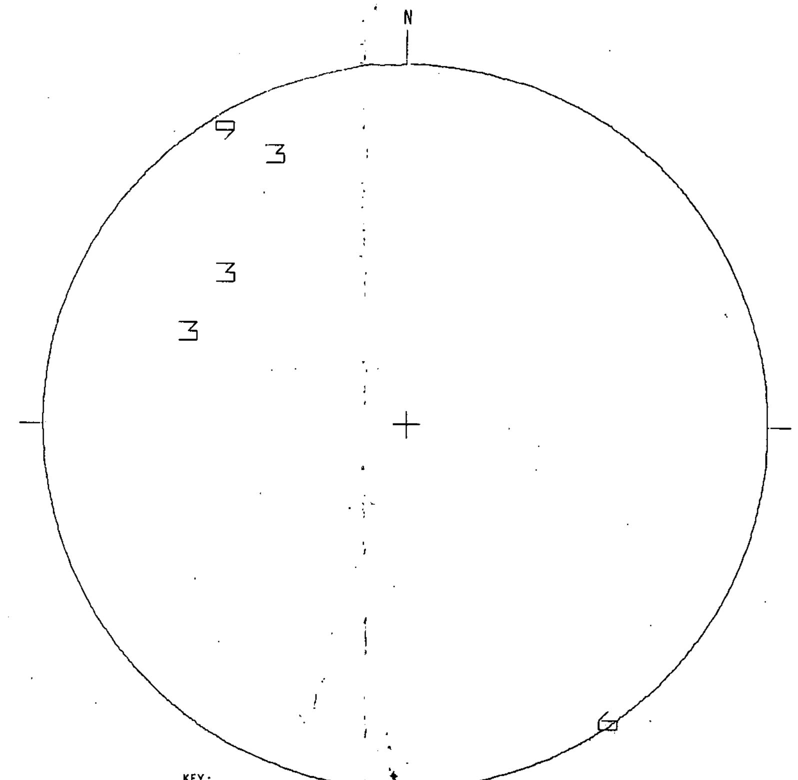

C.4.3 PLOT OF POLES TO SLICKENSIDED PLANES

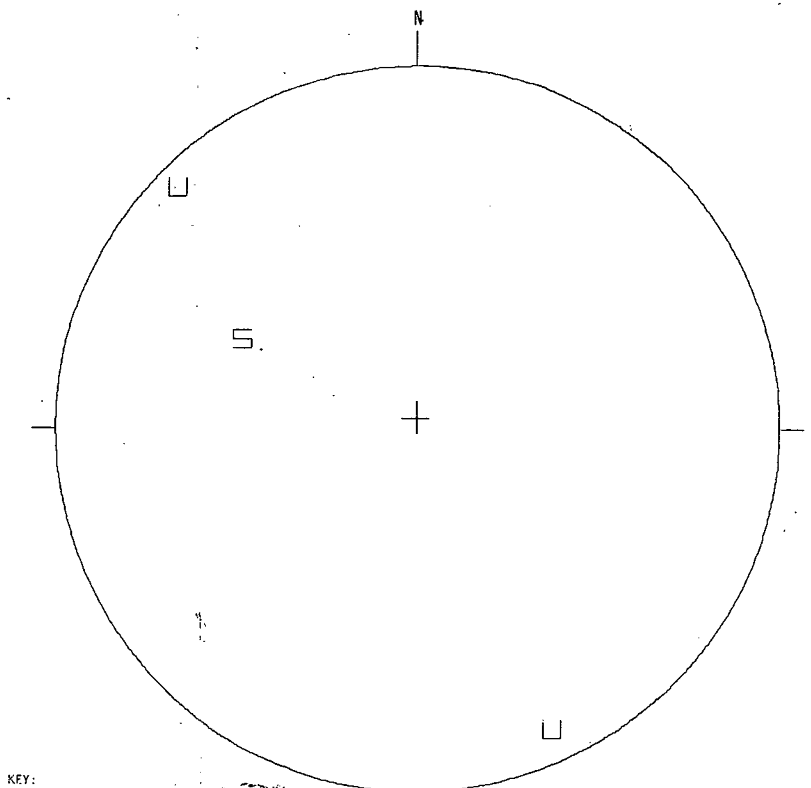

C.4.5 PLOT OF POLES TO FAULT PLANES

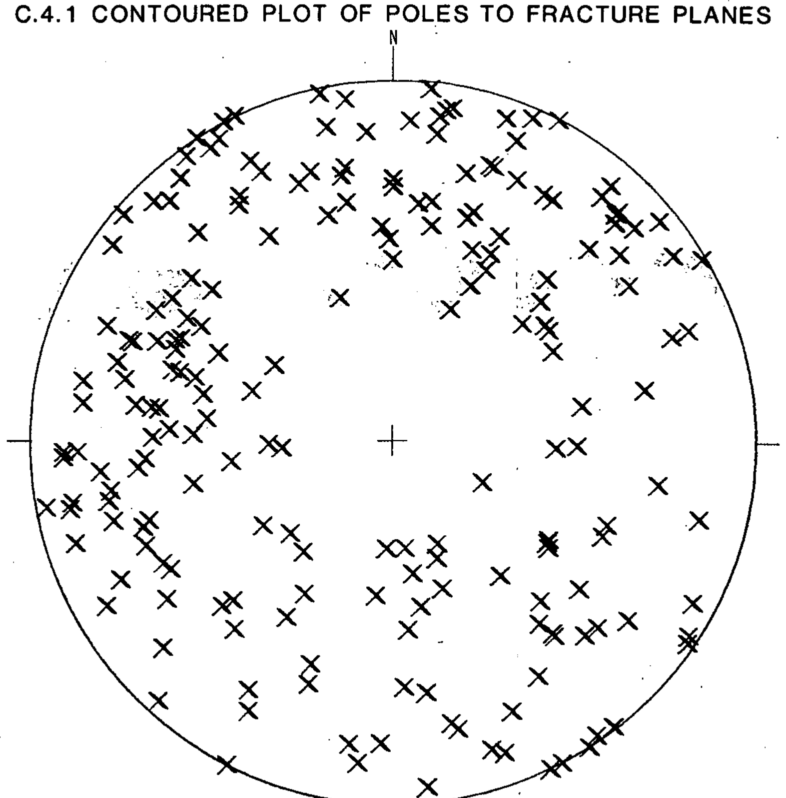

C.4.1 PLOT OF POLES TO ALL FRACTURE PLANES

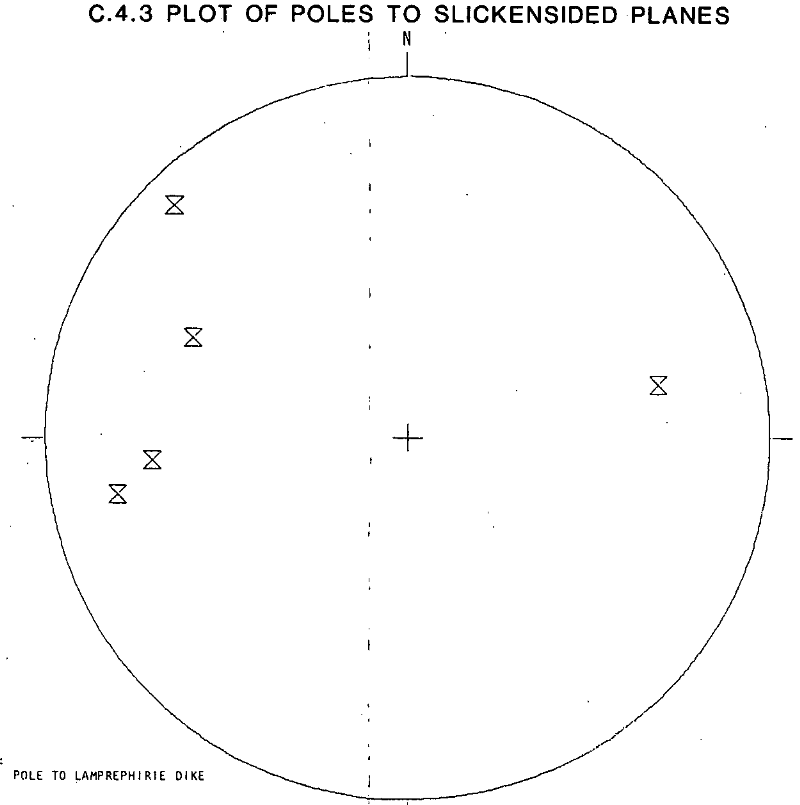

C.4.4 PLOT OF POLES TO MINERALIZED FRACTURE PLANES

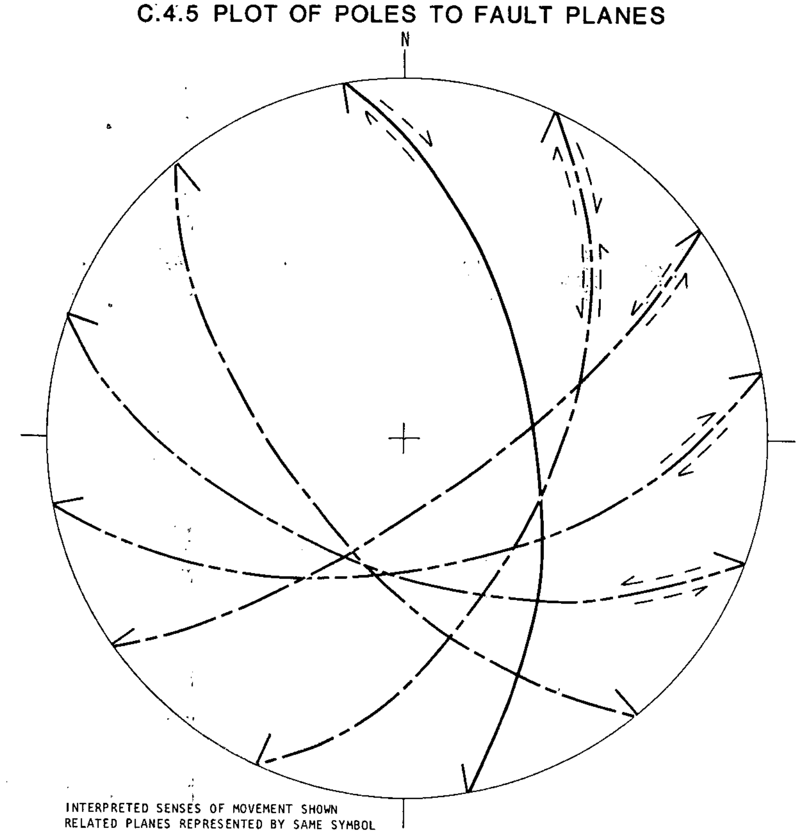

C.4.6 INTERPRETED FAULT AND FRACTURE GEOMETRY

NOTE: STATION LOCATION SHOWN ON PLATE B5.3-1

STRUCTURAL ELEMENTS
STATION C-4 CORTLANDT COMPLEX

(LOWER HEMISPHERE EQUAL AREA PROJECTIONS)

DAMES & MOORE

PLATE B5.3-14

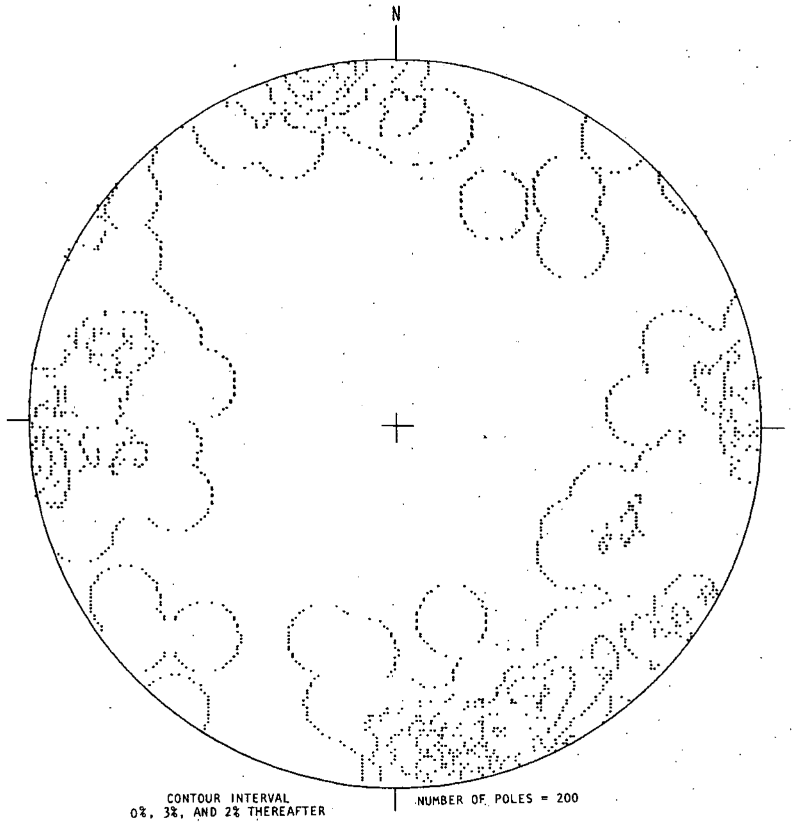

P.1.1 CONTOURED PLOT OF POLES TO FRACTURE PLANES

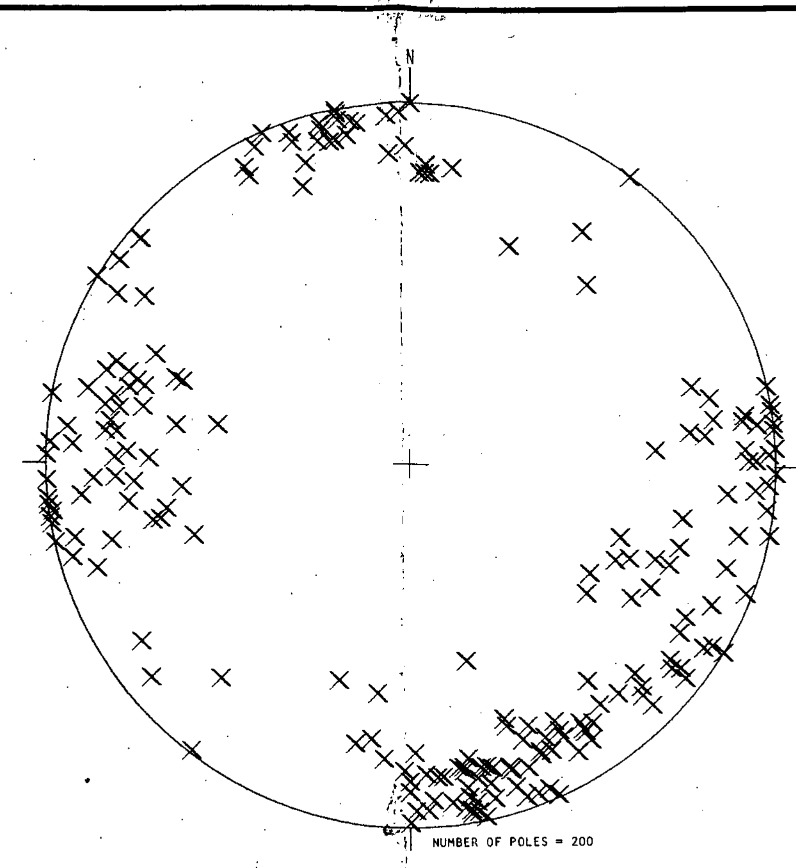

P.1.1 PLOT OF POLES TO ALL FRACTURE PLANES

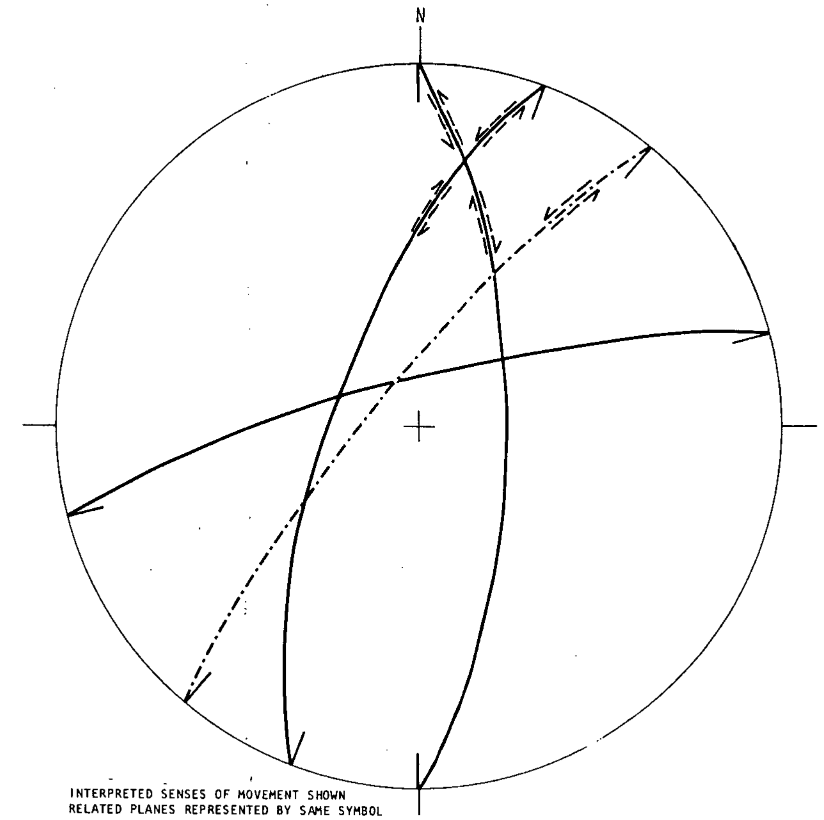

P.1.6 INTERPRETED FRACTURE AND FAULT GEOMETRY

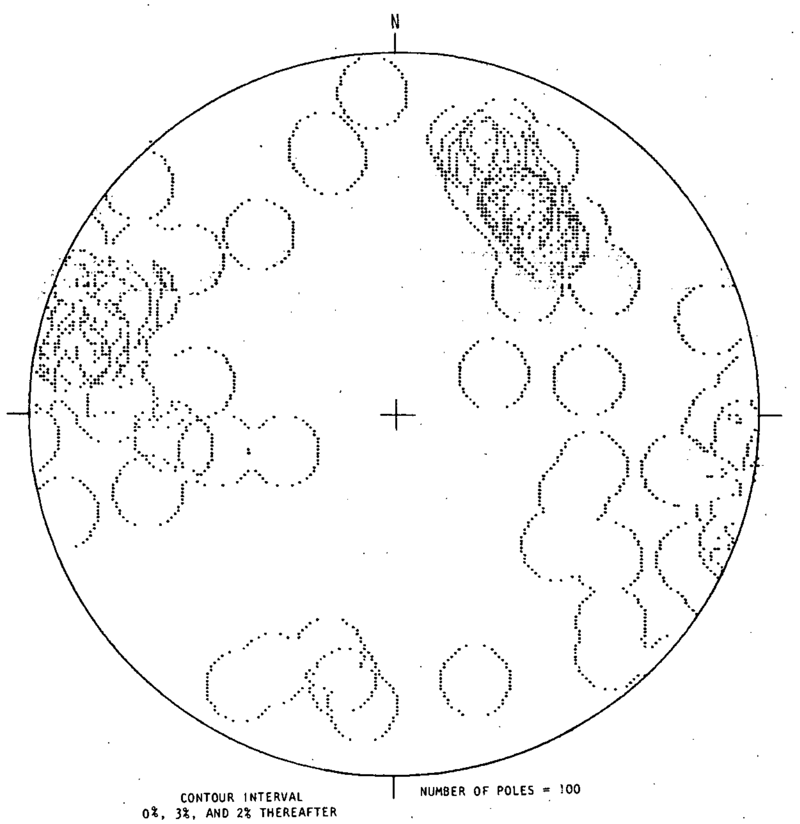

P.2.1 CONTOURED PLOT OF POLES TO FRACTURE PLANES

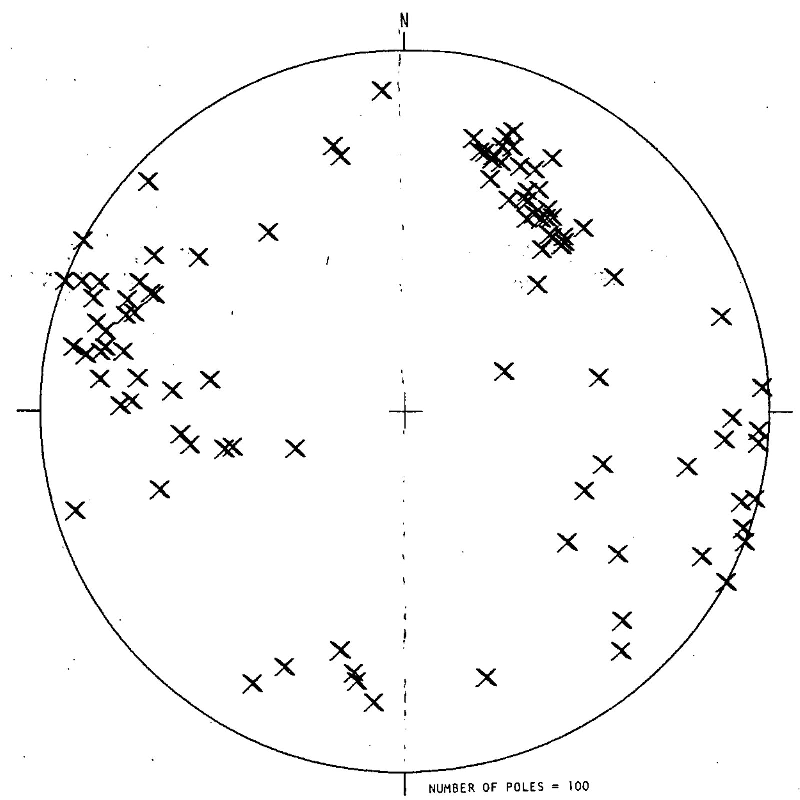

P.2.1 PLOT OF POLES TO ALL FRACTURE PLANES

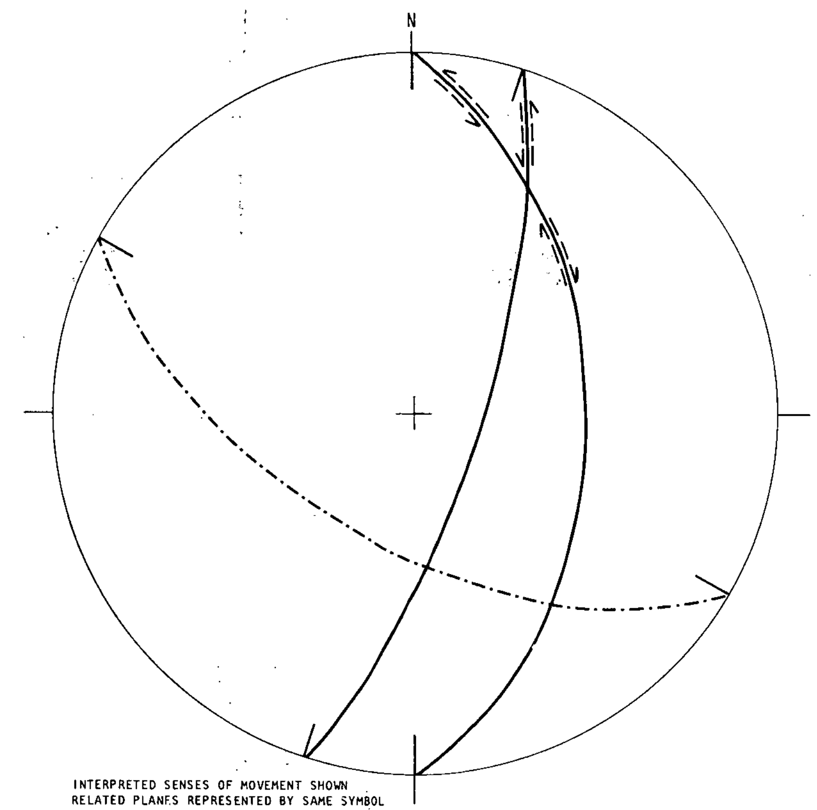

P.2.6 INTERPRETED FRACTURE AND FAULT GEOMETRY

NOTE: STATION LOCATION SHOWN ON PLATE B5.3-1

STRUCTURAL ELEMENTS
STATIONS P-1 AND P-2 PEEKSKILL GRANITE

(LOWER HEMISPHERE EQUAL AREA PROJECTIONS)

DAMES & MOORE

PLATE B5.3-15

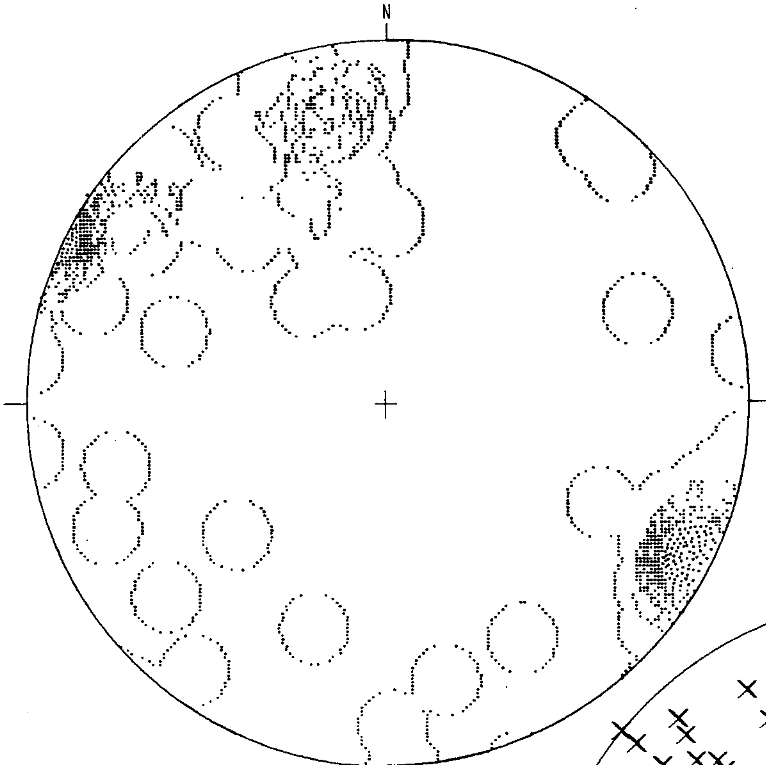

P.3.1 CONTOURED PLOT OF POLES TO FRACTURE PLANES

NOTE: STATION LOCATION SHOWN ON PLATE B5.3-1

CONTOUR INTERVAL 0%, 3%, AND 2% THEREAFTER

NUMBER OF POLES = 150

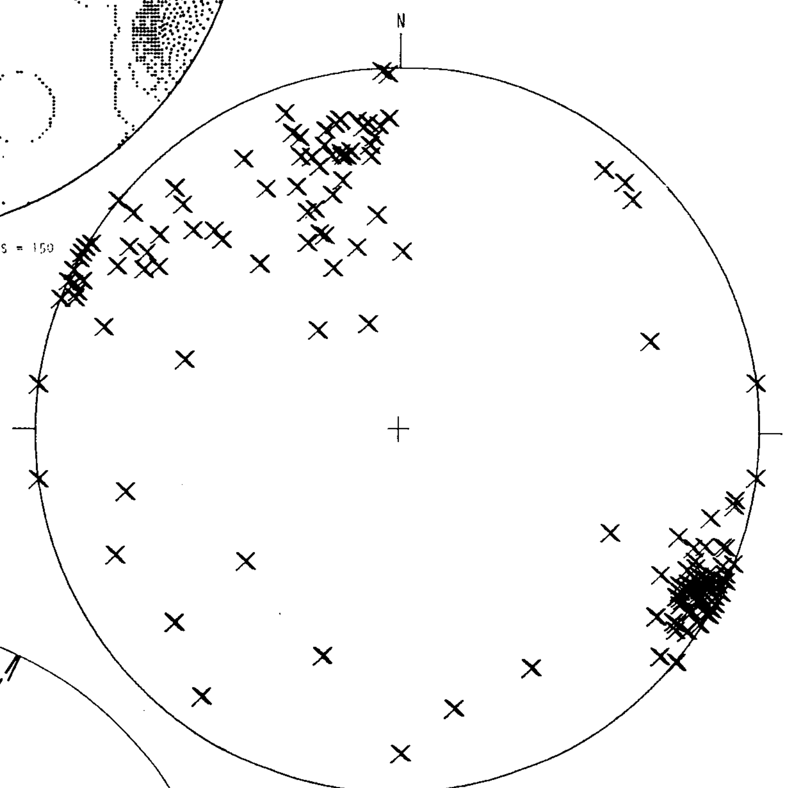

NUMBER OF POLES = 150

P.3.1 PLOT OF POLES TO ALL FRACTURE PLANES

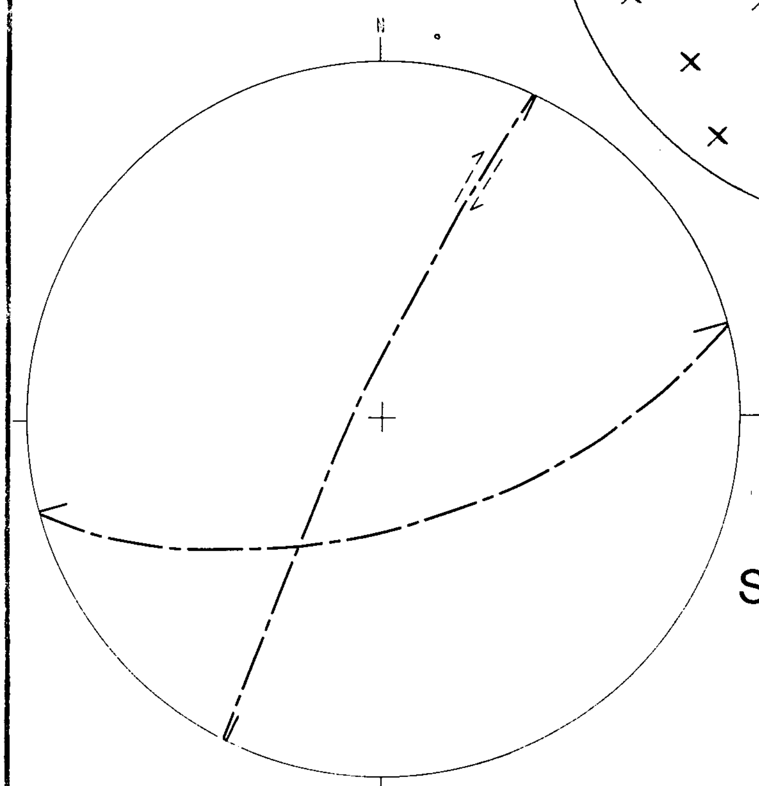

P.3.6 INTERPRETED FRACTURE AND FAULT GEOMETRY

INTERPRETED SENSES OF MOVEMENT SHOWN
RELATED PLANES REPRESENTED BY SAME SYMBOL

STRUCTURAL ELEMENTS
STATION P-3
PEEKSKILL GRANITE

(LOWER HEMISPHERE EQUAL AREA PROJECTIONS)

DAMES & MOORE

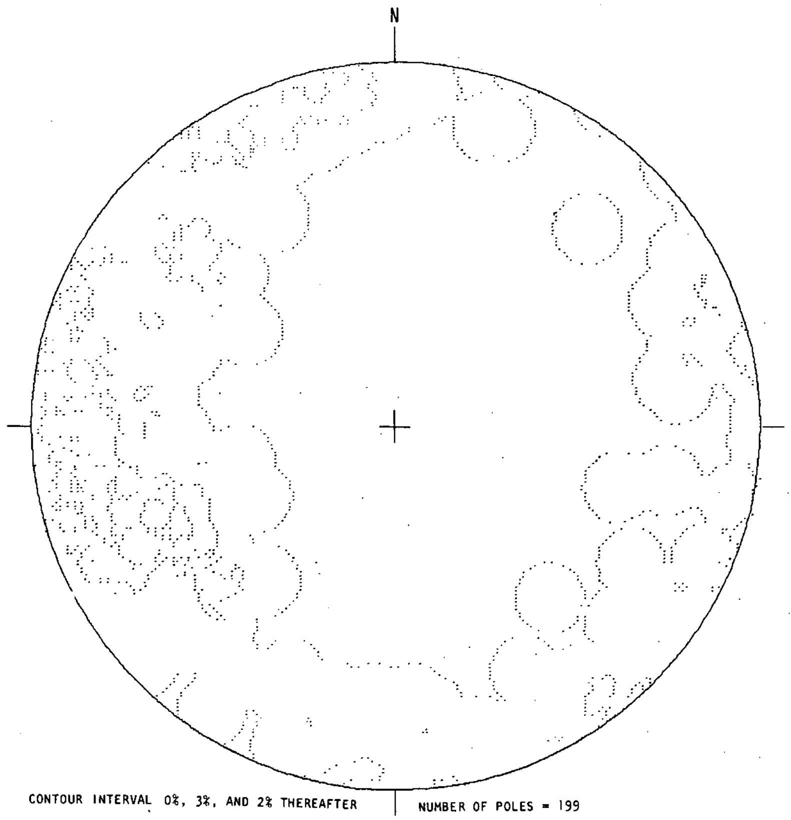

TR.1.1 CONTOURED PLOT OF POLES TO FRACTURE PLANES

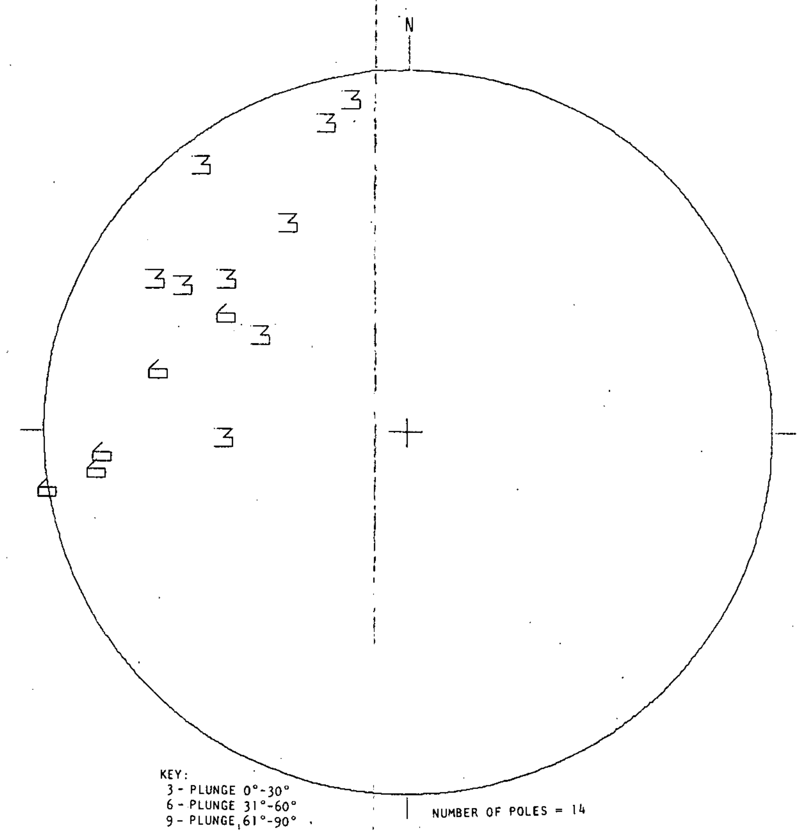

TR.1.3 PLOT OF POLES TO SLICKENSIDED PLANES

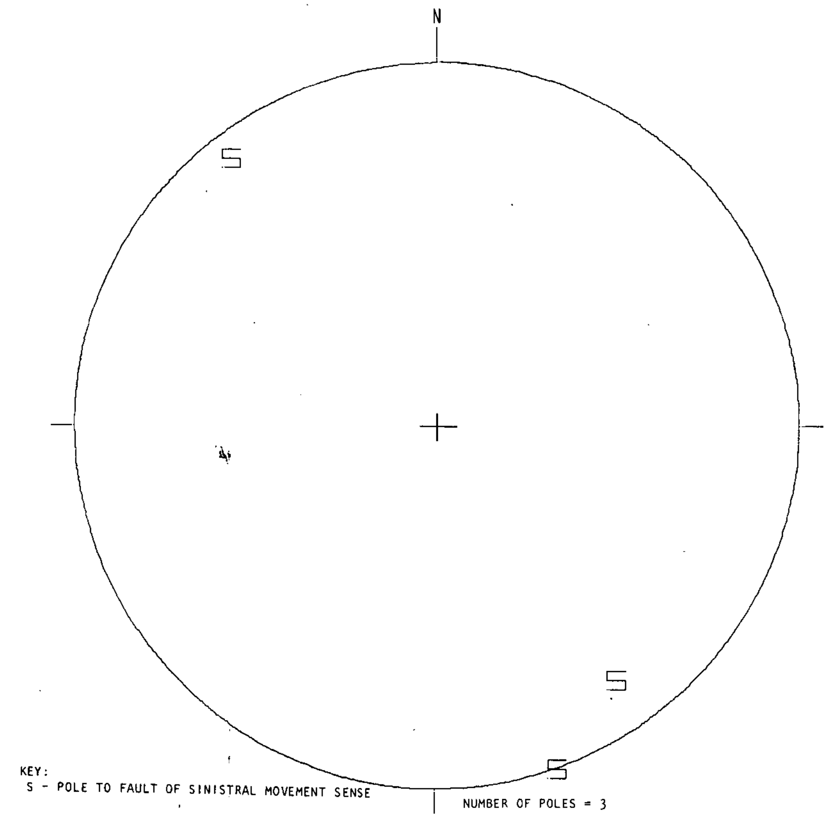

TR.1.5 PLOT OF POLES TO FAULT PLANES

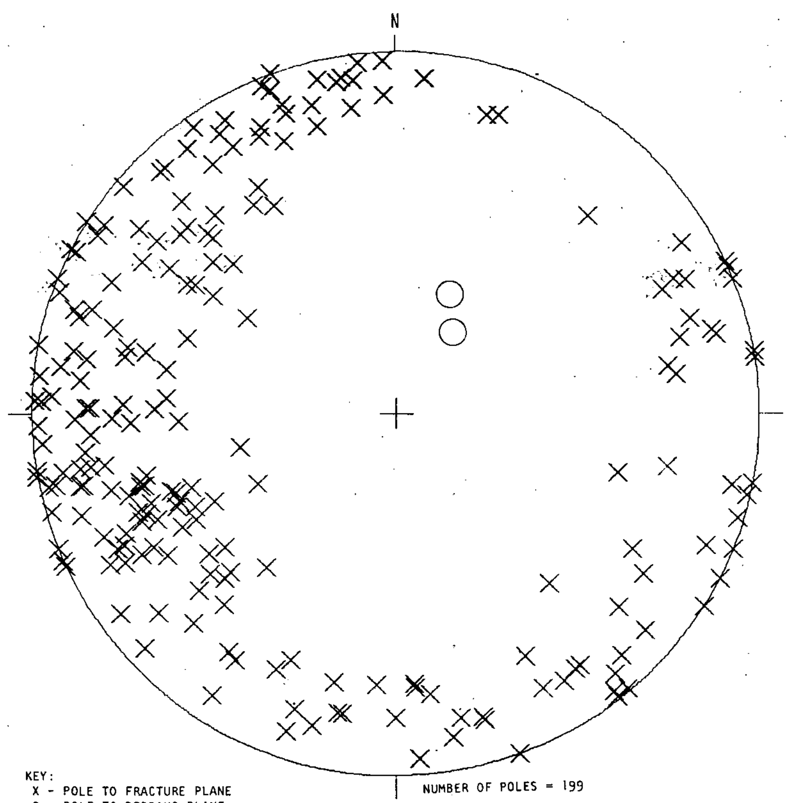

TR.1.1 PLOT OF POLES TO ALL FRACTURE PLANES

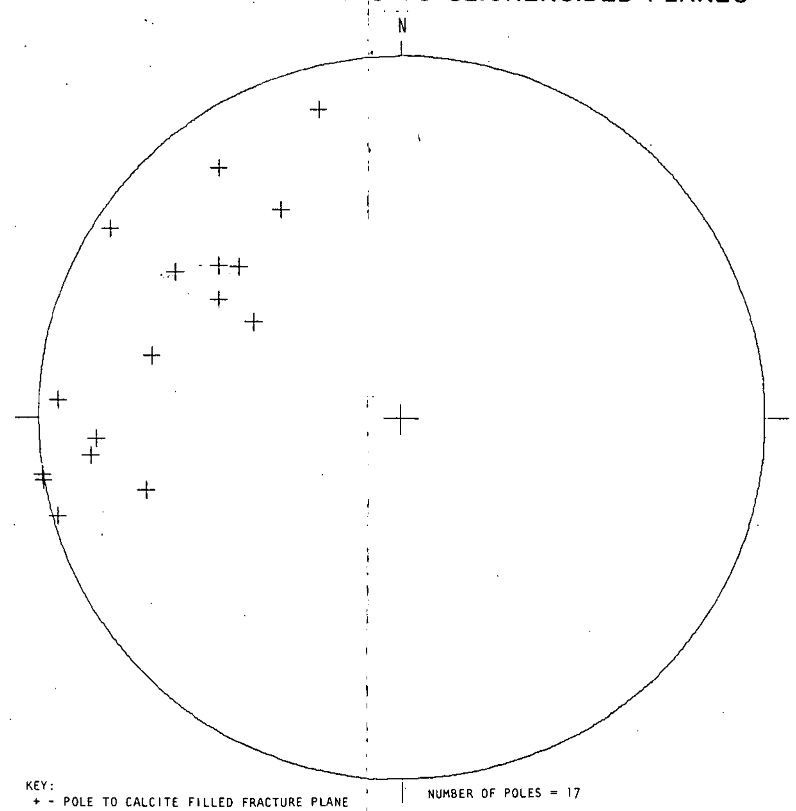

TR.1.4 PLOT OF POLES TO MINERALIZED FRACTURE PLANES

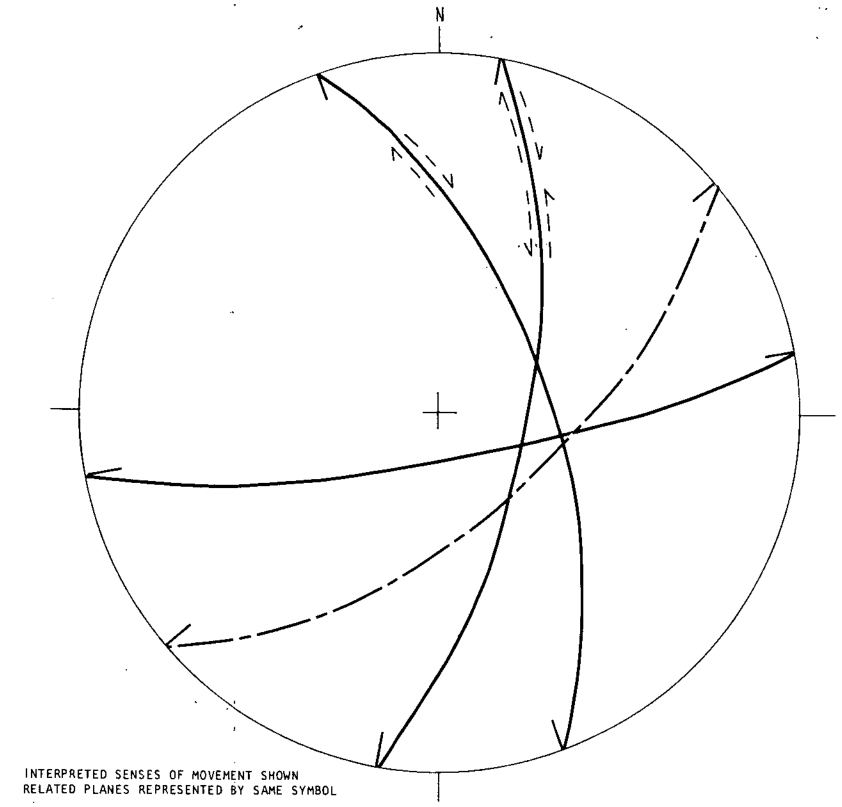

TR.1.6 INTERPRETED FRACTURE AND FAULT GEOMETRY

NOTE: STATION LOCATION SHOWN ON PLATE B5.3-1

STRUCTURAL ELEMENTS
STATIONS TR-1 TRIASSIC SEDIMENTARY ROCKS

(LOWER HEMISPHERE EQUAL AREA PROJECTIONS)

DAMES & MOORE

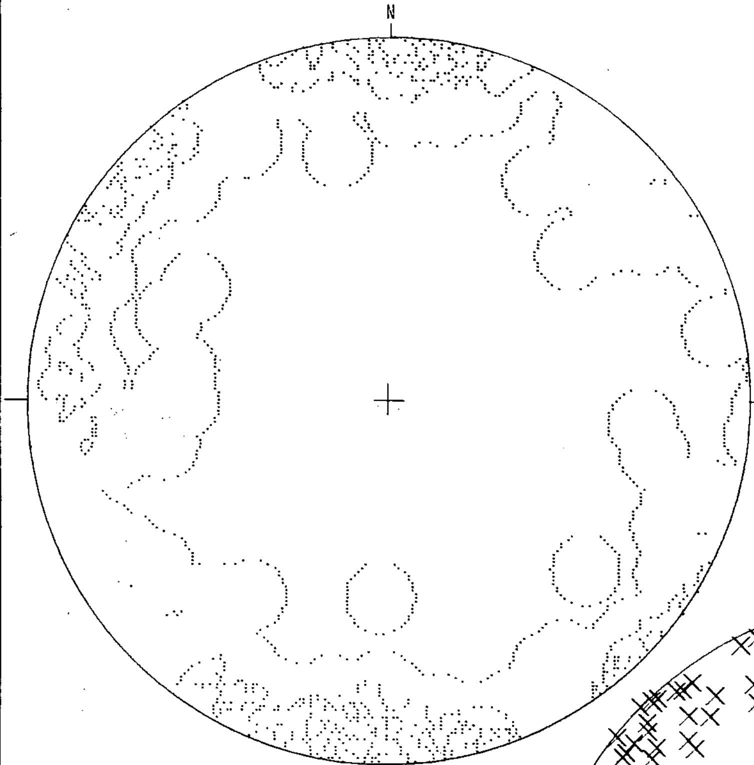

CONTOUR INTERVAL 0%, 3%, AND 2% THEREAFTER

NUMBER OF POLES = 200

TR.2.1 CONTOURED PLOT OF POLES TO FRACTURE PLANES

NOTE: STATION LOCATION SHOWN ON PLATE B5.3-1

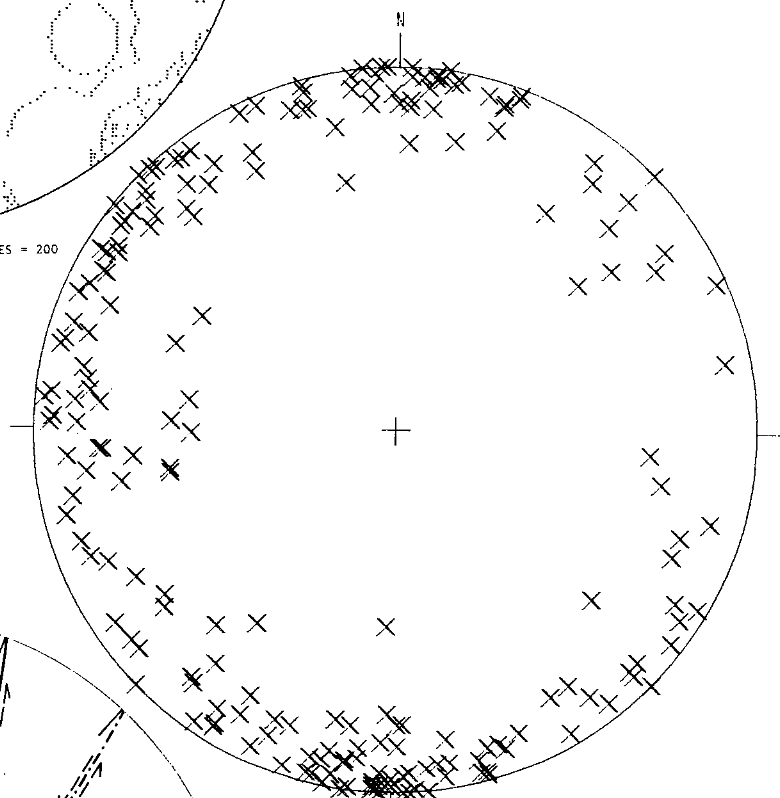

NUMBER OF POLES = 200

TR.2.1 PLOT OF POLES TO ALL FRACTURE PLANES

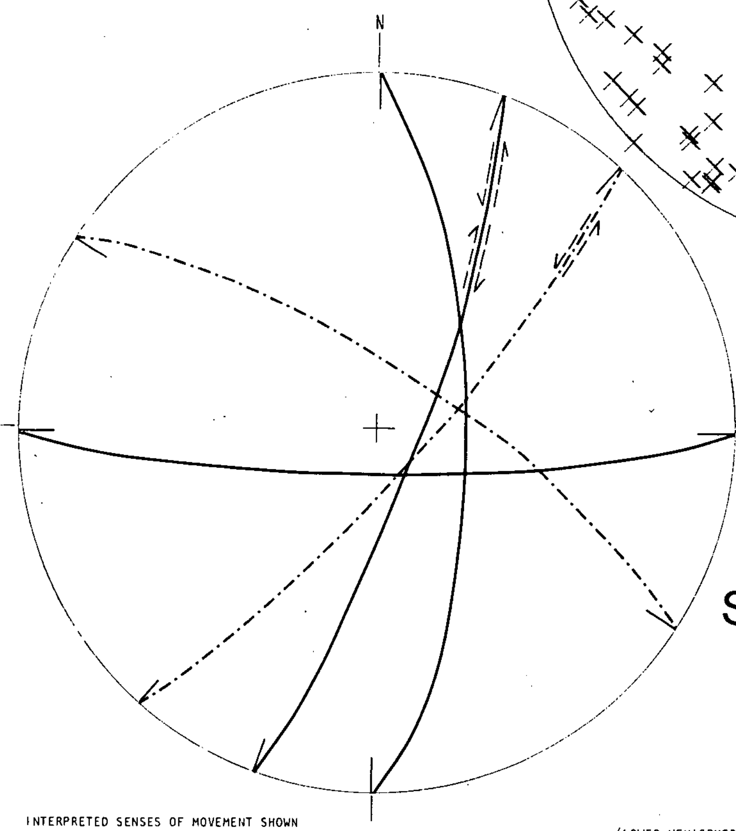

TR.2.6 INTERPRETED FRACTURE AND FAULT GEOMETRY

STRUCTURAL ELEMENTS
STATION TR-2
TRIASSIC SEDIMENTARY ROCKS

INTERPRETED SENSES OF MOVEMENT SHOWN
RELATED PLANES REPRESENTED BY SAME SYMBOL

(LOWER HEMISPHERE EQUAL AREA PROJECTIONS)

DAMES & MOORE

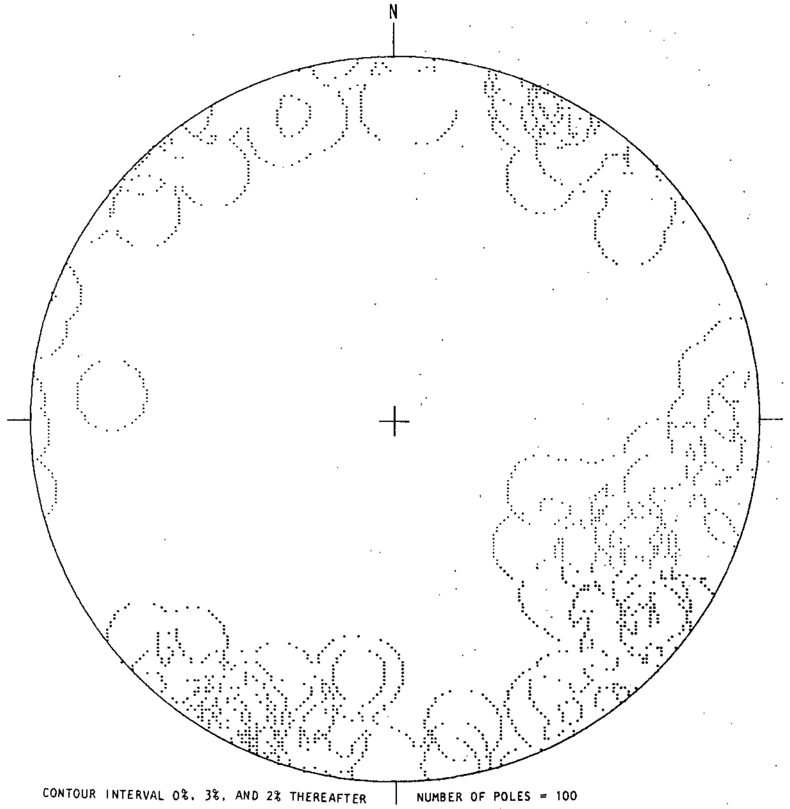

TR.3.1.1 CONTOURED PLOT OF POLES TO FRACTURE PLANES (SEDIMENTARY ROCKS)

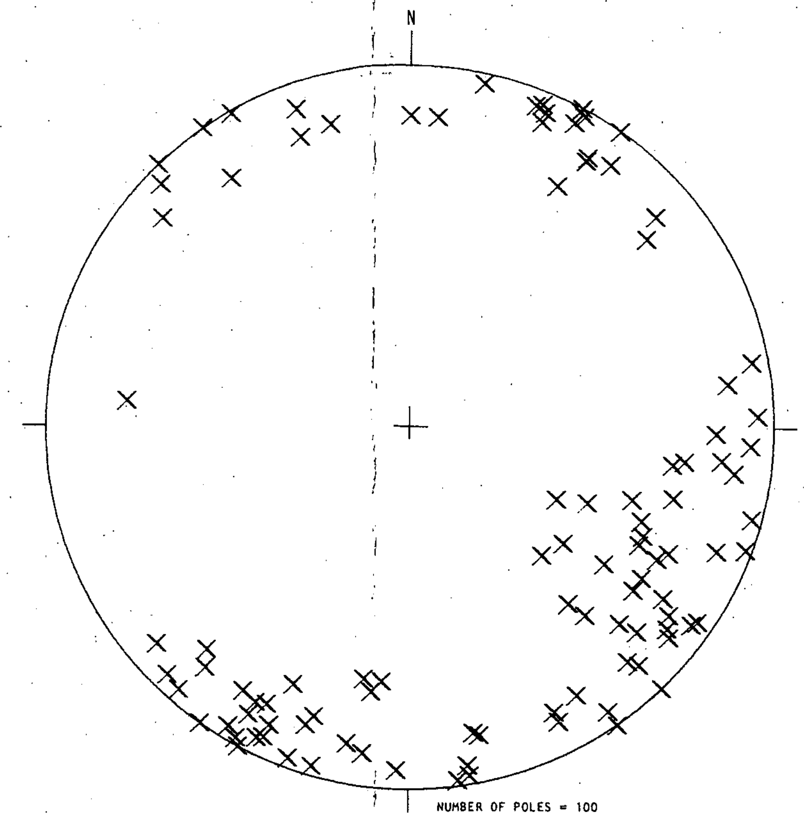

TR.3.1.1 PLOT OF POLES TO ALL FRACTURE PLANES (SEDIMENTARY ROCKS)

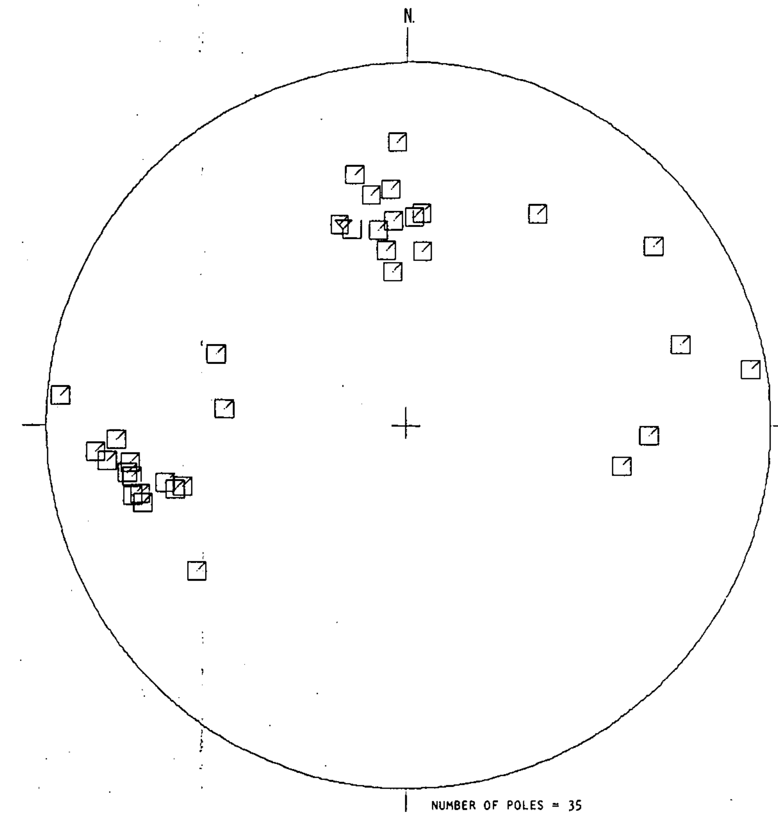

TR.3.4.2 PLOT OF POLES TO MINERALIZED FRACTURE PLANES (DIABASE)

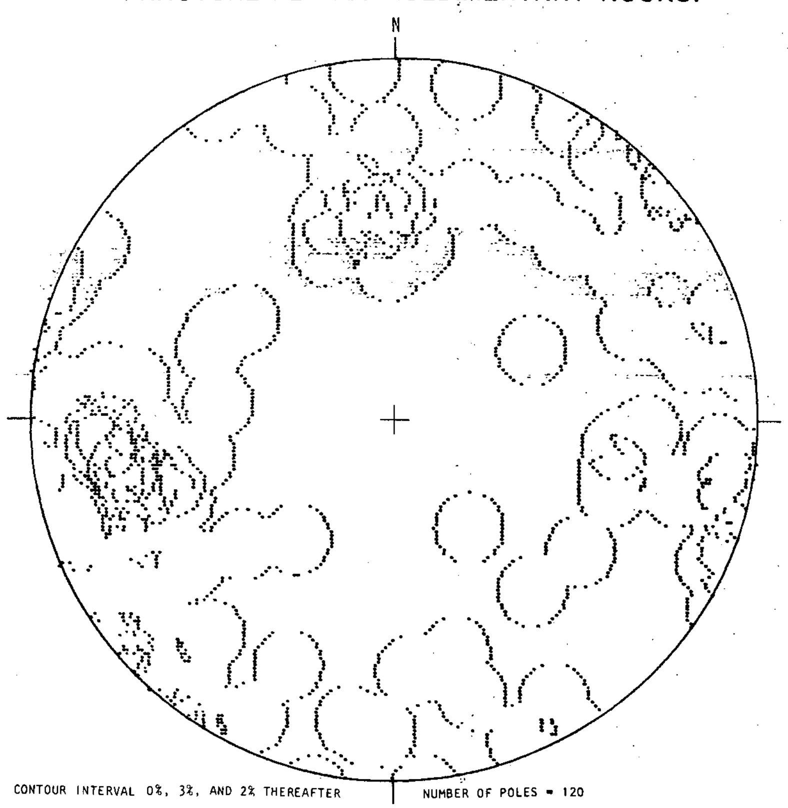

TR.3.1.2 CONTOURED PLOT OF POLES TO FRACTURE PLANES (DIABASE)

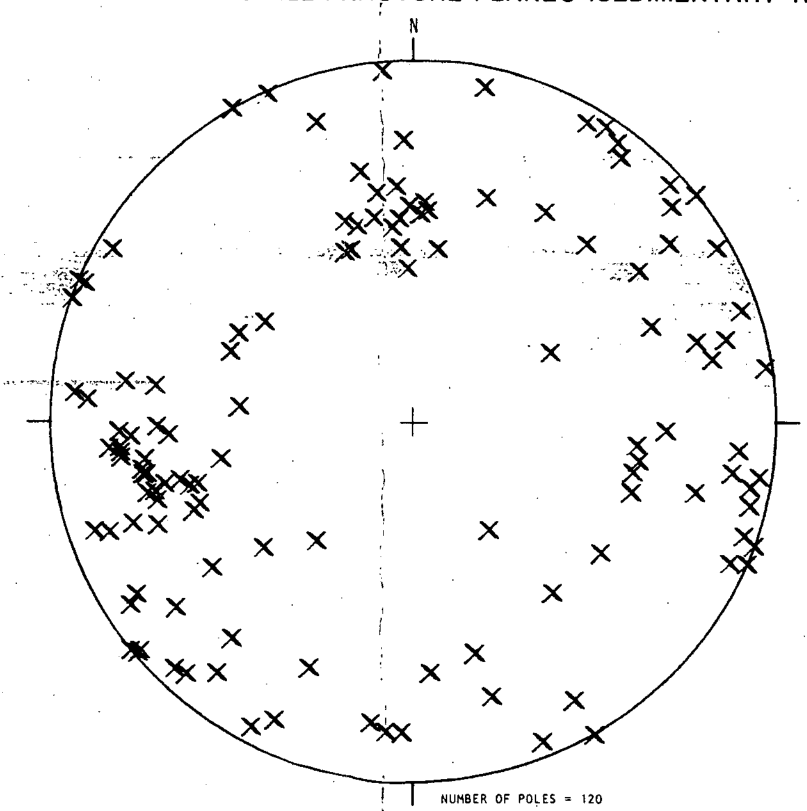

TR.3.1.2 PLOT OF POLES TO ALL FRACTURE PLANES (DIABASE)

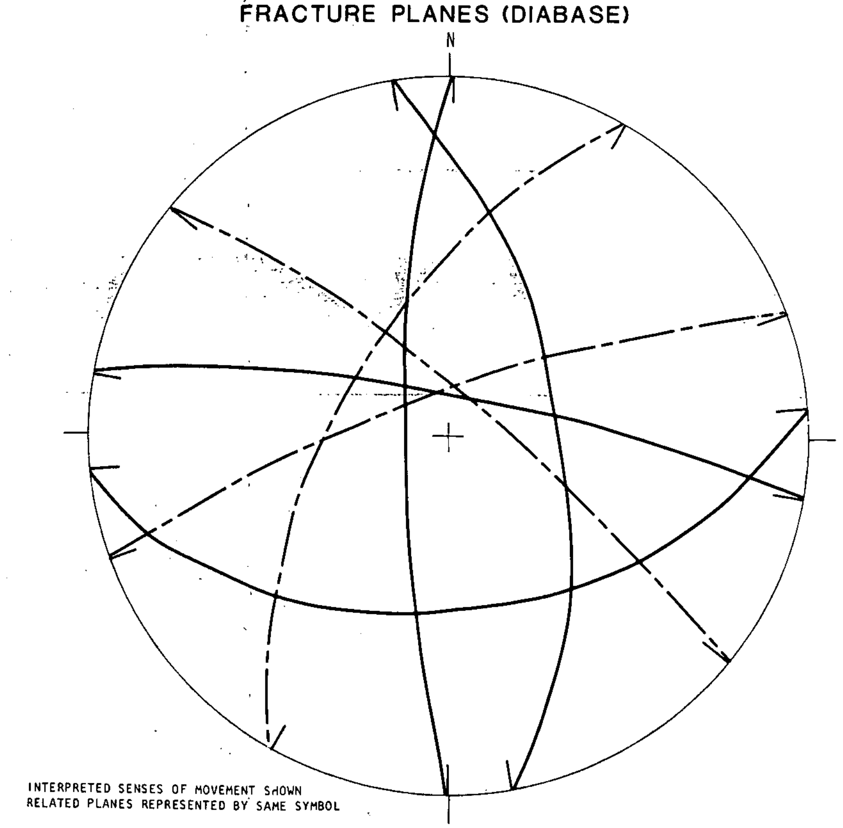

TR.3.6 INTERPRETED FRACTURE AND FAULT GEOMETRY

NOTE: STATION LOCATION SHOWN ON PLATE B5.3-1

STRUCTURAL ELEMENTS

STATION TR-3 TRIASSIC - SEDIMENTARY ROCKS AND DIABASE

(LOWER HEMISPHERE EQUAL AREA PROJECTIONS)

DAMES & MOORE

PLATE B5.3-19

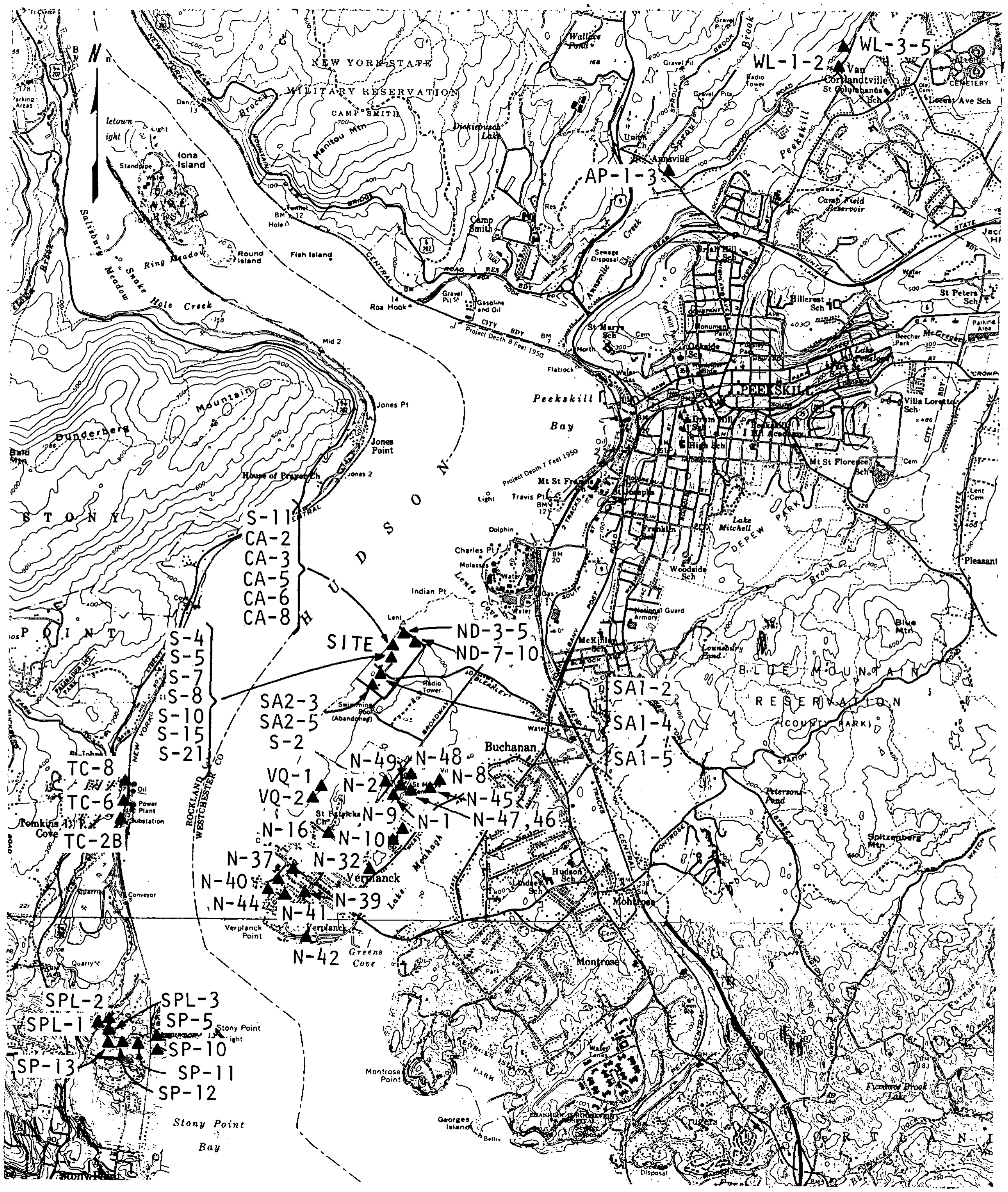

LOCATION MAP

SHOWING LOCATION OF SAMPLES COLLECTED FOR PETROGRAPHIC STUDY

1 0 1

MILES

Reference: The base for this map was produced from the following U.S.G.S. Topographic Maps, Peekskill, N.Y., 1957; Haverstraw, N.Y., 1967.

DAMES & MOORE

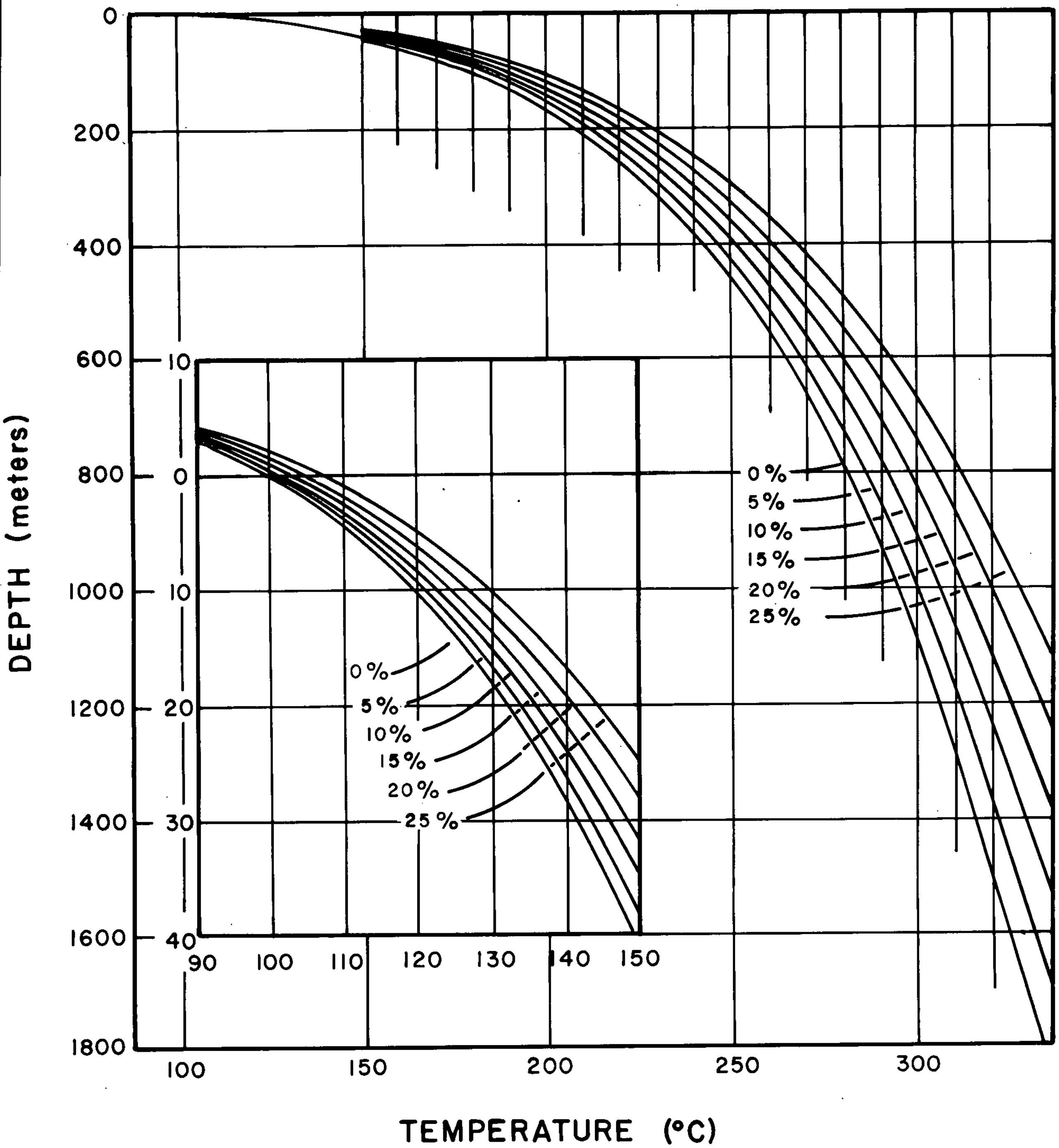

THE TEMPERATURE-DEPTH RELATIONS FOR H_2O LIQUID AND FOR BRINE OF CONSTANT COMPOSITION GIVEN IN WT PERCENT NaCL (J.L. HAAS, JR. 1971).

DAMES & MOORE

APPENDIX C

<u>REGIONAL GEOLOGIC INVESTIGATIONS</u>

APPENDIX C1

INTRODUCTION

C1.1 GENERAL GEOLOGIC STRUCTURE

A regional investigation was conducted within a 10 mile radius of the Indian Point Generating Station. The site is underlain by Lower Paleozoic rocks. It is situated within a geologically complex region comprising Precambrian and Triassic "provinces", each with its own structural history that includes numerous large-scale faults (see Plate C1-1). Ordovician and Devonian intrusives have invaded the older, Lower Paleozoic sedimentary suite, and are part of the total structural evolution of the area. A rock terrace developed during the downcutting of the River channel and remnants of it are exposed along the east and west banks of the Hudson River. Lastly, the entire area, including the river terrace, has been subjected to Pleistocene glaciation.

C1.2 REGIONAL STUDY OBJECTIVES

The objectives of the regional investigation were to:

1) Provide an understanding of the structural framework;
2) Determine which, if any, brittle phenomena were restricted to a given time interval;
3) Understand and logically place the north-south faults and fractures, seen onsite, into their proper regional context; and
4) Identify some of the major or macroscopic regional faults.

The above objectives were accomplished largely by performing fracture and fault studies on an outcrop scale within the three becrock "provinces" (Precambrian, Paleozoic, and Triassic), and by megascopically examining ERTS imagery and aerial photographs (1:60,000 and 1:24,000 scale) within these same provinces. Small-scale structural relationships were established and were extrapolated cautiously to a much larger scale.

Special attention was directed toward establishing a temporal relationship between igneous activity and brittle deformation. Thus, fracture and fault studies were performed in and around the Silurian dikes (which cut the Precambrian rocks), the Cortlandt and Peekskill Plutons (which were emplaced in Lower Paleozoic rocks), and in the Triassic diabase (see Table C1-1).

Glacial deposits and the river terrace were examined to (1) develop a historical framework pertinent to understanding the stability of the area, and (2) to look for features that might be construed as reflecting post-sedimentation tectonism. This part of the study is essential because the terrace and Pleistocene deposits could record any possible present-day tectonic activity, and could provide a limit (perhaps a maximum age) on the date of the last movement.

C1.3 STRUCTURAL DATA PRESENTATION

Structural data obtained from the bedrock studies along with station locations appear on Plates C1-2 and C3-1. Plate C1-2 is a location map on which outcrop-scale structures were plotted. Larger faults, where ground truthed, have been incorporated on this map. Since regional geological mapping was beyond the scope of this study, lithologies are not shown; however they are referenced in this report where pertinent. Plate C3-1 consists of several equal area, lower hemisphere projections of poles to fractures from the three provinces and the two "subprovinces" (the Cortlandt and Peekskill Plutons). Large-scale structural trends obtained from studies of remote sensing imagery and aerial photographs are presented on a topographic base (Appendix G). Information on geomorphic and glacial features is presented in Appendix D.

TABLE C1-1

STATIONS WITHIN GEOLOGIC PROVINCES

Precambrian (Reading Prong)

- All Dr-Stations
- Station JW-21

Lower Paleozoic (Manhattan Prong)

- Station JW-1
- Station JW-2
- Station JW-6
- Station JW-7
- Station JW-13

Triassic Basin

- All CH-Stations

Cortlandt Complex

- Station B-4
- Station B-5
- Station JW-4
- Station JW-11

Peekskill Pluton

- Station B-1
- Station B-2
- Station B-3

APPENDIX C2

REGIONAL TECTONIC SYNTHESIS

C2.1 HUDSON HIGHLANDS

The rocks of the Precambrian Hudson Highlands have had a long and complex deformational history starting some 1100 m.y. ago. Since the Grenvillian (Precambrian) age deformation is incidental to this report, it will not be pursued further.

The importance of the Precambrian rocks lies not in its early deformational history, but in the structural effects of Paleozoic and younger deformations which have been superimposed upon the older rocks. In addition, most of the major faults in the region cut the Precambrian rocks of the Hudson Highlands.

C2.2 MANHATTAN PRONG

The Inwood and Manhattan Formations are considered to be Cambro-Ordovician rocks (Paige, 1956; Ratcliffe, 1969) which were deposited on the Fordham Gneiss basement. These three units consitute the Manhattan Prong within the study area. Following deposition of the sediments, these rocks were subjected to a Lower Paleozoic regional metamorphism about 450 m.y. ago (Mose and Hayes, 1975) which, in general terms, was coincident with ductile deformation, here termed F_1-folding. The rocks continued to cool until about 360 million years ago (ref. Table C5-1).

The Cortlandt Complex was emplaced into the metasedimentary pile about 435 million years ago (Long and Kulp, 1962) following the peak of regional metamorphism. The simple Bouger gravity map of southeastern New York State (Urban, et.al., 1973) shows that the Cortlandt Complex is an irregular elliptical (pear-shaped) body in which the major axis is oriented about N60°W. The west-trending arm of the Cortlandt, which crosses the Hudson River, is not evident on this map, although it does appear on the regional aeromagnetic map (ref. Figure C4-4). This arm is separated from the main mass by a N35°W-trending lineament which is clearly visible on the regional aeromagnetic map. The main mass, recognized on the aeromagnetic map, is approximately coincident with that expressed on the gravity map. It is therefore suggested that the main mass of the Cortlandt is rooted or, at least, deep seated whereas the west-striking arm is a shallow splay off the main body.

C2.3 SILURO-DEVONIAN DIKES

Lamprophyre dikes at Stony Point were mapped as apophyses which were traced from the younger Cortlandt phase of the Cortlandt Complex into both the Annsville Phylite and the older dioritic phase of the Cortlandt (Ratcliffe, 1968). Several lamprophyre dikes, along with numerous dikes ranging from rhyolite to andesite in composition, were recognized throughout the Precambrian rocks of the Hudson Highlands within the study area. For the most part, they have been deuterically altered, although their original igneous texture has been preserved (Mack, 1950). An equal area plot of poles to 50 of these dikes shows distinct concentrations at N64°W and N46°W. Many of these dikes have been subjected to lateral movement(s) following injection. Altered lamprophyre dikes were also recognized in the Monroe quadrangle (Jaffe and Jaffe, 1973) which lies immediately to the west of the Popolopen Lake quadrangle (ref. Figure C1-2). There the dikes occupy only northwest trending fractures in Precambrian through Cambro-Ordovician rocks. Zartman (personal communication to Jaffe and Jaffe), obtained a 398±17 m.y. K/Ar age on a kaersutite from one of the lamprophyre dikes. According to Zartman, this date either reflects the true age of the dike or a cooling age produced by a regional thermal event following dike injection. Recent work by Dallmeyer, et.al. (1975) indicated that there was no post-Grenvillian (1 b.y.) thermal event in the Hudson Highlands. This would, therefore, lend support to the hypothesis expressed by Zartman that the K/Ar date represents the age of emplacement. Based on the preceding information, it is apparent that the dike swarm recognized in the Hudson Highlands is Silurian to Lower Devonian in age. Paleozoic igneous activity in the study area concluded with the emplacement of the Peekskill Pluton 368±27 m.y. ago (Mose, et.al. 1974).

C2.4 EARLY NORMAL FAULTS

West-striking normal faults, which produced monoclinal flexures in the overlying rocks (ref. Figure C5-6), were recognized in the Fordham Gneiss. These faults range in strike from N72°E to N80°W and in dip from 90° to 46°. Due to the ductile behavior of the overlying rocks, these faults are inferred to have formed during cooling following the peak of regional metamorphism. Thus, they probably represent the initiation of brittle deformation within the Manhattan Prong and provided surfaces for subsequent strike-slip displacement.

C2.5 WEST-NORTHWEST AND NORTH-NORTHWEST STRIKE-SLIP FAULTS

C2.5.1 Manhattan Prong

Conjugate pairs of west-northwest and north-northwest strike-slip faults showing right lateral and left lateral displacements respectively were recognized in the Manhattan Prong near the Hudson River. Specifically, right lateral members of observed conjugate pairs recognized in the Inwood Marble at Croton-on-Hudson range in strike from N40°W to N66°W, whereas the left lateral members range in strike from NS to N25°W (ref. Table C5-3).

Three small-scale nearly vertical faults, ranging in strike from N52°-60°W and showing right-lateral slip, cut the Fordham Gneiss just north of Croton-on-Hudson. A fourth fault strikes N05°E and exhibits left lateral slip. These faults are interpreted as defining a conjugate system. Besides these shear surfaces, there are two principal sets of orthogonal vertical fractures which strike N32°W and N64°E, and are respectively perpendicular and parallel to foliation. Geometrically, these orthogonal fractures respectively form acute and obtuse bisectrices to the interpreted conjugate fault system. Therefore, it is inferred that all of these features are cogenetic with the acute and obtuse bisectrices representing extension directions.

C2.5.2 The Cortlandt Complex

In the Cortlandt Complex, shear surfaces, in which the trends are confined to the northwest quadrant of the compass and which show subhorizontal slickensides (less than 35°), vary in strike from N13°W to N52°W. Although lateral slip is indicated for these fractures, no relative movement plans were observed. Nonetheless, it is noteworthy that the spread displayed by generally northwest striking shear fractures in the Cortlandt lies comfortably within the range expressed in the Inwood at Croton and in the Fordham just north of Croton.

C2.5.3 Siluro-Devonian Rocks

At one location within the Hudson Highlands a northwest-trending rhyolite dike, which belongs to the suite of Siluro-Devonian dikes, has been offset left-laterally by faults oriented N10°W - 70°NE and N20°W - 70°SW. These two faults resulted in left-lateral displacements of another northwest-striking rhyolite dike. A small-scale, right-lateral, strike-slip fault which strikes N75°W and dips to the northeast at 74° was identified in the Silurian Green Pond conglomerate just northwest of the Hudson Highlands. Lastly, nearly vertical N05°W-striking fractures define a noticeable concentration of poles to fractures in the Devonian Peekskill Pluton, although no evidence of shearing was apparent along these surfaces.

It is concluded from the previous discussion that conjugate west-northwest and north-northwest oriented strike-slip faults affected the entire study area either during or following the Silurian period. It is even possible that the stress system responsible for these faults endured long enough to produce the north-northwest fractures seen in the Peekskill Pluton.

C2.6 EAST-NORTHEAST STRIKE-SLIP FAULTS

Small-scale and relatively large-scale faulting has occurred along nearly vertical N75° to 80°E fractures which belong to rather prominent fracture maxima developed in both the Cortlandt and Peekskill Plutons (ref. Plates C5-8 and C5-9). One such fault seen in the Cortlandt, displayed right-lateral offset of a hornfels xenolith. A second fault, recognized on a much larger scale, produced intense brecciation in one of the Siluro-Devonian dikes and the host Precambrian trondhjemitic gneiss. The movement sense on this fault could not be determined.

It is not known to what conjugate fault system, if any, these east-northwest faults belong. However, two small intersecting faults oriented N50°W - 88°NE and N60°E - 73°SE, show respective left and right-lateral slip and define a conjugate system in the rocks of the Hudson Highlands. It is possible that this conjugate pair and the east-northeast faults and fractures seen respectively in the Cortlandt Complex and Peekskill Pluton all belong to the same fracture generation.

A small-scale reverse fault seen in the Green Pond conglomerate of Silurian age strikes due north and dips to the east at 30°. Assuming no block rotation since the development of the aforementioned lateral and reverse faults and an acute dihedral angle of 60°, the greatest principal stress would have been nearly the same for both fault systems. Correlation of the lateral faults in the Precambrian rocks with (1) the strike-slip fault seen in the Cortlandt, (2) the reverse fault cutting the Green Pond conglomerate, and (3) the east-northeast fracture set observed in the Peekskill is tenuous. However, such a correlation constitutes a real possibility and, if correct, implies that all of the east-northeast lateral faults and north-south reverse faults are post-Cortlandt and, perhaps, even post-Peekskill in age.

C2.7 REGIONAL FOLDING - ITS GENETIC IMPLICATION

Among the most prominent structural elements present in the study area are the north-northeast to northeast-oriented regional folds which are well developed in both the Hudson Highlands and in the Manhattan Prong. In addition, similarly oriented folds, well expressed by the Schunemunk-Bellvale-Green Pond syncline (Jaffe and Jaffe, 1973), occur in Devonian rocks northwest of the Hudson Highlands. It is not hypothesized that the folding in the Precambrian and Paleozoic rocks was the result of a single period of stress application. Rather, it is suggested that, following the Grenvillian orogeny, the Precambrian rocks were subjected to extension (Precambrian age diabase dikes), uplift, and denudation. Paleozoic sediments were unconformably deposited on this crystalline basement with those to the southwest, having been subjected to regional metamorphism and ductile deformation (F_1-folding). It is theorized that a second protracted period of deformation probably commenced prior to emplacement of the Cortlandt and continued intermittently to at least the Devonian. This deformation, which provided pathways for the invading Cortlandt Complex and the Siluro-Devonian dikes, produced the regional north-northeast to northeast folds, conjugate west-northwest and north-northwest strike-slip faults, as well as northwest and northeast extension fractures.

C2.8 NORTH-NORTHEAST AND EAST-NORTHEAST STRIKE-SLIP FAULTS

C.2.8.1 Manhattan Prong

A second pair of strike-slip faults was first identified in the Inwood Marble at Croton-on-Hudson. Two members of a single, observed pair are oriented N15°E - 80°SE and N43°E - 87°SE, and produced right-lateral and left-lateral displacements, respectively. Other small faults ranging in strike from N43°E to N65°E exhibit left-lateral offsets. Though these faults were not observed as conjugate pairs, they are nonetheless interpreted as having formed in response to the same stress system.

At Croton-on-Hudson nearly vertical N58° to 60°W striking fractures have been displaced right laterally along a fault oriented N15°E - 80°ESE and left-laterally along its conjugate which is oriented N43°E - 87°SE (ref. Figure C5-2). A second example at this location shows a N63°W-trending right-lateral strike-slip fault, marked by a healed breccia zone, offset left-laterally by a second fault which strikes N65°E. It is concluded that conjugate strike-slip faults, dispersed about north-northwest to east-northeast trends, are younger than the conjugate lateral faults striking between about north-northwest to west-northwest.

C2.8.2 Ordovician to Devonian Dikes and Plutons

Members of this younger conjugate pair have also been recognized elsewhere. In the Cortlandt Complex, left-lateral strike-slip movements have occurred along N40° to 60°E striking surfaces. An andesite dike in the Hudson Highlands was displaced left-laterally by a fault striking N70°E and dipping 45° to the south-southeast. Other members of the Silurian-Devonian dike swarm were displaced along N10°E-50° to 80°-dipping right-lateral faults. A N05°E striking right-lateral fault offset the Devonian age Esopus Formation near Highland Mills, New York (Dodd, 1965). A dominant fracture set with an average attitude of N27°E - 80°NW appears in the Peekskill Pluton. No shearing was recognized along members of this set, though it may be postulated that they belong to this younger conjugate fault system. Despite the interpretation of the fractures in the Peekskill Pluton, it is clear that the younger system of strike-slip faults is Devonian or younger.

C2.8.3 The Triassic Basin

In the Triassic Basin, which lies in the southwestern portion of the study area, faults showing similar orientations and movement plans were also noted in beds which strike north-northwest to due north. At one locale, left-lateral displacements occurred along faults oriented N64°-75°SE and N74°E-90°. At the northernmost exposure of the conglomerate, a small north striking right-lateral fault was observed. Elsewhere in the Triassic Basin of Rockland County, New York, small-scale offsets indicate left-lateral movement along a N50°E trend and right-lateral movements along north to northeast surfaces. These features were also observed in the Newark-Gettysburg Triassic Basin near Pottstown, Pennsylvania, where the beds strike generally west to west-northwest.

In a diabase body within the Basin, left-lateral offsets were recognized along surfaces oriented N45°E and right-lateral displacements occurred along N20°E surfaces. In redbeds near Upper Glascow, Pennsylvania, strike-slip faults striking N65° to 70°E show left-lateral movement whereas a fault trending N15°E has produced right-lateral displacement (Dames & Moore, 1974). It is, therefore,evident that north-northeast to east-northeast strike-slip faults are regionally distributed throughout the Triassic age Newark-Gettysburg Basin, and that these structures have been superimposed on the pre-existing curvature expressed by the Basin. This curvature, which is coincident with the Appalachian Salient, was interpreted to have been inherited from a Paleozoic F_3-folding event (Dames & Moore, 1975).

The regional distribution of the previously mentioned conjugate pairs within the Triassic Basin makes it likely that rocks outside of the Basin experienced the same deformation. Hence, it is suggested that the similarly oriented strike-slip fault system seen in the Lower to Middle Paleozoic rocks, and which is also expressed by offset dikes within the Hudson Highlands, is younger than the rocks of the Triassic Basin. Furthermore, it can be postulated that the Ramapo Fault may experienced left-lateral strike-slip movements at this time.

C2.9 THE NEWARK-GETTYSBURG BASIN

The Triassic Newark-Gettysburg Basin extends southwestward from Rockland County, New York to Lancaster County in eastern Pennsylvania, a distance of about 140 miles (Van Houten, 1969). The rocks within the basin, though not as intensely deformed as those within the Hudson Highlands and Manhattan Prong, have nonetheless experienced a complex deformational history.

Conglomerates composed of coarse, clastic material dederived mainly from Paleozoic carbonates, quartz-pebble conglomerates, and orthoquartzites with minor fragments of Siluro-Devonian rhyolite and porphyritic rhyolite, are common, especially near the border zone (The Ramapo Fault in the study area). Away from these zones, conglomeratic units are interlayered with sandstone, siltstone, and shale, indicating variations in the energy level of the stream during deposition. These fluctuations in energy were probably produced by syndepositional normal faulting in the border zone. Following this proposed crustal extension, the Triassic basin was subjected to regional horizontal compression with the greatest principal stress oriented about N25° to 40°E. Extension fractures, parallel to the greatest principal stress northwest to west-northwest-trending folds (Dames & Moore, 1974), and a low-angle, northwest-striking reverse fault (McLaughlin, 1942) were identified near Pottstown, Pennsylvania. These structures, as well as the conjugate north-northeast to east-northeast strike-slip faults described in Section C2.8.3, resulted from this compression.

Subhorizontal slickensides were recognized on the north-northeast to northeast-striking extension fractures, suggesting that a second, differently oriented stress system was operative. Southeast of Pottstown, right-lateral strike-slip along a nearly vertical surface striking N40°E produced a series of en-echelon gash fractures. At this same exposure, two smooth, planar fractures which strike N67°E and dip 81° to the south-southeast are filled with slender, antitaxial calcite fibers (Durney and Ramsey, 1973). The fibrous filling indicates that these fractures formed in extension but were subjected to a very small increment of finite lateral strain. A small, mapped fault, striking N48°E and showing right-lateral displacement, was identified east of Pottstown (Wood, 1963). The geometric and kinematic relations of the coexisting structures suggest that they formed in response to a stress system in which the greatest principal stress was oriented about N68°E. It is suggested that deformation associated with this stress system is younger than that associated with north-northeast compression, and was responsible for the horizontal slickensides seen on the older extension fractures.

Normal faults which strike approximately northwest were identified in the Triassic rocks of Rockland County as well as in the adjacent Hudson Highlands. A northwest-striking normal fault separating Precambrian from Siluro-Devonian rocks was also identified by Dodd (1965, Plate 1).

Numerous northeast-striking normal faults along with lesser numbers of north-, east- and northwest-trending normal faults were identified in the Triassic of eastern Pennsylvania (Dames & Moore, 1974), but no northeast normal faults were observed in the Triassic rocks in Rockland County. Ratcliffe (1971 and 1972), however, stated that post-depositional normal faulting occurred along the northeast-striking Ramapo Fault during the Late Triassic and possibly into the Jurassic. Normal faults striking N50° to 55°E and dipping about 80° to the southeast were recognized in Precambrian trondhjemitic gneiss about 3 miles west of the Ramapo Fault. It is not known if these faults are related to Triassic deformation or to an older event. In any case, it is suggested that normal movement along northeast- and probably north-striking surfaces developed in response to crustal extension attendant upon the Mesozoic opening of the Atlantic Ocean. This deformation is interpreted as having produced the last tectonically induced movements in the study area. The east- and northwest-striking normal faults may have developed during relaxation of the earlier compressive stresses.

C2.10 PLEISTOCENE FAULTS

Normal faults, striking predominantly between west and northwest, cut Pleistocene sediments in the northwestern part of the study area and lie within 1000 feet of the normal fault mapped by Dodd (1965, Plate 1). The fault mapped by Dodd is aligned with a series of parallel topographic lineaments which pass about 2 miles north of the site. One of these lineaments was mapped by Dodd as a shear zone with an unknown movement sense. The origin of the normal faults in the Pleistocene sediments is not presently understood.

APPENDIX C3

REGIONAL OVERVIEW OF FRACTURES

C3.1 NORTH-STRIKING FRACTURES

Fractures belonging to this group have been recognized in all of the major provinces (Precambrian, Lower Paleozoic, and Triassic) as well as in the two subprovinces. In the Precambrian, nearly vertical fractures cut rocks characterized by a steep-dipping northeast foliation at Station DR-8, and a more gently inclined stratiform foliation at Station DR-27 (see Plates C1-2 and C3-1). Steeply inclined, north-northeast fractures at Station DR-12 intersect the foliation at about 90°, and at DR-28 a small group of fractures was recognized. North-striking fractures are either absent from or rare in the Precambrian rocks at Stations DR-4, DR-16, DR-26, and JW-21.

The Inwood Marble within the Manhattan Prong at Croton-on-Hudson is cut by numerous north-striking fractures and faults which belong to two different fault systems (Plate C3-1). A lesser number were recognized in the Fordham Gneiss. At JW-2, and at JW-7, several were seen, the poles of which lie close to the bedding plane. Outside of the site area, north-trending fractures and faults do not appear to be abundant in metasedimentary rocks of the Manhattan Prong. In the Cortlandt Complex, at Stations B-4 and B-5, north to northeast fractures are numerous; however, at Stations JW-4 and JW-11 virtually none were recognized. A large concentration of north to northeast fractures cuts the Peekskill Pluton at Station B-1. At

Station B-2, north-striking fractures are uncommon, though there is a profusion of fractures striking N20°E. A few north-striking fractures were also recorded in the Peekskill at Station B-3. Overall two north-northwest maxima are apparent in this pluton.

In the Triassic diabase (Stations CH-3-5, CH-5-2, and CH-5-3), fractures which strike north are steeply inclined to vertical (Plate C3-1). Triassic sediments also reveal the existence of these structures. At Station CH-10 they range in dip from approximately 60° to nearly 90°. Elsewhere in the sedimentary rocks, the north-striking fractures are generally normal to bedding.

C3.2 NORTHWEST FRACTURES

Northwest striking sets have also been recognized in all of the provinces and subprovinces. In the Precambrian they are commonly nearly vertical, and normal to the foliation or layering (see Plate C3-1, Stations DR-8, DR-12, DR-16, DR-25, and DR-28). At Station DR-4 there is a northwest set in which the members display an average dip of about 60°. Dispersed northwest fractures also occur. Poles to members of this group do not plot on the foliation plane. Northwest fractures at Stations DR-27 and JW-21 are rare.

In the Lower Paleozoic metasedimentary rocks, concentrations of northwest fractures are generally normal to layering (Plate C3-1, Stations JW-6 and JW-7). In the Cortlandt Complex nearly vertical northwest fractures are present despite the absence of layering (Plate C3-1, Stations B-5 and JW-11).

The Peekskill Pluton is devoid of clusters of nearly vertical northwest-striking fractures, although isolated occurrences were recognized. A number of nearly 60° dipping northwest-striking fractures were identified at Station B-2. Within the Triassic, nearly vertical northwest fractures occur both in the sedimentary rock and in the diabase.

C3.3 NORTHEAST FRACTURES

Like the north and northwest fractures, northeast fractures are present throughout the study area. Curiously, their number does not appear to be overwhelming on the equal-area projections, despite the regional northeast grain. This is probably due to the tendency of avoiding repeated measurements of fractures which parallel foliation or bedding. The northeast fractures in the Precambrian Hudson Highlands are coincident with foliation except at Stations DR-12 and DR-28.

Most of the metasedimentary rocks within the study area of the Manhattan Prong strike north-northeast to northeast. Thus, the inherent bedding and foliation planes relieved the strain along this direction. Onsite, the north-northwest striking Inwood Formation displays large northeast fractures, many of which have experienced lateral movement. The Cortlandt Complex also exhibits northeast fractures which are not sufficient in number to define a maximum on a contoured equal area projection. Nevertheless, northeast fractures are important structural elements due to the existence of movements along them. Northeast fractures also appear in the Peekskill Pluton with the greatest concentration evident at Station B-1. At

Stations B-2 and B-3 the major fracture orientation is north-northeast. The northeast trends in the Triassic appear to be more evident in the sedimentary rocks than in the diabase.

C3.4 SUMMARY

A first review of the data suggests that the major fracture trends occur in all the rocks that were studied. These rocks represent a time span of 1,100 m.y. The trends can only be sorted out through geologic time by studying the character and sense of movements along the various fracture and fault sets.

APPENDIX C4

PRECAMBRIAN ROCKS (HUDSON HIGHLANDS)

C4.1 GENERAL STATEMENT

The Hudson Highlands, which lie north and west of the site, consist of Precambrian crystalline rocks which were deformed and metamorphosed about 1 billion years ago. Since that time, these rocks were intruded by diabase dikes about 850 million years ago, and later by a swarm of lamprophyre dikes plus dikes ranging in composition from andesite to rhyolite dated at about 400 m.y. These younger dikes have assisted to unravel a significant part of the pertinent geologic history within the study area. Aside from this later dike swarm, the Hudson Highlands are cut by large-scale, mapped faults and related subsidiary faults (ref. Figure C1-1).

C4.2 SILURO-DEVONIAN DIKES

C4.2.1 Introduction

Rhyolite, andesite, and lamprophyre dikes were recognized at several locations within the Hudson Highlands of the study area. Ratcliffe (1968) suggested that the lamprophyre dikes and the cortlandite phase of the Cortlandt Complex are coeval. In the Monroe Quadrangle just west of the present study area, Jaffe and Jaffe (1962, and 1973) indicated that several northwest striking, vertical to steeply inclined extension fractures are filled with lamprophyre dikes. Many of these dikes intrude Precambrian rocks, the Lower Cambrian Pouqhuag Quartzite and the Cambro-Ordovician Wappinger Dolomite, but have never been recognized in any younger strata.

Zartman (in Jaffe and Jaffe, 1973) reported a K/Ar mineral age (kaersutite) of 398±17 m.y. from a lamprophyre dike in the Monroe Quadrangle. He interpreted the age to represent either the actual time of emplacement or metamorphic overprinting of an older dike during a subsequent regional thermal event. Dallmeyer, et.al. (1975) indicates that the Precambrain rocks were subjected to only one period of regional metamorphism and did not experience a subsequent thermal event. This suggests, then, that the date recorded by Zartman is an emplacement age rather than an indication of argon loss at a later date. This dike swarm is interpreted to have a Siluro-Devonian age of emplacement.

C4.2.2 Relationship of Dikes to Brittle Deformation

The majority of Siluro-Devonian dikes within the study area have intruded northwest-trending fractures, although a few northeast-trending dikes were also recognized (Plate C4-1). An equal area, lower hemisphere plot of poles to 50 dikes (Plate C4-1) shows concentrations about maxima striking N46°W and N64°W. This suggests that fractures displaying these trends (N46°W and N64°W) may have formed as extension fractures during two periods of stress application. However, at one outcrop, fractures which trend N35°W, N58°W, and N80°W cut the Precambrian host rock with right-lateral movement having occurred along the N80°W trend (Plate C4-2). It appears that these three fractures define a conjugate system composed of two shear fractures (N35°W and N80°W) and an extension fracture (N58°W).

A lamprophyre dike follows the N35°W and N58°W fractures. Though this observation was made at a single outcrop, it is likely that both extension and shear fractures were utilized as pathways for the ascending magma during a period of protracted deformation.

Following emplacement of the dikes, continued deformation produced fracturing within the dikes. Lateral movements occurred parallel to dike-wall-rock contacts, and transverse strike-slip faults offset many dikes. A study of 5 dikes at Station DR-26 shows that similar fracture trends exist within each dike. A composite plot of fractures from these 5 dikes show maxima at about an orientation of N32°E-75°SE and nearly N90°E (Plate C4-3). At Station DR-9, a rhyolite dike which trends N60°W has been offset left-laterally about 15 feet along a fault oriented N10°W-70°E. Dikes at Station DR-26 have been displaced right-laterally along faults striking N10°E and N85°E. Northwest trending dikes at Stations DR-15 and DR-25 have been sheared along their contacts, although the movement sense along these dikes could not be determined.

C4.3 MAJOR FAULTS

Many major faults cut the Precambrian rocks of the Hudson Highlands (ref. Plate C1-1). Reconnaissance mapping was performed along some of these faults during the present study to confirm their existence. One of these major features projects north-northeastward from the observed Ramapo Fault and was recognized at Stations CH-18, DR-34, and DR-36 (ref. Plate C1-2). At Stations CH-18 and DR-34, faulting is marked by large-scale brecciation and local zones of cataclastic flow. No fault breccia was recgonized at Station DR-36, but small-scale mylonite zones, paralleling the N30°E trending valley walls, were observed. At Station CH-18, the valley is oriented approximately N30°E, and at Station DR-34 the valley trends about N15°E.

The faults seen at Stations CH-18 and DR-36 lie along the projection of the Ramapo Fault, whereas the fault at Station DR-34 lies just to the west of this projection (ref. Plate C1-2). It is interpreted that the Ramapo bifurcates in the area of these stations with one splay trending about N15°E and the second trending N30°E.

At Station DR-34, breccia and ultramylonite are in contact along a N15°E trend. This contact has been displaced right-laterally along an east-trending fault and left-laterally along a N30°W fault. Furthermore, there is a 1-inch thick gouge zone, oriented N55°W-81°SW, which extends for at least 10 feet across the breccia. It would appear, therefore, that at this locality (DR-34), movement along the N15°E trend predates movement along east-west, N55°W, and N30°W trends.

In light of the observations discussed above, it would seem necessary that any northwest shear zones observed in the area should also be discussed. One such zone lies along Popolopen Creek which trends about N50°W (Dodd, 1965). This shear zone extends to the southeast and lines up with the southeasterly bend seen in the Hudson River Valley just north of Indian Point. To the northwest, the zone is aligned with the Precambrian-Paleozoic contact. This contact is mapped by Dodd (1965) as a normal fault.

The third area investigated is the mapped shear zone that projects through Camp Smith west of Peekskill. At Station SK-23, a massive 75-foot wide shear zone trending approximately N40°E was recognized. Within this zone small north-south fractures display slickensides, indicative of dip-slip movement. A thin section from this zone shows that the rocks are intensely deformed. An aeromagnetic lineament extends southwestward from this area and lines-up with the Ramapo Fault. The continuity of this lineament is interrupted by the Rosetown Pluton (Plate C4-4). A northeasterly projection of this zone should appear just west of Wallace Pond. No shear zone was recognized, although a N30°E trending valley exists along this projection.

APPENDIX C5

LOWER PALEOZOIC (Manhattan Prong)

C5.1 GENERAL STATEMENT

Lower Paleozoic rocks underlie the southeastern third of the study area (Plate C1-2) and consist of the Inwood Marble and the Manhattan Formation. These units together with the Fordham Gneiss have been regionally metamorphosed and constitute the Manhattan Prong in the study area. In general, the degree of metamorphism increases to the east and southeast away from the site. According to Mose and Hayes (1975), the regional metamorphism peaked about 450 m.y. ago. K/Ar determinations from Paleozoic phyllites yielded ages of about 375 m.y. (Table C5-1). Dallmeyer (personal communication) indicated that there was only one period of regional metamorphism in the Manhattan Prong, hence the K/Ar ages probably record the time when the rocks, upon cooling, became retentive to argon.

Fractures and faults have formed at different times within the Manhattan Prong and many have been reactivated during subsequent events. Furthermore, there is abundant evidence of brittle deformation having affected the Triassic Newark - Gettysburg Basin on the west side of the Hudson River. All of these factors complicate the interpretation of the ages and mechanism of brittle deformation. For instance, a surface may show normal movement across it, yet it may have originated as a strike-slip fault. Also, there is evidence of repeated transcurrent movements having occurred in the opposite sense, i.e. right and left-lateral, along the same plane of weakness.

TABLE C5-1

WHOLE-ROCK-K/Ar DATES FROM PALEOZOIC ROCKS

Rock Description	Location	Date
Fine-grained greenish-black phyllite from a fault zone	Cedar Pond Creek north of Thiells, Thiells, Quadrangle	398±15 m.y.
Fine-grained, pale green sericite phyllite, mylonite (?)	Thiells, Thiells Quadrangle	379±13 m.y.
Annsville Phyllite	Route 9 northwest of Peekskill, Peekskill Quadrangle	354±13 m.y.

C5.2 STATIONS JW-1 and JW-2

The Inwood crops out in Croton-on-Hudson (Plate C1-2) and consists of vertically dipping, well-defined layers of carbonate and micaceous carbonate which strike N50° to 55°E. Fractures here appear in two basic groups, the first nearly north-striking and the second trending northwest (Plate C5-1). Within the north-striking group, there are three distinct maxima: the strongest oriented north and dipping 85° to the east; the second striking N09°E and inclined 81° to the east; and the weakest trending N02°W and dipping eastward at 56° (Plate C5-1 and Table C5-2). The dips of the individual north-striking fractures range from 90° to 48° (mostly to the east). The northwest fractures define a single maximum oriented N61°W-77°NE; the dips with this group vary from 90° to about 60°. A third group, subparallel to layering and decidedly subordinate to the north-striking fractures, was also recognized. Strike-slip movement has occurred along members of all three groups (Table C5-3), but no evidence of normal or reverse faulting was recognized. Slickensides and fibrous calcite within the fault planes are subhorizontal with the plunges ranging from 00° to 30°.

Right-lateral offsets have occurred along small faults ranging in strike from N25°E to N75°W. In the interval from NS to N30°W both left and right-lateral shears have developed (Table C5-3). Left-lateral slip was also recognized on surfaces which are subparallel to layering (N43° to 65°E, see Table C5-3). Initially, a rather chaotic picture emerges; however, recognition of several conjugate shear fractures enables this complex pattern to be organized into two well-defined fault systems. The first system comprises steeply inclined to vertically dipping west-northwest and north-northwest (to north) sets, with right-lateral movements evident along the former set and left-lateral displacements apparent along the latter set (Plate C5-2). The second system is composed of steeply dipping north-northeast and northeast fault sets. In this system, the nearly north-striking faults display right-lateral, strike-slip movements, whereas those which nearly parallel bedding exhibit left lateral displacements.

Nearly vertical fractures which strike N58° to 60°W have been offset right-laterally along a fault oriented N15°E-80°SE, and left-laterally along its conjugate which is oriented N43°E-87°SE (Plate C5-2). In a second instance, a right-lateral, strike-slip fault with an attitude of N63°W-76°NE has been left-laterally displaced by transcurrent movement along a steeply inclined fault which strikes N65°E. Despite the absence of offsets of conjugate pairs, the aforementioned observations imply that conjugate lateral movements along north-northeast and northeast faults succeeded conjugate strike-slip movements along west-northwest and north-northwest fault sets.

No evidence exists for establishing the absolute age of faulting here, though fracture data from Station JW-2 (Plate C5-3) appear to provide some qualitative information. At JW-2, 58 fractures were recorded in a quartzofeldspatic phase of the

TABLE C5-2

MAXIMA DEFINED BY FRACTURES IN MANHATTAN PRONG ROCKS

	Station JW-1	Station JW-2	Station JW-6	Station JW-7	Station JW-13	(Composite) Cortlandt Complex	(Composite) Peekskill Pluton
Layering or Foliation	N50°-55°E 90°	N45°-60°E 50°-70°SSE	N60°-75°E 38°-50° NNW	N35°E-90°	N13°E-43°WNW	---	---
Fracture Maxima	*N00°E-86°E	*N06°E-80°W	N40°E-78°SE *N64°E-84°SSE	*N45°E-25°NW	*N07°E-60°ESE	*N11°E-81°ESE	*N27°E-80°WNW N62°E-72°NNW
	*N09°E-81°ESE	N12°E-60°WNW	N70°E-68°SSE	*N61°W-85°SSW	N07°E-75°ESE	*N78°E-82°NNW	*N79°E-74°SSE
	N02°W-56°E	N13°E-22°WNW	N74°E-90°	*N75°W-80°SSW	N70°E-60°NNW	*N38°W-78°NE	*N80°E-79°NNW N05°W-SO°
	N61°W-79°NNE	*N16°W-65°WSW	N90°E-78°S		*N87°E-74°N	*N88°W-80°N	*N10°W-70°ENE
			*N23°W-82°NNE		N15°W-82°ENE		*N61°W-59°WSW
			*N32°W-90°		N54°W-90°		
			*N58°W-85°NNE		*N80°W-80°NNE		

*Strongest Maxima

TABLE C5-3

STRIKE-SLIP FAULTS AT STATION JW-1

Strike	Dip	Movement Sense	Strike	Dip	Movement Sense
N15°W	68°ENE	R.L.	CN55°W	Unknown	R.L.
N05°W	65°E	R.L.	CN15°W	Unknown	L.L.
N06°E	60°E	R.L.	N60°W	76°55W	R.L.
N03°E	60°E	R.L.	N35°W	90°	L.L.
N10°W	82°ENE	R.L.	CN17°W	Unknown	L.L.
N15°W	80°ENE	R.L.	CN66°W	Unknown	R.L.
N40°W	72°ENE	R.L.	N75°W	83°NNE	R.L.
N37°W	65°NE	R.L.	CN25°W	56°ENE	L.L.
N35°W	70°NE	R.L.	CN60°W	70°ENE	R.L.
N06°E	85°E	R.L.	N25°W	72°ENE	R.L.
N45°W	60°NE	R.L.	CN07°W	88°E	L.L.
N30°W	80°ENE	L.L.	CN61°W	88°NNE	R.L.
N08°W	86°E	R.L.	N20°W	86°ENE	L.L.
N08°W	78°E	R.L.	N65°E	78°ESE	L.L.
N25°E	80°ESE	R.L.	CN15°E	80°ESE	R.L.
N14°W	85°ENE	R.L.	CN43°E	87°SE	L.L.
N15°W	85°ENE	R.L.	N63°W	76°NNE	R.L.
N04°W	90°	R.L.	CN00°E	Unknown	L.L.
CN45°W	75°SW	R.L.	CN40°W	Unknown	R.L.
CN18°W	87°WSW	L.L.	N55°E	90°	L.L.

R.L. - Right Lateral
L.L. - Left Lateral
CN45°W
Conjugate pair
CN18°W

Fordham Gneiss in which the foliation strikes N45° to 60°E (parallel to the layering at JW-1) and dips south-southeastward at 50° to 70°, oblique to layering at JW-1 (Plate C5-3 and Table C5-2). Ten of these fractures are nearly vertical and strike north. The combined foliation (layering) and fracture (north-striking) data suggest that the north-striking fractures at both JW-1 and JW-2 formed following the reorientation of the rocks at these two stations.

A small fault striking N09°W and dipping 70° to the east has produced left-lateral displacement of a Silurian porphyritic rhyolite dike seen in the Precambrian Hudson Highlands. Right-lateral offset of layering occurred across a small-scale N75°W-74°NE oriented fault in the Silurian Green Pond Conglomerate. The orientations and movement plans of these two faults appear consistent with those observed in the older fault system at JW-1. If these faults are genetically related to the older system at JW-1, then a maximum age has been established for this system. Further information is also provided from data gathered within the Cortlandt Complex and at Station JW-6.

C5.3 STATION JW-6

The Fordham Gneiss is exposed at Station JW-6 and is composed mainly of a pinkish-gray gneissic granite with lesser amounts of layered paragneiss and amphibolite. Layering and foliation generally strike N60° to 75°E and dip to the north-northwest at 39° to 50°; however, locally, a layering attitude of N75°W-30°NE also occurs. Within the east-northeast striking rocks, the major fracture orientations are N23°W-82°NE, N32°W-90°, and N58°W-85°NE (Plate C5-4 and Table C5-2). Lesser concentrations cluster around N68°E-78°SE and N89°W-75°S maxima, with the remaining fractures being dispersed. Twenty fractures cutting the west-northwest foliation are similarly oriented to those transecting the east-northeast foliation (Plate C5-4).

Four small-scale, nearly vertical strike-slip faults were observed. Three strike N52°W, N55°W, and N60°W, and show right-lateral displacements whereas the fourth strikes N05°E and displays left-lateral offset. The orientations of, and movements along, these faults coupled with the existence of two principal sets of orthogonal, vertical fractures (N32°W and N68°E), which are respectively perpendicular and parallel to foliation, strongly suggest that all of these structures formed in response to the same stress system. It is important to note that the small-scale faults at this location show the same movement plans and nearly the same trends as those belonging to the older system recognized at nearby Station JW-1.

C5.4 STATION JW-7

The Manhattan Formation at Station JW-7 consists predominantly of layered garnetiferous quartz-feldspar-biotite schist with lenses, pockets, and discontinuous layers of white granitic mobilizate surrounded by a selvage of biotite. The entire suite has been affected by passive F_1-folding and flexural-slip F_2-folding, the latter rotated by a later episode of larger-scale F_2-folding (Plate C5-5). F_2-folding was of sufficient scale, relative to the outcrop, to have produced different attitudes of stratiform foliation, thus enabling fractures from differently oriented units to be compared. Foliations from which the fractures were recorded display respective attitudes of about N35°E-90° and N45°E-55°SE. The principal fracture maxima of N45°E-25°NW, N75°W-80°NNE, and N61°W-85°NNE (Table C5-2) were found associated with both foliation orientations, although some east-striking, nearly vertical fractures were recognized in the more gently dipping units. Northwest trending fractures are also affiliated with both foliation orientations, although they do not define a strong maximum. The similar fracture orientations found within differently inclined units suggest that the fractures developed following the formation of the mesoscopic (outcrop scale) F_2-folds.

Three small, nearly vertical shear zones strike N75°W, N75°W, and N64°W. These zones display horizontal slickensides though the movement plans are unknown. The coincidental trends of these zones with those of the major fracture sets suggest that the nearly vertical fractures formed either as incipient strike-slip faults or as extension fractures which were subsequently subjected to shearing.

C5.5 STATION JW-12

This station, seen on Interstate 684, exposes an interlayered sequence of metasedimentary rocks which have experienced passive folding (Plate C5-6). This sequence is cut by a series of small-scale nearly west-striking, north-dipping normal faults which pass upward and, locally, downward into monoclinal flexures (Plate C5-6 and Table C5-4). The overlying, unfaulted metasediments thicken over the hanging wall and thin across the footwall, indicating that this small scale faulting developed when the rocks were still in a semiductile state. This probably developed during incipient uplift of the metasedimentary pile. The importance of these faults is that they may represent, or be among, the earliest formed fracture sets recognized in the Manhattan Prong.

TABLE C5-4

ORIENTATIONS OF NORMAL FAULTS AT STATION JW-12

Strike	Dip
N80° W	70° NNE
N90° W	55° N
N75° E	60° NNW
N72° E	46° NNW

C5.6 STATION JW-13

The rock at Station JW-13, mapped as the Fordham Gneiss, strongly resembles the schist found within the Manhattan Formation, a characteristic of the Fordham recognized by Prucha (1956). Mineralogically, the schist is composed of porphyroblastic xenoblasts of garnet in a matrix of quartz, plagioclase, biotite, muscovite, sillimanite, and an opaque mineral. The foliation strikes N13° E and dips 43° to the west-northwest.

Major fracture maxima are N07°E-60°ESE, N87°E, 74°N, and N80°W-80°NNE (Plate C5-7 and Table C5-2). Lesser concentrations cluster about N07°E-75°ESE, N70°E-60°NNW, N15°W-82°ENE, and N45°W-90°. The N80°W and N07°E fractures are nearly orthogonal with the former striking normal to the foliation and the latter nearly paralleling foliation. These relations suggest that these two fracture sets i.e. N80°W-80°NNE and N07°E-60°ESE may have formed synchronously with, and perhaps just prior to, rotation of this metasedimentary unit. Fractures oriented N54°W-90° and N15°W-82°NE show attitudes similar to those of the earlier fault system recognized at Station JW-1; furthermore, their poles do not lie along the foliation plane (Plate C5-7). It is, therefore, likely that they may have formed as incipient conjugate shears, although no evidence of shearing was apparent.

C5.7 THE CORTLANDT COMPLEX

The Cortlandt Complex consists principally of two plutonic masses, an earlier biotite diorite and a later cortlandtite (Ratcliffe, 1968). Flow layering and foliation are present which define funnel-shaped masses (Balk, 1927 in Dolgoff, 1958). K/Ar determinations yielded a minimum age of 435 m.y. for this complex (Long and Kulp, 1962).

Fractures were recorded at Stations B-4, B-5, JW-4, and JW-11 (Plates C1-2 and C5-8). The 615 poles from these four stations were combined into a single equal area, lower hemisphere projection and contoured; four maxima were defined, three of which are noteworthy (Plate C5-8 and Table C5-2). Although northeast fractures do not define a maximum, they are, nonetheless, important for they define a major transcurrent fault trend within the Cortlandt.

Members of the set oriented N38°W-78°NE closely parallel the nearly vertical N32°W set, interpreted at Station JW-6 as an extension fracture set which formed cogenetically with two sets of strike-slip faults (Appendix C5.3). Despite the implication that this set formed in extension, many northwest-trending fractures display slickensides (Table C5-5). One is a fairly large structure which strikes N30°W and parallels the northwest trendng arm of the New Croton Reservoir (ref. Plate C1-2). Since contouring is an averaging process, it is possible that both extension and conjugate shear fractures with small dihedral angles were included in the northwest set.

Other sets also appear to be geometrically and, in some instances, kinematically related to those identified elsewhere. North-northeast fractures define maxima both in the Cortlandt (N11°E-81°SE) and in the Inwood Marble (N09°E-81°SE and N00°E-86°E) at Station JW-1. Several left-lateral, strike-slip faults trending between N40° to 60°E produced minor offsets in the Cortlandt (Attachment B.5.3). Left-lateral displacement also occurred along N43°-65°E faults belonging to the younger conjugate fault system recognized at JW-1. All of the aforementioned observations made within the Cortlandt Complex appear to establish a maximum age of about 435 m.y. for the conjugate fault systems identified at Stations JW-1 and JW-6.

TABLE C5-5

NORTHWEST-TRENDING SHEAR SURFACES IN THE CORLANDT COMPLEX

Strike	Dip	Slickensides (Pitch)
N13°W	70°WSW	20°NW
N18°W	60°WSW	34°NW
N24°W	85°WSW	18°SE
N25°W	75°ENE	48°NW
N25°W	52°WSW	28°NW
N30°W	75°ENE	30°NW
N30°W	80°ENE	28°NW
N35°W	70°NE	22°NW
N35°W	80°NE	10°SE
N40°W	75°NE	08°NW
N40°W	70°NE	32°NW
N43°W	65°SW	25°SE
N47°W	85°NE	18°NW
N48°W	72°NE	05°NW
N52°W	87°NE	15°SE

The last significant fracture set recognized in the Cortlandt has an average attitude of N78°E-82°NNW and apparently formed as a shear set. Three subparallel shear zones, which are members of this set, were recognized at Station JW-4 (ref. Plate C1-2). One, about 15 feet wide, is oriented N80°E-90° and the other two strike N75°E and N80°E with respective dips of 80° and 85°. Right-lateral strike-slip along with nearly horizontal slickensides were identified along a N80°E-84°NNW fault at Station JW-23 (ref. Plate C1-2). Coexisting with this fault is a 45-foot wide, subparallel zone (N75°E-83°ESE) marked by closely spaced fractures. East-northeast faulting was rather intense and was also observed on a macroscopic scale west of the Hudson River. There, a zone of intensely brecciated Precambrian trondhjemitic gneiss occurs in a valley between Buckberg and Dunderberg Mountains (ref. Plate C1-2, Stations JW-5 and JW-21). Both the gneiss and at least one dike of altered andesite, apparently coeval with the Cortlandt, were affected by this tectonism. The motion sense is not known. A parallel fracture maximum (N80°E-79°NNW) was also recognized in the Peekskill Pluton (Table C5-2), though no evidence shearing was apparent. It is suggested that the stress system producing the lateral east-northeast shear was operative from at least Cortlandt time through Middle Devonian (Peekskill) time, but that the shear strain associated with this system decreased prior to the final crystallization of the Peekskill Pluton. Thus, these fractures in the Peekskill may have formed as incipient strike-slip faults.

C5.8 PEEKSKILL PLUTON

The Peekskill Pluton, consisting of granodioritic and granitic phases, appears as a curving, nearly elliptical body with the major axis swinging from nearly east to approximately north-northeast (ref. Plate C1-2). Both phases are generally massive, though locally the preferred orientation of mica flakes and large crystals of microcline and quartz define a foliation (Espejo, 1969). This foliation, which generally parallels the regional fabric, has been interpreted by Espejo as having developed during emplacement of the pluton. A five-point Rb/Sr whole-rock isochron indicates that this mass invaded the country rocks about 368$\pm$27 m.y. (Mose, et al, 1974).

475 fractures were recorded from three stations (B-1, B-2, and B-3) within this body (ref. Plate C1-2) and were compiled into a single, composite equal area projection, then contoured (Plate C5-9). Several maxima appear on this projection with the most obvious oriented N27°E-80°WNW. This trend is most apparent at Station B-3 where the general outline of the pluton trends nearly NNE (ref. Figure C1-2). At Station B-2 several fractures, striking north-northeast and dipping 70°-90° (ref. Plate C3-1), coexist with a vertically dipping flow foliation which strikes N50° to 60°E. The parallelism between these fractures and the trend of the pluton at B-3 plus the cross-cutting relationships exhibited at B-2 lead to two possible interpretations. The first suggests that the north-northeast fractures may have developed parallel to a pre-existing weakness (the foliation), perhaps during uplift. The

second, which is favored, is that these fractures formed as incipient shear fractures associated with the later north-northeast to east-northeast conjugate pairs recognized in the Inwood Marble at Station JW-1.

In addition to the north-northeast fractures, east-northeast fractures dipping 75° to 80°, north-northwest fractures dipping about 70° and 90°, and west-northwest fractures dipping 60° also cut the Peekskill (Plate C5-9 and Table C5-2).

C5.9 Summary

The rocks of the Manhattan Prong were subjected to elevated temperature-pressure conditions early in their history which induced ductile behavior. Based on studies at JW-12 and possibly at JW-6, ductile properties were apparently still inherent in the rocks when normal faulting, possible as a result of uplift, commenced. This phenomenon of "ductile normal faulting" was only locally recognized, but it is not unreasonable that it affected a fairly significant portion of the Manhattan Prong. If this assumption is correct, then the development of steeply inclined to vertical, nearly west-striking normal faults and associated fractures represent the earliest effects of semi-brittle to brittle deformation recorded in Manhattan Prong.

Regional crustal shortening produced north-northeast to northeast-trending folds which dominate the structural picture in the Lower to Middle Paleozoic rocks seen on either side of the Precambrian Hudson Highlands. These folds, northwest and northeast-striking extension fractures, and conjugate west-northwest right lateral and north-northwest left-lateral faults are apparently cogenetic. No small-scale reverse faults were recognized in the Manhattan Prong, but conjugate pairs, ranging in strike from nearly north to northeast, were recognized in Precambrian rocks and are inferred to have formed during regional Paleozoic compression.

Conjugate east-northeast and west-northwest transcurrent faults, showing respective right and left lateral movements, were recognized both in Precambrian and Lower Paleozoic units (Attachment B.5.3), and have been interpreted as being younger than the regional folds and associated structures (Attachment B.5.3). East-northeast fracture trends appear to affect both the Cortlandt and Peekskill Plutons, but unequivocal evidence of shearing was recognized only in the Cortlandt. It is inferred that the east-northeast fractures and faults in the two plutons are genetically related, but that the percentage of shear strain had diminished sufficiently by Peeksill (Devonian) time so that only incipient faults (fractures), showing no differential slip, developed.

North-northeast and northeast transcurrent faults are younger than the north-northwest and west-northwest faults associated with regional folding. They have been recognized, within the site area, as postdating the east-northeast and west-northwest fault sets (Attachment B.5.3). They are suspected of being related to deformation which affected the Newark-Gettysburg Basin (Appendices C-2 and C-6).

APPENDIX C6

TRIASSIC, NEWARK BASIN

C6.1 INTRODUCTION

The Newark Basin extends southwestward from Stony Point through Rockland County, New York, across New Jersey and into Pennsylvania. The sedimentary strata of continental origin and associated igneous intrusives and flows have been designated the Newark Group. Sedimentation began in Late Triassic time and continued into the earliest part of the Jurassic period. The major intrusive body in Rockland County, the Palisades diabase, has been dated at ≈ 190 m.y. (Dallmeyer, 1975).

In New Jersey and Pennsylvania, four formations of sedimentary rock have been recognized in the Newark Group. Conglomerate along the basin margin (Hammer Creek Formation of Glaeser, 1966) is thought to be the time equivalent to the other three units which are, in ascending order, the Stockton (arkose), Lockatong (argillite), and Brunswick (shale and sandstone) formations.

The Lockatong Formation is a central basin, lacustrine facies which is not present in Rockland County, New York. The greatest part of the area studied during this investigation (from Stony Point to about the latitude of Rockland Lake) is underlain by the Brunswick Formation. Within the study area, the occurrence of arkosic beds appears to be limited to exposures east and north of the Palisades diabase. Major deposits of conglomerate and sedimentary breccia are limited to the northwest and northern basin margins; however, conglomeratic beds and pebbly sandstone within sand-shale sequences were observed across the entire basin.

Structure within the basin (compared to that in the adjacent Reading and Manhattan Prongs) is relatively simple. Early workers (Darton, 1890 and Kümmel, 1898) recognized a major fault along the northwest basin margin, and the absence of major faulting along the northern and eastern margins. Although folding and faulting occur throughout the basin, no major structures have been mapped within Rockland County. Thompson (1959) has postulated several faults crossing and bounding the Palisades diabase. Lowe (1959) has disputed the existence of most of these structures. Their debate on the existence of these structures is centered on the nature of the Palisades intrusion itself.

In New Jersey and southern Rockland County, the Palisades diabase is a sill. Along the Hudson River in Rockland County, the intrusive body begins to migrate up the stratigraphic section within the host sedimentary strata. At Haverstraw, New York, the diabase outcrop makes an abrupt turn to the northwest and then turns southwest to its termination at Mt. Ivy. Changes in elevation of the basal contact of the intrusion coincide with topographic breaks in the ridge formed by the diabase. Darton (1890) and Kümmel (1898) attribute this to the intrusion changing from a sill to a dike, or a sill-dike-sill sequence which migrates upsection to the north and north-west. Lowe

(1959) postulates a ring-dike type configuration. Thompson (1959) believes the intrusion remains a sill and is faulted. All seem to agree that there is a fault at Short Clove. Kümmel (1898) interprets an oblique slip at Sparkill Gap (Overpeck Creek). Lowe (1959) observed N-S faults at West Nyack and conceded the possibility of faults at Long Clove and Trough Hollow. Thompson (1959) interprets all topographic gaps in the ridge as related to normal faulting as well as the southern and western margins of South Mountain. Thompson (1959) and Lowe (1959) note glacial striae in valleys which were eroded in fault zones prior to Pleistocene glaciation.

C6.2 SEDIMENTOLOGY-STRATIGRAPHY

The extreme northeastern portion of the basin (Locations CH-1, CH-2, CH-16, and CH-17) is underlain by conglomerate and sedimentary breccia (Plate C1-2). These deposits, which strike west-northwest to northwest and dip southwest at 10 to 20 degrees, consist of pebble-to-cobble size subangular to subrounded gravel in a medium-to-coarse sand matrix. The pebbles and cobbles are predominantly dolomite and limestone with some quartzite and sandstone.

Less than a mile to the south the conglomerate is limited to a narrow band along the western basin margin which is exposed in Cedar Pond Brook (CH-7-2, Plate C1-2). Eastward, along Cedar Pond Brook, the Triassic section consists of a sequence of interbedded shale, sandy shale and sandstone with several pebbly horizons, and a few zones and interbeds of limestone and sandy limestone. The strata in the lower reaches of Cedar Pond Brook strike N40° to 50°W, and dip 20° to 30°SW. Upstream, the conglomerate adjacent to the border fault strikes N11°W, and dips 07°SW.

The lithologic section in the lower part of Cedar Pond Brook is quite similar to that exposed beneath the diabase along the Hudson River between Haverstraw and Rockland Lake. The latter beds strike about N05W, and dip 10° to 15° to the west.

The interior portion of the basin is underlain primarily by sandstone with some interbedded siltstone and shale and several conglomeratic horizons. Where observed, west and south of the diabase and immediately north of the diabase these strata strike essentially north-south and dip to the west, generally less than 10 degrees. These observations indicate that the diabase is a dike west of Haverstraw (Stations CH-5-1, CH-8, CH-23 and CH-25, Figure C1-2).

Conglomerate is present along the western border in the vicinity of Wesley Chapel and Pomona Heights. These deposits consist of pebble to boulder size, subrounded quartzite, sandstone, and carbonate rock clasts in a medium-to-coarse sand matrix with interbedded sandstone and pebbly sandstone. Along Rt. 202 near Wilder Road (CH-3-3 and CH-4), these beds strike N20° to 42°E, and dip 20° to 26°SE. Further south (CH-4), the beds are essentially horizontal (Figure C1-2).

C6.3 BASIN MARGINS

In the SW quarter of the Thiells 7-1/2 Minute Quadrangle, the Newark Basin is bounded by the Ramapo Fault which is mapped in the valley of the Mahwah River. The actual contact between the Triassic strata and the Precambrian rock to the northwest is covered in this area. Here, the Ramapo Fault strikes about N45°E.

In the vicinity of Ladentown the fault bifurcates or splays with one branch continuing along the Mahwah River striking about N30°E, and the other striking east-northeast. The N30°E branch extends into the Reading Prong where it cuts through Precambrian granite gneiss. There appears to be another bifurcation of this branch in the vicinity of Willow Grove (ref. Appendix C4).

The east-northeast branch is not exposed. All that can be said is that the nearest exposure to the north is Precambrian, whereas that to the south of it is Triassic. A fault between these two outcrops is inferred primarily on the basis of its position between the Ramapo Fault to the south and the border fault of the Newark Basin to the north. A shear zone oriented N80°E-55°NW was observed in the diabase exposed along the Palisades Interstate Parkway at the western end of South Mountain (CH-21, Plate C1-2). The east-northeast fault either turns north-northeast or is terminated at a north-northeast fault(s) in the vicinity of Mt. Ivy. Actually, there are no outcrops along this trend across the Newark Basin. Thus, there are no data to determine if this structure extends into, across, or beneath the Newark Basin. Similarily, the north-northeast trend can only be inferred between Mt. Ivy and Cedar Pond Brook.

The New York State Geological Survey (Fischer, et.al., 1961) and Frimpter (1967) have mapped three faults along the north-northeast trend which have emplaced elongate blocks of Cambro-Ordovician phyllite (Trenton) and dolomite (Inwood) between the Newark strata and the Precambrian granite gneiss. Frimpter (1967) noted the occurrence of quartzite in the vicinity of the town of Thiells and postulated a north-northwest fault within the north-northeast trend. The quartzite exposure could not be found during this investigation.

Exposures along and near Cedar Pond Brook generally support the relationships presented on the state map. At Station CH-7-10 (Plate C1-2), a reddish brown shale grades westward into black argillite. The rock is folded and intensely fractured with polished surfaces, lineations, slickensides, and brecciated zones. The folds trend north-northeast with smaller fold axes oriented about N30°E. A highly fractured dolomite is exposed at Station CH-7-11 (Plate C1-2).

At Cedar Pond itself, Newark conglomerate crops out at the east end of the pond beneath the dam (CH-7-2). The strata at the dam strike N11°W. A short distance downstream the strike of the Newark strata is N63W. Minor faults with left-lateral displacement are visible at Stations CH-7-2 (N64°E-75°SE) and CH-7-6 (N74°E-90°).

A dense, black rock which may be siltstone, but is at least in part a mylonite, crops out at the southwest end of the pond (CH-7-9). A K/Ar whole rock date of 398$\pm$ m.y. was obtained for this rock. The entire exposure is very highly fractured.

Precambrian granite gneiss crops out immediately northwest of the pond (CH-7-8). Further upstream major shearing and brecciation are visible in the Precambrian rock at Station CH-7-15. At Station CH-7-14 several right-lateral displacements are visible within an 8-foot wide shear zone which strikes about N40°W.

The north-northeast trend can be projected across the northwest quarter of the Haverstraw 7-1/2 Minute Quadrangle as a break in topography that trends about N30°E and separates outcrops of Precambrian granite gneiss and the dioritic rocks of the Rosetown Pluton to the northwest from outcrops of Newark strata on the southeast. The Newark conglomerate is not seen north of an unnamed creek which flows generally east-southeast to Stony Point. A small north-south-trending right-lateral fault was observed in the northernmost outcrop of conglomerate (CH-16, Plate C1-2).

The Newark strata unconformably overlie pre-Triassic rocks along the northeastern and eastern margins of the basin. On the east, in the vicinity of Nyack, the 10°W dip of the Newark strata is concordant with the slope of the pre-Triassic surface (Worzel and Drake, 1959). In the northeast, the Newark strata strike roughly parallel to and dip away from the northeastern basin margin. The high percentage of carbonate rock clasts in the conglomerate is presumed to have originated from the Cambro-Ordovician carbonate rocks which crop out to the north-east.

Whether these relationships reflect pre-depositional basin geometry or post-depositional folding and erosion (as suggested by Sanders, 1960 and 1974) has not been conclusively demonstrated.

C6.4 FOLDING

Except for the extreme northwest and northeastern borders, the basin structure is homoclinal with the sedimentary strata striking north and dipping west 5° to 15°.

The southeastward dipping conglomerate along the Ramapo Fault in the southwest quarter of the Thiells Quadrangle create a synform configuration in that area. Kümmel's (1898) interpretation is that the structure is a syncline which was filled with diabase. Sanders (1974) suggests that another fault exists within the basin, possibly parallel to the Ramapo Fault. A simpler explanation would be that the discordant dips are related to movement on the Ramapo Fault. Present exposures do not provide enough information for an unequivocal interpretation.

Similarly, the lack of outcrop between Cedar Pond Brook and the north slope of South Mountain precludes determining a relationship between the northwest strikes in the northern end of the basin and the west-dipping homocline.

The strata in the lower reaches of Cedar Pond Brook strike N40° to 50°W and dip 20° to 30°SW (CH-7-1, CH-7-6, CH-7-7). Upstream the strike rotates to N33°W (CH-7-5) back to N49°W (CH-7-4), then to N63°W (CH-7-3), and finally to N11°W, dipping 07°SW in the conglomerate adjacent to the border fault (Plate C1-2). Whether these variations are due to folding or faulting could not be determined during reconnaissance mapping.

C6.5 FAULTING

Aside from the minor displacements already noted at Cedar Pond Brook and in the conglomerate near Stony Point, actual fault planes were observed at only three localities.

On the north slope of the South Mountain near Little Tor (CH-25), two prominent shear zones are visible in the sandstone and shale beneath the diabase. They strike approximately N50° E. Small-scale offsets indicate left-lateral movement along N50° E and right-lateral movement along north-northeast surfaces (N13° E). Within the eastern shear zone a fault plane oriented N52° E, 83° SE contains 1 to 3 inches of clay and gouge. Slickensided surfaces are visible within the gouge. The footwall face is highly polished with grooves and slickensides plunging 22° SW. Faint horizontal slickensides are superimposed on these surfaces.

These shears are exposed in a rock face above which a glaciated surface is partially exposed. Glacial grooves and striations trend about N15° W. Two gullies in the present surface (one of which is above the eastern shear zone) have glacial striations on their walls, indicating that the gullies existed prior to glaciation. In the vicinity of the eastern shear zone, the striated surface exhibits several vertical displacements of less than one inch. Similiar displacements were not observed in any other areas where the glaciated surface is exposed - including above the western shear zone. The glaciated surface is not well exposed where the displacements are visible, and some of the blocks observed may not actually be in situ. The displacements are more than likely the result of frost heave.

However, in at least one instance the situation is very much like the features described by Oliver, Johnson and Dorman (1970) in Paleozoic rocks to the north. In this instance, the southeast side of a northeast-striking fracture which dips nearly vertically to the southeast is raised about 0.5 inch.

Several shear zones are visible in the diabase quarry between Long Clove and Short Clove. There is no stratigraphy in the diabase with which to determine the sense of movement. A mineralized (calcite) breccia can be traced vertically through the walls of all five levels of the quarry. Its strike is about N20°E. Solution cavities within the breccia are lined with euhedral dolomite. Associated fractures contain smeared calcite, biotite and chlorite (probably altered biotite), and euhedral quartz and dolomite.

A normal fault crosses the southwest edge of the quarry. The same fault is visible at the south portal of the Penn Central R.R. tunnel through Hook Mountain (Plate C1-2, Station CH-5-4). The main fault plane has an average strike of N65°W. The dip is in the range 55° to 75°SW. Several smaller normal faults with strikes in the range N44° to 75°W were observed above the hanging wall. The fault is best exposed in the southeast corner of level 5 in the quarry (Plate C1-2, Station CH-5-6). The main plane consists of 1 to 3 feet of brecciated, slickensided (biotite) diabase, clay and gouge. The gouge zone lies at or near the sandstone-diabase contact within the diabase. Contact metamorphic effects are apparent in the sandstone. Where the fault lies within the diabase, the sandstone-diabase contact is commonly welded. The diabase is brecciated or very highly fractured up to 15 feet away from the gouge zone. The sandstone is highly fractured but not brecciated. A compensatory (?) splay off the main shear zone in the hanging wall block is truncated at the base of the overlying till. Rock along the splay is badly weathered. Its footwall is composed of fresh sandstone, and the material in the hanging wall is weathered sandstone containing somewhat rounded fragments indicating that this may be a colluvial deposit.

A poor exposure of the fault on the west side of level 5 (Plate C.1-2, Station CH-5-7) was examined before and after several days of rain during which slumping occurred. At this location brecciation and clay gouge extend into the sandstone hanging wall as well as the diabase footwall. The footwall block exhibits strong shear fracturing oriented N10°E and N75°E with extension (?) fractures roughly parallel to the main fault trend (N65°W). All three sets are lined with 1/4 to 3 inches of clay and gouge.

On the first examination of this exposure, a hand excavation through a gulley in the diabase footwall revealed weathered sandstone at the base of the excavation which was overlain by gravelly sand and clay. The latter deposit was observed at an elevation directly across the fault from the diabase. Due to its containing rounded fragments of quartz and crystalline metamorphic rocks, it is interpreted as a Pleistocene deposit or fill. Following the slump, this material could not be reached with a hand excavation. The material encountered at a similar elevation was a confused mass of sand, clay and fragments (both rounded and angular) of weathered and relatively fresh sandstone, diabase, and crystalline metamorphic rocks.

C6.6 FRACTURE ANALYSIS

Plate C3-1 presents a summary of fracture data. Table C6-1 lists the movement plans observed. These data were obtained almost entirely from small-scale structures.

Comparison of the plots of poles to fractures and senses of movement suggests that all of the brittle deformation features observed during this investigation could have formed during a single compression, with the maximum principle stress horizontal and oriented approximately N25°E.

It is worthy of note that most of the faults proposed in the study area can be interpreted with this hypothesis. For example, the displacement at Short Clove is interpreted as a normal fault striking N25° to 30°E which is an extension direction (Fischer, et.al., 1961). Another proposed fault at Long Clove strikes N40°E (Thompson, 1959) or N65°E (Lowe, 1959 and Fischer, et.al., 1961). The apparent displacement is down to the north on a horizon which dips WSW; thus, movement can be interpreted as left-lateral. The magnetic anomaly pattern at Long Clove (Plate C4-4) also suggests left-lateral displacement.

The major inconsistencies in the literature center around the east-northeast faults south of the west half of South Mountain proposed by Thompson (1959). These were postulated on the basis of northerly dips in the Newark strata in that area.

The bedding north and south of Lake Lucille (CH-8 and CH-23) strikes N06°W and dips to the west at 13° to 14°.

C6.7 AGE OF MOVEMENT

The fractures and faults described above are younger than 190 m.y.

While the data presented herein are consistant with a hypothesis of one period of deformation, multiple periods of deformation have been interpreted elsewhere in the Newark Basin (Dames & Moore, 1974). Sanders (1971 and 1974) has proposed a complex history of deformation of the Triassic rocks in northern North America which culminates with left-lateral simple shear along northeast-trending faults. According to Sanders, a consequence of this couple is N-S oriented normal faults. de Boer (1967) presented data which indicate that the NE-SW, left-lateral couple occurred during the Jurassic. His data suggest, however, that in the site region the principal horizontal compression had a bearing of about N30°E. This would allow for extension at N30°E to N60°W. North-striking fractures in this model would be right-lateral shear.

There are no data to suggest major tectonic activity since the deformation of the Basin by simple shear or pure shear during the Jurassic or Early Cretaceous periods. Glacial striations in gullies eroded in fault zones indicate a post-faulting, pre-glaciation period of erosion. There are inconclusive data which suggest that post-Triassic and/or Pleistocene material may have been disturbed along the northwest-trending normal fault exposed in the south of the quarry at Haverstraw.

TABLE C6-1

RELATIVE MOVEMENTS OBSERVED DURING BRITTLE DEFORMATION STUDY:

NEWARK BASIN

Location	Orientation	Slickensides (Pitch)	Movement Sense	Filled
*CH-5-4	N66W: 55S		Normal	
CH-5-4	N81W: 60S		Normal	
*CH-5-6	N65W: 74S	64S	Normal	Breccia, Gouge, biotite
CH-5-6	NW: S		Normal	
*CH-5-7	N65W: 70S		Normal	Breccia
CH-5-7	N44W: 53S		Normal	Breccia
CH-7-2	N64E: 75S		Left Lateral	
CH-7-6	N74E: 90		Left Lateral	
CH-16	N13E: 90		Right Lateral	
CH-25	N52E: 83S	22SW & Horiz.	Left Lateral	Clay, Gouge
CH-25	N53E: 87S	12SW	Left Lateral	
CH-25	N53E: 81S	17SW	Left Lateral	
CH-25	N13E: 53S		Right Lateral	

*Probably same fault

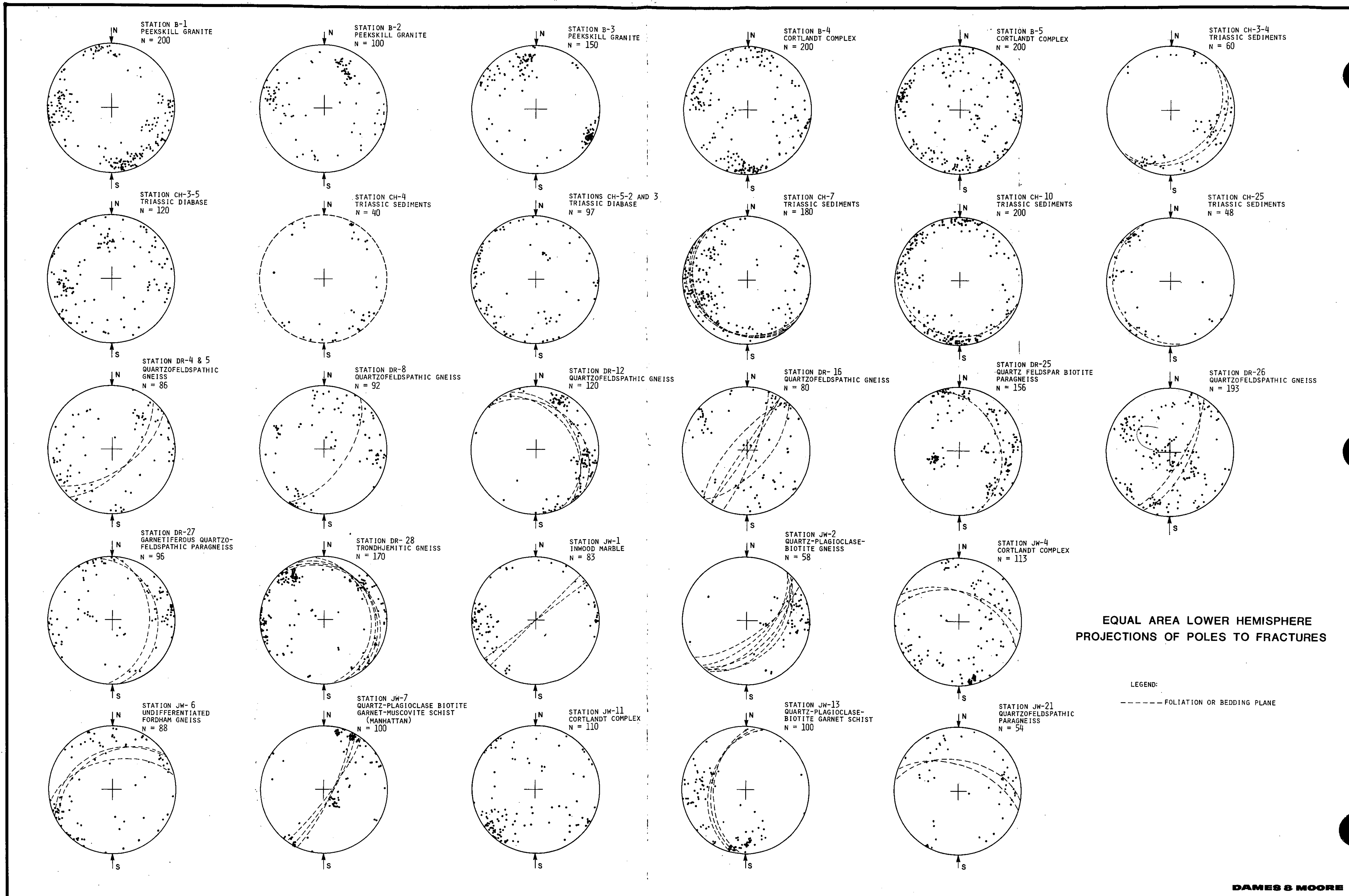

EQUAL AREA LOWER HEMISPHERE PROJECTIONS OF POLES TO FRACTURES

DAMES & MOORE

PLATE C1-1

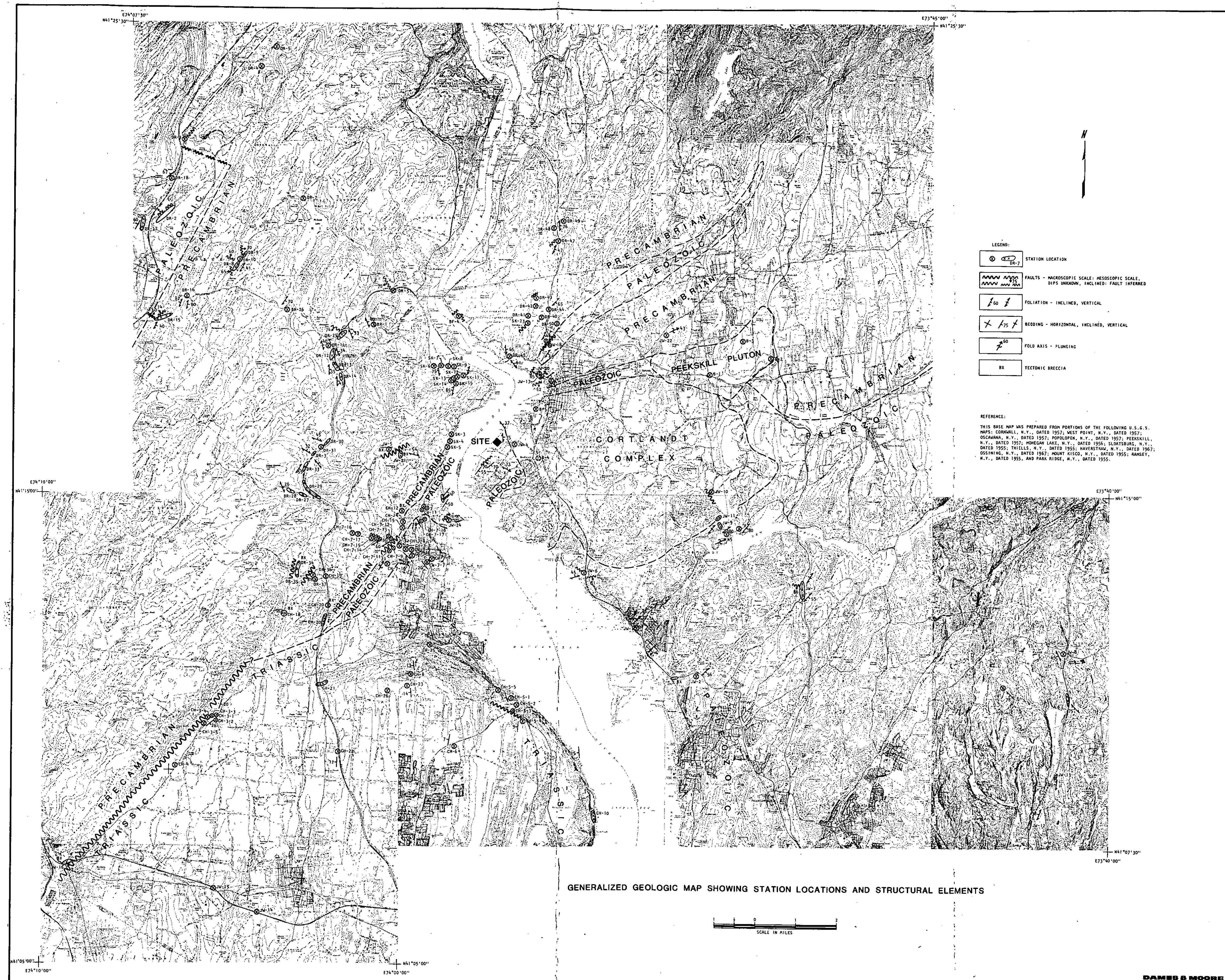

GENERALIZED GEOLOGIC MAP SHOWING STATION LOCATIONS AND STRUCTURAL ELEMENTS

PLATE C1-2

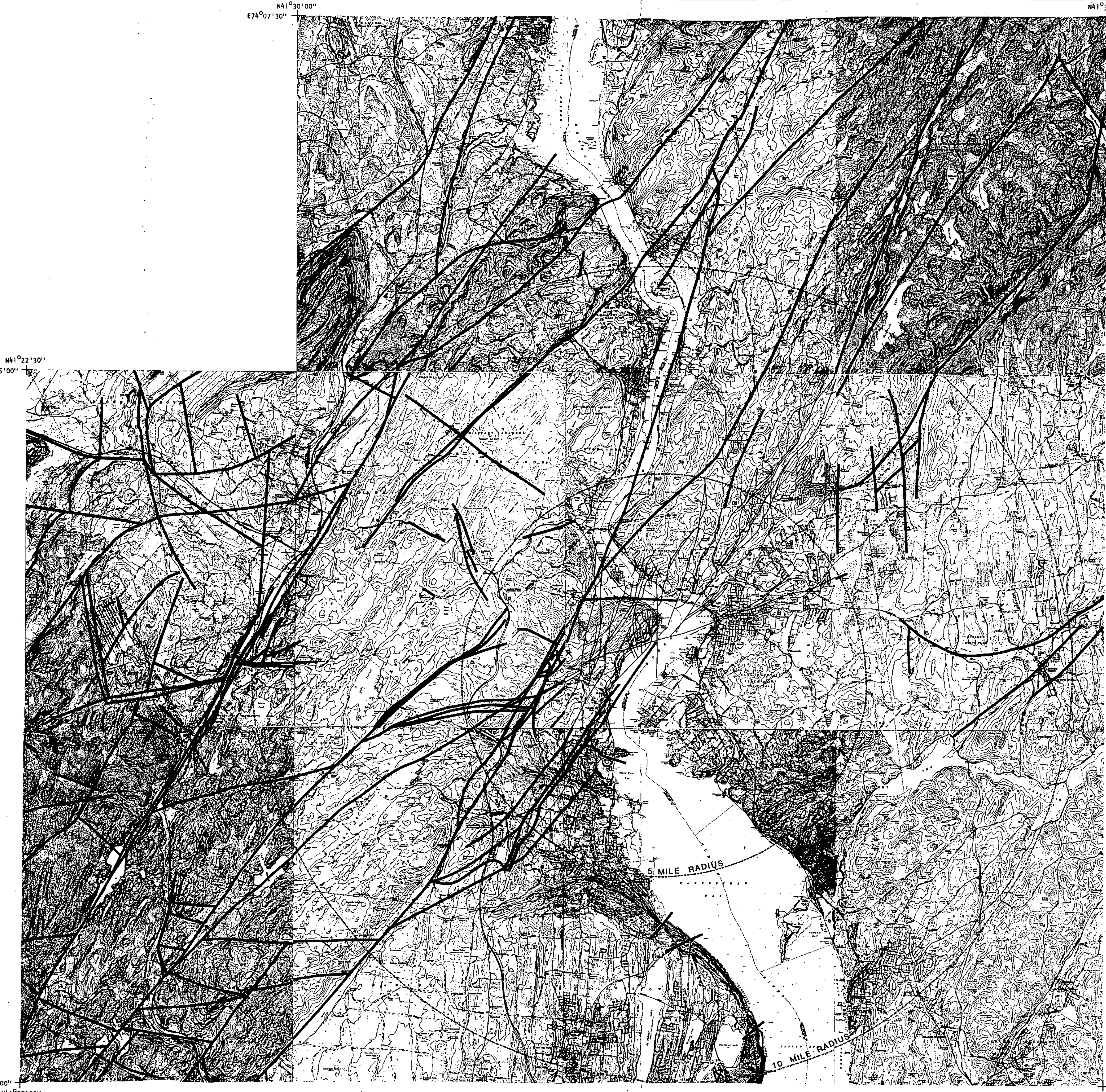

DISTRIBUTION OF MAJOR FAULTS IN SOUTHEASTERN NEW YORK STATE

SCALE IN MILES

LEGEND:

- FAULTS
- UNPUBLISHED DATA (FAULTS)
- MICROSEISMIC STATIONS
- SITE

REFERENCE:

THIS BASE MAP WAS PREPARED FROM PORTIONS OF THE FOLLOWING U.S.G.S. MAPS: CORNWALL, N.Y., DATED 1957; WEST POINT, N.Y., DATED 1957; OSCAWANA, N.Y., DATED 1956; MONROE, N.Y., 1957; POPOLOPEN LAKE, N.Y., DATED 1957; PEEKSKILL, N.Y., DATED 1957; MOHEGAN LAKE, N.Y., DATED 1956; SLOATSBURG, N.Y.-N.J., DATED 1955; THIELLS, N.Y., DATED 1955; HAVERSTRAW, N.Y., DATED 1967, AND OSSINING, N.Y., DATED 1967.

SOURCES OF INFORMATION:

DODD, R.T., 1964; DALLMEYER, R.D., 1972; JAFFE, H.W., AND JAFFE, E.B., 1973; RATCLIFFE, N.M., 1975; COUNTY GROUNDWATER RESOURCES: PUTNAM AND ROCKLAND; NEW YORK STATE GEOLOGIC MAP, 1970.

DAMES & MOORE

PLATE C3-1

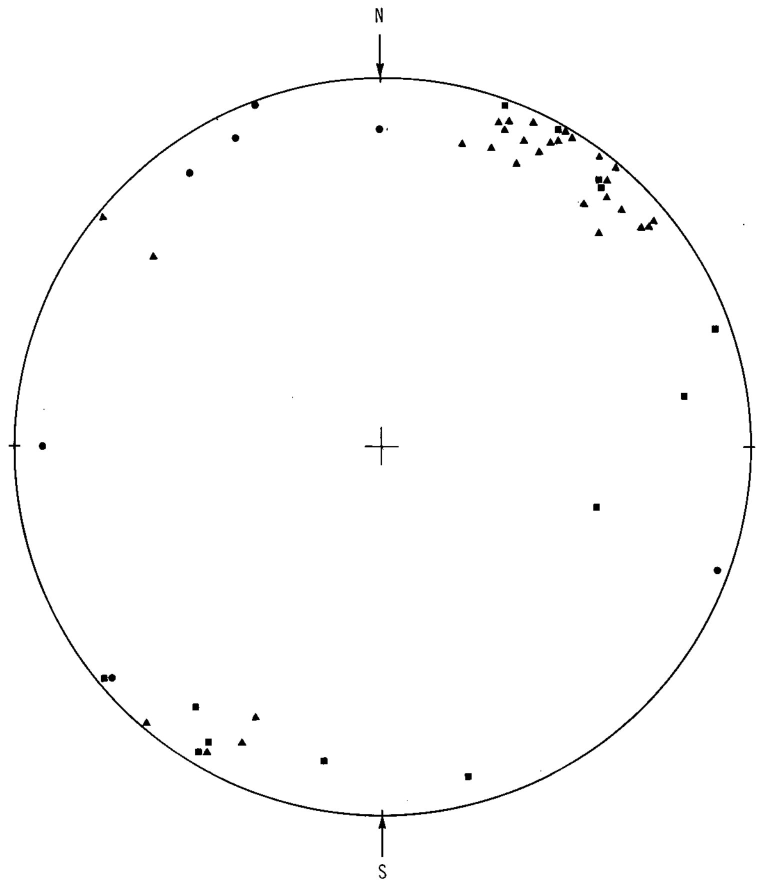

EQUAL AREA LOWER HEMISPHERE
PROJECTION OF POLES TO SILURO-DEVONIAN DIKES
IN THE HUDSON HIGHLANDS
N=50

LEGEND:
- ▲ ANDESITE?
- ■ RHYOLITE?
- ● DIABASE?

DAMES & MOORE

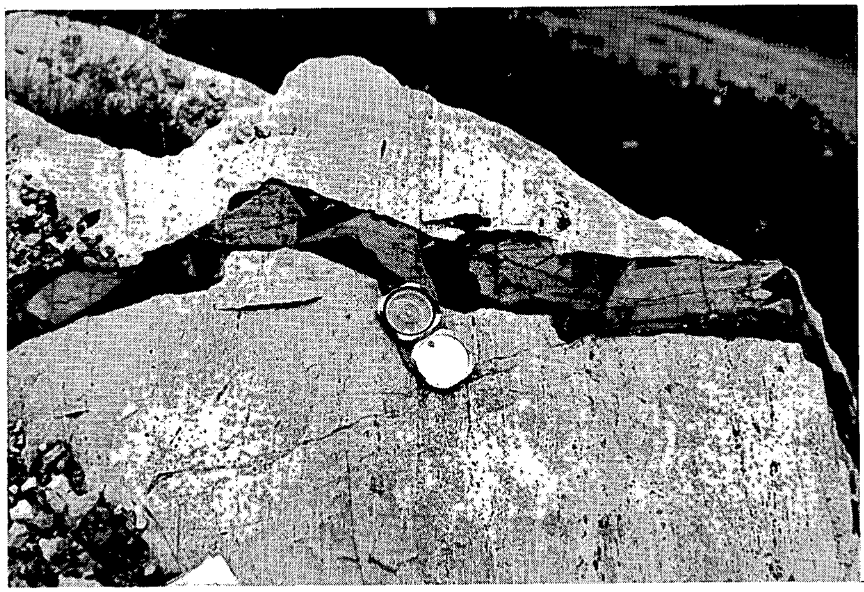

PHOTO A

PLAN VIEW OF AN ANDESITE DIKE CUTTING QUARZ-PLAGIOCLASE LEUCOGNEISS AT STATION DR-26. COMPASS POINTS NORTH. THE DIKE FOLLOWS EXTENSION FRACTURES (LEFT AND RIGHT OF PHOTOGRAPH) AND SHEAR FRACTURE (CENTER)

PHOTO B

CLOSE UP OF PHOTO A

DAMES & MOORE

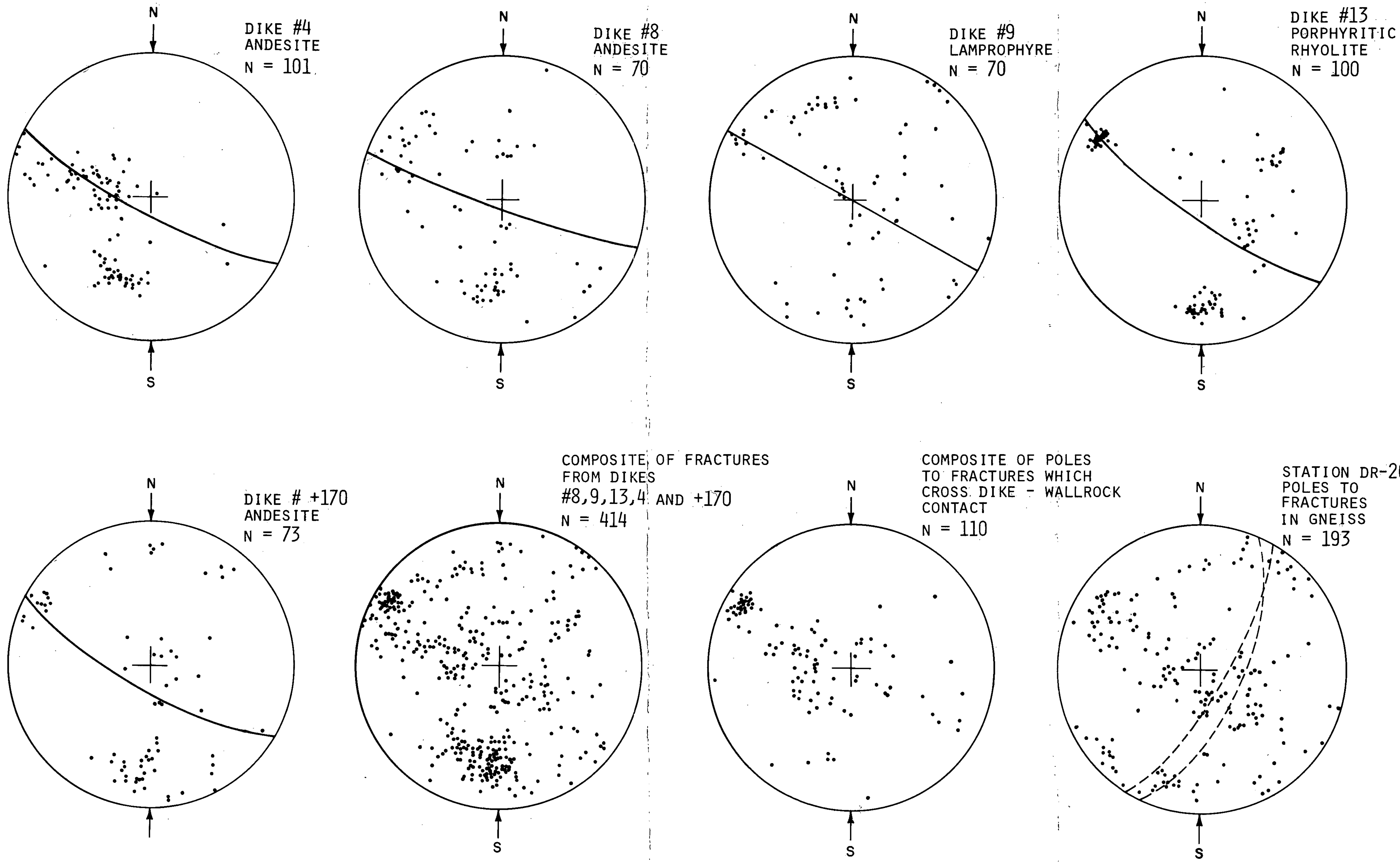

LEGEND:

- - - - - FOLIATION OR BEDDING PLANE

——— DIKE SURFACE

EQUAL AREA LOWER HEMISPHERE

PROJECTION OF POLES TO FRACTURES AT STATION DR-26

(STATION LOCATION ON PLATE C1-2)

DAMES & MOORE

AEROMAGNETIC MAP OF PART OF SOUTHEASTERN NEW YORK STATE

1 0 1

SCALE IN MILES

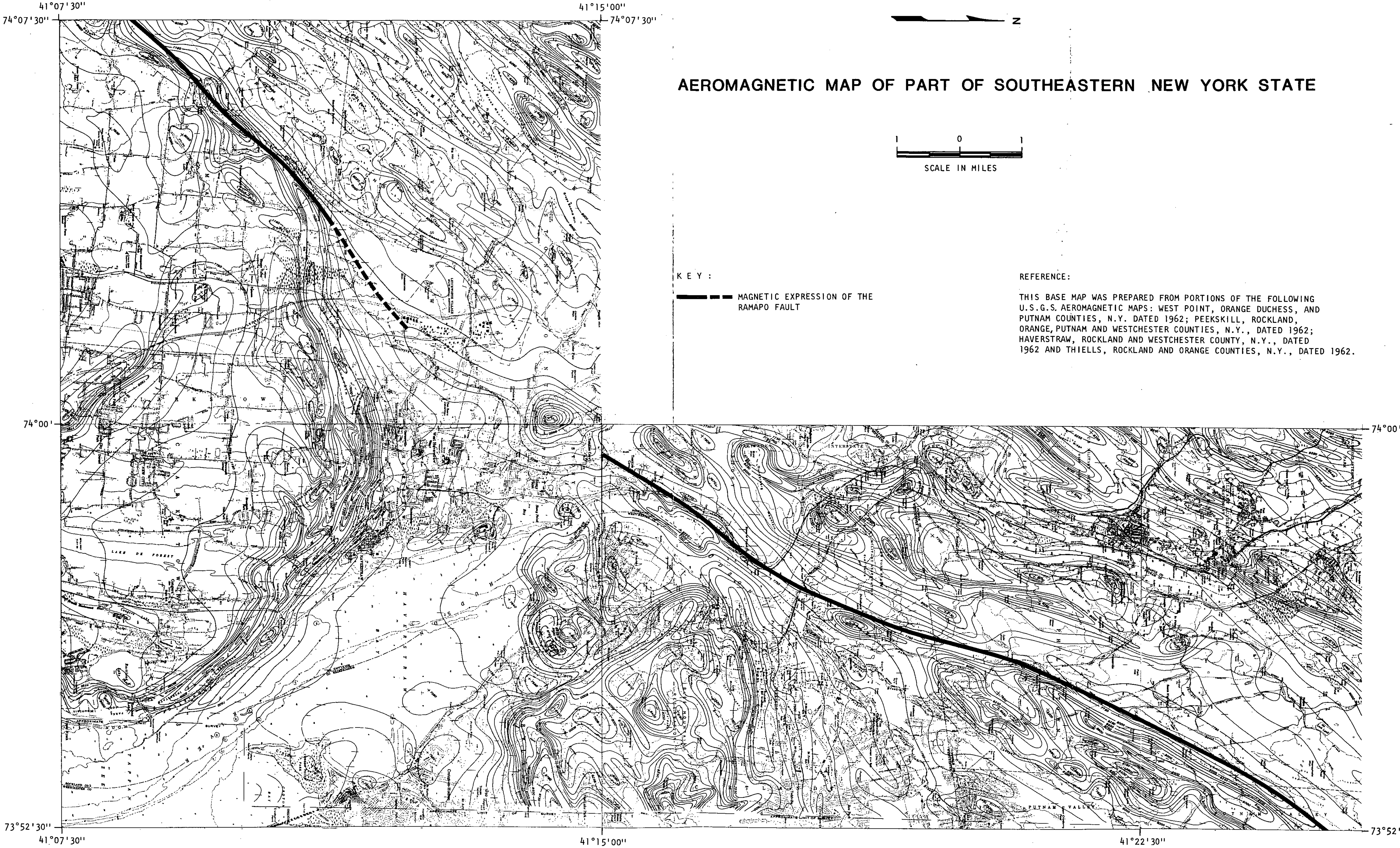

KEY:

MAGNETIC EXPRESSION OF THE RAMAPO FAULT

REFERENCE:

THIS BASE MAP WAS PREPARED FROM PORTIONS OF THE FOLLOWING U.S.G.S. AEROMAGNETIC MAPS: WEST POINT, ORANGE DUCHESS, AND PUTNAM COUNTIES, N.Y. DATED 1962; PEEKSKILL, ROCKLAND, ORANGE, PUTNAM AND WESTCHESTER COUNTIES, N.Y., DATED 1962; HAVERSTRAW, ROCKLAND AND WESTCHESTER COUNTY, N.Y., DATED 1962 AND THIELLS, ROCKLAND AND ORANGE COUNTIES, N.Y., DATED 1962.

DAMES & MOORE

PLATE C4-4

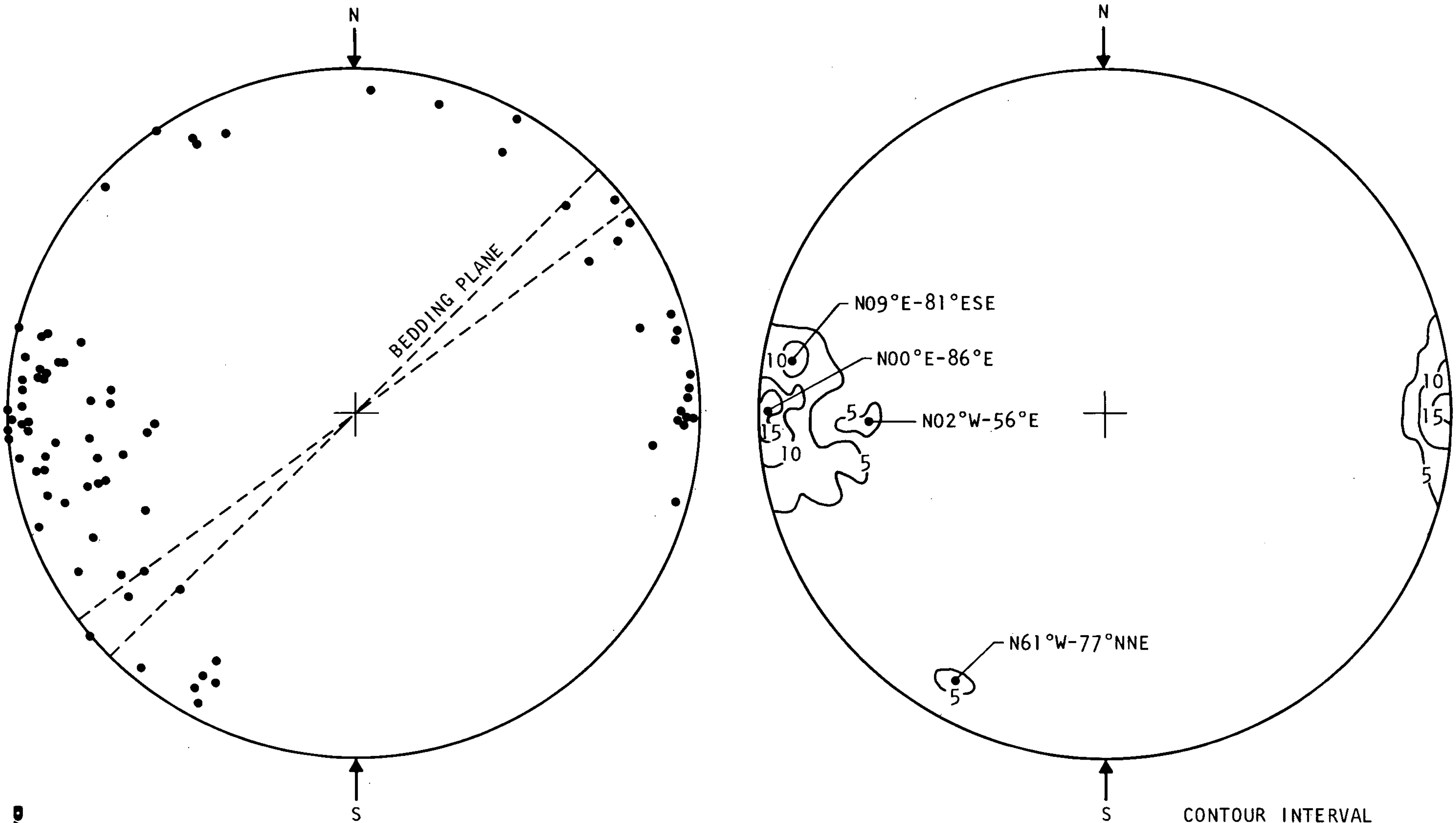

CONTOUR INTERVAL
5,10,15 POINTS/1% AREA

POINT AND CONTOUR DIAGRAMS
OF 83 POLES TO FRACTURES AT STATION JW-1

(STATION LOCATION ON PLATE C1-2)

DAMES & MOORE

PLATE C5-1

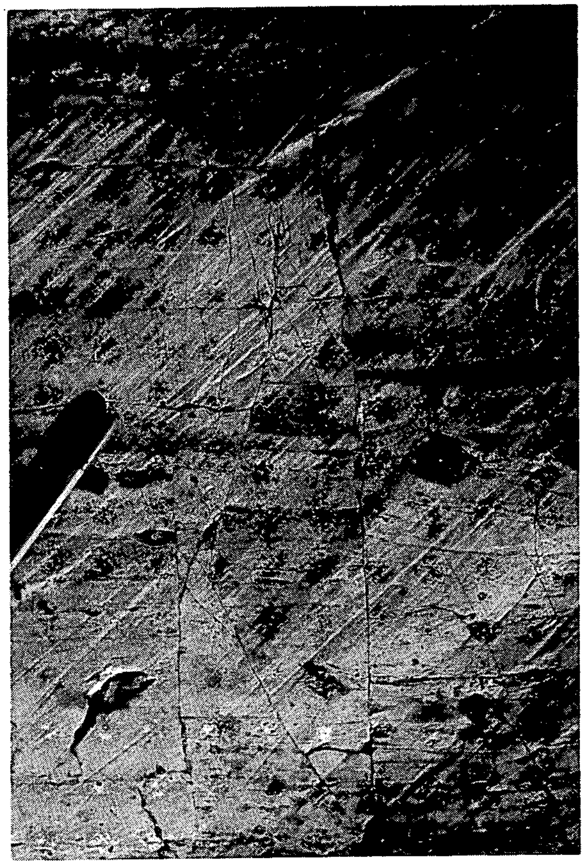

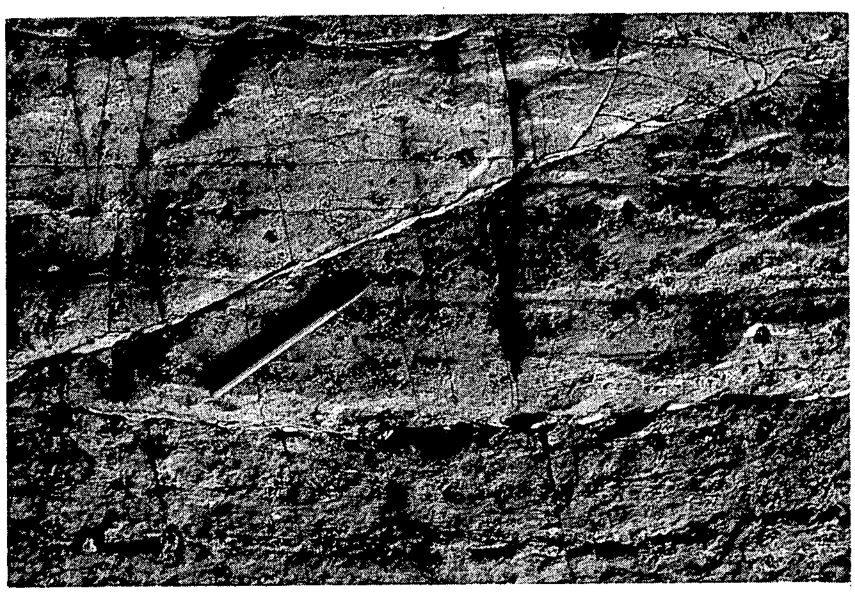

PAIRED CONJUGATE STRIKE-SLIP FAULTS IN THE INWOOD MARBLE AT STATION JW-1.

PEN POINTS NORTH.

DAMES & MOORE

PLATE C5-2

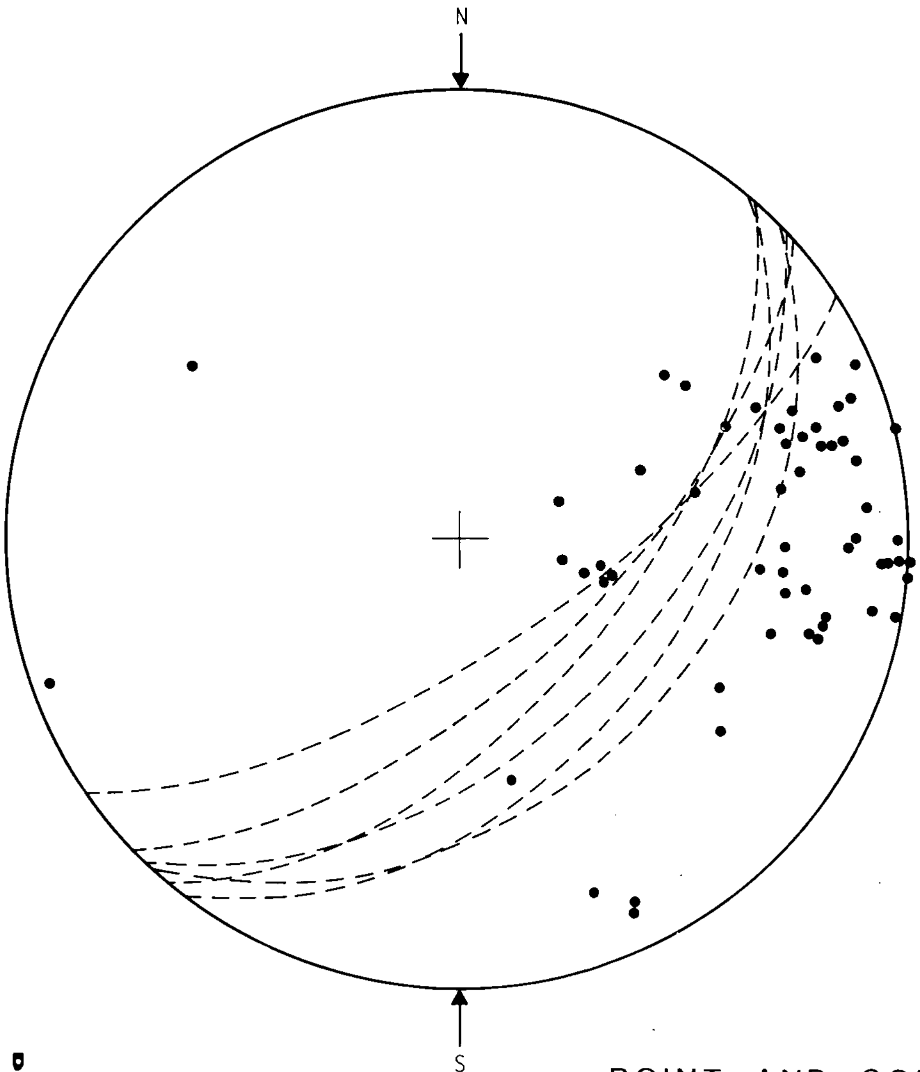

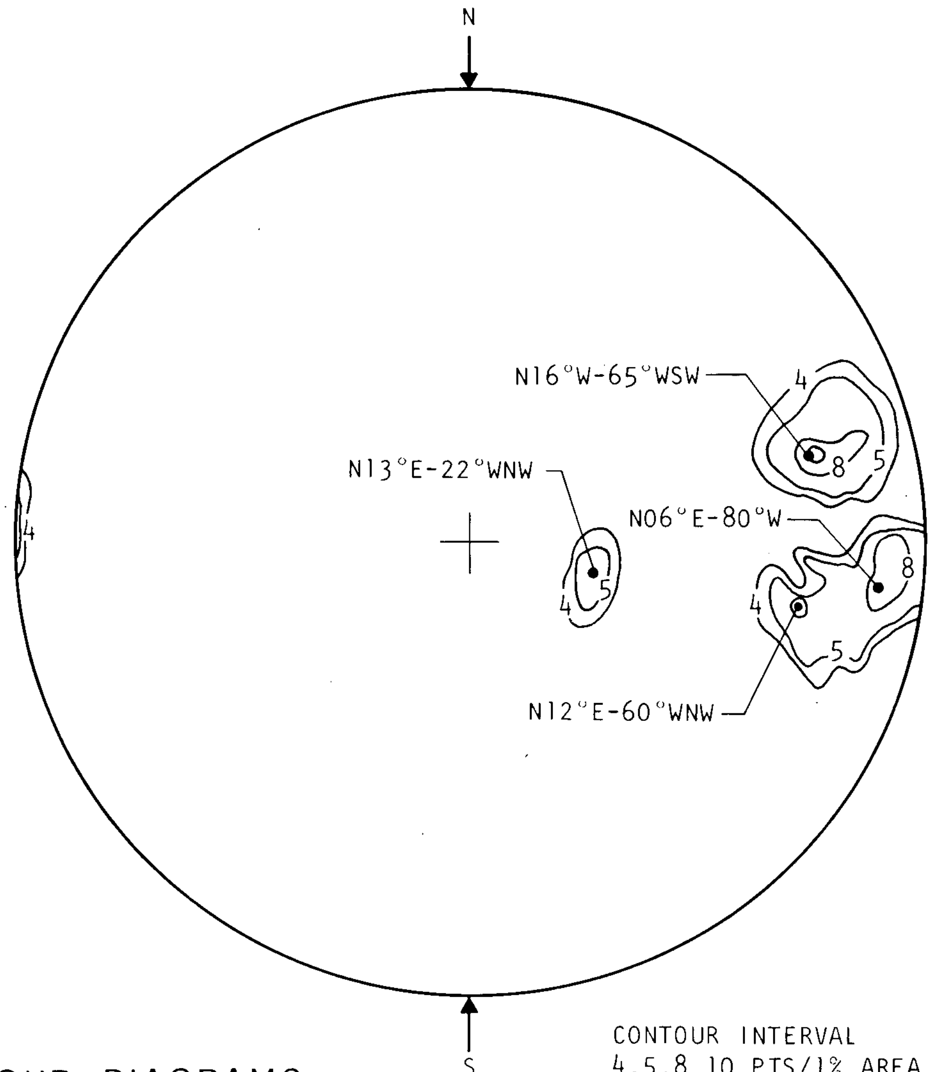

CONTOUR INTERVAL
4,5,8,10 PTS/1% AREA

POINT AND CONTOUR DIAGRAMS
OF 58 POLES TO FRACTURES AT STATION JW-2

KEY:
● POLE REPRESENTING FRACTURE PLANE
– – – – PLANE REPRESENTING FOLIATION SURFACE

(STATION LOCATION ON PLATE C1-2)

DAMES & MOORE

PLATE C5-3

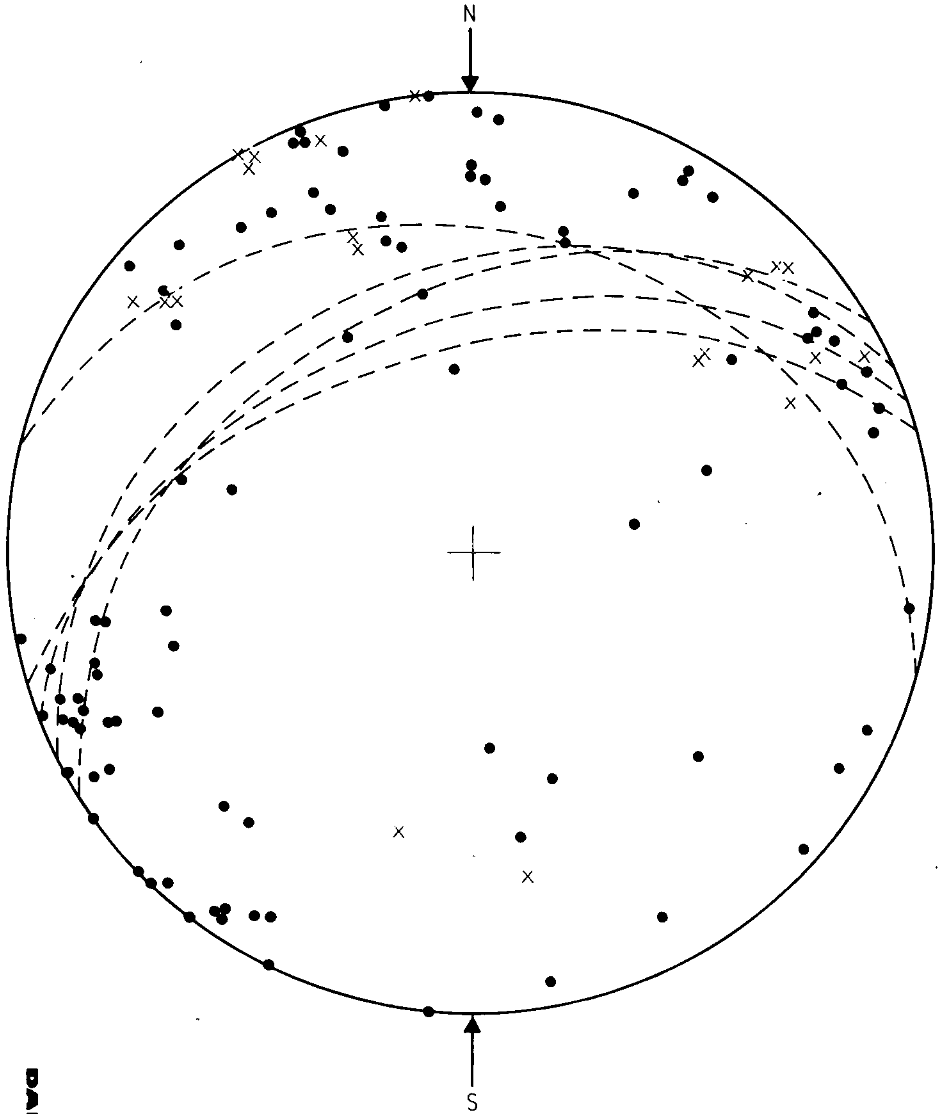

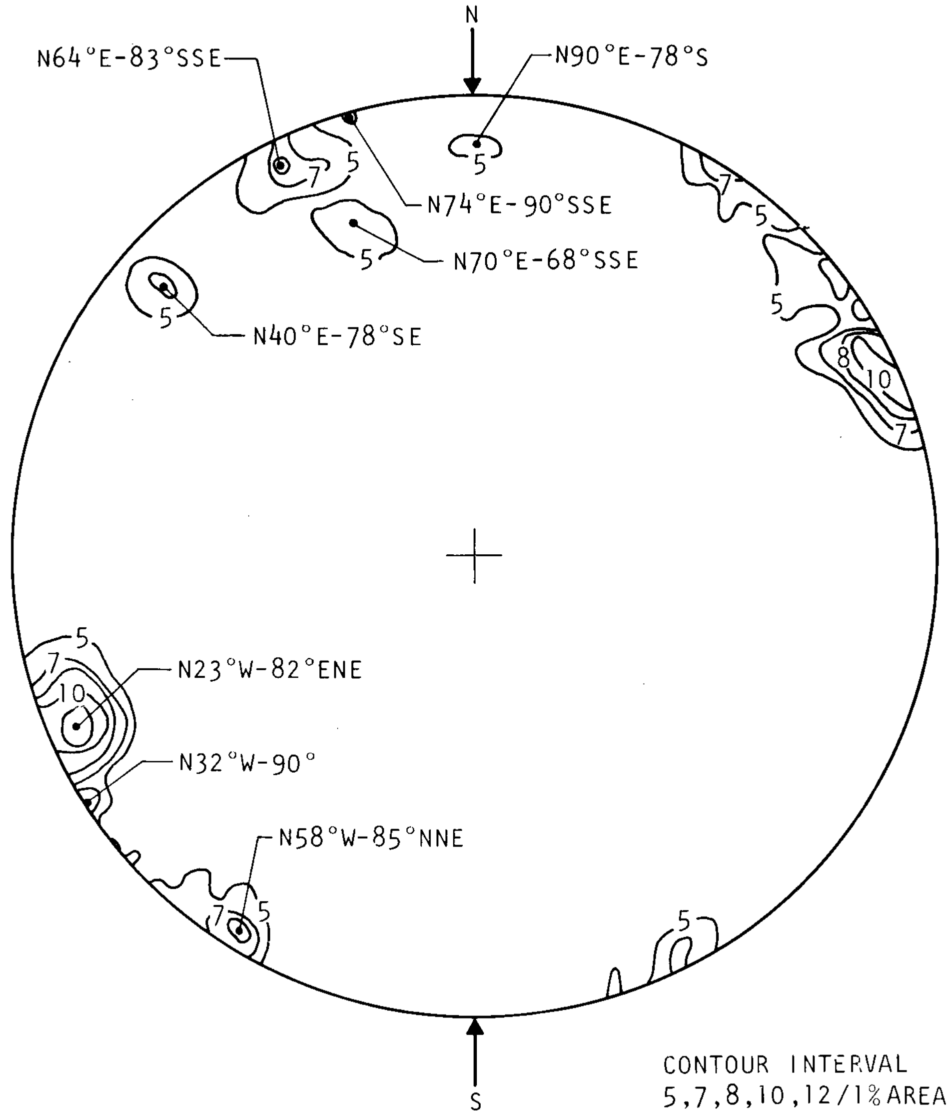

CONTOUR INTERVAL
5,7,8,10,12/1% AREA

KEY:

- ● POLES TO FRACTURES ASSOCIATED WITH FOLIATION ORIENTED N60° TO 75°E - 38° TO 53°NNW
- × POLES TO FRACTURES ASSOCIATED WITH FOLIATION ORIENTED N75°W-30°NNE

(STATION LOCATION ON PLATE C1-2)

POINT AND CONTOUR DIAGRAMS OF 110 POLES TO FRACTURES AT STATION JW-6

DAMES & MOORE

PLATE C5-4

ROTATED MESOSCOPIC F_2-FOLDS IN THE MANHATTAN FORMATION AT STATION JW-7.

NOTE AXIAL PLANE FRACTURES

DAMES & MOORE

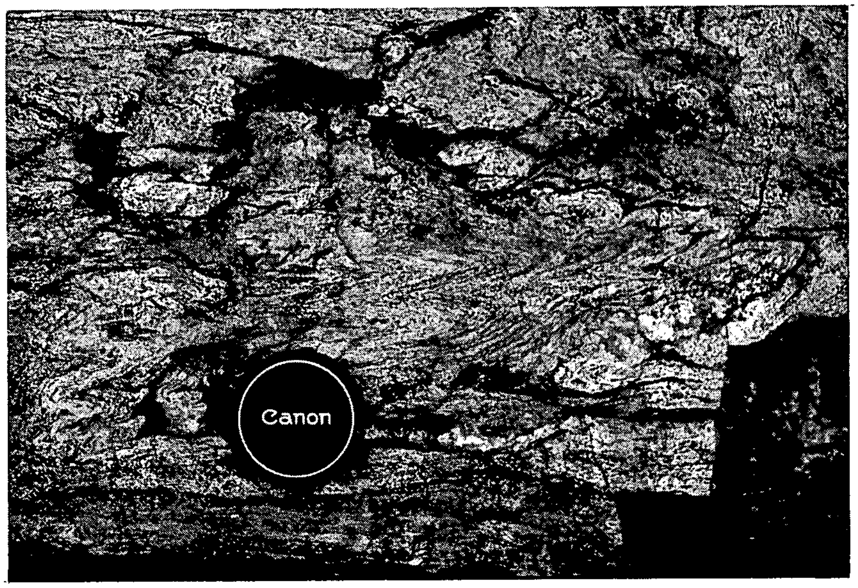

PHOTO A

PASSIVE FOLDING IN THE FORDHAM GNEISS AT STATION JW-12.

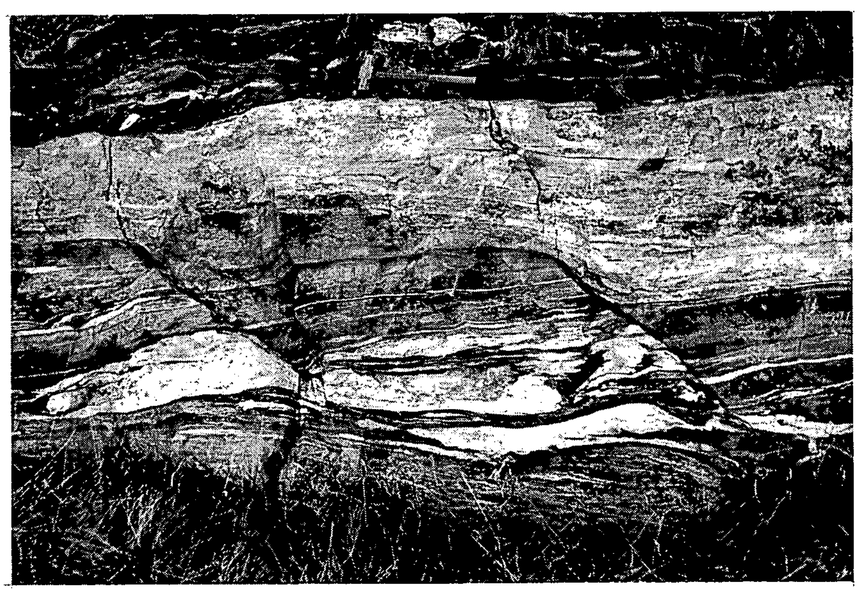

PHOTO B

"DUCTILE" NORMAL FAULTS PRODUCING SMALL MONOCLINAL FLEXURES AT STATION JW-12.

DAMES & MOORE

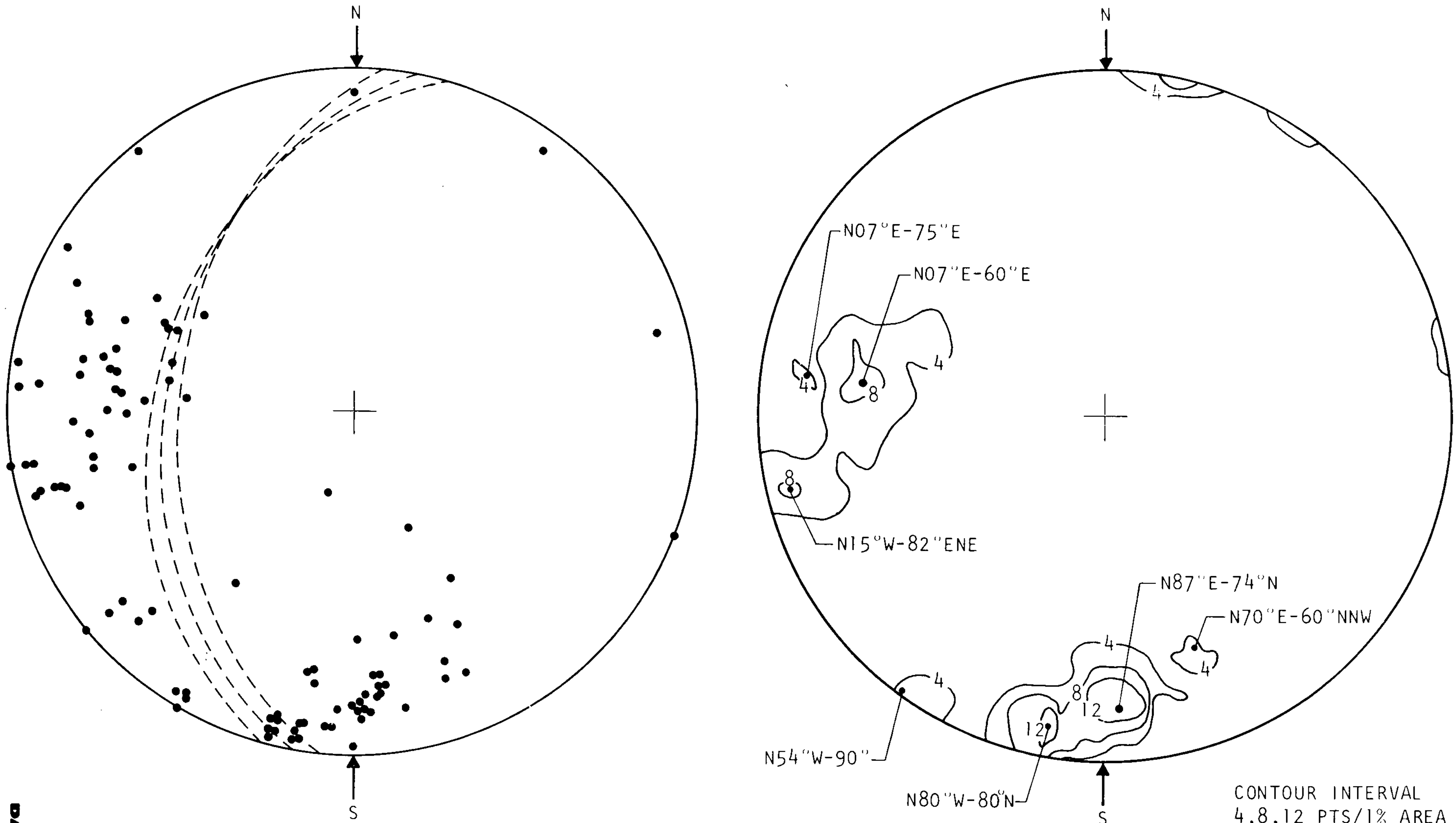

POINT AND CONTOUR DIAGRAMS OF 100 POLES TO FRACTURES AT STATION JW-13

KEY:
- • POLE REPRESENTING FRACTURE PLANE
- ---- PLANE REPRESENTING FOLIATION SURFACE

(STATION LOCATION ON PLATE C1-2)

DAMES & MOORE

PLATE C5-7

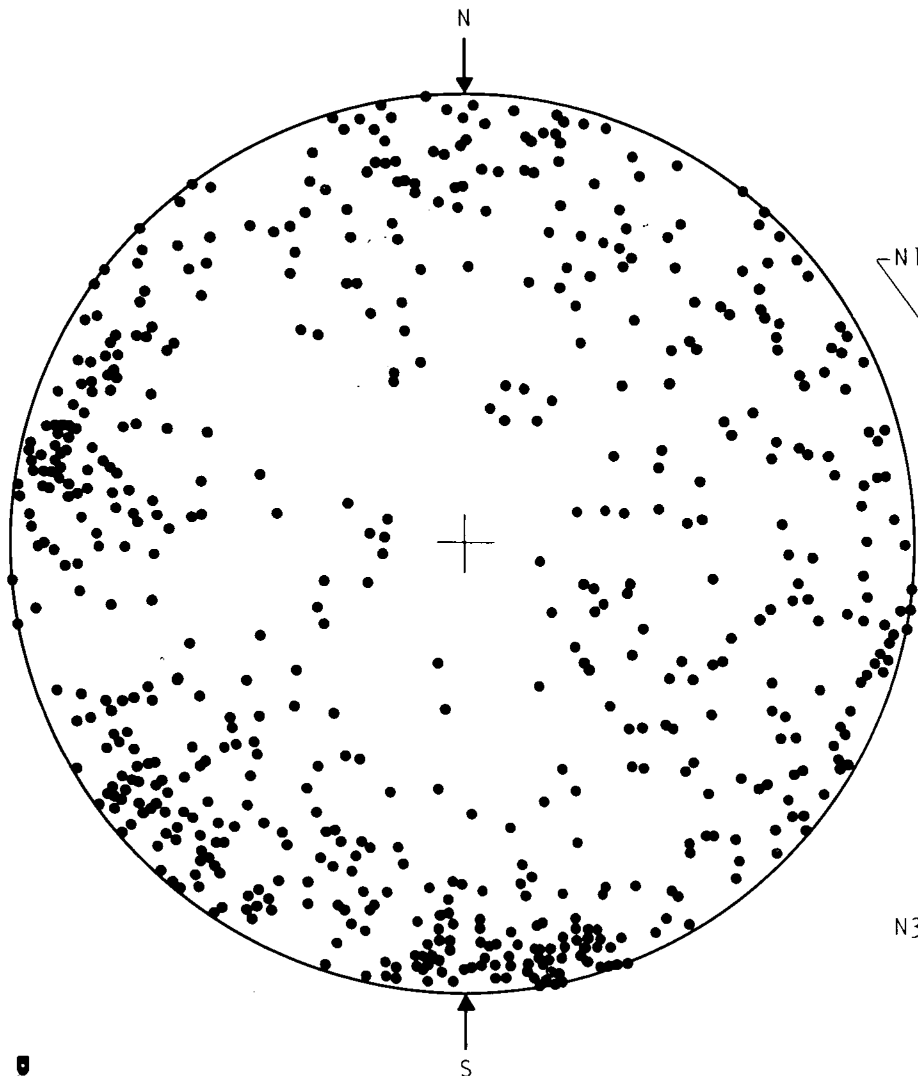

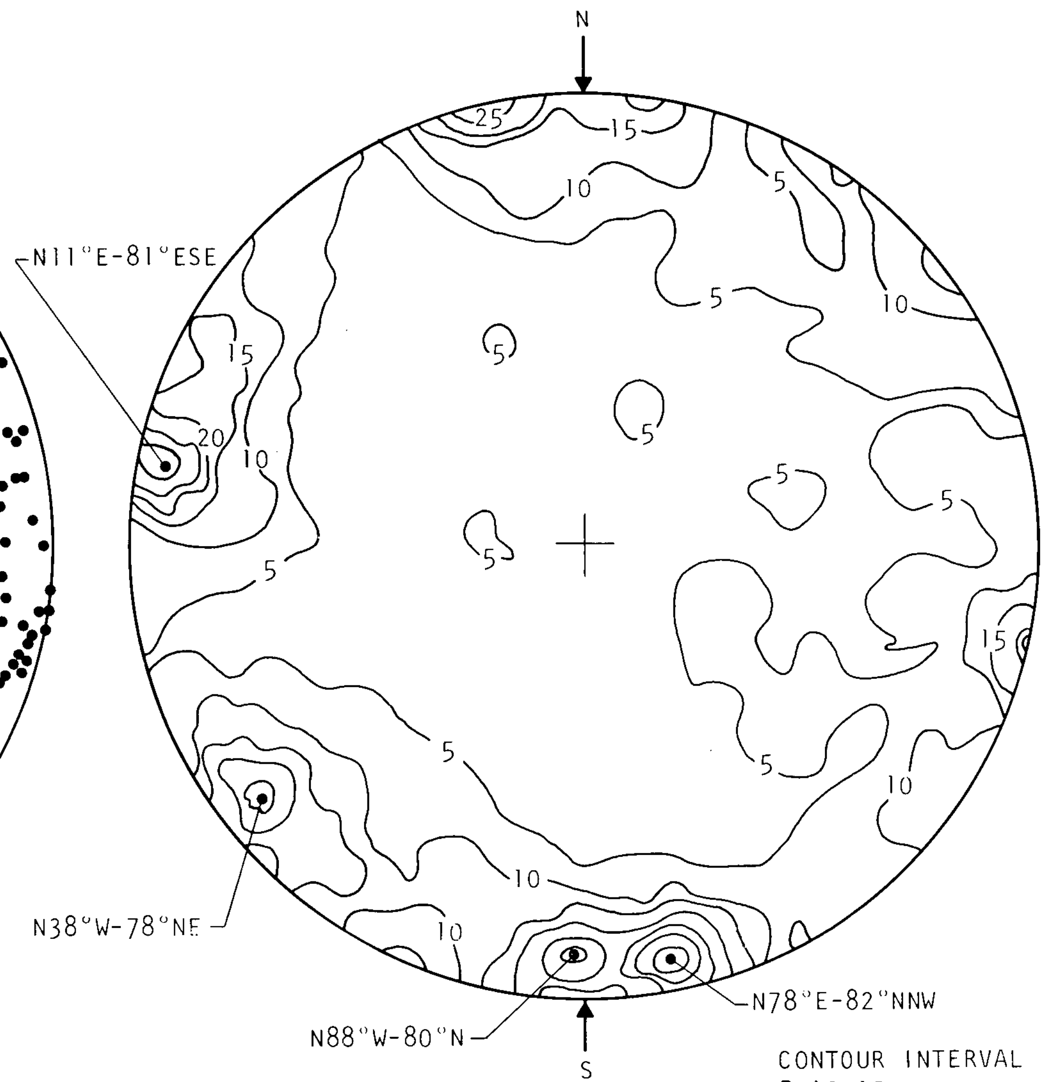

CONTOUR INTERVAL
5,10,15,20,25,
30,35 PTS/1% AREA

COMPOSITE POINT AND CONTOUR DIAGRAMS
OF 615 POLES TO FRACTURES IN THE CORTLANDT COMPLEX

NOTE: DATA FROM STATIONS B-4, B-5, JW-4 AND JW-11 SHOWN ON PLATE C1-2

DAMES & MOORE

PLATE C5-8

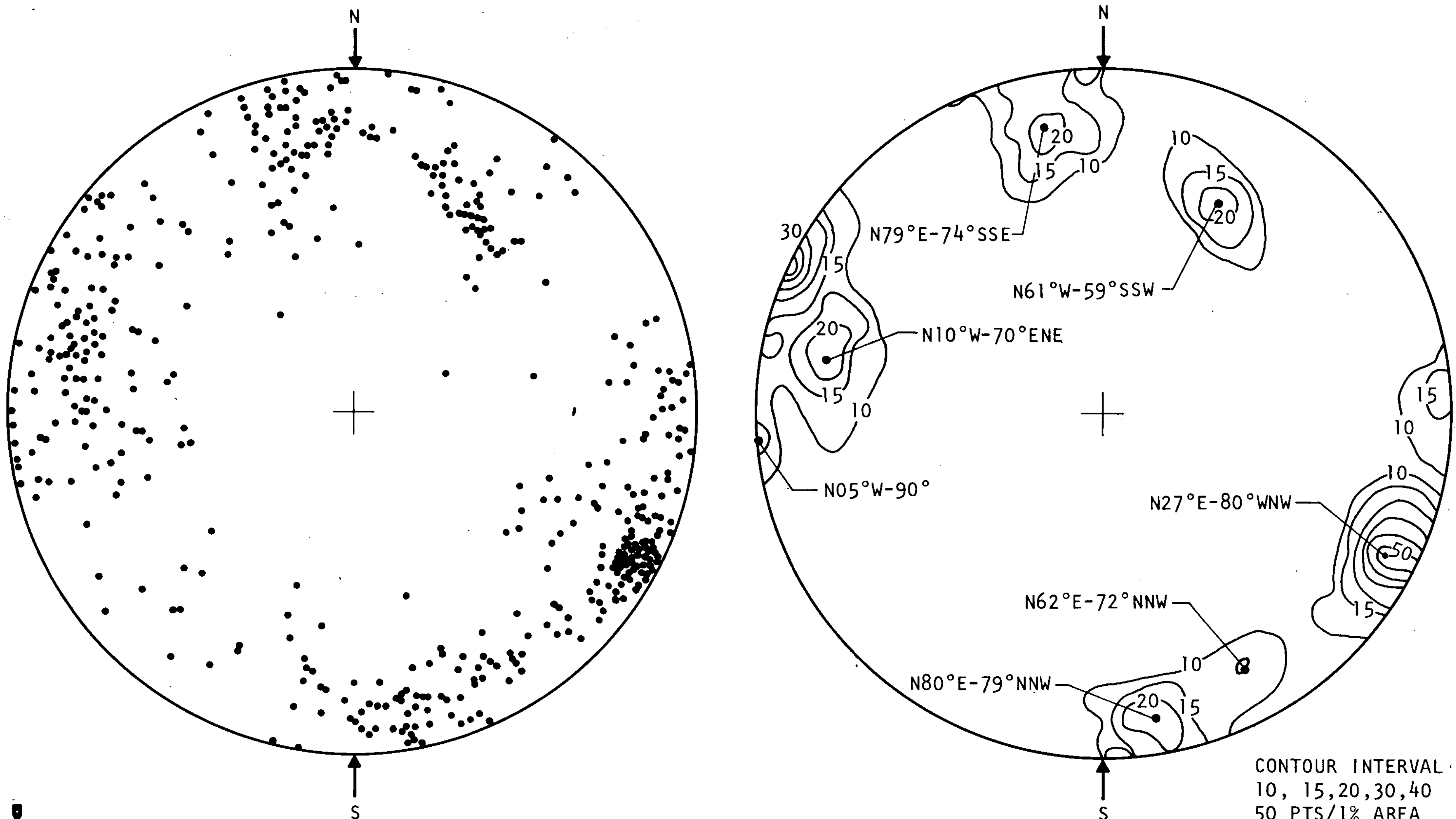

COMPOSITE POINT AND CONTOUR DIAGRAMS
OF 475 POLES TO FRACTURES IN THE PEEKSKILL PLUTON

DAMES & MOORE

PLATE C5-9

APPENDIX D

PLEISTOCENE GEOLOGY AND GEOMORPHOLOGY

APPENDIX D

PLEISTOCENE GEOLOGY AND GEOMORPHOLOGY

D1. INTRODUCTION

The purpose of the present investigation was to examine unconsolidated deposits and geomorphic features within 5 to 10 miles of the Indian Point site to determine if there is any evidence of recent displacement along the north-trending fault system as defined onsite and in the region surrounding the site.

Studies were concentrated on features such as upland surfaces, river terraces, glacial striae, glacial and post-glacial sediments, any materials suitable for radiometric dating, and any other post-Triassic deposit or feature which might directly or indirectly shed light on the question of the age of the last movement of faults in the area. Field work was reconnaissance in nature. It was confined primarily to accessible exposures or those which appeared to be potentially of greatest benefit to the study as determined during the literature search or aerial photographic studies.

The method instituted for completion of the present study involved investigation in three separate directions. First and most basic was a search for exposures of unconsolidated sediments underlain by faulted bedrock, glacially striated and/or polished surfaces on faulted bedrock, or suspect structures in unconsolidated deposits where bedrock is not exposed. The second objective was to respond to those field personnel who were primarily engaged in examining bedrock and bedrock structures by examining exposures of unconsolidated material, striae, polished surfaces, etc., which they felt required further inspection and interpretation. The third objective was to compile information as objectives one and two proceeded for the purpose of developing an understanding of the late glacial history of the region. The latter objective was essential to evaluate the possibilities of using specific geomorphic features or sedimentary deposits to correlate regionally or across specific features found during our studies of the bedrock. If one were not aware of the glacial history and the history of sedimentation within the region, similarities in color, texture, and sedimentary structures through the region might lead to an incorrect correlation of similar appearing yet different materials.

It was necessary to examine in the field the remnants of the previously more extensive deposits, and to compare these observations with those of the earlier writers. In some areas this method has proven satisfactory and even superior, since present exposures may give added information that was not available to the earlier writer. More often, the exposures have been completely destroyed or location information is too meager to allow accurate location of deposits which were described earlier.

D2. PRESERVATION AND EXPOSURE OF GLACIAL AND POST-GLACIAL SEDIMENTS

Preservation and exposure of sediments deposited in the Hudson River Valley and its tributaries are poor. The occurrence of the most extensive deposits unfortunately coincide with those areas which are the most thickly settled, namely Haverstraw and Peekskill. Man-made structures and vegetation cover large portions of the region. Much more detrimental to any comprehensive study of the deposits, however, is the fact that the most extensive and best exposures have been removed by both small and large-scale borrow pit operations. Sand and gravel deposits have been used as fill material and for concrete aggregate, while extensive varved clay deposits, as much as 200 feet in thickness, have been quarried for the making of bricks. Clays were quarried most extensively near Haverstraw, while smaller pits existed near Peekskill, Croton Point, and Crugers. Sand and gravel quarries are ubiquitous, but the largest volume of material appears to have been removed from Jones Point, Roa Hook, Sprout Brook, Peekskill Hollow Brook, and the area between Indian Point and Verplanck. Quarrying in the area has been going on for many years, as is evident from comments by C. E. Peet in 1904 concerning his visit to clay pits at Haverstraw, and his inability to ascertain how much of the flat parade ground surface at State Camp (now Camp Smith), near Peekskill, was a natural bench of sand and gravel and to what extent it had been regraded by man.

D3. LATE GLACIAL AND POST-GLACIAL HISTORY OF THE REGION

Basic to any discussion of surficial deposits in the Hudson River Valley near Peekskill is an understanding of the glacial history of the area, especially the retreat of the Late Wisconsin ice sheet up the valleys of the Hudson River and its tributaries. To date, no unconsolidated deposits or soils older than Late Wisconsin have been identified in the area. Older deposits might be expected to have been preserved in valleys situated transverse to the principal direction of glacial flow, and in those transverse valleys deep enough to have escaped intense glacial scour. In the region around Indian Point, the predominantly northeast and northwest structural grain has resulted in the development of valleys which acted as primary avenues for advance and retreat of glacial ice through the region. The valleys were the first to be affected during glacial advance prior to overtopping of the surrounding elevated areas and the last to become ice-free upon retreat of the ice sheet. They would, therefore, have been subjected to the greatest amount of erosion and deposition by glacial and glacially-related processes.

Absolute dating of the events related to the advance and retreat of the Late Wisconsin ice sheet in the Peekskill area is lacking. However, dates obtained elsewhere serve to bracket the age of these events. Using pollen stratigraphy, Sirkin (1967) inferred that the Late Wisconsin ice sheet began to retreat from the Harbor Hill moraine on Long Island about 17,000 years B.P. Similar work by Connally and Sirkin (1970) indicated that the ice had probably receded from the southern and middle portions of the Wallkill Valley (to a point approximately 25 miles northwest of Peekskill) prior to 15,000 years B.P., and that the Wallkill moraine was formed about 15,000 years B.P. before the ice receded completely from the Wallkill

Valley near Kingston, New York. Thus, any recessional deposits associated with the Late Wisconsin glaciation in the Peekskill area must have been formed between 17,000 years B.P. and 15,000 years B.P., probably closer to the latter date. Glacio-lacustrine and glacio-fluvial outwash deposits should be slightly younger, since they would have been deposited after retreat of the ice from the valley.

Advance of the glacial ice was initially two-pronged in the Haverstraw area, one tongue of ice extended southward around the west side of the South Mountain ridge (Salisbury, 1902; Woodworth, 1904) near Mount Ivy, and into the Hackensack Meadowlands to the south. A second tongue of ice extended down the Hudson Valley east of the Palisades. During the glacial maximum, the uplands were overtopped by the ice. As the ice receded from the terminal moraine, the ice first dropped below the level of the uplands and the lowlands topography again exerted a directional control. The ice retreated first from the west side of the South Mountain ridge in the vicinity of Mount Ivy. It remained in this position for a time, building a morainal complex which extends from the south side of Rider Hill and Collaberg Mountain south and southeastward to South Mountain, and eastward along the base of the mountain to Short Clove. Morainal remnants on the west side of Croton Point east of the Hudson River are thought to be correlative with this recessional moraine, as has been suggested by earlier writers (Woodworth, 1905; Peet, 1904; Markl, 1971). Smaller morainal remnants occur north and south of Minisceongo Creek along U.S.

Route 9W in Haverstraw, West Haverstraw, and northward to the vicinity of the State Rehabilitation Hospital. These smaller morainal remnants may represent a later local readvance of the ice front, the evidence for which was noted by Woodworth (1905), Peet (1904), and Reeds (1927) in the form of clays contorted by overriding ice and clay masses incorporated in till which locally overlies clays near Haverstraw.

The lowland area around Haverstraw, extending from Stony Point on the north to South Mountain on the south and the Palisades Parkway on the west, contains a great diversity of unconsolidated sediments. The stratigraphic relationships of these deposits were not completely unraveled in the past when exposures were better, the deposits well preserved, and the area much more sparsely settled. Description by Pett (1904), Woodworth (1905), and Reeds (1927), together with field observations made during the present study, indicate that the Haverstraw area contains glacial outwash deposits, ice-contact stratified sands and gravels, fluvial/deltaic deposits laid down marginal to the ice front, glacial till, kame deposits, and proglacial lake deposits. The proglacial lake clays were observed by earlier workers to overlie till and kame deposits, and to underlie a local readvance till and extensive deltaic deposits which were laid down by Cedar Pond Creek in an ice marginal lake with a surface elevation of between 100 and 120 feet. Ice-contact deposits observed by Peet (1904) and Woodworth (1905) suggested to them that these deltaic sediments were deposited marginal to an ice front which extended southeastward from the town of Stony Point to Grassy Point and from there out into the Hudson River. When the ice front receded further northward, it appears that a lower lake level was established and that clays, sands and gravels continued to be deposited at lower elevations. The deltaic sediments near Haverstraw, and those occurring at Croton Point and near Peekskill, are thought to have been deposited in glacial Lake Hudson (Markl, 1971; Reeds, 1927) which extended north at least as far as Peekskill. The lake level is thought to have been about 100 feet above the present level of Hudson River.

Some inconsistencies are evident, however, between the observations made by various authors. Both Peet (1904) and Woodworth (1905) identified ice-contact features near North Haverstraw, and concluded that the ice front stood there as the Cedar Pond Creek deltaic deposits were built up in a proglacial lake with a level near 100 feet. If the ice did fill the valley this far south, then the lacustrine and deltaic deposits at Peekskill, Croton Point, and Crugers, which were also built up to an elevation of about 100 feet, could not have been deposited in the same lake at the same time, as has been hypothesized by Reeds (1927) and Markl (1971). Sediments, standing as benches approximately 100 feet high along the periphery of the Hudson River Valley, and the extension of these benches up the valleys of tributary streams such as Annsville Creek, Sprout Brook, Peekskill Creek, Croton River, and Cedar Pond Creek, have been described in the literature by Peet (1904), Woodworth (1905), Reeds (1972), and Markl (1971). The consensus is that these deposits were laid down in a standing body of water. It appears, therefore, that these glacio-lacustrine and deltaic deposits were laid down in a single lake, glacial Lake Hudson, at approximately the same time. The presence of lower benches toward the streams, generally between 20 and 60 feet in elevation, indicates that deposition also may have taken place during lower lake stages which would have resulted either from northward retreat of the ice sheet or downcutting of an outlet channel downstream, probably at The Narrows.

Draining of Lake Hudson was followed by marine encroachment through The Narrows to the south before 12,000 years B.P. (Newman and others, 1969). Isostatic uplift of the lower Hudson River Valley, coupled with an eustatic rise in sea level, caused some fluctuations in salinities near Peekskill and in distance of marine encroachment up the Hudson estuary. Maximum extent of mesohaline water and maximum invasion of foraminifers during post-glacial time occurred 6,500 years ago and are coincident with the end of the period of post-glacial transgression of the Atlantic Ocean along the northeast coast of the United States (Weiss, 1974).

D4. GEOMORPHOLOGY

D4.1 GENERAL

Immediately northwest of the site, the Hudson River emerges from the steep-walled gorge it has cut through the resistant crystalline rocks of the Hudson Highlands. Upon leaving the narrow gorge, the river broadens and flows through the low-rounded knobs and ridges formed on the less resistant schists, gneisses, marbles, and granites of the Manhattan Prong. Ridges and knobs in the Manhattan Prong are generally formed on schists, granities, and gneisses, while the valleys are generally underlain by marble. South of Peekskill, the river follows the contact between the Triassic rocks to the west and the rocks of the Manhattan Prong to the east. Total relief along the Hudson River in the Highlands ranges from 800 to 1500 feet, whereas in the Manhattan Prong, some ridges reach elevations of 500 to 600 feet.

The present course of the Hudson River across a topographic high area of resistant rocks (the Hudson Highlands) is unusual when it is realized that the river might have more easily established a course southwestward down the Valley and Ridge province north of the Highlands. Various authors have tried to explain the present course of the river by resorting to antecedence (Davis, 1891), superposition (Johnson, 1931), and stream capture (Ruedemann, 1932; Thompson, 1936). Whatever its origin, it is generally agreed that the present course of the Hudson River was established before the beginning of the Pleistocene Epoch.

Drainage in the region around Peekskill is poorly integrated with numerous lakes, marshes, and areas of centripetal drainage evident. Many of the through-going valleys, especially in the Highlands, are structurally controlled and partially drift-filled. Many stream valleys, including the Hudson Valley, are underlain by buried, drift-filled bedrock valleys or gorges. Evidence of glacial derangement of drainage is widespread in the region. Instances of apparent stream capture are common and older drainage has been locally blocked by till and other glacially related deposits. The mouths of streams tributary to the Hudson River show evidence of having been drowned as the sea level rose to its present position in post-glacial time. However, further upstream, these tributaries have entrenched the glacial, glacio-fluvial, and glacio-lacustrine deposits along their courses in response to post-glacial isostatic rebound and lowering of the local base level (the Hudson River) as glacial lakes in the Hudson River were drained.

D4.2 BEDROCK TERRACE

Field and aerial photographic examination of the various types of terraces along the Hudson River from Haverstraw to Cold Spring was done in order to determine which, if any, of the terrace types could be used most advantageously in a study related to faulting in the area. The deltaic deposits are of limited suitability for such a study because they generally cannot meet the requirements of accessibility, preservation, lateral continuity, or age. The kame terraces do not meet the requirements of lateral continuity, age, or preservation because they have been quarried extensively, as have the benches of glacio-lacustrine sediment, mainly in the Haverstraw area.

The bedrock terraces which extend along the Hudson River appear to be the only ones which satisfy the requirements sufficiently to warrant further study. The terraces can be definitely shown to predate the Late Wisconsin ice advance because they exhibit abundant evidence that they were galciated in the form of erosional (glacial grooves, polish, and striations) and depositional (glacial till) features. This would indicate a minimum age greater than 20,000 years, the time of the Late Wisconsin maximum on Long Island.

The benches slope gently toward the river and downstream. They end abruptly at steep erosional scarps which descend to the level of the Hudson River. On the side away from the river, the bench terminates at a well-defined knickpoint at the base of steep slopes which ascend to the bordering Highlands summits. The bedrock bench represents an old, relatively flat valley bottom on strath which was cut by lateral planation of the Hudson River at some time in the past. It can be traced on opposite sides of the river at about the same elevation. Some small bedrock irregularities project above the terrace surface and appear to be islands which were never completely removed by erosion. Glacial erosion has modified the surface and left behind a number of small rock basin lakes. Post-glacial stream dissection has locally destroyed the terrace. Although the downstream slope of the terrace is obvious to the casual observer, the exact location of the terrace at any one point, or the change in elevation between any two points along the river, cannot be precisely determined using topographic maps. The 20-foot contour interval of the U.S.G.S. topographic maps and the presence of lateral moraine, ground moraine, talus, and glacial outwash deposits on the bedrock surface do not allow more precise measurements on the bedrock terrace surface. The terrace remnants were mapped and are shown on Plate D-1.

The approximate elevation of the terrace near Cold Spring is 160 to 200 feet, and near Indian Point it is between 100 and 120 feet.

The nature of the terrace changes markedly where the Hudson River leaves the Highlands. Within the Highlands, the break in slope between the upper walls of the gorge and the rock terrace below is very obvious. In the lowlands around Indian Point, the break in slope cannot be pinpointed with extreme accuracy, but that section mapped as the terrace appears to be the result of similar fluvial erosive processes. The slope break becomes much better defined again about a mile to the south at Crugers.

D4.3 UPLAND SURFACES

No upland surfaces were recognized near the Indian Point site. The irregular topography of rounded knobs and low hills is a reflection of the long history of erosion (at least back to the Tertiary) and adjustment to the various lithologies and the bedrock structure within the Manhattan Prong.

D5. UNCONSOLIDATED SEDIMENTS

The locations of significant unconsolidated sedimentary deposits observed in the field are shown on Plate D-1. If no exposures of significance were found, then no location number would appear on the map. A partial list of the stream valleys visited as data was compiled and a "feeling" for the regional distribution of unconsolidated deposits gained, would include the valleys of: Sprout Brook, Annsville Creek, Peekskill Hollow

Brook, and the Hudson River in the Peekskill Quadrangle; Cedar Pond Creek, Minisceongo Creek and the Hudson River in the Haverstraw Quadrangle; Clove Creek in the West Point and Wappinger Falls Quadrangles; Wiccopee Creek in the Hopewell Junction Quadrangle; and Woodbury Creek in the Cornwall Quadrangle. Small unnamed creeks and valleys on the quadrangles were also visited.

These unconsolidated deposits may be divided into five basic groups as described below:

1) <u>Ice-Contact Stratified Drift</u>

Ice-contact stratified drift, as observed during the study, consists of kame terrace deposits and kame delta deposits. These deposits consist mainly of fine-to-coarse grained sands and gravels. They are all similar in that they are stratified and display evidence of having been deposited in contact with or adjacent to a glacier. This evidence is usually in the form of collapsed or distorted bedding where the support of glacial ice has been removed by melting. Deposits of this type often display frequent changes in sediment size and direction of deposition because changes in rate or direction of ice movement may change the course and character of the meltwater streams which deposited the sediment. Large boulders or masses of till are sometimes included in these deposits.

a) Kame terrace deposits are formed by meltwater flowing from a glacier and depositing sediment between the ice mass and a valley wall. Removal of ice support causes collapse of the sediments on the side facing the axis of the valley. These deposits are distinctive in that they often dip outward toward the valley wall and form an irregular terrace surface which may be higher on the side away from the valley wall. In the Peekskill region, these deposits have been almost completely quarried out, but the literature and observation of remnants indicates that they were composed primarily of fine-to-coarse grey-brown sand and gravel which locally grades downdip to light brown or tan silt and fine sand interbedded or interlaminated with dark grey plastic clay (Stations PM-4, PM-5, PM-15, PM-16, PM-22, and CB-21).

b) Kame delta deposits are formed by meltwater flowing off the front of a glacier and building a delta into a proglacial lake, usually moraine-dammed. The deposits are stratified and cross-bedded on both a small and large scale. The sediments are highly variable in grain size, ranging from clays and silts to coarse gravels. In the region around Indian Point, a number of large kame deltas have been preserved as significant topographic highs extending across (or partially across) steep-walled valleys (Stations CB-30, PM-30). Most display excellent ice-contact collapse features on their up-glacier margins.

2) Glacio-Lacustrine Deposits

The glacio-lacustrine deposits consist of stratified or laminated light brown or tan silts and fine-to-medium grained sand (often varved) and light brown to dark grey plastic clays which were deposited mainly in glacial Lake Hudson up to a maximum elevation of approximately 100 feet. The deposits have been extensively quarried, especially the clays, around Haverstraw, Peekskill, Crugers, and Croton Point. Only small pockets remain in a few low areas where they have not been removed or covered by man-made structures (Stations CB-5, CB-10, CB-17, CB-23, and PM-14).

3) Glacio-Fluvial Deposits

Glacio-fluvial outwash deposits consist of stratified deposits laid down by glacial meltwater streams at some distance from the glacial front. Near Indian Point, they consist of yellow or yellow-brown, medium-to-coarse grained sand and gravel. They have been extensively quarried and are generally preserved in small patches or pockets. South and southwest of the Indian Point site, the outwash sands and gravels are thickest along a slight topographic low cut on bedrock and bounded by north-northwest faults. This belt of thicker outwash extends through Verplanck and may represent an old meltwater channel deposit which was laid down across the peninsula marginal to ice within the Hudson River Channel (Stations PM-5, PM-6, and PM-7).

4) <u>Deltaic Deposits</u>

The deltaic deposits were built upward and prograded outward into a standing body of water, glacial Lake Hudson, which was dammed to the south by the Harbor Hill moraine at The Narrows. They are distributed near the mouths of all of the major streams entering this stretch of the Hudson River. They consist of a wide variety of sediment types, and grade both vertically and laterally from one to the other. The most common sediment types are light brown or tan silt and fine-to-medium grained, well sorted sand with lesser amounts of grey or light brown clay and grey or grey-brown fine-to-coarse gravel. The most extensive deltaic deposits were laid down at Croton Point and in the Haverstraw-Stony Point area. They have been extensively quarried and built-over (Stations CB-2, CB-18, CB-19, CB-22, and CB-29).

5) <u>Till</u>

Glacial till deposits are distributed over the entire region, mainly as a thin blanket less than 10 feet thick. Thicker concentrations often occur on north-facing slopes of bedrock highs, along the walls of valleys and in end moraines such as those near Haverstraw. The composition of the till is quite variable and generally reflects the type of bedrock which underlies it. The two most common end members are a relatively loose, sandy matrix surrounding rounded fine-to-coarse gravel (probably an ablation till) and a hard, compact lodgement till consisting of a matrix of silt or sandy silt surrounding fine-to-coarse gravel ranging from angular to subrounded (Stations CB-1, CB-2, CB-3, CB-6, CB-7, CB-14, CB-15, CB-16, CB-20, CB-28, CB-31, CB-32, CB-33, CB-34, CB-36, PM-19, PM-23, PM-24, PM-27, and PM-32).

D6. STRUCTURES IN SEDIMENTS

Both primary and secondary sedimentary structures were found in nearly every outcrop of stratified, unconsolidated sediments. Primary structures observed include sheet laminations, current laminations, large and small-scale cross stratification, and topset, foreset, and bottomset beds associated with deltaic deposits. Secondary structures observed in outcrop include various types of folds, faults (predominantly normal), and decollement.

In the County Asphalt Quarry at the southwest corner of the Cornwall quadrangle (Plate D-1, Station CB-30), numerous faults were observed in layered silts, sands, and gravels of possible Pleistocene age. An equal area lower hemisphere plot of the poles to these faults (Plate D-2) shows a preferred orientation from N25°W to N85°W, dipping 60° to the northeast and southwest. Most of these faults show small-scale normal movement on the order of a few inches (Plate D-3, Photo A); however, one fault trending N70°W-58°W (Plate D-3, Photo B) exhibits about four feet of normal displacement and can be traced laterally for at least 50 feet. The faults may be the result of syngenetic and epigenetic processes such as slumping, loading, or melting of buried ice blocks which remained after the glacier retreated. However, due to the proximity of this exposure to a mapped west-northwest striking normal fault (Dodd, 1965), it may require further investigation.

Most folding appears to be the result of slumping or loading. The greatest number of folds were found in a kame delta deposit (Station CB-30) where rapid deposition and changes in water level and rate of ice melting engendered unstable conditions in soft sediment. Near the upstream margin of this deposit, glacial overriding is indicated by the presence of a large recumbent fold (5 feet high x 12 feet long) in unconsolidated sand and gravel, with its axis trending nearly east-west at right angles to the direction of ice-movement in the valley and overturned toward the south (downstream) (Plate D-4). Some smaller scale folds within the deposit are also suggestive of overriding or downslope movement of sediment toward the southward with resultant wrinkling of silt and clay beds.

In two outcrops (Stations CB-30 and PM-4), small-scale (1 to 4 inches) convolute laminations and diapiric structures were recognized, resembling structures formed experimentally on a shake table by Coates and others (1975, and personal communication), suggesting that such features may be related to seismic shocks. Similar features have also been attributed to collapse by ice meltout, glacial readvance, lateral displacement by sliding, loading, flooding, and water level changes. To date, definitive criteria have not been developed by which these various causative mechanisms can be distinguished.

D7. SEDIMENTS AND GLACIAL FEATURES ON BEDROCK

D7.1 GENERAL

Faulted bedrock at a number of localities is exposed at the surface or in artificial cuts where either unconsolidated material or a glacially smoothed and/or striated surface extends across the fault. Such exposures often display indisputable proof that the faulting at that point occurred prior to formation of the overlying surface or surficial material. Because of the rarity of such ideal exposures and their importance to the present study, they are herein described in greater detail. (These stations are located on Plate D-1.)

D7.2 STATION CB-37

This location is an excellent bedrock exposure on Route 9A near Croton Point in the parking lot of an automobile dealer. The outcrop is a white marble which exhibits very fine glacial polish, grooves, and two distinct sets of striae. A number of cross-cutting faults are also present and the striae and polished surfaces extend across them (Plate D-5). No vertical or horizontal displacement has affected the glacial features which extend across the faults. A detailed discussion of the faulting is included in Section C5.2. Striae trending N20°E are also present at this outcrop.

D7.3 NEAR GEORGIA-PACIFIC PROPERTY

A bedrock fault is exposed in the bed of a small northeast-flowing stream at the southern limit of the Consolidated Edison property, 10 to 20 feet north of a chain-link fence surrounding the Georgia-Pacific plant. The fault is exposed in the rockface beneath a waterfall and runs subparallel to the stream banks. It extends beneath unconsolidated material both north and south of the stream. The south bank is composed of sand and gravel which appears to be slumped or slope-washed material used as fill under the Georgia-Pacific parking lot upslope. Along the north bank, the unconsolidated material appears to be colluvium. It is made up of angular rock fragments and some rounded gravels in a sand and silt matrix. The material composing the north bank of the stream exhibits abundant evidence of having undergone recent slumping. The slump is in the form of a downdropped bench which is subparallel to the bedrock fault in the stream. The bench ranges in width from 2 to 6 feet, has a sloping surface (≈30°-35°) toward the stream, and has dropped downward 2 to 3 feet toward the stream and in a downstream direction. Trees and bushes on the bench are bent over toward the stream, roots are exposed in the slump scar and subvertical, slightly curved slabs of bedrock, which underlie the bench and intersect the stream bank at an oblique angle, have become separated by 2 to 4 inches in the downstream direction. No relationship between the slump and the fault is apparent in present exposures.

D7.4 SOUTH END OF VERPLANCK QUARRY

At the south end of the Verplanck quarry, a sediment-filled gully is exposed. The gully trends at this point west of north and is approximately 20 feet deep. Bedrock is not exposed in the gully, but is thought to be not far below the clays exposed in the gully bottom. The gully is cut into the bedrock of the south quarry wall and exposes a sedimentary section about 15 feet thick as a result of modern erosion by an intermittent stream. The gully appears to be aligned with a fault found further to the north in a quarry wall. Strikes of N20° to N30° W and dips ranging from 5° to 14° to the southwest were measured in the sediments filling the gully.

The stratigraphic section consists of grey plastic clay grading upward to grey gravelly clay which is overlain by yellow medium-grained sand, grey clayey sand, brown medium grained sand, grey sand-clay-gravel, and finally 7 feet of fill material. Examination of the weakly laminated grey clay and gravelly clay uncovered no evidence which would indicate that the clays have been faulted or otherwise disrupted. Rotational slumping of unconsolidated material has truncated the stratigraphic section toward the quarry on the west and possibly also on the east side of the gully.

D7.5 STATION CB-35

An outcrop of Traissic, red beds and diabase dikes are present behind the Dowd Apartments south of Route 202 at South Mountain. The fine-grained sandstone has a glacially polished, grooved and striated bedrock surface exposed at the top of a 12-foot high cliff which is mostly the result of blasting. Striations are trending N35°W. Faults with sub-horizontal slickenslides are exposed in the cliff face. At the top of the cliff a polished red sandstone surface, partially covered with slopewash, has an irregular fracture extending across it subparallel to a nearby fault. Striations extend obliquely across the fracture which shows about 1/2-inch of relief from one side to the other. The irregular nature of the fracture, the relation of the surface to nearby polished surfaces, and the presence of loose fragments nearby with polished surfaces indicate that the offset of the striated surface is not the result of fault displacement. It appears the apparent offset is due to some other agency such as frost-heaving, root wedging, downslope movement, or possibly blasting when the cliff face was excavated.

D7.6 MARTIN MARIETTA TRAP ROCK QUARRY

Two faults in the Triassic diabase were examined where they were overlain by unconsolidated material. The first exposure was in the cliff face at the northwest corner of the lower quarry level. A northwest-trending fault occurs in the diabase, and has a 2-to 3-foot wide breccia zone which has been partially eroded out. The resultant void is partially filled with slump material from above. A second northwest-trending fault is exposed in the cliff face at the south end of the lower quarry level. The fault is overlain by 10 to 15 feet of red till. The lower two-thirds of the till appears to be in place across the fault. At the cliff top, the upper few feet are gravel fill used to form a flat roadway on the top of the quarry bench. Beneath the till and in the fault zone, unconsolidated material, composed of angular broken fragments of diabase in a red sand and clay matrix, is present. The fragments are generally less than one inch in diameter. An occasional subangular to subrounded fragment occurs in the material. This material resembles colluvium which probably washed into a small depression where fault breccia had been removed. Very short transport, if any, is indicated. The contact of the till across the fault and the infilled colluvium appeared undisturbed. The fault, therefore, must be older than the till.

D7.7 TRENCHES AT INDIAN POINT

Trenches were excavated north of Reactor No. 3 to determine whether undisturbed soils or glacially striated or polished surfaces have been preserved on the bedrock extending across faults. The trenches encountered only artificial fill as overburden underlain by a weathered sandy dolomite with no preserved glaciated surfaces.

D7.8 STATION PM-23

A large fault plane on Mott Farm Road is exposed in a road cut. It trends N63°E and dips 65°SE. There are subvertical slickensides and remnants of a thick breccia which still adhere to the fault face at the base of the cliff. There is also a thin wedge of loose, sandy till plastered against the fault. The outcrop relations can be explained in a number of ways, including faulting of the till against the bedrock fault plane. A landslide scar exposed at the top of the cliff above the till against the fault indicates that the observed field relations are most likely the result of till sliding down the cliff face and coming to rest at the base of the scarp against the fault plane.

D7.9 STATION PM-16 (JONES POINT)

Along Ayer's Road, dark brown gravelly sand (unstratified) interbedded with light yellow-brown clay overlies a prominent N20-30°E, 60-70°SE joint or fault in crystalline bedrock. No disturbance of the overlying sediments was observed.

D7.10 STATION PM-21 (CEDAR POINT CREEK)

Approximately 5 feet of pebble to cobble-size gravel overlies faulted Triassic red beds with subhorizontal slickensides. No evidence of faulting was observed to extend upward from the bedrock into the overlying gravels. The position of the gravels at the base of the dam, however, indicates that they may have been placed there by man.

D7.11 SUMMARY

The locations discussed above depict the types of outcrop situations which are encountered in the field. They run the gamut from outcrops, where definitive evidence can be recognized on a faulted and glaciated bedrock surface, to outcrops where it cannot be determined whether the unconsolidated materials or even the exposed bedrock surface are in their natural state. Intermediate between the two are those instances where some circumstantial evidence can be gleened from an outcrop and a probable conclusion reached.

D8. GEOMORPHOLOGY AND SURFICIAL DEPOSITS WITHIN THE SITE AREA

An examination of the security area at the Indian Point nuclear power plant site was conducted to determine whether any geomorphic features or undisturbed surficial deposits are preent within the inner security boundaries at the site, and whether any such features or undisturbed deposits extend across bedrock structures mapped at the site.

Judging from boring logs, surrounding terrain, and topographic maps produced before plant construction, the site originally consisted of a gently westward-sloping upper area (landward from the present reactor locations) which extended westward to a steep bedrock incline, and finally to a nearby flat expanse of marshy ground leading to the river's edge. Bedrock was present within a few feet (2 to 8 feet) of the surface over most of the site, with the exception of the flat area along the Hudson River where fluvial silts and sands were overlain by marsh and river deposits containing organic remains. Total thicknesses of sediment as great as 50 feet were encountered in borings drilled in the river.

The reactor excavations were blasted into the steeply sloping bedrock surface which marks the transition from the river to a relatively flat bedrock terrace east of the site at an elevation of approximately 110 feet. The bedrock configuration within the site itself suggests the remains of a terrace and scarp which have been modified by glacial and postglacial erosion and weathering. Only two outcrops remain within the security area, one immediately north of Reactor No. 3 and a second along the road south of Reactor No. 3. Weathered rock was observed in the outcrop south of Reactor No. 3. The outcrop is a road cut trending nearly east-west. At two points the rock grades vertically, over a thickness of 1 to 2 feet, from sound rock to rock that responds to hammer blows with a dull thud, and finally to completely weathered rock which crumbles and disaggregates to a sand. The latter is in sharp contrast with a dark red-brown, sandy soil which appears to be a result of more advanced weathering of rock. At the west end of the outcrop, the red-brown sandy soil is overlain by a dark brown and a black organic-rich soil layer approximately 6 to 8 inches thick which is, in turn, overlain by fill. At the east end of the outcrop, the weathered materials are partially covered by fill and a wood retaining wall. It is not certain, therefore, whether the sequence at this point represents an old rock surface or weathering along a vertical fracture zone.

On the north side of Reactor No. 3 a vertical scarp of dolostone is exposed. The cliff face has been blasted and no natural bedrock surfaces have been preserved. A number of faults and fractures are exposed along the face, and zones of broken rock appear to have been weathered to depths as great as 5 to 10 feet below the top of the cliff at two places near the north end of the exposure. The bedrock at the top of the cliff was covered with fill ranging from approximately one foot to nearly 5 feet in thickness. Trenches were dug east-west and nearly north-south through the fill to determine a weathering profile; glacial striations or a glacially polished surface extend across the faults where they intersect the bed-rock surface. A third trench was dug at the base of the cliff and fill material was removed from a bedrock spur at the top of the cliff at its south end. No glacially striated or polished surfaces were found. A number of fracture zones were exposed, however. The trench at the base of the cliff exposed only fresh, blasted rock, while those at the top of the cliff exposed a weathered sandy dolomite which has decom-posed to a sugary unconsolidated sand. The depth of weathering was variable and ranged from a few inches on sloping surfaces to 3 or more feet where fracture zones were intersected by the trenches on flat surfaces.

In summary, it appears that the Indian Point security area is located on the margin of a glacially modified bedrock terrace remnant which is approximately 110 feet above river level. Any exposed bedrock surfaces or undisturbed surficial materials which existed prior to construction have been covered, removed, modified, or destroyed with the exceptions noted above. The bedrock surface is weathered to varying degrees and was not seen to preserve glacial striae or polish where exposed in trenches.

D9. SUBREGIONAL MAP

The generalized map (Plate D-6) shows the distribution of surficial deposits within a four-mile radius of the Indian Point Generating Station. Mapping was done on U.S.G.S. 7-1/2 min. topographic maps at a scale of 1/24,000 using parts of the following quadrangles: Peekskill, Haverstraw, Popolopen Lake and Thiells. Aerial photographs at scale of 1/6,000, 1/24,000, and 1/60,000 were used to aid in mapping, interpretation, and to pinpoint areas of special interest for field visit. The types of deposits encountered within the four-mile radius have been presented on the surficial map under the following headings:

1) Fill or Densely Populated Areas - Denotes areas where surficial materials have been removed, replaced, disturbed by regrading or obscured by man-made structures, or coverings. Where it was determined that sufficient undisturbed materials remain, an attempt was made to identify the type and origin of the materials and to map their distribution accurately.

2) Glacial Till - Thicker concentrations of unstratified and unsorted sediment (generally greater than 10 feet thick) which was deposited directly by glacial ice. Within the mapped area, these deposits generally consist of a silty, fine-to-medium grained, light-to-dark brown sandy matrix containing fine gravel to

boulder size (angular to rounded) rock fragments.

3) Thin Till over Bedrock - Glacial till distributed in patches or as a thin blanket, generally less than 10 feet in thickness, lying on bedrock which crops out in many places either naturally or in artificial cuts.

4) Glacio-fluvial, Fluvial/deltaic, and Glacio-lacustrine - Brown to grey clay, sand and gravel, generally confined to valley bottoms and valley walls generally at elevations below 200 feet. Glacio-fluvial deposits in the region are mainly composed of medium-to-coarse sand and gravel with minor silt, while the glacio-lacustrine sediments are predominantly finely laminated varved clays grading upward to fine-to-medium grained sand. The fluvial/deltaic sediments consist of mixtures of both the coarser grained sands and gravels and the finer grained clays and sands.

5) Kame Terrace Deposits - Generally consist of brown to grey stratified clay, sand and gravel. The deposits are of limited extent, characterized by the presence of ice-contact features, and are situated on valley walls at elevations above 100 feet.

6) Recent Fluvial and Marsh Deposits - Low-lying floodplain or marsh deposits along the Hudson River and its tributaries or in small, closed drainage basins in the surrounding uplands.

D10. CONCLUSIONS

The present investigation has confirmed that unconsolidated deposits are abundant and widespread in the region surrounding the Indian Point site. These consist mainly of thin glacial deposits on interstream uplands, and thicker and more extensive morainal, glacio-fluvial, glacio-lacustrine, and ice-contact deposits which are confined to the bottoms and walls of the principal valleys. The uplands were subjected to glacial erosion as is evidenced by the exposure of numerous scoured and polished surfaces, rock-basin lakes, and glacially grooved and striated bedrock surfaces. Thin sandy or silty glacial till, generally less than 10 feet in thickness, predominates in the interstream uplands. Bedrock crops out over large parts of the area. Locally, thicker till occurs where it has been banked against steep north-facing bedrock slopes. Some streamlined hills, such as the one between Pleasantside and Crompond Road (Peekskill Quad), appear to be either rock-cored drumloidal hills or morainal remnants.

The valleys of the Hudson River, Annsville Creek, Peekskill Hollow Brook, Cedar Pond Brook, and Sprout Brook contain large amounts of sediment deposited directly or indirectly as a result of glacial processes. Valley bottoms are occupied by till, glacial lake deposits, glacial outwash, delta and kame deposits, in addition to recent marsh and flood-plain deposits. The glacial lake clays and sands and associated deltaic deposits generally occur as remnants at elevations below 100 to 120 feet, the approximate level of glacial Lake Hudson. The remnants are only a small part of the deposits which reached thicknesses of more than 200 feet before being quarried by man earlier in this century and during the last. Kame terrace deposits are found high up on valley walls, often between 100 and 160 feet in elevation.

The unconsolidated sediments in this area are not useful, however, for conventional stratigraphic correlation purposes over large areas because they consist mainly of isolated erosional remnants of sediments which were deposited at different times as a result of different processes. Only in a small area, possibly within a single outcrop, is it feasible to trace or correlate units to determine if they could have been disrupted by bedrock faulting. Even then, only in the rare case where both faulted bedrock and overlying sediments are exposed, can it be decided whether there is a relationship between the structures in the two mediums.

The exposures that were studied showed no faulting that was traceable from bedrock upward into overlying unconsolidated materials. Published studies indicate that glacial deposits in the region are probably a maximum of 15,000 years. No evidence has yet been found in the field to indicate that deposits older than Late Wisconsin have been preserved.

Most of the faulting and folding observed in unconsolidated sediments can be attributed to sedimentary and early diagenetic processes. At least two possible exceptions may exist. The diapiric structures and convolute which were noted at two localities indicate that some layers of sediment have undergone liquefaction at some time during their post-depositional history. It is not known whether these features are the result of seismic shocks, ice meltout, glacial re-advance, loading, lateral displacement sliding, water level changes, or some other, as yet, unrecognized process. The second possible exception is the large fault noted at Location CB-30 which has been traced vertically for about 25 feet and laterally for 40 to 50 feet. Although large-scale slumping cannot be ruled out, it has not been proven.

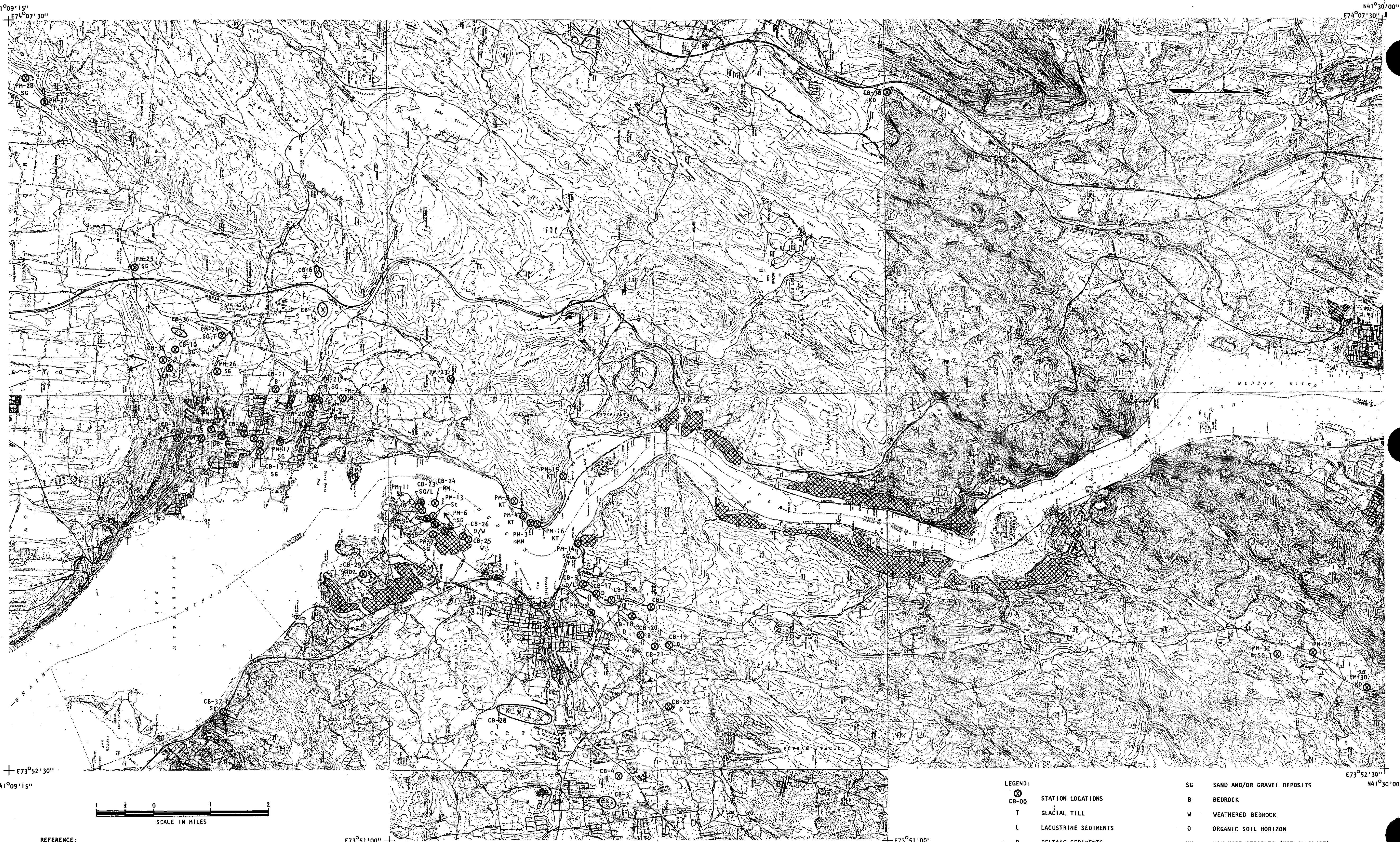

REFERENCE:

THIS BASE MAP WAS PREPARED FROM PORTIONS OF THE FOLLOWING U.S.G.S. MAPS: CORNWALL, N.Y., DATED 1957; WEST POINT, N.Y., DATED 1957, POPOLOPEN, N.Y., DATED 1957; PEEKSKILL, N.Y., DATED 1957; MOHEGAN LAKE, N.Y., DATED 1956; THIELLS, N.Y., DATED 1955, AND HAVERSTRAW, N.Y., DATED 1967

LOCATION MAP SHOWING SURFICIAL DEPOSITS IN SOUTHEASTERN NEW YORK STATE AND BEDROCK (STRATH) TERRACE ALONG THE HUDSON RIVER

LEGEND:

⊗ CB-00	STATION LOCATIONS	SG	SAND AND/OR GRAVEL DEPOSITS
T	GLACIAL TILL	B	BEDROCK
L	LACUSTRINE SEDIMENTS	W	WEATHERED BEDROCK
D	DELTAIC SEDIMENTS	O	ORGANIC SOIL HORIZON
KD	KAME DELTA DEPOSITS	MM	MAN-MADE DEPOSITS (NOT IN PLACE)
KT	KAME TERRACE DEPOSITS	St	GLACIAL STRIAE
IC	ICE-CONTACT STRATIFIED DRIFT	↙	ORIENTATION OF STRIAE
			BEDROCK TERRACE

DAMES & MOORE

PLATE D-1

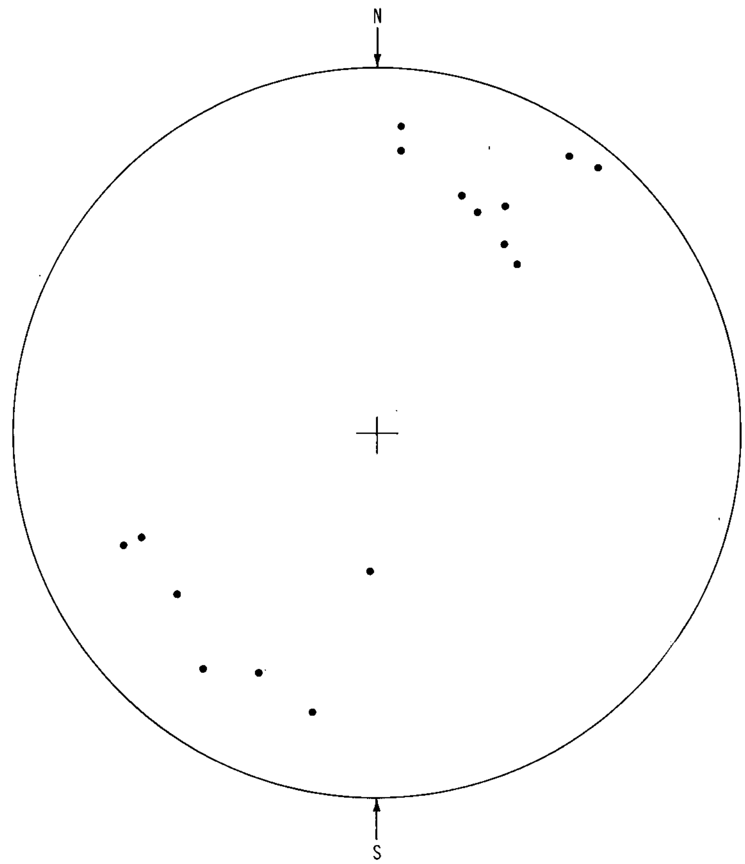

STATION CB - 30
EQUAL AREA LOWER HEMISPHERE
PLOT OF POLES TO FAULTS IN
UNCONSOLIDATED SEDIMENTS
N=16

NOTE: STATION LOCATION SHOWN ON PLATE D-1

DAMES & MOORE

PLATE D-2

PHOTO A

CROSS-SECTION OF N 60°W - 60°NE AND N63°W-59°SW CONJUGATE NORMAL FAULTS IN INTERLAYERED SILTS AND SANDS AT STATION CB-30

PHOTO B

CROSS-SECTION OF A N 70°W - 58°SW ORIENTED NORMAL FAULT WHICH OFFSETS INTERLAYERED SILTS, SANDS, AND GRAVELS AT STATION CB-30

DAMES & MOORE

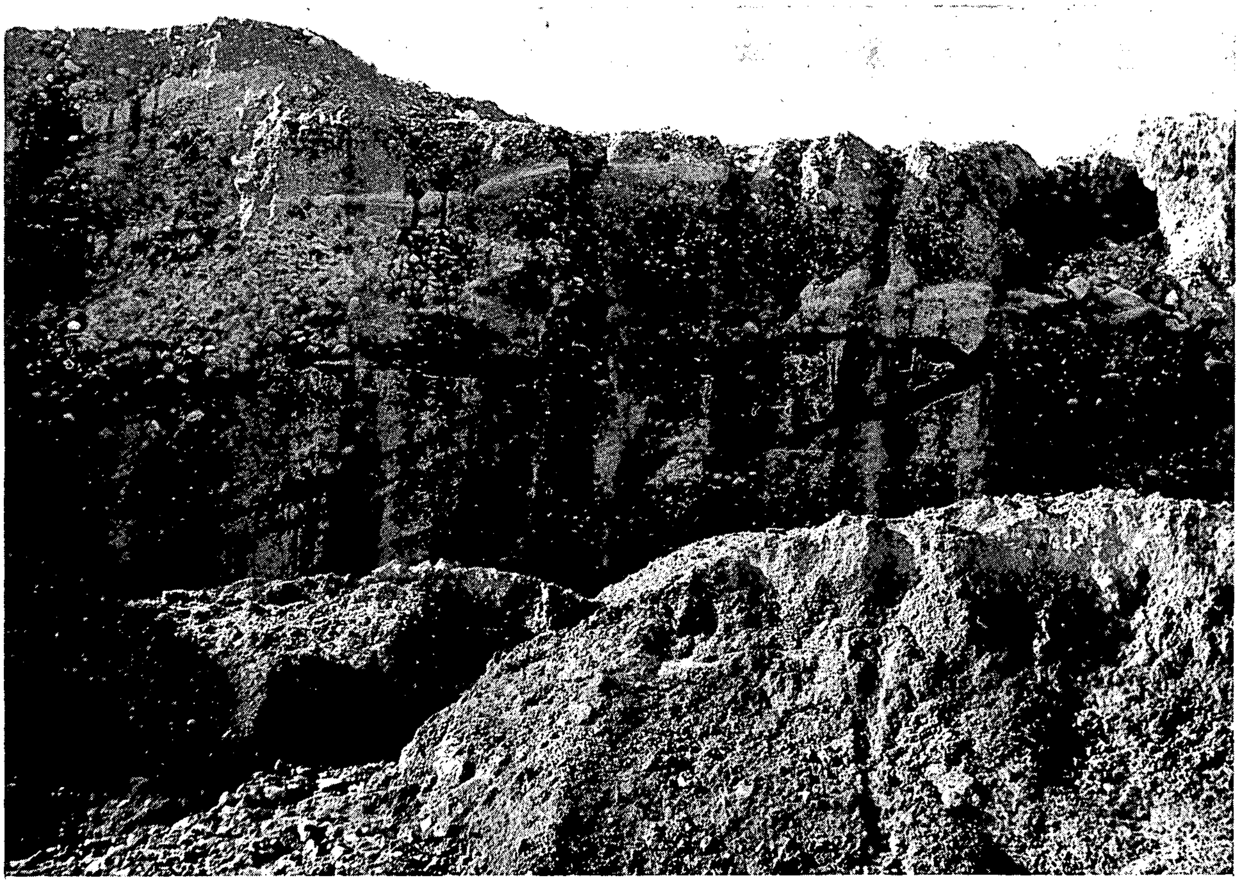

RECUMBENT FOLD IN LAYERED UNCONSOLIDATED PLEISTOCENE SEDIMENTS.
VIEW LOOKING WEST.

DAMES & MOORE

PLATE D-4

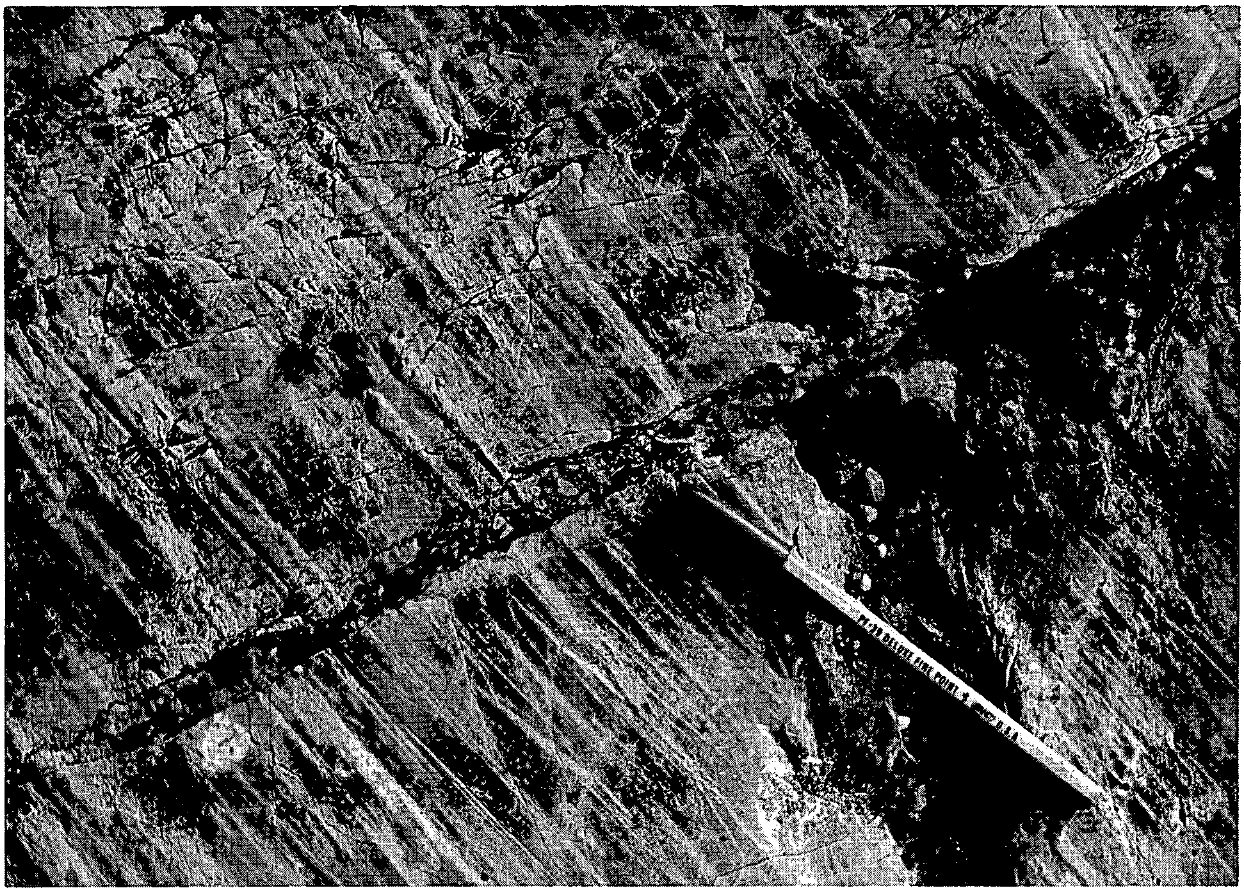

GLACIAL STRIATIONS CROSSING A FAULT ZONE MARKED BY BRECCIATION.
PEN POINTS NORTH.

DAMES & MOORE

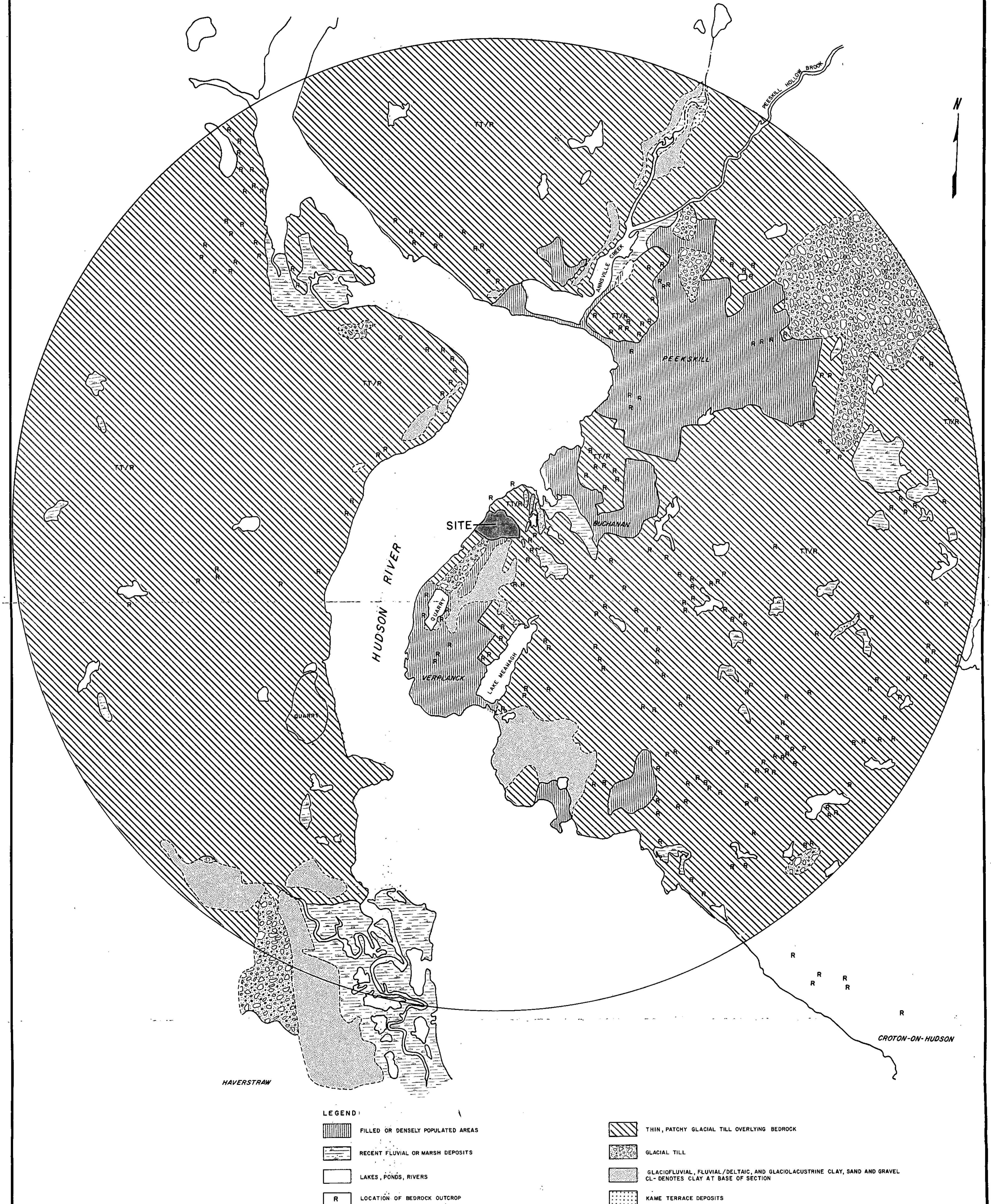

GENERALIZED MAP SHOWING SURFICIAL DEPOSITS WITHIN FOUR MILE RADIUS OF INDIAN POINT

1 0 1
MILES

DAMES & MOORE

PLATE D-6

Appendix E

PEDOLOGY

Lowell A Douglas

Interim Report of Soils Investigations at the Indian Point Reactor Site of Consolidated Edison

Lowell A. Douglas, Ph.D.

A study of the soils found on the site of the Indian Point Reactor Site of Consolidated Edison was undertaken. The study was limited to the immediate area of Reactor No. 3. The study had three objectives:

1. To determine the age of the soil;
2. To find out if the soil undergoes creep; and
3. To find out if the soil has been displaced by faulting.

Figure 1 is a highly generalized and idealized sketch of the study area. The numbers on this figure represent the positions where samples were collected for characterization studies. Profiles 3020, 3010 and 3030 were sampled on the exposure adjacent to Reactor No.3. Profiles 3000, 3050 and 3060 were sampled in pits back on the slope. Their relative positions have been projected (Figure 1) to the exposure of the general study to facilitate comparisons.

AGE OF SOIL

The study area was glaciated some 15 000 years ago. It is thought that soil 3060 represents normal post-glacial soil development. Soil profiles 3020, 3010, 3030 and 3000 may be diagnostic regarding last movement of the faults.

These soils are located on steep slopes. Although the depths of these profiles are comparable to the depth of profile 3060, the clay accumulation in the B horizons of these soils is much less than the accumulation in profile 3060 (Table 1). The development of these soil profiles, and accumulation of clay, is a time dependent property that has been altered by erosion or creep. Profiles 3020, 3010, and 3000 may represent a time span of 3/4 to ½ of the post-glacial time span.

TABLE 1

PARTICLE SIZE DISTRIBUTION OF B HORIZONS OF SOME SOILS AT INDIAN POINT.[1]

Profile	Sand	Silt	Clay
	%	%	%
3000	80	16	4
3020	84	14	2
3060	68	12	20

1. Analysis by a rapid approximate method.

CREEP

Some type of foreign object (or objects) has been found in every A horizon we have studied from the Indian Point site. They include pieces of glass, rusty nails, coal, cinders, etc. Much of the A horizons of these soils have been effected by man's activities, erosion, and probably creep. However, in a few locations (at the present time not defined) creep may not have altered the A horizon on this slope.

Profile 3050 was over dolomite which contained three thin (4 to 6 inches), parallel, contrasting beds. The saprolitized dolomite beds and the upper portions of the B horizons, and the A horizon over each bed were sampled. Figure 2 shows the side of the trench at site 3050, and the approximate locations where samples were taken. In the field the dolomite at 3057, and overlying soil, had a reddish cast; at 3052 and overlying soil, a blueish cast; and at 3056 a pale yellow cast. The organic matter in the soil's A horizon imports a brownish black color so that any color of A horizons that might have been inherited from the dolomite was masked by the organic matter. Foreign material was found in samples 3053, 3050 and 3055.

The samples were taken to the laboratory and fractionated into several size fractions. The greater than 2 mm fractions from samples 3051, 3052 and 3056 could not be separated on basis of gross appearance. As these samples have weathered they have assumed a pale cream to light gray color. Samples 3054 and 3057 showed the effects of oxidation of iron during weathering. Sample 3054 ($>$2 mm fraction) had a Munsel color of 7.5 YR 7/6 (orange) and sample 3057 ($>$2 mm fraction) had a Munsel color of 7.5 YR 7/3 (dull orange). Comparable colors from sample 3052 was 7.5 YR 6/1 (brownish gray) and sample 3051 was 7.5 YR 6/3 (dull brown). The color intensity in the B horizon of the soil is proportional to the color of the dolomite immediately under the B. If creep had occurred in the B horizon it is highly unlikely that this color relationship would exist.

SOILS AND FAULTING

At B (Figure 1) the horizonation of the soil indicate that the soil horizons (lower portion of the A and the B horizon) have not been displaced by faulting. (This determination has a precision of about ± 2 inches). At point A, all of the soil over the dolomite has possibly been effected by creep. No conclusion could be arrived at relative to last movement of the fault at A, from soil information.

The deep soil immediately upslope from A (Figure 1) and shallow soil downslope from A might be related to slope and rate of weathering. Above A, the slope is about 22%. Below A, the slope is somewhat steeper. The dolomite upslope from A has been brecciated and the zone healed by crystallization of carbonates. The dolomite below A has not been brecciated. Two rock samples (3070 and 3071, Figure 1) were collected by Ned Tillman of Dames & Moore. Sample 3070 was near the foot of the slope, and 23 feet west of the two walls. Sample 3071 was from the foot of the slope and three feet west of two walls. Sample 3071 did not include any of the carbonate that has reprecipitated to heal the breccia zone.

A simple experiment was devised to compare the rates these two dolomite samples would weather. Duplicate 1 gm. samples of ground dolomite were placed in beakers and 100 cc. of distilled water added. Then periodically 5 ml. of 0.020 N HCl was added to each beaker, the sample allowed to sit a while, and the pH determined. Higher pH values indicated a faster rate of dissolution of dolomite. This experiment is outlined in Table 2. In all cases the pH's of dolomite 3071 were greater than the corresponding value for dolomite 3070, indicating that dolomite 3071 may weather faster than dolomite 3070. The contrasting soils above and below A may be caused by a combination of erosion rate and rates of dissolution of two slightly different rock types.

All of the results presented here must be considered tentative. Mineralogical studies are underway to give us better knowledge about the age of the soil. Microscopic studies are underway to give us a better grasp of creep on this slope and of the soil-faulting interactions.

TABLE 2

RATE OF DISSOLUTION OF GROUND DOLOMITES 3070 AND 3071

Sample No.	3070A	3070	3071A	3071
add 100 ml H_2O				
pH	9.59	9.58	9.51	9.50
add 5 ml 0.02 N HCl, sit 20 minutes				
pH	6.6	7.15	7.59	7.70
sit 45 minutes, add 5 ml 0.02 N HCl sit 30 minutes,				
pH	6.21	5.92	6.55	6.70
sit 17 hours				
pH	8.05	8.07	8.20	8.31
add 5 ml 0.02 N HCl, sit 1 hour				
pH	6.30	6.48	6.61	6.65

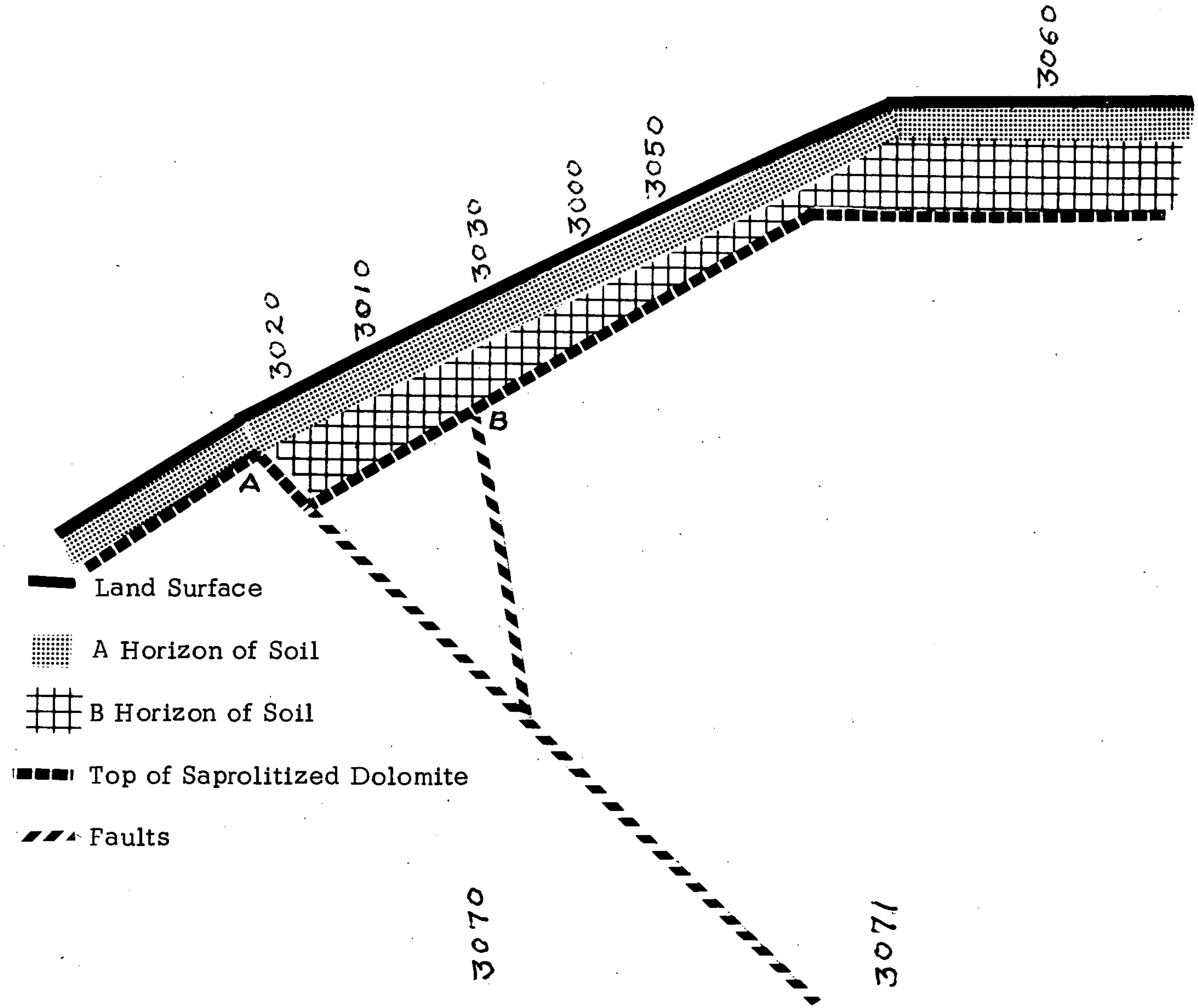

Figure 1. Generalized sketch of soils and underlying rocks, near Reactor No. 3.

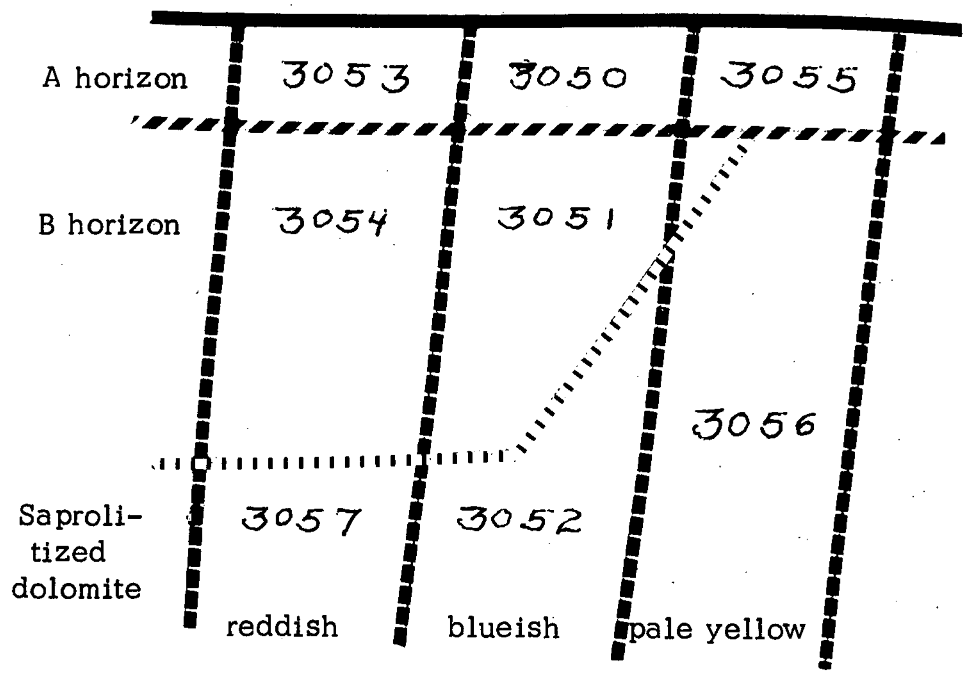

Figure 2. Highly generalized sketch of soils and saprolitized dolomite at site 3050. Numbers identify sampling locations.

APPENDIX F

GEOPHYSICS

APPENDIX F1

INTRODUCTION AND SUMMARY

F1.1 INTRODUCTION

A geophysical program, consisting of approximately 27 miles of reflection seismic profiling and bathymetric surveying, was performed in the Hudson River between the Bear Mountain Bridge and a point several miles south of the Consolidated Edison Indian Point Generating Station. The field portion of the survey started August 18, 1975 and was completed August 22, 1975.

E.G.& G., environmental consultants and marine seismic contractors, performed the actual field work under contract to, and under direct supervision of, Dames & Moore geophysicists. The interpretation of the seismic data was accomplished by Dames & Moore geophysicists.

F1.2 SUMMARY

From Jones Point northwest to the Bear Mountain Bridge, there are few sediments present in the main channel. The shape of the river bed is indicative of a scoured river valley with steep rock walls and a hard bottom (see Plate F-12). No anomalous conditions were observed in this area.

From Jones Point southwest past the site, sediments are present on the river bottom. Subbottom reflections are absent in this area. This may be due to a hard river bottom condition or a lack of an acoustic contrast in the subbottom materials. There are a few areas of limited penetration

(See Plate F-4); however, those areas are scattered and no correlation between them is possible.

Two anomalies are observed on the river bottom in the area from Jones Point southwest past the site. The major anomaly is characterized by irregularities on the river bottom, and by a distinctive character or signature of the seismic signal as seen on the seismograms (see Plates F-8 through F-14 and map overlay, Plate F-1). This anomaly strikes approximately north 35° east and trends from the quarries on the west bank of the river north of Tomkins Cove toward Peekskill Bay.

The second anomaly, characterized by a break in, and possible offset of, the surface of the river bottom, is found on two lines of survey close to Lents Cove on the eastern bank of the river just north of the site (see Plates F-5 and F-6 and map overlay, Plate F-1). This anomaly is topographic in nature and is recognized on both the bathymetric record and the seismic section. Since this anomaly is found only on two closely spaced lines, it is not possible to define what it represents on the basis of these data only.

APPENDIX F2

SEISMIC INVESTIGATION

F2.1 PURPOSE AND SCOPE

The purpose of the geophysical seismic investigation was to:

1) Define the gross features of the crystalline basement, if possible;
2) Locate areas of anomalous acoustic reflections in the basement;
3) Profile acoustic horizons in the post-glacial material, looking especially for offsets or anomalous zones which may be related to faulting; and
4) Try to correlate observed fault zones onsite to other zones on the opposite side of the river.

F2.2 FIELD PROCEDURES

Consolidated Edison provided a 28-foot aluminum work boat for the seismic survey. This vessel was suitable for this work, having a large open deck area aft, ample cabin space for the recording instruments, and full head room. It was necessary to construct a wooden platform to cover the afterdeck. The recording system produces very high voltages and amperages, and the wooden platform insulated this equipment from the aluminum deck.

The Motorola Mini-Ranger navigation system, used on this survey, consists of two transponders located at known points ashore and a receiver aboard the boat. The transponders were placed so that the geometry of the three points (two shore transponders and a shipboard receiver) allowed accurate positioning. The transponder locations chosen for this survey were the fixed navigation beacon in Peekskill Bay, a benchmark located on the northeast shore upriver from Roa Hook (labeled "Tunnel"; see map overlay, Plate F-1) and a point just downstream from Jones Point (labeled "Jones"; see map overlay, Plate F-1). It was necessary to survey in the "Jones" transponder location; this task was accomplished by a Consolidated Edison survey crew.

E.G.& G. provided both a sparker and a boomer seismic energy source. The sparker is a medium to high-power, low-resolution energy source with deep penetration capabilities. The boomer is a moderate-power energy source with moderate resolution and penetration capabilities.

It was expected that the sparker system would work since the portion of the river in which the survey area is located is tidal. It was found, however, that the salinity was not high enough to allow the spark between electrodes. The sparker system was tested both at the dock and in the river without success. This left the boomer, which will work in fresh water, as our only energy source.

Two 500-joule boomers were mounted on a single sled so that either 500 joules or 1000 joules of energy could be used. Both were tested and it was found that a single unit of 500 joules gave a cleaner record. This power setting was used on the production runs.

Two E.G.& G. technicians worked aboard the survey boat. An instrument technician monitored the record as it was produced on the recorder, ensuring that the proper instrumental settings were maintained for maximum record quality. At the same time, the surveyor monitored the Mini-Ranger and fathometer equipment and placed fiducial marks on both the seismic record and fathometer charts at one-minute intervals to correspond with Mini-Ranger fixes. In this way, particular points on the seismic record and fathometer chart can be related to points on the ground along the lines of survey.

The survey information was plotted on the map (Map overlay, Plate F-1), and the interpretation was related to the plotted lines of survey.

Equipment used in this survey consisted of:

1) Motorola 3-element Mini-Ranger system;
2) Raytheon Model DE719 Precision Survey Fathometer;
3) Model 254 E.G.& G. Seismic Recorder;
4) Model 232-A E.G.& G. Power Supply, 2 each;

5) Model 231 E.G.& G. Triggered Capacitor Bank, 2 each;

6) Model 265 E.G.& G. Eight-Element Hydrophone;

7) Model 402-7 E.G.& G. Nine-Electrode Sparkarray; and

8) Model 230-1 E.G.& G. Uniboom Boomer System, 2 per sled.

F2.3 INTERPRETATION OF RESULTS

F2.3.1 Record Quality

Record quality is considered to be good. A strong bottom reflection was recorded at all points along the lines of survey. Such river bottom conditions as dredged channels and rubble from constructon (see Plate F-3) were well delineated.

F2.3.2 Penetration of Seismic Energy

The penetration of the seismic signal into the river bottom seems to be limited. There are two possible reasons for this:

1) The northwestern leg of the river from Jones Point to the Bear Mountain Bridge appears to have a predominantly rock bottom. The "U" shaped cross section of the river valley, just downstream from the Bear Mountain Bridge (Plate F-2), indicates that the river channel has hard rock sides and a hard rock bottom. The seismic signal generated by the Boomer System cannot penetrate this type of bottom; and

2) The portion of the survey area from Jones Point southwest is underlain by sediments of apparently seismically homogeneous material with a hard river bottom. The few areas of limited penetration, showing scattered subbottom reflections (as characterized by Plate F-4) and the characteristic strong, initial reflection with up to 10 sharp multiples as seen (with few exceptions) over the whole survey area, reinforce this interpretation. There are no cores of the river bottom sediments, with the exception of cores taken directly adjacent to the power plant; thus, the exact nature of the river bottom and the material above bedrock is not known.

F2.3.3 Anomalies

Because of the apparently poor penetration of the seismic energy, only a single bottom reflection was recorded over the majority of the survey area. This single, strong bottom reflection and the bathymetric data indicate three different bottom types:

1) Smooth - a more or less even bottom topography;
2) Irregular - small, abrupt differences in elevation; and
3) Disturbed - larger topographic differences than 2), with more of a non-homogeneous appearance.

A large disturbed area is located adjacent to and downstream from the power plant site. This bottom condition is probably caused by the dumping of waste material in the river during plant construction.

A large area of disturbed river bottom occurs around Roa Hook. However, since this area is at the bend of the river and the bottom condition is localized, it is felt that this disturbed area is caused by normal river current action.

An important zone of disturbed bottom material occurs opposite the site. This zone strikes approximately N35^{o}E and trends from the quarry on the west side of the river north of Tomkins Cove toward Peekskill Bay (Plates F-8 through F-14 and map overlay, Plate F-1).

This anomalous zone is best characterized by the events marked on Plates F-8 through F-12. The event on Plate F-12 occurs between stations 0935 and 0937 (recorded October 21, 1975). A shallow depression in the hard bottom is indicated, and a small hump in the center of this depression is also noted. This same depression with a hump in the center is noted between stations 0926 and 0928 (recorded October 21, 1975) and shown on Plate F-13. These anomalies are located at the northeast end of the anomalous zone.

Plate F-8 shows the anomaly located at the southwest end of the anomalous zone between stations 1444 and 1446 (recorded October 21, 1975). This anomaly indicates a greater disturbance than the anomalies at the northeast end of the zone, and the depression and hump in the center of the depression are striking.

The reflection signature indicated by arrows on Plates F-8, F-9, F-11, F-12 and F-13 are significant because they do not seem to occur anywhere else on the seismic section. They appear to be characteristic of this anomalous zone.

The similarity of the anomalies at the extremes of the zone, and the characteristic seismic signature observed at the extremes, in conjunction with the much less distinct anomalies between, indicate that the zone is continuous from the southwest to the northeast.

A second anomalous condition exists close to the east bank of the river, upstream from the power plant site in the vicinity of Lents Cove. This feature, indicated by the arrows on Plates F-5 and F-6, shows a discontinuity of the primary reflection from the river bottom. Since this anomaly appears only on two closely spaced lines of survey, it is not possible to determine its trend on the basis of the data available.

The results of the bathymetric survey (Plate F-5a confirm the shape and orientation of the anomalies noted above.

An attempt was made to correlate the scattered subbottom reflections seen on the sections. This was done by making overlays of each survey line and orienting the overlays in their proper relationship to each other. No correlation was possible, however, as the events are too small and widely scattered. It was also not possible to determine which, if any, of the reflections represented bedrock.

The topography of the river bottom was contoured from the southern limit of the survey to Jones Point and Peekskill Bay (map overlay, Plate F-1), using the bathymetric data. The resulting map shows a topography that, as expected, is dominated by the gradient of the river. However, where the channel turns NW around Jones Point, this pattern is disturbed by a N35E-trending, anomalous feature that is coincident with the features described from the seismic records.

F2.4 CONCLUSIONS

The seismic reflection survey did not provide answers to the four tasks outlined in Section F2.1. With the possible exception of the river channel between Jones Point and the Bear Mountain Bridge, the top of the crystalline bedrock was not defined. Since bedrock was not defined, anomalies in bedrock, if present, could not be recognized. Two topographic anomalies were found on the river bottom:

(1) The major N35E-trending anomaly between the quarries on the westside of the river downstream of the power plant site and Peekskill Bay, and

(2) The feature near Lents Cove, just upstream of the power plant site.

These features were found only on the surface of the river bottom. Caution must be exercised in attaching significance to these anomalies since their exact nature is not known.

The failure to penetrate the bottom materials of bedrock may have been caused by the lack of power in the seismic signal source. If this is the case, then a sparker system, encased in a salt water sleeve, or an airgun signal source might work. It might be, however, that the acoustic impedence of the bottom material is such that the reflection method will not work with any signal source. In that case, the refraction seismic method would have to be used.

Until the bedrock surface is mapped, no positive statements, as to structural features under the river bottom, can be made. The two anomalous features found on the surface of the river bottom mentioned above should be investigated further. This could be done by a diver, side-scan sonar, further geophysical investigation or, possibly, by drilling. No definite structural significance should be given to these anomalies until some further investigation is accomplished.

APPENDIX F3

MAGNETOMETER SURVEY

F3.1 SITE SURVEY

F3.1.1 General

The survey was conducted in a wooded area just northeast of the site. It followed a baseline which began at Broadway Avenue, crossed Bleakley Avenue near parking lot number 9, and ended at the Hudson River. The strike of the baseline was approximately N25°W.

The purpose of the survey was to better define the throughgoing nature of faults seen in exposures at the site and in the immediate vicinity of the site. The magnetic survey was initiated due to lack of rock exposures near the site. The location selected for the survey was along the contact between the Cortlandt Complex and the Manhattan Schist. The Cortland Complex is a magnetite rich igneous rock and the Manhattan Schist contains little magnetite. This creates a good contrast in the magnetic susceptibility between these two rock types which is easily distinguished by magnetometer measurements. The contact between these two rock types strikes approximately west-northwest. The strike and magnetic contrast of these rocks afford an exceptional opportunity to indirectly evaluate the horizontal component of movement of the postulated and observed north-south and northeast faulting seen on site.

F3.1.2 Establishment of the Survey Baseline

A survey baseline was determined for use as a reference for the magnetometer work. The baseline begins at Broadway Avenue and ends at the Hudson River. The contact of the two rock types can be seen at the end points of the baseline. The baseline strikes approximately N25°W and has a staked station every 50 feet along its 2,500-foot length. Dames & Moore personnel constructed crosslines at the 50-foot stations and staked them for 100 feet both east and west of the baseline. This 100-foot length on either side of the baseline was a first approximation and was modified as the work progressed; some lines were lengthened while some of the western lines were eliminated. To expedite the work from Station 0+00 to Station 14+00, the Con Edison surveyors were used to construct and stake the crosslines. Plate F-15 shows the location of the baseline used. No crossline was run at Station 6+00 because of materials, i.e. guardrail, overhead wires, etc., which interfered with the magnetometer readings.

F3.1.3 Procedures and Instrumentation

The Geometrics Model G816 Portable Proton Magnetometer was used for the survey. This instrument is a total field measuring device with a digital readout.

To check for magnetic storms, the magnetometer was read at a specific base station before and after running survey lines. It was also read at the base station at intervals throughout the day to collect data and to plot a diurnal curve for correcting the day's survey data to a chosen datum. The base station readings did not vary a great deal over the course of the survey. Mangetometer readings were taken on the crosslines at predominately 25-foot intervals, although in areas where wider spacing seemed appropriate, 50-foot spacing was used.

Topographic corrections for horizontal distances were not employed in the survey; therefore, positions on the cross-lines are not precise.

F3.1.4 Magnetic Susceptibility

The contrast between the magnetic susceptibilities of the Manhattan Schist and Cortlandt Complex is large. The magnetite rich Cortlandt Complex is characterized by magnetometer total field readings on the order of 57,000^{+} gammas while in the Manhattan Schist total field readings appear predominately below 56,500 gammas. The contact area between the two rock types has been interpreted using the difference in magnetic susceptibility. Plate F-16 shows the 57,000 gamma and 56,500 gamma contours. The readings between the two contoured values are indicative of some overlapping of the intruded Cortlandt on the Schist. In a few areas, the Cortlandt appears to give relatively low readings, on the same order as the Schist; however, these areas are located where the Cortlandt is suspect of being severely sheared. Deep weathering and leaching of magnetic minerals may account for the lower readings. The Cortlandt can be physically made to read lower by alteration of the magnetite; however, the Schist cannot be made to read higher.

F3.1.5 Contour Map

The concentrated effort of the completed magnetic survey was to locate apparent offsets of the Cortlandt-Manhattan contact; therefore, the contouring was done in this area, and a completely contoured map was not drawn. The first 57,000 gamma points seen on the traverse lines, going from west to east, were interpreted as the higher limiting boundry of the contact; the closest 56,500 gamma value to the 57,000 gamma value was interpreted as the lower boundry of the contact. The contact, therefore, is shown as a zone between 57,000 gammas and 56,500 gammas.

F3.1.6 Interpretation

Step offsets of the 57,000 gamma contour are easily seen. The step offsets (or discontinuities) are more easily seen along this contour because of the more pronounced nature of the magnetic readings as the survey lines approach the Cortlandt. The ambiguity of the contact zone becomes less pronounced here. Seven discontinuities are seen along the length of the reference baseline. Only the most pronounced of these seven will be discussed. Two major discontinuities are seen at Station 4+50 and Station 22+50. These discontinuities may very well be indicative of the horizontal component of faulting; however, two assumptions must first be made:

1) The Cortlandt-Manhattan contact was, to begin with, a smooth continuous contact; and

2) Weathering along an overlapping contact has not produced the discontinuities.

The two major offsets appear to have right-lateral movment. This is indicated by the apparent displacement of the contact face and apparent drag of the two contour values.

Another relatively large discontinuity is seen between Stations 6+50 and 7+00. This appears left lateral with an apparent offset of approximately 130 feet. No drag of the contour lines are seen near this presumed structural feature.

F3.2 REGIONAL SURVEY

A reconnaissance magnetometer survey was conducted near the old Tiorati Brook Road, located on Thiells Quadrangle. The area of the survey was at the junction of two valleys: an east-west valley, and a southwest valley. It is believed that the east-west valley is faulted and offsets the southwest valley. A diabase dike seen in a road cut at the junction of the valleys strikes approximately N55°E. The trend of the dike would place it within the southwest valley. The magnetometer survey was attempted to follow the dike from the road cut up the southwest valley to determine if any apparent offset of the dike, and, therefore, the valley, could be detected.

It was concluded, however, that the apparently small difference in the magnetic susceptibility of the diabase dike and county rock (gneiss), and the large amount of anomalous "noise" from the glacial deposits in the area, precluded a positive identification of the dike. The investigation was, therefore, terminated.

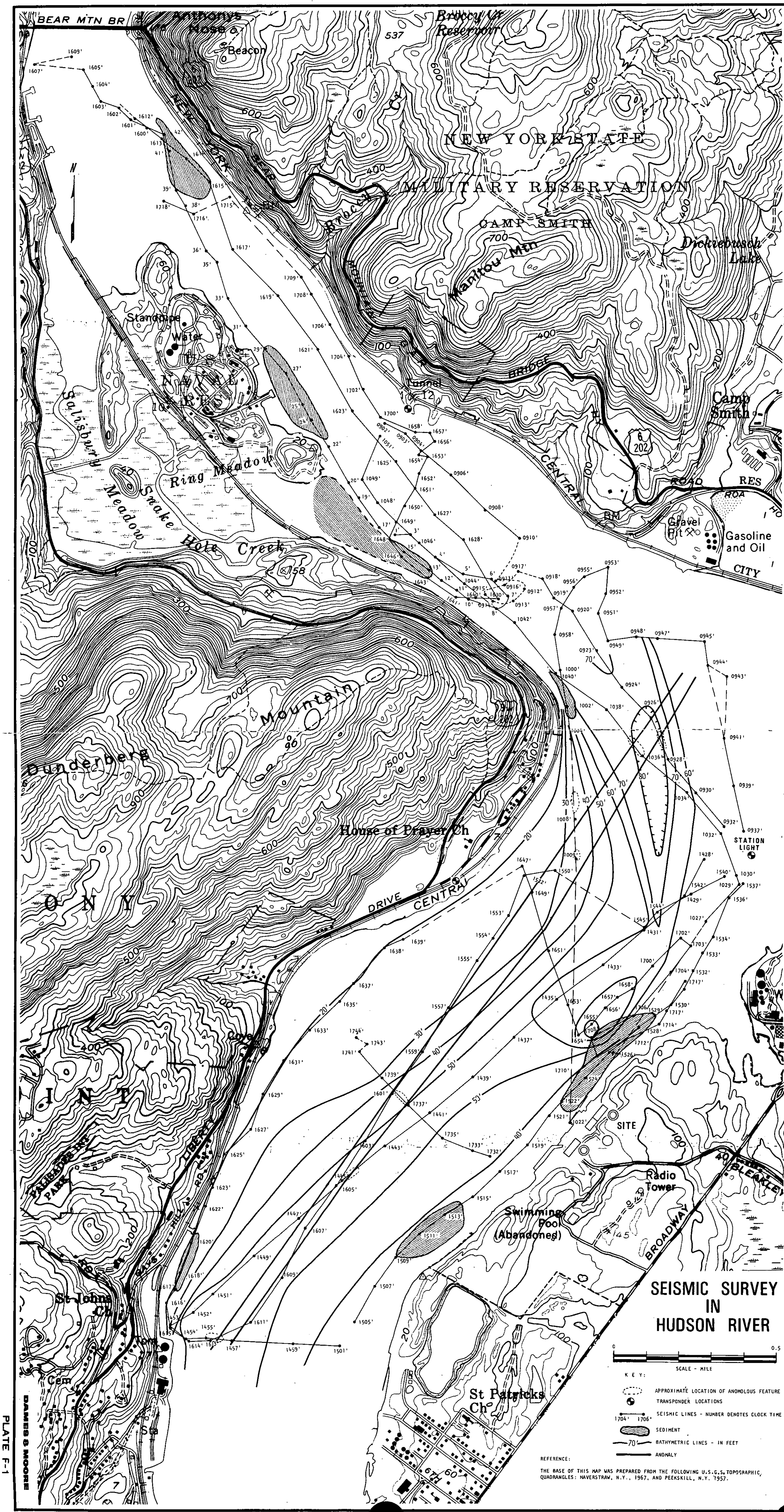
SEISMIC SURVEY
IN
HUDSON RIVER
0
0.5
SCALE - MILE
KEY:
APPROXIMATE LOCATION OF ANOMOLOUS FEATURE
TRANSPONDER LOCATIONS
1704' 1706'
SEISMIC LINES - NUMBER DENOTES CLOCK TIME
SEDIMENT
70'
BATHYMETRIC LINES - IN FEET
ANOMALY
REFERENCE:
THE BASE OF THIS MAP WAS PREPARED FROM THE FOLLOWING U.S.G.S. TOPOGRAPHIC QUADRANGLES: HAVERSTRAW, N.Y., 1967, AND PEEKSKILL, N.Y. 1957.
BEAR MTN BR
Anthonys Nose
Beacon
Broccy Cr Reservoir
NEW YORK STATE
MILITARY RESERVATION
CAMP SMITH
Manitou Mtn
Dickiebusch Lake
Camp Smith
Tunnel
Standpipe
Water
U.S. NAVAL RES
Salisbury Meadow
Ring Meadow
Snake Hole Creek
Gravel Pit
Gasoline and Oil
CENTRAL
CITY
STATION LIGHT
Dunderberg
Mountain
House of Prayer Ch
DRIVE
Cove
SITE
Radio Tower
Swimming Pool (Abandoned)
BROADWAY
BLEAKLEY
St Johns Ch
St Patricks Ch
DAMES & MOORE

PLATE F-1

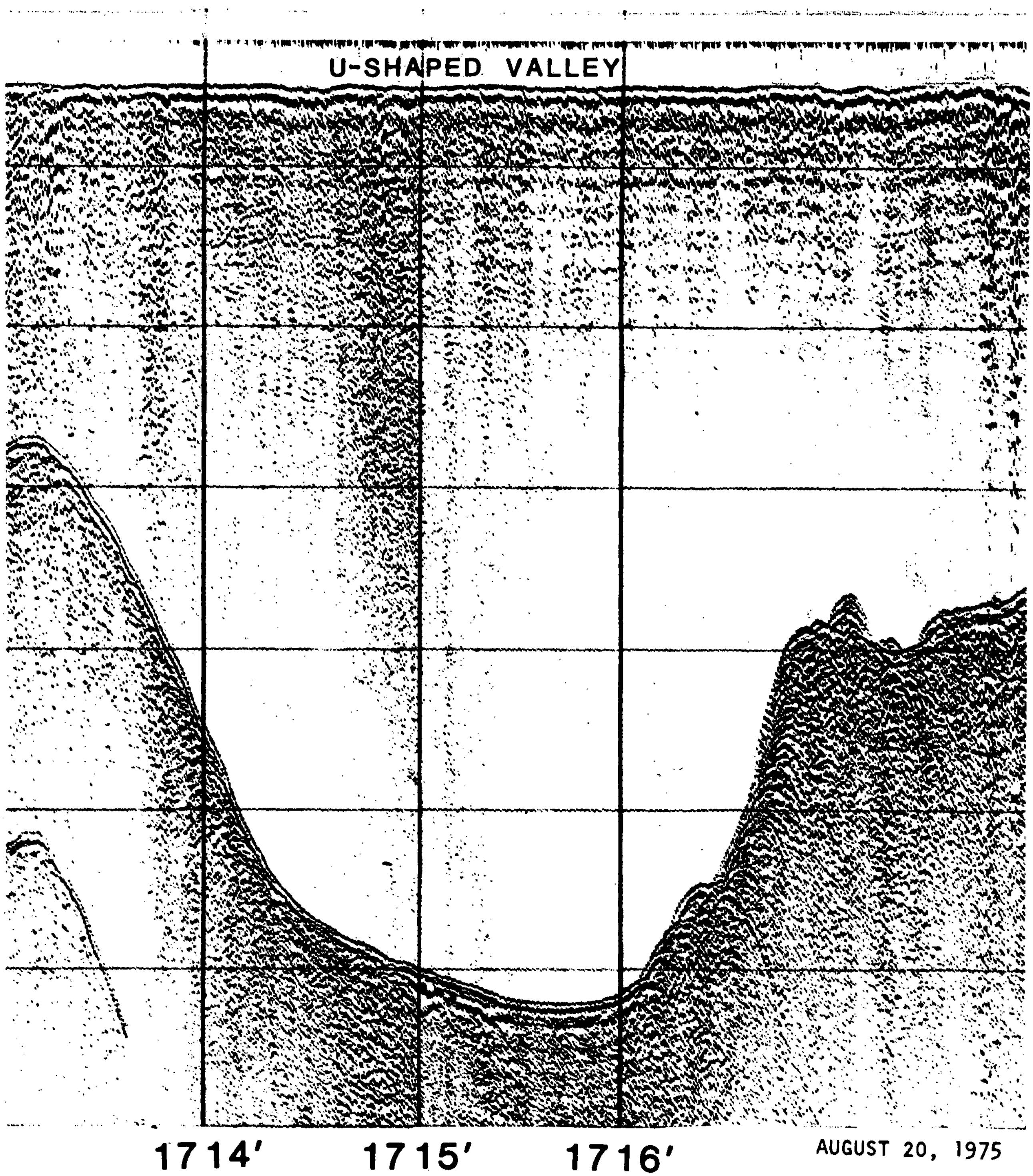

SEISMIC REFLECTION PROFILE

DAMES & MOORE

PLATE F-2

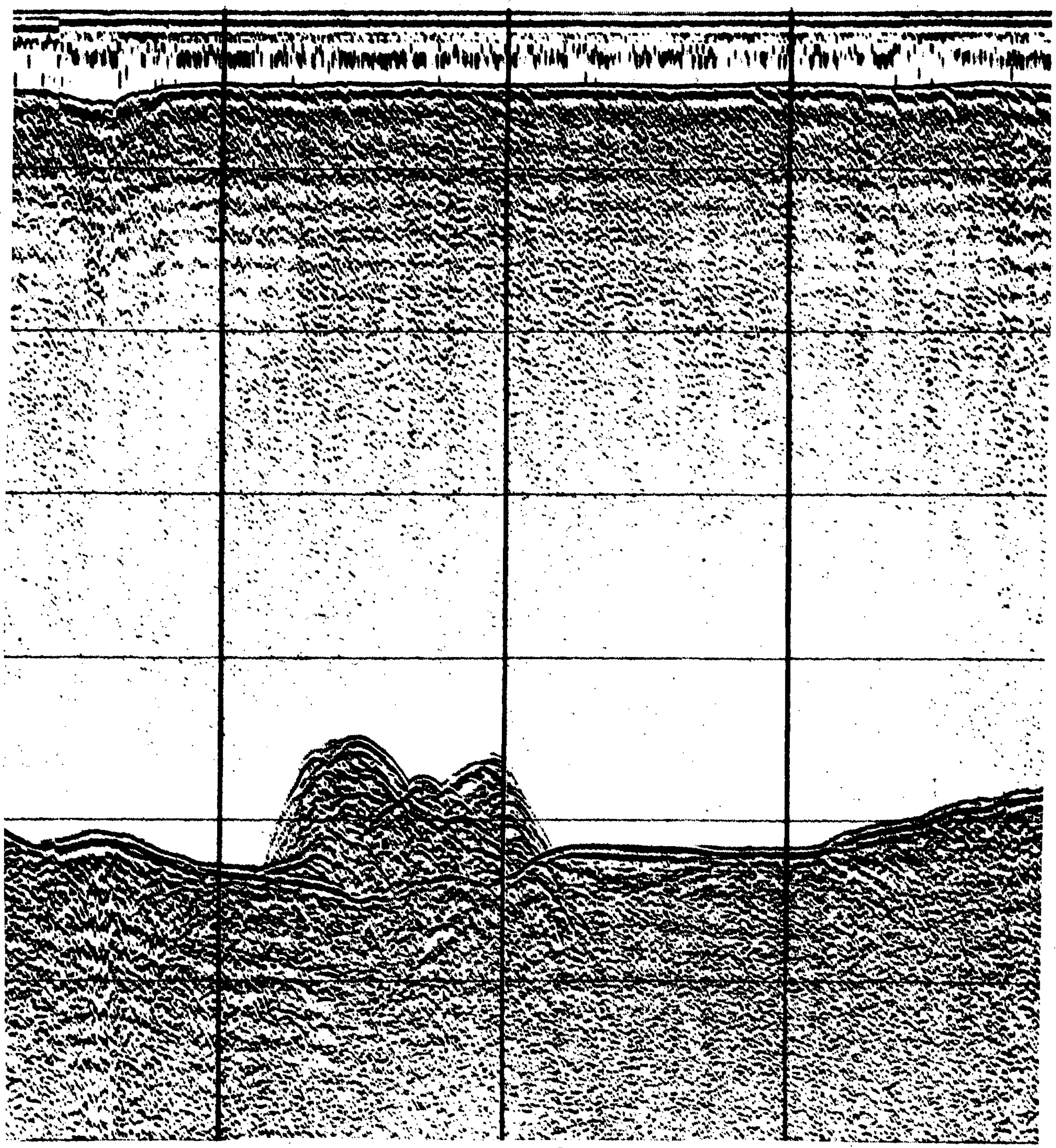

AUGUST 20, 1975

SEISMIC REFLECTION PROFILE

DAMES & MOORE

PLATE F-3

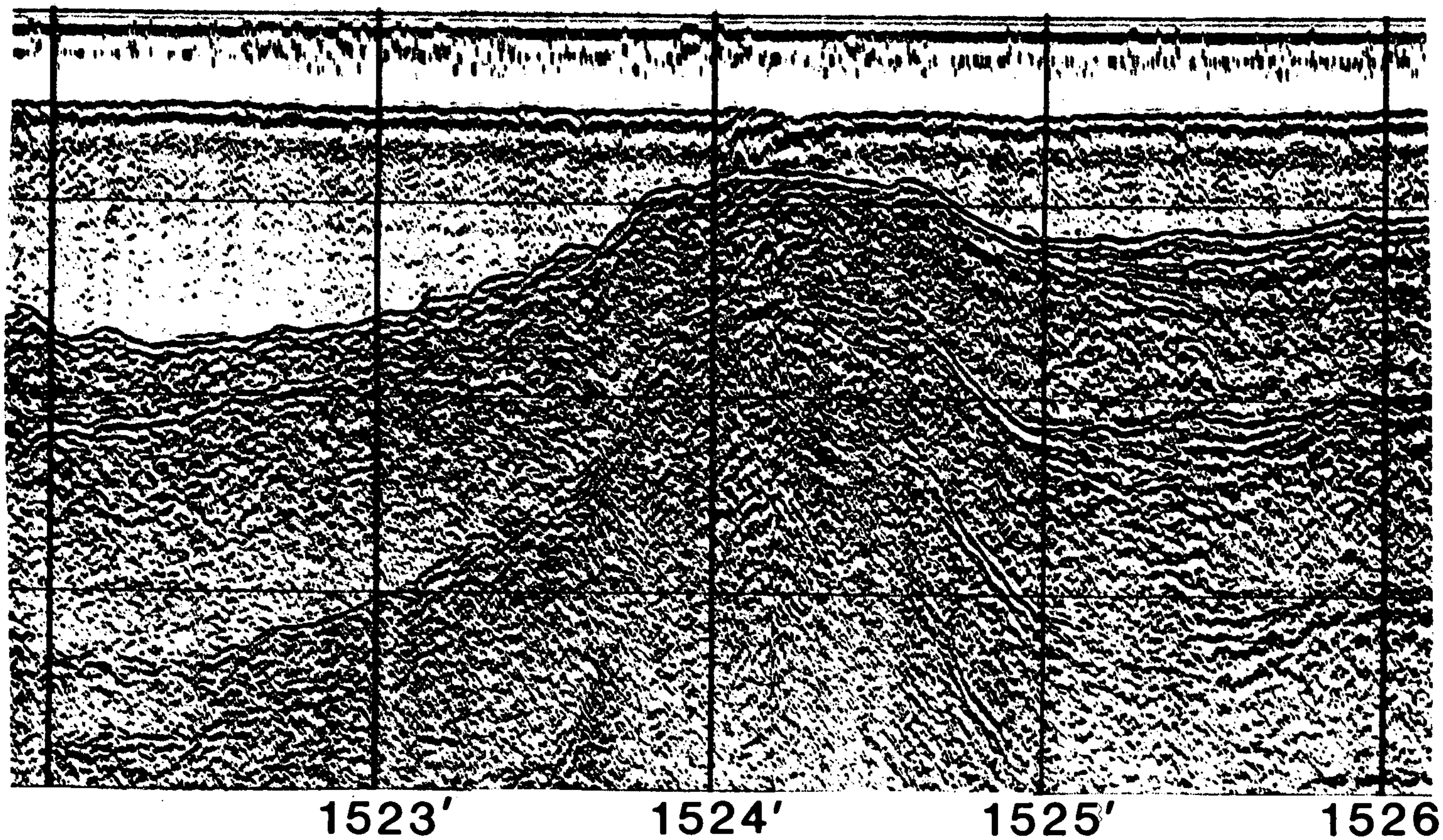

AUGUST 21, 1975

SEISMIC REFLECTION PROFILE

DAMES & MOORE

PLATE F-4

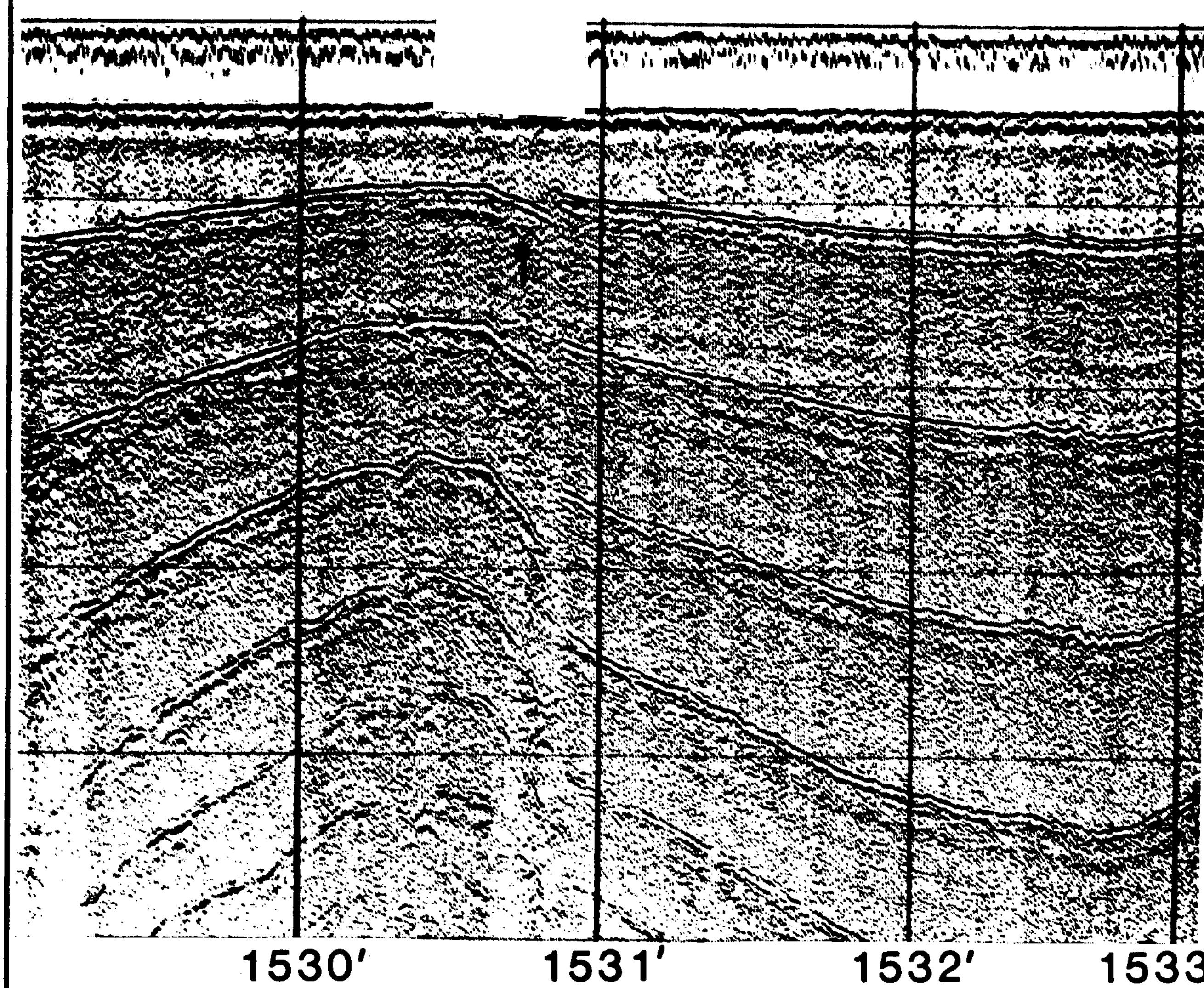

AUGUST 21, 1975

SEISMIC REFLECTION PROFILE

DAMES & MOORE

PLATE F-5

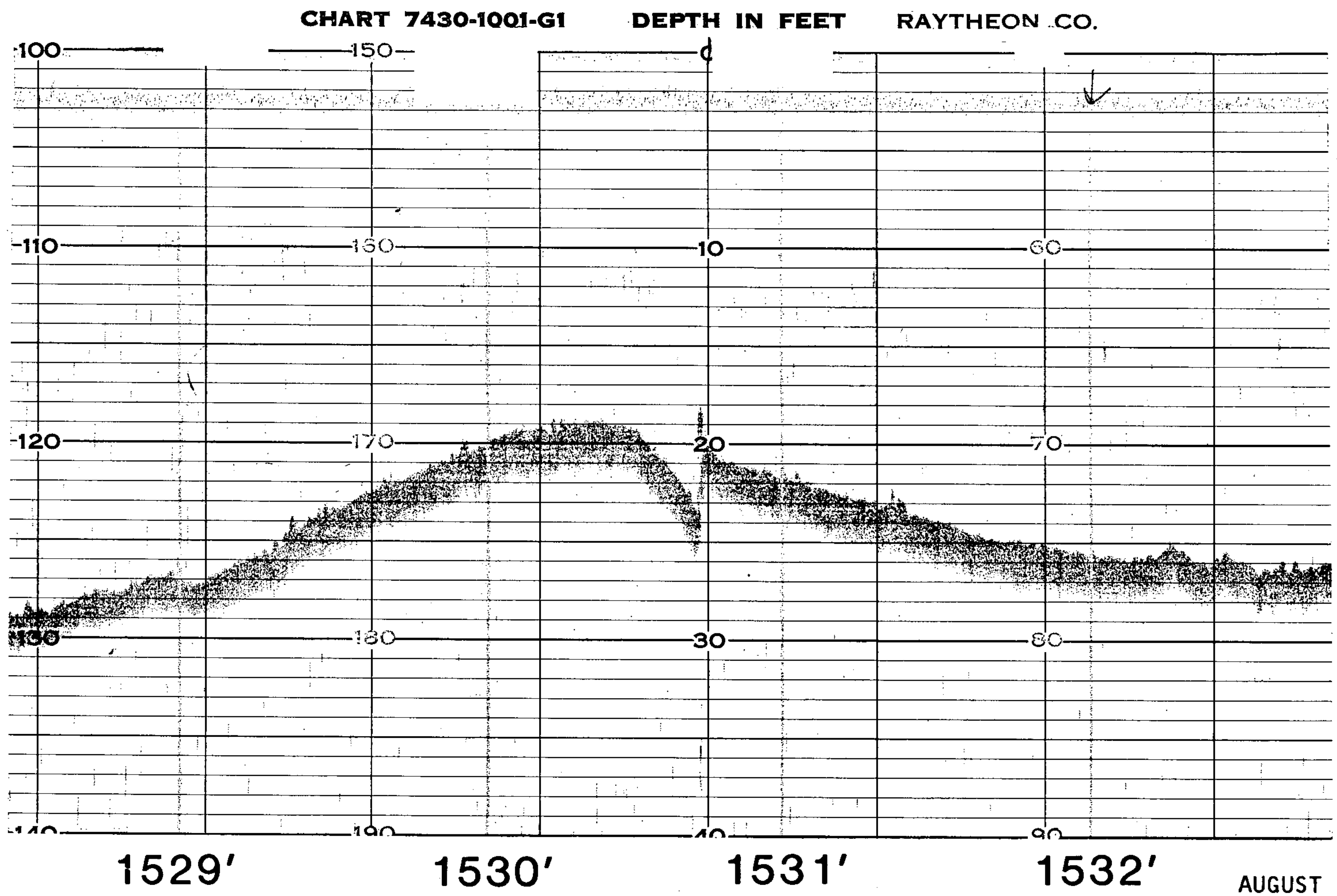

AUGUST 21, 1975

BATHYMETRIC PROFILE

DAMES & MOORE

PLATE F-5a

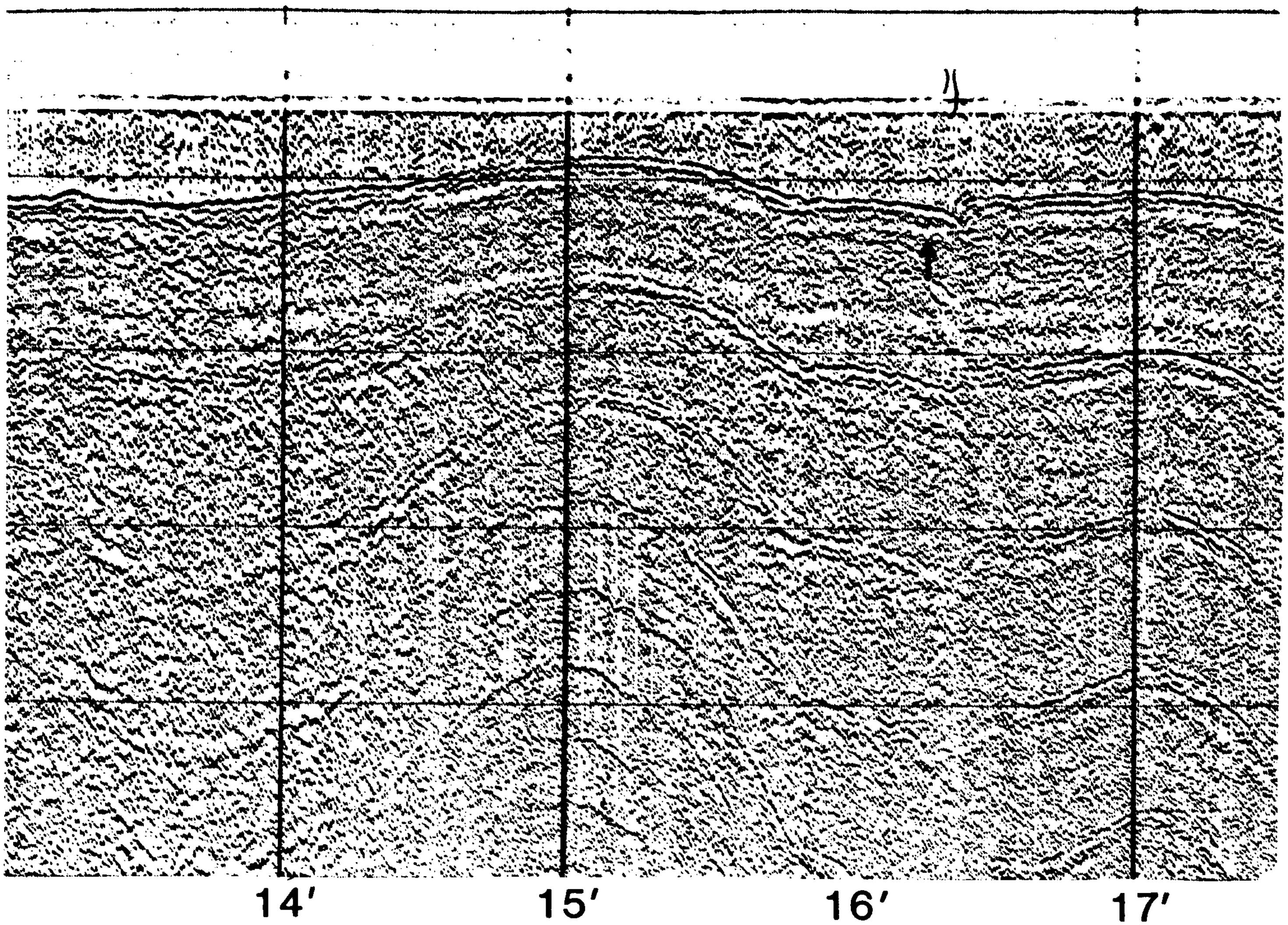

AUGUST 21, 1975

SEISMIC REFLECTION PROFILE

DAMES & MOORE

PLATE F-6

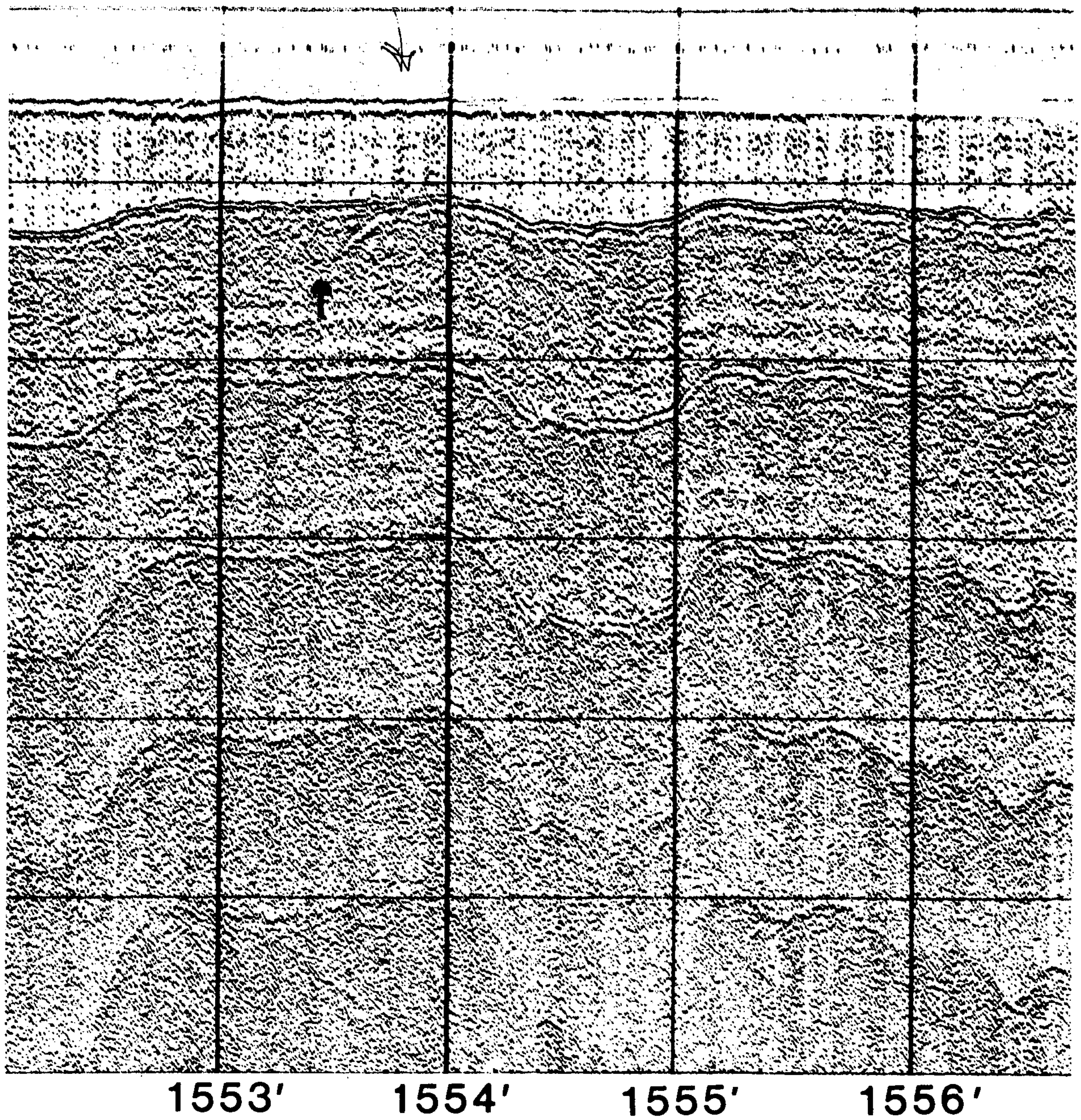

AUGUST 21, 1975

SEISMIC REFLECTION PROFILE

DAMES & MOORE

PLATE F-7

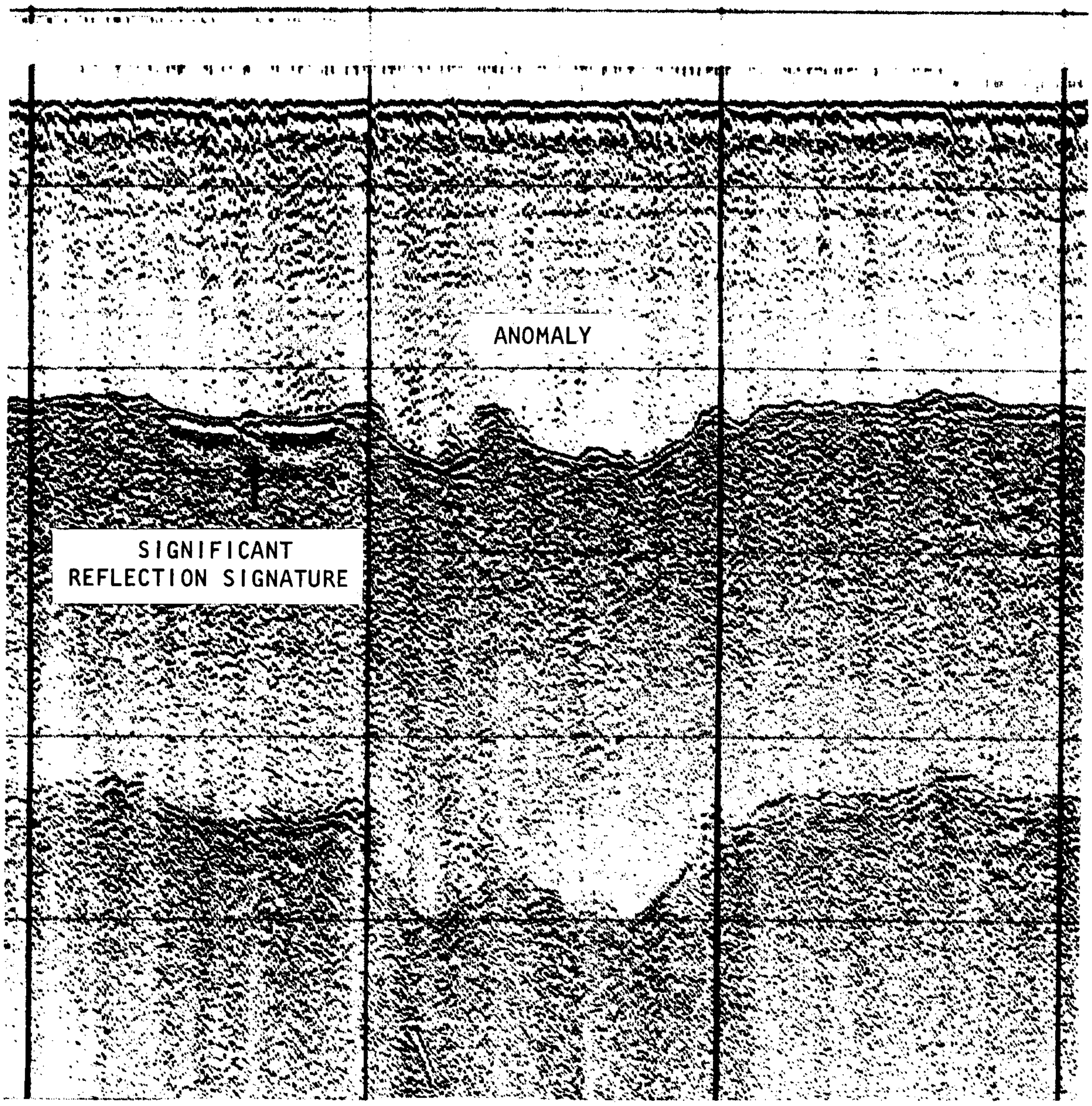

1444′ 1445′ 1446′ 1447′

AUGUST 21, 1975

SEISMIC REFLECTION PROFILE

DAMES & MOORE

PLATE F-8

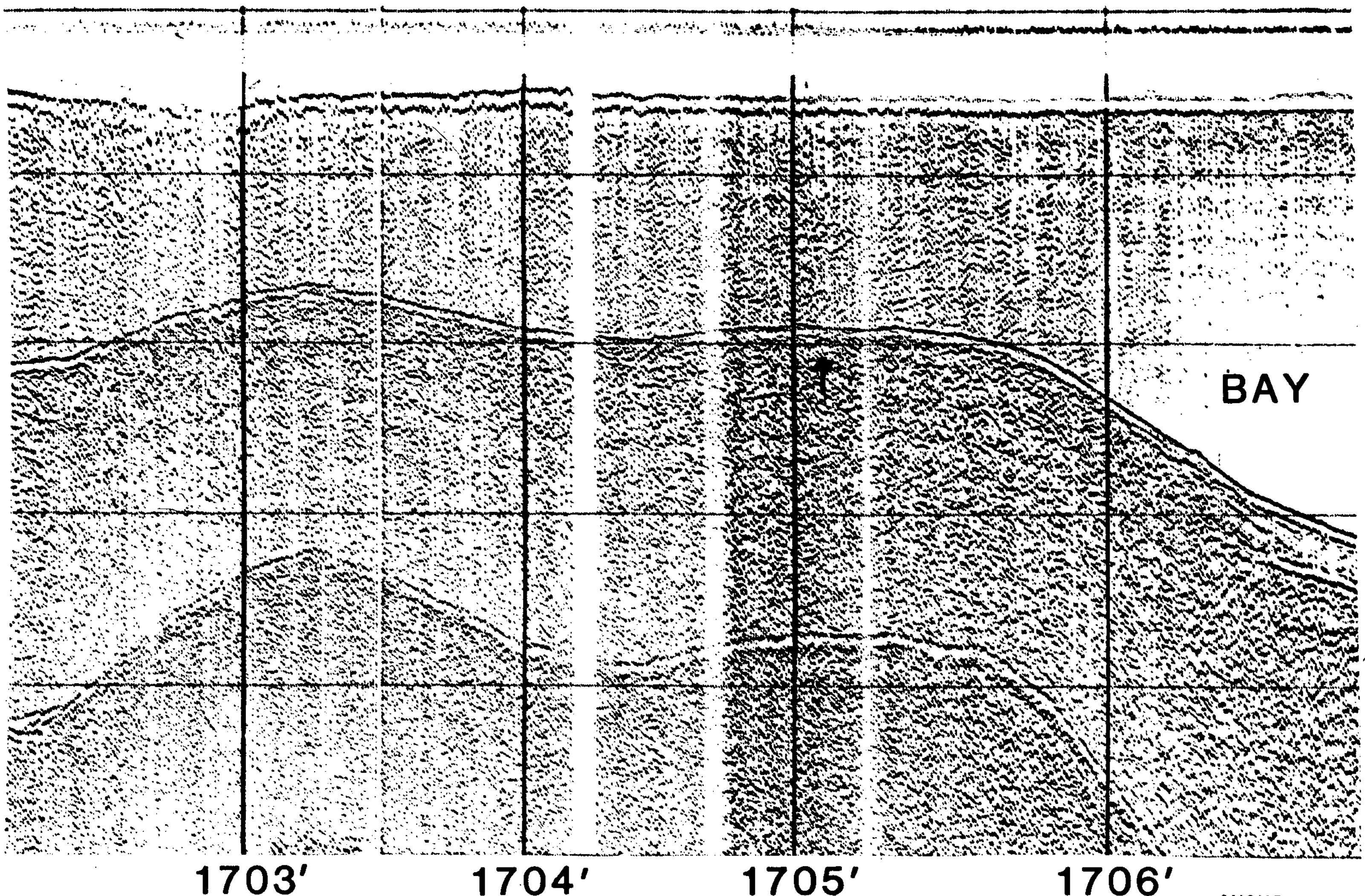

AUGUST 21, 1975

SEISMIC REFLECTION PROFILE

DAMES & MOORE

PLATE F-9

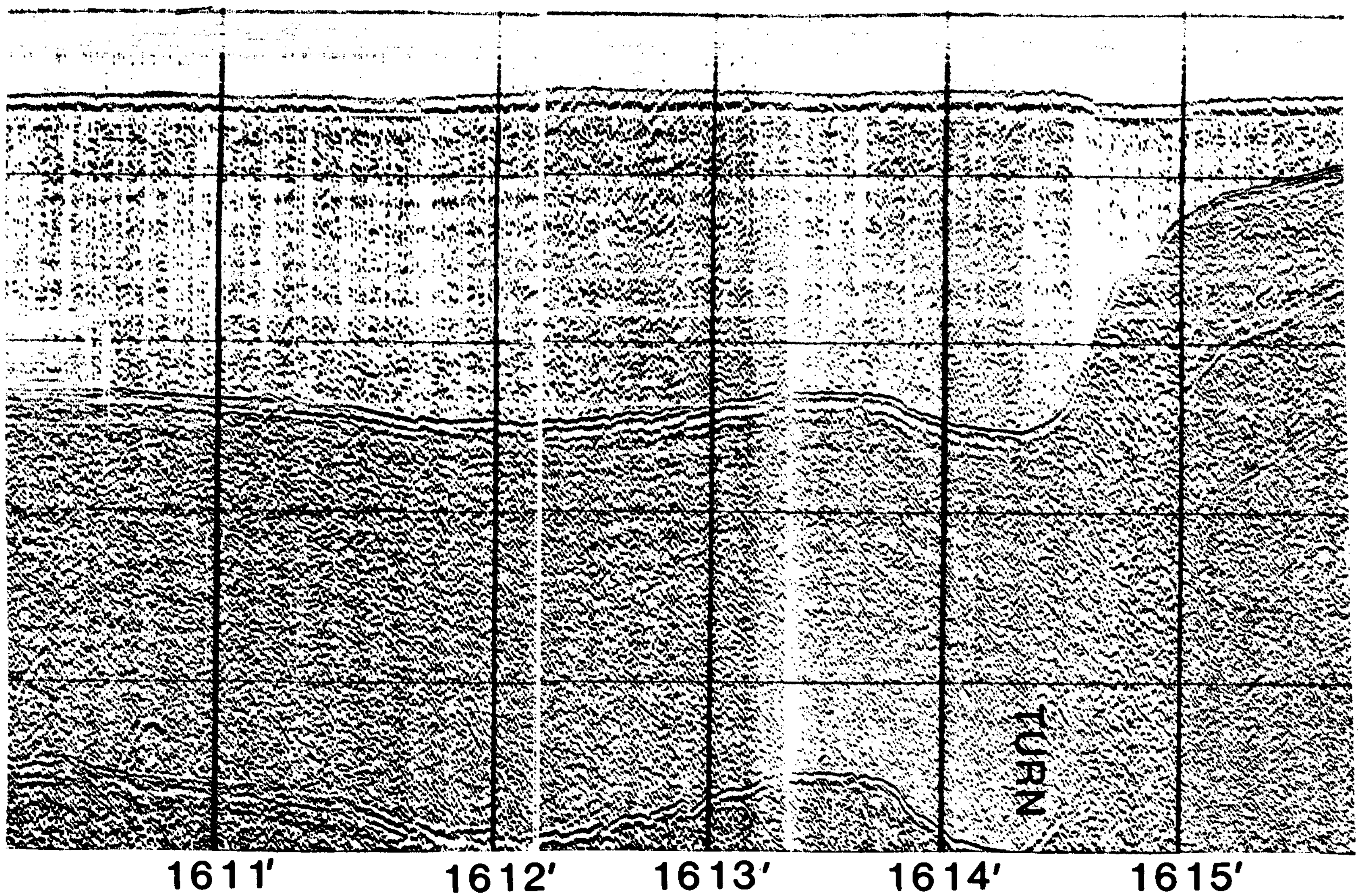

AUGUST 21, 1975

SEISMIC REFLECTION PROFILE

DAMES & MOORE

PLATE F-10

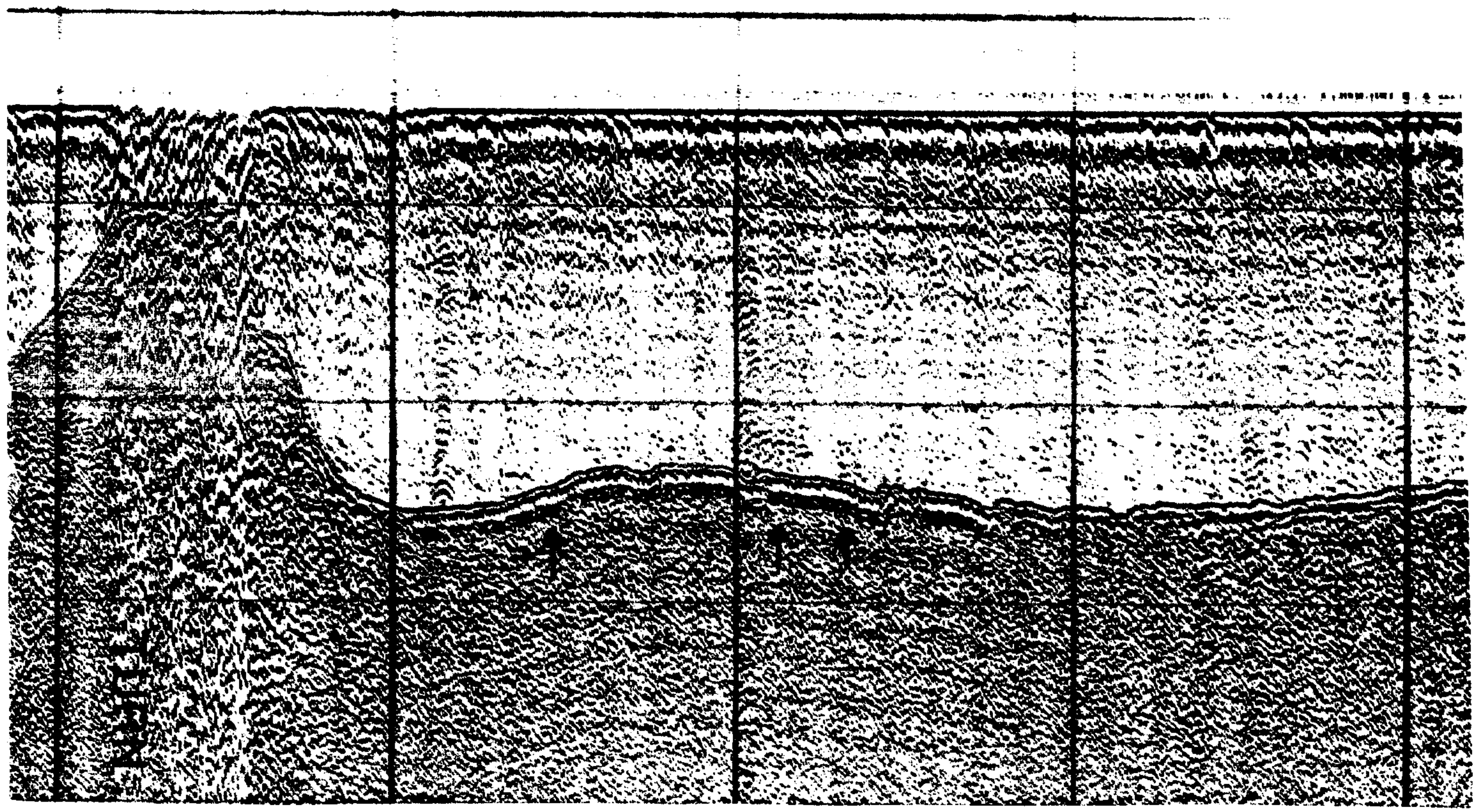

AUGUST 21, 1975

SEISMIC REFLECTION PROFILE

DAMES & MOORE

PLATE F-11

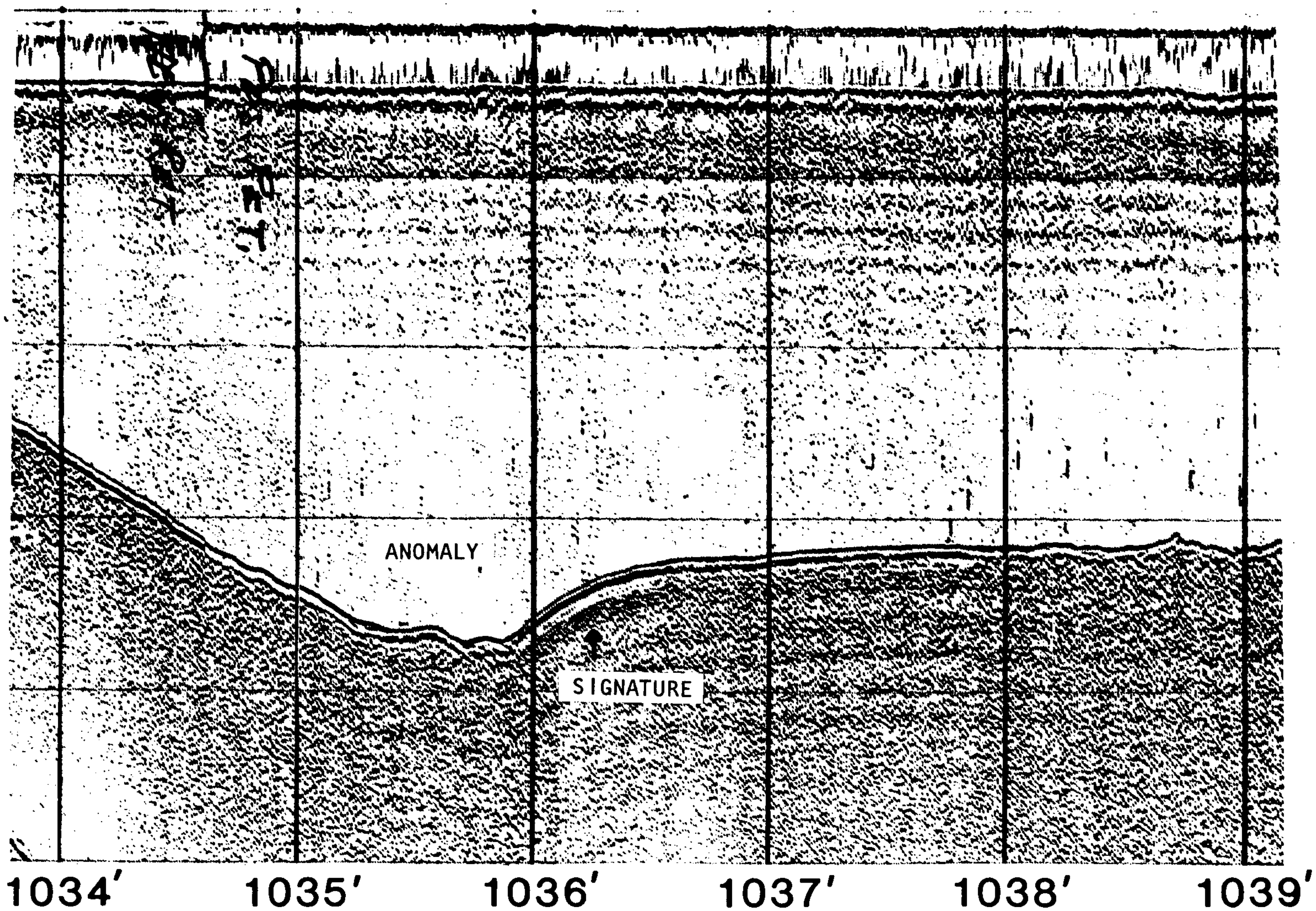

AUGUST 21, 1975

SEISMIC REFLECTION PROFILE

DAMES & MOORE

PLATE F-12

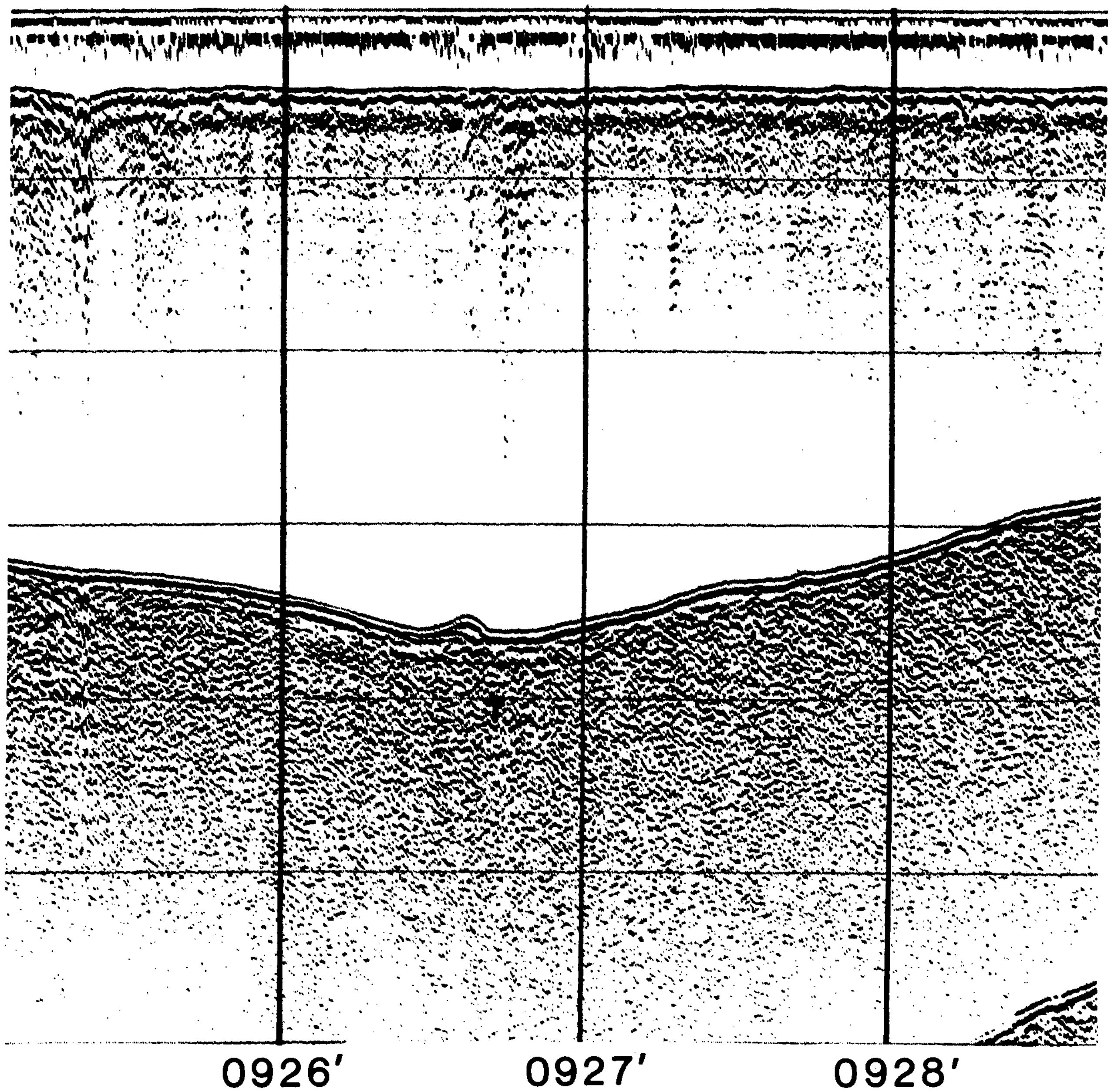

AUGUST 21, 1975

SEISMIC REFLECTION PROFILE

DAMES & MOORE

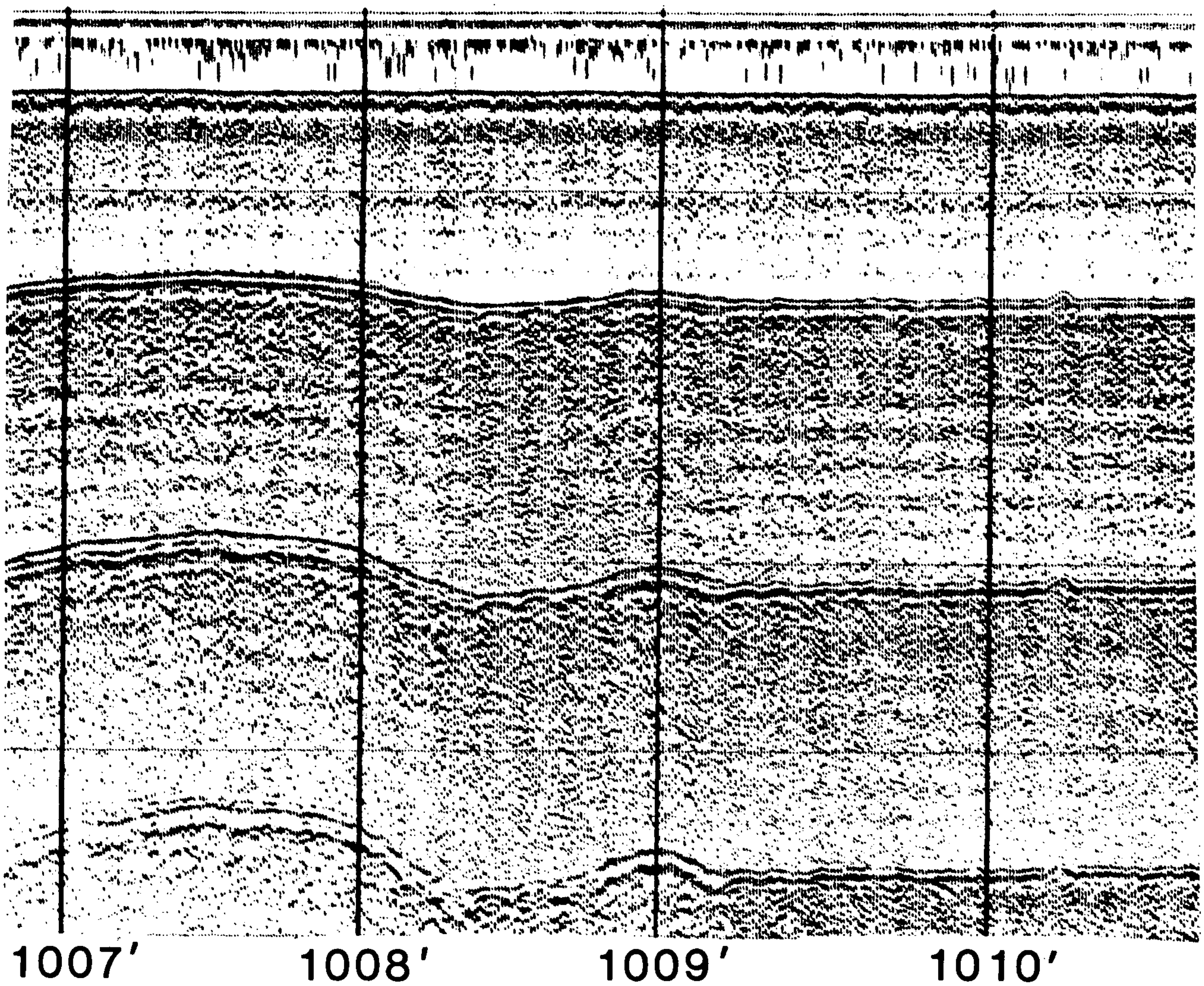

AUGUST 21, 1975

SEISMIC REFLECTION PROFILE

DAMES & MOORE

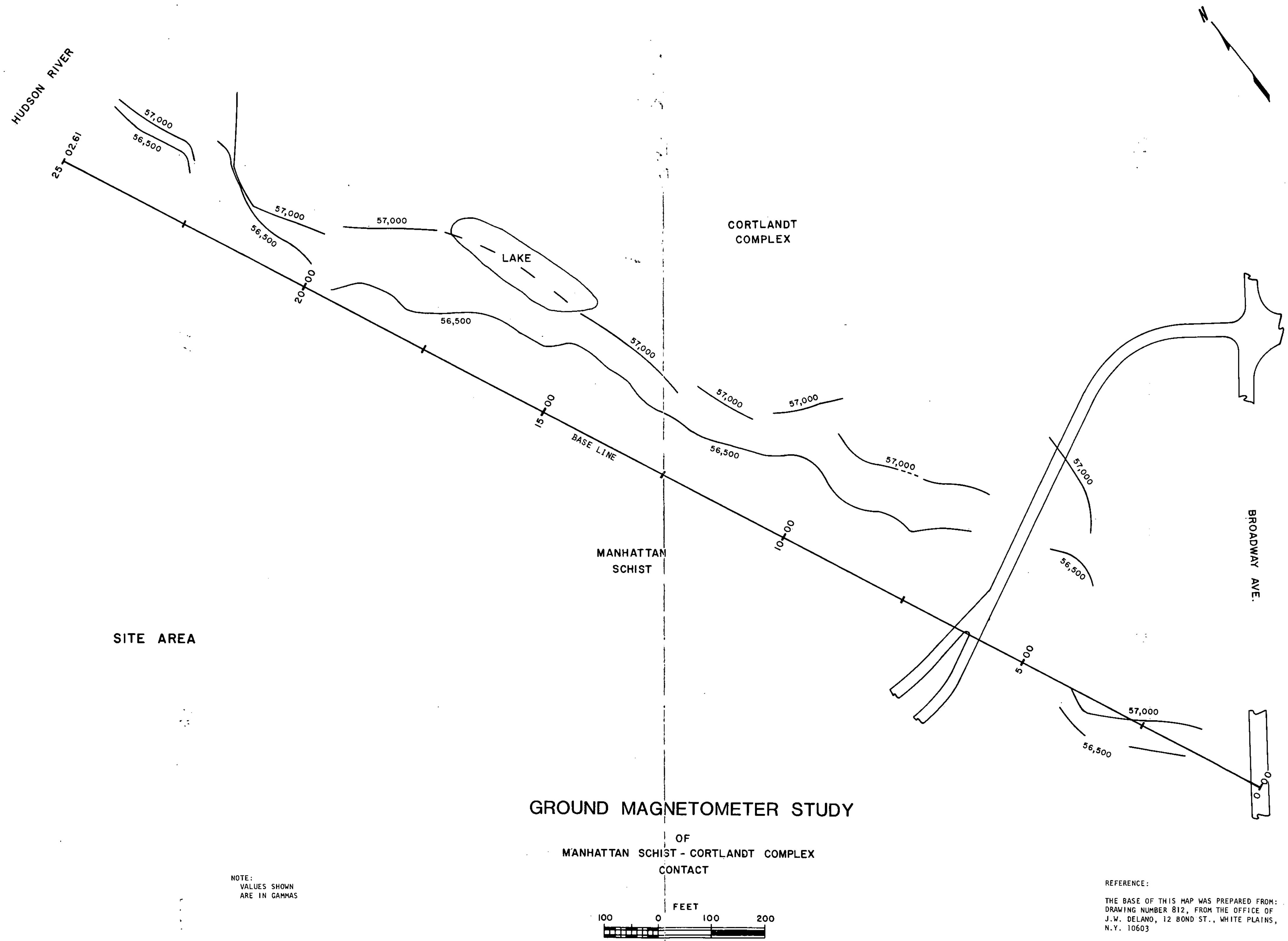

GROUND MAGNETOMETER STUDY
OF
MANHATTAN SCHIST - CORTLANDT COMPLEX
CONTACT

NOTE:
VALUES SHOWN
ARE IN GAMMAS

REFERENCE:

THE BASE OF THIS MAP WAS PREPARED FROM: DRAWING NUMBER 812, FROM THE OFFICE OF J.W. DELANO, 12 BOND ST., WHITE PLAINS, N.Y. 10603

GENERAL LOCATION OF STUDY DENOTED BY CORTLANDT-MANHATTAN CONTACT ON PLATE B3-3.

DAMES & MOORE

PLATE F-15

APPENDIX G

PHOTOGEOLOGY

APPENDIX G

PHOTOGEOLOGY

G1 INTRODUCTION

The photogeology study for the Indian Point fault investigation involved remote sensing work utilizing both satellite imagery and aerial photography.

The area investigated on the satellite imagery encompassed some 1,200 square miles. The purpose of the investigation was to delineate the major lineaments within this area. Lineaments of interest are rectilinear topographic features which are structurally controlled. Frequently, lineaments are the surface manifestation of faulting. To ensure that all the major lineaments were observed, all bands available for each frame were analyzed. This approach is necessary because the different bands emphasize different geologic/geomorphic conditions. For example, band No. 7 shows drainage much better than the other bands.

The area investigated on the 1/60,000 aerial photographs encompassed some 400 square miles. The purposes of this investigation was to provide a higher resolution view of the lineaments detected on the satellite imagery and to detect additional lineaments not observable on the satellite imagery. With a higher resolution view, a more confident assessment of the cause of the lineaments was made. This is desirable because there are geomorphic and geologic conditions, not related to faulting, that will cause a lineament to be expressed at the earth's surface. For example, bedding changes are frequently expressed as sharp lineaments on the imagery. Better resolution obtainable on the 1/60,000 aerial photographs also permits accurate placement of the satellite lineaments onto base maps. With these base maps (1/24,000 topographic maps), the lineaments from both the satellite imagery and the 1/60,000 photos can be checked in the field.

The 1/24,000 aerial photographs have a corresponding higher resolution than the 1/60,000 photographs. An inherent difficulty, however, is that the higher resolution is obtained at the expense of losing the broad view of the terrain. It becomes difficult, therefore, to track features for long distances with the 1/24,000-scale photography. The 1/24,000 photos were used only when higher resolution was required. For example, the photos were used: (1) when specific problem areas were pointed out by the field geologist; (2) when a questionable lineament from the 1/60,000 photo analysis needed a higher resolution analysis; or (3) when specific areas deemed essential to our understanding of the regional or site geology needed a more detailed analysis. Analyses of Dunderberg Mountain, the immediate vicinity of the site, Hook Mountain, and Cedar Brook Creek were some of the areas that required the use of these 1/24,000 photos.

G2 IMAGERY AND AERIAL PHOTOGRAPHY USED

G2.1 Imagery

The satellite imagery used for the study was obtained from Photo Science Corporation of Gaithersburg, Maryland. Imagery was in the form of 20" x 20" black-and-white prints at a scale of 1/500,000 (Imagery I.D. Nos. 1258-15080, 1979-15124). A 30' x 30' false-color composite print at a scale of 1/250,000 (imagery I.D. No. 1079-15124) was also obtained.

Images from the ERTS satellite comprise individual scenes (frames) recorded in different parts (bands) of the electromagnetic spectrum. Each frame covers an area of approximately 13,225, square miles. Bands 4, 5, 6, and 7 of each frame and the false-color composite were used in the interpretation. Band 4 is recorded in the 0.5 to 0.6 micrometer part of the visible spectrum (green light); band 5 is recorded in the 0.6 to 0.7 micrometer part of the visible spectrum (red light); band 6 is recorded in the 0.6 to 0.7 part of the near-infrared spectrum; and band 7 is recorded in the 0.8 to 1.1 micrometer part of the near-infrared spectrum. False-color composites are made by overlaying and printing 3 bands of the same frame. The three bands are assigned three different colors (yellow, cyan, and magenta) that do not correspond to the part of the spectrum recorded by the bands and, hence, these composites are termed "false color".

G2.2 Aerial Photography

The high-altitude aerial photos used for the study were obtained from the Eros Data Center at Sioux Falls, South Dakota. These photographs are in standard 9" x 9" black-and-white print format at a scale of 1/60,000. Low-altitude aerial photos were obtained from Lockwood, Kessler and Bartlett, Syosset, New York. These photographs were also in standard 9" x 9" black-and-white print format at a scale of 1/24,000.

G3 METHODOLOGY

In the satellite imagery analysis an acetate overlay was initially prepared showing all of the lineaments for band 7 of each frame. These overlays were then registered to bands 4, 5, and 6 of their corresponding frames, and any additional lineaments observed on these frames were added to the overlays. It was possible to observe the study area in stereo due to the sufficient number of adjacent frames. Using a mirror stereoscope, corresponding bands of the adjacent frames with their previously analyzed overlays were studied stereoscopically. This added a three-dimensional view of the lineaments, providing a more confident assessment of the lineaments. This assessment was further refined when the analysis of the 1/60,000 aerial photographs was completed. The assessment, presented in Table G3-1 shows: (1) the number of each lineament, (2) the strength (by which is meant how easily the feature is recognized on the imagery), (3) the length in miles, (4) the strike of the lineament, and (5) the geologic/geomorphic conditions which appear to be controlling the lineament. These conditions are:

(a) Topographic Alignments (TA) - anomalously straight sections of ridges and valleys or more subtle topographic highs and lows;

(b) Drainage Alignments (DA) - anomalously straight stretches of streams, lakes or rivers;

(c) Topographic Offset (TO) - distinct offset of ridges and valleys or more subtle topographic highs and lows;

(d) Stratigraphic Offset (SO) - distinct offset in key beds and other stratigraphic units or offset of folds or intrusives; and

(e) Tonal Anomalies (TN) - changes in photographic tones which may reflect changes in vegetation slope, or drainage.

Another very important conditions noted in Table G3-1 is the coincidence with a mapped fault (CMF). This determination was arrived at by transferring the lineaments from the 1/500,000 scale black-and-white ERTS frames to the 1/250,000-scale false-color composite ERTS frames. Any additional lineaments seen at 1/250,000 scale were then added to the overlay and the table. Prominant natural and cultural features were traced from the 1/250,000-scale frame onto the overlay for control. This overlay was then fitted to the 1/250,000-scale Geologic Map of New York State (1970), and the determination of whether a lineament was coincident with mapped faults was made and noted in Table G3-1.

Before analyzing the 1/60,000-scale aerial photography, a print laydown of all the photographs was made. The laydown served as a large photo index and was useful in maintaining a regional overview. It also aided in positioning ERTS lineaments on individual 1/60,000 photos. In analyzing the 1/60,000 photos, acetate overlays were prepared and the ERTS lineaments transferred. The photos were then examined with a mirror stereoscope, and additional lineaments seen only on the 1/60,000 photos were delineated. The same procedure was followed when specific areas were analyzed on 1/24,000-scale photographs.

The lineaments observed on the ERTS imagery and on the 1/60,000 and 1/24,000-scale photographs, and the mapped faults of the area, are all shown on Plate G-1. This base map was made from photographically reduced topographic maps onto which the lineaments and mapped faults had been transferred. A zoom transfer scope, manufactured by Bausch and Lomb, was used to transfer the data to the base map. The base map also served as a means of filtering out spurious, culturally controlled lineaments such as transmission lines.

The 1/60,000 and 1/24,000 lineaments were compiled onto the base map, and the strike of each was recorded. These trends are grouped by the physiographic region in which they occurred. There are three of these major regions within the area of study: the Hudson Highlands, the Manhattan Prong, and the Triassic Basin. The trends of the ERTS lineaments, previously recorded in Table G3-1, were also grouped into these three regions. A plot of the frequency versus trend was then made for each physiographic region. A 5°-interval in recording the trends was chosen as the best compromise between graphic representation and data compression. Some 317 lineaments were recorded in the Hudson Highlands; 105 were recorded in the Manhattan Prong, and 58 were recorded in the Triassic Basin.

G4 RESULTS OF ANALYSES

G4.1 Regional Analysis Results

The Precambrian rocks of the Hudson Highlands are the oldest rocks of the area and have been affected by many deformational events. The dominant fold trends observed on remote sensing imagery in the Hudson Highland range from about N30° to 45°E. The trend versus frequency histogram define the following dominant lineament directions: N2°E, N12°E, N23°E, N33°E, and N43°E. Noticeably smaller peaks are centered N14°W, N27°W, N67°W, N75°W, N62°E, N72°E, and N82°E. It is obvious that the major peaks in the Hudson Highlands occur between N7°W and N47°E. The NNW, WNW, ENE, and E-W directions represent subordinate trends (see Plate G-2).

The Manhattan Prong consists of deformed Cambro-Ordovician metasedimentary rocks. In the vicinity of the site, the dominant fold trend is N30° to 35°E. North of the site near Kingston and Poughkeepsie and south of the site near Dobbs Ferry, the dominant fold trend is N10° to 20°E (New York State Geologic Map, 1971). The histogram of trend versus frequency of lineaments defines a broad peak between N10°W and N15°E. A strong peak also occurs at N37°E. Other subsidiary peaks occur at N5°E, N67°E, N35°W, N47°W, N64°W, N74°W, and E-W (see Plate G-2).

No fold trend was recognized on the remote sensing imagery in the Triassic rocks of Rockland County, New York. One dominant linear trend (N3°E) is apparent on the trend versus frequency histogram. Other subsidiary peaks occur at N13°E, N22°E, N35°E, N50°E, N87°E, N7°W, N17°W, N40°W, N57°W, and N82°W.

It is interesting to note that the dominant lineament trends, striking between N10°W and N45°E, occur in all three regions. These trends decrease in intensity from the Precambrian to the Triassic. Therefore, it may be reasonable to conclude that the lineaments developed genetically during the Precambrian and propagated into the younger rocks by reactivation of movement along pre-existing trends during the deformation of the younger rocks. This observation seems to apply also to the subsidiary peaks. Alternatively, the style of deformation of the younger rocks may have been controlled by the position of the Precambrian block. The development of new fractures in both the Precambrian and younger rocks, during the Paleozoic and Triassic tectonic events, occurred along the same old established trends.

G4.2 Results of Specific Areas Analyses

G4.2.1 Peekskill Hollow Fault

On ERTS imagery and the 1/60,000 aerial photographs, the Peekskill Hollow Fault (lineament 1) appears to be offset (see Plate G-1). The Peekskill Hollow Fault trends N41°E. The lineaments which appear to offset it trend N41°W and N12°W. Both of these offsetting lineaments are coincident with mapped faults (New York State Geologic Map, 1970). However, on the state map the more northerly trending lineament trends N5°E, and on the photos and ERTS it appears to trend N12°W. The N12°W lineament appears to offset the Peekskill Hollow Fault right-laterally as seen in the vicinity of Adams Corners. The opposite sense of movement is seen on the state map.

The N41°W lineament, as seen in the vicinity of Boyd Corners Reservoir, suggests a right-lateral displacement of the Peekskill Hollow Fault. This concurs with the sense of movement on the state map. This sense of movement is also seen at South Branch Reservoir. At the reservoir, an Upper Proterozoic biotite gneiss is also right-laterally offset by the N41°W lineament.

It seems that, at least, at these locations the N41°W and N12°W (N5°) faults are younger than the N41°E Peekskill Hollow Fault.

G4.2.2 Dunderberg Mountain

A detailed analysis of Dunderberg Mountain was done on 1/60,000 and 1/24,000 aerial photographs (see Plate G-1, inset A). The analysis revealed north-south and north-northeast lineaments, many of which were coincident with those mapped by Ratcliffe (1975). The offsets of the northeast faults by these north-south and north-northeast faults were not observed on the photographs (as mapped by Ratcliffe). It is possible that these offsets are not observable at the scales of the aerial photographs used.

It was observed, however, that a major northwest-trending lineament appears to offset a major northeast-trending lineament. The northeast-trending lineament (3) is located near the base of Dunderberg Mountain, and has been interpreted by Ratcliffe (1975) as an extension of the Peekskill Fault. Several smaller northwest, north-northwest, and east-west lineaments were also observed on Dunderberg Mountain.

G4.2.3 Ramapo Fault

Analysis of 1/60,000 aerial photographs and ERTS imagery suggests that beginning at about Ladentown, New Jersey (see Plate G-1) the Ramapo Fault splays into many parallel to subparallel branches. One mapped branch, which is just east of Thiells, appears to align up with and extend to the site. Specifically, it appears to align with a lineament trending N38°E that extends from Verplanck Point to Uriah Hill School. If this is one continuous branch, then a splay of the Ramapo Fault extends through the vicinity of the site.

Strong northwest trending lineaments are apparent at Cedar Brook Creek, Suffern, and Bensons Point; north-south-trending lineaments are also observed in these areas. These northwest and north-south lineaments cross the northeast trend of the many splays of the Ramapo. No offsets of the Ramapo splays by the northwest and north-south lineaments were observed at Bensons Point or at Cedar Brook Creek. It may be that such offsets exist but cannot be observed at the scale of the photographs. It is suggested that at these locations the northwest and north-south lineaments may have formed due to movement on the Ramapo and, thus, represent antithetic shears.

However, at Suffern, there is some indication, although rather weak, that the Ramapo may be offset by northwest and north-south lineaments. This suggests that north-south and northwest lineaments, at least in the vicinity of Suffern, may possible postdate movement on the Ramapo.

G4.2.4 <u>County Asphalt Quarry</u>

When this area was first analyzed on ERTS imagery, a major N55°W lineament was recognized which parallels Popolopen Brook. This area is of concern because northwest-striking normal faults within Pleistocene deposits (see Appendix D) have been recognized in County Asphalt Quarry. This lineament passes within 500 feet of the quarry, which may imply a genetic relationship. The lineament was observed with greater resolution on the 1/60,000-scale photos and extended further to the northwest and southeast. To the southeast, this lineament extends at least to a topographic feature named the Torne (see Plate G-1), and possibly extends through the Torne to the Hudson River. To the northwest, it extends to the crest of a hill about 1-1/2 miles east of County Asphalt Quarry. On the western side of this hill, in the parallel adjoining valley, is a major northeast-trending lineament. This lineament is coincident with mapped faults that appear on the New York State Geologic Map (1970). Dodd (1965) mapped the northwest-trending lineament as a megashear whose movement sense is unknown.

Two additional northwest-trending lineaments were observed between County Asphalt Quarry and the hill to the east of the quarry. Both of these lineaments appear to terminate against the northeast-trending lineament that parallels the western side of the hill. The more southerly of these lineaments extends within 1,000 feet of the quarry and was mapped by Dodd (1965). It is aligned with the major northwest lineament that parallels Popolopen Brook. The more northerly of these northwest-trending lineaments is about 1 mile north of County Asphalt Quarry, and appears as a mapped fault on the N.Y.S. Geologic Map.

It appears, on the basis of the photo analysis, that these two lineaments are two separate features, the alignments of which do not necessarily imply a genetic relationship. It must be emphasized, however, that the southernmost lineament, which appears to align with the Popolopen Brook lineament, could be one continuous feature.

G4.2.5 Site

A major N59°W-trending ERTS lineament (15) was observed only at the scale of the satellite imagery. This lineament, which passes within three miles of the site, is rather weak on the imagery, and is expressed as a topographic and drainage alignment. However, this feature extends from the New Croton Reservoir to the Hudson River, a distance of some 13.1 miles, and aligns approximately with lineament (43) which is coincidental with the mapped fault that trends towards County Asphalt Quarry. It is not known if this lineament (15) can be joined to lineament (43) as one continuous feature, or whether two separate features are indicated. More importantly, it is not at all certain that lineament (15) is structurally controlled.

Another weak feature observed on the satellite imagery is lineament (14) which extends from Lents Cove to Chimmery Corners (see Plate G-1). This feature trends N16°W to N36°W and is some 4.4 miles long and passes within one mile of the site. It appears that the lineament may be the contact between the Manhattan Prong and the Cortland Complex rocks for a portion of its length. However, to the northeast it appears to cut across Cortland rocks. Again, it is not at all certain that this feature is structurally controlled.

At the scale of the 1/60,000 and 1/24,000 aerial photographs in the immediate vicinity of the site, the dominant trends observed are north-northwest, north-northeast, and east-west. Of the lineaments observed, the most prominent extends from Verplanck Point to the Uriah Hill School. The lineament trends N38°E and portions of it have been observed in the field. It is tentatively suggested that this lineament may be a continuation of a splay off the Ramapo Fault, as discussed previously.

G4.3 Remote Sensing Interpretation

A multitude of structural elements has resulted from Precambrian, Paleozoic and Mesozoic tectonism (Appendix C2, C4, C5, and C6). Partial resolution of the complex pattern of lineaments, which resulted from these successive events, was achieved by comparing the orientations of the major folds to those of the lineaments seen in both Precambrian and Paleozoic rocks. The areas underlain by each of these two groups were analyzed separately, yet because the regional grain seen within the Precambrian and Paleozoic terrain is parallel, the following discussion is fundamental to both areas. This discussion is predicated upon the mechanical behavior of rocks in which folds, extension fractures, and conjugate transcurrent faults are predictable products of regional horizontal compression. Furthermore, the stress system responsible for the deformation can be inferred from the two-dimensional fold geometry, assuming no block rotation about a vertical axis subsequent to the folding. Fold traces should be perpendicular to the greatest principal stress. Extension fractures should be parallel and perpendicular to the greatest principal stress. Conjugate strike-slip faults will be inclined at about 30° or less to the greatest principal stress (e.g. Hubbert, 1951, and Muehlberger, 1961).

Major folds in the study area were observed on aerial photographs and ERTS imagery to trend N30°-45°E in the Precambrian Hudson Highlands and N30°-35°E in the Lower Paleozoic Manhattan Prong. Many major lineaments show trends coincident with the axial traces of folds (Plate G-2) and are thus interpreted as expressions of upturned beds and extension fractures which formed as a direct consequence of folding. Based on the assumptions presented in the previous paragraph, conjugate strike-slip faults should strike about N15°W, N30°W, N75°W, and N90°W. Large-scale linear features in the Hudson Highlands define peaks oriented N15°W, N30°W, N69°W, and N85°E. Lineaments trending N30°W and N85°E can, therefore, be interpreted as respective left- and right-lateral strike-slip faults associated with folds which trend N30°E, whereas N15°W lineaments are inferred to be left-lateral faults related to N45°E folding. The lineaments which define the N68°W peak may be interpreted alternatively as extension fractures related to the N30°E fold or as right-lateral faults which are cogenetic with N45°E folding. No distinct N45°E peak was defined, although lineaments showing this orientation were recognized. Movement plans, which correspond to these predicted, were recognized on the ground by the field geologists (ref. Appendix C2, C4, and C5). Fractures which formed during Precambrian orogenesis and those attributed to Paleozoic or younger tectonism cannot be differentiated by utilizing remote sensing imagery, though it is likely that Paleozoic features have been superimposed on Precambrian rocks. This interpretation was confirmed by field work done in the Hudson Highlands.

Many lineaments in the Manhattan Prong cluster about N35°W, N48°W, N64°W, N75°W, N87°W, and N87°E peaks (Plate G-2). Based on the predicted relationships of cogenetic development of folds and fractures, the strikes of left-lateral shears in the Manhattan Prong should range between N25°W and N30°W, those of right-lateral shears between N85°W and N90°W, and those of extension fractures between N55°W and N60°W. Though the fit of predicted trends to actual trends is not as good in the Manhattan Prong as in the Hudson Highlands, the following interpretations are nonetheless suggested: N35°W lineaments correspond to left-lateral shears, N87°W and N87°E to right-lateral shears, and N48°W to N64°W to extension fractures. These interpretations are consistent with field observations (ref. Appendix C2 and C5). Based on an acute dihedral angle of 60°, no explanation can be offered for the linear features which trend N75°W. However, they have been identified on the ground as right-lateral faults; thus, they probably formed with a smaller acute dihedral angle (see Muehlberger, 1961). Though the N48°W and N64°W trends are inferred to have formed as extension fractures, they have experienced lateral movements (ref. Appendix C2, C4 and C5). This apparent discrepancy may be explained by slight changes in the stress sytem during the protracted deformation which affected the study area.

Peaks corresponding to lineaments trending N03°E, N12°E, N23°E, N60°E, and N75°E in the Hudson Highlands along with those oriented N03°E, N53°E, and N67°E in the Manhattan Prong (Plate G-2) represent residual sets which are apparently unrelated to the regional N30°-45°E folding. It is, therefore, likely that they may be, at least in large part, due to a younger event.

In the Triassic Basin many lineaments define rather strong N03°E and N12°E peaks with lesser concentrations at N22°E, N35°E, and N45°-67°E (Plate G-2). Within the interval from N45°-67°E, there is a distinct peak at N50°E. Right-lateral faults, striking between N03° and 25°E in both the Manhattan Prong (N03°-25°E, ref. Table C5-3) and in the Triassic Basin (N13°E, Ref. Table C6-1), correspond to lineaments identified in the Triassic Basin. The lineaments in the interval N45°-67°E compare favorably with left-lateral faults recognized in the Manhattan Prong (N43°-65°E, ref. Table C5-3) and in the Triassic Basin (N52°-74°E, ref. Table C6-1). It was established in the Manhattan Prong that these faults are younger than those associated with regional folding (ref. Section C2). Due to the fact that similarly oriented and kinematically related strike-slip faults were also observed within the Triassic Basin, it was suggested that the faults in the Manhattan Prong and those within the Triassic Basin are cogenetic and, therefore, younger than the Triassic rocks (ref. Section C2). Thus, the residual peaks seen in the Hudson Highlands and in the Manhattan Prong, along with a large number recognized in the Triassic, are interpreted as, at least in part, representing the expressions of a fault system which is Triassic or younger in age.

North-northwest to west-northwest lineaments along with nearly east-trending lineaments have also been identified in the Triassic Basin. Normal faults in the Triassic of Rockland County strike N44°-81°W (ref. Table C6-1); thus, the northwest to nearly east-trending lineaments may be megascopic expressions of these faults. No explanation can presently be offered for the north-northwest trending lineaments.

TABLE G.3-1

TABULATION OF ERTS LINEAMENTS [1]

Frames 1258-15080 Bands 4,5,6,7
1079-15124

Number	Strength	Length (mi)	Evidence[1]	Weight	Trend	Comments[2]
1	very strong	6.6 9.6	DA + TA CMF	fault	N51E N41E	Extends Peekskill Hollow Brook fault to South Canopus Valley
2	very strong	9.3 3.9 5.0	SO + TA CMF	fault	N31E N20E N34E	
3	very strong	2.5	DA + TA SO to the SW CMF	fault	N73E	Extends Peekskill fault to the west
4	strong	3.6	TA, CMF	fault	N12W	Possible right lateral movement of along 4
5	strong	6.0 3.4	TA + DA CMF	fault	N41E N47E	Appears to truncate S limb of fold
6	strong	5.6	DA, CMF	fault	N41W	Appears to terminate 1
7	strong	6.3 5.0	SA, CMF	possible fault and fault	N45E N51E	Only portion is coincident with mapped fault
8	medium	2.4 3.8	TA	possible fault	N4W N6E	Possible right lateral offset of lineament 2 by 8

1 TA - topographic alignment, DA - drainage alignment, TO - topographic offset, SO - stratigraphic offset, TN - tonal anomalies, CMF - coincident with mapped fault

2 Unless noted in comments lineaments are with Hudson Highlands

TABLE G.3-1 (Continued)

Frames 1258-15080 Bands 4,5,6,7
1079-15124

Number	Strength	Length (mi)	Evidence[1]	Weight	Trend	Comments[2]
9	strong	9.3	TA + DA CMF	fault	N31E	
10	strong	7.5 3.3	SA, CMF	possible fault and fault	N25E N13E	Only small southern portion coincident with fault
11	strong	11.4	SO, CMF	possible fault and fault	N54E	Only small southern portion coincident with fault
12	weak	2.8	TA	possible	N12E	Appears to offset 10
13	moderate	2.3	DA + TA	possible	N22E	
14	weak	4.4	TA	possible	N28W	In Manhattan Prong
15	very weak	13.1	TA + DA	possible	N59W	In Manhattan Prong Portion Might join 43 may be coincident with mapped fault
16	weak	3.8	TA	possible	N80W	Appears offset
17	moderate	5.1	TA	possible	N37E	
18	moderate	2.0	SO + TO	probable	N11E	Appears to offset 16.

TABLE G.3-1 (Continued)

Frames 1258-15080 Bands 4,5,6,7
1079-15124

Number	Strength	Length (mi)	Evidence[1]	Weight	Trend	Comments[2]
19	moderate	3.5	TA, CMF	fault	N54E	In Manhattan Prong
20	weak	5.8	DA	possible	N46W	
21	moderate	1.9	DA	possible	N34W	In Manhattan Prong
22	weak	9.6	DA + TA	possible	N22E	
23	moderate	3.6	TO + SO	fault	N73E	Trace of Peekskill fault
24	moderate	0.61 1.3	DA	possible	N10E N50E	In Manhattan Prong
25	strong	3.4 1.9	TA, CMF	fault	N53E N31E	
26	weak	8.9 2.9	TA + DA	possible	N81E N85E	
27	very strong	5.3	SO	probable	N38E	Appears to offset Schunnemunk Mt.

TABLE G.3-1 (Continued)

Frames 1258-15080 Bands 4,5,6,7
1079-15124

Number	Strength	Length (mi)	Evidence[1]	Weight	Trend	Comments[2]
28	very strong	6.4	TA, SA, CMF	fault	N31E	Off base map greater than 15 mi from site
29	moderate	7.5	SO, CMF?	probable	N73E	
30	strong	3.3	SO	probable	N40E	
31	very strong	5.2 2.3	SO, CMF	fault	N77E N85E	Extends a mapped fault
32	strong	7.9 2.6	SO, CMF	fault	N18E N42E	Trace of Ramapo
33	moderate	4.1 1.4	TA, CMF	fault	N35E N23E	
34	strong	20.9 2.9	SA, CMF	fault	N31E N37E	May join 25
35	moderate	1.8 3.8 2.5	SO + TA	possible	N84E N47E N80W	
36	strong	5.3	SA	possible	N12W N32E	Offsets 42

TABLE G.3-1 (Continued)

Frames 1258-15080 Bands 4,5,6,7
1079-15124

Number	Strength	Length (mi)	Evidence[1]	Weight	Trend	Comments[2]
37	moderate	4.0	SA	possible	N31E	
38	strong	3.4	SO + TA	probable	N39W	
39	moderate	3.0	SA	possible	N84E	
40	moderate	4.3 3.3 1.5	DA + TA OMF	possible	N31E N37E N48E	Only portion coincident with mapped fault
41	moderate to strong	1.8 4.3 3.3	SO, CMF	fault	N80E N61E N42E	
42	weak	6.6 2.3	TA	possible	N54E N83W	
43	strong	3.1	TA, CMF	fault	N55W	May join 15? Heads towards County Asphalt Quarry
44	moderate	4.5 2.9	TA + SO CMF	probable	N68W N74W	Manhattan Prong Triassic and Highlands; trends across Ramapo splays

TABLE G.3-1 (Continued)

Frames 1258-15080 Bands 4,5,6,7
1079-15124

Number	Strength	Length (mi)	Evidence[1]	Weight	Trend	Comments[2]
45	moderate	4.3 2.5	TA + DA	possible	N71E N82W	In Manhattan Prong, Highlands and Triassic; trends across Ramapo splays
46	strong	4.3 4.3	SO, DA + TA	possible	N70E N85E	
47	strong	5.1	TA + DA	possible	N31E	Off base map, greater than 14 mi from site
48	moderate	1.6 1.9	TA + DA CMF	possible	N30E N23E	
49	strong	1.6	TA	fault	N18E	Splay off Ramapo?
50	very strong	3.3 1.5 1.8	TA, CMF	fault	N32E N23E N40E	Off Ramapo?
51	strong	4.4 3.6	TA, CMF	fault	N40E N77E N84E	Extension 55, offset by 41?
52	strong	8.5	TA + DA CMF	fault	N37E	

TABLE G.3-1 (Continued)

Frames 1258-15080 Bands 4,5,6,7
1079-15124

Number	Strength	Length (mi)	Evidence[1]	Weight	Trend	Comments[2]
53	strong	2.3	TA	possible	N11E	In Manhattan Prong
54	strong	2.9	TA	possible	N50E	In Manhattan Prong
55	medium	3.8	TA	possible	N72E	Extension of Peekskill?
56	weak	1.9	TA	possible	N81W	Off base map in Triassic Basin over 10 mi from site
57	weak	4.3	TA	possible	N31W	Off base map in Triassic Basin over 10 mi from base
58	weak	1.9	TA	possible	N15E	Off base map in Triassic Basin over 10 mi from base
59	weak	3.0	TA	possible	N1W	Off base map in Triassic Basin over 10 mi from base
60	medium	2.4	TA, CMF	fault	N47E	Off base map in Triassic Basin over 10 mi from base
61	medium	4.6 3.9	TA + SA CMF	fault	N30E N39E	Off base map over 10 mi from site

TABLE G.3-1 (Continued)

Frames 1258-15080 Bands 4,5,6,7
1079-15124

Number	Strength	Length (mi)	Evidence[1]	Weight	Trend	Comments[2]
62	medium	2.6	TA + SA CMF	fault	N41E	Off base map over 12 mi from site
63	medium	5.1	TA + SA CMF	fault	N41E	Off base map over 12 mi from site
64	medium	2.3	TA CMF	fault	N36E	
65	medium	0.81	TA	possible	N22E	Appears to offset 45 and trend across a (Ramapo splay?)
66	weak	1.9	TN	slightly possible	N89E	Off base map in Triassic Basin
67	weak	3.0	TN	slightly possible	N7E	Off base map in Triassic Basin over 10 mi from site
68	medium	1.5 2.4	TA	possible	N88W N80W	
69	medium	2.6	TA, CMF	fault	N84E	Off base map in High-lands over 10 mi from site

TABLE G.3-1 (Continued)

Frames 1258-15080 Bands 4,5,6,7
1079-15124

Number	Strength	Length (mi)	Evidence[1]	Weight	Trend	Comments[2]
70	weak	1.3	TA	slightly possible	N1E	Off base map in Triassic Basin over 10 mi from site
71	weak	3.8	TA	slightly possible	N5W	

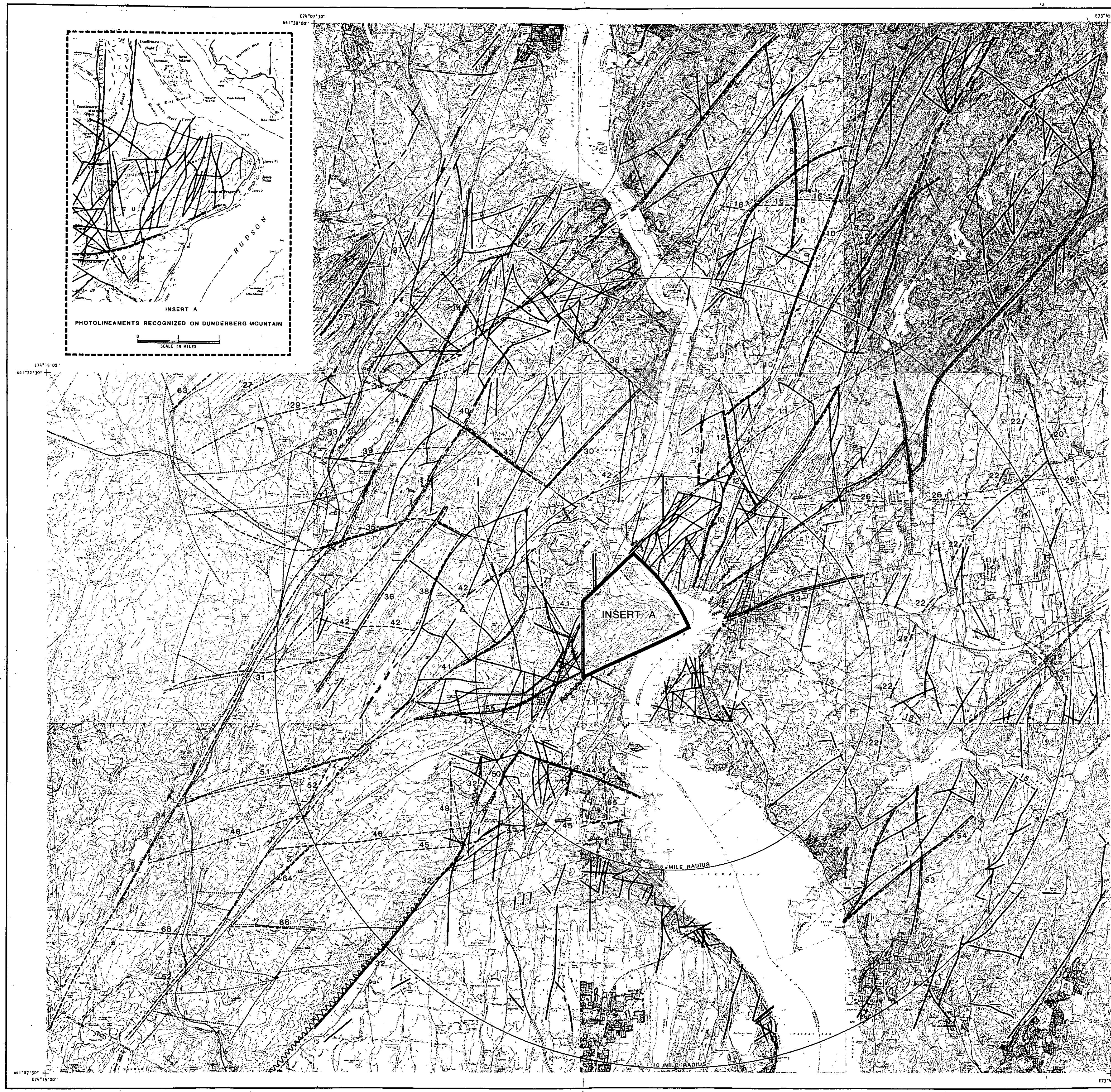

REGIONAL PHOTOLINEAMENT AND FAULT MAP

SCALE IN MILES

SCALE IN KILOMETERS

LEGEND:

- MAPPED FAULTS FROM THE LITERATURE
- FAULTS RECOGNIZED IN THE FIELD DURING THIS INVESTIGATION
- 15 ERTS LINEAMENTS
- LINEAMENTS FROM 1/60,000 AND 1/24,000 PHOTOGRAPHS

REFERENCE:

THIS BASE MAP WAS PREPARED FROM PORTIONS OF THE FOLLOWING U.S.G.S. MAPS: CORNWALL, N.Y., DATED 1957; WEST POINT, N.Y., DATED 1957; OSCAWANA, N.Y., DATED 1956; MONROE, N.Y., DATED 1957; POPOLOPEN N.Y., DATED 1957; PEEKSKILL, N.Y., DATED 1957; MOHEGAN LAKE, N.Y., DATED 1956; SLOATSBURG, N.Y.-N.J., DATED 1955; THIELLS, N.Y., DATED 1955; HAVERSTRAW, N.Y., DATED 1975, AND OSSINING, N.Y., DATED 1957.

DAMES & MOORE

PLATE G-1

TRIASSIC BASIN N=58

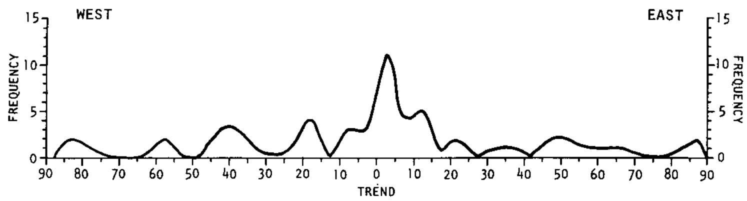

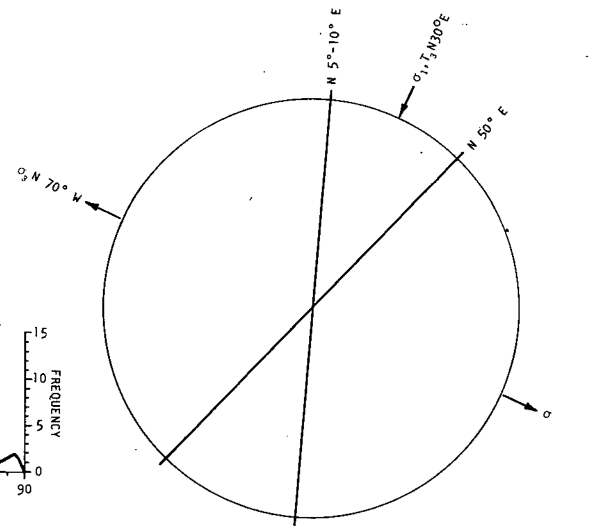

T_3 TRIASSIC (JURO-CRETACEOUS ?)

MANHATTAN PRONG N=105

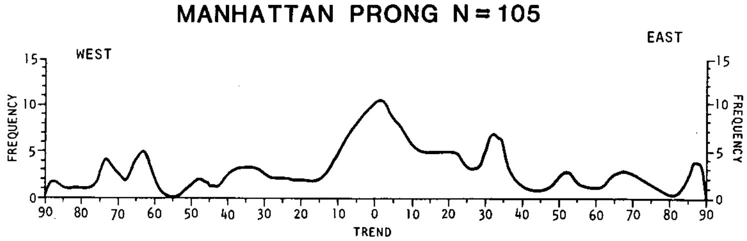

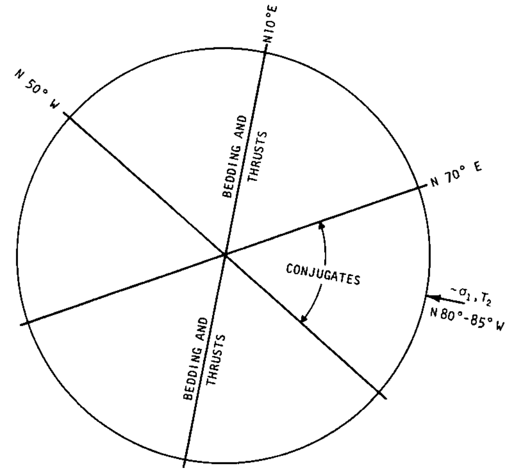

T_2 ACADIAN-APPALACHIAN

HUDSON HIGHLANDS N=317

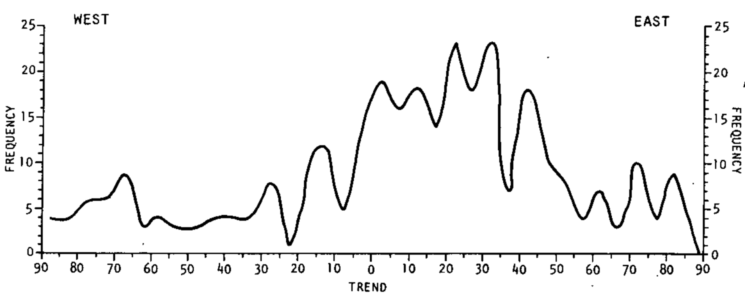

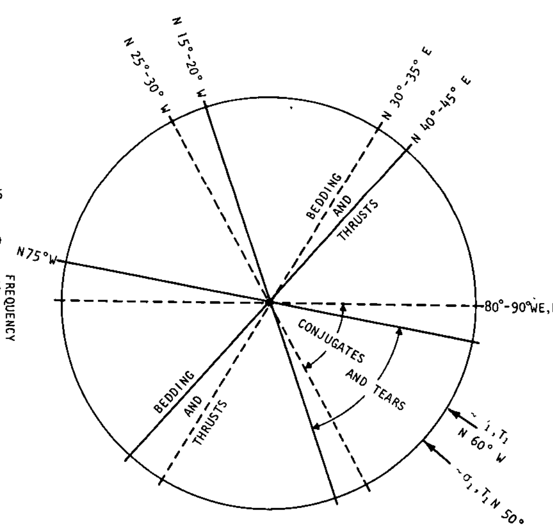

T_1 GRENVILLIAN AND TACONIC

HISTOGRAM OF TREND VS. FREQUENCY COMPILED FROM ERTS AND AERIAL PHOTOGRAPHY

DAMES & MOORE

APPENDIX H

CONSULTANTS' REPORTS

H1 Mineralogy - Andreas H. Uassilion

MINERALOGICAL REPORT for

Slavomir A. Zalewski of
Dames & Moore

Samples

Nine samples described as representing "fracture" mineralization from the general vicinity of the Cortlandt complex (New York) were submitted by Mr. Zalewski for mineral content analysis. A preliminary physical description of the samples is as follows:

SCA-2 - A massive dark gray carbonate (dolomitic) rock, somewhat friable, with irregular patches or veinlets of light-colored carbonate (calcite) and associated silica, brown mica, and sulfides. Parts of sample weathered or stained (limonite).

SCA-10 - General matrix of sample similar to SCA-2. Sliced portion of sample shows very clearly the presence of pink calcite veins or veinlets (some with very sharp vein walls) and associated sulfieds (generally disseminated small grains) and silica.

SB-3 - Generally light gray, highly friable, medium to coarse-grained rock that seems to consist mainly of carbonate material(dolomite) and associated silvery-white mica (multiple orientation of flakes) and a light-gray silicate (feldspar?)

S2 - The matrix is a fine-grained light-colored carbonate (with some small patches of silica); associated dark-colored material seems to represent fracture filling in the matrix. The vein consists mainly of a greenish prismatic to fibrous material (tremolite-actinolite?) with associated micaceous material.

SB-30 - Dense or fine-grained dolomitic rock with some shallow or film-like secondary deposition on what seems to be the wall of a joint surface. The secondary material is dark-brown and very fine-grained but crystals (dodecahedrons) are visible (under magnification) exhibiting submetallic to metallic luster.

ND-7 - Matrix: fine-grained mica schist
Vein: Zeolite crystals(white radiating, prismatic, and light gray short prismatic individuals)

SA2-6 - Matrix: Fine-grained, light gray dolomitic rock
Vein material(dark layer): calcite crystals, mica and silicates.

SA2-3 - Very light-gray dense carbonate matrix with some vein mineralization: mostly fine micaceous material and associated disseminated sulfide grains.

SA2-4 - Matrix generally similar to SA2-3 ; the fracture deposition is mainly a micaceous material with other associated silicates.

Analytical Procedure and Techniques

Weighted mineral fractions from each sample were obtained through crushing, sieving, separation into lights and heavies with bromoform, and separation on the basis of magnetic susceptibility (Frantz). Identification ofeach weighted mineral fraction was based on:

1. specific gravity
2. magnetic susceptibility
3. microscopic (optical) properties
4. x-ray diffraction (diffractometer and powder camera)

In addition, the identification of some minerals was based in part on special tests:

1. weight percent of whole rock soluble in 1:1 HCl = percent carbonate (calcite and dolomite).
2. percent orthoclase feldspar (or k-feldspar) determined on basis of sodium cobaltinitrite stain.
3. x-ray fluorescence analysis of mineral separates to determine chemical composition.

Results of Analysis (All pertinent x-ray charts enclosed)

The mineral composition of the samples was found to be as follows:

SCA-2 (bulk):

40 - 45 % carbonate (predom. dolomite with some calcite)
30 - 35 % phlogopite
10 - 12 % quartz
5 % muscovite
2 % pyrite

plus trace of limonite, magnetite, k-feldspar, and chlorite or amphibole.

Note: On the basis of ratio of soluble (HCl 1:1) to non-soluble, the carbonate content of sample was calculated as 42 percent.

SCA-10:

Generally similar in bulk composition to sample SCA-2. Veins of pink calcite were specifically x-rayed to determine the exact nature of its composition. The analysis suggests the presence of ordinary and relatively pure calcite.

SB-3 (bulk):

72 % carbonate (dolomite with minor calcite)
20 % muscovite
7 % K-feldspar (microcline structure)

plus trace of quartz and phlogopite

S2:

Matrix - 97 % dolomite
3 % quartz
Vein - 45 % pyroxene-amphibole*
38 % calcite
10 % muscovite
4 % pyrite
3 % phlogopite

plus trace of quartz

* The greenish prismatic to fibrous "pyroxene-amphibole" (in general appearance suggesting tremolite-actinolite) was found, on the basis of x-ray diffraction, to be poorly crystalline in spite of its apparent physical crystallinity. The x-ray spectra suggest that the mineral is altering to a clay-like substance; the nature of the soft alteration product is suggested to be a hydrous Mg/ Al silicate.

SB-30:

Matrix - dolomite
Secondary mineralization - pyrite crystals (with some limonite staining)

ND-7:

Secondary (vein) mineralization, all zeolites:
stilbite (fibrous, radiating; also, some limonite-stained individual prisms)
heulandite (prismatic, clear)

SA2-6:

Matrix - 85 % dolomite
15 % calcite
Vein - 35 % carbonate (dolomite and calcite , including some large pink crystals of the latter)
19 % phlogopite
9 % muscovite
36 % K-feldspar (microcline structure)

SA2-3:
Vein deposition - mostly muscovite and pyrite (trace of silica)

SA2-4:
Mainly dolomite with shallow vein deposition of muscovite, calcite, and traces of silica nad phlogopite.

Discussion

On the basis of bulk mineralogical analysis of samples submitted (especially SCA-2, SCA-10, SB-3, and S2), the rocks represent a metamorphic environment and appear to fall into the quartz - albite - epidote -- biotite subfacies of the greenschist facies (Fig. 1) or is equivalent contact metamorphic facies, the albite - epidote - hornfels facies (Fig. 2). Thus, the rocks formed within a 300 - 500° C range and a P_{H2O} range of 3000 to 8000 bars. This facies assignment to the general area of the samples agrees with that reported by Ratcliffe (1969).

The comparison of mineralogy with experimental data suggest a 450°C as the maximum temperature for such an assemblage even if the rock is hydrothermal.(Kerrick, 1970, based his experimental data on hydroghermal conditions.) This temperature has to be lowered considerably when one considers the P - T conditions of vein filling associated with the bulk samples. A close examination of the mineralogy of the associated vein material reveals the predominant presence of minerals such as carbonates, pyrite, silica (fine-grained), zeolites, fine-grained muscovite, and coarse-grained K-feldspar (microcline-adularia).

The latter assemblage (together with the presence of clay material forming as alteration product of a silicate) suggest epithermal+ conditions of deposition with temperatures between 50 - 200°C and pressure relating to a maximum burial of 3000 feet from the surface.

Most of the clay material is believed to be kaolin although a hydrous Mg silicate association is also suggested by the x-ray pattern. If this is the case, then the conditions relating to the formation of kaolin suggest epithermal temperatures, acidic interstitual water and shallow burial in a region receiving high rainfall and having good drainage.

+ The epithermal hydrothermal deposits of Lindgren:
Depth: slight (within 3000 feet of surface)
Temp.: 50-200 °C
Pres. : Moderate

In these deposits, open-space filling is predominant, and although replacement is generally recognized it is nevertheless subordinate. The characteristic mineralogy: the absence of high temp. minerals such as tourmaline, topaz, Vassilim – p. 5

 (Winkler, 1967)

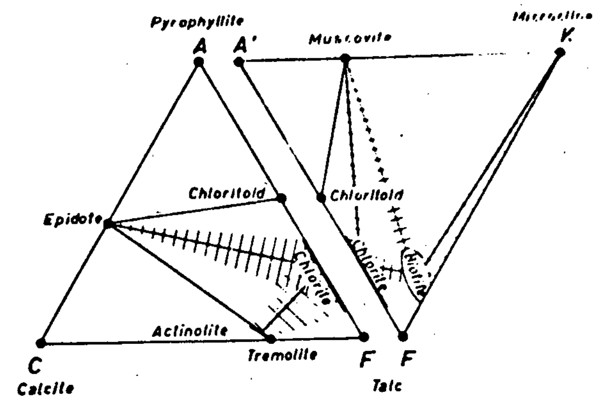

← Fig. 1

FIG. 24 (B 1.2) Quartz-albite-epidote-biotite-subfacies of the greenschist facies. Paragonite may appear as well, not, however, in conjunction with biotite and only seldom with albite (A. L. ALBEE, *et al.*, 1965). Chloritoid originates only if proper bulk chemical compositions are provided, otherwise the tie lines to chloritoid disappear from this as well as from Fig. 22. If K-feldspar, albite and/or biotite are present in a metamorphite, chloritoid cannot be generated, a fact that can be readily seen from this diagram.

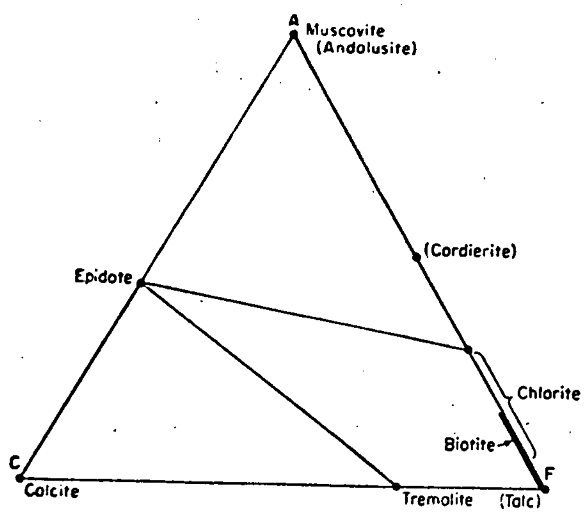

← Fig. 2

FIG. 67. Albite-epidote-hornfels facies: ACF diagram for assemblages with excess SiO_2. Quartz and albite are possible members of each assemblage. Minerals in brackets are stable only in K_2O-deficient assemblages (lacking potash feldspar).

(Turner & Verhoogen, 1960 – Igneous & Metamorphic Petrology garnet, etc.; the presence of minerals such as carbonates, zeolites, clays, chlorites, and often sericite (fine-grained muscovite) as well as alunite, adularia, silica and pyrite.

A.V.

MINERALOGICAL REPORT

A. H. Kautz – Mineralogist

TO: S. Zalewski
c/o Dames & Moore

Job # 0874-044 (Buchanan, N.Y. - Con. Ed.)

Samples

5 samples were provided (B-30; B-31; B-32; B-33; B-34) with specific test instructions as per attached copy of Dames & Moore "Sample Shipment & Test Instruction Form".

Analysis

1) Sample B-30

Test instructions: Identify all sulfides present

Procedure & Results

Areas of the rock sample displaying macroscopic and microscopic (20X) sulfide minerals were mechanically extracted. The sulfide-bearing samples were then separated by means of bromoform into two fractions. The essentially pure sulfide fraction was analyzed by x-ray diffraction.

Pyrite (FeS_2) - was identified as the only sulfide phase present. (See attached x-ray pattern - ASTM 6-070).

2) Samples B-31; B-32; B-33; B-34

Although specific test instructions are given for each of these samples (see attached form), the tests relate either directly or indirectly to whether clay minerals are present in the fractions; therefore , besides the specific tests designated, each of these samples was tested for the presence of clay minerals. The basic mineralogy of each of the samples was also determined.

Test Procedure (all above samples)

All samples were mechanically disaggregated (no grinding). Fine silt to clay size particles were suspended in water-filled 100 ml graduated cylinders where glass slides were also suspended allowing clay-size particles to be sedimented on the slides. This procedure enhances basal reflections of clays (and other phyllosilicates). Slides were air-dried and analyzed by x-ray diffraction; in same cases slides were heated or glycolated to differentiate clays.

a) Sample B-31

Test Instructions: origin of dark fines?

Results of Analysis

Basic mineral phases identified in the fine portion are:

muscovite
dolomite
quartz
feldspar (microcline)

No clay minerals were dected.

Also No pyrite or other sulfides were detected. The dark "fines" in the sample are represented by a dark colored, high-luster material that resembles chlorite/or other fine-grained phyllosilicate/or perhaps some amphibole. (No chlorite or amphibole were detected in the fine fractions). Test for coarser fractions (dark fines extracted - silt or coarser).

X-ray analysis:

Muscovite (fine-grained) paragonite-phengite

b) Sample B-32

<u>Test Instructions</u>: what caused lamination? (dark & light fine layers)

<u>Results and Analysis</u>

Basic mineral phases in <u>fine</u> fractions:

dolomite (ankerite)
muscovite
quartz
feldspar (microcline)
Paragonite - phengite
<u>No</u> clay minerals identified
<u>No</u> sulfides in fines
<u>No</u> chlorite

Dark lamination? Microscopic examination suggests dark gray (luster) chloritic material, similar to B-31 dark fines. The microscopic particles <u>(not</u> clay size) indicate the presence of gypsum (selenite) plus irridescent pyrite (insipient alteration - to limonite).

The association of gypsum (sulfate) and <u>pyrite</u> (sulfide) in the same environment suggests that the accumulation represents <u>mechanical</u> mixture (not deposited in same environment). Also the absence of clay minerals suggests absence of chemical (hydrothermal) deposition to any mentionable extent.

Cause of lamination: Mostly mechanical separation of particles on basis of orientation (pressure orients phyllosilicates with flat planes or directions at right angles ($\perp$) to pressure directions. Dark layers seem to be phyllosilicate.

c) Sample B-33

<u>Test Instructions</u>: General Mineralogy

<u>Results</u>:

Basic mineral phases (fine fraction)

Dolomite
Gypsum
Quartz
presence of minor Kaolin clay.

Microscopic: presence of dark (chlorite-like) fragments, gypsum, some calcite (?)

No sulfides

Coloration: same as that of B-31

Presence of some clay suggests some hydrothermal (low-temp) activity in this portion otherwise mostly mechanical accumulation (mylonitization).

d) Sample B-34

Test Instructions: Dark colorations (?)

Analysis: (fine-fractions)

Muscovite
gypsum
calcite-dolomite
quartz
feldspar (m)
paragonite-phengite
No clays; No sulfide

Dark coloration - similar to B-31, B-32

Albert H. Vaudi

H2 Fluid Inclusion Analyses - H. L. Barnes

Fluid Inclusion Analyses

for Dames & Moore

Job #0874-044

Submitted By:

Roger K. McLimans, Graduate Assistant
H. L. Barnes, Professor of Geochemistry

H-11

H. L. Barnes

Oct. 9, 1975

INTERPRETATION

There are several implications to these measurements (see Table 1).

1. The temperatures found for sample ND-6 are significantly higher than for all other samples which suggests that local hydrothermal activity was present.

2. Virtually all primary inclusions lie between 130°C and 260°C, regardless of orientation. Deformation may lower the apparent temperatures of homogenization of primary inclusions and also causes very irregular shapes, as shown best by sample SA-22.

3. The termperatures shown by free standing crystals and by filled veins are indistinguishable so that there is no value to separating these measurements into separate categories.

4. There is a strong possibility that all six inclusions found in sample ND-1 are secondary due to their low homogenization temperatures.

5. The broad uniformity of the primary inclusion temperatures suggests that they are the product of a regional metamorphic event (excepting ND-6). This possibility might be evaluated further by checking the areal distribution of these temperatures for evidence of any regional temperature gradients that often accompany regional metamorphism.

6. The facts that there are no temperature differences in the primary inclusions from different orientations and that deformation may have slightly lowered the temperature of some suggests that the deformation associated with the large crystals and veins with primary inclusions accompanied a regional metamorphic event.

TABLE 1

SUMMARY (RANGE (NO. SAMPLES) AVERAGE, IN °C)

Sample	Primary Inclusions	Secondary Inclusions	Veins
B-6	none visible	∿ 118 + °C (poor)	
B-35	141-195 (3) 171°	93 (1)	
ND-1	94- 95 (2) 95°	50-75 (4) 63°	
ND-2	171-226 (12) 194°	----	225-250 (5) 232°
ND-6	274-352 (3) 317°	106-209 (3) 171°	
SA-21	131-188 (8) 168°		
SA-22	92-167 (5) 139° (deformed)	50- 72 (3) 62°	
SB-31	151-169 (7) 161°	69- 98 (5) 82°	
4-B	171-187 (7) 177°		98° (secondary)
30-03	159-201 (5) 174°		

ANALYSES OF SAMPLES

GENERAL COMMENTS

With the exception of a few of the crystal samples (such as ND-2), measurements of filling temperature of the samples were complicated by the milky nature of the calcite and its common habit of containing many cavities, solid inclusions, and other imperfections. The B-6 vein sample was particularly difficult because the calcite is only translucent, not transparent, and has a mosiac-like texture not well suited to fluid inclusion study.

Normally in fluid inclusion examinations, the sample is thoroughly studied under the microscope to determine the types of inclusions present and to mark areas containing primary inclusions which are then observed in the heating stage apparatus. In the majority of the samples studied in this project, fluid inclusions of sufficient size were extremely difficult to locate and thus the analyses reported represent only those inclusions which were found in the sample sections, a barest minimum population. To determine thoroughly the variability of each population of inclusions in these samples and to obtain their filling temperatures would require several days per sample. Within the time available and reasonable cost restraints, this was not possible.

Detailed comments on each sample are included in the following text. The order is first alphabetical and then numerical:

B-6	SA-21
B-35	SA-22
ND-1	SB-31
ND-2	4-B
ND-6	30-03

All microscopic measurements were carried out by Roger K. McLimans.

B-6

1. crystals - so fine and fragile unable to make good sections that hold up. Would probably have to impregnate crystal area or make several cuts and sections.

2. vein - so milky, "dirty", and has grainy "mosiac" texture not well suited to fluid inclusion study.

   1 inclusion found but vapor bubble moves to dark side of inclusion upon heating.

   $T_{min.} \cong 118°$

B-35

6 inclusions

2 leaked at (172°)

4 inclusions

Range: 93° - 195°

Secondary inclusion - #3 (93°)

Possible primary: #1 (176°), #2 (195°), #6 (141°)

(average 171°)

FLUID INCLUSION SKETCHES

SAMPLE # B6

CHIP # 1

MINERAL: Cc

Inclus. # 1
Position:
Mag:

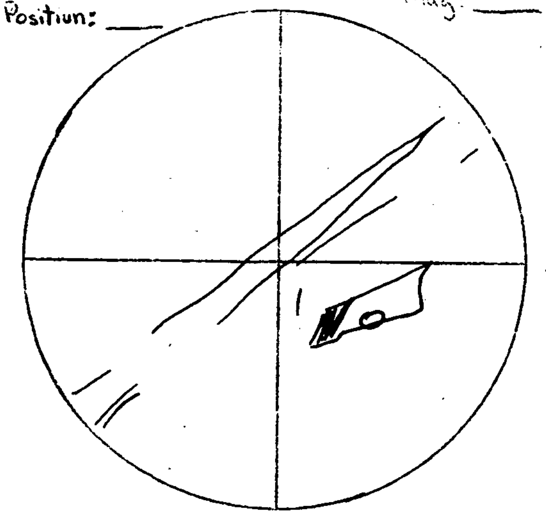

REMARKS

1mv= 475 but bubble into dark
uncertain

Inclus #
Postn.
Mag

Inclus #
Pos.
Mag

Inclus #
Pos.
Mag

Inclus. #
Pos.
Mag

Inclus #
Pos.
Mag

REMARKS

FLUID INCLUSION SKETCHES

SAMPLE # B-35

CHIP # 1

MINERAL: Calcite

Inclus. # 1-3
Position:
Mag:

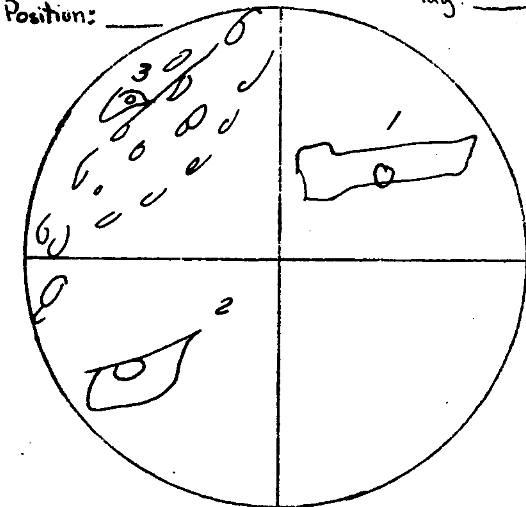

1 - 718 mv (176°)
2 - 792,790 (195°)
3 - 380 mv (93°)

Inclus # 4-5
Postn.
Mag

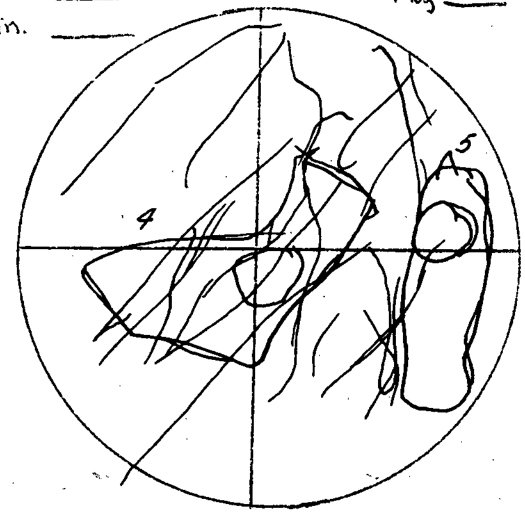

4,
5, = Both leaked at 7.00
w/o filling (172°)

Inclus # 6
Pos.
Mag

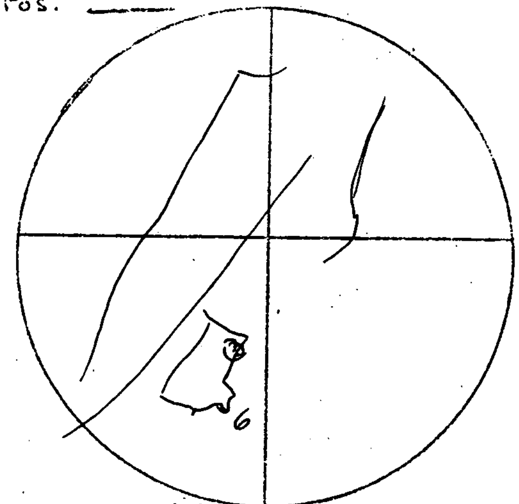

6 - 575 mv (141°)

REMARKS

H-17

Inclus #
Pos.
Mag

Inclus. #
Pos.
Mag

Inclus #
Pos.
Mag

ND-1

Few inclusions found; therefore, any interpretation must be tentative.

2 possible populations

A. Secondary (inclusions located in zone)

#1 75°

#2 58°

#3 70°

#4 50°

Range 50-75°

Average 63°

B. Primary or Pseudo-Secondary

#5 94°

#6 95°

Average: 95°

Range all data: 50-95°

FLUID INCLUSION SKETCHES

SAMPLE #: ND - 1 | CHIP #: 1 | MINERAL: Calcite

Inclus #: 1-4 | Mag: 500
Position: ___

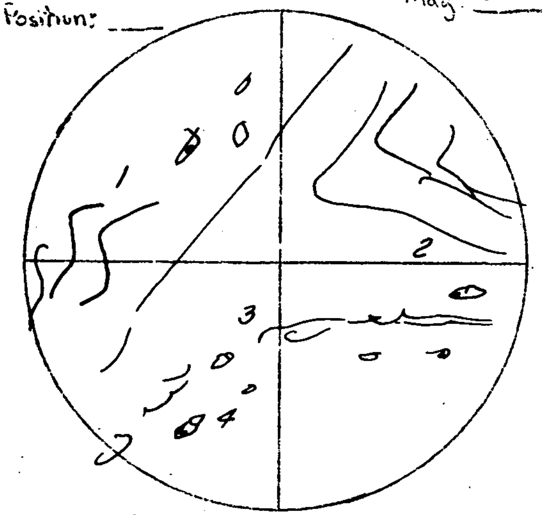

REMARKS

1 - 75°
2 - 58°
3 - 70°
4 - 50°

Inclus #: 5-6 | mag: 500
Postn.: ___

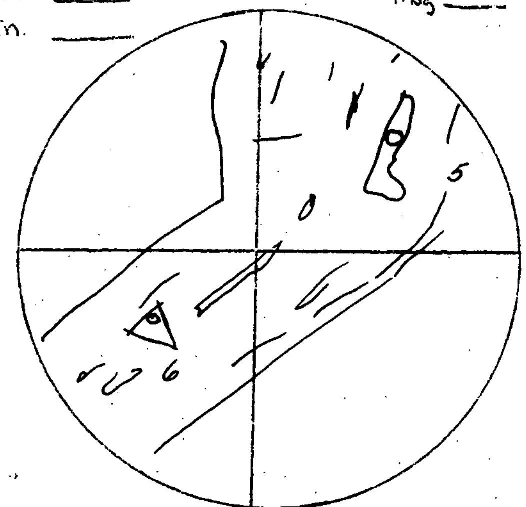

5 - 386 mv (94°)
6 - 388 mv (95°)

Inclus #: ___ | Mag: ___
Pos.: ___

Inclus #: ___ | mag: ___
Pos.: ___

Inclus. #: ___ | Mag: ___
Pos.: ___

Inclus #: ___ | Mag: ___
Pos.: ___

H-19

N-D-2 - Large Crystal

Most inclusions appear to belong to same population.

12 inclusions (See notes on inclusions #9 and #13, both are unreliable and not used)

Range: 171° - 226°

Average: 194°

95% I: 177° - 224°

ND2 - Vein

All inclusions are apparently from the same population.

5 inclusions

Range: 225 - 250°

Average: 232°

FLUID INCLUSION SKETCHES

SAMPLE # ND -2 Large   CHIP # 1   MINERAL: Calcite

Inclus. #1-2   Mag: 500
Position: ____

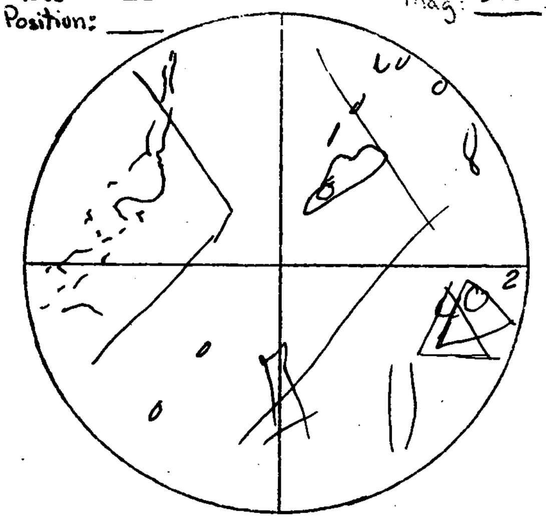

1 mv - 738, 739 (181°)
2 mv - 700, 690 (171°)

Inclus # 3-5   Mag 500
Postn. ____

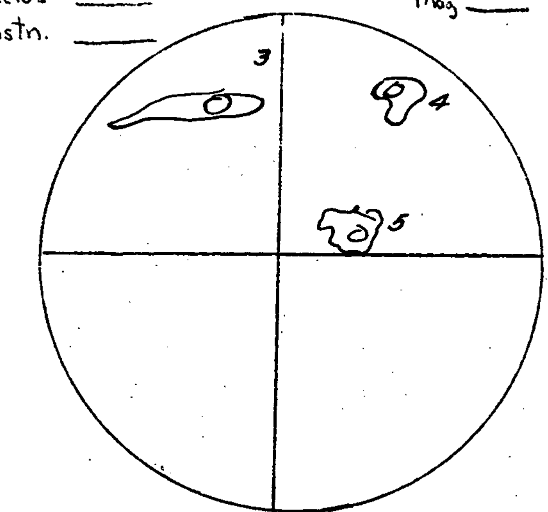

3 mv - 776 (191°)
4 mv - 807 (198°)
5 mv - 809 (199°)

Inclus # 6   Mag 500
Pos. ____

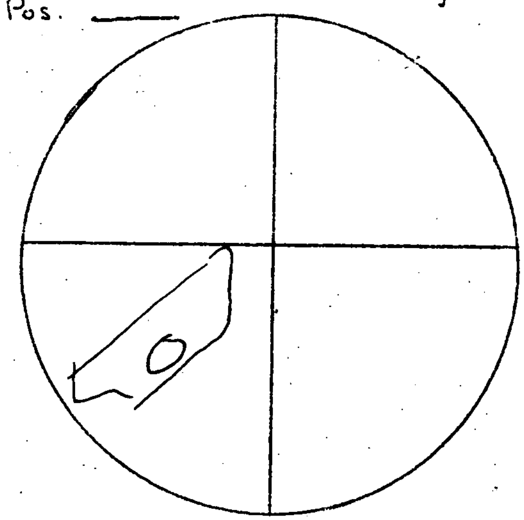

6 mv - 910 (224°)

REMARKS

Inclus # 7,8   Mag ____
Pos. ____

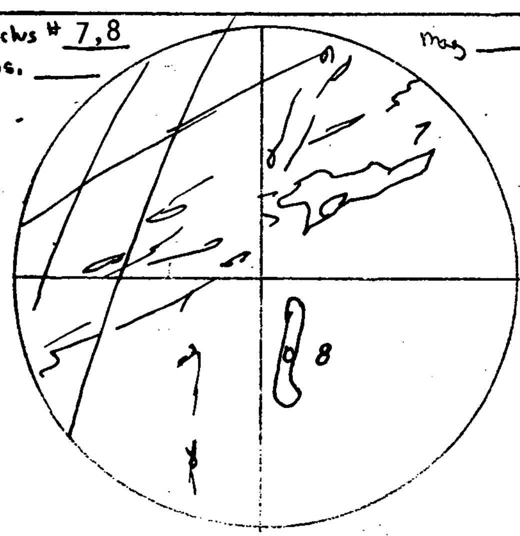

7 mv - 730 (179°)
8 mv - 778 (191°)

Inclus. # 9-13   Mag ____
Pos. ____

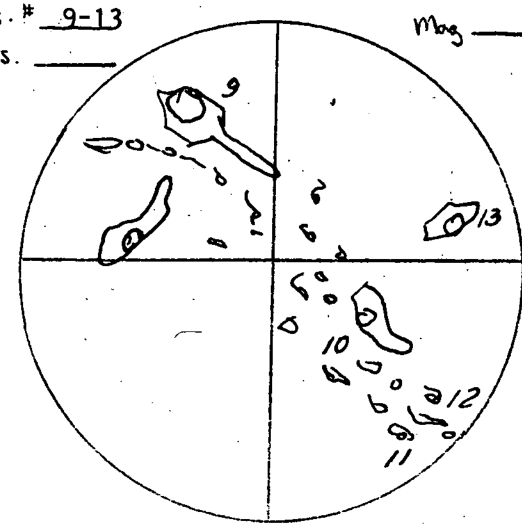

9 necked   11 - 758 (186°)
10 mv 812 (200°)   12 - 720 (177°)
13 heated to 300°, sample begin to decrep. inclusion not filled yet.

Inclus # 14   Mag 500
Pos. ____

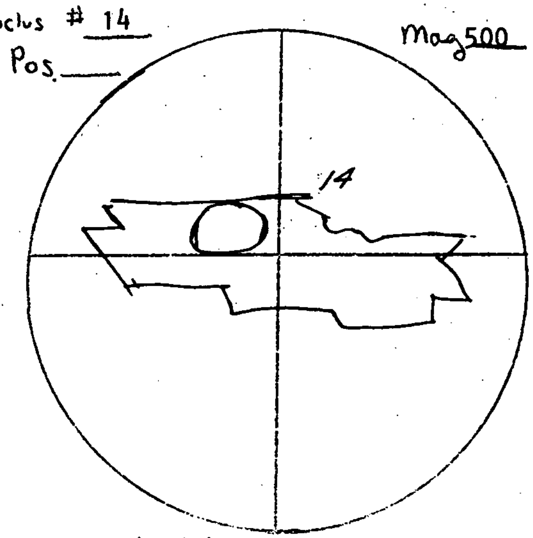

14 - 919 (226°)

Fluid Inclusion Sketches

Sample # ND2 - vein | Chip # 2 | Mineral: Calcite

Inclus. # 1
Position:
Mag: 500

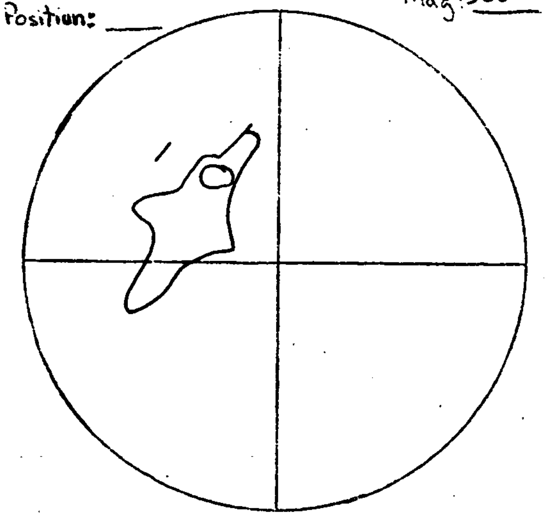

Inclus # 2-3
Postn.
Mag 500

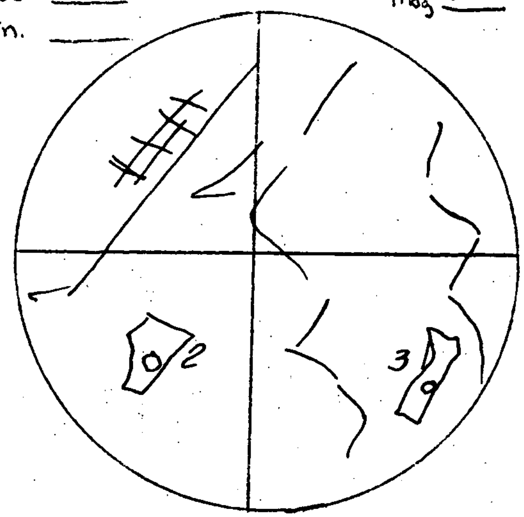

Inclus # 4-5
Pos.
Mag

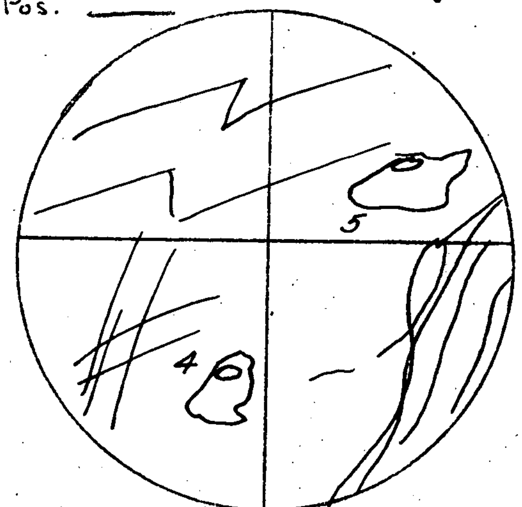

REMARKS

1 mv - 1018, 1010 (250°)

2 mv - 912 (225°)
3 mv - 920 (226°)

4 mv - 922 (227°)
5 mv - 942 (232°)

Inclus #
Pos.
Mag

Inclus. #
Pos.
Mag

Inclus #
Pos.
Mag

REMARKS

N-D-6 - Crystals

8 inclusions

Range: 106° - 354°

Average: NA

95% I: NA

Probable secondary inclusions: #4, #7, #8.

Range: 106 - 209°C

Probable primary omitting odd shaped #6, #2 although #2, #6 are probably o.k.

3 inclusions

Range: 274° - 352°

Average: 317°

N-D-6 - Vein

Summary:

9 inclusions

Range: 159° - 232°

Average: 195°

95% I: 171° - 222°

Most inclusions were not part of a zone of inclusions and are considered primary for this reason.

FLUID INCLUSION SKETCHES

SAMPLE # ND6 - Crystal

CHIP # 1

MINERAL: Calcite

Inclus # ____ Position: ____ Mag: ____

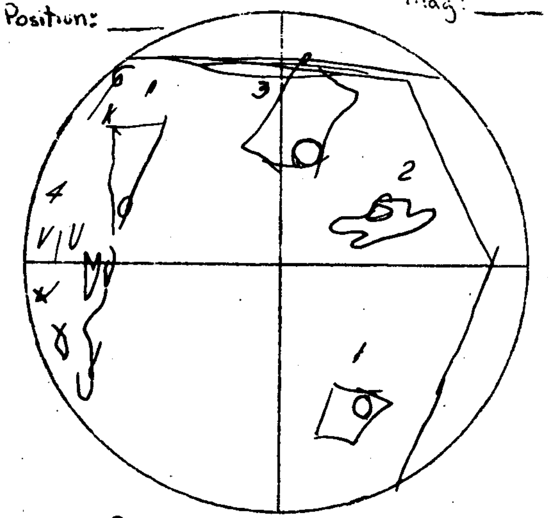

REMARKS

1 - 352°C
2 - 343°C
3 - 274°C
4 - 197°C

Inclus # ____ Postn. ____ Mag ____

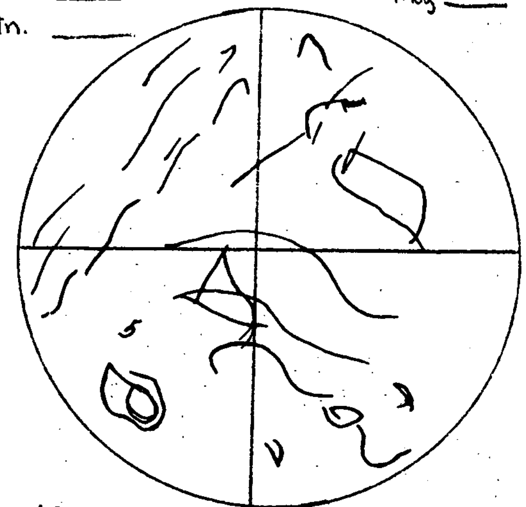

5 - 324° C

Inclus # ____ Pos. ____ Mag ____

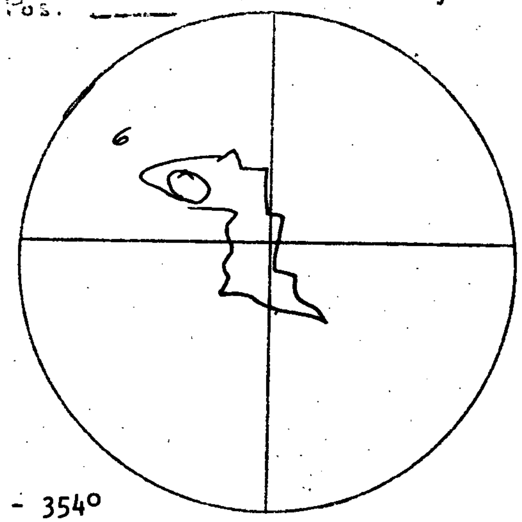

6 - 354°
Questionable, odd shape

Inclus # ____ Pos. ____ Mag ____

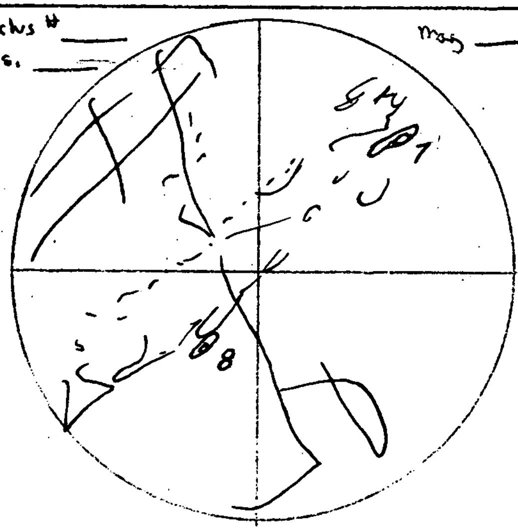

7 - 209°
8 - 106°

Inclus # ____ Pos. ____ Mag ____

Inclus # ____ Pos. ____ Mag ____

H-24

Fluid Inclusion Sketches

Sample # ND6 - vein | Chip # 1 | Mineral: Calcite

Inclus. # ____ Position: ____ Mag: ____

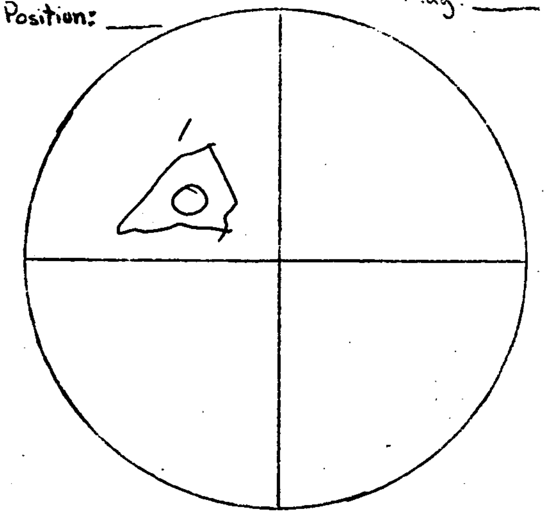

1 - 892 mv - (220°)

Inclus # ____ Postn. ____ Mag ____

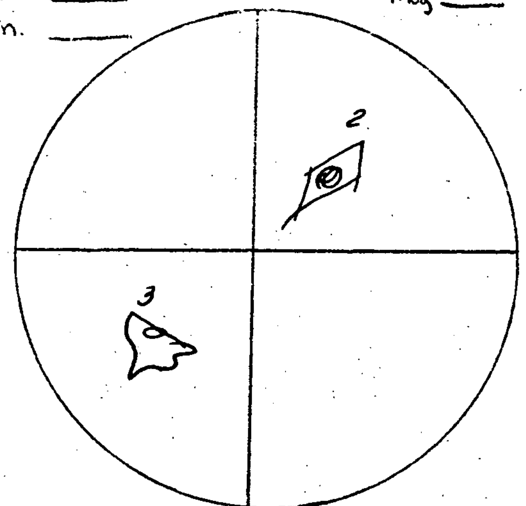

2 - 176°
3 - 200°

Inclus # ____ Pos. ____ Mag ____

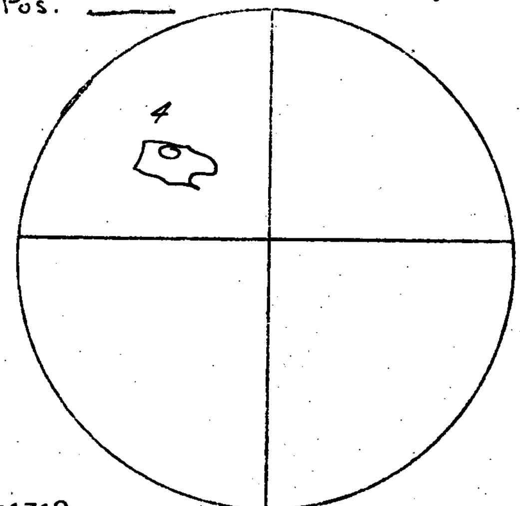

4-171°

REMARKS

H-25

Inclus # ____ Pos. ____ Mag ____

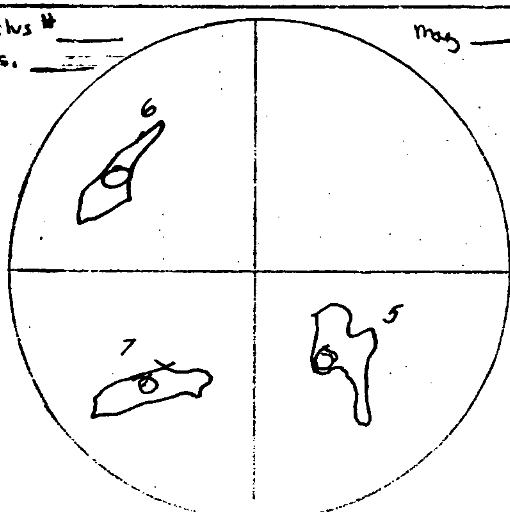

5 - 232° C
6 - 200° C
7 - 222° C

Inclus. # ____ Pos. ____ Mag ____

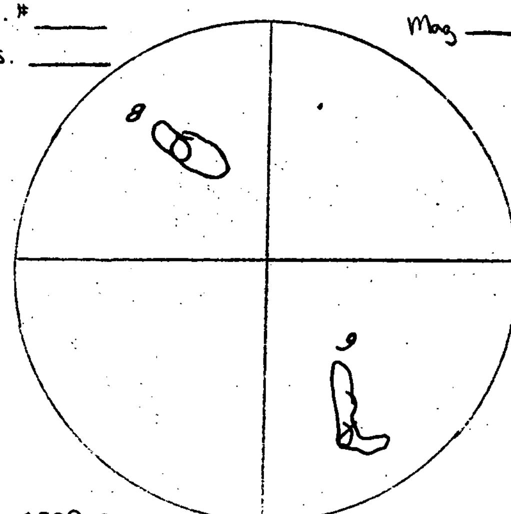

9 - 159° C
8 - 171° C

Inclus # ____ Pos. ____ Mag ____

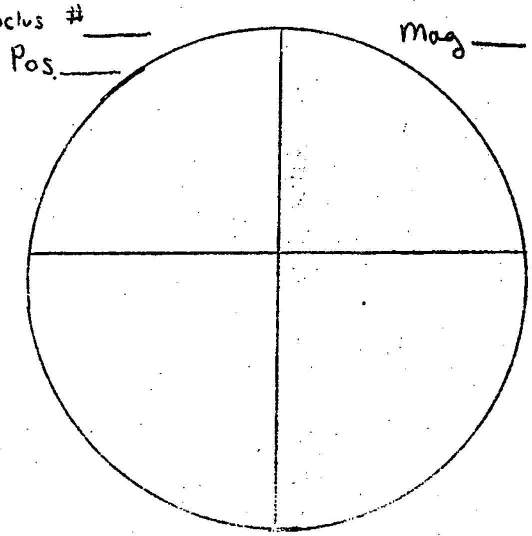

REMARKS

SA-21

8 inclusions

Range: 131° - 188°

95% I: 148° - 184°

Average: 168°

SA-22

8 inclusions

2 possible populations

A. Secondary #1 - 50°

#2 - 65°

#3 - 72°

R = 50 - 72°

A = 62°

B. Primary? (But deformed see sketches)

#4 - #8

R = 92° - 167°

A = 139°

Fluid Inclusion Sketches

Sample # SA2-1 | Chip # 1 | Mineral: ______

Inclus. # 1 | Position: ______ | Mag: 500

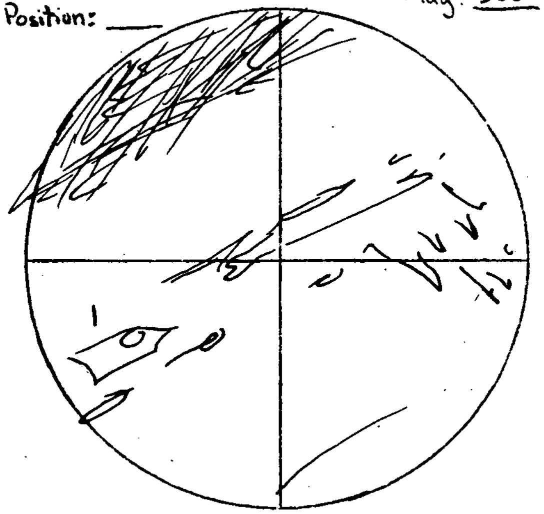

1 mv - 434 (131°)

Inclus # 2-5 | Postn. ______ | Mag 500

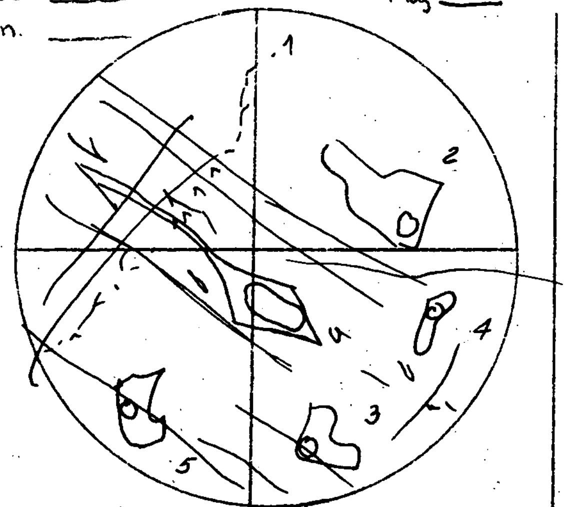

2 mv - 653, 669 (162°)
3 mv - 748 (184°)
4 mv - 725 (178°)
5 mv - 717 (176°)

Inclus # 6-8 | Pos. ______ | Mag 500

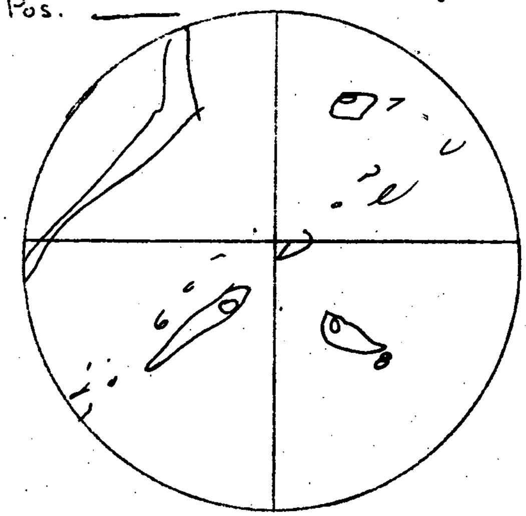

6 mv - 719 (176°)
7 mv - 766 (188°)
8 mv - 603 (148°)

REMARKS

Inclus # ______ Pos. ______ Mag ______

Inclus. # ______ Pos. ______ Mag ______

Inclus # ______ Pos. ______ Mag ______

H-27

FLUID INCLUSION SKETCHES

SAMPLE #: SA-22   CHIP #: 1   MINERAL: Calcite

Inclus. # 1-2   Position: ____   Mag: ____

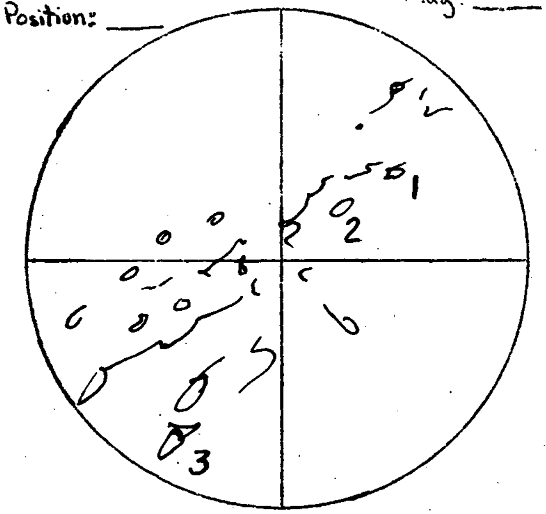

REMARKS

1 - 50^oC
2 - 65^oC = Secondary ?
3 - 72^oC

Inclus # 4-6   Postn. ____   Mag ____

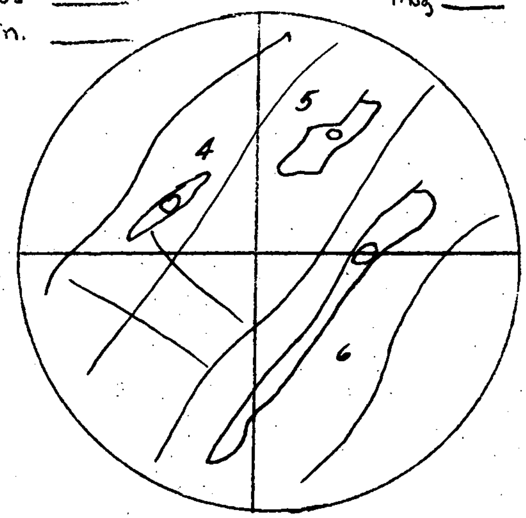

4 - 680 mv (167°)
5 - 377 mv (92°)
6 - 637 mv (156°)

Inclus # 7-8   Pos. ____   Mag ____

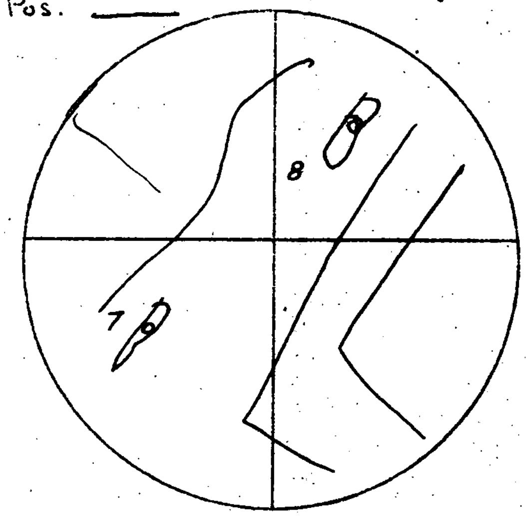

7 - 467 mv (114°)
8 - 680 mv (167°)

Inclus # ____   Pos. ____   Mag ____

Inclus. # ____   Pos. ____   Mag ____

Inclus # ____   Pos. ____   Mag ____

REMARKS

All from mainly zones of inclusions, secondary or pseudo- sec.
Most inclusions oval shaped as if deformed somewhat

SB-31

No really good isolated primary inclusions. All inclusions from zones of inclusions. From cut of section and small population, we cannot readily determine whether secondary or pseudo-secondary. Possibility listed below.

12 inclusions

Range: 69° - 169°

2 possible populations

A. secondary?

\# 8 - 69°

\# 9 - 74°

\#10 - 72°

\#11 - 98°

\#12 - 98°

R: 69° - 98°

Av: 82°

B. pseudo-secondary?

\#1 - 167°

\#2 - 169°

\#3 - 151°

\#4 - 157°

\#5 - 156°

\#6 - 159°

\#7 - 167°

R: 151° - 169°

Av: 161°

FLUID INCLUSION SKETCHES

Sample # SB-31 | Chip # 1,2 | Mineral: Calcite

Chip #1

Inclus # 1 Mag: 500
Position: ___

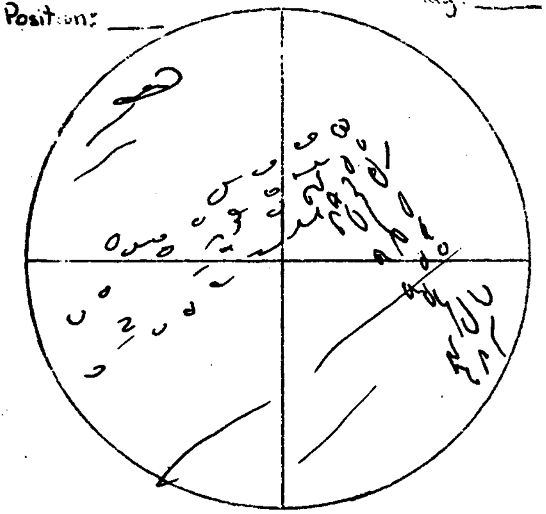

1, mv 682 (167°)

Inclus # 2-7 Mag 500
Postn. ___

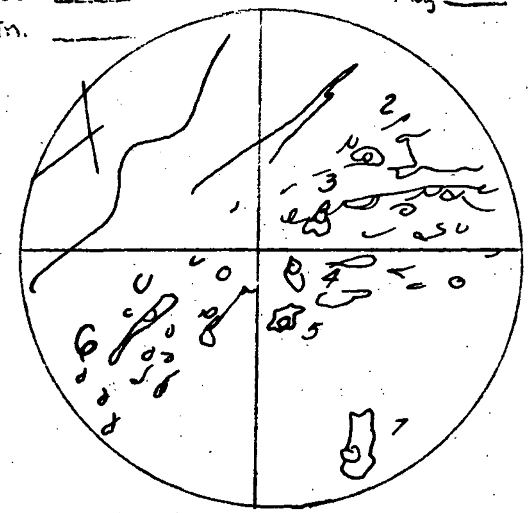

2 mv - 689 (169°)
3 mv - 618 (151°)
4 mv - 642 (157°)
5 mv - 638, 642 (156°)
6 mv - 650 (159°)
7 mv - 680 (167°)

Inclus # 8-10 Mag 500
Pos. ___

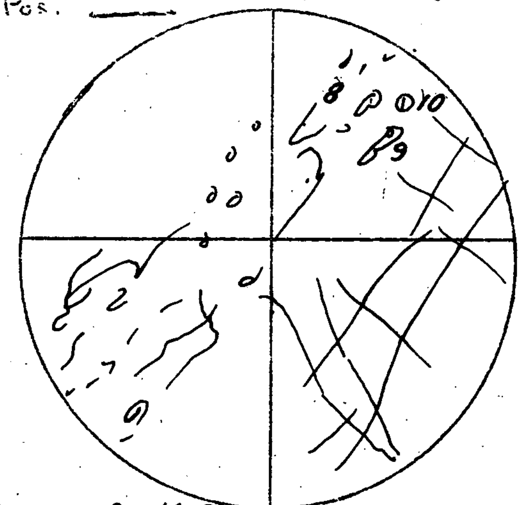

8 mv - 280 (69°)
9 mv - 302 (74°)
10 mv - 295 (72°)

REMARKS

H-30

Chip #2

Inclus # 11-12 Mag 500
Pos. ___

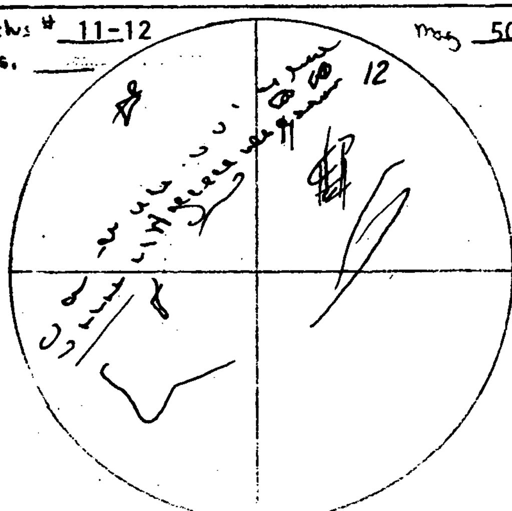

11 mv - 401 (98°)
12 mv - 403 (98°)

Decrep. noted at

13.80 mv

Inclus. # ___ Mag ___
Pos. ___

Inclus # ___ Mag ___
Pos. ___

4B

All inclusions appear to be good primaries.

7 inclusions

Range: 171° - 187°

Average: 177°

95% I: 172° - 182°

4B - Vein

Difficult to find inclusions.

One noted:

1 inclusion

Possible secondary T = 98°

Fluid Inclusion Sketches

Sample # 4B

Chip # 1,2

Mineral: Cc

Inclus. # 1-2
Position: ___
Mag: ___

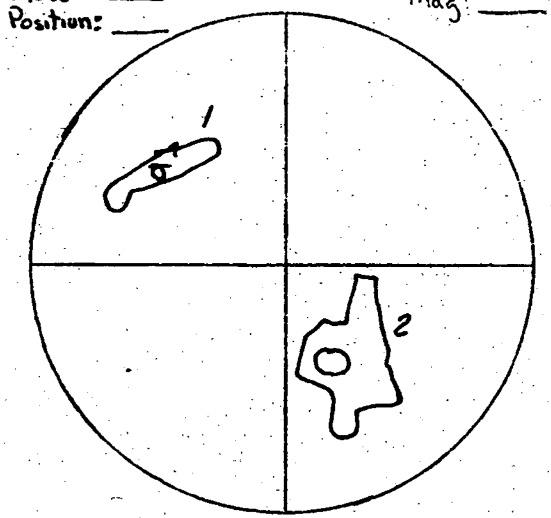

1 - 178°C
2 - 177°C

Inclus # 3-5
Postn. ___
Mag ___

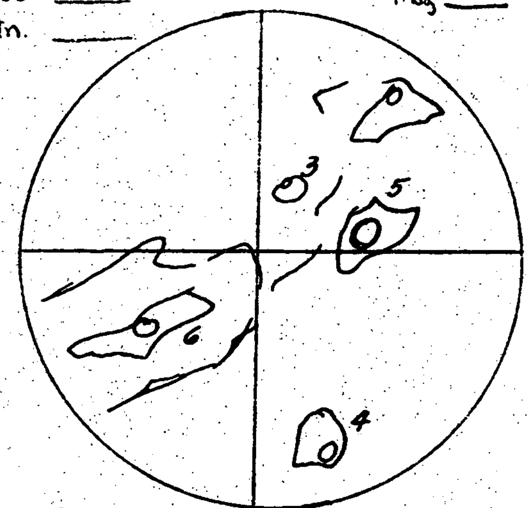

3 - 172°C
4 - 171°C
5 - 182°C
5 - 174°C

Inclus # 7
Pos. ___
Mag ___

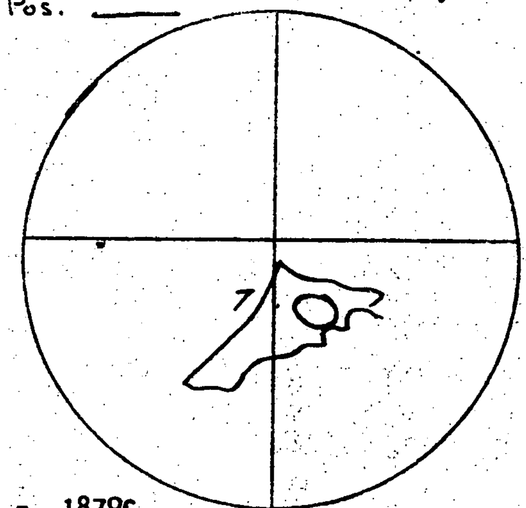

7 - 187°C

REMARKS

H-32

Inclus # ___
Pos. ___
Mag ___

Inclus. # ___
Pos. ___
Mag ___

Inclus # ___
Pos. ___
Mag ___

REMARKS

FLUID INCLUSION SKETCHES

SAMPLE # 4B vein

CHIP # 1

MINERAL: Calcite

Inclus. # 1
Position:

Mag:

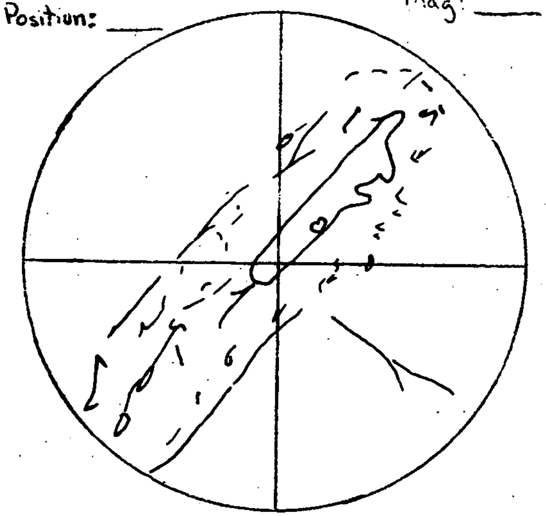

1 mv - 401 (98°)

Secondary

REMARKS

H-33

Inclus #
Postn.

mag

Inclus #
Pos.

Mag

Inclus #
Pos.

Mag

Inclus. #
Pos.

Mag

Inclus #
Pos.

Mag

REMARKS

30-03

5 inclusions

R - 159° - 201°

A = 174°

30-03 - Slickensides

One section made, but was not suitable for study. It would not polish sell and yielded few clear areas.

Fluid Inclusion Sketches

Sample # 30-03

Chip # 1 ⊥ to C Axis

Mineral: Calcite

Inclus. # 1
Position:
Mag: 500

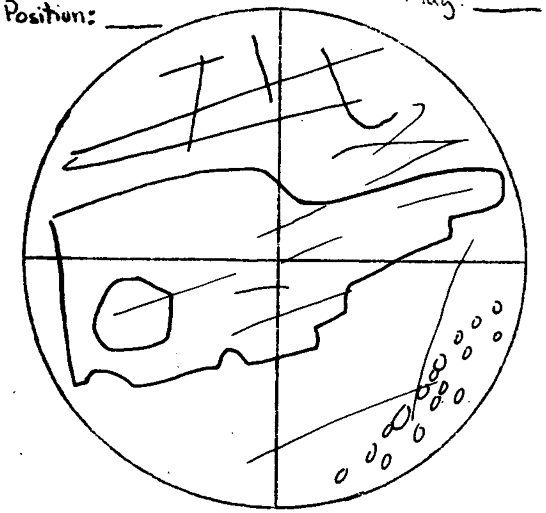

1 mv - 818 (201°C)

Inclus # 2-4
Postn.
Mag

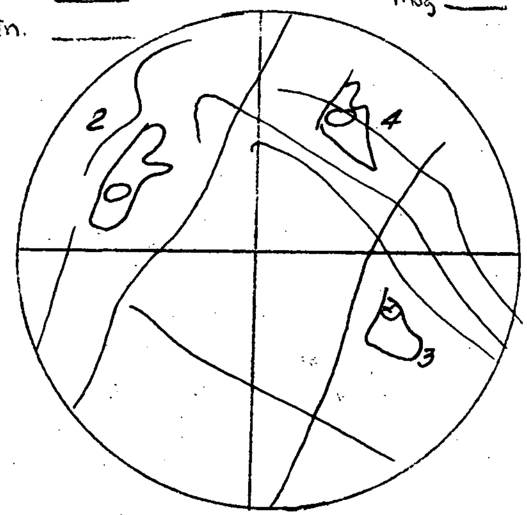

2 mv - 650 (159°)
3 mv - 680 (167°)
4 mv - 700 (172°)

Inclus # 5
Pos.
Mag

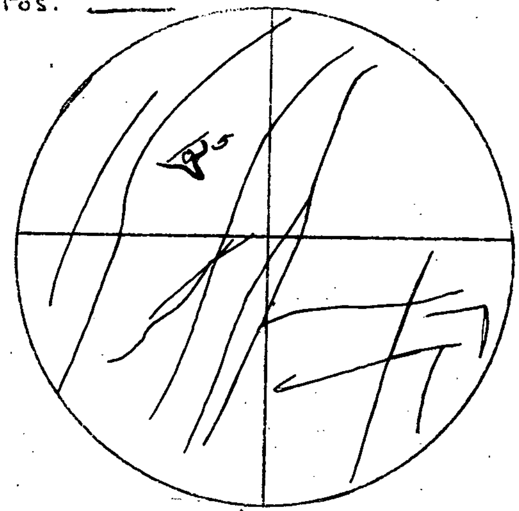

5 mv - 700 (172°)

REMARKS

H-35

Inclus #
Pos.
Mag

Inclus. #
Pos.
Mag

Inclus #
Pos.
Mag

REMARKS

FLUID INCLUSION DATA

R McLimans

SAMPLE #:	MINERAL:	ORE BODY: ?	DATES:

Sample Sketch: N.A.

Chip Sketches: N.A.

H-36

Position of Inclusion	No. of Inclus. Measured	Type of Inclus.	FILLING TEMP	No. Inclus. Measured	FREEZING TEMP	SALINITY % NaCl
Indicated by yellow marker on examined sections.					N.A.	N.A.

Remarks:

Sample Description: ?

Notes:

H3 Radiometric Dating

H3.1 Kurger Enterprises Inc.

H3.2 Edward Farrer

KRUEGER ENTERPRISES, INC.
GEOCHRON LABORATORIES DIVISION
24 BLACKSTONE STREET • CAMBRIDGE, MA. 02139 • (617)-876-3691

POTASSIUM–ARGON AGE DETERMINATION **REPORT OF ANALYTICAL WORK**

Our Sample No. B-3399 **Date Received:** 29 Sept 75

Your Reference: S-8A J.O. 0874-047 **Date Reported:** 17 October 1975

Submitted by: Thomas E. Mills
Dames & Moore
6 Commerce Drive
Cranford, NJ 07016

Sample Description & Locality: Silicate rich marble with coarse grained calcite veinlet, sample S-8A.

Material Analyzed: Phlogopite mica concentrate, -40/+200 mesh. Estimated purity is about 90%, with the impurities mainly muscovite and traces of carbonates. (Total sample recovered was only 430 milligrams.)

Ar^{40*}/K^{40} = .03457 AGE = 514 ± 18 M.Y.

Argon Analyses:

Ar^{40*}, ppm.	Ar^{40*}/ Total Ar^{40}	Ave. Ar^{40*}, ppm.
.3228	.773	.3149
.3070	.272	

Potassium Analyses:

% K	Ave. %K	K^{40}, ppm
7.487	7.466	9.108
7.445		

Constants Used:

$\lambda_\beta = 4.72 \times 10^{-10}$/ year

$\lambda_e = 0.585 \times 10^{-10}$/ year

$K^{40}/K = 1.22 \times 10^{-4}$ g./g.

$$AGE = \frac{1}{\lambda_e + \lambda_\beta} \ln \left[\frac{\lambda_\beta + \lambda_e}{\lambda_e} \times \frac{Ar^{40*}}{K^{40}} + 1 \right]$$

Note: Ar^{40*} refers to radiogenic Ar^{40}.
M.Y. refers to millions of years.

KRUEGER ENTERPRISES, INC.
GEOCHRON LABORATORIES DIVISION

24 BLACKSTONE STREET • CAMBRIDGE, MA. 02139 • (617)-876-3691

POTASSIUM-ARGON AGE DETERMINATION | **REPORT OF ANALYTICAL WORK**

Our Sample No. F-3399 | **Date Received:** 29 Sept 1975

Your Reference: S-8A J.O. 0874-047 | **Date Reported:** 17 October 1975

Submitted by: Thomas E. Mills
Dames & Moore
6 Commerce Drive
Cranford, NJ 07016

Sample Description & Locality: Silicate-rich marble with coarse-grained carbonate veinlet. Sample S-8A.

Material Analyzed: Feldspar concentrate, -80/+200 mesh. Density less than 2.70; greater than 2.60. Calcite removed by digestion in cold, very dilute acid, in an ultrasonic cleaner. Probably some quartz present.

Ar^{40*}/K^{40} = .01792

AGE CORRECTED FOR PROBABLE ARGON LOSS = 421 ± 14 M.Y.
MEASURED **AGE =** 284 ± 10 **M.Y.**

Argon Analyses:

Ar^{40*}, ppm.	Ar^{40*}/ Total Ar^{40}	Ave. Ar^{40*}, ppm.
.2688	.741	.2570
.2452	.653	

Potassium Analyses:

% K	Ave. %K	K^{40}, ppm
11.687	11.752	14.338
11.818		

Constants Used:

$\lambda_\beta = 4.72 \times 10^{-10}$/ year

$\lambda_e = 0.585 \times 10^{-10}$/ year

$K^{40}/K = 1.22 \times 10^{-4}$ g./g.

$$AGE = \frac{1}{\lambda_e + \lambda_\beta} \ln\left[\frac{\lambda_\beta + \lambda_e}{\lambda_e} \times \frac{Ar^{40*}}{K^{40}} + 1\right]$$

Note: Ar^{40*} refers to radiogenic Ar^{40}.
M.Y. refers to millions of years.

KRUEGER ENTERPRISES, INC.
GEOCHRON LABORATORIES DIVISION
24 BLACKSTONE STREET • CAMBRIDGE, MA. 02139 • (617)-876-3691

POTASSIUM-ARGON AGE DETERMINATION **REPORT OF ANALYTICAL WORK**

Our Sample No. M-3399 **Date Received:** 29 Sept 75

Your Reference: S-8A J.O. 0874-047 **Date Reported:** 17 October 1975

Submitted by: Thomas E. Mills
Dames & Moore
6 Commerce Drive
Cranford, NJ 07016

Sample Description & Locality: Silicate rich marble with coarse grained calcite veinlet, sample S-8A.

Material Analyzed: Muscovite concentrate, -40/+80 mesh. Estimated purity exceeds 95% muscovite with a few percent of calcite and other silicates.

Ar^{40*}/K^{40} = .02405 **AGE** = 372 ± 13 **M.Y.**

Argon Analyses:

Ar^{40*}, ppm.	Ar^{40*}/ Total Ar^{40}	Ave. Ar^{40*}, ppm.
.2649	.747	.2704
.2758	.775	

Potassium Analyses:

% K	Ave. %K	K^{40}, ppm
9.220	9.215	11.242
9.211		

Constants Used:

$\lambda_\beta = 4.72 \times 10^{-10}$/ year

$\lambda_e = 0.585 \times 10^{-10}$/ year

$K^{40}/K = 1.22 \times 10^{-4}$ g./g.

$$AGE = \frac{1}{\lambda_e + \lambda_\beta} \ln \left[\frac{\lambda_\beta + \lambda_e}{\lambda_e} \times \frac{Ar^{40*}}{K^{40}} + 1 \right]$$

Note: Ar^{40*} refers to radiogenic Ar^{40}.
M.Y. refers to millions of years.

KRUEGER ENTERPRISES, INC.
GEOCHRON LABORATORIES DIVISION
24 BLACKSTONE STREET • CAMBRIDGE, MA. 02139 • (617)-876-3691

POTASSIUM-ARGON AGE DETERMINATION — REPORT OF ANALYTICAL WORK

Our Sample No. R-3409 — **Date Received:** 6 October 1975

Your Reference: PK 764 A   J.O. 0874047 — **Date Reported:** 17 October 1975

Submitted by: Thomas E. Mills
Dames & Moore
6 Commerce Drive
Cranford, NJ 07016

Sample Description & Locality: Fine grained greenish-gray sericite(?) schist, sample PK 764 A. Chips taken from each of the three pieces and made into a composite for analysis.

Material Analyzed: Whole rock, -60/+200 mesh.

Ar^{40*}/K^{40} = .02456 — AGE = 379 ± 13 M.Y.

Argon Analyses:

Ar^{40*}, ppm.	Ar^{40*}/ Total Ar^{40}	Ave. Ar^{40*}, ppm.
.2618	.984	.2611
.2604	.982	

Potassium Analyses:

% K	Ave. %K	K^{40}, ppm
8.693	8.715	10.632
8.737		

Constants Used:

$\lambda_\beta = 4.72 \times 10^{-10}$/ year

$\lambda_e = 0.585 \times 10^{-10}$/ year

$K^{40}/K = 1.22 \times 10^{-4}$ g./g.

$$AGE = \frac{1}{\lambda_e + \lambda_\beta} \ln\left[\frac{\lambda_\beta + \lambda_e}{\lambda_e} \times \frac{Ar^{40*}}{K^{40}} + 1\right]$$

Note: Ar^{40*} refers to radiogenic Ar^{40}.
M.Y. refers to millions of years.

KRUEGER ENTERPRISES, INC.
GEOCHRON LABORATORIES DIVISION

24 BLACKSTONE STREET • CAMBRIDGE, MA. 02139 • (617)-876-3691

POTASSIUM–ARGON AGE DETERMINATION | **REPORT OF ANALYTICAL WORK**

Our Sample No. R-3383 | **Date Received:** 15 Sept 75

Your Reference: JW-16B Job 0874-047 | **Date Reported:** 10 October 1975

Submitted by: Thomas E. Mills
Dames & Moore
6 Commerce Drive
Cranford, NJ 07016

Sample Description & Locality: Dark gray to black mylonite(?), sample JW-16B.

Material Analyzed: Selected fresh material, homogenized at -40/+100 mesh, and analyzed as a whole rock sample.

Ar^{40*}/K^{40} = .03720 AGE = 548 ± 29 M.Y.

Argon Analyses:

Ar^{40*}, ppm.	Ar^{40*}/ Total Ar^{40}	Ave. Ar^{40*}, ppm.
.01474	.699	.01446
.01417	.725	

Potassium Analyses:

% K	Ave. %K	K^{40}, ppm
.322	.318	.388
.315		

Constants Used:

$\lambda_\beta = 4.72 \times 10^{-10}$/ year

$\lambda_e = 0.585 \times 10^{-10}$/ year

$K^{40}/K = 1.22 \times 10^{-4}$ g./g.

$$AGE = \frac{1}{\lambda_e + \lambda_\beta} \ln\left[\frac{\lambda_\beta + \lambda_e}{\lambda_e} \times \frac{Ar^{40*}}{K^{40}} + 1\right]$$

Note: Ar^{40*} refers to radiogenic Ar^{40}.
M.Y. refers to millions of years.

KRUEGER ENTERPRISES, INC.
GEOCHRON LABORATORIES DIVISION
24 BLACKSTONE STREET • CAMBRIDGE, MA. 02139 • (617)-876-3691

POTASSIUM-ARGON AGE DETERMINATION — REPORT OF ANALYTICAL WORK

Our Sample No. R-3384 **Date Received:** 15 Sept 75

Your Reference: JW-20-1 Job 0874-047 **Date Reported:** 10 October 1975

Submitted by: Thomas E. Mills
Dames & Moore
6 Commerce Drive
Cranford, NJ 07016

Sample Description & Locality: Black micaceous schist or mylonite(?), sample JW-20-1.

Material Analyzed: Whole rock, selected fresh material homogenized at -40/+100 mesh and analyzed as a whole rock sample.

Ar^{40*}/K^{40} = .04738 AGE = 674 ± 24 M.Y.

Argon Analyses:

Ar^{40*}, ppm.	Ar^{40*}/ Total Ar^{40}	Ave. Ar^{40*}, ppm.
.1861	.964	.1877
.1893	.974	

Potassium Analyses:

% K	Ave. %K	K^{40}, ppm
3.278	3.247	3.961
3.216		

Constants Used:

$\lambda_\beta = 4.72 \times 10^{-10}$/ year

$\lambda_e = 0.585 \times 10^{-10}$/ year

$K^{40}/K = 1.22 \times 10^{-4}$ g./g.

$$AGE = \frac{1}{\lambda_e + \lambda_\beta} \ln \left[\frac{\lambda_\beta + \lambda_e}{\lambda_e} \times \frac{Ar^{40*}}{K^{40}} + 1 \right]$$

Note: Ar^{40*} refers to radiogenic Ar^{40}.
M.Y. refers to millions of years.

KRUEGER ENTERPRISES, INC.
GEOCHRON LABORATORIES DIVISION
24 BLACKSTONE STREET • CAMBRIDGE, MA. 02139 • (617)-876-3691

POTASSIUM-ARGON AGE DETERMINATION **REPORT OF ANALYTICAL WORK**

Our Sample No. R-3385 **Date Received:** 15 Sept 75

Your Reference: JW-18-B Job 0874-047 **Date Reported:** 10 October 1975

Submitted by: Thomas E. Mills
Dames & Moore
6 Commerce Drive
Cranford, NJ 07016

Sample Description & Locality: Dark gray mylonite (?), sample JW-18-B.

Material Analyzed: Selected fresh material, homogenized at -40/+100 mesh and analyzed as a whole rock sample.

Ar^{40*}/K^{40} = .02278 AGE = 354 ± 13 M.Y.

Argon Analyses:

Ar^{40*}, ppm.	Ar^{40*}/ Total Ar^{40}	Ave. Ar^{40*}, ppm.
.07914	.395	.08076
.08238	.767	

Potassium Analyses:

% K	Ave. %K	K^{40}, ppm
2.946	2.906	3.545
2.866		

Constants Used:

$\lambda_\beta = 4.72 \times 10^{-10}$/ year

$\lambda_e = 0.585 \times 10^{-10}$/ year

$K^{40}/K = 1.22 \times 10^{-4}$ g./g.

$$AGE = \frac{1}{\lambda_e + \lambda_\beta} \ln\left[\frac{\lambda_\beta + \lambda_e}{\lambda_e} \times \frac{Ar^{40*}}{K^{40}} + 1\right]$$

Note: Ar^{40*} refers to radiogenic Ar^{40}.
M.Y. refers to millions of years.

KRUEGER ENTERPRISES, INC.
GEOCHRON LABORATORIES DIVISION
24 BLACKSTONE STREET • CAMBRIDGE, MA. 02139 • (617)-876-3691

POTASSIUM–ARGON AGE DETERMINATION — REPORT OF ANALYTICAL WORK

Our Sample No. R-3375 **Date Received:** 9 Sept 75

Your Reference: DR-27B Job 0874-047 **Date Reported:** 16 Sept 75

Submitted by: Thomas E. Mills
Dames & Moore
6 Commerce Drive
Cranford, NJ 07016

Sample Description & Locality: Medium-grained dark gray basalt or diorite, sample DR-27B (no locality).

Material Analyzed: Whole rock. Selected material crushed to -40/+100 mesh.

Ar^{40*}/K^{40} = .06277 AGE = 849 ± 37 M.Y.

Argon Analyses:

Ar^{40*}, ppm.	Ar^{40*}/ Total Ar^{40}	Ave. Ar^{40*}, ppm.
.04945	.883	.04890
.04834	.880	

Potassium Analyses:

% K	Ave. %K	K^{40}, ppm
.653	.638	.778
.624		

Constants Used:

$\lambda_\beta = 4.72 \times 10^{-10}$/ year

$\lambda_e = 0.585 \times 10^{-10}$/ year

$K^{40}/K = 1.22 \times 10^{-4}$ g./g.

$$AGE = \frac{1}{\lambda_e + \lambda_\beta} \ln\left[\frac{\lambda_\beta + \lambda_e}{\lambda_e} \times \frac{Ar^{40*}}{K^{40}} + 1\right]$$

Note: Ar^{40*} refers to radiogenic Ar^{40}.
M.Y. refers to millions of years.

KRUEGER ENTERPRISES, INC.
GEOCHRON LABORATORIES DIVISION

24 BLACKSTONE STREET • CAMBRIDGE, MA. 02139 • (617)-876-3691

POTASSIUM–ARGON AGE DETERMINATION **REPORT OF ANALYTICAL WORK**

Our Sample No. R-3369 **Date Received:** 29 August 1975

Your Reference: CH 7-9 Job. 0874-047 **Date Reported:** 9 Sept 75
P.O. NJ 3237

Submitted by: Thomas E. Mills
Dames & Moore
6 Commerce Drive
Cranford, NJ 07016

Sample Description & Locality: Greenish-black, fine-grained mylonite. Sample CH 7-9. From fault zone, possibly the Ramapo fault zone, near Cedar Pond Creek, W of Stony Point, NY.

Material Analyzed: Whole rock. Freshest material selected and crushed to -40/+100 mesh to insure homogeniety.

Ar^{40*}/K^{40} = .02590 **AGE =** 398 $\pm$ 15 **M.Y.**

Argon Analyses:

Ar^{40*}, ppm.	Ar^{40*}/ Total Ar^{40}	Ave. Ar^{40*}, ppm.
.08295	.913	.08517
.08738	.881	

Potassium Analyses:

% K	Ave. %K	K^{40}, ppm
2.708	2.695	3.287
2.682		

Constants Used:

$\lambda_\beta = 4.72 \times 10^{-10}$/ year

$\lambda_e = 0.585 \times 10^{-10}$/ year

$K^{40}/K = 1.22 \times 10^{-4}$ g./g.

$$AGE = \frac{1}{\lambda_e + \lambda_\beta} \ln \left[\frac{\lambda_\beta + \lambda_e}{\lambda_e} \times \frac{Ar^{40*}}{K^{40}} + 1 \right]$$

Note: Ar^{40*} refers to radiogenic Ar^{40}.
M.Y. refers to millions of years.

DEPARTMENT OF
GEOLOGICAL SCIENCES

Queen's University
Kingston, Canada
K7L 3N6

October 7, 1975

Dr. J. Wallach
1089 Field Avenue
Plainfield, N.J.
U.S.A. 07060

Dear Joe:

I have enclosed the computer printouts of the K and Ar analyses, and explanation of the ages, an invoice for Dames and Moore and an outline of my analytical procedures as required by your Quality Assurance people.

Thanks for this opportunity to do some consulting. If you ever need further geochronological assistance don't hesitate to ask.

Yours sincerely,

Edward Farrar

EF/jj

Report on the K-Ar analyses of rock samples JW 20-1 and JW 16B

JW 20-1

Examination of a thin section made from this rock revealed that there was abundant fine-grained, unaltered biotite. The rock was crushed and sieved and a -40+80 mesh fraction was obtained. The biotite was separated using a shaking table and a Frantz Isodynamic Separator. The final concentrate was better than 80% biotite, the remaining 20% being extremely fine grained quartz. Since quartz has no deleterious effect on either the K or Ar analysis, further separation was considered unnecessary.

Flame photometric analysis for potassium was done in duplicate and gave values 5.048 and 5.034% K.

Isotope dilution analysis for argon showed that the sample contained 1.596×10^{-4} cm^3 S.T.P. radiogenic Ar^{40}/gm. The atmospheric contamination was 0.5%. The model age calculated from these values is <u>661 ± 18 m.y.</u> The error represents the analytical precision at the 95% confidence level.

JW 16B

Examination of a thin section prepared from this rock showed that it was very fine grained and contained approximately 40% plagioclase, 40% pyroxene, 10% epidote, 5% amphibole + minor amounts of other minerals. Unfortunately, separation of the amphibole from the other minerals in the rock was virtually impossible and a 'whole rock' sample had to be analysed. The mesh size was -40+80.

Analysis for potassium in triplicate gave results 0.260, 0.257, 0.262% K. In view of this relatively high potassium content, the deleterious effects (initial argon) of the presence of pyroxene will be minimal.

The argon analysis showed the presence of 1.110×10^{-5} cm^3 S.T.P. radiogenic Ar^{40}/gm. The atmospheric contamination was 3.4%.

The above K and Ar values combine to give a model age of <u>847 ± 22 m.y.</u> Again the quoted error only represents the analytical precision at the 95% confidence level. A rough calculation suggests that the presence of 40% pyroxene could have led to a slight increase in the apparent age of the rock. However it is not considered likely that this increase would exceed 50 m.y.

In Summary:

Sample	K %	Ar^{40}rad cm^3STP/gm	Atmos %	Age and error m.y.
JW 20-1	5.041	1.596×10^{-4}	0.5	660 ± 18
JW 16B	0.260	1.110×10^{-5}	3.4	847 ± 22

Interpretation of the model ages of these rocks must be made in the light of the geological relationships that exist in the areas from which they were collected.

E. Farrar

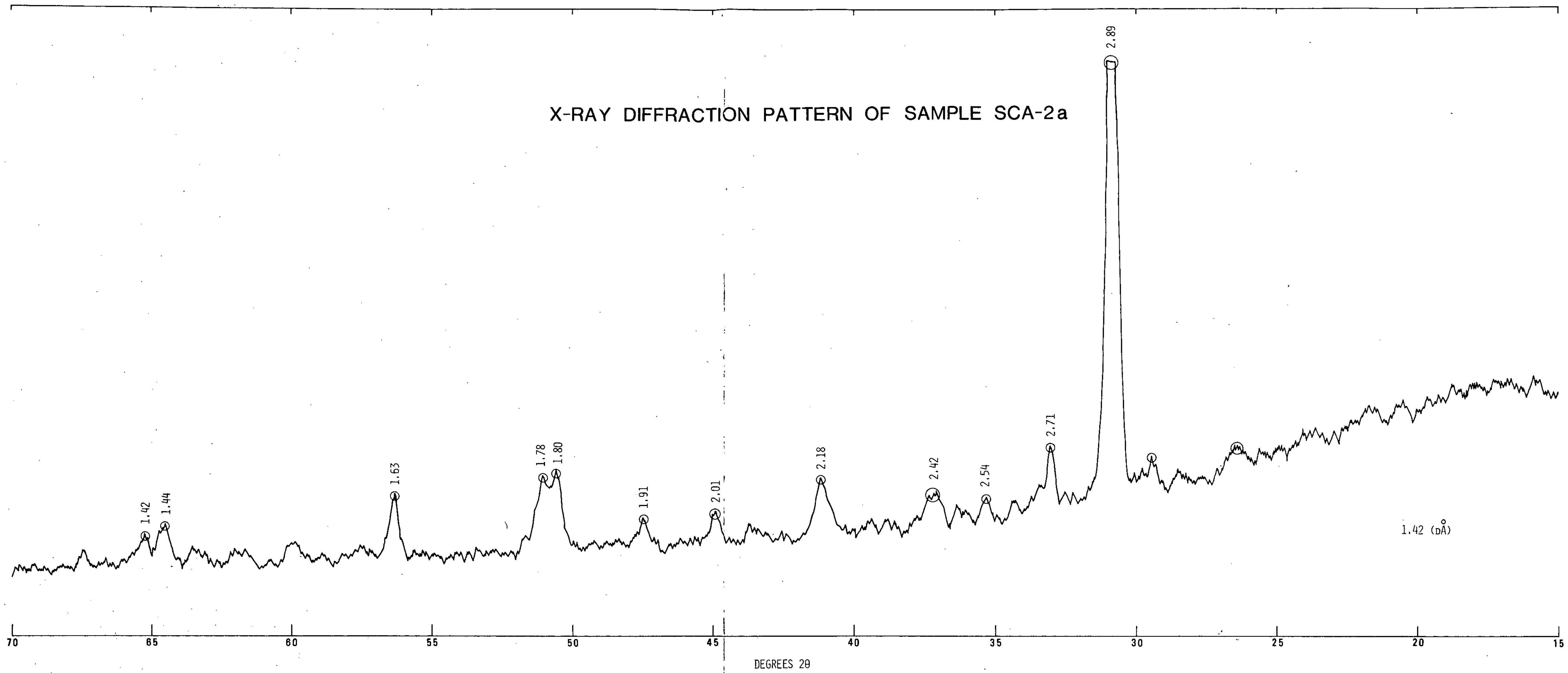
X-RAY DIFFRACTION PATTERN OF SAMPLE SCA-2a
2.89
2.71
2.54
2.42
2.18
2.01
1.91
1.80
1.78
1.63
1.44
1.42
1.42 (DÅ)
70
65
60
55
50
45
40
35
30
25
20
15
DEGREES 2θ

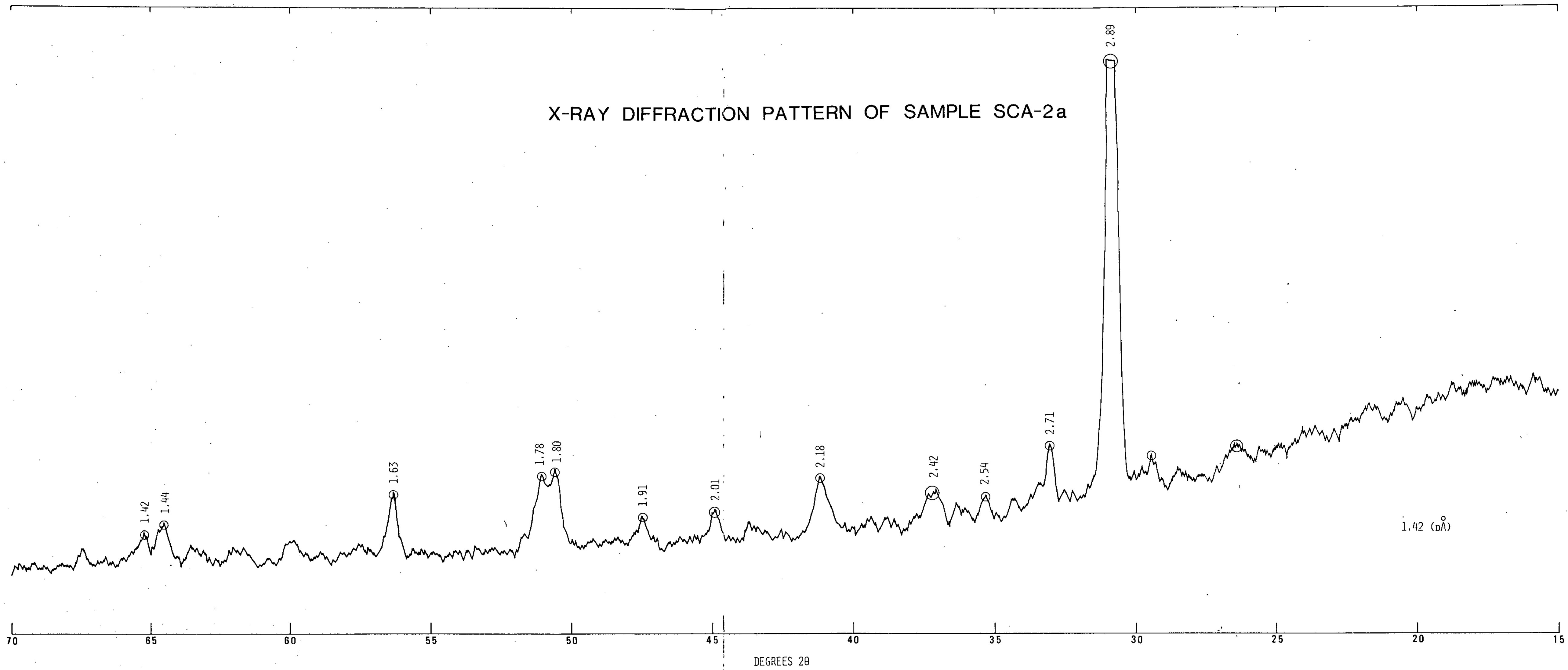

DAMES & MOORE

PLATE H1-1

X-RAY DIFFRACTION PATTERN OF SAMPLE SCA-2b

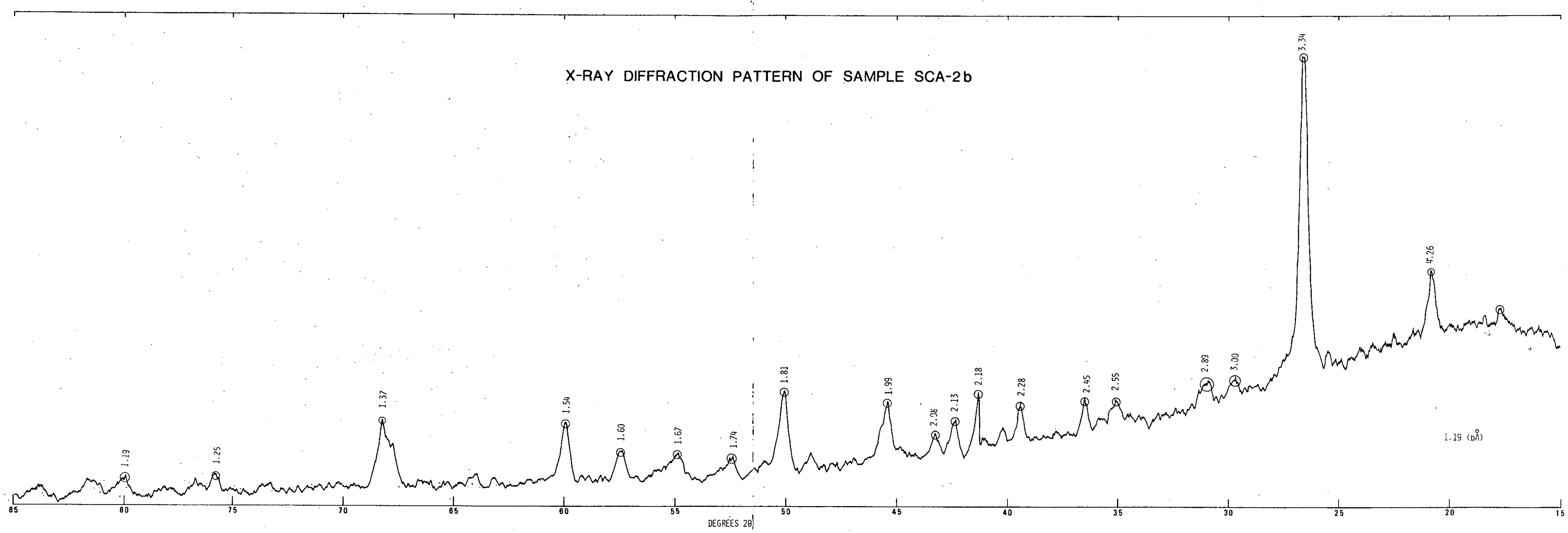

DAMES & MOORE

PLATE H1-2

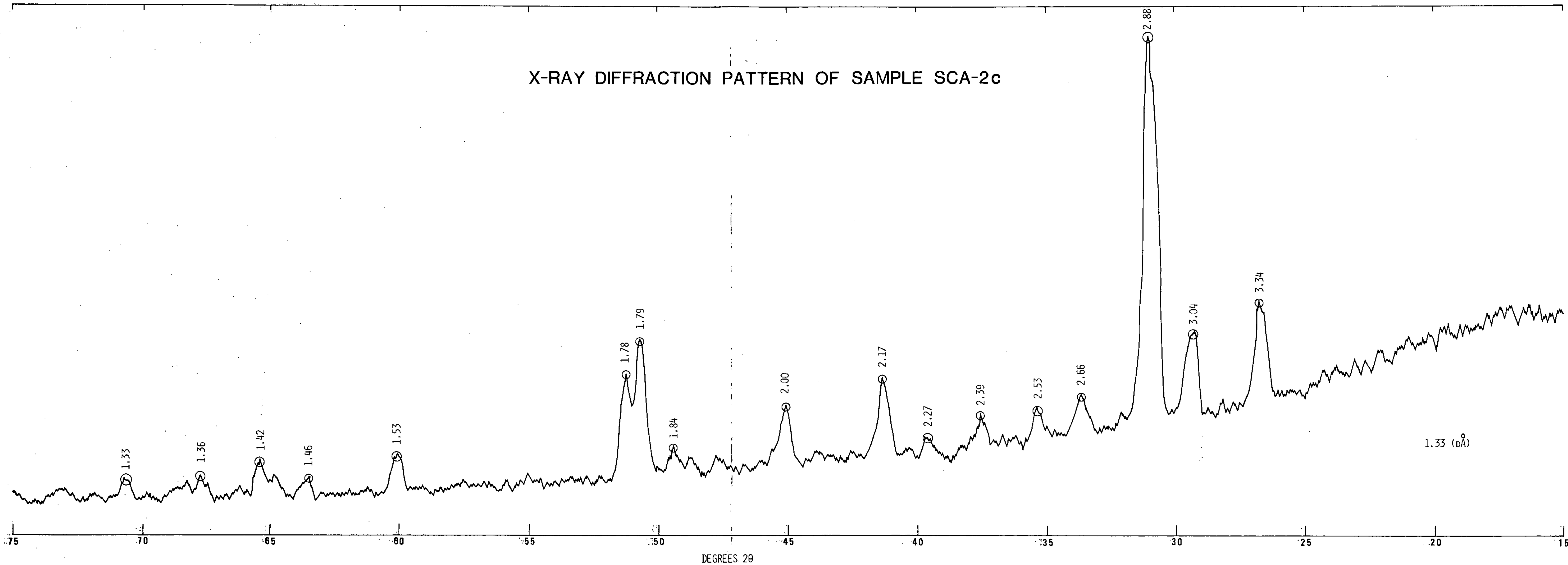
X-RAY DIFFRACTION PATTERN OF SAMPLE SCA-2c
2.88
3.34
3.04
1.79
1.78
2.17
2.00
2.66
2.53
2.39
2.27
1.84
1.53
1.42
1.36
1.46
1.33
1.33 (dÅ)
75
70
65
60
55
50
45
40
35
30
25
20
15
DEGREES 2θ

X-RAY DIFFRACTION PATTERN OF SAMPLE SCA-2d

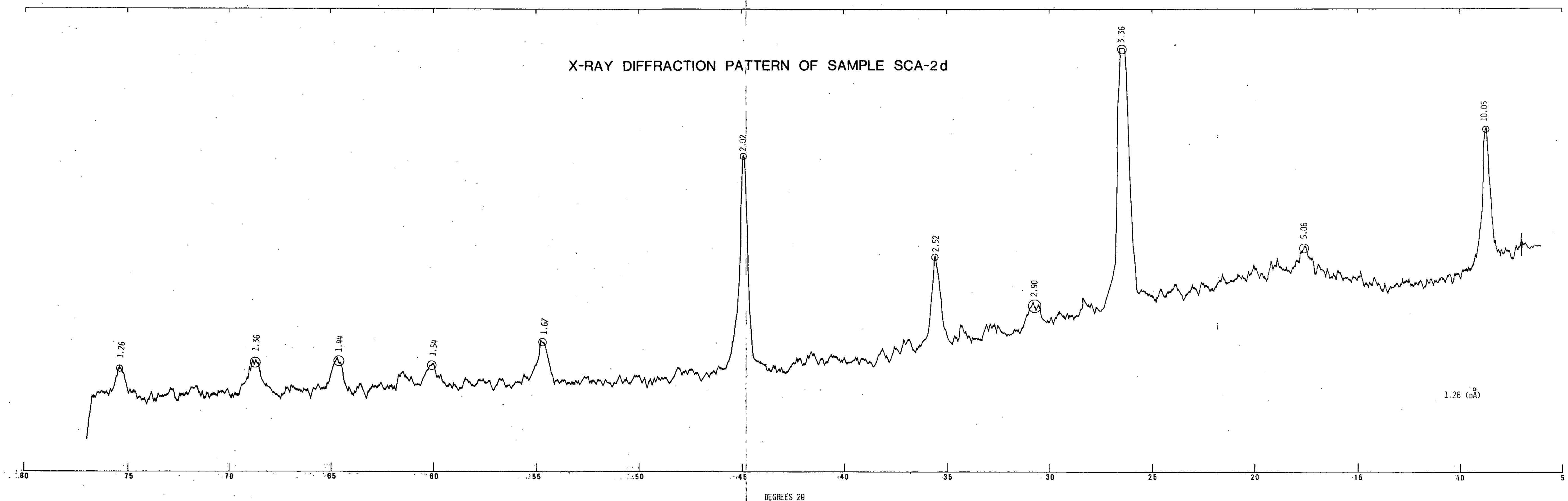

DAMES & MOORE

PLATE H1-4

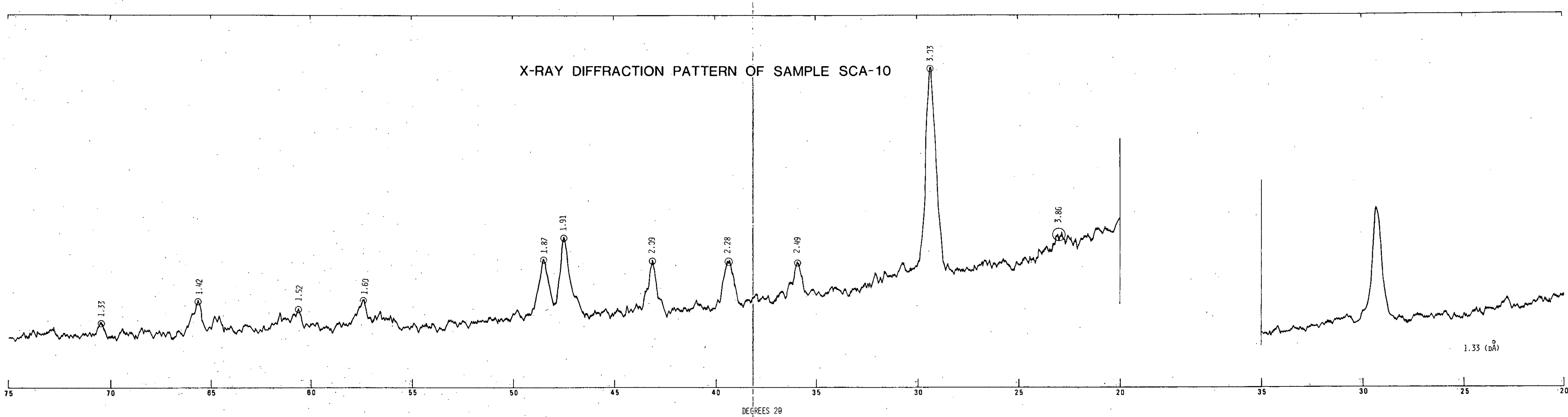

DAMES & MOORE

PLATE H1-5

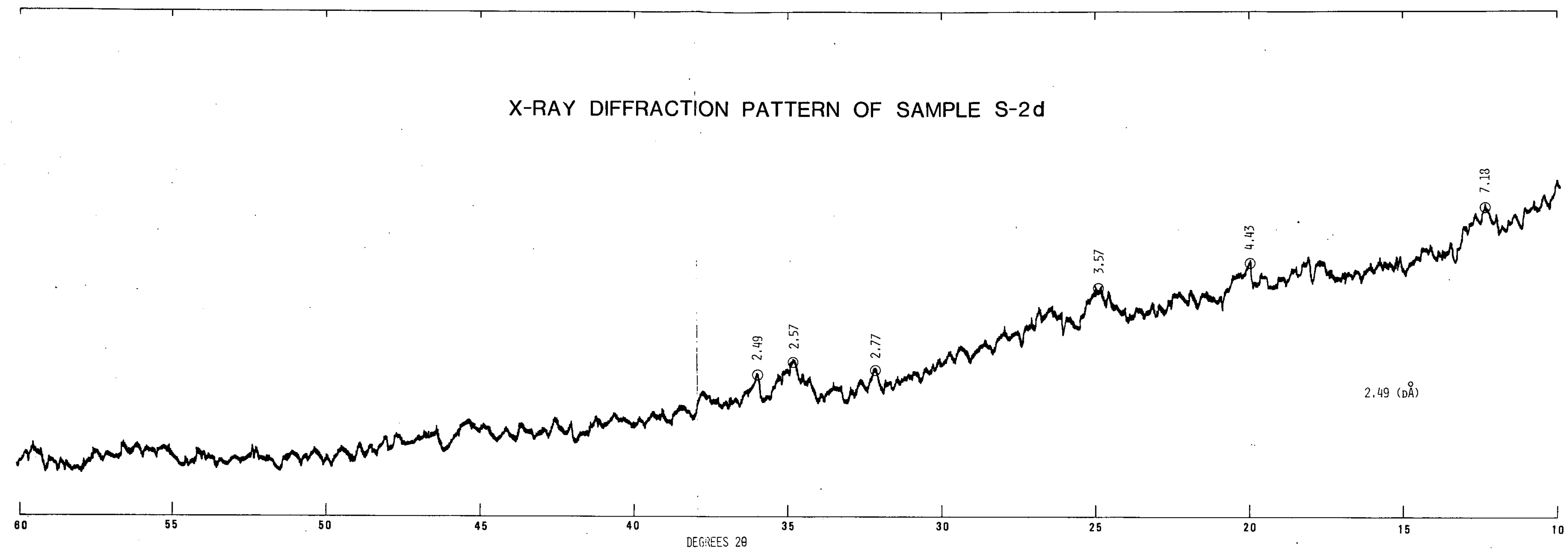
X-RAY DIFFRACTION PATTERN OF SAMPLE S-2d
7.18
4.43
3.57
2.49
2.57
2.77
2.49 (dÅ)
60
55
50
45
40
35
30
25
20
15
10
DEGREES 2θ

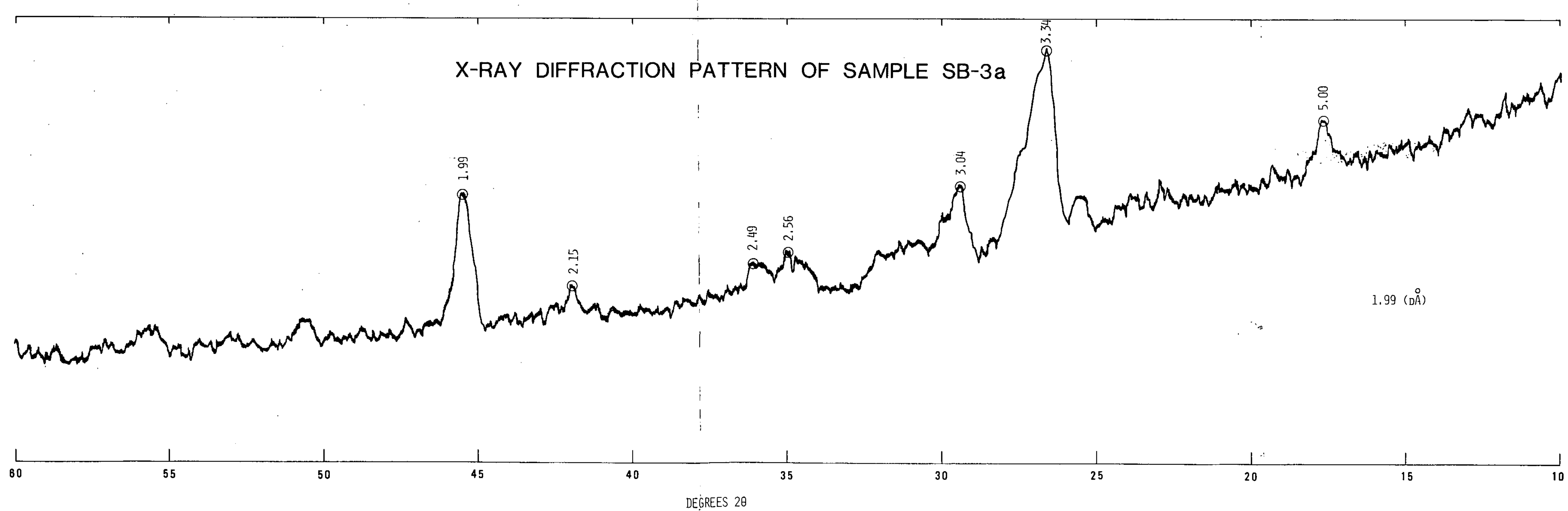
X-RAY DIFFRACTION PATTERN OF SAMPLE SB-3a
3.34
5.00
1.99
3.04
2.15
2.49
2.56
1.99 (dÅ)
60
55
50
45
40
35
30
25
20
15
10
DEGREES 2θ

DAMES & MOORE

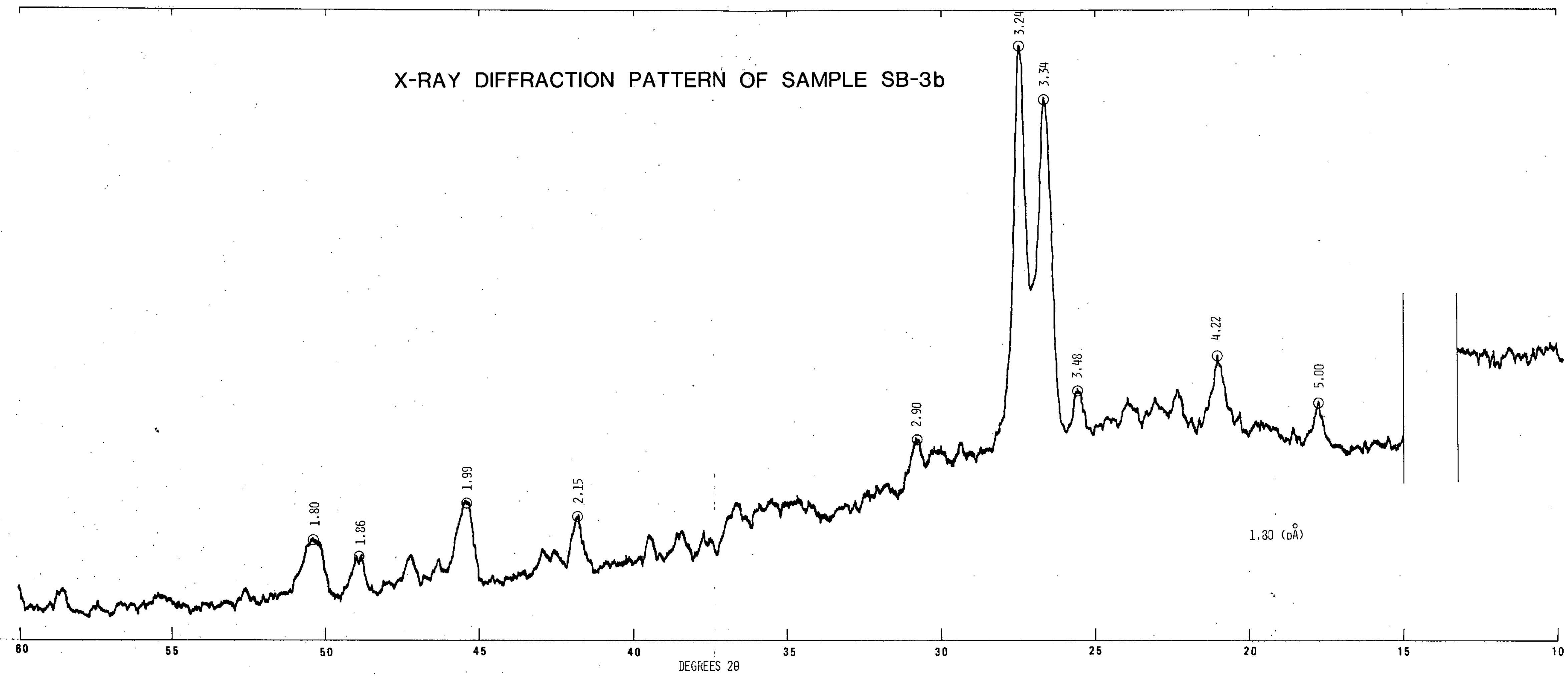
X-RAY DIFFRACTION PATTERN OF SAMPLE SB-3b
3.24
3.34
4.22
3.48
5.00
2.90
1.99
2.15
1.80
1.86
1.80 (DÅ)
60
55
50
45
40
35
30
25
20
15
10
DEGREES 2θ

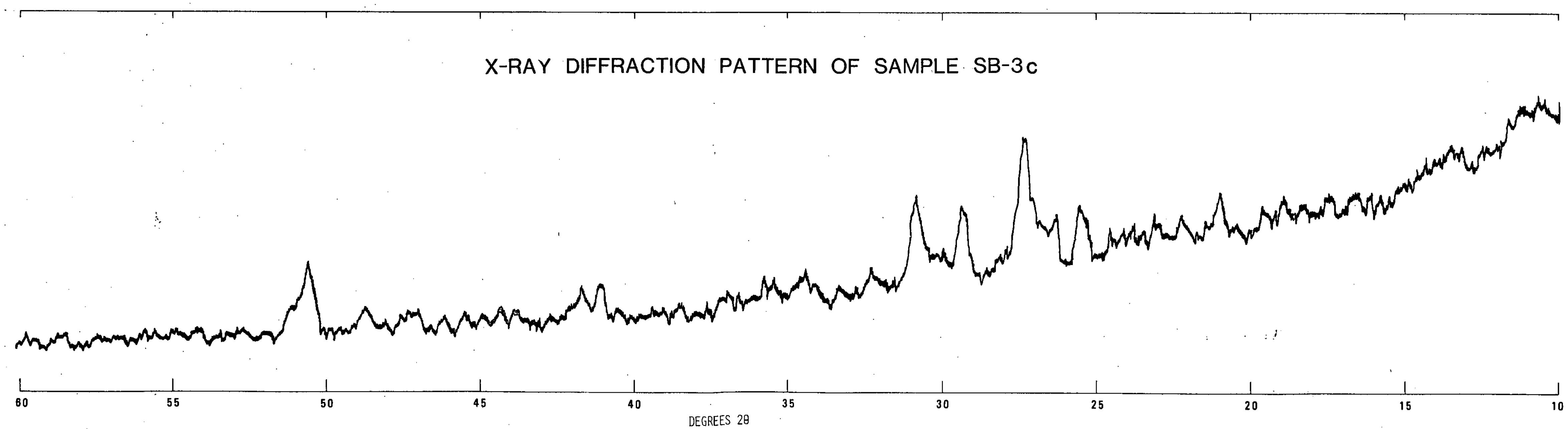
X-RAY DIFFRACTION PATTERN OF SAMPLE SB-3c
60
55
50
45
40
35
30
25
20
15
10
DEGREES 2θ

DAMES & MOORE

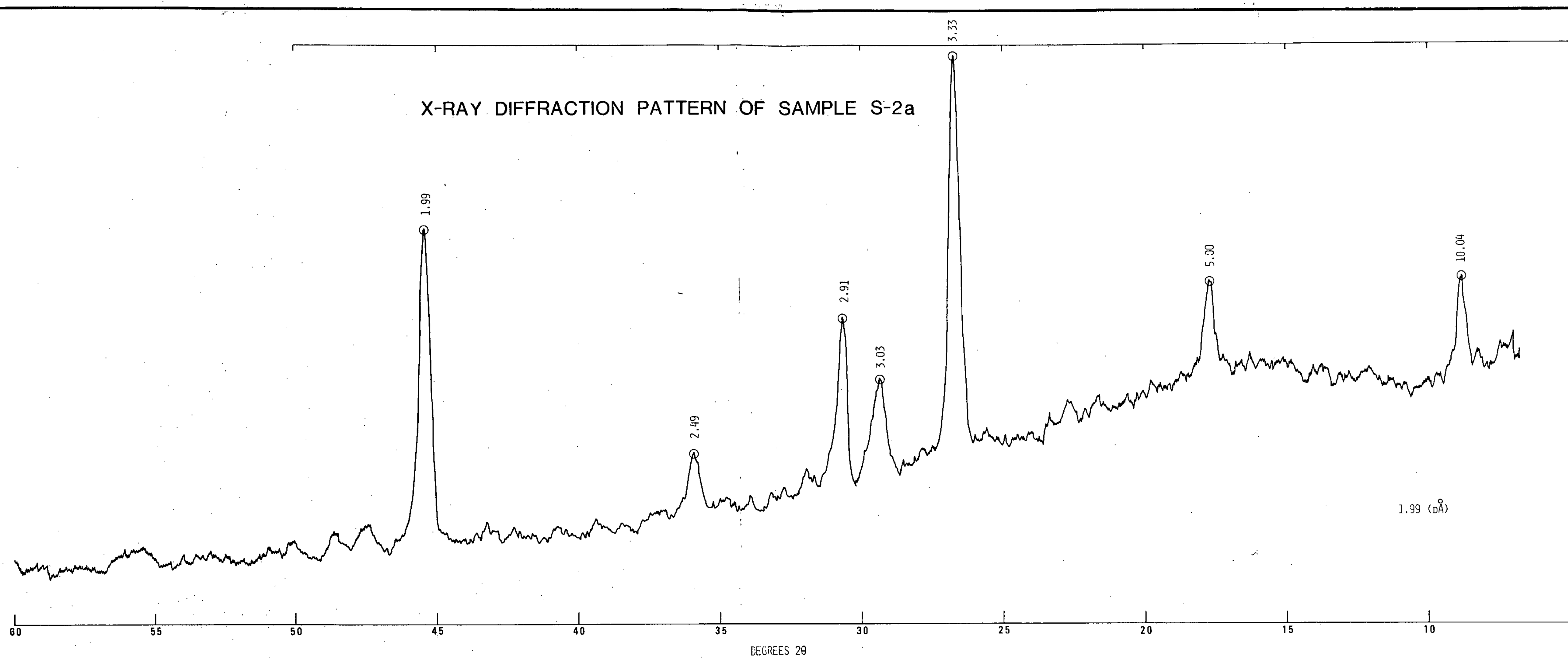
X-RAY DIFFRACTION PATTERN OF SAMPLE S-2a
3.33
1.99
10.04
5.30
2.91
3.03
2.49
1.99 (dÅ)
60
55
50
45
40
35
30
25
20
15
10
5
DEGREES 2θ

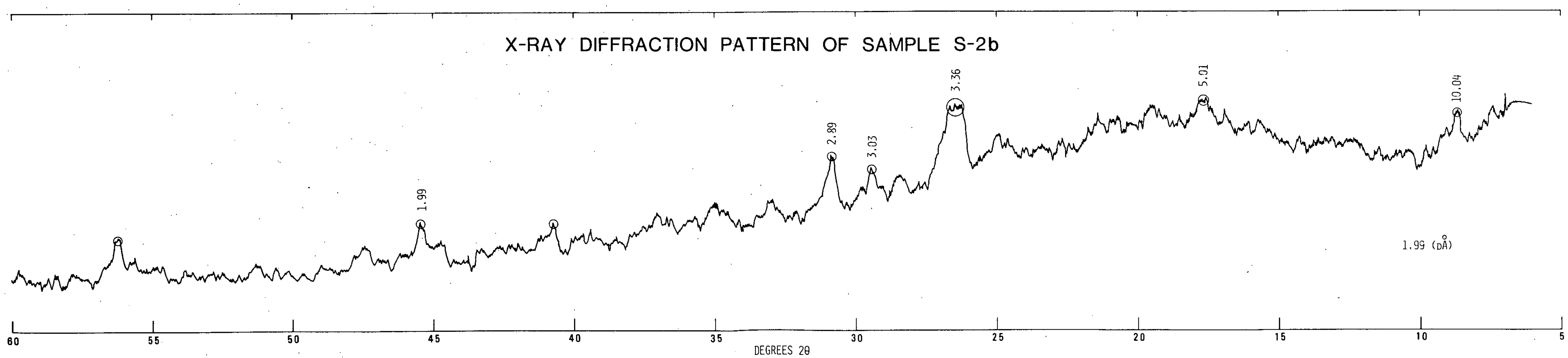
X-RAY DIFFRACTION PATTERN OF SAMPLE S-2b
3.36
5.01
10.04
2.89
3.03
1.99
1.99 (dÅ)
60
55
50
45
40
35
30
25
20
15
10
5
DEGREES 2θ

DAMES & MOORE

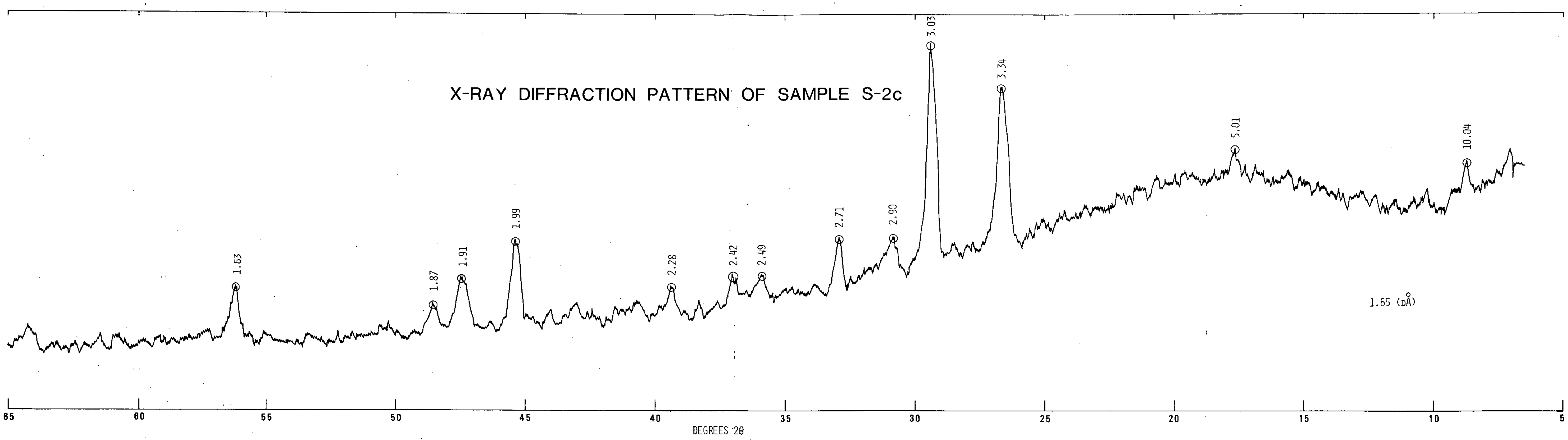
X-RAY DIFFRACTION PATTERN OF SAMPLE S-2c
3.03
3.34
5.01
10.04
1.99
2.71
2.90
1.63
1.87
1.91
2.28
2.42
2.49
1.65 (DÅ)
65
60
55
50
45
40
35
30
25
20
15
10
5
DEGREES 2θ

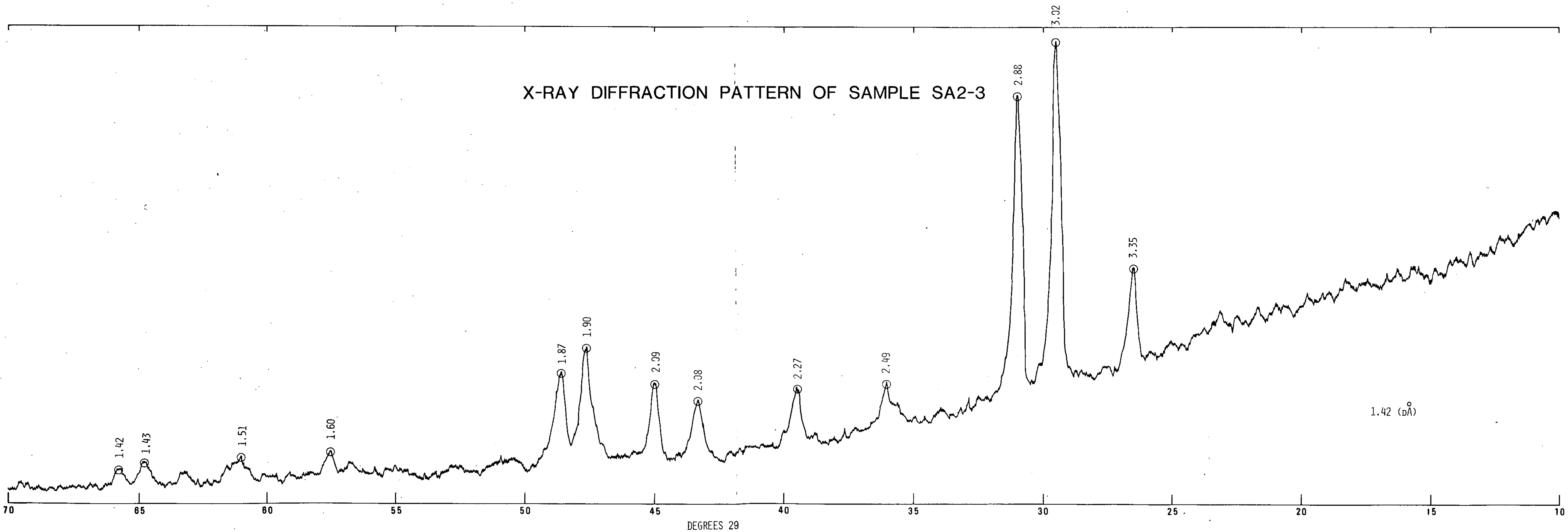
X-RAY DIFFRACTION PATTERN OF SAMPLE SA2-3
3.02
2.88
3.35
1.90
1.87
2.09
2.38
2.27
2.49
1.42
1.43
1.51
1.60
1.42 (DÅ)
70
65
60
55
50
45
40
35
30
25
20
15
10
DEGREES 2θ

DAMES & MOORE

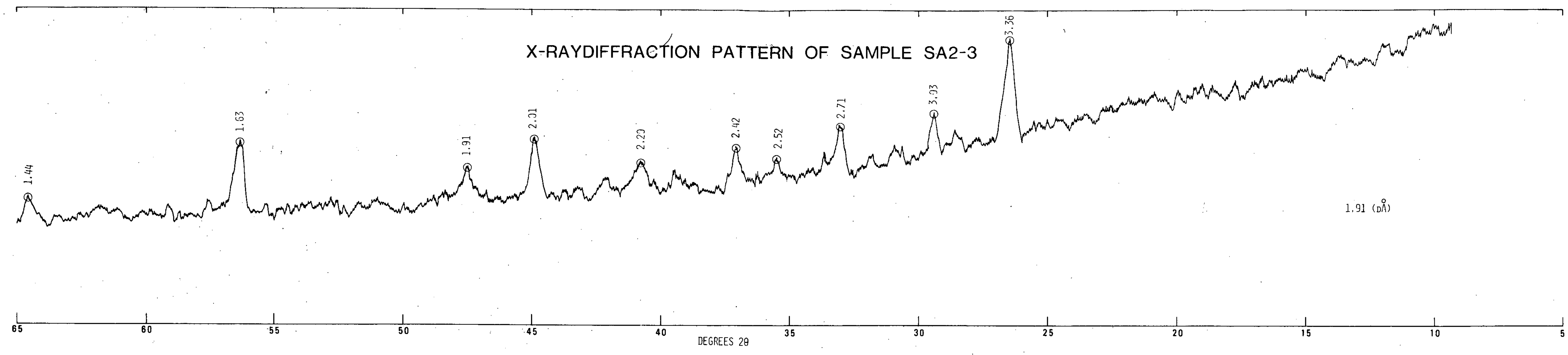

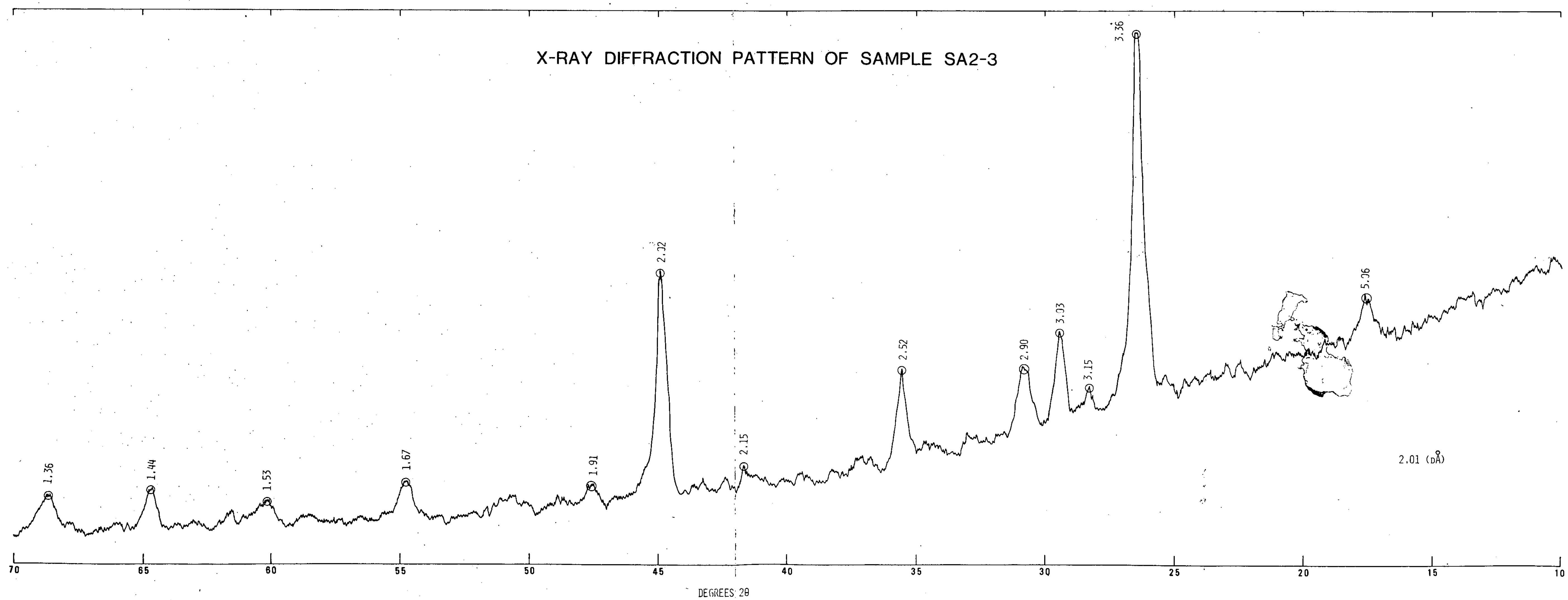

DAMES & MOORE

PLATE H1-10

X-RAY DIFFRACTION PATTERN OF SAMPLE SA2-6

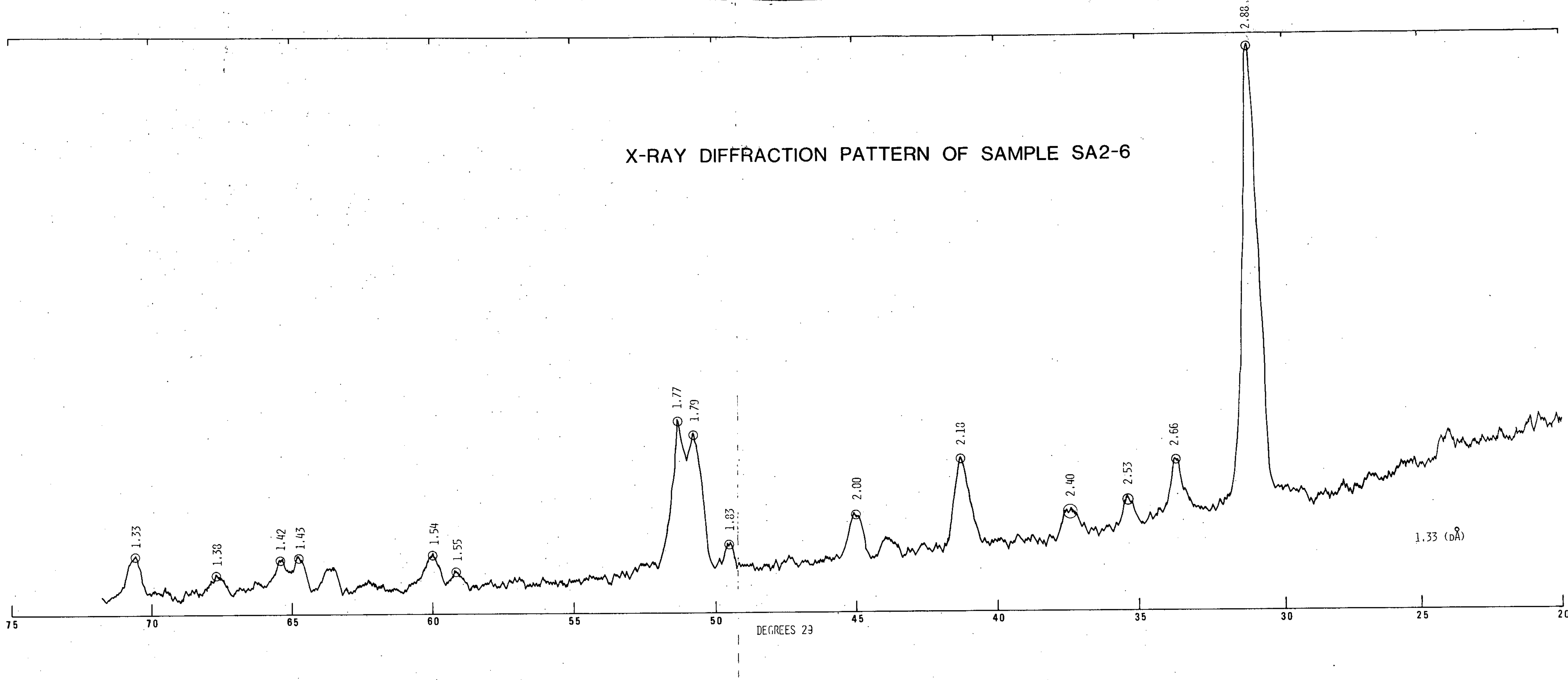

X-RAY DIFFRACTION PATTERN OF SAMPLE SB-30

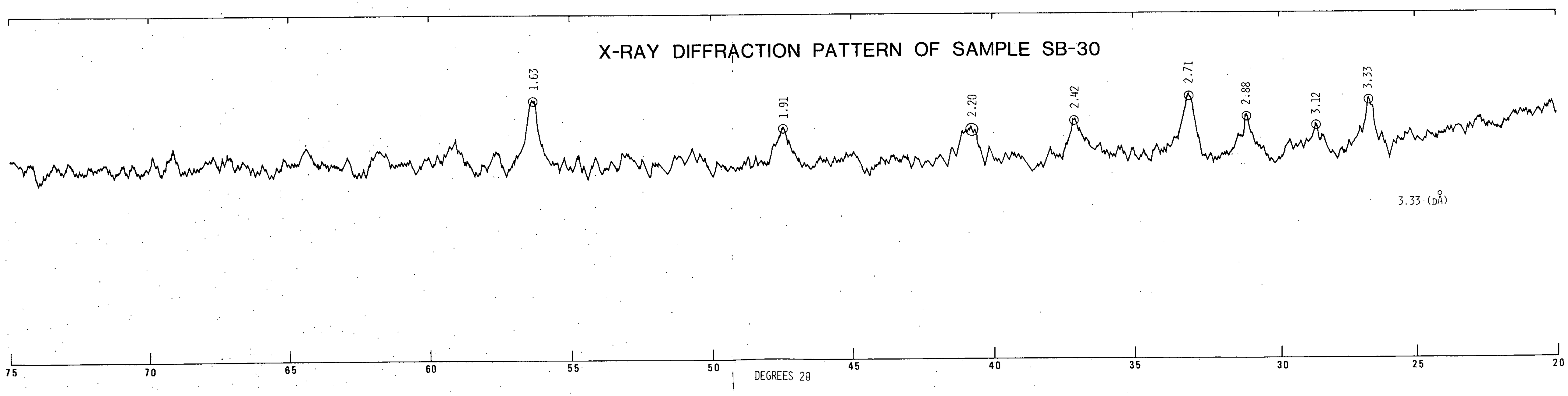

DAMES & MOORE

PLATE H1-11

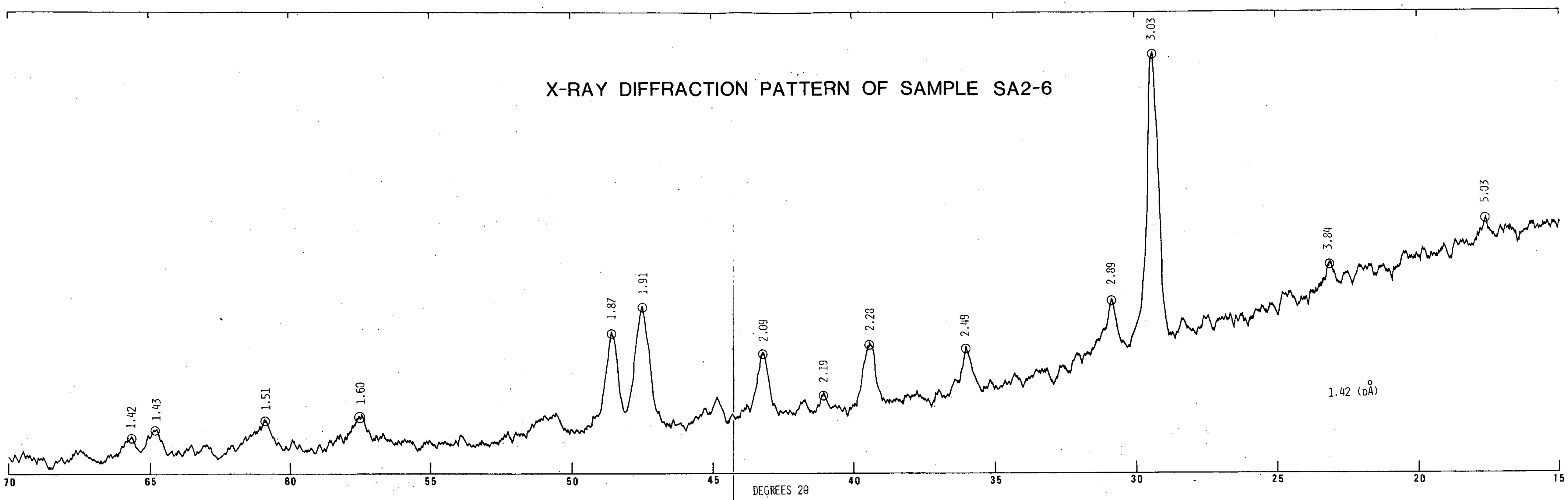
X-RAY DIFFRACTION PATTERN OF SAMPLE SA2-6
3.03
5.03
3.84
2.89
1.87
1.91
2.09
2.28
2.49
2.19
1.51
1.60
1.42
1.43
1.42 (dÅ)
70
65
60
55
50
45
40
35
30
25
20
15
DEGREES 2θ

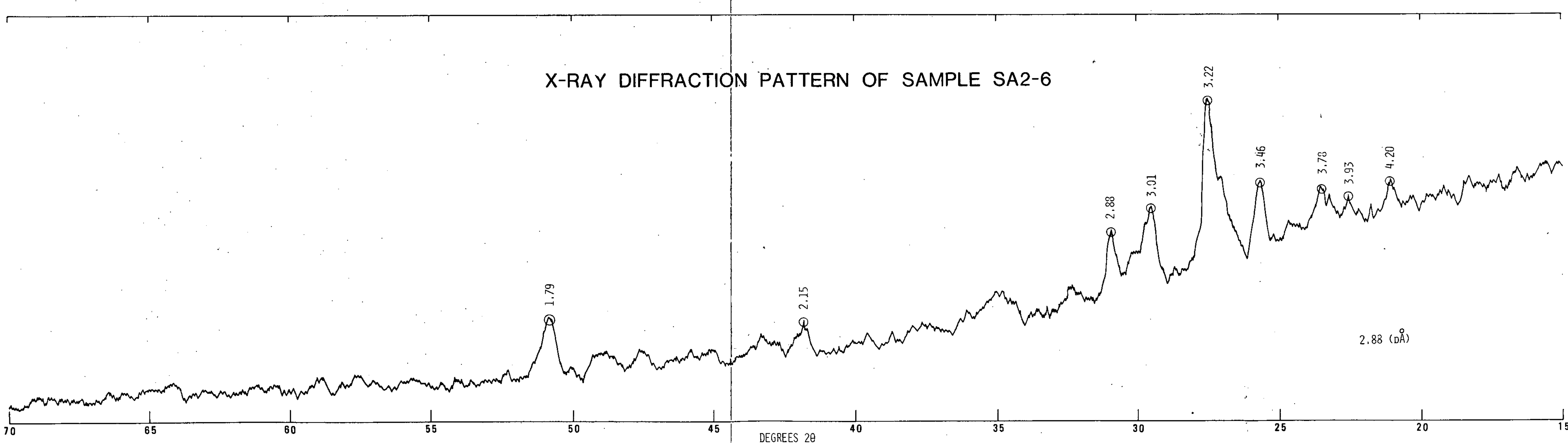
X-RAY DIFFRACTION PATTERN OF SAMPLE SA2-6
3.22
3.46
3.78
3.93
4.20
2.88
3.01
1.79
2.15
2.88 (dÅ)
70
65
60
55
50
45
40
35
30
25
20
15
DEGREES 2θ

DAMES & MOORE

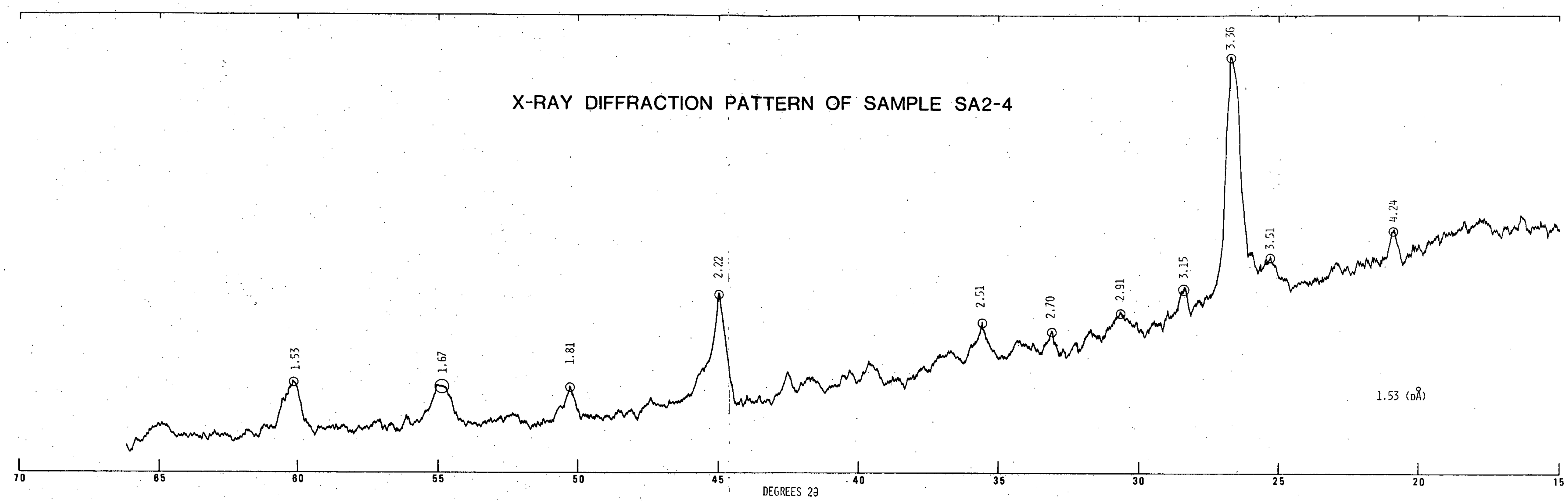

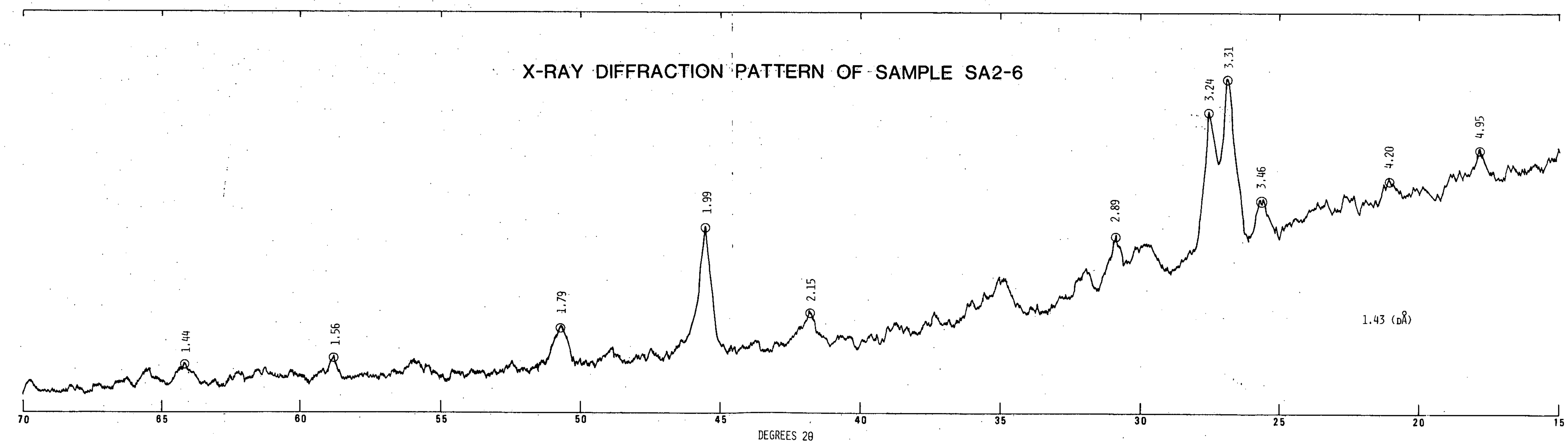

DAMES & MOORE

PLATE H1-13

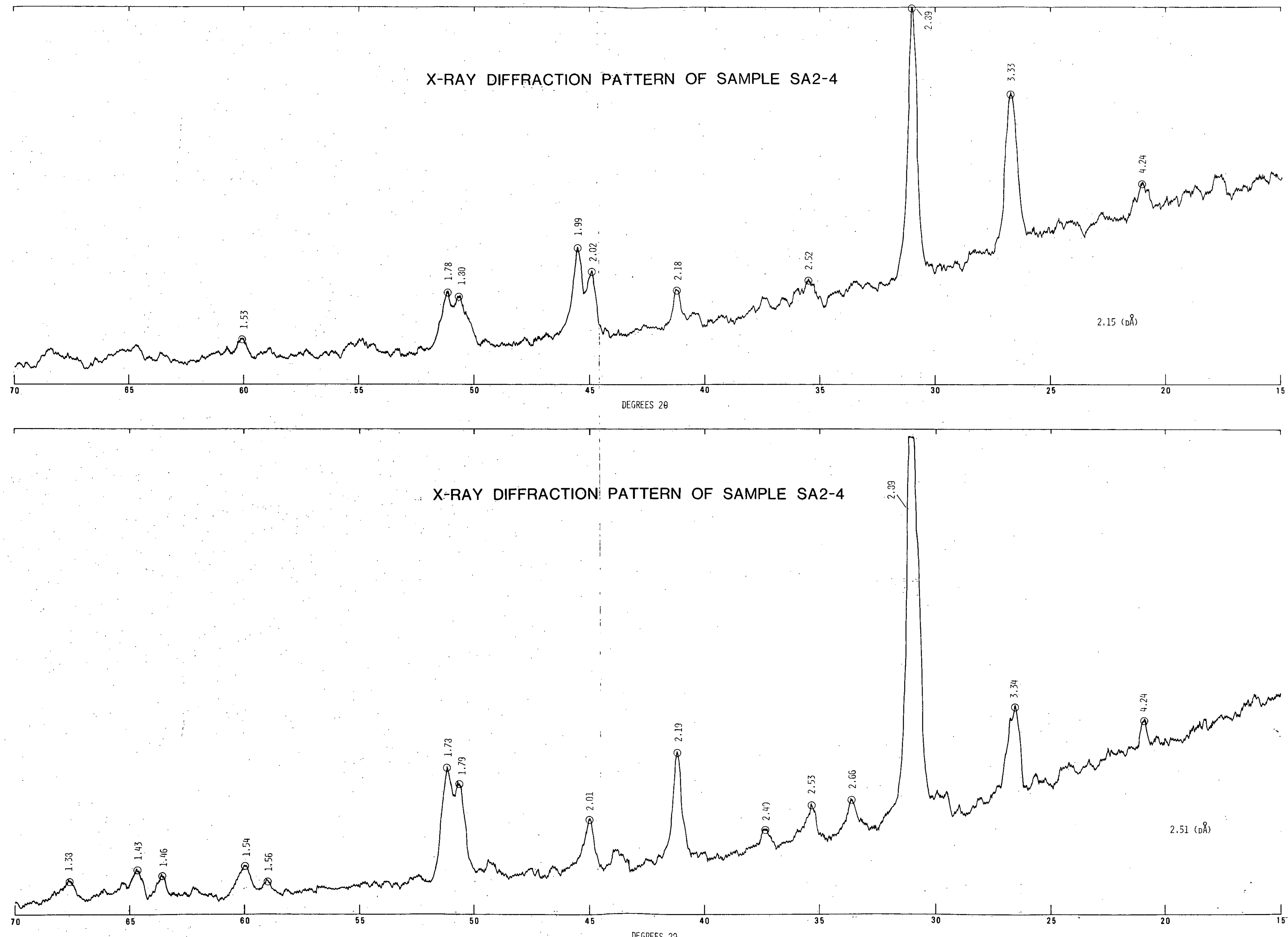
X-RAY DIFFRACTION PATTERN OF SAMPLE SA2-4
2.39
3.33
4.24
1.99
2.02
1.78
1.80
2.18
2.52
1.53
2.15 (DÅ)
70
65
60
55
50
45
40
35
30
25
20
15
DEGREES 2θ
X-RAY DIFFRACTION PATTERN OF SAMPLE SA2-4
2.39
3.34
4.24
2.19
1.73
1.79
2.01
2.66
2.53
2.49
1.33
1.43
1.46
1.54
1.56
2.51 (DÅ)
DEGREES 2θ

DAMES & MOORE

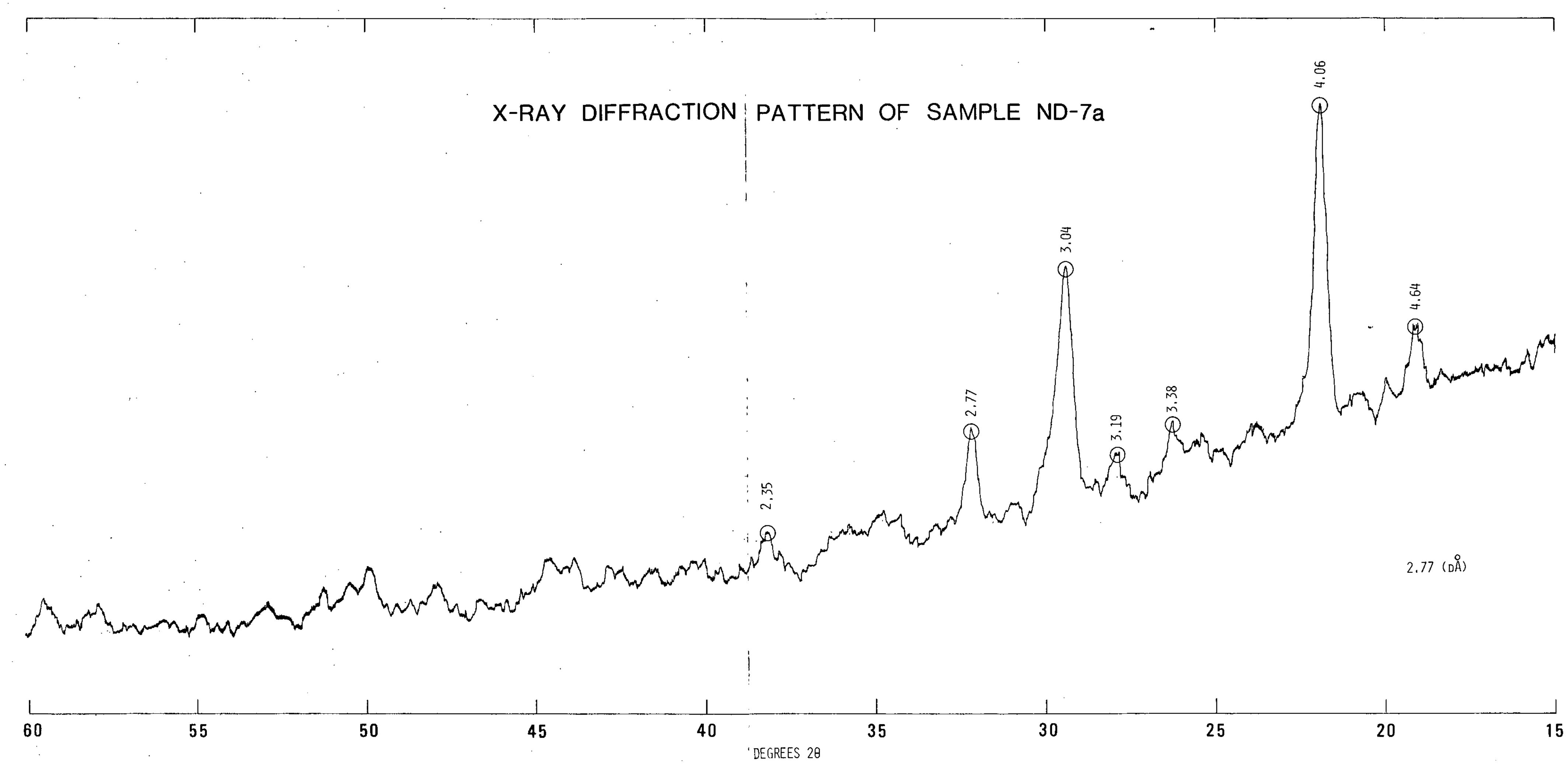

DAMES & MOORE

PLATE H1-15

X-RAY DIFFRACTION PATTERN OF SAMPLE ND-7b

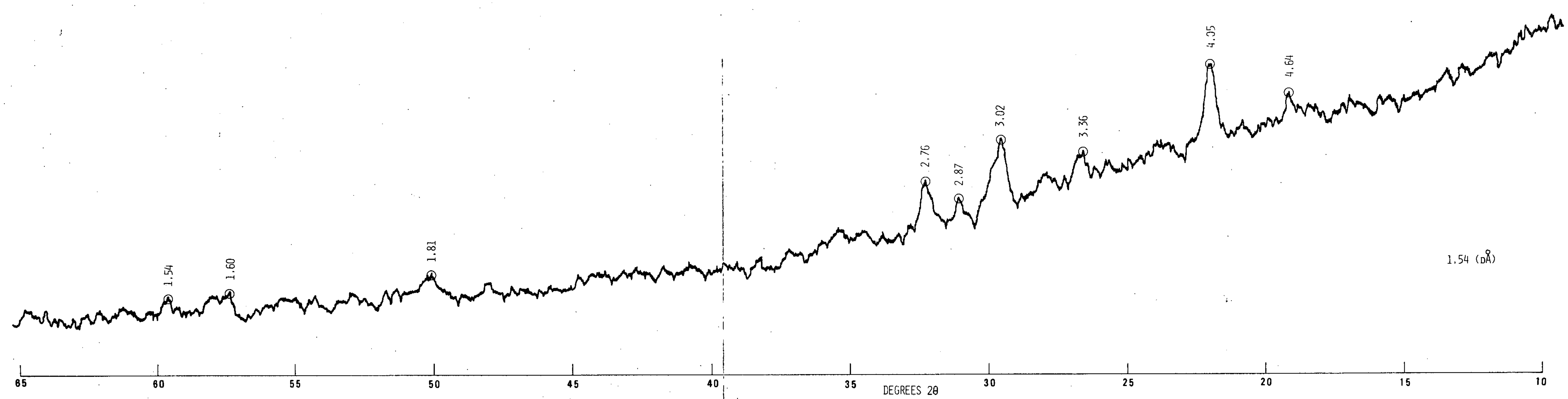

X-RAY DIFFRACTION PATTERN OF SAMPLE ND-7c

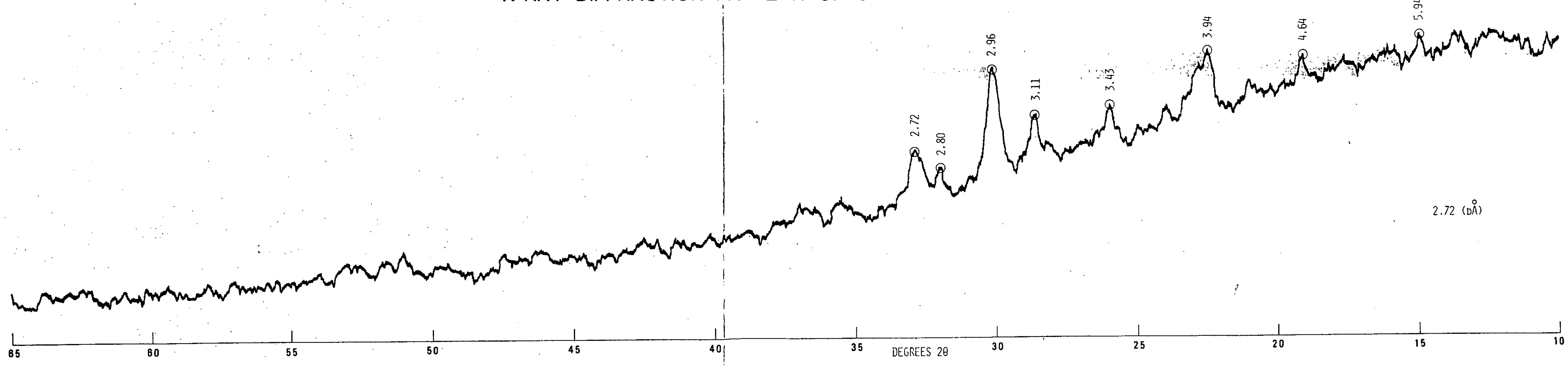

DAMES & MOORE

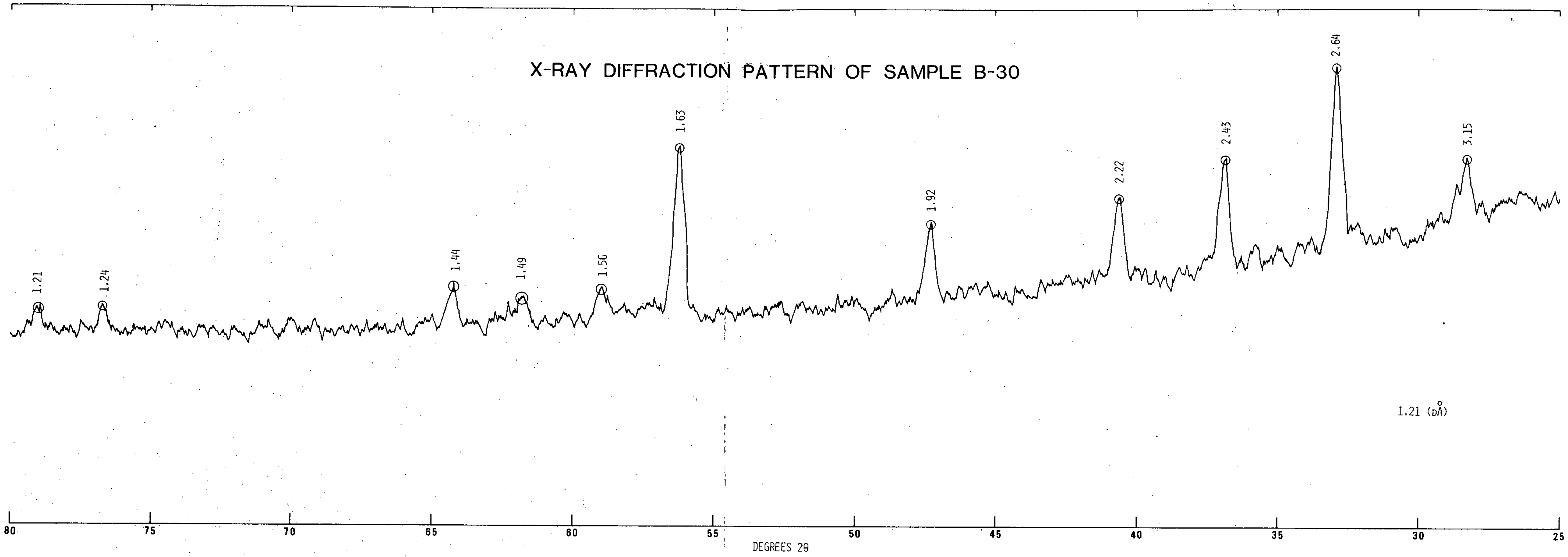
X-RAY DIFFRACTION PATTERN OF SAMPLE B-30
1.21
1.24
1.44
1.49
1.56
1.63
1.92
2.22
2.43
2.64
3.15
1.21 (dÅ)
80
75
70
65
60
55
50
45
40
35
30
25
DEGREES 2θ

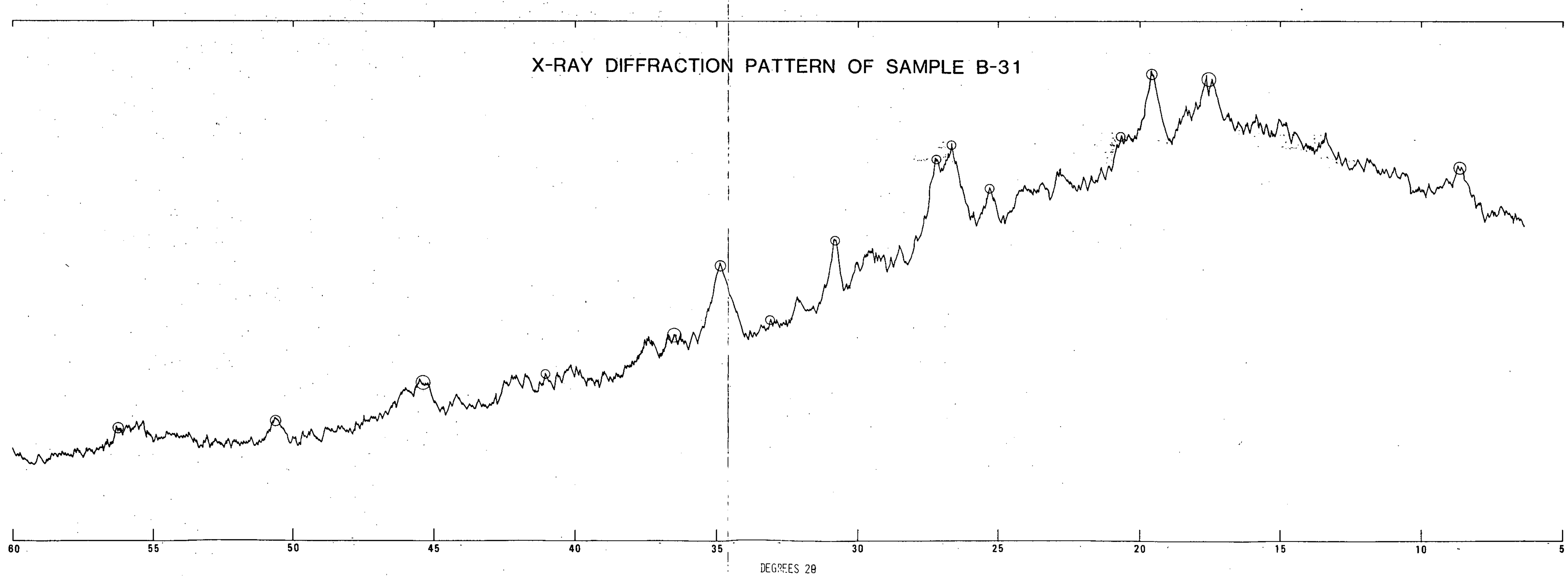
X-RAY DIFFRACTION PATTERN OF SAMPLE B-31
60
55
50
45
40
35
30
25
20
15
10
5
DEGREES 2θ

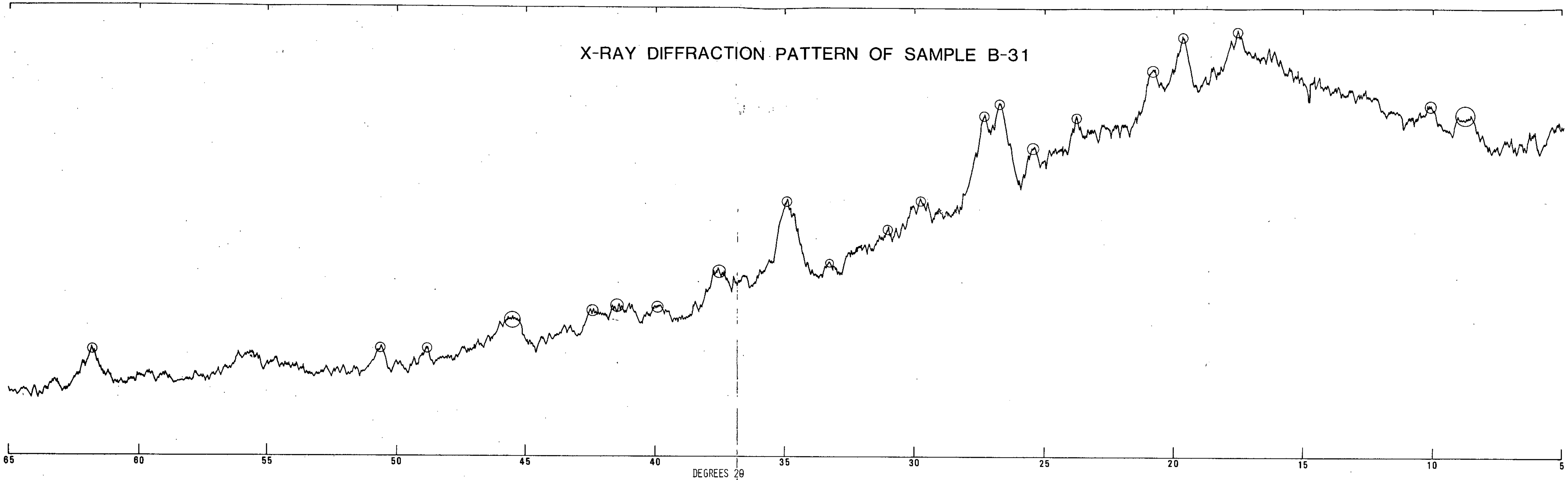
X-RAY DIFFRACTION PATTERN OF SAMPLE B-31
65
60
55
50
45
40
35
30
25
20
15
10
5
DEGREES 2θ

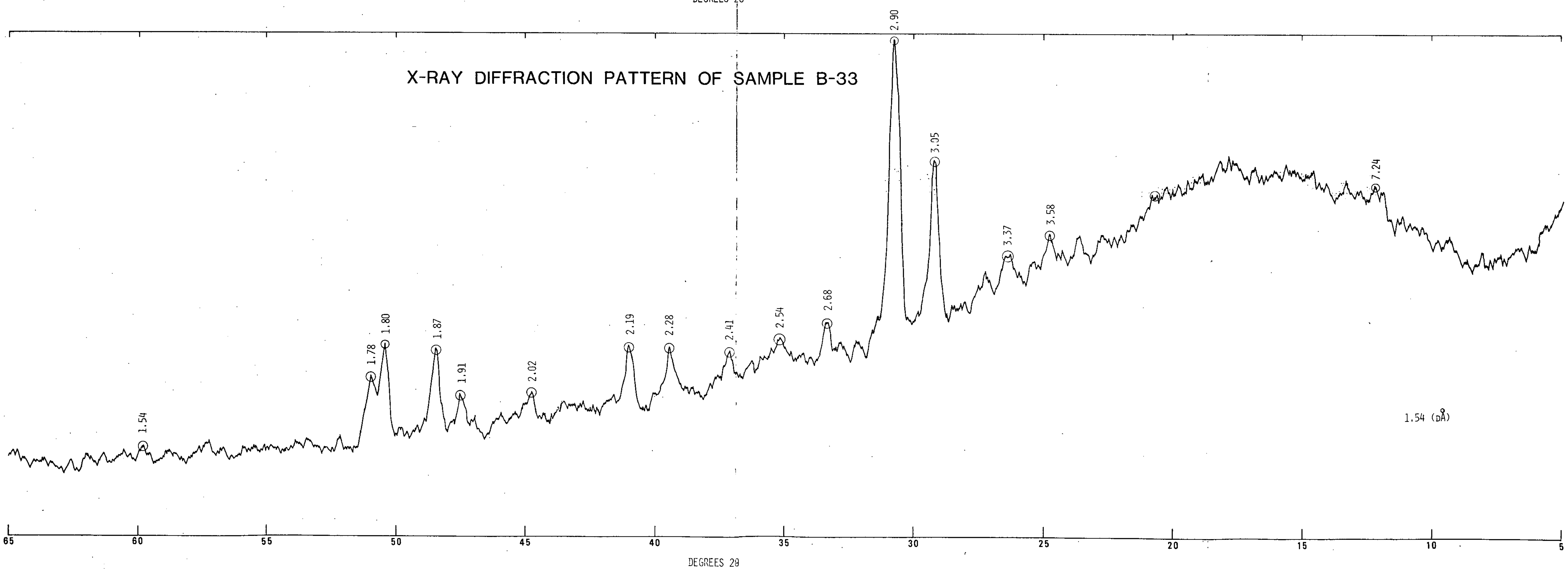
X-RAY DIFFRACTION PATTERN OF SAMPLE B-33
2.90
3.05
7.24
3.58
3.37
2.68
2.54
2.41
2.28
2.19
2.02
1.91
1.87
1.80
1.78
1.54
1.54 (dÅ)
65
60
55
50
45
40
35
30
25
20
15
10
5
DEGREES 2θ

DAMES & MOORE

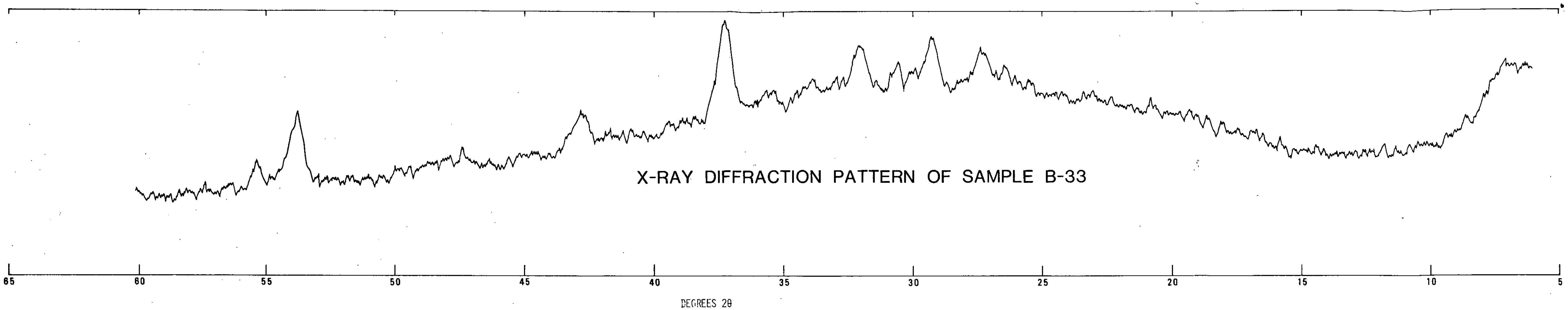
X-RAY DIFFRACTION PATTERN OF SAMPLE B-33
65
60
55
50
45
40
35
30
25
20
15
10
5
DEGREES 2θ

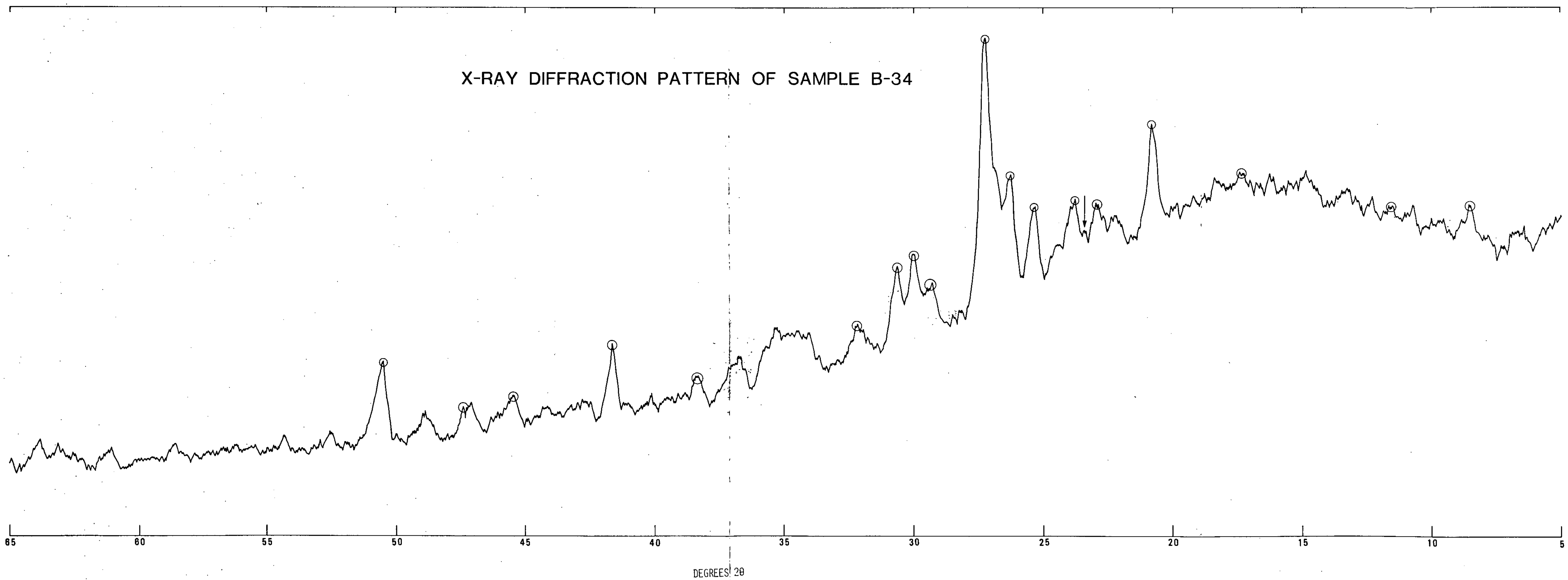
X-RAY DIFFRACTION PATTERN OF SAMPLE B-34
65
60
55
50
45
40
35
30
25
20
15
10
5
DEGREES 2θ

DAMES & MOORE

APPENDIX J

BIBLIOGRAPHY

APPENDIX J

BIBLIOGRAPHY

Balk, R. 1927, DiePrimaere Struktur des Noritmassive von Peekskill am Hudson, Noerdlich New York, Neves Jahab f. Mineral Beilageband 57, p. 253-255.

Berkey, C.P. and Rice, M., 1919, Geology of the West Point Quadrangle, New York: N.Y. State Mus. and Sci. Service Bull., no. 225-226, 152 p.

Bowes, D.R. and Langer, A.M., 1969, Polyphase Deformation in the Schists of the Bronx, New York City, p. 17-33 in Alexandrov, E., (ed.), Simposium of the New York City Group of Formations: Geological Bull. no. 3, Queens College Press, New York, 83 p.

de Boer, J., 1967, Paleomagnetic-Tectonic Study of Mesozoic Dike Swarms in the Appalachians: Jour. Geophys. Res. v. 72, no. 8, p. 2237-2250.

Broughton, J.G., Fisher, D.W., Isachsen, Y.W. and Rickard, L.V., 1966, Geology of New York: A Short Account from Geologic Map of New York State Mus. Educational Leaflet 20, p. 17-21.

Brown, J.S., 1968, Ore Deposits of the United States 1933-1937: in Graton-Sales Vol., Ridge, J.D., ed., Amer. Inst. Mining, Metallurgical and Petroleum Eng., New York, p. 1-19.

Bucher, W.H., 1951, Infolded mid-Ordovician Limestone on Precambrian North of Peekskill, N.Y., and its Bearing on the Region's Orogeny (Abstract): Geol. Soc. America Bull., v. 62, p. 1426-1427.

Bucher, W.H., 1957, Taconic Klippe: A Stratigraphic-Structural Problem, Geol. Soc. America Bull., v. 68, p. 657-674.

Coates, D.R., and others, 1975, Quaternary Sediment Deformation as a Seismic Indicator in the St. Lawrence Lowland, New York: Geol. Soc. America Bull., Abs. with Programs, v. 7, no. 7, p. 1030-1031.

Connally, G.G. and Sirkin, L., 1970, Late Glacial History of the Upper Wallkill Valley, New York: Geol. Soc. America Bull., v. 81, p. 3297-3306.

Dallmeyer, R.D., 1969, Structural and Metamorphic History of the Precambrian Gneisses at Bear Mountain, New York: M.S. Thesis, State University of New York, Stony Brook, N.Y., 56 p.

Dallmeyer, R.D., 1972, Precambrian Structural History of the Hudson Highlands Near Bear Mountain, New York: Geol. Soc. America Bull., v. 83, p. 895-904.

Dallmeyer, R.D., 1975, The Palisades Sill: A Jurassic Intrusion? Evidence from 40 Ar/29 Ar Incremental Release Ages: Geology, v. 3, no. 5, p. 243-245.

Dallmeyer, R.D., Baker, D.J. and Sutter, J.F., 1974, 40 Ar/39 Ar Incremental Release Ages of Biotite and Hornblende from Retrograded Grenville Gneisses in the Northeastern Reading Prong., New York (Abstr.): Geol. Soc. America, Abstr. with Prog. v. 6, no. 7, p. 703-704.

Dallmeyer, R.D., Sutter, J.F. and Baker, D.J., 1975, Incremental 40 Ar/39 Ar Ages of Biotite and Hornblende from the Northeastern Reading Prong: Their Bearing on Late Proterozoic Hermal and Tectonic History: Geol. Soc. America Bull., v. 86, p. 1435-1443.

Dames & Moore, 1974, Geologic Report, Limerick Generating Station, Limerick, Pennsylvania.

Dames & Moore, 1975, Supplemental Geological Investigation of the Fulton Generating Station, Appendix B.9.

Darton, N.H., 1890, The Relations of the Traps of the Newark System in the New Jersey Region: U.S. Geol. Survey, Bull., 67, 82 p.

Davis, W.M., 1891, Dates of Origin of Certain Topographic Forms on the Atlantic Slope: Geol. Soc. America Bull., v. 2, p. 570-571.

Dodd, R.T., Sr., 1965, Precambrian Geology of the Popolopen Lake Quadrangle, Southeastern New York: N.Y. State Mus. & Sci. Service Map and Folio Series no. 9, 39 p.

Dolgoff, A., 1958, The Cortlandt Complex: New York State Geol. Ass'n Guidebook, 30th Ann. Meeting, p. 18-22.

Durney, D.W. and Ramsey, J.G., 1973, Incremental Strains Measured by Syntectonic Crystal Growths: in DeJong, K.A. and Schelton, R., (eds.) Gravity and Tectonics, John Wiley and Sons, p. 67-96.

Espejo, A.C., 1969, Pluton (Precambrian), New York: MS Thesis Queens College of CUNY.

Faill, R.T., 1973, Tectonic Development of the Triassic Newark-Gettysburg Basin in Pennslyania: Geol. Soc. America Bull., v. 84, p. 725-740.

Fisher, D.W., Isachsen, Y.W., and Rickard, L.V., 1970, Geologic Map of New York: New York State Mus. and Sci. Serv., Map and Chart Series no. 5.

Flint, R.F., 1963, Probable Wisconsin Substages and Late-Wisconsin Events in Northeastern United States and Southern Canada: Geol. Soc. America Bull., v. 64, p. 897-920.

Frimpler, M., 1967, Geology of the Thiells Quadrangle, N.Y., with Emphasis on the Igneous and Metamorphic Rocks: Ph.D. Dissertation, Boston University, 146 p.

Glaeser, J.D., 1966, Provenance, Dispersal and Depositional Environments of Triassic Sediments in the Newark-Gettysburg Basin: Penn. Geol. Survey, Rept. G-43, 168 p.

Haas, J.L., 1971, The Effect of Salinity on the Maximum Thermal Gradient of a Hydrothermal System at Hydrostatic Pressure, Economic Geology, v. 66, p. 940-945.

Hadley, J.B., 1964, Correlation of Isotopic Ages, Crustal Heating, and Sedimentation in the Appalchian Region, in Lowry, W.D., ed., Tectonics of the Southern Appalachians: VPI Dept. of Geol. Sciences, Mem. 1, p. 33-45.

Hall, L.M., 1968, Times of Origin and Deformation of Bedrock in the Manhattan Prong; p. 117-127 in Zen, E-an, White, W.S., Hadley, J.B. and Thompson, J.B., Jr., (eds.), Studies of Appalachian Geology - Northern and Maritime, New York, Wiley - Interscience, 475 p.

Harwood, D.S., and Zietz, I., 1974, Configuration of Precambrian Rocks in Southern New York and Adjacent New England from Aeromagnetic Data: Geol. Soc. America Bull., v. 85, p. 181-188.

Helenek, H.L., 1971, An Investigation of the Origin, Structure and Metamorphic Evolution of Major Rock Units in the Hudson Highlands: Ph.D. Dissertation, Brown University, 244 p.

Hubbert, M.K., 1951, Mechanical Basis for Certain Familiar Geologic Structures: Geol. Soc. America Bull., v. 70, p. 355-372.

Jaffe, H.W. and Jaffe, E.B., 1962, Geology of the Precambrian Crystalline Rocks, Cambro-Ordovician Sediments, and Dikes of the Southern Part of the Monroe Quadrangle; p. B-1 - B-11 in Valentine, W.G., (ed.), Guidebook to Field Trips - N.Y. State Geological Assoc. - 34th Ann. Mtg. - Port Jervis.

Jaffe, H.W. and Jaffe, E.B., 1973, Bedrock Geology of the Monroe Quadrangle, New York: State Mus. and Sci. Serv., Map and Chart Series no. 20.

Johnson, D.W., 1931, Stream Sculpture on the Atlantic Slope: Columbia Univ. Press, New York, 142 p.

Judson, S. and Ritter, P., 1964, Rates of Denudation in the United States: Jour. Geophys. Research, v. 69, no. 16, p. 3395-3401.

Klein, G. deVries, 1969, Deposition of Triassic Sedimentary Rocks in Separate Basins, Eastern North America: Geol. Soc. America Bull., v. 80, p. 1825-1832.

Kümmel, H.B., 1898, The Newark or New Red Sandstone Rocks of Rockland County, N.Y.: (1900) New York State Museum, 52nd Annual Report of the Regents, p. 9-50.

Langer, A.M., and Bowes, D.R., 1969, Polyphase Deformation in the Manhattan Island, N.Y. City, p. 361-377 in Larsen, L.H.; Prinz, M. and Manson, V., (eds.), Igneous and Metamorphic Geology: Geol. Soc. America Memoir, no. 115, 561 p.

Long, L.E., 1969, Whole-rock Rb-Sr. Age of the Yonkers Gneiss, Manhattan Prong: Geol. Soc. America Bull., v. 80, no. 10, p. 2087-2090.

Long, L.E., and Kulp, J.L., 1962, Isotopic Age Study of the Metamorphic History of the Manhattan and Reading Prong: Geol. Soc. America Bull., v. 73, p. 969-996.

Lowe, K.E., 1950, Storm Key Granite at Bear Mountain, New York: Geol. Soc. America, Bull., v. 61, p. 137-190.

Lowe, K.E., 1959, Structure of the Palisades Intrusion at Haverstraw and West Nyack, New York: N.Y. Acad. Sci. Annale v. 90, p. 1127-1147.

McLaughlin, D.B., 1942, The Distribution of Minor Faults in the Triassic of Penn: Mich. Acad. Science Paper, v. 27, p. 465-479.

Mack, S., 1950, Petrography and Structure of Some Non-Pegmetite Dikes in the Hudson Highlands of New York: M.S. Thesis, Syracuse University, Syracuse, New York, 80 p.

Markl, R.G., 1971, Pleistocene Geology of Croton Point: N.Y. Acad. Sci. Trans., v. 33, no. 5, p. 505-515.

Meade, R.H. "Errors in Using Modern Streamload Data To Estimate Natural Rates of Denudation", Geol. Soc. Amer. Bull. 1969 Vol. 80 p. 1265-1274.

Mose, D. Hayes, J., and Odom, A.L., 1974, Pound Ridge Granite Gneiss and Peekskill Granite: Rb/Sr Whole-rock Age Determinations in the Manhattan Prong (Abstr.): Geol. Soc. America Abstr. with Prog. v. 5, no. 1, p. 58.

Mose, D. and Baiamonte, M., Haynes, J., and LoBello, L., 1975, Rb/Sr Age Determination of a Multiple Intrusion in the Ramapo Fault Zone, Southeastern New York (Abstr.): Geo. Soc. America Abstr. with Prog. v. 7, no. 1, p. 97.

Mose, D. and Hayes, J., 1974, Rb/Sr Whole Rock Age Determination in the Precambrian Reading Prong, New York and New Jersey (Abstr.): Geol. Soc. America Abstr. with Prog. v. 6, no. 7, p. 878-879.

Mose, D. and Hayes, J., 1975, Avalonian Igneous Activity in the Manhattan Prong, Southeastern New York: Geol. Soc. America, v. 86, p. 929-932.

Muehlberger, W.R., 1961, Conjugate Sets of Small Dihedral Angle: Jour. Geol., v. 69, p. 211-219.

Newman, W.S., Thurber, D.H., Zeiss, H.S., Rokack, A. and Musich, L., 1969, Late Quaternary Geology of the Hudson River Estuary: A Preliminary Report: Trans. N.Y. Acad. Sci., p. 548-570.

Oliver, J., Johnson, T. and Dorman, J., 1970, Postglacial Faulting and Seismicity in New York and Quebec: Canadian Jour. Earth Sci., v. 7, p. 579-590.

Paige, S., 1956, Cambro-Ordovician Age of the "Inwood" Limestone and "Manhattan" Schist Near Peekskill, New York: Geol. Soc. America Bull., v. 67, p. 391-394.

Parker, J.M., 1942, Regional Systematic Jointing in Slightly Deformed Sedimentary Rocks; Geol. Soc. America Bull., v. 53, p. 381-408.

Peet, C.E., 1904, Glacial and Post-Glacial History: Jour. Geol., v. 12, p. 415-453.

Peterson, J.R., 1970, The Mineral Industries of New York State: New York State Dept. of Commerce, Division of Commerce and Industry, Albany, New York, p. 102.

Prucha, J.J., 1956, Stratigraphic Relationships of the Metamorphic Rocks in Southeastern New York: Amer. Jour. Sci., v. 254, p. 672-684.

Ratcliffe, N.M., 1968, Contact Relations of the Cortlandt Complex at Stony Point, N.Y. and Their Regional Implications: Geol. Soc. America Bull., v. 79, p. 777-786.

Ratcliffe, N.M., 1969, Stratigraphic Relations Along the Western Edge of the Cortlandt Intrusives and Their Bearing on the Inwood-Manhattan Problem: Geol. Bull., no. 3, Queens College Press, p. 49-54.

Ratcliffe, N.M., 1970, Ancient Strike-Slip Fault Tectonics in the Hudson Highlands and Manhattan Prong: New York Acad. Sci., Trans. Ser. 11, v. 32.

Ratcliffe, N.M., 1971, The Ramapo Fault System in New York and Adjacent Northern New Jersey: A Case of Tectonic Heredity: Geol. Soc. America Bull., v. 82, p. 125-142.

Ratcliffe, N.M., 1972, Geology of the Ramapo Fault System: in Averill, S.P. (ed.), Field Trip Guidebook Eastern Section, Nat. Ass'n Geol. Teachers, Fairleigh Dickenson University, Rutherford, N.J., p. 1-1 to 1-13.

Ratcliffe, N.M., 1975, Preliminary Report on Fault Systems, in Vicinity of Indian Point, Peekskill and Haverstraw Quadrangles, N.Y.: Report to Consolidated Edison Co. of N.Y., Inc.

Ratcliffe, N.M. and Knowles, R.R., 1969, Stratigraphic Relations Along the Western Edge of the Cortlandt Intrusives and Their Bearing on the Inwood-Manhattan Problem: Geol. Bull., no. 3, Queens College Press.

Ratcliffe, N.M., Armstrong, R.L., Chai, B.H.T. and Senechal, R.G., 1972, K-Ar and Rl-Se Geochronology of the Canopus Pluton, Hudson Highlands, New York: Geol. Soc. America Bull., v. 83, p. 523-530.

Reeds, C.A., 1927, Glacial Lakes and Clays Near New York City: National History: v. 27, p. 54-64.

Ruedemann, R., 1932, Development of Drainage of Catskills: Am. Jour. Sci., v. 223, p. 337-349.

Salisbury, R.D., 1902, Pleistocene Formations, U.S. Geol. Surv. Folio no. 83, New York City.

Sanders, J.E., 1960, Structural History of Triassic Rocks of the Connecticut Valley Belt and its Regional Implications: N.Y. Academy Science, Trans., Series II, v. 23, p. 119-132.

Sanders, J.E., 1971, Triassic Rocks, Northeastern North America: Regional Tectonic Significance in Light of Plate Tectonics: Geol. Soc. America Bull., Abstracts with Programs, v. 3, no. 7, p. 781-783.

Sanders, J.E., 1974, Guidebook to Field Trip in Rockland County, N.Y.: Petroleum Exploration Society of New York, New York, 87 p.

Shand, S.J., 1942, Phase Petrology of the Cortlandt Complex: Geol. Soc. America Bull., v. 53, p. 409-428.

Sirkin, L.A., 1967, Late-Pleistocene Pollen Stratigraphy of Western Long Island and Eastern Staten Island, New York; in Cushing, E.J. and Wright, H.E., Jr., eds., Quaternary Paleoecology: 7th Internat. Cong. Assoc. Quaternary Res., 1965 Proc., v. 7; New Haven, Yale Univ. Press, p. 249-274.

Sutter, J.F. and Dallmeyer, R.D., 1972, of $^{40}Ar/^{39}Ar$ and K-Ar Ages of Biotites Comparison and Hornblendes from the Precambrian of Southeastern New York, and North-Central New Jersey, Geol. Soc. America Bull. Abst., 1972 Annual Meeting.

Thompson, H.D., 1936, Hudson Gorge in the Highlands: Geol. Soc. America Bull., v. 47, p. 1831-1848.

Thompson, H.D., 1959, The Palisades Ridge in Rockland County, N.Y.: N.Y. Academy Science, Annals, v. 80, p. 1106-1126.

Urban, T.C., 1971, Terrestrial Heat Flow in the Middle Atlantic States, 1970, PhD. Dissertation, Univ. of Rochester, N.Y.

Urban, T.C., Bromery, R.W., Revetta, F.A., and Dimert, W.H., 1973, Simple Bouger Gravity Anomaly Map of Southeastern New York and Contiguous States: New York State Mus. and Sci. Service, Geol. Survey, Map and Chart Series no. 17C.

Van Houten, F.B., 1969, Late Triassic Newark Group North-Central New Jersey and Adjacent Pennsylvania and New York: in Subitzky, S., (ed.) Geology of Selected Areas in New Jersey and Eastern Pennsylvania and Guidebook of Excursions: New Brunswick, New Jersey, Rutgers University Press, p. 314-347.

Weiss, D., 1974, Late Pleistocene Stratigraphy and Paleoecology of the Lower Hudson River Estuary: Geol. Soc. America Bull., v. 85, p. 1561-1570.

Wood, C.R., 1963, Geologic Map of the Brunswick and Lockatong Formations in Berks and Montgomery County, Pennsylvania.

Woodworth, J.B., 1905, Ancient Water Levels of the Champlain and Hudson Valleys: N.Y. State Mus. Bull., no. 84, p. 85-265.

Worzel, J.L. and Drake, C.L., 1959, Structure Section Across the Hudson River at Nyack, N.Y. from Seismic Observation. Ann. N.Y. Acad. Sci., v. 80, p. 1092-1105.

34-1

3